Scientific Programming

Optimization Models and Algorithms for Services and Operations Management 2021

Lead Guest Editor: Lu Zhen
Guest Editors: Xiaobo Qu and Tingsong Wang

Optimization Models and Algorithms for Services and Operations Management 2021

Scientific Programming

Optimization Models and Algorithms for Services and Operations Management 2021

Lead Guest Editor: Lu Zhen
Guest Editors: Xiaobo Qu and Tingsong Wang

Copyright © 2022 Hindawi Limited. All rights reserved.

This is a special issue published in "Scientific Programming." All articles are open access articles distributed under the Creative Commons Attribution License, which permits unrestricted use, distribution, and reproduction in any medium, provided the original work is properly cited.

Chief Editor

Emiliano Tramontana, Italy

Academic Editors

Marco Aldinucci, Italy
Daniela Briola, Italy
Debo Cheng, Australia
Ferruccio Damiani, Italy
Sergio Di Martino, Italy
Sheng Du, China
Basilio B. Fraguela, Spain
Jianping Gou, China
Jiwei Huang, China
Sadiq Hussain, India
Shujuan Jiang, China
Oscar Karnalim, Indonesia
José E. Labra, Spain
Maurizio Leotta, Italy
Zhihan Liu, China
Piotr Luszczek, USA
Tomàs Margalef, Spain
Cristian Mateos, Argentina
Zahid Mehmood, Pakistan
Roberto Natella, Italy
Diego Oliva, Mexico
Antonio J. Peña, Spain
Danilo Pianini, Italy
Jiangbo Qian, China
David Ruano-Ordás, Spain
Željko Stević, Bosnia and Herzegovina
Kangkang Sun, China
Zhiri Tang, Hong Kong
Autilia Vitiello, Italy
Pengwei Wang, China
Jan Weglarz, Poland
Hong Wenxing, China
Dongpo Xu, China
Tolga Zaman, Turkey

Contents

Hindawi
Scientific Programming
Volume 2022, Article ID 6994700, 11 pages
https://doi.org/10.1155/2022/6994700

Research Article

Joint Ordering and Selling Policy for Storable Agricultural Products in Contract Farming

Shui Wenbing and Xinrui Chen

Faculty of Transportation Engineering, Kunming University of Science and Technology, Kunming 650500, China

Correspondence should be addressed to Xinrui Chen; 20192206005@stu.kust.edu.cn

Received 23 April 2021; Revised 25 October 2021; Accepted 27 January 2022; Published 15 February 2022

Academic Editor: Shah Nazir

Copyright © 2022 Shui Wenbing and Xinrui Chen. This is an open access article distributed under the Creative Commons Attribution License, which permits unrestricted use, distribution, and reproduction in any medium, provided the original work is properly cited.

With the farming mode widely promoted in many countries around the world, agricultural enterprises need to face risks from both supply and sales at the same time. Especially for storable agricultural products, it is also necessary to consider the potential profits and losses brought about by the sales of multi-period. This paper establishes a joint ordering and selling decision model under multiperiod random supply and demand. The model takes the maximum expected profit of agricultural enterprises as the goal, considers the constraints of production capacity and the risk preference coefficient of shortage, and makes decisions on the order and sales quantity in each cycle. The feasibility of the model was verified by taking China Yunnan Pu'er tea as a specific example. Finally, through numerical examples, the influence of important parameters on the joint ordering and selling strategy is as follows: order cost is the main factor affecting the order quantity. When the order cost increases to a certain level, the solving algorithm will make a decision that would rather be out of stock than to order. With the increase in selling price, inventory holding cost, and shortage cost, there will be an increasing trend of the sales quantity allocated to this period. Compared with other parameters, selling price and inventory holding cost have a more remarkable impact on sales quantity. In addition, enterprises can increase their expected profits of storable agricultural products by controlling the inventory holding cost, appropriately reducing the risk preference coefficient, and increasing the level of the selling price.

1. Introduction

To solve the conflicts between individual farmers and huge markets, contract farming has been widely promoted in many countries. Contract farming means that farmers and enterprises or intermediary organizations sign a contract with a legal effect that determines the rights and obligations of both parties before the production process. This type of agricultural cooperative business form requires the farmers to organize production according to the contract and the enterprises or intermediary organizations to acquire products produced by farmers following the contract. In China, the primary participants in agricultural planting are mostly self-employed farmers. They can obtain more economic benefits through stable sales channels provided by contract farming. Huge market development space and strong promotion from the government are also the driving force of this mode. Because of individual agriculture mode occupying a dominant position, China's contract farming industry is still in the initial stage of development [1]. However, contract farming has huge development potential in China and is worth studying under the trend of large-scale industrial production and farmers' professional cooperatives.

According to the storage performance in physiological characteristics, agricultural products can be roughly divided into fresh agricultural products and storable agricultural products. Storable agricultural products generally have longer storage periods and lower storage requirements, such as grain, cotton, soybeans, coffee beans, ginseng, rubber, tea, and herbal medicines, many of which have high unit product value or huge circulation. These products can be sold for a long period without processing or after simple processing. Because of their huge market share, the industry of such

products is an important part of supporting the rural economy. In 2020, which was severely affected by the COVID-19 pandemic, the Chinese export volume of some storable agricultural products with nutritional or medicinal value has increased significantly, which decreased the economic losses of agricultural enterprises caused by the epidemic [2]. Excellent storage performance makes storable agricultural products suitable for the mode of contract farming. Based on the above discussions, this paper chooses storable agricultural products as the research objects. To research these products under contract farming, it is necessary to clarify their characteristics.

The supply and demand uncertainty are the common characteristics of storable agricultural products and even all agricultural products. On the one hand, the factors that affected the yield of agricultural production are complicated. Controllable factors, including capital, labor, land input, and planting technology, affect the overall scale of agricultural production. Uncontrollable factors included weather, season, and natural disasters, which cause output fluctuation. These elements together influence the uncertainty in supply [3]. On the other hand, the demand uncertainty of storable agricultural products is mainly reflected in the uncertain factors during the demand accumulation process. Unlike industrial production that can start the machine at any time, the planting cycle of agricultural products is long and fixed. Orders accumulate during the planting period and sharply increase in the product harvest season. These orders will not be processed until the agricultural products are harvested. The total demand of the whole sales cycle is difficult to accurately predict. However, compared with fresh agricultural products, storable agricultural products have the inventory to meet uncertain demand, which greatly reduces the probability of shortages.

Another characteristic of storable agricultural products is the randomness of price changes. We divide storable agricultural products into two types according to this nature. One is a product whose value decreases slowly during the storage period, such as grain and cotton. The price change of this product fluctuates randomly during long-term sales, and this change is most obvious when similar new products are harvested. The other category is products whose value will increase by the storage process, such as tea and ginseng. Different from other agricultural products that exhibit price fluctuations related to the harvest season, storable agricultural products with large value-added space are easy to become the target of investors' price speculation, which leads to price instability. In addition, the price fluctuations of storable agricultural products are related to the market capacity of the products and depend on the circulation volume of the market, and they are similar to general products.

The characteristics and risks mentioned above bring complex challenges to suppliers and distributors of storable agricultural products. The main problem faced by the management is how to predetermine the production scale and reserve inventory for each sales cycle. Ordering too much in advance may bring about a large inventory backlog and costs. The shortage of predetermined amounts may also lead to the loss of sales opportunities and lack of stock. Too large an inventory volume may result in the loss of opportunity to sell products at high prices. The insufficient inventory volume may cause excessive inventory costs and the risk of low-price selling.

Many scholars conducted research on the problems in the production, sales, and inventory of storable agricultural products mentioned above. Katagiri et al. studied the ordering decision problem of simultaneously ordering perishable and storable products under uncertain demand and solved the optimal order quantities using Kuhn–Tucker conditions [4]. Li and Hou proposed a two-stage supply chain model composed of manufacturers and retailers for storable products, both of which determine yield and manage inventory by demand forecasting, to improve the overall performance of the supply chain [5]. Deng and Yano studied the multiperiod pricing decision problem of storable agricultural products affected by seasonal demand. The yield constraints were considered in the model, and the optimal price changes and dynamic price strategies were also studied [6]. Shi et al. established a random and dynamic inventory model of storable agricultural products with exogenous supply and prices. Farmers' cooperatives use this model to determine the best sales and inventory strategies and obtain the maximum expected profit [7].

Because of the characteristics of fixed order time, uncertain output, and uncertain demand, the newsboy model under random supply can be used for research on storable agricultural products. Merzifonluoglu and Feng simultaneously considered the supplier's fixed contract cost and production capacity constraints, designed a branch and bound algorithm based on Karush–Kuhn–Tucker conditions (KKT) conditions, and solved the optimal order quantities and supplier selection decisions [8]. Okyay et al. studied the single-period newsboy model of products with a correlational relationship between market demand and supply. Under three random supply situations, they solved the optimal order quantities under the condition that supply and demand are not necessarily independent of each other [9]. Zhen established two kinds of multiperiod models under the uncertainty of demand, which are used to make the scheme of tactical berth allocation [10]. Wen et al. studied the optimal initial inventory and multiperiod inventory allocation strategy for storable products whose inventory cannot be replenished. They considered the autoregressive process of price and fluctuations in demand and used the Markov decision process to solve the model [11].

Storable agricultural products also have the characteristics of production, storage, and sales decision for a multiperiod. The multiperiod model that meets the above characteristics can be used to solve the decision-making problem of this product. Matsuyama established a multiperiod newsboy model considering the stock-up and out-of-stock and studied the ordering strategy in these two situations [12]. Farahvash and Altiok introduced the auction theory and constructed a multiperiod newsboy model using stochastic dynamic programming to solve the optimal inventory level [13]. Mardaneh and Caccetta proposed a multiperiod dynamic pricing and production planning model for multispecies storable

agricultural products based on the newsboy model to solve the optimal production volume and optimal pricing strategy [14]. Zhen et al. proposed a mixed-integer programming model to integrate the berth template and the yard template planning and a heuristic algorithm for solving the problem in large-scale realistic environments [15]. Based on previous research, they further studied the multiperiod yard template planning in container terminals and daily berth planning problems [16, 17]. Kim et al. applied the multiperiod newsboy model to perishable products with a short shelf life to optimize the total logistics cost and proposed an effective method to optimize inventory holding, handling, and delivery costs [18]. Zhen built a container handling and storage berth allocation model based on the mixed-integer programming method. This model met the uncertainty of port transit demand and improved operational efficiency [19]. Deng et al. established a newsboy model for two suppliers, taking into account the randomness of product demand and aiming at buyers with a risk-averse attitude. Based on Copulas theory, this paper proposed an effective algorithm to optimize orders [20].

The above-mentioned kinds of literature studied the multiperiod newsboy model under different element combinations, which included periods, backgrounds, demand and supply situations, and solving methods. However, most studies only considered the strategic decision of order quantities and rarely introduced inventory decisions or other variables. Decision objectives most focused on single-period and double-period issues, and hypotheses rarely considered the uncertainty of supply, demand, and price fluctuation together. Therefore, according to the characteristics of storable agricultural products, this paper establishes an optimized joint decision model for multiperiod production and sales based on the newsboy model framework. Based on the above three uncertainty dimensions, the objective of this model is simultaneously determining the optimal order and sales quantities of all periods. We also introduce the sequential quadratic programming algorithm (SQP) to solve the proposed model, which is always used to solve the quadratic linear optimization problem. Moreover, this article uses a kind of Chinese storable agricultural product called Pu'er tea to verify the effectiveness of the model by analyzing the impact of price, cost, and risk preference on the order and sales quantities in each period.

The remainder of this paper is organized as follows: in Section 2, the descriptions and assumptions of the problems, followed by the ordering-selling joint decision model and the sequential quadratic programming algorithm for model solving are introduced. Section 3 is the analysis of numerical examples, which take Pu'er tea as the research object. We conduct a series of parameter analyses on order and sales decisions under different variables. Finally, section 4 summarizes the major conclusions of this research and gives several suggestions for further research.

2. Materials and Methods

2.1. Problem Description and Assumptions. In this part, we introduce the basic problem description and assumptions. This paper studies an agricultural enterprise engaged in contract farming. It means that this enterprise signs agricultural contracts with farmers before production. The contracts define the purchase price, quality level, and quantities. The farmers plant and harvest crops, and the agricultural enterprises provide technical support. During the product harvest season, the enterprise acquires agricultural products following the contracts. Since storable agricultural products can be stored and sold for a multiperiod, enterprises choose different ordering and selling strategies based on price fluctuations. The decisions faced by the enterprise in each sales period with time are shown in Figure 1. At the beginning of each period, it is necessary to allocate the sales quantities of the products ordered in the last period. Then, at the end of this period, decision-makers decide the order quantities of the next period. These two periods are relatively short compared to the whole sales period, and we assume that these two decisions are completed instantaneously. At the same time, decision-makers need to face two types of risks: supply uncertainty caused by product characteristics and demand uncertainty beause of market size changes. Therefore, to reduce shortage cost, excessive inventory holding cost, and order cost caused by unmet demand and excessive inventory, it is necessary to make more reasonable ordering and selling decisions to achieve the optimal profit of the system. Because of the differences in the market rules of different types of storable agricultural products, this paper puts forward assumptions before constructing the model, which are as follows:

(1) This model considers the multiperiod order and sales of only one type of storable agricultural product in each solving process.

(2) The market demand for storable agricultural products in each period is uncertain, which is defined by random variables. Moreover, the market demand for agricultural products in each period is different and mutually independent.

(3) The supply of farmers in each period is uncertain, which is described as the supply rate. The final supply of agricultural products is equal to the total order quantity multiplied by the supply rate.

(4) The unit order cost, inventory holding cost, shortage cost, and sales price in each period are known and determined by practical or hypothetical data.

2.2. Multiperiod Order and Sales Decision Model. In this part, we introduce the model-building process. We consider a type of storable agricultural product A. There are a total of N selling periods for this product. Decision-makers make order decisions at the end of the sales period and calculate the sales volume of the current period. Moreover, the supply volume ordered in the last period arrives instantaneously at the beginning of the current sales period.

The order quantity in period i is q_i, and the unit order cost is c_i. Suppliers provide products according to the order quantity q_i, which depends on the supply rate u_i. We assume that u_i is an independent random variable with probability density function $h(u_i)$, distribution function $H(u_i)$,

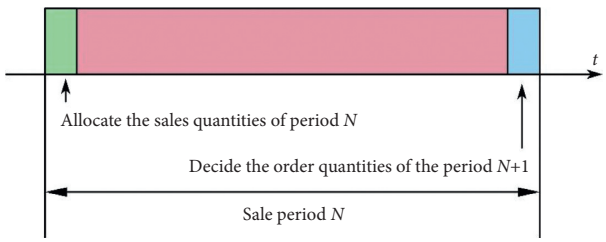

Figure 1: Decisions that enterprises face over time in sales period i.

expectation μ_i, and variance σ_i. Hence, the practical product quantity of period i obtained by ordering is $q_i u_i$.

These products purchased in period i will circulate to the market immediately after arrival, and the sales quantity in period j is x_{ij}. p_{ij} denotes the unit sales price. h_{ij} denotes the unit inventory holding cost. s_{ij} denotes the unit shortage cost. Assumption (4) shows that the values of these parameters will change according to the order period of the product and the sales period in which it is located.

Finally, we denote w_{ij} as the market demand of period j for the products ordered in period i, and its probability density function, distribution function, expectation, and variance are, respectively, $g(w_{ij}), G(w_{ij}), w_{ij}, \theta_{ij}$. According to the above parameter settings, the calculation functions for profit and cost are as follows:

Let P denote the total expected profit of products for all sales periods. Then,

$$P = E\left(\sum_{j=1}^{N}\sum_{i=1}^{j} p_{ij}x_{ij}\right). \tag{1}$$

At the end of each sale period, the inventory holding cost of the remaining products needs to be calculated. Denoting C_h as the total expected inventory holding cost of products for all sales periods, we have,

$$C_h = E\left[\sum_{j=1}^{N}\sum_{i=1}^{N} h_{ij}\left(q_i u_i - \sum_{n=i}^{j} x_{ij}\right)^+\right]. \tag{2}$$

Similarly, at the end of the sales period, if the inventory does not meet the demand of this period, there will be a shortage cost for unmet needs. Let C_s denote the total expected shortage cost of demands for all sales periods. We have,

$$C_s = E\left[\sum_{j=1}^{N}\sum_{i=1}^{j} s_{ij}\left(w_{ij} - x_{ij}\right)^+\right]. \tag{3}$$

In addition, C_c denotes the total expected order cost for all sales periods. It is worth noting that C_c is related to the order quantity q_i rather than the practical product quantity obtained through ordering. Hencce, we have the following:

$$C_c = E\left(\sum_{i=1}^{N} c_i q_i\right). \tag{4}$$

Upon integrating the above formulas, we obtain the total objective function for solving the net profit, which is as follows:

$$\begin{aligned}\max W &= \max E\left(P - C_h - C_s - C_c\right)\\ &= \max E\left[\sum_{j=1}^{N}\sum_{i=1}^{j} p_{ij}x_{ij} - \sum_{j=1}^{N}\sum_{i=1}^{j} h_{ij}\left(q_i u_i - \sum_{n=i}^{j} x_{ij}\right)^+\right.\\ &\quad \left. - \sum_{j=1}^{N}\sum_{i=1}^{j} s_{ij}\left(w_{ij} - x_{ij}\right)^+ - \sum_{i=1}^{N} c_i q_i\right].\end{aligned} \tag{5}$$

Since different decision-makers have different acceptance levels of shortage risk, this paper introduces the risk preference coefficient α $(0 < \alpha < 1)$. Generally, the low value of α indicates that the decision-maker can accept more shortage risk, and high value of α explains that the enterprise is more inclined to have sufficient inventory for avoiding shortage. Therefore, this paper has the functions about α, which are as follows:

For all $i, j \in N$,

$$\begin{gathered} p\left(x_{ij} + \sum_{m=i}^{j-1} x_{im} \leqslant q_i u_i\right) \geqslant \alpha, i < j, \mathfrak{M} \\ p\left(x_{ij} \leqslant q_i u_i\right) \geqslant \alpha, i < j. \end{gathered} \tag{6}$$

Function (6) indicates the probability that sales quantity for each subsequent period does not exceed the order quantity in the current period cannot be lower than α. Function (7) indicates the probability that the sales quantity does not exceed the order quantity in the current period cannot be lower than α. Obviously, function (6) contains the condition of function (7). To determine the random variable u_i in function (6), we assume that it obeys normal distribution. Then, function (6) can be rewritten as follows:

$$1 - p\left(\frac{u_i - \mu_i}{\sigma_i} \leqslant \frac{x_{ij} + \sum_{m=i}^{j-1} x_{im}/q_i - \mu_i}{\sigma_i}\right) \geqslant \alpha. \tag{7}$$

After deduction and simplification, we have the following:

$$x_{ij} + \sum_{m=i}^{j-1} x_{im} - \left(\mu_i - \phi^{-1}(\alpha)\sigma_i\right)q_i \leqslant 0. \tag{8}$$

Similarly, considering the limitation of supply capacity, we denote M_i as the maximum quantity that the supplier can provide in period i. Then, we have the following constraints:

$$0 < E\left(q_i u_i\right) \leqslant M_i. \tag{9}$$

The model of the optimal solution in this paper is a complex multiperiod model with nonlinear constraint optimization problems, which has many decision variables and complex forms. Its concavity and convexity cannot be judged by the Hessian Matrix, and the optimal solution cannot be obtained by conventional mathematical methods. Therefore, we use the SQP algorithm to acquire the optimal solution. SQP is a solving algorithm for problems with quadratic objective functions and linear inequality constraints. It can solve the optimal order and sales quantity of

the model in this paper. The specific flow chart of the SQP algorithm is shown in Figure 2.

The detailed iterative process of the SQP algorithm is as follows [21]:

(1) Define the values of initial iteration point X^0 and the convergence precision ε. Let $H^0 = I$ (I denotes the unit matrix) and $k = 0$ (k denotes the number of iteration).

(2) Utilize the Taylor formula to simplify the original objective function to the quadratic programming relation at the point X^k. Simultaneously, simplify the constraints into linear functions. Convert the original question into the question about the variable S ($S = X - X^k$).

(3) Solve the simplified quadratic programming problem and let $S^k = S^*$ (S^* denotes the locally optimal solution obtained from this solution).

(4) Perform a constraint one-dimensional search on the objective function of the original problem in direction S^k and get the next iteration point X^{k+1} from this solution.

(5) If X^{k+1} meets the accuracy standard of the convergence precision, the calculation will terminate, and the solving algorithm will output the optimal solution $X^* = X^{k+1}$. Otherwise, proceed to step (6).

(6) Modified second derivative matrix is H^{k+1}, and let $k = k + 1$. Back to step (2) and continue iterating.

Based on the above algorithm process, it is necessary to set the number of iterations. The iterative process cannot stop until the iterative point X^{k+1} meets the requirements. The setting of the maximum number of iterations is particularly important. Therefore, this paper sets the maximum number of iterations to 1000, which can satisfy the solving of the optimal solution of a certain period range.

3. Numerical Example

3.1. The Pu'er Tea. In this section, we use a numerical example to analyze the effect of using this decision model of this paper. We select a storable agricultural product called Pu'er tea as the research object. Pu'er tea is a kind of storable agricultural product made from a characteristic *Camellia sinensis* species in Yunnan, China. It is generally divided into three series: raw tea, aging tea, and ripe tea [22]. Raw tea can be drunk directly after fixation and sunning, and the raw tea material can be made into aging tea and ripe tea through microbial fermentation. On the one hand, like other teas, Pu'er tea has physiological characters and nutritive value, such as antioxidation, antivirus, anticancer, and hypoglycaemic. On the other hand, the quality of Pu'er tea will be improved during the long term of storage. Its collection value has made it favored by investors. This product has the advantages of storable and large value-added space. However, the market sales of this product have the risk of erratic prices, random supply, and demand.

We also collect the data on the yields and export prices of Pu'er tea from 2015 to 2020 to introduce some basic market situation of this product. Figure 3 exhibits that the total annual yields of Pu'er tea in China have been showing relatively stable growth. Its main production area is still mainly in Yunnan Province of China, however, the supply situation for different areas is still complicated. The average export price of Pu'er tea in China fluctuates irregularly every year. Especially in 2020, because of its nutritional value and government policies in the context of the COVID-19 pandemic, the average export price has increased by 98.94% compared to 2019.

3.2. Parameter Settings and Computation Results. We assume that a certain amount of Pu'er tea products will be sold in three cycles ($N = 3$). Then, the specific total objective function can be shown as follows:

$$\begin{aligned}
E(\pi) = {} & \sum_{j=1}^{3}\sum_{i=1}^{j} p_{ij}x_{ij} - \sum_{j=1}^{3}\sum_{i=1}^{j} h_{ij}\left(q_i u_i - \sum_{n=i}^{j} x_{ij}\right)^+ \\
& - \sum_{j=1}^{3}\sum_{i=1}^{j} s_{ij}\left(W_{ij} - x_{ij}\right)^+ - \sum_{i=1}^{3} c_i q_i \\
= {} & p_{11}x_{11} + p_{12}x_{12} + p_{13}x_{13} + p_{22}x_{22} + p_{23}x_{23} + p_{23}x_{23} \\
& - \int_{x_{11}/q_1}^{1} h_{11}(q_1u_1 - x_{11})h(u_1)\mathrm{d}u_1 \\
& - 2\int_{x_{11}+x_{12}/q_1}^{1} h_{12}(q_1u_1 - x_{11} - x_{12})h(u_1)\mathrm{d}u_1 \\
& - 2\int_{\frac{x_{22}}{q_2}}^{1} h_{22}(q_2u_2 - x_{22})h(u_2)\mathrm{d}u_2 \\
& - 4\int_{x_{11}+x_{12}+x_3/q_1}^{1} h_{13}(q_1u_1 - x_{11} - x_{12} - x_{13})h(u_1)\mathrm{d}u_1 \\
& - 4\int_{x_{22}+x_{23}/q2}^{1} h_{23}(q_2u_2 - x_{22} - x_{23})h(u_2)\mathrm{d}u_2 \\
& - 4\int_{x_{33}/q_3}^{1} h_{33}(q_3u_3 - x_{33})h(u_3)\mathrm{d}u_3 \\
& - \int_{x_{11}}^{\infty} s_{11}(w_{11} - x_{11})g(w_{11})\mathrm{d}w_{11} \\
& - 2\int_{x_{12}}^{\infty} s_{12}(w_{12} - x_{12})g(w_{12})\mathrm{d}w_{12} \\
& - 2\int_{x_{22}}^{\infty} s_{22}(w_{22} - x_{22})g(w_{22})\mathrm{d}w_{22} \\
& - 4\int_{x_{13}}^{\infty} s_{13}(w_{13} - x_{13})g(w_{13})\mathrm{d}w_{13} \\
& - 4\int_{x_{23}}^{\infty} s_{23}(w_{23} - x_{23})g(w_{23})\mathrm{d}w_{23} \\
& - 4\int_{x_{33}}^{\infty} s_{33}(w_{33} - x_{33})g(w_{33})\mathrm{d}w_{33} - c_1q_1 - c_2q_2 - c_3q_3.
\end{aligned} \tag{10}$$

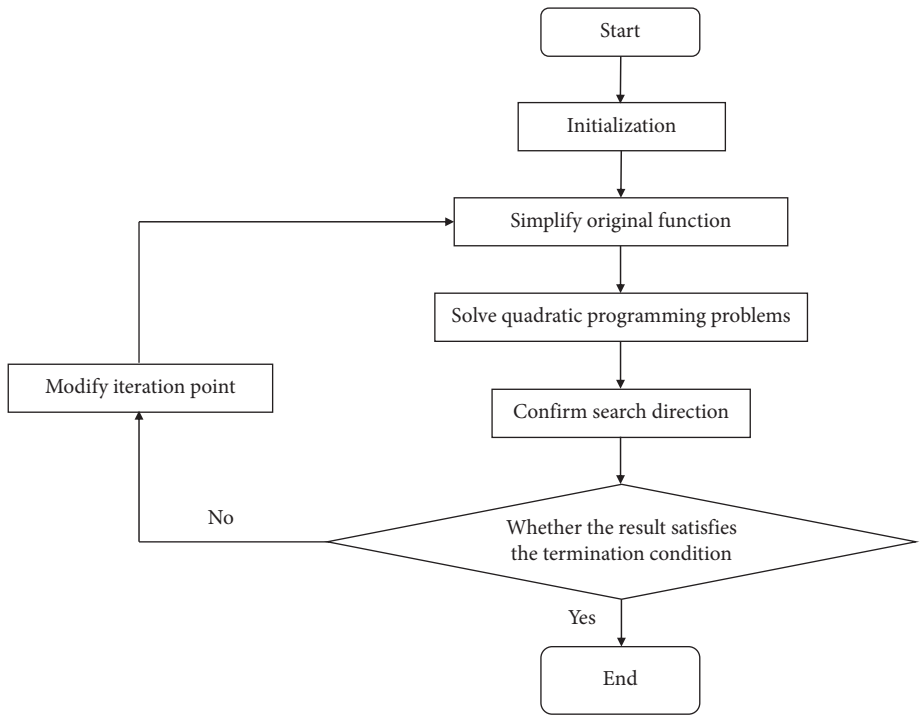

Figure 2: Flow chart of the SQP algorithm.

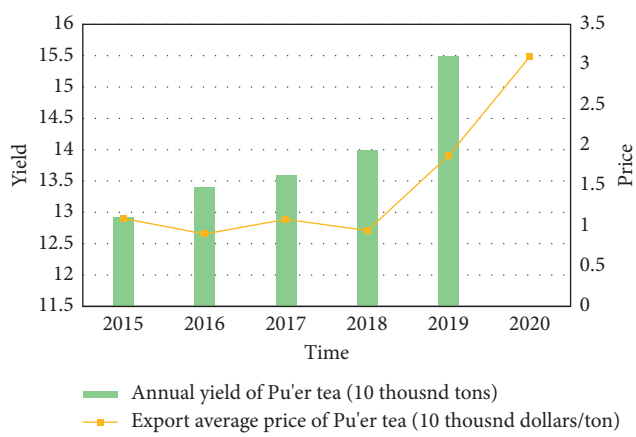

Figure 3: Change curves of yield and price with time (Pu'er tea).

S.T.

$$\begin{aligned}
&0 < E(q_1u_1) \leqslant M_1,\\
&0 < E(q_2u_2) \leqslant M_2,\\
&0 < E(q_3u_3) \leqslant M_3, 0 < E(q_2u_2) \leqslant M_2,\\
&0 \leqslant x_{11} + x_{12}x_{13} - \left(\mu_1 - \phi^{-1}(\alpha)\sigma_1\right)q_1 \leqslant 0,\\
&0 \leqslant x_{22} + x_{23} - \left(\mu_2 - \phi^{-1}(\alpha)\sigma_2\right)q_2 \leqslant 0,\\
&0 \leqslant x_{33} - \left(\mu_3 - \phi^{-1}(\alpha)\sigma_3\right)q_3 \leqslant 0.
\end{aligned} \tag{11}$$

Products can be ordered in all periods but need to be sold out at the end of the third period. The value of the risk preference coefficient we set is 0.99 ($\alpha = 0.99$). The solving target is to find the optimal order quantity and sales quantity of every period to maximize the net profit. Set the input parameters as shown in Table 1.

One point that needs to be explained about the above parameters is that i represents the ordering period of products and j represents the selling period of products. We use the MATLAB nonlinear optimization toolbox to solve the complicated model. According to the parameter settings of the above numerical examples, the optimal order quantity and sales quantity are calculated. The results are shown in Table 2.

The explanation of the solution result is as follows: the order quantities of the three periods are, respectively, 7000, 6400, and 3900. Products ordered in the first period are all allocated to the third sales period. Products ordered in the second period are allocated to the second and third sales periods. Moreover, the third period is the last period that the ordered products must be sold in this period. The total expected profit is 2398064. After our analysis, we believe that this result is caused by the dissimilarities of parameters. The prices of the products ordered in the first period that we set will gradually increase in the next two periods and reach a maximum value of 300 in the third period. To maximize the sales profit, the solving algorithm chooses to sell all the products in the third period, with the highest unit sales price, even if it caused shortages and storage costs of the first period. The difference between prices and costs makes the net profit still the highest. On the contrary, the price of the products ordered in the second period only increased slightly in the third period. Taking into account the shortage cost and storage cost of the last two periods, the final result of the solving algorithm allocates more sales to the second period. In addition, the products ordered in the third period

Table 1: Parameter setting of the optimal model.

Parameter	Value					
	Period 1			Period 2		Period 3
	$i = 1, j = 1$	$i = 1, j = 2$	$i = 1, j = 3$	$i = 2, j = 2$	$i = 2, j = 3$	$i = 3, j = 3$
c_i	40			36		38
u_i	N (0.9,0.01)			N (0.95,0.04)		N (0.97,0.09)
p_{ij}	200	220	300	180	210	210
s_{ij}	41	48	52	40	44	40
h_{ij}	10	11	12	10	11	10
w_{ij}	N (4000,200)	N (2000,280)	N (1000,300)	N (4100,220)	N (2300,260)	N (3900,250)

Table 2: Optimal solution results.

Parameter	Value					
	Period 1			Period 2		Period 3
	$i = 1, j = 1$	$i = 1, j = 2$	$i = 1, j = 3$	$i = 2, j = 2$	$i = 2, j = 3$	$i = 3, j = 3$
q_i	7000			6400		3900
x_{ij}	0	0	6137	3092	2392	2966
$E(W)$	2398064					

need to be sold in time. To study the optimal order and sales quantity changes of storable agricultural products under contract farming, we conduct a numerical analysis of the price and cost parameters related to the price fluctuations or the uncertainty of supply and demand. We selected several parameters that were significantly affected. The purpose is to find the variation laws of these parameters and provide some suggestions for enterprises that participate in the sale of storable agricultural products and contract farming.

3.3. Impact of Selling Price on Order and Sales Quantity. In this part, we research the changes in order and sales quantity of the products purchased in the first period with the increase in selling price. We suppose that while keeping the other parameters of products ordered in period 1 unchanged, the value of selling price in period 1 is increased from 200 to 300, and the effects of the selling price on order and sales quantity are shown in Table 3. We also observed the situation that the selling price of the second period is increased from 220 to 320 or the selling price of the third period is increased from 300 to 400 under the previous assumption. The calculation results are also shown in Table 3.

Then, we have the following observation results: firstly, as the selling price increases, the corresponding optimal sales quantities and expected total profit gradually increase, and the optimal order quantities remain constant regardless of the sales price. Moreover, when the sales quantity changes with the selling price, there are maximum and minimum values. The sales quantity is continuously changing in the interval between these two values. In this numerical example, when the selling price is less than the value point 240 in period 1 or 2, the solving algorithm will not allocate sales quantity to this period. The minimum value point of the first period or the second period is within the interval between 240 and 260. When the selling price reaches the value point 300 in period 3, the solving algorithm allocates all sales quantities to this period. The maximum value point of the third period is less than 300. Outside this interval, sales quantity will remain unchanged. Finally, under the same selling price in the change interval, the distribution of sales quantity to different periods is different. It is related to the setting values of other parameters, especially the difference in the selling prices of other periods.

3.4. Impact of Order Cost on Order and Sales Quantity. In this part, we research the changes in order and sales quantity of products with the increase of the order cost. We suppose that while keeping other parameters unchanged, the value of the unit order cost in period 1 is increased from 40 to 320, and the effects of the order cost on the order and sales quantity are shown in Table 4. We also observe the situation that the order cost of the second period is increased from 36 to 276 or the order cost of the third period is increased from 38 to 278 under the previous assumption. The calculation results are also shown in Table 4.

Then, we have the following observation results: Firstly, with the increase of the unit order cost, the corresponding optimal order quantity and sales quantity drop sharply. When the cost increases to a certain extent, the order quantity drops to 0, and the solving algorithm would rather choose to be out of stock than to order products. Moreover, there is a change interval for the influence of order cost on optimal order quantity and sales quantity. Before reaching the interval, the order quantities or sales quantities of the three periods made by the solving algorithm will not change. When the change interval is reached, the order quantity or sales quantity under the solving algorithm will drop sharply. Until the order cost exceeds the interval, these values will drop to 0. In addition, for different periods, the interval ranges are also different.

3.5. Impact of Inventory Holding Cost on Order and Sales Quantity. In this part, we research the changes in order and sales quantity of the products with the increasing unit

Table 3: Effects of p_{ij} on order and sales quantity.

Parameter		Value					
Group 1	p_{11}	200	220	240	260	280	300
	q_1	7000	7000	7000	7000	7000	7000
	x_{11}	0	0	0	3977	4308	5003
	$E(W)$	2398064	2398064	2398064	2469409	2551776	2646924
Group 2	p_{12}	220	240	260	280	300	320
	q_1	7000	7000	7000	7000	7000	7000
	x_{12}	0	0	1899	2213	4855	5176
	$E(W)$	2398064	2398064	2427548	2468860	2537486	2638020
Group 3	p_{13}	300	320	340	360	380	400
	q_1	7000	7000	7000	7000	7000	7000
	x_{13}	6137	6137	6137	6137	6137	6137
	$E(W)$	2398064	2520804	2643544	2766284	2889024	3011764

Table 4: Effects of c_i on order and sales quantity.

Parameter		Value					
Group 1	c_1	40	160	200	240	280	320
	q_1	7000	7000	7000	7000	945	0
	x_{11}	0	0	0	0	0	0
	x_{12}	0	0	0	0	0	0
	x_{13}	6137	6137	6137	6137	828	0
Group 2	c_2	36	116	156	196	236	276
	q_2	6400	6400	6400	2637	0	0
	x_{22}	3092	3092	3092	0	0	0
	x_{23}	2392	2392	2392	2260	0	0
Group 3	c_3	38	118	158	198	238	278
	q_3	3900	3900	3900	0	0	0
	x_{33}	2966	2966	2966	0	0	0

inventory holding cost. We suppose that while keeping the other parameters of products ordered in period 1 unchanged, the unit inventory holding cost of sales period 1 is increased from 10 to 210 or its value of sales period 2 is increased from 11 to 211. The changes in order and sales quantities are shown in Table 5. The change curve of sales quantities that is affected by the increase of h_{12} is shown in Figure 4.

Then, we have the following observation results: firstly, as the unit inventory holding cost increases, the optimal sales quantity of this period will also increase. It will affect the optimal sales quantities of other periods and reduce their values. In addition, the optimal order quantities remain unchanged regardless of the change of inventory holding cost. Moreover, there is a change interval for the influence of unit inventory holding cost on sales quantity. Before reaching the change interval, the sales quantity will not change under the solving algorithm. The change interval can be divided into two parts. In the first half part, the unit inventory holding cost of this period is less than that of other periods. The solving algorithm is more inclined to store the product until later sales. In the latter half part, the unit inventory holding cost is much higher than in other periods, and the solving algorithm is more inclined to sell the products in this period. It is worth noting that the absolute value changes of the slope in the first half part is higher than that of the latter half part. Finally, as the unit inventory holding cost increases, the total expected profit will gradually decrease, and the variation trend is changing too. This variation trend will gradually slow down, and it is also related to the division of change parts.

3.6. Impact of Inventory Holding Cost on Order and Sales Quantity. In this part, we research the changes in order and sales quantity of the products with the increasing unit inventory shortage cost. We suppose that while keeping other parameters unchanged, the unit shortage cost of products ordered in period 1 sold in period 2 increased from 48 to 98, and the effects of the selling price on order and sales quantity are shown in Table 6. We also observe the situation that the shortage cost of products ordered in period 2 sold in period 2 is increased from 40 to 90 under the previous assumption. The calculation results are also shown in Table 6.

Then, we have the following observation results: firstly, as the unit shortage cost increases, the optimal order quantities are not affected by it, and the optimal sales quantities will slightly change. Moreover, if the unit shortage cost of this period increases, the order quantity allocated to this period will increase, and the order quantity of other periods will decrease accordingly. We did not find a significant change interval or extreme value.

3.7. Impact of Inventory Holding Cost on Order and Sales Quantity. Finally, we research the changes in order and sales quantity of the products with the decreasing of risk preference coefficient. Since this parameter has a huge impact on the investment decision behavior of an enterprise, we also observe the impact on the total expected profit. We suppose that while keeping other parameters unchanged, the risk preference coefficient is decreased from 0.99 to 0.5. The final calculation results are shown in Table 7.

Then, the observation results we have are as follows: firstly, as the risk preference coefficient decreases, the differential value between the order quantity and the total sales quantities allocated to each period gradually decreases. In other words, enterprises' attitudes toward shortage risk have become more radical. The decision-maker is unwilling to keep more inventory for later sales periods, and the shortage risks in the later periods have also increased. Moreover, it can be seen that as the value of the risk preference coefficient

Table 5: Effects of h_{ij} on order and sales quantity.

Parameter		Value					
Group 1	h_{11}	10	50	90	130	170	210
	q_1	7000	7000	7000	7000	7000	7000
	x_{11}	0	0	4062	4964	5318	5621
	x_{12}	0	0	0	0	0	0
	x_{13}	6137	6137	2075	1173	820	516
	$E(W)$	2398064	2196820	2088431	2035011	2002830	1979737
Group 2	h_{12}	11	51	91	131	171	211
	q_1	7000	7000	7000	7000	7000	7000
	x_{11}	0	0	3135	3503	3753	3862
	x_{12}	0	1791	1935	1939	1999	2080
	x_{13}	6137	4347	1067	695	386	195
	$E(W)$	2398064	2214889	2146510	2117334	2098733	2085668

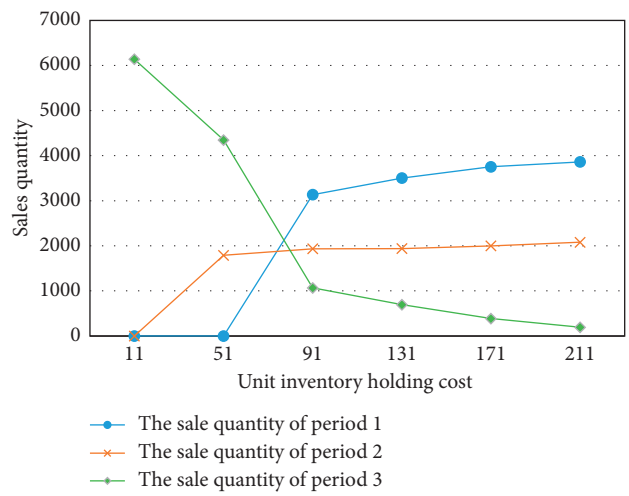

Figure 4: Change curves of order and sales quantities with h_{12}.

Table 6: Effects of s_{ij} on order and sales quantity.

Parameter		Value					
Group 1	s_{12}	48	58	68	78	88	98
	q_1	7000	7000	7000	7000	7000	7000
	x_{11}	3835	3800	3779	3764	3753	3744
	x_{12}	1724	1833	1905	1958	1999	2033
	x_{13}	578	504	454	415	385	360
Group 2	s_{22}	40	50	60	70	80	90
	q_2	6400	6400	7000	7000	7000	7000
	x_{22}	3092	3242	3415	3709	3869	3945
	x_{23}	2392	2242	2069	1776	1615	1540

Table 7: Effects of α on order and sales quantity.

Parameter	Value					
α	0.99	0.9	0.8	0.7	0.6	0.5
q_1	7000	7000	7000	7000	7000	7000
x_{11}	0	0	0	0	0	0
x_{12}	0	0	0	0	0	0
x_{13}	6137	6210	6241	6263	6282	6300
q_2	6400	6400	6400	6400	6400	6400
x_{22}	3092	3358	3469	3547	3612	3668
x_{23}	2392	2394	2395	2398	3404	3412
q_3	3900	3900	3900	3900	3900	3900
x_{33}	2966	3333	3488	3599	3694	3783
$E(W)$	2398064	2574169	2647961	2700604	2745724	2787045

decreases, the total expected profit of product sales becomes higher. It demonstrates that the more the market environment risks, the more opportunities to get a higher expected profit. Because of the existence of random variables in the decision function, the variance of the actual total profit will continue to increase as the risk increases. It also means that the range of actual profit becomes larger as the risk preference coefficient increases.

4. Conclusions

This paper proposes a joint optimization model for the multiperiod order and sales quantities of storable agricultural products, with the target of obtaining the optimal total net profit, and it solves the model by the SQP algorithm. Then, we set up the numerical examples with a type of storable agricultural product named Pu'er tea as the research object, and we used MATLAB to solve the model. Finally, we conducted a parameter analysis for the solution results.

From the analysis of the parameters, the subsequent conclusions are drawn. Firstly, the optimal order quantity is not affected by the sales price and the unit shortage cost, however, it is affected by the unit order cost and inventory holding cost. Order cost is the main factor affecting the order quantity. The optimal sales quantity is affected by the unit selling price, order cost, shortage cost, and inventory holding cost. Compared with other parameters, selling price and inventory holding cost have a more remarkable impact on sales quantity. Moreover, when the optimal order quantity is affected by the unit order cost and the unit inventory holding cost, there is an obvious changing interval. Within the changing interval, the order quantity will keep changing. Outside the interval, the order quantity reaches the maximum value or the minimum value, and it will no longer change. The above conclusions about the changing interval are also available when the unit sales price, unit order cost, and unit inventory holding cost affect the allocation of the optimal sales quantity in each period. In addition, the solving algorithm will make a decision that would rather be out of stock than to order when the order cost increases to a certain level. Thirdly, the expected profit is affected by the unit selling price, unit inventory holding cost, and risk preference coefficient. When it is affected by these parameters, the variation trend is also related to the changing interval.

For enterprises, we have some suggestions for them when dealing in storable agricultural products under contract farming. Firstly, the suppliers and enterprises can better adjust the order quantity and storage capacity in the contract agricultural model to ensure that the cooperative parties obtain the optimal profit of the system. Therefore, contract farming is worth promoting, and the model proposed in this paper can be used for the optimal decision, especially in China, where individual farmers occupy the main position of agricultural production. Moreover, the risk preference coefficient is very important for enterprises participating in contract farming. Enterprises should choose an appropriate value to balance the relationship of shortage risk and inventory cost. It depends on the current stage of enterprise development. The expected optimal total net profit does not necessarily mean the optimal decision. Furthermore, it is a valuable sales strategy for companies to maintain the stocks of storable agricultural products to sell them in the later periods with higher sales prices. To ensure sufficient supply, enterprises must sign more attractive contracts to obtain supplies from more individual farmers. Finally, to obtain a better optimal total net profit, enterprises can consider looking for the inflection intervals for the parameters they can control, such as sales prices. We can keep them at an appropriate value to obtain more stable and better profits using agricultural contracts. We suggest that enterprises make longer-term decisions to allocate the storable agricultural products to the more suitable sales periods with more net profits.

Like other studies, this article has some limitations. Firstly, the uncertainty function of supply and demand is relatively simple. The supply function can be replaced by the production function that considers more deterministic factors to make the theoretical model closer to actual agricultural production in future research. Moreover, in this study, the price is introduced as an input variable. In the actual agricultural product market, there is a correlation between price and demand. In future research, the demand formula should be modified to a price-oriented function. In addition, the model can be improved by replacing some elements with more specific random functions and considering the dynamic changes of the inventory in each period so that the optimal solution can be directly calculated from the functions.

Data Availability

The data used to support the findings of this study are available from the corresponding author upon request.

Conflicts of Interest

The authors declare that there are no conflicts of interest regarding the publication of this paper.

Acknowledgments

The authors acknowledge the National Natural Science Foundation of China (Grant no. 71462024).

References

[1] H. H. Wang, Y. Wang, and M. S. Delgado, "The transition to modern agriculture: contract farming in developing economies," *American Journal of Agricultural Economics*, vol. 96, no. 5, pp. 1257–1271, 2014.

[2] CNNIC, "46th Statistical Report on China's internet development is a report published by China Internet Network Information Center (CNNIC)," 2020, http://www.cnnic.com.cn/IDR/ReportDownloads/202012/P020201201530023411644.pdf.

[3] Z. J. Yuan, "Analysis of agricultural input-output based on Cobb-Douglas production function in Hebei Province, North China," *African Journal of Microbiology Research*, vol. 5, no. 32, pp. 5916–5922, 2011.

[4] H. Katagiri, H. Ishii, and M. Sakawa, "An inventory problem with a perishable commodity and a nonperishable one," *Asia Pacific Management Review*, vol. 8, no. 4, pp. 499–507, 2003.
[5] X. Li and Y. Hou, "Repeating contract research on nonperishable product with random demand," in *Proceedings of the International Conference on Management and Service Science*, pp. 1–4, Wuhan, China, August 2011.
[6] S. Deng and C. A. Yano, "Joint production and pricing decisions with setup costs and capacity constraints," *Management Science*, vol. 52, no. 5, pp. 741–756, 2006.
[7] J. Shi, Y. Zhao, R. B. K. Kiwanuka, and J. Chang, "Optimal selling policies for farmer cooperatives," *Production and Operations Management*, vol. 28, no. 12, pp. 3060–3080, 2019.
[8] Y. Merzifonluoglu and Y. Feng, "Newsvendor problem with multiple unreliable suppliers," *International Journal of Production Research*, vol. 52, no. 1, pp. 221–242, 2014.
[9] H. K. Okyay, F. Karaesmen, and S. Özekici, "Newsvendor models with dependent random supply and demand," *Optimization Letters*, vol. 8, no. 3, pp. 983–999, 2014.
[10] L. Zhen, "Tactical berth allocation under uncertainty," *European Journal of Operational Research*, vol. 247, no. 3, pp. 928–944, 2015.
[11] X. Wen, C. Xu, and Q. Hu, "Dynamic capacity management with uncertain demand and dynamic price," *International Journal of Production Economics*, vol. 175, pp. 121–131, 2016.
[12] K. Matsuyama, "The multi-period newsboy problem," *European Journal of Operational Research*, vol. 171, no. 1, pp. 170–188, 2006.
[13] P. Farahvash and T. Altiok, "A multi-period inventory model with multi-dimensional procurement bidding," *Annals of Operations Research*, vol. 186, no. 1, pp. 101–118, 2011.
[14] E. Mardaneh and L. Caccetta, "Optimal pricing and production planning for multi-product multi-period systems with backorders," *Journal of Optimization Theory and Applications*, vol. 158, no. 3, pp. 896–917, 2013.
[15] L. Zhen, E. P. Chew, and L. H. Lee, "An integrated model for berth template and yard template planning in transshipment hubs," *Transportation Science*, vol. 45, no. 4, pp. 483–504, 2011.
[16] L. Zhen, Z. Xu, K. Wang, and Y. Ding, "Multi-period yard template planning in container terminals," *Transportation Research Part B: Methodological*, vol. 93, pp. 700–719, 2016.
[17] L. Zhen, Z. Liang, D. Zhuge, L. H. Lee, and E. P. Chew, "Daily berth planning in a tidal port with channel flow control," *Transportation Research Part B: Methodological*, vol. 106, pp. 193–217, 2017.
[18] G. Kim, K. Wu, and E. Huang, "Optimal inventory control in a multi-period newsvendor problem with non-stationary demand," *Advanced Engineering Informatics*, vol. 29, no. 1, pp. 139–145, 2015.
[19] L. Zhen, "Modeling of yard congestion and optimization of yard template in container ports," *Transportation Research Part B: Methodological*, vol. 90, pp. 83–104, 2016.
[20] S. Deng, Z. Wan, Z. Wan, and Y. Zhou, "Optimization model and solution method for dynamically correlated two-product newsvendor problems based on copula," *Discrete & Continuous Dynamical Systems - S*, vol. 13, no. 6, pp. 1637–1652, 2020.
[21] S. H. R. Pasandideh, S. T. A. Niaki, and A. Gharaei, "Optimization of a multiproduct economic production quantity problem with stochastic constraints using sequential quadratic programming," *Knowledge-Based Systems*, vol. 84, pp. 98–107, 2015.
[22] N. Li, Y. Zhang, H. Zhu, D. Wang, and C. Yang, "Chemical and dominant microbial studies on Pu-er tea and its original plants," *Modernization of Traditional Chinese Medicine and Materia Medica--World Science and Technology*, vol. 21, no. 6, pp. 1173–1188, 2019.

Hindawi
Scientific Programming
Volume 2022, Article ID 8971882, 11 pages
https://doi.org/10.1155/2022/8971882

Research Article

Assessing the Influence Level of Food Safety Public Opinion with Unbalanced Samples Using Ensemble Machine Learning

Bo Song,[1] **Kefan Shang**,[1] **Junliang He**,[2] **and Wei Yan**[1]

[1]*China Institute of FTZ Supply Chain, Shanghai Maritime University, Shanghai 201306, China*
[2]*Institute of Logistics Science and Engineering, Shanghai Maritime University, Shanghai 201306, China*

Correspondence should be addressed to Junliang He; jlhe@shmtu.edu.cn

Received 23 April 2021; Accepted 22 December 2021; Published 14 February 2022

Academic Editor: Xiaobo Qu

Copyright © 2022 Bo Song et al. This is an open access article distributed under the Creative Commons Attribution License, which permits unrestricted use, distribution, and reproduction in any medium, provided the original work is properly cited.

Assessing the public opinion on food safety events constitutes an important job of government regulators. To optimize the government's management of food safety affairs, a promising way is to use artificial intelligence to improve the efficiency of food safety public opinion assessment. In this paper, we model the assessment of public opinion influence as a text classification task. The whole model adopts the ensemble learning framework, and it integrates naive Bayes, support vector machine, extreme gradient boosting, convolutional neural network, long- and short-term memory network, FastText, and BERT classification methods into the framework to form an ensemble learner. The ensemble learner is able to classify textual public opinion into high, medium, and low influence levels by learning from the samples assessed by human experts. To overcome the problem of unbalanced samples, we propose a sample generation method consisting of synonym replacement and semantic filtering to increase the number of high-influence samples. Real public opinion data collected from the Food Safety Department of the Chinese government are used for experiment. Extensive comparison of the proposed method with baseline methods proves the effectiveness of the ensemble learner and the sample generation steps.

1. Introduction

Nowadays, people are used to expressing opinions on the Internet, which leads to an explosive growth in the amount of online public opinions. Because food safety is closely related to everyone's daily life, public opinions with this topic are very likely to develop into hot events in the society. For example, La Tourangelle is a walnut oil brand welcomed by the most discerning customers in China. In 2019, the news of this brand of oil containing plasticizer exceeding the standard triggered vast public opinion on the Web, as this oil was mainly used for feeding babies. It has been shown that the interaction of government agencies with public opinions through social media can help the government to respond to public events efficiently [1]. The government can use public opinion assessment to explore people's attitudes towards an event [2–4] and predict events that may lead to serious consequences [5]. Therefore, it is meaningful to assess the influence of food safety public opinion in the early stage of its formation.

The importance of food safety public opinion has been pointed out in various regulatory documents issued by the government [6, 7]. However, unlike many other management optimization fields which have been intensively studied [8, 9], currently there is not much research dedicated to food safety public opinion assessment. Instead of analyzing research on food safety public opinion assessment, we survey the literature of general public opinion assessment. Moreover, since we formalize the public opinion assessment problem as a text classification problem, the literature of text classification is also analyzed to show the character of our research.

2. Related Works

2.1. Public Opinion Assessment. For assessing the influence of general public opinion, researchers often construct an index system to carry out public opinion evaluation. For example, considering the influence of microblog messages

and the dynamic role of the target audience of online public opinion, a microblog public opinion indicator system is established based on the Information Source Index (ISI), Geographic Index (GI), Subject Index (SI), and Industry Index (II) [10]. Simple analysis methods such as principal component analysis and analytic hierarchy process [11] are also often used in the construction of public opinion index systems. However, the manually selected indexes in this kind of studies cannot fully measure the characteristics of public opinion influence. At the same time, the index selection has a strong dependence on the opinions of experts and thus has a strong subjectivity. Some scholars believe that user behaviors such as forwarding and commenting can be used as the basis for evaluating the future development of public opinion. Li and Li use cloud models and analytic hierarchy processes to analyze user behaviors in public opinion dissemination, and they use this method to accurately predict hot public opinions [12]. Considering the impact indicators that affect the amount of user forwarding, Zheng et al. build a prediction model of network public opinion forwarding behavior using BP neural networks [13]. Due to the randomness and ambiguity of user forwarding behavior, Liu et al. used cloud theory to optimize the activation function of RBF neural networks [14]. When the information publisher has some professional authority or high popularity, users may ignore the actual content of the information when forwarding it [15]. Therefore, only relying on the statistics of user behavior to assess the influence of public opinion will produce a certain deviation. Seeing the problems with using user behaviors and artificial indexes, scholars begin to resort to the textual content of public opinion to assess its influence.

2.2. Text Classification for Public Opinion Assessment. Text classification plays an important role in public opinion assessment. Some scholars use text classification to identify the sentiment of public opinion, as sentiment affects the behavior of people interacting with public opinion [16, 17]. Other scholars use text classification to directly classify public opinion into different influence categories [18]. Text classification is an intensively studied field in recent years. When text underwent feature extraction and turned into numerical features, various machine learning methods can be used to classify text. Al-Tabbakh et al. use support vector machine, k-nearest neighbors, naive Bayes, and decision trees to classify the same text collection, whose results show that k-nearest neighbors perform the best in the experiment [19]. In contrast, deep learning algorithms do not require text feature extraction [20]. Deep learning models complete text classification by autonomously acquiring the relationship between text and label [21]. Another way to enhance text classification performance is to use multiple classifiers, which is called ensemble learning. Ensemble learning can effectively improve the accuracy and generalization ability of machine learning by accommodating more model assumptions. Cotelo et al. use a stacking framework of ensemble learning to integrate the content feature and structure feature of text to do classification [22]. Song et al. propose an ensemble learner to assess the impact of food safety news, which improves the accuracy of impact prediction [18]. However, their work does not take into consideration the unbalanced sample distribution across different impact levels, so the result is not satisfactory for high-impact news.

2.3. Dealing with Unbalanced Samples in Text Classification. Using machine learning for public opinion classification must pay attention to the distribution of data samples, as high-influence samples take only a very small part of the whole. Studies have shown that when the imbalance of the data set reaches 4 : 1 or higher, the predictive ability of the model will be lost [23]. Methods of processing unbalanced samples can be divided into oversampling and undersampling. Oversampling tries to enrich the minority type of samples by generating more samples of this type, and undersampling uses a subset of the majority type to make the number of each type equal. The classic oversampling method SMOTE maps the original samples to a certain vector space and then uses the samples in the space that are close to each other to construct new samples [24]. SMOTE-IPF [25] optimizes the classic method considering noisy and borderline examples. ADASYN [26] considers the distribution of minority data and generates new samples corresponding to the actual distribution of minority samples. In addition to oversampling and undersampling, classification algorithms themselves can be adapted to fit unbalanced samples. Datta and Das propose an approximate Bayesian support vector machine based on boundary transition and asymmetric cost to minimize the classification error [27]. Ando proposes a nearest neighbor model based on class weighting to compensate for the sparsity of minority classes by adjusting the k radius [28]. Cheng et al. introduce cost-sensitive marginal mean, variance, and penalty to adjust the proportional distribution between different categories, so as to obtain a balanced detection rate [29]. Despite the usefulness of adapting algorithms to unbalanced data, the adapted algorithms are often only applicable to a specific model. Under the framework of ensemble learning, adapting different base models one by one to unbalanced samples will increase complexity and cost of the framework.

3. Ensemble Learning Framework

In this paper, we propose a food safety public opinion assessment model that considers unbalanced sample distribution using the ensemble learning framework. The structure of the model is shown in Figure 1. In order to make full use of the data samples labeled by domain experts, we retain all the available data and adopt a "replacement-filtering" oversampling method to replenish the minority samples. The first step of oversampling is to build a synonym dictionary based on the vectorized word representation acquired through word embedding operation. Then, we replace some words in a sample with similar words to generate more samples of the minority type. At the last step of oversampling, we train a Siamese LSTM network to filter

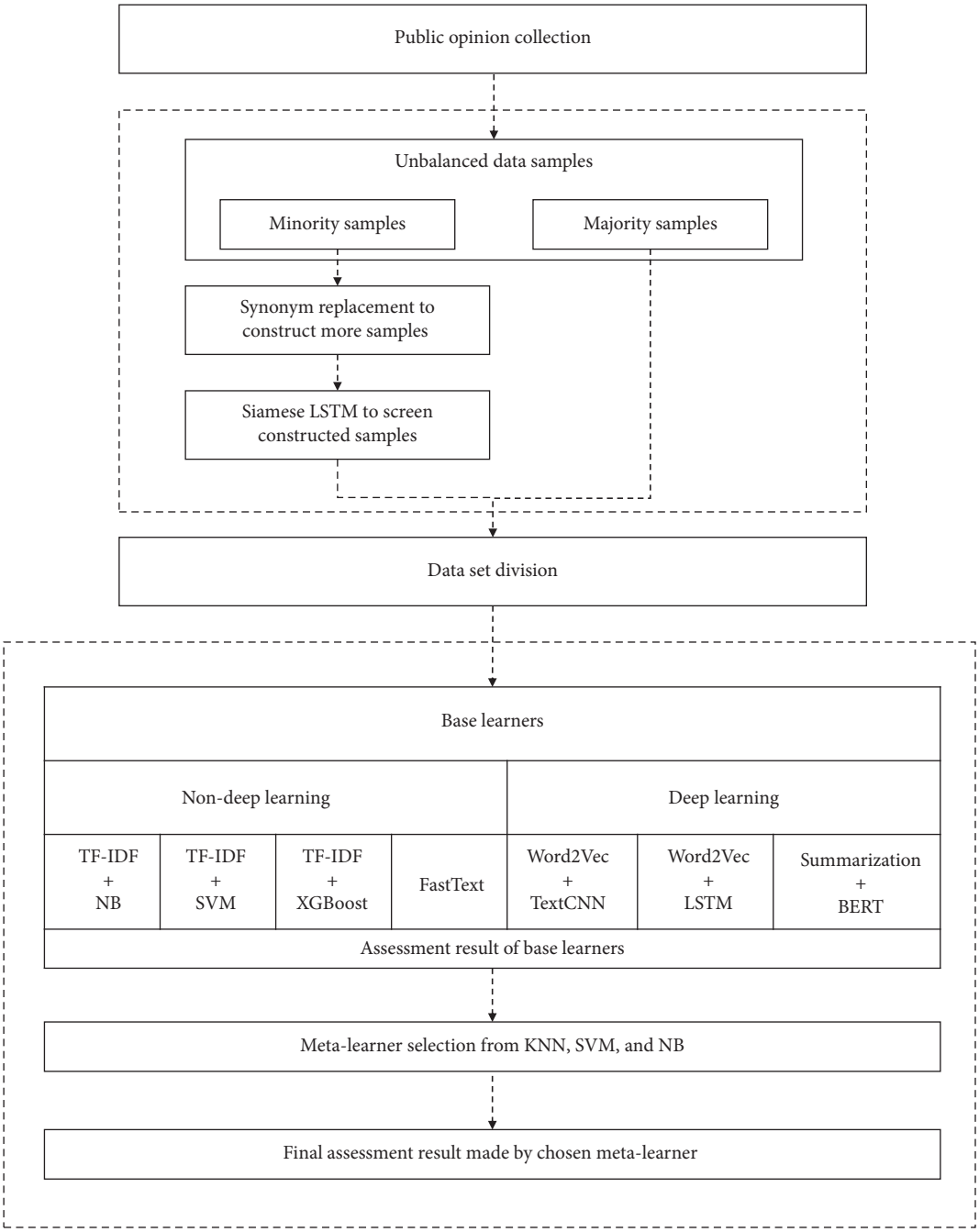

Figure 1: Ensemble model of food safety public opinion assessment with unbalanced samples.

out the newly constructed samples that are too dissimilar to real samples. To improve the accuracy and robustness of influence level classification, we use the stacking ensemble learning framework. The framework integrates naive Bayes (NB), support vector machine (SVM), extreme gradient boosting (XGBoost), convolutional neural network (CNN), long- and short-term memory network (LSTM), FastText, and BERT as base learners. Each base learner has its corresponding text preprocessing step: for NB, SVM, and XGBoost, each public opinion sample is turned into a vector of TF-IDF weights, together with the influence level label of this sample; for CNN and LSTM, each public opinion sample is turned into a matrix whose columns correspond to the embedding of words; for FastText, it takes the original text as input; for BERT, as it limits the length of input text for efficiency consideration, we apply automatic summarization to shorten oversized public opinion samples.

The stacking ensemble learning framework includes a meta-learner to synthesize the influence level rated by each of the base learners. We test k-nearest neighbors (KNN), SVM, and NB as three candidate meta-learners and select the best to use. To test the method proposed in this paper, we obtain food safety public opinion samples from the Risk Control Department of China Customs. Each sample has a

piece of text showing the original content of the public opinion, and an influence label ranging from high, medium, and low influence levels.

4. Processing Unbalanced Samples

In this study, we propose a "replacement-filtering" oversampling method to deal with the unbalanced data. The flowchart of the proposed oversampling method is shown in Figure 2. Details of the method are introduced in the following sections.

4.1. Minority Sample Generation Based on Synonym Replacement. In order to retain the information in the original data to the greatest extent, this paper uses the method of increasing minority samples to balance the sample set. To ensure that a newly added sample can achieve the purpose of equalizing the sample set, the new sample and the corresponding original sample should have similar characteristics. From the perspective of textual samples, the new sample and the corresponding original sample should be highly similar in terms of content and semantic meaning. Using synonym replacement to modify the original sample serves the goal of keeping text content similar. Synonym replacement is to replace each word in the original sample with a synonym of the word in the synonym dictionary and then obtain a new sample corresponding to the original sample. Although there is an existing platform that can do Chinese synonym replacement [30], the synonyms in this platform only include common terms and lack professional vocabulary such as law, medicine, and food safety. In this paper, we propose a synonym replacement method based on computed word vectors. The implementation steps are as follows:

4.1.1. Word Vector Computation. We use the Python package jieba to segment the original Chinese text. Then, we input the segmented text to the Word2Vec model realized in the Python package gensim to get word vectors. This step is also called word embedding. Word2Vec is a widely used word embedding model capable of capturing word meaning through self-supervised learning.

4.1.2. Top N Synonym Dictionary Construction. The cosine similarity of two words is calculated according to (1), where $\mathbf{x} = (x_1, \ldots x_i, \ldots, x_n)$ and $\mathbf{y} = (y_1, \ldots y_i, \ldots, y_n)$ represent two word vectors.

$$\cos(\mathbf{x}, \mathbf{y}) = \frac{\sum_{i=1}^{n} (x_i \times y_i)}{\sqrt{\sum_{i=1}^{n} (x_i)^2} \times \sqrt{\sum_{i=1}^{n} (y_i)^2}}. \quad (1)$$

The closer the cosine similarity value is to 1, the higher the similarity between the two words. We calculate the cosine similarity of each word pair and choose the top N word most similar to a specific word to construct the synonym dictionary.

4.1.3. Generating Samples for a Minority Sample. We traverse each word in the minority sample and replace the word with its ith similar word in the synonym dictionary, where i is a random number ranging from 1 to N. A new minority sample is generated after each word in the original minority sample has been replaced.

4.2. Sample Filtering Based on Siamese LSTM. Using the above method, we can generate any number of new samples for a given sample. However, this process only pays attention to the similarity of words but not the similarity of semantic meaning between the new samples and the original sample. To improve the quality of generated samples, we use Siamese neural networks to filter the new samples to ensure the semantic similarity between the new samples and the original sample.

The Siamese neural network [31] is composed of two identical neural networks with shared weights. It can be used to assess the similarity of two samples. Due to the excellent performance of the LSTM model in text understanding, this paper uses the Siamese LSTM model to complete sample filtering. The process is as follows:

4.2.1. Construction of a Siamese LSTM Model. Construct two LSTM models with identical structure and shared weights. This is done by training a LSTM text classifier using the original public opinion samples and duplicating the trained classifier.

4.2.2. Sample Filtering. For each newly generated sample, we input it with its corresponding original sample to the Siamese LSTM model. We can obtain the vector representation of the two samples at the LSTM layer prior to the softmax layer. Then, we compute the cosine similarity between the two vectors and see if the similarity value exceeds a predefined threshold. If so, we retain the generated sample, otherwise the generated sample is discarded.

5. Construction of an Ensemble Learner

To construct an ensemble learner includes three basic steps. The first is to select a group of base learners that are differently structured or differently trained. The second step is to divide the data set to properly train the base learners. The last step is to select a meta-learner to synthesize the results of base learners to get the final prediction result.

5.1. Base Learner Selection. To ensure the superiority and robustness of the final result, the selection of base learners follows the principle of accurate result and model diversity. The chosen base learners include those listed below.

5.1.1. Naive Bayes. Naive Bayes (NB) is a classic machine learning model based on the Bayes theorem and assumption of independent sample features. If the sample features meet the requirement of such assumption, a NB learner will have superior performance. In food safety public opinion

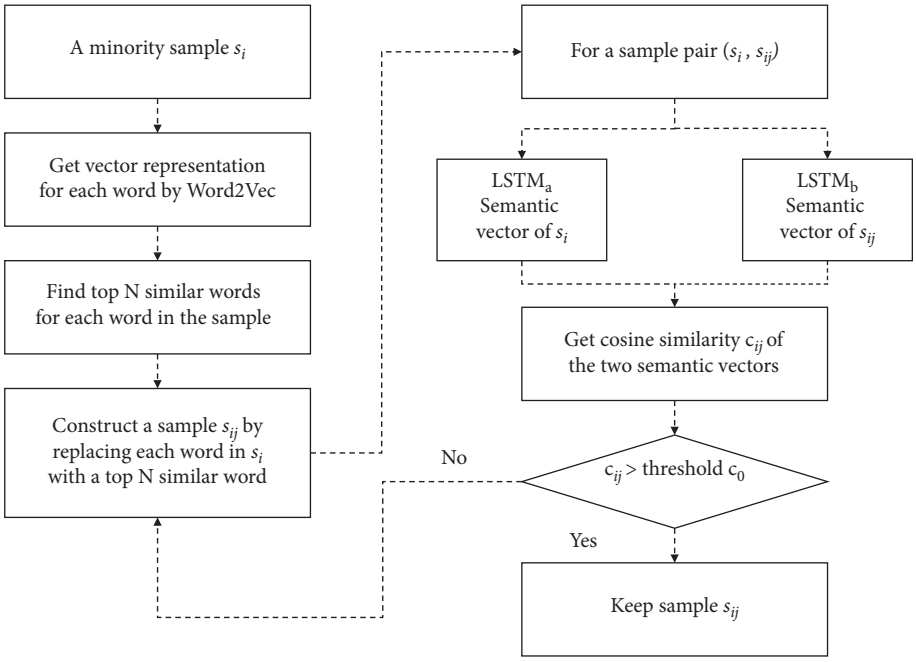

Figure 2: Flowchart of unbalanced sample processing.

assessment, a NB learner uses TF-IDF weighted words in the public opinion as features, and we use the sklearn package to carry out the training and predicting with the NB learner.

5.1.2. SVM. SVM learns to classify by solving a optimization problem. It maximizes the distance between a cutting hyperplane and the support vectors in the sample space. Due to its good performance, SVM has been used as a benchmark in many classification tasks. When there are more than two classes, a one-versus-rest method is usually adopted: by treating one class of the total n classes as a class, and the other $n-1$ classes as another class, totally n SVM classifiers will be constructed for an n-class classification problem.

5.1.3. XGBoost. XGBoost itself is an ensemble learner integrating multiple CART (classification and regression tree) models based on the boosting mechanism. The training process of XGBoost is to create a series of CARTs and let each tree learn to fit the prediction error of a previous tree. Leveraging the different assumptions in the constructed trees, XGBoost can improve the generalization ability of a learned model.

5.1.4. FastText. FastText is a simple three-layer neural network deliberately trained for accomplishing natural language processing tasks. FastText can achieve text classification precision comparable to that of deep neural networks but is many orders of magnitude faster in training time. At the input layer of FastText, n-grams in the text undergo a bucket hashing process and become embedding vectors. Since FastText generate word vectors by itself, we do not apply Word2Vec to the FastText classifier.

5.1.5. CNN. CNN is a deep neural network architecture originally proposed for image classification. Yoon Kim proposed a variant of CNN, namely TextCNN, for text classification [32]. In this paper, we use the word vectors generated by Word2Vec to replace the random word embedding used in TextCNN, so as to incorporate more prior knowledge in the classification model.

5.1.6. LSTM. LSTM adds an input gate, a forgetting gate, an output gate, and a memory unit to a RNN neuron, making the modified model capable of memorizing important information and forgetting unimportant information in a time series [33]. LSTM is very useful for modeling text as the word sequences in text represents time series signals. The training of LSTM requires vector representation of each word in the text, which in this paper is acquired using Word2Vec.

5.1.7. BERT. BERT [34] and its variations are among the state-of-the-art techniques for natural language processing. BERT is based on Transformer [35], an encoder-decoder architecture built on multihead self-attention mechanism. BERT is structured as a multilayer bidirectional Transformer encoder and is deliberately pretrained with two types of tasks: masked language model and next sentence prediction. Using BERT to classify is called fine-tuning, which is to learn only the weight matrix of the softmax layer. BERT consumes significantly more resources to compute as the length of input text grows. To fit the capacity of our computing resources, we set 128 Chinese characters as the max length of input text for BERT and use TextRank [36] to summarize the food safety public opinion, so as to keep as much information in the original text as possible.

5.2. Data Processing for the Ensemble Model. To train the 7 base learners and the meta-learner, the sample data set should be properly divided and fed to the model following the process depicted in Figure 3.

The overall training set is divided into 7 sets of equal size, shown as $a_1, \ldots, a_7$ in Figure 3. For each base learner, it is trained 7 times. In the first time, a_1 is used as the inner test set and the rest sets are used as the training set; in the second time, a_2 is used as the inner test set and the rest sets are used as the training set, and so on. The predicted class labels for inner test set a_i by base learner j is denoted as b_{ij}. By merging $b_{i1}, \ldots, b_{i7}$ along the same test samples, we get B_i, and $B_1, \ldots, B_7$ comprise the training set for the meta-learner. Since each base learner has 7 differently trained versions, and when testing the ensemble learner the meta-learner needs a determined class label from each base learner, we test the seven versions of a base learner one by one using the overall test set and choose the most frequently appearing class label for each test sample to get T_i, the test result of base learner i. Finally, by merging $T_1, \ldots, T_7$, we get T, the test set for the meta-learner.

5.3. Meta-Learner Selection. A meta-learner uses the output of all the base learners as input and makes final decision on the class label of a sample. Since the output of base learners for a given sample comprises a digital vector, and the results of different base learners do not affect each other, the meta-learner predicting with this vector needs not to be complicated. In this paper, we choose KNN, SVM, and NB as the candidate meta-learners. They have good performance in the ensemble learning framework and relatively short training time. We will test the performance of the three models and select the best model to use.

6. Experiment

6.1. Data Collection. The experiment data in this article come from the Food Safety Department of China Customs. Each public opinion has been manually rated by the customs officers. The original data collection includes 21,145 samples of food safety public opinion. After deleting invalid information, the total number of data sample is 21,065, including 10,247 low-influence samples, 10,314 medium-influence samples, and 504 high-influence samples.

6.2. Model Settings. The settings of each compositional machine learning model are shown in Table 1. Among the models, TextCNN, LSTM, and BERT need to set the reading length of the text. As samples with the length of less than 1000 characters account for 98% of the total samples, the reading length of TextCNN and LSTM is set to 1000 characters, and the excessive text is cut off. Due to the reason explained in Section 5.1, the reading length of the BERT model is set to 128 characters, and we apply automatic summarization to compensate for the information loss.

6.3. Evaluation Index. To conduct a comprehensive evaluation of the model results, four evaluation indexes are used: accuracy, precision, recall, and F1-score. The calculation of these indicators is listed below, where TP, TN, FP, and FN stand for the number of true positive, true negative, false positive, and false negative predictions of sample influence level.

$$\begin{aligned} \text{accuracy} &= \frac{\text{TP} + \text{TN}}{\text{TP} + \text{TN} + \text{FP} + \text{FN}}, \\ \text{precision} &= \frac{\text{TP}}{\text{TP} + \text{FP}}, \\ \text{recall} &= \frac{\text{TP}}{\text{TP} + \text{FN}}, \\ \text{F1} &= \frac{2 \times \text{precision} \times \text{recall}}{\text{precision} + \text{recall}}. \end{aligned} \tag{2}$$

Accuracy reflects the overall performance of a model. Precision and recall reflect the ability of the model to correctly predict class labels regarding all classified samples and samples of a certain type respectively. The F1 value is the harmonic average of precision and recall.

6.4. Minority Sample Generation and Filtering. We use Word2Vec to train a word vector table of $88{,}296 \times 50$ from the original 21,145 public opinion samples. After removing useless words such as punctuations and numbers, we get a table of $62{,}981 \times 50$. Each row in the table corresponds to a Chinese word, and its similarity with another word is calculated through cosine similarity. For a real minority sample, we traverse each word in it and replace the word with its ith similar word in the word vector table. By ranging i from 1 to 20, we obtain 10,080 new samples.

Word replacement only ensures the word-level similarity between a generated sample and the original sample, but in fact we need the semantic meaning between the two samples to be similar. To achieve this goal, we train Siamese LSTM networks to filter out the generated samples whose semantic similarity with the original sample is low. Adopting a semantic similarity threshold of 0.8, we retain 5544 high-influence samples constructed from word replacement. The final set of high-influence samples has a size of 6048.

6.5. Meta-Learner Selection Based on Performance. Three types of meta-learner have been tested using the balanced samples. Their performances are shown in Table 2. From Table 2 we can see that NB has the best accuracy, which is 0.8530. So we choose NB as the meta-learner in our ensemble learning model.

7. Result and Analysis

To show the effectiveness of the proposed ensemble learning framework and sample balancing method, we present results of influence assessment in three scenarios. The first is the result of base learners and ensemble model with original and

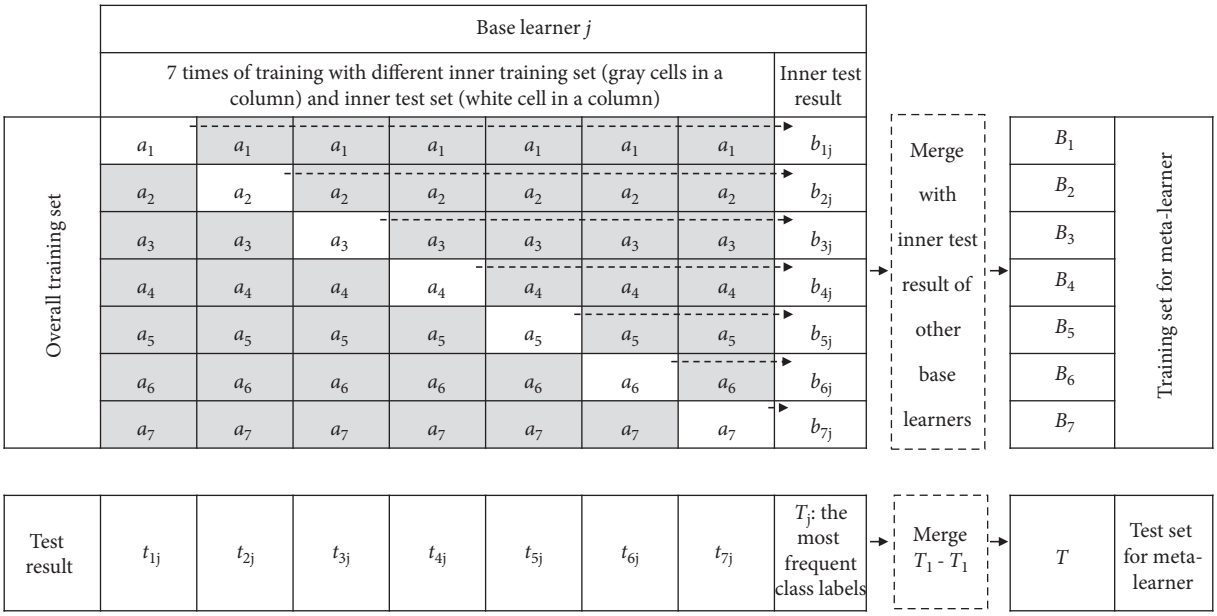

Figure 3: Construction of training and test data sets.

Table 1: Model settings.

Model	Settings
NB	Uniform prior probability of classes; other parameters follow the default setting of sklearn MultinomialNB model.
SVM	Parameters follow the default setting of sklearn LinearSVC model.
XGBoost	Early stopping rounds = 10; eval_metric = "logloss"; other parameters follow the default setting of the Python package XGBoost.
FastText	Minimal number of word occurrences = 2; other parameters follow the default setting of the Python package FastText.
TextCNN	Keras-based implementation of a TextCNN [11]-like CNN, with a dropout layer after the embedding layer (dropout rate = 0.2); the 1D convolutional layer has 250 filters (kernel length = 3); a 3-max pooling layer follows and is followed by a flatten layer, a 50-unit dense layer, and a 3-unit softmax layer; the activation function of the convolutional layer and the dense layer is ReLU; input length = 1000, batch size = 256, epochs = 5.
LSTM	Keras-based implementation of LSTM; the embedding layer is connected to a LSTM layer with 200 neurons, where a 0.2 dropout rate of the input and recurrent state is applied; following the LSTM layer is a dropout layer (dropout rate = 0.2), a 64-unit dense layer (ReLU activation function) and a 3-unit softmax layer; input length = 1000, batch size = 128, epochs = 5, Adam optimizer, learning rate = 0.01.
BERT	Chinese pretrained model, $L = 12$, $H = 768$, $A = 12$; batch size = 32, epochs = 5, learning rate = $2e-5$; input length = 128.
KNN	Parameters follow the default setting of the sklearn neighbors model.

Table 2: Comparison of meta-learners.

Meta-learner	Evaluation index			
	Accuracy	Precision	Recall	F1
KNN	0.8357	0.8364	0.8357	0.8360
SVM	0.8500	0.8506	0.8500	0.8502
NB	0.8530	0.8541	0.8530	0.8534

balanced samples as input (Table 3). The second is the result of some base learners under 3 ways of sample balancing: none, SMOTE, and replacement-filtering (Table 4). The third is the performance of influence assessment for each sample class (Figure 4).

It can be seen from Table 3 that before sample balancing, only FastText and LSTM achieve accuracy more than 0.8. After using replacement-filtering measure to process unbalanced samples, all base learners achieve accuracy more than 0.8, and the ensemble model proposed by this paper has the highest score of 0.8530. After processing unbalanced samples, the best performance of a single learner is 0.8494 of accuracy achieved by LSTM. BERT represents a more advanced model than LSTM in processing text, but the performance of BERT predicting public opinion influence in this paper is only better than the NB model. This is due to the limitation of input text length caused by hardware constraints. From the above result we can see that both the ensemble learning framework and the replacement-filtering oversampling measure improve the performance of public opinion assessment. While the ensemble learning framework achieves a 0.42% improvement regarding the best single learner, the oversampling measure achieves an improvement of 5.8%. Moreover, in real application of artificial intelligence, people usually consider an accuracy above 0.85 as the baseline, so in this sense, only the result of ensemble learning model with balanced samples meets the requirement of real application.

To verify the advantage of the proposed oversampling method versus traditional oversampling methods, we

Table 3: Influence assessment results.

Model		Evaluation index			
		Accuracy	Precision	Recall	F1
NB	Original sample	0.7587	0.7615	0.7587	0.7592
	Balanced sample	0.8126	0.8127	0.8126	0.8124
SVM	Original sample	0.7968	0.7990	0.7968	0.7972
	Balanced sample	0.8435	0.8439	0.8435	0.8434
XGBoost	Original sample	0.7902	0.7918	0.7902	0.7905
	Balanced sample	0.8491	0.8490	0.8491	0.8490
FastText	Original sample	0.8027	0.8037	0.8027	0.8030
	Balanced sample	0.8470	0.8468	0.8469	0.8469
TextCNN	Original sample	0.7870	0.7907	0.7870	0.7879
	Balanced sample	0.8392	0.8417	0.8392	0.8393
LSTM	Original sample	0.8018	0.8064	0.8018	0.8024
	Balanced sample	0.8494	0.8513	0.8494	0.8494
BERT + summarization	Original sample	0.7919	0.7934	0.7919	0.7921
	Balanced sample	0.8300	0.8298	0.8300	0.8299
Ensemble model (ours)	Original sample	0.8062	0.8071	0.8062	0.8052
	Balanced sample	0.8530	0.8541	0.8530	0.8534

Table 4: Comparison of oversampling methods.

Model		Evaluation index			
		Accuracy	Precision	Recall	F1
NB	Original sample	0.7312	0.7652	0.7312	0.7321
	SMOTE	0.7714	0.7703	0.7714	0.7697
	Replace-filter	0.8052	0.8167	0.8052	0.8030
SVM	Original sample	0.7532	0.7563	0.7532	0.7535
	SMOTE	0.8235	0.8257	0.8235	0.8242
	Replace-filter	0.8064	0.8070	0.8064	0.8063
XGBoost	Original sample	0.7986	0.7992	0.7986	0.7984
	SMOTE	0.8384	0.8389	0.8384	0.8385
	Replace-filter	0.8485	0.8488	0.8485	0.8486
TextCNN	Original sample	0.7782	0.7882	0.7782	0.7806
	SMOTE	0.8153	0.8171	0.8153	0.8157
	Replace-filter	0.8375	0.8375	0.8375	0.8372
LSTM	Original sample	0.7845	0.7852	0.7845	0.7848
	SMOTE	0.8054	0.8080	0.8054	0.8054
	Replace-filter	0.8332	0.8339	0.8332	0.8331

conduct experiments with three types of samples, saying the original samples without oversampling, the balanced samples using SMOTE oversampling method, and the balanced samples using the proposed replacement-filtering oversampling method. Since the SMOTE method generates new samples by locating points between two original sample points in the hyperspace, only learners using vectorized representation of input text are suitable for testing with this oversampling method. From Table 4 we can see that both oversampling methods can improve the accuracy of influence level prediction. From the perspective of improved performance, the SMOTE method has a better improvement effect on non-deep learning models, and the replacement-filtering method proposed in this paper has good improvement effect on both non-deep learning models and deep learning models.

An important capability of a public opinion assessment model is to recognize high-influence samples, as these samples are more likely to trigger public events. Figure 4 shows the class level results of influence assessment. It can be seen that the abilities of different models to distinguish between low- and medium-influence-level samples are close. But for high-influence-level samples, the performances of different models vary greatly. For single models, SVM and LSTM are better than NB and CNN in recognizing high-influence public opinion with unbalanced samples. For the ensemble model, it has high precision and low recall when recognizing high-influence public opinion with unbalanced samples, but when the samples are balanced, it has the highest precision, recall, and overall performance when recognizing high-influence public opinion.

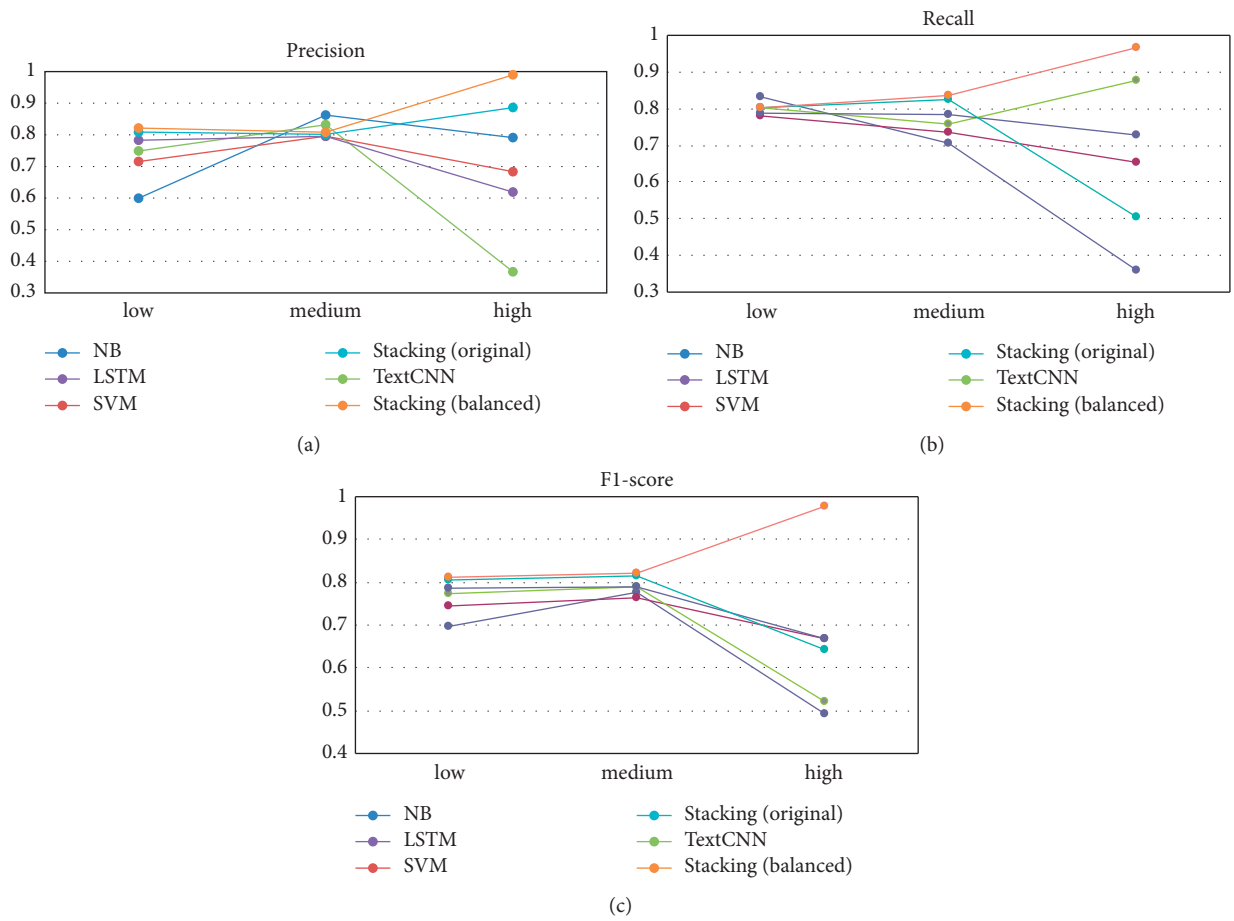

Figure 4: Comparison of class level results.

8. Conclusion

In this paper we study the problem of assessing the influence level of food safety public opinion. An ensemble machine learning model is proposed to classify food safety public opinions into three influence levels: high, medium, and low. Given that the number of high-influence public opinion samples is much smaller than that of low-influence samples, an oversampling method is proposed to balance the sample number and improve the assessment accuracy. The oversampling method includes using synonym replacement to generate pseudo-high-influence samples and using Siamese LSTM neural network to filter out low-quality pseudo-samples. Experiments with real data collected from the Food Safety Department of China Customs show that the ensemble machine learning model outperforms single machine learning model including NB, SVM, XGBoost, FastText, TextCNN, LSTM, and BERT in terms of assessment accuracy. The oversampling operation is also tested to be beneficial, as after sample balancing, the accuracy of recognizing high-influence samples reaches more than 0.9 and the F1-score raises from below 0.7 to above 0.9. The result of the study shows that the proposed method can be used in real life to optimize the trade-off between accuracy and efficiency of food safety public opinion assessment.

As pointed out by Zheng [37], it is important to do reproducible research by making the data and model definite. Regarding the oversampling model and ensemble learning model proposed in this paper, the result can be made reproducible if the random seeds used in these models were set definite. However, we have not studied how to tactically eliminate the randomness of the model to achieve beneficial effects such as avoiding the selection of outliers during sampling [38]. This kind of study will be done in the future research.

Data Availability

Data are available upon request.

Conflicts of Interest

The authors declare that there are no conflicts of interest regarding the publication of this paper.

Acknowledgments

This work was sponsored by the National Natural Science Foundation of China (71601113 and 72072112), Shanghai Science and Technology Committee Project (21010501800), and Shanghai Rising-Star Program (19QA1404200).

References

[1] D. Wu and Y. Cui, "Disaster early warning and damage assessment analysis using social media data and geo-location information," *Decision Support Systems*, vol. 111, pp. 48–59, 2018.

[2] E. D'Andrea, P. Ducange, and F. Marcelloni, "Monitoring negative opinion about vaccines from tweets analysis," in *Proceedings of the 2017 Third International Conference on Research in Computational Intelligence and Communication Networks*, Kolkata, India, November 2017.

[3] E. D'Andrea, P. Ducange, A. Bechini, A. Renda, and F. Marcelloni, "Monitoring the public opinion about the vaccination topic from tweets analysis," *Expert Systems with Applications*, vol. 116, pp. 209–226, 2019.

[4] B. O'Connor, "From tweets to polls: linking text sentiment to public opinion time series," in *Proceedings of the Fourth International Conference on Weblogs and Social Media, ICWSM 2010*, ICWSM, Washington, DC, USA, May 2010.

[5] J. Chen, H. Zhou, H. Hu et al., "Research on agricultural monitoring system based on convolutional neural network," *Future Generation Computer Systems*, vol. 88, pp. 271–278, 2018.

[6] European Food Safety Authority, "EFSA Image Qualitative Research Report," 2020, http://www.efsa.europa.eu/sites/default/files/event/2010/mb100318-ax4.pdf.

[7] US Food and Drug Administration, "DFA's Strategic Plan for Risk Communication," 2020, http://www.fda.gov/Food/default.htm.

[8] L. Zhen, Z. Liang, D. Zhuge, L. H. Lee, and E. P. Chew, "Daily berth planning in a tidal port with channel flow control," *Transportation Research Part B: Methodological*, vol. 106, pp. 193–217, 2017.

[9] J. He, Y. Wang, C. Tan, and H. Yu, "Modeling berth allocation and quay crane assignment considering QC driver cost and operating efficiency," *Advanced Engineering Informatics*, vol. 47, Article ID 101252, 2021.

[10] L. Zhao, X. Zhang, M. He, D. Zhang, W. Liu, and C. Liu, "Research on public opinion index system of Chinese microblog," in *Proceedings of the 2014 IEEE 5th International Conference on Software Engineering and Service Science*, pp. 385–388, IEEE, Beijing, China, June 2014.

[11] H. Xing, J. Huidong, and Z. Yu, "Risk assessment of earthquake network public opinion based on global search BP neural network," *PLoS One*, vol. 14, 2019.

[12] Y. Li and S. Li, "The propagation behavior prediction of Tibetan network public opinion based on cloud model," in *Proceedings of the: 2nd International Conference on Information Science and Control Engineering, ICISCE 2015*, pp. 992–995, Shanghai, China, April 2015.

[13] C. Zheng, Y. Song, and Y. Ma, "Public opinion prediction model of food safety events network based on bp neural network," *IOP Conference Series: Materials Science and Engineering*, vol. 719, no. 1, Article ID 012078, 2020.

[14] Y. Liu, J. Zhao, and Y. Xiao, "C-RBFNN a user retweet behavior prediction method for hotspot topics based on improved RBF neural network," *Neurocomputing*, vol. 275, pp. 733–746, 2018.

[15] L. Zhang, H. Li, C. Zhao, and X. Lei, "Social network information propagation model based on individual behavior. Wireless Communication over ZigBee for automotive inclination measurement," *China Communications*, vol. 14, no. 7, pp. 78–92, 2017.

[16] M. Zhang, R. Zheng, J. Chen et al., "Emotional Component analysis and forecast public opinion on micro-blog posts based on maximum entropy model," *Cluster Computing*, vol. 22, 2018.

[17] L. Servi and S. B. Elson, "A mathematical approach to gauging influence by identifying shifts in the emotions of social media users," *IEEE Transactions on Computational Social Systems*, vol. 1, no. 4, pp. 180–190, 2015.

[18] B. Song, K. Shang, J. He, W. Yan, and T. Zhang, "Impact assessment of food safety news using stacking ensemble learning," *Advances in Transdisciplinary Engineering*, vol. 12, pp. 353–362, 2020.

[19] S. M. Al-Tabbakh, H. M. Mohammed, and H. El-Zahed, "Text mining techniques for intelligent grievances handling system: WECARE project improvements in EgyptAir," *International Journal of Advanced Computer Science and Applications*, vol. 10, no. 2, pp. 603–614, 2019.

[20] Y. Bengio and Y. Lecun, "Scaling learning algorithms towards AI," in *Proceedings of the Large-Scale Kernel Machines*, vol. 34, no. 5, pp. 1–41, 2007.

[21] B. Zhong, X. Xing, P. Love, X. Wang, and H. Luo, "Convolutional neural network: deep learning-based classification of building quality problems," *Advanced Engineering Informatics*, vol. 40, pp. 46–57, 2019.

[22] J. M. Cotelo, F. L. Cruz, F. Enríquez, and J. A. Troyano, "Tweet categorization by combining content and structural knowledge," *Information Fusion*, vol. 31, pp. 54–64, 2016.

[23] L. Victoria, F. Alberto, G. Salvador, P. Vasile, and H. Francisco, "An insight into classification with unbalanced data: empirical results and current trends on using data intrinsic characteristics," *Information Sciences*, vol. 250, pp. 113–141, 2013.

[24] G. E. A. P. A. Batista, R. C. Prati, and M. C. Monard, "A study of the behavior of several methods for balancing machine learning training data," *ACM SIGKDD Explorations Newsletter*, vol. 6, no. 1, pp. 20–29, 2004.

[25] A. S. José, L. Julián, J. Stefanowski, and H. Francisco, "SMOTE–IPF: addressing the noisy and borderline examples problem in unbalanced classification by a re-sampling method with filtering," *Information Sciences*, vol. 291, 2015.

[26] H. He, Y. Bai, E. A. Garcia, and S. Li, "ADASYN: adaptive synthetic sampling approach for unbalanced learning," in *Proceedings of the IEEE International Joint Conference on Neural Networks*, IEEE, Hong Kong, June 2008.

[27] S. Datta and S. Das, "Near-Bayesian support vector machines for imbalanced data classification with equal or unequal misclassification costs," *Neural Networks*, vol. 70, pp. 39–52, 2015.

[28] S. Ando, "Classifying imbalanced data in distance-based feature space," *Knowledge and Information Systems*, vol. 46, no. 3, pp. 707–730, 2016.

[29] F. Cheng, J. Zhang, C. Wen, Z. Liu, and Z. Li, "Large cost-sensitive margin distribution machine for unbalanced data classification," *Neurocomputing*, vol. 224, pp. 45–57, 2016.

[30] W. Che, Z. Li, and T. Liu, "LTP: a Chinese language technology platform// COLING 2010," in *Proceedings of the 23rd International Conference on Computational Linguistics, Demonstrations*, pp. 23–27, Beijing, China, August 2010.

[31] S. Chopra, R. Hadsell, and Y. Lecun, "Learning a similarity metric discriminatively, with application to face verification," in *Proceedings of the 2005 IEEE Computer Society Conference on Computer Vision and Pattern Recognition (CVPR'05)*, IEEE, San Diego, CA, USA, June 2005.

[32] Y. Kim, "Convolutional neural networks for sentence classification," 2014, https://www.researchgate.net/publication/265052545_Convolutional_Neural_Networks_for_Sentence_Classification.

[33] J. Chung, C. Gulcehre, K. H. Cho, and B. Yoshua, "Empirical evaluation of gated recurrent neural networks on sequence modeling," 2014, https://www.semanticscholar.org/paper/Empirical-Evaluation-of-Gated-Recurrent-Neural-on-Chung.

[34] J. Devlin, M. W. Chang, K. Lee, and T. Kristina, "BERT: pre-training of deep bidirectional transformers for language understanding," 2018, https://www.semanticscholar.org/paper/BERT%3A-Pre-training-of-Deep-Bidirectional-for-Devlin-Chang.

[35] A. Vaswani, N. Shazeer, N. Parmar et al., "Attention Is All You Need," 2017, https://papers.nips.cc/paper/7181-attention-is-all.

[36] R. Mihalcea and P. Tarau, "Textrank: bringing order into texts," in *Proceedings of the EMNLP*, pp. 404–411, Barcelona, Spain, July 2004.

[37] Z. Zheng, "Reasons, challenges, and some tools for doing reproducible transportation research," *Communications in Transportation Research*, vol. 1, Article ID 100004, 2021.

[38] J. Zhang, X. Qu, and S. Wang, "Reproducible generation of experimental data sample for calibrating traffic flow fundamental diagram," *Transportation Research Part A: Policy and Practice*, vol. 111, pp. 41–52, 2018.

Hindawi
Scientific Programming
Volume 2021, Article ID 6189075, 12 pages
https://doi.org/10.1155/2021/6189075

Research Article

Traffic Game Model with the Contract Model

Lin Zhang [1] **and Xinquan Liu** [2]

[1] *School of Economics and Management, Nanchang Hangkong University, Nanchang 330063, Jiangxi, China*
[2] *School of Logistics Management and Engineering, Nanning Normal University, Nanning 530001, Guangxi, China*

Correspondence should be addressed to Lin Zhang; 773651827@qq.com and Xinquan Liu; gxsfxy80@163.com

Received 14 April 2021; Accepted 10 October 2021; Published 23 October 2021

Academic Editor: Jiwei Huang

Copyright © 2021 Lin Zhang and Xinquan Liu. This is an open access article distributed under the Creative Commons Attribution License, which permits unrestricted use, distribution, and reproduction in any medium, provided the original work is properly cited.

To distribute the right-of-way of intersection reasonably, the game model between each adjacent agent was obtained through agent technology. The Nash equilibrium model to measure the negotiation effects was proposed, and the existence of the Nash equilibrium solution was proved. We obtained the game equilibrium solution between each adjacent agent and thus got the equilibrium price (cost) in the network. According to the equilibrium price, travelers will choose the best path in transportation networks by adopting the path strategy with the minimum cost or fuzzy-comparison strategy. The results indicate that the contract mode algorithm makes signal control of each intersection coordinated and unified and shows subjective initiative of traffic control and management fully. The contract-based algorithm combining the management initiatives with the driver's rational behavior will make the control effectiveness of the road network system increase by 55.58%. Hence, it is an effective measurement for studying coordination between system optimality and user optimality.

1. Introduction

The target of an Intelligent Transportation System is to configure the actual traffic demand rationally in time and space by a certain control means and the induction strategies, so that the distribution equilibrium of traffic flow can be reached in the road network, and the overall resources and the traffic capacity of the road network can be fully utilized. The effectively induced information should consider the traveler's response to the information and choice preferences, which can estimate the expected benefits of both the traveler and transport system. Furthermore, the expected benefits are optimized and integrated. Then, an intelligent transport system will give the inducing advice to accord with the transport system and the driver's choices. At this point, the behavior between managers and travelers is a game.

The first application of game theory in transportation is in the form of Wardrop equilibrium in 1952, where Wardrop analyzed the traffic phenomena comprehensively and then proposed two basic principles of the user optimal equilibrium and the system optimal equilibrium about traffic flow, which was similar to Nash equilibrium of noncooperative game about N agents. After that, the game theory is increasingly applied to the field of transportation.

Game theory is the study of mathematical models of no cooperation and cooperation between rational agents. In these two kinds of game modes, players have two choices: to cooperate or to defect. In terms of traffic control at an intersection, some control strategy using a game-theoretic approach, the basic theory of independent and interdependent decision-making, has been introduced for intelligent traffic light control problem. Dong et al. [1] applied a two-person static game model in multi-intersection coordinate control problem. Technically, they proposed some concepts of game theory such as pure strategy Nash equilibrium, mixed strategy Nash equilibrium, Pareto efficiency solution, and Pareto improvement solution of Nash equilibrium for solving traffic control at multi-intersection coordination. Qi [2] establishes the congestion model of intersection between drivers and traffic administration based on the benefit-tending characteristics of the drivers and traffic administrations, an incorrect inducement for traffic administration to take the strategy that prevents vehicles from crossing the intersection during the amber light, where each intersection is regarded as a noncooperative game.

Regarding the noncooperative game, Dai et al. [3] proposed an algorithm to solve the multi-intersection coordinated control problem, which combines the maximal flow theory with the game theory and considers both the individual interests of one intersection and the interests of the whole traffic network. After that, Bel and Cassir [4], Zhou et al. [5], and Li [6] discussed the game equilibrium about ticket price between the transport operators and passengers. Transport operators made decisions on the ticket price, which is responded by passengers from changing the travel means. It is concluded that transport operators can get a competitive advantage by improving the service quality, and transport operators' strategy may benefit local targets. But it may be harmful to the whole road network target. Then Miyagi et al. [7] and Zhen [8] formulated this traffic game as a stochastic congestion game and proposed a naive user algorithm for finding a pure Nash equilibrium. An analysis of the convergence is based on the Markov chain. Finally, using a single origin-destination network connected by some overlapping paths, the validity of the proposed algorithm is tested.

Recently, in terms of the development of Internet of Things, intersections coordinate controls are regarded as smart agents which can communicate and coordinate with each other. The control of several signalized intersections in a network is decomposed into multiple subnetworks and each subnetwork is considered as a region agent. These studies explored the benefits of reducing problem complexity and improving system performance and learning efficiency when cooperation between agents is enabled. Some scholars have studied the integrated management system on the traffic management system and the traveler information system based on the agent technology, and the information communication platform between them is constructed (Ezzedine et al. [9, 10]; Liu and Wang [11]; Zhang et al. [12]; Zhen [13]; Yuan et al. [14]; Zhou et al. [15]; Zhang and Gao [16]). According to the noncooperative game between two agents, the reliability of transportation network performance was measured by Bel [17] in 2000. Miyagi et al. [18] showed a pure user Nash equilibrium which describes the route-choice behavior of a user in a traffic network comprising several discrete, interactive decision-makers, and the agents use only the utility information of the previous action to get a congestion game. It is a multiagent distributed traffic routing problem with both linear and nonlinear link cost functions. Bui et al. [19] applied a cooperative game-theoretic approach among agents to improve traffic flow with a large network. Thereby, a distributed merge and split algorithm for coalition formation is presented. However, both the timely reflection on the traffic conditions and the actions for adapting to the environment are not considered in these systems.

If traffic management can take proactive actions to adapt to the environment according to the drivers' behavior, the traffic condition will be improved significantly. Thus, we can use agent technology to make signal control system in the intersection abstract and ideological, which is conducive to the implementation of intelligent traffic management, and the analysis of multiagent behavior is more easily transformed into traffic network management.

Regarding the intersection of the road network as an agent, where the agent is the signal control system of an intersection, we adopt bid and bargain between every two adjacent agents and then obtain the equilibrium strategy price for the traffic flow in the road network. According to the latest equilibrium strategy price information provided by the intelligent traffic information system, the drivers further optimize their path selection strategy and get the most favorable path for themselves. At the same time, better system goals are achieved, and the coordination between system optimality and user optimality is retained.

2. Negotiation Model Based on Contract

2.1. Price Game between Adjacent Agents. Let a city traffic network be

$$G = (V, E), \tag{1}$$

where V is the set of intersections in the traffic network and E is the set of directed roads between two adjacent intersections. Assuming that one intersection corresponds to a signal control system, the set of signal control system in the intersection can be also denoted by V. The control system of each intersection in the traffic network represents an agent. For any agent $j \in V$, V_j is the set of the adjacent agents with j.

Denote the phase set of signal control system of intersection j by

$$S_j = \{1, 2, \ldots, s\}, \tag{2}$$

where s is the phase number of a signal control system of intersection j. Each signal phase of signal control system of intersection j gets the green light time alternately. For any $i \in V_j$, let ij be the directed road from agent i to j, and the lane set of road ij controlled by phase k of intersection j can be expressed as

$$R_{ij}^k = R_{ij} \cap R_j^k, \tag{3}$$

where R_{ij} is the lane set of the directed road ij and R_j^k is the import lane set controlled by phase k of intersection j.

Let

$$f_{ij} = \sum_{k \in S_{ji}} f_{ij}^k, \tag{4}$$

be the real-time traffic flow of road ij, where S_{ji} is the phase composition set of S_j that controls lanes of road ij, that is, $S_{ji} \subseteq S_j$, k is the phase of intersection j, and f_{ij}^k is the real-time traffic flow on lane set R_{ij}^k.

Assume that any agent i can get real-time traffic information on road ij by using the Intelligent Transportation System. Each agent i is both a traffic flow sender and a receiver except for it is the origin and destination in the network and hopes to send traffic volume to lane set R_{ij}^k at the moment of t. According to the real-time traffic flow f_{ij}^k of lane set R_{ij}^k, free flow speed, traffic volume and length of

road ij, signal cycle T_j of intersection j, and corresponding phase green time of lane set R_{ij}^k, agent i will calculate the real-time traffic impedance of road ij and intersection j and is willing to quote the receiving end j for traffic impedance.

Since, on the one hand, f_{ij}^k, f_{ij}, and the green time of the phase that corresponded to lane set R_{ij}^k are changing over time and, on the other hand, free flow speed, traffic capacity and length of road ij, and signal cycle T_j of intersection j all have fixed values, we can consider the offering price of agent i to be the function of f_{ij}^k, f_{ij}, and the green time of phase k of lane set R_{ij}^k. Hence, the acceptable traffic impedance price that agent i prefers to give to phase k of receiving end agent j can be expressed as

$$p_{ij}^k = p\left(f_{ij}^k, f_{ij}, \lambda_{jk}\right), \tag{5}$$

where λ_{jk} is green time of the $k-$th phase in intersection j and p is the function formula of offering price p_{ij}^k from i to j.

Each agent i hopes to send certain traffic flow to lane set R_{ij}^k at the moment of t. If road ij accepts the traffic flow from i, then the traffic volume of road ij changes to

$$f_{ij}^{k1} = f_{ij}^k + f_0^k, \tag{6}$$

where f_0^k is the traffic volume that agent i sends to lane set R_{ij}^k at the moment of t.

According to the traffic flow f_{ij}^{k1}, where after road ij accepts traffic flow f_0^k, green time λ_{jk}, and static property of road ij, the traffic impedance of road ij and the delay of intersection j are calculated by the receiving end agent j, furthermore, the impedance bargain q_{ji}^k of intersection j which is willing to accept traffic flow f_0^k from i can be obtained as

$$q_{ji}^k = q\left(f_{ij}^{k1}, f_{ij}, \lambda_{jk}\right), \tag{7}$$

where q is the function of that j bargaining q_{ji}^k to i. When agent i makes an offer p_{ij}^k above or equal to bargaining q_{ji}^k of agent j, the two sides will reach an agreement which leads to the successful negotiations.

As set S_{ji} may contain several elements, it means the traffic flow of road ij can be controlled by multiple phases of j intersection signal control system. For any $k \in S_{ji}$, there exists a corresponding bid p_{ij}^k. Hence, there exists one set of bids from i to j, which will form a bid fracture surface, and it is denoted by

$$p_{ij} = \left(\ldots, \left(p_{ij}^k\right)_{k\in S_{ji}}, \ldots\right), \tag{8}$$

where $(p_{ij}^k)_{k\in S_{ji}}$ is the set of bids from i to j. For example, if $S_{ji} = \{1, 2, 3\}$, then p_{ij} can be got as

$$p_{ij} = \left(p_{ij}^1, p_{ij}^2, p_{ij}^3\right). \tag{9}$$

For any $k \in S_{ji}$, p_{ij}^k is a function of f_{ij}^k, f_{ij}, and λ_{jk}, where f_{ij} is given by

$$f_{ij} = \sum_{k\in S_{ji}} f_{ij}^k, \tag{10}$$

and then a bid fracture surface p_{ij} from i to j is indeed a function of f_{ij}^k and λ_{jk}; that is,

$$p_{ij} = p\left(\ldots, \left(f_{ij}^k\right)_{k\in S_{ji}}, \ldots, \left(\lambda_{jk}\right)_{k\in S_{ji}}, \ldots\right), \tag{11}$$

where $(f_{ij}^k)_{k\in S_{ji}}$ is the traffic flow group of road ij controlled by different phases before road ij accepts f_0^k, and $(\lambda_{jk})_{k\in S_{ji}}$ is the green time group of traffic flow phase on the control road ij. Similarly, the bargain fracture surface and the function of bargain fracture surface from j to i can be deduced as follows:

$$q_{ji} = \left(\ldots, \left(q_{ji}^k\right)_{k\in S_{ji}}, \ldots\right), \tag{12}$$

$$q_{ji} = q\left(\ldots, \left(f_{ji}^{k1}\right)_{k\in S_{ji}}, \ldots, \left(\lambda_{jk}\right)_{k\in S_{ji}}, \ldots\right), \tag{13}$$

where $(q_{ji}^k)_{k\in S_{ji}}$ is the bargain group from j to i and $(f_{ji}^{k1})_{k\in S_{ji}}$ is the traffic flow group by different phases control on road ij after road ij accepts f_0^k.

If the traffic volume of road ij is f_{ij}, the traffic impedance of road ij is thus

$$t_{ij} = \frac{l_{ij}}{v\left(f_{ij}\right)}, \tag{14}$$

where l_{ij} is the length of road ij and $v(f_{ij})$ is the vehicle speed on road ij. Let

$$u_{ji}^k = t_{ij} + d_{ij}^k, \tag{15}$$

where u_{ji}^k is the traffic impedance of vehicle going through road ij and d_{ij}^k is the red light delay of the import lanes of road ij by the $k-$th phase control, and the traffic impedance u_{ji}^k can also be referred to as the status quo point from agent j to i, which is on road ij by the $k-$th phase control. Agent i quotes impedance p_{ij}^k by the $k-$th phase control lane of signal control system of intersection j, which should be higher than or equal to the status quo point u_{ji}^k from agent j to i; that is,

$$p_{ij}^k \geq u_{ji}^k. \tag{16}$$

Otherwise, agent j will refuse to continue negotiations with agent i on the $k-$th phase.

After j receives traffic flow f_0^k from i, we denote M_{ij}^k to be the status quo point from agent i to agent j on road ij controlled by the $k-$th phase, and it holds

$$M_{ij}^k = t_{ij}^1 + d_{ij}^{k1}, \tag{17}$$

where M_{ij}^k is the traffic impedance that vehicles pass the directed road ij after j received traffic flow f_0^k from i, t_{ij}^1 is the traffic impedance of road ij after j receives traffic flow f_0^k from i, and d_{ij}^{k1} is the red light delay on the import lanes of road ij by the $k-$th phase control after j receives traffic flow f_0^k from i. Agent j counteroffers q_{ji}^k to agent i which should not be higher than the status quo point M_{ij}^k from agent i to j, and agent i will refuse negotiation with j if not; that is,

$$q_{ji}^{k} \leq M_{ij}^{k}. \tag{18}$$

As S_{ji} may have several elements and $k \in S_{ji}$, the status quo points from j to i and from i to j will form an individual fracture surface, respectively, which are expressed as

$$u_{ji} = \left(\ldots, \left(u_{ji}^{k}\right)_{k \in S_{ji}}, \ldots\right), \tag{19}$$

$$M_{ij} = \left(\ldots, \left(M_{ij}^{k}\right)_{k \in S_{ji}}, \ldots\right), \tag{20}$$

where $(u_{ji}^{k})_{k \in S_{ji}}$ is the status quo point group from j to i, $(M_{ij}^{k})_{k \in S_{ji}}$ is the status quo point group from i to j, u_{ji} is the status quo point fracture surface from j to i, and M_{ij} is the status quo point fracture surface from i to j. Quotes fracture surface p_{ij} should be preferable to u_{ji}; that is to say,

$$p_{ij} \succ u_{ji}, \tag{21}$$

where $\succ$ means it holds that, for any $k \in S_{ji}$,

$$p_{ij}^{k} \geq u_{ji}^{k}. \tag{22}$$

Furthermore, the bargain fracture surface from j to i should meet the demand of

$$q_{ji} \prec M_{ij}. \tag{23}$$

2.2. Nash Equilibrium of the Negotiation between Agents. Assume that all the agents in V are individually rational; that is to say their acquisition is as good as before after knowing the final results of the negotiation. Agent i quotes each fracture surface p_{ij} which will compare own status quo point fracture surface M_{ij} to j, and agent j counteroffers each fracture surface q_{ji} which will compare own status quo point fracture surface u_{ji} to i as well. For any $k \in S_{ji}$, the utilities obtained by i and j are $M_{ij}^{k} - p_{ij}^{k}$ and $q_{ji}^{k} - u_{ji}^{k}$, respectively, under each bid and bargain. If the negotiation reaches an agreement, the arithmetic product of utility with agents i and j in phase k can be got as

$$U_{ij}^{k} = \left(M_{ij}^{k} - p_{ij}^{k}\right)\left(q_{ji}^{k} - u_{ji}^{k}\right), \tag{24}$$

where it must meet

$$p_{ij}^{k} \geq q_{ji}^{k}. \tag{25}$$

Thus, we have

$$\begin{aligned} U_{ij} &= \sum_{k \in S_{ji}} U_{ij}^{k}, \\ p_{ij}^{k} &\geq q_{ji}^{k}, \\ j &\in V, \\ i &\in V_j, \end{aligned} \tag{26}$$

where U_{ij} can be regarded as the measurement of negotiation price agreements effect between i and j. The negotiators are all individually rational, and they hope the final price agreement is preferable to that of their status quo points, and the parties have the will to reach an agreement. Now, let us talk about the final agreement.

The bid price strategy between every two adjacent agents in the traffic network forms a fracture surface, which can be expressed as

$$R = \left(\ldots, \left(p_{ij}, q_{ji}\right)_{j \in V, i \in V_j}, \ldots\right), \tag{27}$$

where $(p_{ij}, q_{ji})_{j \in V, i \in V_j}$ is a bid and bargain strategy for any two adjacent agents in the traffic network. We denote $\mathfrak{R}$ to be the set of all strategy fracture surfaces R and B^{+} to be the set of all possible traffic distributions. For any traffic distribution $B \in B^{+}$ and $R \in \mathfrak{R}$, if there does not exist $B^{/} \in B^{+}$ and $B^{/} \succ B$ is made, we conclude that traffic distribution B is valid to strategy fracture R. Let $P(R)$ be the valid set (Pareto set) of all traffic distributions to R.

Definition 1 (validity). The validity means all agents' strategy fracture surface R, of which the results of traffic distribution are $B \in P(R)$; that is to say, all the agents always choose the most advantageous strategy.

Theorem 1. *If any two adjacent agents in the network are individually rational and follow the validity, the following hold: ① the negotiation between them can reach an agreement; ② the final agreement price reaches Nash equilibrium; that is,*

$$p_{ij}^{k^*} = p_{ij}^{k} = q_{ji}^{k} = \frac{M_{ij}^{k} + u_{ji}^{k}}{2}, \quad k \in S_{ji}. \tag{28}$$

Proof. ① According to individual rationality, let the initial bid price of agent i be the status quo point u_{ji}^{k} from j to i for any $k \in S_{ji}$. Then, agent i increases his bid price according to the bargain price from agent j. On the other hand, the initial bargain price of agent j is the status quo point M_{ij}^{k} from i to j, and agent j then decreases his bargain price according to the increasing value size of bid price of agent i. Since both sides' bid prices are preferable to their status quo points, respectively, they both wish to reach an agreement. In order to do this, the bid price of i will be higher as long as the bargain price of j will be lower. When the n-th bid and bargain price of them is

$$p_{ij}^{kn} \geq q_{ji}^{kn}, \tag{29}$$

they finally achieve an agreement with the price:

$$p_{ij}^{k^*} = p_{ij}^{kn}. \tag{30}$$

Thus, their negotiation can achieve an agreement.

② Assume that both sides achieve an agreement at the l-th bid p_{ij}^{kl} and bargain q_{ji}^{kl}; that is,

$$p_{ij}^{kl} \geq q_{ji}^{kl}. \tag{31}$$

If

$$p_{ij}^{kl} > q_{ji}^{kl}, \tag{32}$$

according to formula (26), the effect of the price agreement of their negotiation is

$$U_{ij}^{k} = \left(M_{ij}^{k} - p_{ij}^{kl}\right)\left(q_{ji}^{kl} - u_{ji}^{k}\right). \tag{33}$$

As

$$p_{ij}^{kl} > q_{ji}^{kl}, \tag{34}$$

we can get that

$$U_{ij}^{k} < \left(M_{ij}^{k} - p_{ij}^{kl}\right)\left(p_{ji}^{kl} - u_{ji}^{k}\right). \tag{35}$$

If the agreed price of both sides is

$$p_{ij}^{k^*} = p_{ij}^{k} = q_{ji}^{k} = \frac{M_{ij}^{k} + u_{ji}^{k}}{2}, \tag{36}$$

the arithmetic product of effectiveness for their negotiation is

$$U_{ij}^{k^*} = \left(M_{ij}^{k} - p_{ij}^{k^*}\right)\left(p_{ij}^{k^*} - u_{ji}^{k}\right) = \left(\frac{M_{ij}^{k} - u_{ji}^{k}}{2}\right)^2. \tag{37}$$

Since

$$\begin{aligned} U_{ij}^{k^*} - U_{ij}^{k} &> \left(\frac{M_{ij}^{k} - u_{ji}^{k}}{2}\right)^2 - \left(M_{ij}^{k} - p_{ij}^{kl}\right)\left(p_{ij}^{kl} - u_{ji}^{k}\right) \\ &= \frac{\left(M_{ij}^{k}\right)^2 + \left(u_{ji}^{k}\right)^2 - 2M_{ij}^{k}u_{ji}^{k}}{4} - \left[M_{ij}^{k}p_{ij}^{kl} - M_{ij}^{k}u_{ji}^{k} - \left(p_{ij}^{kl}\right)^2 + p_{ij}^{kl}u_{ji}^{k}\right] \\ &= \frac{\left(M_{ij}^{k}\right)^2 + \left(u_{ji}^{k}\right)^2 + 2M_{ij}^{k}u_{ji}^{k}}{4} - \left(M_{ij}^{k} + u_{ji}^{k}\right)p_{ij}^{kl} + \left(p_{ij}^{kl}\right)^2 \\ &= \left(\frac{M_{ij}^{k} + u_{ji}^{k}}{2}\right)^2 - \left(M_{ij}^{k} + u_{ji}^{k}\right)p_{ij}^{kl} + \left(p_{ij}^{kl}\right)^2 \\ &= \left(\frac{M_{ij}^{k} + u_{ji}^{k}}{2} - p_{ij}^{kl}\right)^2 \geq 0, \end{aligned} \tag{38}$$

that is,

$$U_{ij}^{k^*} > U_{ij}^{k}, \tag{39}$$

the Nash equilibrium price of both sides is thus

$$p_{ij}^{k^*} = p_{ij}^{k} = q_{ji}^{k} = \frac{M_{ij}^{k} + u_{ji}^{k}}{2}. \tag{40}$$

Hence, for any $k \in S_{ji}$, if

$$p_{ij}^{k^*} = p_{ij}^{k} = q_{ji}^{k} = \frac{M_{ij}^{k} + u_{ji}^{k}}{2}, \tag{41}$$

it holds that

$$U_{ij} = \sum_{k \in S_{ji}} U_{ij}^{k}, \tag{42}$$

reaches maximum, and then $p_{ij}^{k^*}$ is the Nash equilibrium price of both agents i and j. According to the validity, bid price of both sides will be selected in the Pareto set, which yields that the final agreement price must be the Nash equilibrium price.

For agent j at any receiving side, it will receive many adjacent agents' quotation. Whose quotation will be prioritized is directly related to the utility obtained by j. So the priority will be given to the specific traffic route, which obtains the largest system utility. Thus, agent j has to balance all agents' transportation requests in V_j and use the available resources (such as adjusting the green signal ratio of imported lanes, etc.) to meet the prior request. □

Theorem 2. *If the traffic flow receiver agent j and the traffic flow sender agent i in V_j are all individually rational and follow the validity, we can get the following: ① each agent in V_j can reach an agreement with agent j, respectively; ② the Nash equilibrium of all agents utility arithmetic product,*

$$U_j = \prod_{i \in V_j} U_{ij}, \tag{43}$$

is the final agreement price, which is expressed as

$$p_{ij}^{k^*} = p_{ij}^{k} = q_{ji}^{k} = \frac{M_{ij}^{k} + u_{ji}^{k}}{2}, \quad k \in S_{ji}, i \in V_j. \tag{44}$$

Proof. (1) According to Theorem 1, for any agent i and agent j, they can achieve a final agreement. Hence, each agent in V_j can reach an agreement with agent j, respectively.

(2) According to Theorem 1, for any agent $i \in V_j$, $k \in S_{ji}$, if the final agreement price between two agents is

$$p_{ij}^{k^*} = p_{ij}^k = q_{ji}^k = \frac{M_{ij}^k + u_{ji}^k}{2}, \tag{45}$$

we can obtain

$$\left(M_{ij}^k - p_{ij}^{k^*}\right)\left(p_{ij}^{k^*} - u_{ji}^k\right) > \left(M_{ji}^k - p_{ji}^k\right)\left(q_{ji}^k - u_{ji}^k\right), \tag{46}$$

where

$$p_{ij}^k > q_{ji}^k, \tag{47}$$

that is,

$$\begin{aligned} U_{ij}^* &= \sum_{k\in S_{ji}} \left(M_{ij}^k - p_{ij}^{k^*}\right)\left(p_{ij}^{k^*} - u_{ji}^k\right) > \sum_{k\in S_{ji}} \left(M_{ij}^k - p_{ij}^k\right)\left(q_{ij}^k - u_{ji}^k\right) \\ &= U_{ij}. \end{aligned} \tag{48}$$

This leads to

$$U_j^* = \prod_{i\in V_j} U_{ij}^* > \prod_{i\in V_j} U_{ij} = U_j, \tag{49}$$

that is,

$$U_j^* > U_j. \tag{50}$$

Thus, the Nash equilibrium of

$$U_j = \prod_{i\in V_j} U_{ij}, \tag{51}$$

is

$$p_{ij}^{k^*} = p_{ij}^k = q_{ji}^k = \frac{M_{ij}^k + u_{ji}^k}{2}, \tag{52}$$

where $k \in S_{ji}$ and $i \in V_j$. According to the validity, the bid prices of all agents in V_j and agent j will be selected in the Pareto set, and the final agreement price between j and his adjacent agents must be the Nash equilibrium price:

$$p_{ij}^{k^*} = p_{ij}^k = q_{ji}^k = \frac{M_{ij}^k + u_{ji}^k}{2}, \quad k \in S_{ji}, i \in V_j. \tag{53}$$

Agent j can change the price by adjusting the split ratio to achieve the purpose of regulating road traffic and control the traffic volume of the up-down stream. For example, according to the existing number of vehicles in the upstream road and the traffic volume that prepare to enter the road, the agent decreases the traffic volume that is prepared to enter the road by increasing the bargain price to the adjacent agent in the upper stream road and increase outflow by improving the quotation to the downstream adjacent agents. This may guarantee the entire road network traffic flow to be balanced. □

Theorem 3. *If every two adjacent agents in V have a price negotiation with each other and they are all individually rational and follow the validity, we can get the following: ① all adjacent agents of both sides will reach an agreement; ② the entire road network has Nash equilibrium price, and the final price agreement is the Nash equilibrium solution to*

$$U = \prod_{j\in V} U_j, \tag{54}$$

which is expressed as

$$p_{ij}^{k^*} = p_{ij}^k = q_{ji}^k = \frac{M_{ij}^k + u_{ji}^k}{2}, \quad k \in S_{ji}, j \in V, i \in V_j. \tag{55}$$

Proof. (1) According to Theorem 2, for any $j \in V$ and all the agents in V_j, they can reach an agreement. By the arbitrariness of j, all adjacent negotiations of both sides can reach an agreement in the road network.

(2) According to Theorem 2, for any $j \in V$, $i \in V_j$, and $k \in S_{ji}$, if

$$p_{ij}^k > q_{ji}^k, \tag{56}$$

it holds that

$$U_j^* > U_j, \tag{57}$$

and we thus get that

$$U^* = \prod_{j\in V} U_j^* > \prod_{j\in V} U_j, \tag{58}$$

that is,

$$U^* > U. \tag{59}$$

This yields that the Nash equilibrium solution of U is

$$p_{ij}^{k^*} = p_{ij}^k = q_{ji}^k = \frac{M_{ij}^k + u_{ji}^k}{2}, \quad k \in S_{ji}, j \in V, i \in V_j. \tag{60}$$

According to the validity, every two adjacent agents select their quotation price in the Pareto set, and the final agreement price must be Nash equilibrium solution in the road network. That is, the entire road network forms the Nash equilibrium price. □

2.3. Confirming the Green Time of the Signal Control System in the Intersection. It follows from Theorem 3 that j could obtain the largest utility by adjusting the green time λ_{jk} in the k-th phase when facing any agent i in V_j. Due to the individual rationality, for any $i \in V_j$ and $k \in S_{ji}$, j will increase the green time λ_{jk} in the k-th phase if j can obtain larger utility from i and reduce λ_{jk} conversely if not. Meanwhile, to prevent conflict of green light, we assume that when any phase in an intersection is a green light or yellow one, the others are all red light. Notice that the vehicle may get through the intersection on the yellow time; we fix the green time λ_{jk} here including the yellow time in the k-th phase for discussing conveniently. Therefore, it holds that

$$\sum_{k\in S_j} \lambda_{jk} = T_j, \tag{61}$$

where T_j is the signal circle of the signal control system in intersection j. On the grounds of Theorem 1, together with the status quo point

$$u_{ji}^{k} = t_{ij} + d_{ij}^{k}. \tag{62}$$

from j to i and the status quo point

$$M_{ij}^{k} = t_{ij}^{1} + d_{ij}^{k1}. \tag{63}$$

from i to j, we thus obtain the equilibrium price as follows:

$$p_{ij}^{k^*} = \frac{M_{ij}^{k} + u_{ji}^{k}}{2}, \tag{64}$$

where the traffic impedance of the intersection part is $p_{ij}^{k^*} - (t_{ij} + t_{ij}^{1})/2$. Taking the maximum of intersection stop delay controlled by the k-th phase in different roads as an example, that is, $\vee_{R_{ij}^{k} \in R_{j}^{k}} (p_{ij}^{k^*} - (t_{ij} + t_{ij}^{1})/2)$, the green time of the k-th phase in intersection j can then be denoted by

$$\lambda_{jk} = \min\left\{\lambda_1, \max\left\{\frac{\bigvee_{R_{ij}^{k} \in R_{j}^{k}} \left(p_{ij}^{k^*} - \left(t_{ij} + t_{ij}^{1}\right)/2\right)}{\sum_{k \in S_j}\left[\bigvee_{R_{ij}^{k} \in R_{j}^{k}} \left(p_{ij}^{k^*} - \left(t_{ij} + t_{ij}^{1}\right)/2\right)\right]} T_j, \lambda_0\right\}\right\}, \tag{65}$$

where λ_0 is the minimum green time to make sure vehicles and pedestrians get through the intersection safely and λ_1 is the maximum green time of signal phase for intersection j.

3. The Driver Path Selection Rules Based on the Price Information

Let K be the origin set of the OD and let S be the destination set of the OD; it is obvious that $K \subset V$ and $S \subset V$, and all the path set between origin site and the destination one is

$$Z^{\kappa\ell} = \{z_1, z_2, \ldots, z_m\}, \tag{66}$$

where $\kappa \in K$, $\ell \in S$, and z_m is the m-th path from origin κ to destination ℓ. For any path $z_\lambda \in Z^{\kappa\ell}$, it can be expressed as

$$z_\lambda = \left\{\kappa = k_0, k_1, \ldots, k_{m_\lambda} = \ell\right\}, \tag{67}$$

where k_0 is the first intersection on path z_λ from κ to ℓ and k_{m_λ} is the last intersection on path z_λ. The driver hopes to pay the least expenditure for starting from the origin site κ to the destination site; that is to say, he will choose the path with the lowest equilibrium strategy price in the network. Theorem 3 tells that all the adjacent agents in the network can reach an agreement and get an equilibrium price, and thus the intelligent traffic system can continuously provide the driver with the real-time equilibrium price between every two adjacent agents. With the equilibrium strategy price at hand, the driver calculates all path prices from κ to ℓ, which is indeed a price function that can be expressed as follows:

$$U^{\kappa\ell} = \left\{U_{z_\lambda}^{\kappa\ell} \mid U_{z_\lambda}^{\kappa\ell} = \sum_{i \in z_\lambda} p_{ij}^{k^*}, \text{and } i = k_a, j = k_{a+1}, k_a, k_{a+1} \in z_\lambda, z_\lambda \in Z^{\kappa\ell}\right\}, \tag{68}$$

where $p_{ij}^{k^*}$ is the Nash equilibrium price from i to j and $U_{z_\lambda}^{\kappa\ell}$ is the price of path z_λ.

Let the driver set with traffic demand between origin κ and destination ℓ be

$$N = \{1, 2, \ldots, n\}, \tag{69}$$

where n is the total number of the drivers with traffic demand between origin κ and destination ℓ. The price information in the Intelligent Transportation System is updated with a certain period of time which is assumed to be T_0. Assume that the equilibrium price information of Intelligent Transportation Systems is updated once at the moment of t_1. Now, during the period from moment t_1 to $t_1 + T_0$, the equilibrium price of each path between origin κ and destination ℓ has changed with vehicles entering the road network, which is in sharp contrast to the price information in the Intelligent Transportation System that did not update in time. In this case, if the driver selects the path with the least sum of the price which is provided by Intelligent Transportation Systems, the actual price of the path may not be the lowest. As the received price information is not exactly coincided with the actual information, the different path strategies may be selected by different drivers according to their age, gender, education level, and other factors. Assume that the driver has two strategies to choose: the first one is to choose the path with the lowest price offered by the Intelligent Transportation Systems at the moment of t_1; the second one is based on the path price of the Intelligent Transportation System offered at the moment of t_1, and choose the path in $Z^{\kappa\ell}$ by using fuzzy-comparison strategy.

Let

$$Z^{\kappa\ell} = \left\{z_{\pi(1)}, z_{\pi(2)}, \ldots, z_{\pi(m)}\right\}, \tag{70}$$

where π is a rearrangement of all the paths in $Z^{\kappa\ell}$, which makes the price relationship of each path as follows:

$$U_{z_{\pi(1)}}^{\kappa\ell} \le U_{z_{\pi(2)}}^{\kappa\ell} \le \cdots \le U_{z_{\pi(m)}}^{\kappa\ell}. \tag{71}$$

Hence, the equilibrium price for path $z_{\pi(1)}$ is

$$U_{z_{\pi(1)}}^{\kappa\ell} = \min U^{\kappa\ell}. \tag{72}$$

If the driver adopts the first strategy, then path $z_{\pi(1)}$ will be chosen.

The theoretic basis of the driver adopting the second strategy is that drivers calculate the price of each path by the Intelligent Traffic Information System at the moment of t_1, and price $U_{z_{\pi(1)}}^{\kappa\ell}$ of path $z_{\pi(1)}$ with the smallest traffic impedance between κ and ℓ was obtained by calculating. With the vehicles entering and exiting the path, the price on the path has been changed in the period of time of $[t_1, t_1 + T_0)$. Indeed, this yields the fuzziness of the price. Next, let the fuzzy price interval of $z_{\pi(1)}$ be

$$\tilde{U}_{z_{\pi(1)}}^{\kappa\ell} = \left[(1-\eta)U_{z_{\pi(1)}}^{\kappa\ell}, (1+\eta)U_{z_{\pi(1)}}^{\kappa\ell}\right], \tag{73}$$

where $0 \le \eta \le 1$ represents the fuzzy degrees of the path price provided by the Intelligent Transportation Information System. The probability of choosing path z_r for the drivers adopting the second strategy is as follows:

$$\left\{\varphi(z_r)\colon Z^{\kappa\ell} \longmapsto [0,1], \text{and} \sum_{z_r \in Z^{\kappa\ell}} \varphi(z_r) = 1\right\}, \tag{74}$$

where $\varphi(z_r)$ is the probability of the driver chosen path z_r.

In general, the driver of the second strategy regards only parts of the paths between κ and ℓ in the period of time of $[t_1, t_1 + T_0)$, but not all of them, as a candidate one. Consequently, the driver should choose the path whose price belongs to $\widetilde{U}^{\kappa\ell}_{z_{\pi(1)}}$ in $Z^{\kappa\ell}$ before entering the network; and we denote these paths to be a set as follows:

$$A = \left\{z_{\pi(e)} \mid z_{\pi(e)} \in Z^{\kappa\ell}, 2 \le e \le h\right\}, \tag{75}$$

where h is a positive integer lesser than or equal to m which satisfies

$$U^{\kappa\ell}_{z_{\pi(h)}} \in \widetilde{U}^{\kappa\ell}_{z_{\pi(1)}}, \tag{76}$$

$$U^{\kappa\ell}_{z_{\pi(h+1)}} \notin \widetilde{U}^{\kappa\ell}_{z_{\pi(1)}}. \tag{77}$$

And m is the total number of paths between κ and ℓ. The driver randomly selects the path in set C by a certain probability, where C is expressed as

$$C = A \cup \left\{z_{\pi(1)}\right\}. \tag{78}$$

If A is empty, the driver chooses path $z_{\pi(1)}$ unconditionally. If A is not empty, the path will be chosen with much higher probability as the gap between the path price in A and $U^{\kappa\ell}_{z_{\pi(1)}}$ is smaller. According to the specificity of $z_{\pi(1)}$ in $Z^{\kappa\ell}$, we define the probability of $z_{\pi(1)}$ to be chosen as

$$\varphi'\left(z_{\pi(1)}\right) = 1 - \varphi'\left(z_{\pi(2)}\right), \tag{79}$$

where $z_{\pi(2)}$ is the lowest-price path in set A and φ' is the probability of $z_{\pi(1)}$ to be chosen. Recalling that

$$U^{\kappa\ell}_{z_{\pi(1)}} \le U^{\kappa\ell}_{z_{\pi(e)}} \le (1+\eta) U^{\kappa\ell}_{z_{\pi(1)}}, \tag{80}$$

it holds that the probability of path $z_{\pi(e)}$ to be chosen is

$$\begin{aligned}\varphi'\left(z_{\pi(e)}\right) &= \frac{(1+\eta)U^{\kappa\ell}_{z_{\pi(1)}} - U^{\kappa\ell}_{z_{\pi(e)}}}{(1+\eta)U^{\kappa\ell}_{z_{\pi(1)}} - U^{\kappa\ell}_{z_{\pi(1)}}} \\ &= \frac{(1+\eta)U^{\kappa\ell}_{z_{\pi(1)}} - U^{\kappa\ell}_{z_{\pi(e)}}}{\eta U^{\kappa\ell}_{z_{\pi(1)}}}.\end{aligned} \tag{81}$$

When $2 \le e \le h$, thus

$$\varphi'\left(z_{\pi(e)}\right) = \begin{cases} 1 - \varphi'\left(z_{\pi(2)}\right), & e = 1, \\ \dfrac{(1+\eta)U^{\kappa\ell}_{z_{\pi(1)}} - U^{\kappa\ell}_{z_{\pi(e)}}}{\eta U^{\kappa\ell}_{z_{\pi(1)}}}, & 2 \le e \le h, \\ 0, & h < e \le m. \end{cases} \tag{82}$$

Furthermore, we obtain after normalizing (82) that the probability of each path chosen by the driver is

$$\varphi\left(z_{\pi(e)}\right) = \frac{\varphi'\left(z_{\pi(e)}\right)}{\sum_{k=1}^{m} \varphi'\left(z_{\pi(k)}\right)}, \quad 1 \le e \le m. \tag{83}$$

This is the resulting path selection rule for the drivers of the second strategy by applying the fuzzy-comparison method. More precisely, the Intelligent Transportation System updates all path prices in the network at the moment of $t_1 + T_0$. Next, the drivers in the network choose the path by the latest information of path price in the period of time of $[t_1 + T_0, t_1 + 2T_0)$. Then, the network price will be updated again at the moment of $t_1 + 2T_0$. The above steps repeat indefinitely to be a circle.

4. Algorithm

According to Theorem 3, the driver obtains the Nash equilibrium price of each path in the network by using an Intelligent Transportation System. Based on the equilibrium price, the algorithm of the dynamic traffic game model can be given as follows:

Step 1: We will give some initial data as follows: the initial value of traffic volume of all the paths in the network is $f_{\pi(e)} = f_0$, the initial value of green time is λ_{jk}, the driver ratio of the first strategy is γ, the traffic volume of entering the network in the period of time of T_0 is $f^{\kappa\ell}$, and the demand of all OD in the network is $d^{\kappa\ell}$; let $d_0^{\kappa\ell} = 0$ and $t_0^{\kappa\ell} = 0$, where $\kappa \in K$ and $\ell \in S$.

Step 2: Calculate t_{ij}, d_{ij}^k, t_{ij}^1, and d_{ij}^{k1}, respectively, and then also

$$u_{ji}^k = t_{ij} + d_{ij}^k, \tag{84}$$

$$M_{ij}^k = t_{ij}^1 + d_{ij}^{k1}. \tag{85}$$

This leads to

$$p_{ij}^{k^*} = \frac{M_{ij}^k + u_{ji}^k}{2}. \tag{86}$$

We will calculate λ_{jk} by formula (65), where $j \in V$, $i \in V_j$, and $k \in S_{ji}$.

Step 3: Calculating $U^{\kappa\ell}$ on the basis of formula (68) and ranking all the elements in $U^{\kappa\ell}$, it holds that

$$\left\{U^{\kappa\ell}_{z_{\pi(1)}}, U^{\kappa\ell}_{z_{\pi(2)}}, \ldots, U^{\kappa\ell}_{z_{\pi(m)}}\right\}. \tag{87}$$

Step 4: If an OD is

$$d_0^{\kappa\ell} \ge d^{\kappa\ell}. \tag{88}$$

We ignore distributing it, and if

$$d_0^{\kappa\ell} < d^{\kappa\ell}. \tag{89}$$

$\varphi'(z_{\pi(e)})$ will be got by using formula (82). Then, $\varphi(z_{\pi(c)})$ can be calculated by formula (83). Here, c is a positive integer satisfying $1 \le c \le m$.

Step 5: Let

$$f_{\pi(1)}^{\kappa\ell} := f_{\pi(1)}^{\kappa\ell} + \gamma f^{\kappa\ell}, \tag{90}$$

$$f_{\pi(e)} := f_{\pi(e)} + (1-\gamma) f^{\kappa\ell} \varphi\left(z_{\pi(e)}\right), \tag{91}$$

where $1 \le e \le m$. Set

$$d_0^{\kappa\ell} := d_0^{\kappa\ell} + f^{\kappa\ell}, \tag{92}$$

$$t_0^{\kappa\ell} := t_0^{\kappa\ell} + T_0. \tag{93}$$

Step 6: If all the OD meet the condition

$$d_0^{\kappa\ell} \ge d^{\kappa\ell}, \tag{94}$$

we thus stop calculating; otherwise, we get back to Step 2.

This algorithm cycles on the basis of cycle time T_0. There is a traffic distribution to the entire network in each cycle and to test the distribution of each OD demand in the network. If the distribution of an OD demand is finished, the allocation of the next cycle will skip the OD demand, until all OD demand allocations come to an end. The price information in the algorithm is constantly updated over time, and it also reflects the human behavior factors in the distribution. Hence, it is much closer to the actual traffic distribution.

5. Example

Figure 1 is a simple road network, which consists of 7 points and 20 directed roads. Each road has 3 lanes, points 2–6 are signalized intersections, where points 2, 3, 5, and 6 are T-intersections, and point 4 is the crossed intersection. All the T-intersections adopt three-phase control scheme, and the signal cycle is 90 s. The crossed intersection adopts four-phase control scheme, and the signal cycle is 120 s. The phase and phase sequence in each intersection can be expressed in Figures 2 and 3.

The initial green times of phases 1, 2, and 3 for the T-intersection are 50 s, 20 s, and 20 s, respectively. The initial green times of phases 1, 2, 3, and 4 for the crossed intersections are 40 s, 20 s, 40 s, and 20 s, respectively. The length, traffic capacity, and free-flow speed of each road are shown in Table 1.

There are two cases in finding the solution of average delay on the lanes of import road ij of the k-th phase control in a time cycle. On the one hand, if the arrival rate is less than signal traffic capacity, it can be calculated by the steady-state delay model. On the other hand, if the arrival rate is higher than signal traffic capacity, it can be calculated by fixed number delay model. The steady-state delay model and fixed-number delay model (Wang and Yan) [20] can be, respectively, expressed as

$$d_{ij}^k = \frac{c_{ij}^m \left(T_j - \lambda_{jk}\right)^2}{2T_j\left(c_{ij}^m - f_{ij}^{k1}\right)}, \tag{95}$$

$$d_{ij}^k = \frac{c_{ij}^m \left(T_j - \lambda_{jk}\right)}{2 f_{ij}^{k1}} + \frac{\left(f_{ij}^{k1} - c_{ij}^m\right) T_j}{2}, \tag{96}$$

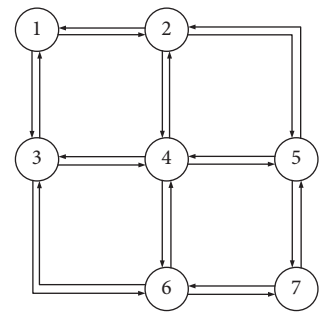

Figure 1: Simple traffic network.

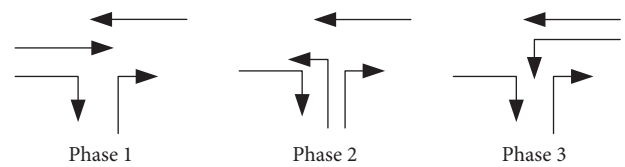

Figure 2: T-intersection design phase and phase sequence diagram.

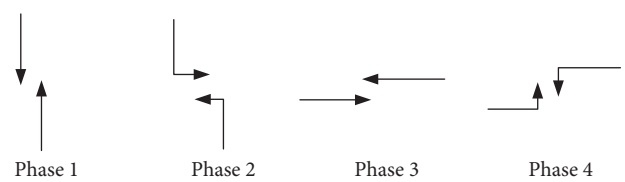

Figure 3: Cross-intersection design phase and phase sequence diagram.

where v_{ij}^m is the free flow speed on road ij. The traffic impedance of each road is obtained by the numerical correspondence relationship between (traffic volume/traffic capacity) and (average speed/free flow speed), which is shown in Table 2 (Markose et al.) [21].

There are three OD pairs in the network, that is, (1, 7), (7, 1), and (4, 7), and the OD demands are $d_{17} = 3000\,\text{veh}\cdot\text{h}^{-1}$, $d_{71} = 4000\,\text{veh}\cdot\text{h}^{-1}$, and $d_{47} = 1020\,\text{veh}\cdot\text{h}^{-1}$. There are six paths between OD pair (1, 7), that is, $a_1: 1 \longrightarrow 2 \longrightarrow 5 \longrightarrow 7$, $a_2: 1 \longrightarrow 2 \longrightarrow 4 \longrightarrow 5 \longrightarrow 7$, $a_3: 1 \longrightarrow 2 \longrightarrow 4 \longrightarrow 6 \longrightarrow 7$, $a_4: 1 \longrightarrow 3 \longrightarrow 4 \longrightarrow 5 \longrightarrow 7$, $a_5: 1 \longrightarrow 3 \longrightarrow 4 \longrightarrow 6 \longrightarrow 7$, and $a_6: 1 \longrightarrow 3 \longrightarrow 6 \longrightarrow 7$. There are two paths between OD pair (4, 7); that is, $a_7: 4 \longrightarrow 5 \longrightarrow 7$ and $a_8: 4 \longrightarrow 6 \longrightarrow 7$. There are six paths between OD pair (7, 1), that is, $a_9: 7 \longrightarrow 5 \longrightarrow 2 \longrightarrow 1$, $a_{10}: 7 \longrightarrow 5 \longrightarrow 4 \longrightarrow 2 \longrightarrow 1$, $a_{11}: 7 \longrightarrow 6 \longrightarrow 4 \longrightarrow 2 \longrightarrow 1$, $a_{12}: 7 \longrightarrow 5 \longrightarrow 4 \longrightarrow 3 \longrightarrow 1$, $a_{13}: 7 \longrightarrow 6 \longrightarrow 4 \longrightarrow 3 \longrightarrow 1$, and $a_{14}: 7 \longrightarrow 6 \longrightarrow 3 \longrightarrow 1$. The traffic flows on these fourteen paths are represented by $f_{a_1}, f_{a_2}, \ldots, f_{a_{14}}$, respectively.

The fuzzy degree of the path price provided by the Intelligent Transportation Information System is $\eta = 0.2$; the ratio of drivers adopting the first strategy is $\gamma = 0.5$. We carry out road network traffic assignment by the dynamic traffic game model based on the contraction algorithm and the shortest path algorithm, respectively. We conduct

Table 1: Static attributes of simple traffic network.

Road	$1 \longrightarrow 2$ $2 \longrightarrow 1$	$2 \longrightarrow 5$ $5 \longrightarrow 2$	$1 \longrightarrow 3$ $3 \longrightarrow 1$	$2 \longrightarrow 4$ $4 \longrightarrow 2$	$3 \longrightarrow 4$ $4 \longrightarrow 3$	$4 \longrightarrow 5$ $5 \longrightarrow 4$	$3 \longrightarrow 6$ $6 \longrightarrow 3$	$4 \longrightarrow 6$ $6 \longrightarrow 4$	$5 \longrightarrow 7$ $7 \longrightarrow 5$	$6 \longrightarrow 7$ $7 \longrightarrow 6$
Length/(km)	2.9	5	2.875	0.65	0.94	1.18	4	0.975	2.72	3.2
Traffic capacity/(veh·h^{-1})	3000	3000	2500	3000	3000	3000	2500	3000	3000	2500
Free flow speed/(km·h^{-1})	50	50	40	40	40	30	40	40	50	40

Table 2: Relationship between vehicle average speed and path flow.

(Traffic volume)/(traffic capacity)	≤0.3	0.4	0.5	0.6	0.7	0.8	0.9	1.0	1.1	1.2	≥1.3
(Average speed)/(free flow speed)	1	34/35	31/35	24/35	19/35	14/35	9/35	4/35	3/35	2/35	0

Table 3: Assignment results of link flow/(veh·h^{-1}).

Path flow	f_{a_1}	f_{a_2}	f_{a_3}	f_{a_4}	f_{a_5}	f_{a_6}	f_{a_7}	f_{a_8}	f_{a_9}	$f_{a_{10}}$	$f_{a_{11}}$	$f_{a_{12}}$	$f_{a_{13}}$	$f_{a_{14}}$
Shortest path algorithm	4	2988	0	4	4	0	1016	4	4	3988	0	0	4	4
Contraction model algorithm	4	864	732	736	664	0	688	332	0	1028	1000	1040	932	0

Table 4: The red light total delay of all vehicles at the intersection/(s).

Intersection	2	3	4	5	6	Red light delay	Increased utility (%)
Shortest path algorithm	2.2307×10^8	2.6634×10^2	1.2521×10^8	2.2313×10^8	1.1258×10^2	5.7141×10^8	55.58
Contraction algorithm	5.7744×10^7	2.7525×10^7	6.6767×10^7	5.9933×10^7	4.1850×10^7	2.53819×10^8	

simulation by MATLAB2006a, and the simulation time is 15 minutes. The result of traffic assignment in each path is shown in Table 3.

In Table 3, the traffic assignment result has been given based on the contract model and the shortest path algorithm. On the one hand, the assignment results based on the shortest path algorithm are listed as follows: there is 2988 veh·h^{-1} traffic flow choosing path a_2 among the traffic demand volume of 3000 veh·h^{-1} of OD pair (1, 7); there is 3988 veh·h^{-1} traffic flow choosing path a_{10} among the traffic demand volume of 4000 veh·h^{-1} of OD pair (7, 1); there is 1016 veh·h^{-1} traffic flow choosing path a_7 among the traffic demand volume of 1020 veh·h^{-1} of OD pair (4, 7). On the other hand, the traffic assignment results based on the contract model algorithm are stated as follows: the traffic demands of OD pair (1, 7) distributing the traffic flow to paths a_2, a_3, a_4, and a_5 are 864 veh·h^{-1}, 732 veh·h^{-1}, 736 veh·h^{-1}, and 664 veh·h^{-1}, respectively; the traffic demands of OD pair (7, 1) distributing the traffic flow to paths a_{10}, a_{11}, a_{12}, and a_{13} are 1028 veh·h^{-1}, 1000 veh·h^{-1}, 1040 veh·h^{-1}, and 932 veh·h^{-1}, respectively; the traffic demands of OD pair (4, 7) distributing the traffic flow to paths a_7 and a_8 are 688 veh·h^{-1} and 332 veh·h^{-1}, respectively. Compared with the contract model algorithm, the traffic flow is overconcentrated on the shortest path algorithm and it does not respond to the human behavior factor in transportation route choice. For the contract model algorithm, according to the characteristic of traffic flow, every two adjacent intersections have a game, and the equilibrium price of the road network is obtained. It adjusts the intersection signal phase green time and meets the condition of the equilibrium price for the road network. Finally, it induces by an Intelligent Transportation Information System and considers behavior factors of the driver, which succeed in distributing the traffic flow to the road network equally. Therefore, the contract model algorithm promotes traffic to be distributed more evenly to the road network and makes a more rational distribution of traffic flow in the network and thus avoids the phenomenon of overconcentration of the traffic flow.

It is shown from Table 4 that the red light delays of intersections 3 and 6 for the traffic flow assigned by shortest path method are far below the one assigned by the contract model algorithm. Indeed, since OD traffic demand distribution is overconcentrated on certain paths by the shortest path method, there is little traffic flow passing intersections 3 and 6, and the red light delays of intersections 3 and 6 by using the shortest path algorithm are fewer correspondingly. From the total red light delay of all the intersections in the network, we find that the total red light delay of all the intersections in the network by using the contract model algorithm is 2.53819×10^8 s, which is significantly lower than the total delay of 5.7141×10^8 s by using the shortest path algorithm. Hence, it has improved the total utility of the network signal control by 55.58%. Thus, the contract model algorithm makes the signal control of each intersection coordinated and unified by agent technology. It is a full initiative of traffic management and control and thus improves greatly the system utility in the road network.

The contract model algorithm obtains the least price path by coordinating and unifying the control system of the road network. Furthermore, this combined with the positive inducement by the Intelligent Transportation System, and the uncertainty of driver's choosing the path, the system

utility in the network thus plays its role effectively. By the simulation example, we can find that the dynamic traffic game model based on contract considers fully the system optimization of the road network and also the utility maximization of the driver's choosing the path which achieves coordination between system optimization and user optimization and thus improves greatly the effectiveness of the system in the road network.

6. Conclusions

This paper combines the manager's initiatives with the driver's personal rational behavior closely by using agent technology and thus studies intensively the allocation of each intersection traffic right in the road networks. Based on the fact that the Intelligent Transportation Systems provides continually the real-time traffic information of road network, it is much easier for agents to achieve equilibrium strategy price. Next, the equilibrium strategy price will be given to the driver through the information system. Then, the driver takes the corresponding path selection strategy by the latest price information of the road network, which succeeds in making the traffic flow assignment more reasonable in the road network. The example shows that the network utility will be greatly increased by using a dynamic traffic game model based on the contract model. The model gives full consideration to the system optimality and takes into account the user optimality, which conforms to the actual situation.

The next step is based on the traffic conditions of the road network, to which agents (intersection) price control strategy makes the appropriate dynamic response, and pricing strategies influence each other between the various agents and so forth.

Data Availability

The data used to support the study are included within the article.

Conflicts of Interest

The authors declare that there are no conflicts of interest.

Acknowledgments

This research are supported by the National Natural Science Foundation of China (no. 52062038) and Jiangxi Province Educational Science Planning Project of China (no. 19YB099).

References

[1] H. Dong and Z. Dai, "A multi intersections signal coordinate control method based on game theory," in *Proceedings of the International Conference on Electronics, Communication and Control (ICECC)*, pp. 1232–1235, IEEE, Vienna, Austria, November 2016.

[2] W. W. Qi, H. Y. Wen, C. Y. Fu, and M. Song, "Game theory model of traffic participants within amber time at signalized intersection," *Computational Intelligence and Neuroscience*, vol. 2014, Article ID 756235, 7 pages, 2014.

[3] Z. Dai, H. Dong, and Q. Wang, "A multi-intersection coordinated control algorithm based on game theory and maximal flow," in *Proceedings of the 39th Annual Conference of the IEEE on Industrial Electronics Society (IECON)*, pp. 3258–3263, IEEE, Vienna, Austria, November 2013.

[4] M. G. H. Bell and C. Cassir, "Risk-averse user equilibrium traffic assignment: an application of game theory," *Transportation Research Part B: Methodological*, vol. 36, no. 8, pp. 671–681, 2002.

[5] J. Zhou, W. H. K. Lam, and B. G. Heydecker, "The generalized Nash equilibrium model for oligopolistic transit market with elastic demand," *Transportation Research Part B: Methodological*, vol. 39, no. 6, pp. 519–544, 2005.

[6] Z. C. Li and Z. K. Li, "Pricing model of parking facilities under different market regimes," *China Journal of Highway and Transport*, vol. 24, no. 4, pp. 80–86, 2011.

[7] T. Miyagi, G. Peque, and J. Fukumoto, "Adaptive learning algorithms for traffic games with naive users," *Procedia-Social and Behavioral Sciences*, vol. 80, no. 3, pp. 806–817, 2013.

[8] L. Zhen, "Tactical berth allocation under uncertainty," *European Journal of Operational Research*, vol. 247, no. 3, pp. 928–944, 2015.

[9] H. Ezzedine, A. Trabelsi, and C. Kolski, "Modeling of an interactive system with an agent-based architecture using Petri-nets, application of the method to the supervision of a transport system," *Mathematics and Computers in Simulation*, vol. 70, no. 5, pp. 358–376, 2006.

[10] H. Ezzedine, T. Bonte, C. Kolski, and C. Tahon, "Integration of traffic management and traveller information systems: basic principles and case study in intermodal transport system management," *International Journal of Computers, Communications and Control*, vol. 3, no. 3, pp. 281–294, 2008.

[11] X. M. Liu and X. Y. Wang, "Vehicle-cross action model in intersection without traffic light based on reduplicate game," *China Journal of Highway and Transport*, vol. 24, no. 4, pp. 94–100, 2011.

[12] L. Zhang, W. Du, and Q. Q. Guo, "Negotiation mechanism model of relationship between residential location and traffic system," *Journal of Traffic and Transportation Engineering*, vol. 10, no. 6, pp. 102–109, 2011.

[13] L. Zhen, "Modeling of yard congestion and optimization of yard template in container ports," *Transportation Research Part B: Methodological*, vol. 90, pp. 83–104, 2016.

[14] C. W. Yuan, X. X. Yu, H. P. Lu, and C. Bian, "Road network equilibrium traffic assignment method based on Stackelberg game," *China Journal of Highway and Transport*, vol. 22, no. 5, pp. 89–93, 2009.

[15] Y. F. Zhou, H. Z. Zhang, K. Zhang, and J. Wu, "Research on dynamic traffic information strategy model based on game-based coordination," *China Journal of Highway and Transport*, vol. 22, no. 1, pp. 89–96, 2009.

[16] B. Q. Zhang and J. Gao, "Research on critical state of sub-phase setting between right-turn motor vehicles and pedestrians for new urban zone intersections," *China Journal of Highway and Transport*, vol. 32, no. 2, pp. 99–104, 2010.

[17] M. G. H. Bell, "A game theory approach to measuring the performance reliability of transport networks," *Transportation Research Part B: Methodological*, vol. 34, no. 6, pp. 533–545, 2000.

[18] T. Miyagi and G. C. Peque, "Informed-user algorithms that converge to Nash equilibrium in traffic games," *Procedia-Social and Behavioral Sciences*, vol. 54, no. 4, pp. 438–449, 2012.

[19] K.-H. Nam Bui and J. J. Jung, "Cooperative game-theoretic approach to traffic flow optimization for multiple intersections," *Computers & Electrical Engineering*, vol. 71, pp. 1012–1024, 2018.

[20] D. H. Wang and B. J. Yan, *Traffic Flow Theory*, China Communications Press, Beijing, China, 2002.

[21] S. Markose, A. Alentorn, D. Koesrindartoto, P. Allen, P. Blythe, and S. Grosso, "A smart market for passenger road transport (SMPRT) congestion: an application of computational mechanism design," *Journal of Economic Dynamics and Control*, vol. 31, no. 6, pp. 2001–2032, 2007.

Hindawi
Scientific Programming
Volume 2021, Article ID 4924708, 10 pages
https://doi.org/10.1155/2021/4924708

Research Article

Hybrid Approach for Resource Allocation in Cloud Infrastructure Using Random Forest and Genetic Algorithm

Madhusudhan H S,[1] **Satish Kumar T**,[2] **S.M.F D Syed Mustapha**,[3] **Punit Gupta**,[4] **and Rajan Prasad Tripathi**[5]

[1]*Department of Computer Science and Engineering, NIE Institute of Technology, Mysuru, Karnataka, India*
[2]*Department of Computer Science and Engineering, BMS Institute of Technology and Management, Bengaluru, Karnataka, India*
[3]*College of Technological Innovation, Zayed University, Dubai, UAE*
[4]*Department of Computer and Communication Engineering, Manipal University Jaipur, Jaipur, India*
[5]*Department of Electronics and Communication, Amity University Tashkent, Tashkent, Uzbekistan*

Correspondence should be addressed to Punit Gupta; punit.gupta@jaipur.manipal.edu

Received 18 April 2021; Revised 2 September 2021; Accepted 29 September 2021; Published 16 October 2021

Academic Editor: Marco Aldinucci

Copyright © 2021 Madhusudhan H S et al. This is an open access article distributed under the Creative Commons Attribution License, which permits unrestricted use, distribution, and reproduction in any medium, provided the original work is properly cited.

In cloud computing, the virtualization technique is a significant technology to optimize the power consumption of the cloud data center. In this generation, most of the services are moving to the cloud resulting in increased load on data centers. As a result, the size of the data center grows and hence there is more energy consumption. To resolve this issue, an efficient optimization algorithm is required for resource allocation. In this work, a hybrid approach for virtual machine allocation based on genetic algorithm (GA) and the random forest (RF) is proposed which belongs to a class of supervised machine learning techniques. The aim of the work is to minimize power consumption while maintaining better load balance among available resources and maximizing resource utilization. The proposed model used a genetic algorithm to generate a training dataset for the random forest model and further get a trained model. The real-time workload traces from PlanetLab are used to evaluate the approach. The results showed that the proposed GA-RF model improves energy consumption, execution time, and resource utilization of the data center and hosts as compared to the existing models. The work used power consumption, execution time, resource utilization, average start time, and average finish time as performance metrics.

1. Introduction

Cloud computing is a form of distributed computing that brings in utility models to deliver measurable and scalable resources remotely. Cloud is also a materialistic implementation of parallel computing, grid computing, and distributed computing [1]. The cloud environment offers a shared pool of resources to users as a service on an "on-demand" approach [2]. Effective computing capability and enormous storage capacity allow the users to access services of the cloud anytime and anywhere. A cloud data center comprises IT resources like databases, servers, communication devices, network, and software systems. More user's demand for cloud resources makes the cloud providers scale up the number of servers or required hardware. As a result, the creation of more physical nodes will lead to an increase in power consumption by the data center. Data centers consume 2% of today's worldwide electricity. It is expected to reach 8% by 2030. There are three power consumers in a data center, namely cooling systems, data center networks, and servers. 10 to 25% of power is consumed by the network, cooling systems consume 15 to 30% power, and servers will consume power around 40 to 55% [3].

IaaS (Infrastructure as a Service) offers computing resources like RAM, CPU, Network, and Storage as a service and their use is likely abided by SLA (Service Level Agreement). Resource utilization is also having an impact on energy consumption. Low resource utilization is one of the

reasons for the energy inadequacy of the data center [4]. If the CPU utilization is as low as 10%, that means the workload is less and energy consumption is above 50% of the peak power. The virtualization techniques in IaaS play a vital role here, which efficiently improve resource or cloud utilization [5]. Virtualization offers resource sharing which allows virtual machines (VMs) to execute physical machines (PMs) to process user requests. Three possible operations performed using virtualization are VM isolation, VM migration, and VM consolidation. VM migration technique shifts the running virtual machines from a physical machine to another. In the VM consolidation process, virtual machines running on different hosts will leave that host and gather on fewer ones to reduce energy wastage by switching off the initial running host or moving it to hibernate mode [6]. Virtual Machine Placement (VMP) is a technique of executing virtual machines on suitable physical machines. To enhance power efficiency and maximize resource utilization, an efficient VMP technique is very much necessary [7]. The VMP problem is an NP-hard optimization problem [8].

In this work, efficient hybrid VMP technique is using the genetic algorithm (GA) and random forest (RF) algorithm. Our objective is to reduce the energy consumption of the data center while maintaining the load across several physical machines. Maximizing resource utilization of the physical machines is also taken as one of the key parameters for the evaluation of the proposed method. Cloud demands the least waiting time and least request completion time; therefore, minimizing execution time, average start time, and average finish time is the objective of this work. Another objective of the proposed model is to reduce the time to find the optimal solution which takes maximum time iterative metaheuristic algorithms like GA, ACO, PSO, and many more. The model is aimed to train the machine learning model with the best optimal solution and then, in the next iteration, the trained model can be used to predict the optimal solution in a constant time removing the time taken by evolutions in search of the global best solution.

One of the metaheuristic techniques used to find a globally optimal solution is the genetic algorithm. Firstly, the GA focuses on generating an optimized schedule for resource allocation which acts as training dataset that contains the mapping of virtual machines to the physical machines. Next, the dataset derived from GA is used to train the random forest algorithm and then it performs the classification, i.e., allocation of virtual machines to the physical machines. Classification accuracy of the RF is tested using the subset of the dataset obtained from the GA.

The random forest is a supervised machine learning technique and it can perform the placement of virtual machines on the best physical machines with good accuracy as it reduces overfitting in decision trees. Figure 1 represents the system model. It comprises several physical machines within a data center. Each physical machine can execute many virtual machines. The Virtual Machine Monitor (VMM), also known as Hypervisor, is a software program that facilitates the creation, managing, and monitoring of virtual machines. It also manages a virtualized environment on top of physical machines. When a request for VM execution is received by the data center manager, firstly it gathers the status information from all available physical machines and delivers it to the VM scheduler. The VM scheduler is developed using GA-RF technique. In the next step, VM scheduler analyzes status information and then allocates virtual machines to apt physical machines.

The rest of the work is organized as follows: Section 2 brings in a literature survey with existing models and their comparison. The proposed method is discussed in Section 3, Section 4 gives an evaluation of the proposed method with experimental setup and results, and, lastly, conclusion and future work are given in Section 5.

2. Literature Review

This section brings in some of the work done by researchers. Table 1 depicts different approaches in the field of virtual machine placement and the parameters they have considered for the performance evaluation. Authors in [9] propose VMP technique using a combination of genetic algorithm and Tabu search algorithm. The authors have focused on achieving energy efficiency with an increase in load balance. They have also taken execution time for comparison of different algorithms in their work. Abohamama et al. [10] presented a VMP algorithm using an improved permutation-based genetic algorithm to improve energy consumption rate by reducing the number of active hosts that run VMs. The proposed method is compared with the Flow Shop Scheduling Problem and Traveling Salesman Problem. Yao et al. [11] introduced a VM placement procedure based on Weighted PageRank. They focused on minimizing the number of active physical machines and also increased resource utilization of all hosts in the data centers. To avoid the proposed method falling in local optimum solution, the impact of nonplaced virtual machines is considered. During the process of selecting a physical machine for VM, Weighted PageRank covers unplaced VMs of several types and the algorithm measures the possibility of a physical machine making complete use of resources under different conditions.

Authors in [12] proposed a stochastic VMP approach to increase energy efficiency and resource utilization of the data center. Here resource requirements are modeled as random variables instead of taking deterministic values to denote resource requirements. Due to variation in the resource requirements, the proposed optimization model is subject to a probabilistic restriction on resource overflow probability on every physical machine [13]. VMP in the heterogeneous data center using a Binary gravitational search algorithm (BGSA) was proposed. The aim of this work is to decrease energy consumption. The proposed method uses agents as objects and their mass is used to measure the performance. The object having a higher mass has a better solution [14]. Authors have proposed an evolutionary approach to increase energy efficiency. Here the proposed approach incorporates the reserved virtual machines also. Both simulation and real-time cloud environments were used to evaluate the performance of different techniques.

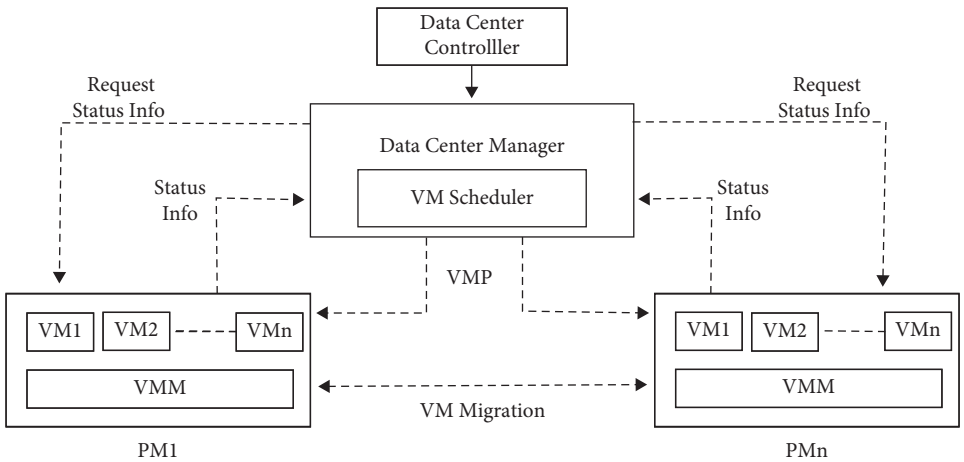

Figure 1: System model in cloud infrastructure for VM placement.

Table 1: Classification of different approaches in existing literature.

Reference	Technique/algorithm used	Energy consumption	Resource utilization	Load balance	SLA	No. of hosts shutdown/no. of active PM	Execution time/ elapsed/ simulation time
[9]	Metaheuristic (genetic and tabu search algorithm)	✓		✓			✓
[10]	Optimization (permutation-based genetic algorithm and multidimensional resource-aware best fit)	✓	✓				✓
[11]	Heuristic/Weighted PageRank		✓			✓	
[12]	Metaheuristic/stochastic VM placement algorithm	✓					
[13]	Heuristic/binary gravitational search algorithm	✓					
[14]	Optimization/evolutionary approach	✓					✓
[15]	Machine learning/reinforcement learning		✓	✓		✓	✓
[16]	Machine learning and metaheuristic/ (Naive Bayesian Classifier and Random Key Cuckoo Search)	✓			✓	✓	
[17]	Heuristic/HeporCloud	✓					✓
[18]	Heuristic	✓					✓
[19]	Optimization/game theory	✓					✓

Consolidation of VMs on lesser hosts resulted in a decrease in energy consumption.

Ghasemi et al. [15] have designed a reinforcement learning-based approach to address VM placement. The authors focused on load balancing while maximizing resource utilization and a number of hosts shutdown. The proposed method chooses an action from available acceptable actions and executes it on a cloud environment. It receives a reinforcement signal conforming to the suitability of the virtual machine placement solution by using that action [16]. The authors proposed a hybrid approach based on Naive Bayesian Classifier and Random Key Cuckoo Search for VM consolidation problem to minimize energy consumption. Here Naïve Bayes is used for detecting the future state of the hosts which is necessary to perform virtual machine placement in an efficient manner. Khan et al. [17] presented HeporCloud, a framework for a hybrid cloud platform that includes an integrated, workload-aware single resource scheduler and orchestrator. The proposed resource management may assign and forecast the placement and transfer of effective workloads. The empirical study shows that HeporCloud can efficiently plan and consolidate various types of workloads in terms of energy, performance, and cost. An extended version of the cloudsim simulator was proposed [20] to improve the accuracy and precision of the cloudsim. The evaluation of the extended version proved that it performed better in terms of energy, the performance of resource allocation, and even consolidation in heterogeneous data centers. Authors in [18] presented a consolidation approach that prioritizes the most efficient migration, which could be a VM, a container, or a specific application running within a container. Here authors modeled the

heterogeneity of cloud applications and resources and demonstrated how the consolidation of heterogeneous apps, containers, and virtual machines affects heterogeneous data center performance and energy efficiency. In [19], game-theoretic resource management techniques for multiaccess edge computing were developed. Google's workload traces were used to evaluate the proposed work. The goal is to develop a resource management technique that is efficient in terms of energy, performance, and cost. [21] Ilias Mavridis and Helen Karatza proposed an approach to combine virtual machines and containers to enhance the isolation and extended functionality of the cloud. The authors highlighted the benefits of running containers on virtual machines, as well as an investigation of how different virtualization approaches and configurations influence the method's performance. Docker containers were made to run on KVM and XEN virtual machines, and Linux containers were run on Windows Server to see how they performed. By running multiple benchmarks and installing real-world apps as use cases, authors were able to estimate the performance cost caused by the additional virtualization layer of virtual machines. Lastly, the authors investigated several operating systems designed to host containers, as well as techniques for storing persistent data, to see how isolation is implemented on virtual machines and containers.

3. Proposed Method

The proposed virtual machine placement technique in this work is a hybrid model using a genetic algorithm and random forest technique. A genetic algorithm is an optimization technique and here it will generate the dataset required for training the random forest algorithm. The training dataset comprises allocation or mapping of virtual machines to physical machines.

3.1. Genetic Algorithm. A genetic algorithm (GA) is a metaheuristic technique that generates a global optima solution. Here we use the genetic algorithm to generate a mapping of VM to available physical machines.

The following steps are incorporated in our work:

(1) Initialize the population.

The population is initially generated in a random manner and all the virtual machines VMi ($i = 1$ to n) are mapped to physical machines PM_j ($j = 1$ to m). Figure 2 shows the sample of the initial population.

(2) Fitness function: fitness values of the host is derived as

$$\text{Fitness}(i) = \beta * \text{Power Efficiency}, \quad (1)$$

where β is the random constant. The individuals having higher fitness values are used for the reproduction process.

(3) Selection: the fittest individuals are selected from the population using the tournament selection method. Tournament size is taken as N (individuals) and they are chosen randomly from the population. The winner of the tournament is taken for crossover operation.

VM_2	VM_1	VM_3	VM_5	VM_7	VM_4	VM_6
PM_3	PM_7	PM_1	PM_2	PM_4	PM_6	PM_5

Figure 2: Initial population generation in a random manner.

(4) Crossover: in this work, a 2-point crossover is used to generate new individuals/offspring from the selected best individuals. Crossovers like single-point crossover, multipoint, and uniform crossover are also available. To improve the diversity, a newly generated individual is added back to the population. An example of a 2-point crossover is given in Figure 3.

(5) Mutation: mutation operation can be accomplished using swap, move, move and swap, and rebalancing; we have used swap operation to mutate individuals. Two points are identified and their values are swapped to create a new individual. Here swap operation will swap the physical machine allocated to the virtual machine as shown in Figure 4.

The pseudocode of the proposed genetic algorithm is shown in Figure 5. We have used 100 evolutions to get better results. The final result will have a mapping of virtual machines to physical machines.

3.2. Random Forest Classifier. Random forest is one of the supervised machine learning techniques used for both regression and classification. It is one of the flexible and easy-to-use algorithms. A random forest is made up of trees, and the more trees there are, the more resilient the random forest is. The random forest creates each decision tree by first selecting at random, at each node, a small set of features to split on and, secondly, by calculating the best split based on these features in the training set. Finally, it gets a prediction from each tree and chooses the best solution either by means of 'majority voting' or 'performance voting' as expressed in Figure 6.

Module 1 (dataset creation): the dataset is created using the genetic algorithm. The dataset consists of mapping of VM allocation to the best possible physical machine. The procedure to create the dataset using GA is discussed in the previous Section 3.1. Here, the dataset is divided into 2 sets. The first set consists of 80% of the dataset which is used as the training dataset to train the model and the remaining 20% of the dataset is used for testing.

Module 2 (training): consider a training dataset $T = \{(x_1, y_1), \ldots (x_N, y_N)\}$ consist of N observations from the random vector (x, y). Vector $x = (x^1, \ldots, x^P)$ contains predictors or independent variables and $y \in C$ where C is the class label. Using this training set, the developed random forest will be an ensemble of B trees$\{(t_1(x), \ldots, t_b(x))\}$. The ensemble results in B outputs $\{y_1 = t_1(x), \ldots, y_b = t_b(x)\}$, where y_b, $b = \{1, 2, \ldots, B\}$ is

Parent 1: 2 point crossover

VM_2	VM_1	VM_3	VM_5	VM_7	VM_4	VM_6
PM_3	PM_7	PM_1	PM_2	PM_4	PM_6	PM_5

Parent 2:

VM_2	VM_1	VM_3	VM_5	VM_7	VM_4	VM_6
PM_4	PM_5	PM_2	PM_6	PM_1	PM_3	PM_7

(a)

Child (Offspring):

VM_2	VM_1	VM_3	VM_5	VM_7	VM_4	VM_6
PM_3	PM_7	PM_2	PM_6	PM_1	PM_6	PM_5

VM_2	VM_1	VM_3	VM_5	VM_7	VM_4	VM_6
PM_3	PM_7	PM_1	PM_2	PM_4	PM_6	PM_5

(b)

Figure 3: Crossover operation in the proposed model.

Before Mutation:

VM_2	VM_1	VM_3	VM_5	VM_7	VM_4	VM_6
PM_3	PM_7	PM_2	PM_6	PM_1	PM_6	PM_5

After Mutation:

VM_2	VM_1	VM_3	VM_5	VM_7	VM_4	VM_6
PM_3	PM_7	PM_6	PM_6	PM_1	PM_2	PM_5

Figure 4: Swap operation in mutation process of the proposed model.

```
Input : population_size, mutation_rate, generation_size, virtual machine (VM) list, physical machine (host) list
Output: New population (Assignment of VM to PM)
begin
While(stopping criteria(generation_size)) do
  new_population←select fittest individuals
  for i←1 to new_population_size
      parent1, parent2←select two best individuals
      child←crossover(parent1, parent2)
      add child to new population
    newchild←mutate (child, mutation_rate)
  end for
end while
end
```

Figure 5: Pseudocode of genetic algorithm.

```
Input : Training Data set
Output: Classification tree
for b=1 to B
  Draw a Sample Z of size N from the training data.
  Derive a random-forest tree T_b to the data, by recursively repeating the following steps for each
  terminal nod of the tree, until the either minimum node size n_min is reached or given depth is reached
      i. Select m variables at random from the p variables.
      ii. Pick the best variable/split-point among the m.
      iii. Split the node into two daughter nodes.
  Output the ensemble of trees {T_b}_1^B
  Classification: Let Ĉ_b(x) be the class prediction for the bth random forest tree.
  Then Ĉ_rf^B(x) = majority vote {Ĉ_b(x)}_1^B
end for
```

Figure 6: Pseudocode of random forest algorithm for the proposed model.

the prediction for the classified data object by the Bth tree. All the trees outputs are combined to produce the final class y which receives the maximum votes by all the trees.

3.2.1. Tree Construction. The training dataset is used in tree building and it follows a top-down approach. We use information gain to identify the attribute that best splits the given training set. "Best" is measured using information gain:

$$\Delta E = -\sum_i \frac{|D_i|}{|D|} E(D_i). \tag{2}$$

It is produced by partitioning the set D of examples into two subsets D_i according to the given attribute. Here E(d) is the entropy $-\sum_{i=1}^{N} q_i \log_2(q_i)$ with q_j as the proportion of examples in d belonging to class i and |.| is the size of the set. The process of selecting the attribute is repeated for each nonterminal node; the process is stopped when the node receives less examples or when it reaches the given depth.

Module 3 (testing): once the training of the model using the training set is over, prediction is performed on the test set. After training, the accuracy is checked using actual values and predicted values. If the obtained accuracy is less than the desired value, some tuning will be done and again the model is trained and tested. This repeats until the desired accuracy is achieved.

3.2.2. Flow Diagram. Figure 7 depicts the block diagram of the proposed hybrid technique. The genetic algorithm reads the PlanetLab dataset, which is a real-time dataset. The genetic algorithm goes through all the processes prescribed in Section 3.1 to generate the dataset having mapping of virtual machines to physical machines. This dataset is used as the dataset for a random forest classifier. Random forest classifier splits the dataset into training and testing datasets. Using training data, RF generates a specified number of random trees for each subsamples. The test dataset is used to test the classification process. Finally, majority voting decides the final class label (output value). Here the output value consists of a physical host number which is used to execute the required virtual machines on it.

Once the virtual machines are placed on the physical machines, it starts the execution. After some time, a physical machine may get more VMs to execute, in this situation, the physical machine which gets overloaded. We have used a VM migration technique to handle this kind of scenario. When a PM gets overloaded, some of the virtual machines will be selected and migrated to other PMs having less load, thereby maintaining load balance across all the physical machines in the data center. Interquartile range (IQR) is used to detect overloaded physical machines in the data center, which is one of the available overload detection methods [22]. Next, maximum correlation policy is used to select the VMs to be migrated from the overloaded PM. It selects the VMs having the maximum correlation of the CPU utilization with other VMs.

4. Simulation Results

Experimental setup, performance metrics, and experimental results are discussed in this section.

4.1. Experimental Setup. We have used the CloudSim 3.0 toolkit simulator to evaluate the proposed algorithm. Cloudsim provides different VM provisioning techniques and virtualized resources. To carry out the experiment, we have taken real workload traces from PlanetLab. PlanetLab is part of the CoMon project, which consists of CPU utilization from more than 1000 virtual machines running on various hosts in more than 500 locations around the world. In our experimental setup, we used 4 different types of virtual machines, Micro, Small, Medium, and Extra-Large instances. 800 heterogeneous hosts are deployed which belong to HP ProLiant G4 and HP ProLiant G5 category. Characteristics of these servers are shown in Table 2. For simulation, 500 hosts and VM vary from 500 to 650 with data center configuration as shown in Table 2. PlanetLab dataset is a log file of a real word data center with incoming traffic, task size, size of VM requested by task with VM configuration like RAM, number processor, and MIPS count.

4.2. Performance Metrics and Results. The following metrics are used to evaluate the proposed algorithm and other algorithms.

4.2.1. Energy Consumption. It denotes the total energy consumed by all the physical machines (PMs) in the data center. PMs energy consumption is calculated according to the linear cubic power consumption model. In this power model, the power consumption of the physical host grows linearly with an increase in the CPU utilization.

Let us consider the following parameters for the power model:

(i) $P_k^{\max}$: maximum power consumed when the host k is completely utilized

(ii) P_k^{idle}: idle power value of the host k

(iii) U_k : current CPU utilization host k

(iv) T: total number of hosts in the data center

The power consumption of host P_k can be expressed as

$$P_k = P_k^{\text{idle}} + \left(P_k^{\max} - P_k^{\text{idle}}\right) * U_k^3. \tag{3}$$

Our goal is to minimize power consumption of the data center; then, we aim to minimize

$$\sum_{k=1}^{T} P_k = \sum_{k=1}^{T} \left[P_k^{\text{idle}} + \left(P_k^{\max} - P_k^{\text{idle}}\right) * U_k^3\right]. \tag{4}$$

Figure 8 shows the energy consumption of different algorithms. The energy consumption of our proposed algorithm GA-Random Forest (RF) has declined on an average by 17%, 31%, and 39% compared to default GA (genetic algorithm), ACO (ant colony optimization), and

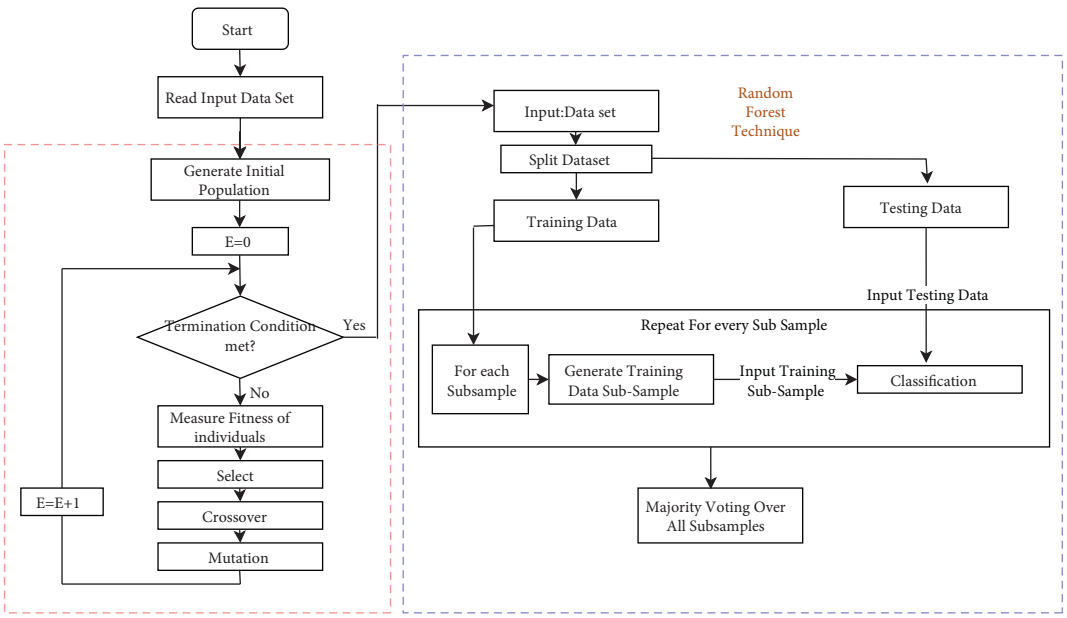

Figure 7: Block diagram of the hybrid proposed approach using GA and random forest.

Table 2: Characteristics of servers.

Machine type	Description
HP G4	1860 MIPS, 4 GB RAM, 2 GB network bandwidth 1.5 GB storage
HP G5	2660 MIPS, 4 GB RAM, 2 GB network bandwidth, 1.5 GB storage

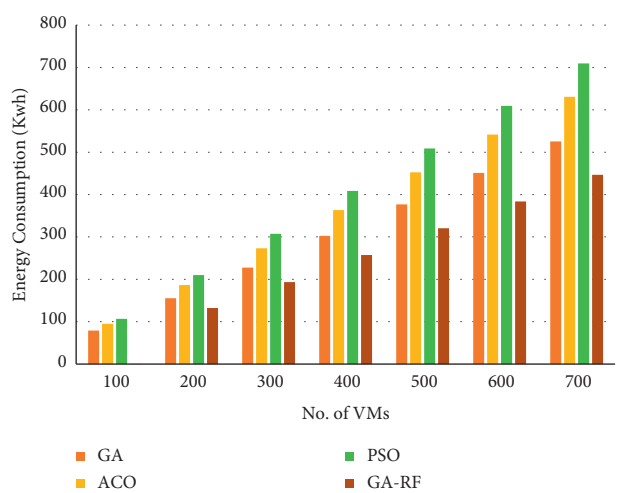

Figure 8: Comparative analysis of energy consumption of the proposed and existing approaches.

PSO (particle swarm optimization), respectively, for PlanetLab "20110409/planetlab-1_amst_nodes_planet-lab_org_Arizona_beta and 20110409/pl1_rcc_uottawa_ca_Google _ highground.

4.2.2. Execution Time. Executing all the user requests in lesser time is indeed an important factor from the cloud provider perspective. So, execution time is taken as one of the key performance factors to evaluate the algorithms.

Let $T = \{T_1, T_2, \ldots T_N\}$ be the set of tasks. $|T|$ represents the total number of tasks in the set. $VM = \{VM_1, VM_2, .., VM_M\}$ denotes a set of virtual machines. $T_E(i, j)$ represents the execution time of task Ti on virtual machine j. It is expressed as

$$T_E(i, j) = \frac{t_l(i, j)}{VM_c}, \tag{5}$$

where $t_l(i, j)$ represents the time required to execute the instruction of length l on virtual machine j and VM_c denotes

the computational ability of virtual machine j which can be expressed as

$$VM_c = VM_{\text{pesNum}b} * VM_{\text{MIPS}}. \quad (6)$$

So, task i runtime on virtual machine j can be represented as

$$\text{Task Run Time}(i, j) = T_E(i, j). \quad (7)$$

The completion time of virtual machine j is the sum of the task run time of all tasks on that virtual machine.

$$CT\_VM_j = \sum_{i=1}^{N} \text{Task Run Time}(i, j). \quad (8)$$

Total execution time represents the time required to execute all the virtual machines thereby completing the execution of all the user requests. It can be expressed as

$$\text{execution time} = \sum_{j=1}^{M} CT\_VM_j. \quad (9)$$

As shown in Figure 9, the average execution time of GA-RF is less by 15%, 29%, and 37% compared to GA, ACO, and PSO, respectively; i.e., GA-RF has a faster execution time.

4.2.3. Resource Utilization. To process a user's request based on the resource requirement by the user, the Cloud data center creates various types of VMs. VMP technique aims to place a virtual machine on a suitable physical machine to improve resource utilization. The resource type we have considered is CPU. Suppose there are N PMs and M VMs. Let $PM = \{PM_1, PM_2, \ldots, PM_N\}$ denote the set of PMs, where $PM_i \in PM$. PMC_i represents the CPU capacity of PM_i. Let $VM = \{VM_1, VM_2, .., VM_M\}$ denote a set of virtual machines, where $VM_j \in VM$. VMC_j represents the CPU requirement of VM_j.

Let P_{ij} denote whether VM_j is placed on PM_i. If VM_j is placed on PM_i, then $P_{ij} = 1$ or else if VM_j is not placed on PM_i, then $P_{ij} = 0$. Equation (9) represents the requirements of all the virtual machines placed on a physical machine that cannot exceed the resource capacity of the physical machine.

$$\sum_{j=1}^{M} VMC_j \cdot P_{ij} \leq PMC_i \forall PM_i \in PM. \quad (10)$$

Once the virtual machine types are determined, the resource utilization of all the physical machines needs to be maximized. The CPU utilization of physical machine PMi is expressed as

$$UCPU_i = \frac{\sum_{j=1}^{M} VMC_j \cdot P_{ij}}{PMC_i}. \quad (11)$$

Maximizing the CPU utilization of all the physical machines can be expressed as

$$\text{maximize} \sum_{i=1}^{N} UCPU_i. \quad (12)$$

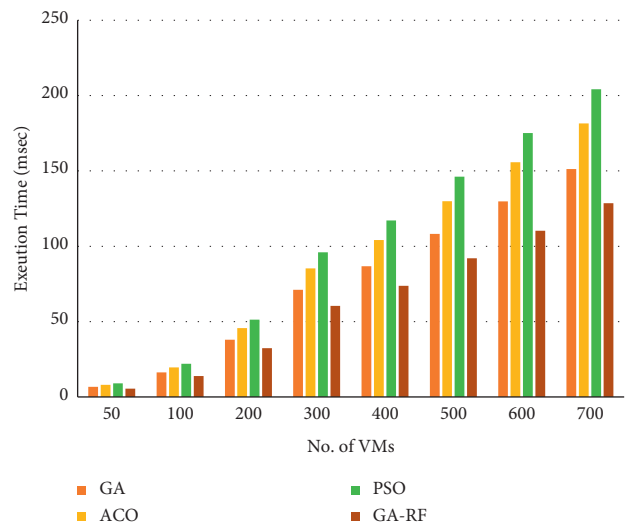

Figure 9: A comparative study of execution time for the proposed and existing approaches.

Figure 10: Comparative analysis of CPU Utilization using proposed and existing approaches.

Figure 10 shows the average CPU utilization of all the active PMs. Average CPU utilization of GA with the random forest is higher by 6%, 10%, and 11% compared to GA, ACO, and PSO, respectively.

4.2.4. Average Start Time and Finish Time. Delivering high performance to the cloud user is becoming an important criterion for the cloud provider. In this regard, parameters like start time and finish time of the user request/task can be considered as major factors. Figure 11 and 12 show the average start time and finish time of different algorithms. As a result, GA-RF can finish the user's requests/tasks in less time compared to other existing algorithms.

In cloud computing, time complexity plays an important role in studying the performance of the algorithm. There exist various studies which show the comparative analysis of the complexity of GA, ACO, and PSO [23,24]. The study shows that GA finds the best global optimal solution at the

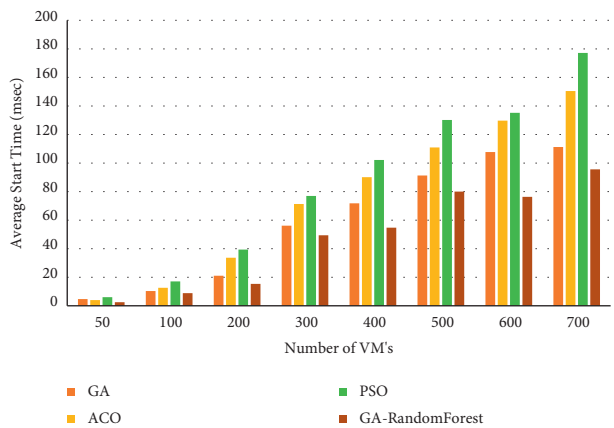

Figure 11: Comparison of average start time (msec) of GA-RF and existing approaches.

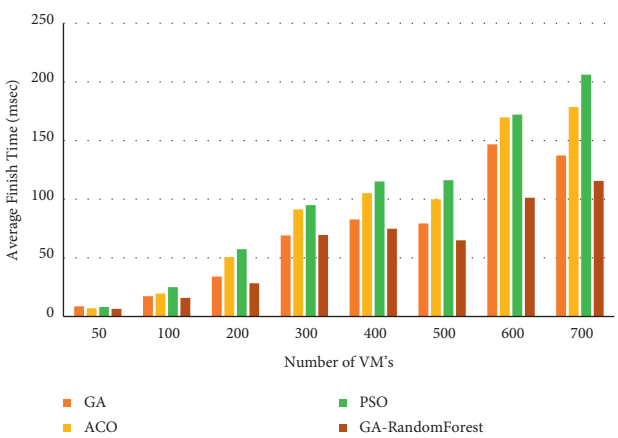

Figure 12: Comparison of average finish time (msec) of GA-RF and existing approaches.

cost of high searching time but finds a solution better than ACO and PSO. In order to reduce the searching time of GA, the optimal solution is trained to a random forest model for training and further prediction which gives an optimal solution in constant time. The cost overhead is only one time overhead, that is optimal solution generation using GA and training the model.

5. Conclusion

With the development of virtualization technology, designing a multiobjective virtual machine placement technique has become a hot research topic. Our work is two-fold. Firstly, a hybrid approach for VMP using a genetic algorithm and random forest algorithm is proposed to reduce the search time to find the best optimal solution. The genetic algorithm is used to find an optimal solution as a dataset that contains the mapping of the virtual machines to the physical machines. This dataset is used to train the random forest algorithm to place the virtual machines on apt physical machines and also the placement accuracy of RF is evaluated with the test data. Secondly, the trained model is used for load balancing through migrating the virtual machines from overloaded physical machines to underloaded physical machines. This is accomplished using IQR technique to detect overloaded physical machines and VMs to be migrated are selected using the maximum correlation policy. The result shows that the proposed model provides an energy-efficient placement scheme by reducing power consumption, execution time, average start time, and finish time as compared to the existing approaches. In the future, the model can be tested with various machine learning and deep learning approaches for better solutions and performance study.

Data Availability

The dataset for simulation is supported by parallel workload.com for real-time analysis.

Conflicts of Interest

The authors have no conflicts of interest to declare

Authors' Contributions

Madhusudhan H. S., Satish Kumar T., and Punit Gupta developed the theory and proposed model. Dr. S.M.F. D. Syed Mustapha and Rajan Prasad Tripathi worked on data preparation, ML model for the dataset, and verified the analytical methods. All authors discussed the results and contributed to the final manuscript. All authors confirm sole responsibility for the following: study conception and design, data collection, analysis and interpretation of results, and manuscript preparation. All coauthors have seen and agreed with the contents of the manuscript.

References

[1] I. Foster, Y. Zhao, I. Raicu, and S. Lu, "Cloud computing and grid computing 360-degree compared," in *Proceedings of the Grid Comput. Environ. Workshop*, pp. 1–10, Austin, TX, USA, November 2008.

[2] R. Buyya, A. Beloglazov, and J. Abawajy, "Energy-ef_cient management of data center resources for cloud computing: a vision, architectural elements, and open challenges," *Eprint Arxiv*, vol. 12, no. 4, pp. 6–17, 2010.

[3] K. Zheng, X. Wang, L. Li, and X. Wang, "Joint power optimization of data center network and servers with correlation analysis," in *Proceedings of the IEEE INFOCOM 2014 - IEEE Conference on Computer Communications*, pp. 2598–2606, Toronto, ON, Canada, May 2014.

[4] A. Beloglazov, R. Buyya, Y. C. Lee, and A. Zomaya, "A taxonomy and survey of energy-efficient data centers and cloud computing systems," *Advances in Computers*, vol. 82, pp. 47–111, 2011.

[5] V. Petrucci, O. Loques, and D. Mossé, "March. A framework for dynamic adaptation of power-aware server clusters," in *Proceedings of the 2009 ACM symposium on Applied Computing*, pp. 1034–1039, Honolulu, Hawaii, USA, March 2009.

[6] M. Masdari, S. S. Nabavi, and V. Ahmadi, "An overview of virtual machine placement schemes in cloud computing," *Journal of Network and Computer Applications*, vol. 66, pp. 106–127, 2016.

[7] G. Hadi and M. Pedram, "Energy-efficient virtual machine replication and placement in a cloud computing system," in *Proceedings of the 2012 IEEE Fifth International Conference on Cloud Computing*, pp. 750–757, Honolulu, HI, USA, June 2012.

[8] J. D. Ullman, "NP-complete scheduling problems," *Journal of Computer and System Sciences*, vol. 10, no. 3, pp. 384–393, 1975.

[9] D.-M. Zhao, J.-T. Zhou, and K. Li, "An energy-aware algorithm for virtual machine placement in cloud computing," *IEEE Access*, vol. 7, pp. 55659–55668, 2019.

[10] A. S. Abohamama and E. Hamouda, "A hybrid energy-Aware virtual machine placement algorithm for cloud environments," *Expert Systems with Applications*, vol. 150, Article ID 113306, 2020.

[11] W. Yao, Y. Shen, and D. Wang, "A weighted PageRank-based algorithm for virtual machine placement in cloud computing," *IEEE Access*, vol. 7, Article ID 176369, 2019.

[12] J. Zhou, Y. Zhang, L. Sun, S. Zhuang, C. Tang, and J. Sun, "Stochastic virtual machine placement for cloud data centers under resource requirement variations," *IEEE Access*, vol. 7, Article ID 174412, 2019.

[13] F. Abdessamia, W.-Z. Zhang, and Y.-C. Tian, "Energy-efficiency virtual machine placement based on binary gravitational search algorithm," *Cluster Computing*, vol. 23, no. 3, pp. 1577–1588, 2020.

[14] X. Zhang, T. Wu, M. Chen et al., "Energy-aware virtual machine allocation for cloud with resource reservation," *Journal of Systems and Software*, vol. 147, pp. 147–161, 2019.

[15] A. Ghasemi and A. Toroghi Haghighat, "A multi-objective load balancing algorithm for virtual machine placement in cloud data centers based on machine learning," *Computing*, vol. 102, pp. 2049–2072, 2020.

[16] Y. Moaly and B. A. Youssef, "Hybrid algorithm naive bayesian classifier and random key Cuckoo search for virtual machine consolidation problem," *International Journal of Advanced Computer Science and Applications*, vol. 11, no. 1, 2020.

[17] A. A. Khan, M. Zakarya, I. U. Rahman, R. Khan, and R. Buyya, "HeporCloud: an energy and performance efficient resource orchestrator for hybrid heterogeneous cloud computing environments," *Journal of Network and Computer Applications*, vol. 173, Article ID 102869, 2021.

[18] A. A. Khan, M. Zakarya, R. Khan, I. U. Rahman, and M. Khan, "An energy, performance efficient resource consolidation scheme for heterogeneous cloud datacenters," *Journal of Network and Computer Applications*, vol. 150, Article ID 102497, 2020.

[19] M. Zakarya, G. Lee, H. Ali et al., "Epcaware: a game-based, energy, performance and cost efficient resource management technique for multi-access edge computing," *IEEE Transactions on Services Computing*1 page, 2020.

[20] M. Zakarya and L. Gillam, "Modelling resource heterogeneities in cloud simulations and quantifying their accuracy," *Simulation Modelling Practice and Theory*, vol. 94, pp. 43–65, 2019.

[21] I. Mavridis and H. Karatza, "Combining containers and virtual machines to enhance isolation and extend functionality on cloud computing," *Future Generation Computer Systems*, vol. 94, pp. 674–696, 2019.

[22] A. Beloglazov and R. Buyya, "Optimal online deterministic algorithms and adaptive heuristics for energy and performance efficient dynamic consolidation of virtual machines in cloud data centers," *Concurrency and Computation: Practice and Experience*, vol. 24, pp. 1397–1420, 2012.

[23] X. Zhu, N. Li, and Y. Pan, "Optimization performance comparison of three different group intelligence algorithms on a SVM for hyperspectral imagery classification," *Remote Sensing*, vol. 11, no. 6, p. 734, 2019.

[24] M. K. Patel, M. R. Kabat, and C. R. Tripathy, "A hybrid ACO/PSO based algorithm for QoS multicast routing problem," *Ain Shams Engineering Journal*, vol. 5, no. 1, pp. 113–120, 2014.

Hindawi
Scientific Programming
Volume 2021, Article ID 9168504, 11 pages
https://doi.org/10.1155/2021/9168504

Research Article

Job Value and Organizational Socialization of the Youth of Guangdong-Hong Kong-Macao Greater Bay Area: The Mediation of Career Exploration?

Zhihua Lian [1] **and Nana Feng** [2]

[1] *Xiamen University, Tan Kah Kee College, Zhangzhou 363105, China*
[2] *Nanning Normal University, School of Logistics Management and Engineering, Nanning 530299, China*

Correspondence should be addressed to Nana Feng; violet3676@163.com

Received 22 April 2021; Accepted 23 August 2021; Published 13 September 2021

Academic Editor: Xiaobo Qu

Copyright © 2021 Zhihua Lian and Nana Feng. This is an open access article distributed under the Creative Commons Attribution License, which permits unrestricted use, distribution, and reproduction in any medium, provided the original work is properly cited.

This paper took the social exchange and social cognitive perspectives to examine the effects between job values and organizational socialization and how to play a mediation in career exploration and moderating effect in demographic characteristics. The research collected 700 valid samples of the youth of Guangdong-Hong Kong-Macao Greater Bay Area for statistical analysis and then subjected them to job value scale, career exploration, and organizational socialization scale. With structural equation model and correlation analysis, it verified that the proposed scale had demonstrated acceptable reliability and validity, a theoretical model of a good overall fit. In the final part, this paper used hierarchical regression analysis and path analysis. The results indicated that career exploration plays a mediation role between job value and organizational socialization, demographic characteristics are moderating effect between job value and career exploration, and demographic characteristics make a moderating effect between career exploration and organizational socialization, but demographic characteristics are not moderated on work value and organizational socialization.

1. Introduction

With the construction and promotion of Guangdong-Hong Kong-Macao Greater Bay Area in China, major industries are facing opportunities for development. However, the COVID-19 pandemic has brought a serious impact on the global economy, and at the same time, it has once again exposed the problems of a single industrial structure and insufficient economic resilience in some areas of the Greater Bay Area. In addition, the retail, catering, hotel, and other industries have also suffered great losses. Young people in Greater Bay Area are faced with unemployment, career loss, social status pressure, and instability. Due to geocultural reasons, Greater Bay Area has integrated the characteristics of Chinese and Western cultures, and a series of historical events, such as the return of Hong Kong and Macao, the opening of gambling rights, and the financial crisis, have also left a deep imprint on the growth of young people in Guangdong, Hong Kong, and Macao, which have also had a far-reaching impact on the formation of young people's personal career development in Guangdong, Hong Kong, and Macao, showing significant differences in professional values between the younger generation in Greater Bay Area and intergenerational groups in other regions; Moreover, most young people also show maladjustment in career and fail to properly evaluate themselves and analyze the external environment. They often do not have a clear concept of career exploration and do not think it can affect their cognition of career prospects or even regard it as irrelevant and redundant behavior with career development. Based on the current situation, this paper attempts to explore the intermediary effect of the career exploration behavior of young people in Guangdong, Hong Kong, and Macao from the perspective of social cognition and social exchange

between professional values and organizational socialization, and how they play a role under the regulation of population attributes, in order to explore strategies to promote the career development of young people in Guangdong, Hong Kong, and Macao, so that they can better seek the matching between individuals and organizations and individuals and occupations after entering the workplace and provide corresponding enlightening ideas and reference for academic circles.

2. Literature Review

2.1. Career Exploration. The theory of career exploration first appeared in the 1960s, and at first, it was only regarded as a common exploration behavior [1]. However, with the development of society, career exploration has gradually evolved a variety of meanings. (1) The first definition is also a relatively simple one, which comes from the theories of career choice and career consultation, such as Krumboltz's learning theory [2]. This definition regards career exploration as an information-seeking behavior or a career problem-solving behavior. For example, Greenhaus and Sklarew [3] directly define career exploration as the collection and analysis of information related to career development. (2) The second definition comes from the career decision-making theory, which regards career exploration as an important stage in the process of career decision-making, which includes information collection behavior and identification and evaluation of various possible choices (e.g., Gelatt [4]). (3) The third definition comes from the theory of career development, which regards career exploration as an important career stage, that is, adolescence (14–24 years old). The important task of this stage is to finalize, clarify, and implement career choices [5]. (4) The fourth and final definition regards career exploration as a process of career learning and career development that runs through the whole career [1, 6, 7].

This paper holds that career exploration is a series of professional behaviors which integrate the internal professional psychology and the external professional reaction. According to the definition proposed by Jordaan [1] and Super [5], career exploration should be regarded as a process throughout the whole career and career development. The core of it is self-evaluation and external environment analysis.

2.2. Connotation of Career Exploration. Career exploration can enhance people's awareness of themselves and their environment. The purpose of career exploration is to help people establish a more realistic career development goal and more appropriate development strategy. According to the types of information obtained, most researchers, such as Taveira and Moreno [7], divide career exploration into two parts: self-exploration and environmental exploration. For example, Luo [8] used "confidant" and "Zhibi" to express the task of career exploration. However, there is no big difference between its content and the classification methods of self-exploration and environmental exploration. The real-time "self-exploration" corresponding to "confidant" corresponds to "environmental exploration." Therefore, this study intends to use the classification method of self-exploration and environmental exploration to review the content of career exploration.

2.2.1. Self-Exploration. When a person is collecting personal characteristics related to career decision-making, we can think that he is exploring himself. In order to set a suitable career goal, a person needs to have a clear understanding of what he/she hopes to obtain from his/her working and nonworking roles and what his/her skills and abilities can be engaged in (or develop in his/her work). In the specific content of self-exploration, researchers mentioned more about professional values, professional interests, personality characteristics, professional ability, preferred lifestyle, and so on (Greenhaus and Sklarew [3], Song and Fai Tso [9], etc.).

(1) Professional Interest. Professional interest refers to whether a person likes a specific work activity or work goal. Professional interest is the embodiment of the following factors, such as professional values, family lifestyle, social class, accepted culture, and material conditions, etc. Professional interests are associated with specific activities. Studies have shown that when a person chooses a career field that is consistent with his /her own professional interests, his/her satisfaction is significantly higher than that of those who choose a career field that is not consistent with his /her interest and is willing to continue to engage in this occupation [10].

Holland [11] identified six career interest orientations that reflect a person's personality, values, and preferred lifestyle. Holland's theory assumes that professional interest is an important embodiment of a person's personality. Therefore, the six interest orientations he listed are consistent with specific personality characteristics. These six career interest orientations are realistic, research-oriented, social-oriented, conventional, entrepreneurial, and artistic.

(2) Personality. Personality is a person in the social life adaptation process, for himself, others, or other things, in the body and mind behavior of the unique personality. This unique personality is influenced by many congenital factors and an acquired environment. It is formed by the interaction of heredity, maturity, environment, and learning. It has relative continuity and stability. Therefore, personality factor is very important to one's career choice. Personality theory has made great progress in the past ten or twenty years. One of them is the preliminary study of the big five-factor structure of personality traits. Cattell [12] designed a 16-factor personality questionnaire in 1943, which laid a foundation for the study of the big five factors. Goldberg and Hillier [13] formally proposed the big five-factor model. Costa and McCrae [14] and others put forward the big five personality trait theory on the basis of previous studies. The personality scale developed by McCrae and Costa [15] reflects the connotation of these five factors: extraversion, adjustment, friendliness, rigor, and curiosity. Some studies

have shown that these five factors have a good predictive ability for individual job performance and career development.

(3) Professional Ability. The professional abilities mentioned here include not only one's innate ability but also the acquired skills, which reflect what one can do or accomplish. Therefore, professional ability sets a certain limit for one's career development. Therefore, before making a career decision, an individual must carefully examine his own professional ability. With the development of the social division of labor, people are engaged in more and more professional fields, so the specific professional ability model is very rich. The American general aptitude test has identified nine abilities: general learning ability, speech ability, arithmetic ability, judgment ability, figure perception ability, symbol perception ability, motor coordination ability, finger dexterity, and wrist dexterity. The test can help to determine the professional ability in 8 categories and 32 subcategories of occupational fields and is considered to be a better test in career guidance.

The Canadian vocational classification system divides professional competence into 11 aspects, including intelligence and ten basic special abilities. The first nine abilities are obviously influenced by the American GATB. Each of these 11 abilities is suitable for a certain occupation type.

(4) Preferred Lifestyle. Because the work role is only one of the many roles one plays in one's life, one must also consider nonworking life when making career decisions, such as what kind of family life you want to live, what kind of leisure and entertainment you need, and so on. We can call these issues the preferred lifestyle.

2.2.2. Environmental Exploration. Because a person's career exists in a certain industry and organization, personal professional values, interests, talents, etc., are bound to be related to a certain working environment, and the matching between personal characteristics and environmental characteristics will inevitably affect a person's job satisfaction and career success. Therefore, professional exploration must include active exploration of the environment. Environmental exploration includes many contents, but four aspects are often mentioned by researchers: occupation, position, organization, and family (such as Blustein and Phillips [16], etc.).

(1) Occupation and Position. Occupation refers to a series of jobs with similar job requirements or parallel responsibilities in different organizations and at different times. For example, teachers, workers, and engineers are different occupations. A position is a job, which is a job with equivalent responsibilities according to regulations or a clear work behavior to achieve a certain purpose. For example, the deputy general manager in charge of production and the deputy general manager in charge of marketing in the same enterprise are different positions. The exploration of occupation includes occupation task activities, ability/training requirements, remuneration, safety, social relations, physical environment, lifestyle (working time commitment, working pressure), and so on. The exploration of the position includes the diversity of tasks, importance of tasks, ability/training requirements, remuneration, safety, social relations, physical environment, lifestyle (working time commitment, work pressure), independence/autonomy, relationship with other positions, and so on.

(2) Organization. Generally speaking, an organization has a different attraction to different students. The exploration of an organization should include its industrial prospect, financial status, organizational strategy, promotion opportunities within the organization, the flexibility of career channels, career management practices/policies, organizational scale and structure, remuneration system, and human resource needs. In addition, some researchers mentioned the analysis of the external environment of the organization, such as its position and development trend in the industry and market conditions faced, etc. Some researchers also mentioned the ownership nature of the organization (such as whether the organization is state-owned or private), the subordinate relationship (if it is a subordinate unit; it is necessary to find out the situation of the higher authorities at the same time), the geographical location and environment of the organization, and the social security provided by the organization.

(3) Family. The exploration of the family should include spouse's career expectation, spouse's emotional needs, children's emotional needs, other family members' needs, family financial needs, family's expected lifestyle, family stage, career stage of oneself and spouse, etc. For college students, family influencing factors should mainly include the needs of family members or male/female friends, family financial needs, expected family lifestyle, etc. These factors often affect salary expectations, career choices, or geographical choices, etc.

In addition to the above, Yang and Ji [17] also mentioned the understanding and analysis of the social environment. Because China is in the process of social reform, college students should pay attention to the current social, political, and economic development trends when exploring their careers. Distribution and demand of social hot occupational categories. The status of one's chosen profession in current and future society. The influence of social development trend on one's occupation is analyzed.

2.3. Job Values, Career Exploration, and Organizational Socialization. As a predictive variable, career exploration behavior has many related factors, such as professional values, organizational socialization, personality factors, family environment, demographic characteristics, and so on. Among them, professional values, organizational socialization, and demographic characteristics are the related influencing variables that this study tries to pay attention to.

The discussion of professional values began around the 1950s. It is generally believed that personal work attitude and performance are closely related to personal, professional values, and personal views on work values will affect career choice, development, and performance [18]. Professional values are the results that individuals expect through their careers. Professional values emphasize the differences between people in terms of remuneration, reputation, security, self-satisfaction, and realization. Super [19] once summarized people's professional values into 15 types: helping others, aestheticism, creation, intellectual stimulation, independence, achievement, reputation, management, economic return, safety, things around, relationship with superiors, social interaction, diversification, and lifestyle. Allport [20] proposed a classification system of professional values, including six types: theoretical, economic, aesthetic, religious, social, and political. Each person may focus on a certain type of professional values, and each occupation or job can provide people with different value satisfaction. Therefore, people tend to choose a career that can meet their own value needs, so it is very helpful to know their own professional values for their career aspirations.

Since the concept of professional values was put forward, scholars have devoted themselves to exploring the influencing factors and resulting variables of professional values. Studies have shown that the correlation between professional values and career exploration attitude has been widely supported, among which Rounds [21] found that there is a correlation between professional values and work attitude. Many experts' studies, such as Kidron [22], also show that individual job values are related to organizational commitment, and job values are also related to job engagement. Elizur [23] pointed out that professional values and motivation are two related but different concepts. Therefore, previous studies have found that there is a high correlation between career values and career exploration. In addition, "organizational socialization" is a very important process because it ensures to provide a framework for new employees to respond to their working environment and cooperate with other members and continuously conveys the values and norms of the organizational center. When the socialization process makes the new members' "personal value" and "organizational value" closely linked, they will become more committed to the organization, and will not easily try to leave, so as to ensure that the organization has more benefits and save investment in recruitment, selection, and training [24].

This paper argues that professional values will lead to professional exploration behavior and then have an impact on organizational socialization. When the individual's professional values are clearer, the career exploration is more involved and the career planning is more comprehensive; that is, the individual may know more about himself and his chosen career. If a person does more career exploration activities before setting career goals, then the career goals he sets may be more suitable for himself, the higher his career satisfaction will be, and the matching with the organizational level will be more suitable. At the same time, the degree of career exploration developed by different professional values is also different, and the simple and complex professional values also influence or guide individual career exploration activities to varying degrees; The process of organizational socialization urges employees to subtly match the environment with individuals, thus influencing individual professional values by constantly scanning, perceiving, and exploring professional behaviors. It can be seen that career exploration is an indispensable and irreplaceable important element in the process of personal career development, which is not only affected by the formation and structure of professional values but also affects the process of organizational socialization in the long run. Organizations should plan and develop employees' professional behaviors from the strategic level and based on professional exploration activities, so as to promote the perfect match between individuals and organizational goals. Based on the above literature, this paper establishes the following research hypothesis. See Figure 1 for details:

H1: career exploration has a mediating effect between job values and organizational socialization

H2: demographic characteristics have a moderating effect between job values and career exploration

H3: demographic characteristics have a moderating effect between career exploration and organizational socialization

3. Methodology

This paper mainly adopts the method of combining theoretical research with empirical statistics. With the help of statistical software tools such as IBM AMOS 24.0 and IBM SPSS 24.0, descriptive statistical analysis, reliability analysis, correlation analysis, confirmatory factor analysis, path analysis, multiple regression analysis, etc., so as to obtain rigorous and standardized research results. The Richter scale 5 was used in the survey, in which 1 means totally disagree, 5 means totally agree, and the subjects are required to fill in the answers according to their actual situation.

3.1. Sampling Design. This study adopts a convenient sampling method. The sampling objects are young people aged 20–30 in Guangdong, Hong Kong, and Macao, including students and enterprise employees. This group was born in 1991–2000. Society defines this generation as the post-90s generation, which has many different characteristics from previous generations. The total sample size is designed to be 710. The data are collected in the form of street visits, business visits, and school visits in Guangzhou, Shenzhen, Zhuhai, Hong Kong Island, Macao Peninsula, and Taipa Island. The distribution of regions, industries, occupations, and identities is taken into account according to the sample quota design.

3.2. Variable Measurement. The contents of this research questionnaire are mainly divided into four parts. The first part is a survey of job values, the second part is a survey of occupational exploration activities, the third part is a survey

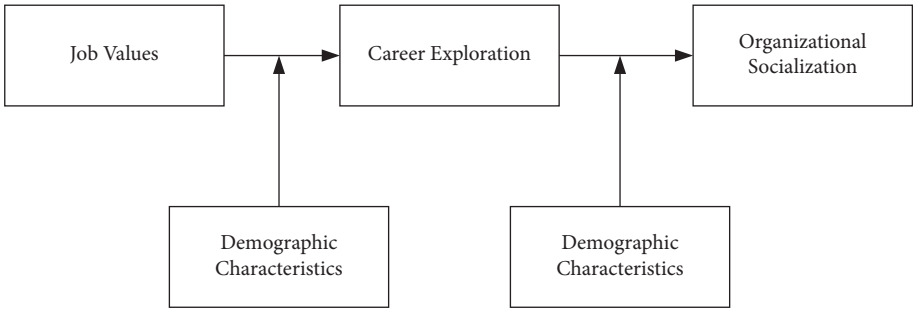

Figure 1: Theoretical model.

of organizational socialization, and the fourth part is demographic variables. In the measurement method of the questionnaire, the comprehensive scale of Likert is adopted to measure the problems, and the scale is five points. In the preliminary questionnaire, the specific items of professional values refer to the scale of Manhardt [25], and its A coefficient is 0.84. The specific items of career exploration refer to the scale of Lovelace and Rosen [26], and its A coefficient is 0.88. The scale of Cable and Judge [27] is adopted as the specific item of organizational socialization, and its A coefficient is 0.88. Demographic variables are mainly gender, age, education, major, industry, enterprise scale, position, working status, seniority, salary, and other items. After pretesting the questions and testing the reliability and validity of the contents, the items that do not conform to the empirical results were eliminated. There were 56 items in the formal questionnaire, among which 16 items examined the professional values of young people in Guangdong, Hong Kong, and Macao, 12 items examined the career exploration behavior of young people, and 16 items examined the organizational socialization.

4. Data Analysis and Results

4.1. Sample Distribution. In this study, 710 samples were collected, 10 invalid questionnaires such as missing items were deleted, and 700 actual valid questionnaires were collected. Among them, there were 282 males, accounting for 40% of the total sample size; there are 418 females, accounting for 60% of the total sample size. In terms of age structure, the youth aged 20–25 accounted for 74% of the total sample. Observing the educational background of the research subjects, the proportion with undergraduate level is the highest, with a total of 472, accounting for 67.4% of the total number of samples; The high school level ranks second, with a total of 188, accounting for 26.9% of the total number of samples. There are 19 graduate students, accounting for 2.7% of the total number of samples. There are 15 junior high school students, accounting for 2.1% of the total samples. There are 6 students below junior high school, accounting for only 0.9% of the total number of samples. In addition, from the distribution of the industries in which the respondents are located, there are 196 tourism and hotel industries, accounting for 28% of the total number of samples. There are 117 people in the gaming industry, accounting for 16.7 of the total number of samples. There are 190 people in financial and insurance services, accounting for 27.1% of the total number of samples. There are 113 people in public administration, accounting for 16.1% of the total sample number; 27 people in the manufacturing industry, accounting for 3.9% of the total number of samples; 24 people in the communication industry, accounting for 3.4% of the total number of samples. Transportation and warehousing 20 people, accounting for 2.9% of the total number of samples. There are 13 people in the construction industry, accounting for only 1.9% of the total samples.

4.2. Reliability Analysis. The Cronbach's a coefficient is used to analyze the questionnaire coefficient in order to measure the correlation of common factors among variables and also to measure the degree of internal consistency among variables. When Cronbach's αcoefficient is greater than 0.70, it means that the correlation between the measurement items is stronger, and the reliability of this dimension is quite good [28].

According to the analysis in Table 1, Cronbach's α coefficient is 0.84 for the professional values, 0.88 for the professional exploration, and 0.88 for the organizational socialization. All of them are greater than the standard value of 0.70, which also accords with the standard value of the reliability test proposed by Hair et al. [28]. Therefore, the aspects of "professional values, professional exploration and organizational socialization" in this study have high reliability.

4.3. Exploratory Factor Analysis. The paper adopts Harman's single factor test, incorporates all kinds of job values, professional exploration, and organizational socialization into exploratory factor analysis. Through the main component factor test, results found that 3 feature values can be selected 1 of the factor accumulated variance interpretation of 65%, and the first-factor explanation force of the nonrotating shaft is only 20%, which is much less than 50%, which can be seen that the study has no common method deviation problem.

4.4. Confirmatory Factor Analysis. In terms of validity, the contents of the questionnaire in this study are based on theory, revised with reference to the contents of similar studies by scholars in the past, discussed with practical and

Table 1: Confirmatory factor analysis.

Variables	a	AVE	Reliability	GFI	AGFI	RMR	RMSEA	NFI	RFI	CFI	IFI
Job values	0.84	0.56	0.928	0.948	0.908	0.034	0.07	0.919	0.873	0.936	0.936
Career exploration	0.88	0.51	0.887	0.971	0.932	0.028	0.068	0.944	0.889	0.956	0.956
Organizational socialization	0.88	0.55	0.925	0.945	0.908	0.026	0.068	0.92	0.881	0.937	0.937

Note. AVE = average variance extracted, GFI = goodness of fit index, AGFI = adjusted goodness of fit index, RMR = root mean square residual, RMSEA = root mean square error of approximation, NFI = Normed fit index, CFI = comparative fit index, and IFI = incremental fit index.

academic experts, and conducted with a trial test, providing suggestions for improving the contents and format of the questionnaire, so as to effectively integrate theory with the opinions of experts and scholars, so it should have a certain degree of face validity and content validity.

In terms of constructive validity, this study uses Confirmatory Factor Analysis (CFA) to test the scale of job values, occupational exploration, and organizational socialization and measure the overall fitness and aggregation validity of the model. The three potential variables included in the experiential research scale are "professional values, professional exploration and organizational socialization," which can explain the relationship between the factors of the measured variables.

According to Wu [29], three types of overall adaptation indexes, such as absolute adaptation index, value-added adaptation index, and simple adaptation index, are used as the evaluation criteria of measurement mode adaptation degree in this study. Among them, the absolute adaptation index: the smaller the test value of chi-square, the better the overall fit. GFI > 0.90, AGFI > 0.90, RMSEA < 0.05, and RMSEA < 0.08. In terms of value-added adaptability, NFI > 0.90 and CFI > 0.90. If the value is equal to 1, the mode is completely suitable, and if it is equal to 0, it is totally unsuitable. In terms of simple fitness, PCFI value > 0.50, PGFI value > 0.50, PNFI value > 0.50, CAIC value must be lower than independent model value and lower than saturated model value.

In the CFA analysis results of this study, there is no negative error variance in the nonstandardized parameter estimation model diagram, which means that there is no problem in model definition. In the overall summary of pattern adaptation degree, X^2 (Chi-square) is 218.879, $P < 0.05$; RMR value is $0.02 < 0.05$; The RMSE value of $0.07 < 0.08$ indicates that the mode adaptation is good. GFI value is $0.942 > 0.90$; The AGFI is 0.90; The NFI value is $0.908 > 0.90$; IFI value is $0.921 > 0.90$; CFI value is $0.920 > 0.90$; PCFI value is $0.654 > 0.50$; the value of PGFI is $0.548 > 0.50$; the value of PNFI is $0.646 > 0.50$; while CAIC values are $392.554 < 415.309$ and $392.554 < 2466.528$. At the same time, the factor load value is more than 0.5 except the working stability factor of 0.39, which belongs to the acceptable and reasonable range. It can be seen from the above that the research scale has good construction validity and the model is well adapted.

4.5. Correlation Analysis. Through Pearson coefficient correlation analysis, we further explore the correlation analysis between pairwise variables such as "professional values," "professional exploration," "organizational socialization," "education level," "gender distribution," "working years," "industry distribution," and "position situation." From Table 1, it is not difficult to see that all the research variables involved in this paper are related. In this study, Pearson product-moment correlation is used to analyze the data of which both variables are equidistant variables, Spearman rank correlation is used to analyze the sequential variables, and if the statistical correlation coefficient r reaches the significant level of 0.05, the determination coefficient is obtained [30]. After the preliminary correlation analysis, in order to test whether the hypotheses put forward in this study are valid, the hierarchical regression analysis is used to verify the causal relationship between variables.

4.6. Hierarchical Regression Analysis. In this study, the hypothesis is verified by class regression analysis, in which H1: career exploration has a mediating effect between job values and organizational socialization, and the hypothesis holds; H2: demographic characteristics have interference effect between job values and career exploration, and the hypothesis holds; H3: demographic characteristics have interference effect between career exploration and organizational socialization, which is assumed to be true. The analysis results are shown in Tables 2 and 3.

4.6.1. Mediating Effect of Career Exploration. According to Baron and Kenny [31], when the mediation effect is verified by hierarchical regression analysis, the conditions for the mediation effect are as follows: First, independent variables and mediation variables are significantly related to dependent variables. Secondly, there is a significant relationship between independent variables and intermediary variables. Finally, the relationship between the independent variable and the dependent variable should be weaker when the intermediate variable is put in.

In order to verify whether career exploration is the intermediary variable between career values and organizational socialization, taking organizational socialization as the dependent variable, the control variable (demographic characteristics) is put in first, and then the independent variable job values are put in. The results show that there is a significant positive correlation between job values and organizational socialization (β value is 0.161, $P < 0.001$, ΔR^2 is 0.042). Then, taking career exploration as the dependent variable, the control variable (demographic characteristics) and independent variable job values are inserted. The results show that there is a significant positive correlation between job values and career exploration (β value is 0.327, $P < 0.001$,

Table 2: Descriptive statistics and correlation analysis.

Serial number	Variable	Average value	Standard deviation	1	2	3	4	5	6	7	8	9
1	Gender	1.597	0.491	1								
2	Age	22.877	2.658	0.026	1							
3	Education	4.681	0.646	−0.040	0.311**	1						
4	Major	1.111	0.315	−0.033	0.095*	−0.029	1					
5	Seniority	2.243	1.091	0.055	0.394**	−0.038	0.009	1				
6	Income	2.194	1.095	0.010	0.315**	−0.131**	0.041	0.267**	1			
7	Job values	3.741	0.467	0.050	−0.035	0.038	0.086*	−0.020	−0.020	1		
8	Career exploration	3.278	0.544	−0.044	0.003	0.167**	0.058	−0.104**	−0.013	0.335**	1	
9	Organizational socialization	3.208	0.481	0.003	0.081*	0.105**	0.041	0.046	0.100**	0.164**	0.401**	1

Note. $N = 700$. $^{*}P < 0.05$; $^{**}P < 0.01$; $^{***}P < 0.001$.

Table 3: Analysis of intermediary role.

Explanatory variable	Model 1 Organizational socialization	Model 2 Organizational socialization	Model 3 Career exploration	Model 4 Organizational socialization
Gender	0.007	−0.002	−0.047	0.016
Age	−0.004	0.007	−0.013	0.012
Education	0.123**	0.112**	0.160***	0.050
Major	0.040	0.025	0.033	0.012
Seniority	0.023	0.022	−0.096*	0.059
Income	0.110**	0.109**	0.044	0.092
Job values		0.161***	0.327***	0.034*
Career exploration				0.388***
R^2	0.026***	0.051***	0.150***	0.180***
ΔR^2	0.018***	0.042***	0.141***	0.170***
F	3.099***	18.511***	85.674***	64.741***
D-W		2.004	2.121	2.010

Note. $N = 700$. $^{*}P < 0.05$; $^{**}P < 0.01$; $^{***}P < 0.001$.

ΔR^2 is 0.141). At last, with career exploration as an independent variable, Model 4 shows that the mediation of career exploration is significant ($\beta = 0.388$, $P < 0.001$, $\Delta R^2 = 0.170$), while the β value of career values decreases from 0.161 ($P < 0.001$) to 0.034 ($P < 0.05$), which accords with the third condition proposed by Baron and Kenny. Therefore, it can be seen that career exploration has a mediating effect on the correlation between career values and organizational socialization, so it is assumed that H1 is supported.

4.6.2. Moderation of Demographic Characteristics. In this study, H2 and H3 discussed the moderation of demographic characteristics on job values, career exploration, and organizational socialization, which were all important interference variables considered in the study. The details of empirical analysis data for every indicator can be found in Tables 4 and 5. However, the direct effect before the interference variables are added confirmed that there are significant positive roles between job values, career exploration, and organizational socialization.

Figures 2 and 3 further report the changes in moderating effect of demographic characteristics for career exploration and organizational socialization. The results of hierarchical regression analysis show that only the interaction between seniority situation and job values has a significant interference effect on career exploration in the demographic characteristics of Model 3, and its β value is −0.128 ($P < 0.01$) and ΔR^2 is 0.159, so H2 hypothesis holds. In the demographic characteristics of Model 6, only the interactive items, including gender and career exploration, have a significant interference effect on organizational socialization, and its β value is 0.071 ($P < 0.05$) and ΔR^2 is 0.187, so the H3 hypothesis holds.

5. Discussion and Suggestion

5.1. Theoretical Contribution and Practical Significance. To sum up, although the causes and consequences of career exploration have been confirmed by many studies, it is rare to discuss the effect of comediation and referral based on the vision of youth's professional values, organizational socialization, and population attributes. In the theoretical model constructed in this paper, the internal consistency among the measurement items has been verified by Cronbach's *a*, and the three dimensions of professional development, such as professional values, professional exploration, and organizational socialization, have reached more than 0.8, and have passed the validity test, which meets the requirements of basic research; This scale and theoretical model are of great theoretical significance for the government and academic circles to further explore the career

Table 4: Regulation analysis 1.

Predictor variable	Career exploration		
	Model 1	Model 2	Model 3
Job values	0.335***	0.327***	0.346***
Gender		−0.047	−0.053
Age		−0.013	0.002
Education		0.160***	0.149***
Major		0.033	0.024
Seniority		−0.096*	−0.117**
Income		0.044	0.053
Job values × gender			−0.002
Job values × age			0.101*
Job values × education			−0.009
Job values × major			0.017
Job values × seniority			−0.128**
Job values × income			0.102**
R^2	0.112***	0.150***	0.175***
ΔR^2	0.111***	0.141***	0.159***
F	88.372***	17.409***	11.202***
D-W	2.046	2.121	2.100

Note. $N = 700$. $^{*}P < 0.05$; $^{**}P < 0.01$; $^{***}P < 0.001$.

Table 5: Regulation analysis 2.

Predictor variable	Organizational socialization		
	Model 4	Model 5	Model 6
Career exploration	0.401***	0.400***	0.399***
Gender		0.019*	0.018*
Age		0.010	0.000
Education		0.050	0.053
Major		0.014	0.034
Seniority		0.060	0.041
Income		0.091*	0.111**
Career exploration × gender			0.071*
Career exploration × age			−0.099*
Career exploration × education			−0.019
Career exploration × major			−0.041
Career exploration × seniority			−0.040
Career exploration × income			−0.021
R^2	0.161***	0.179***	0.202***
ΔR^2	0.159***	0.171***	0.187***
F	133.527***	21.529***	13.382***
D-W	2.008	2.010	2.009

Note. $N = 700$. $^{*}P < 0.05$; $^{**}P < 0.01$; $^{***}P < 0.001$.

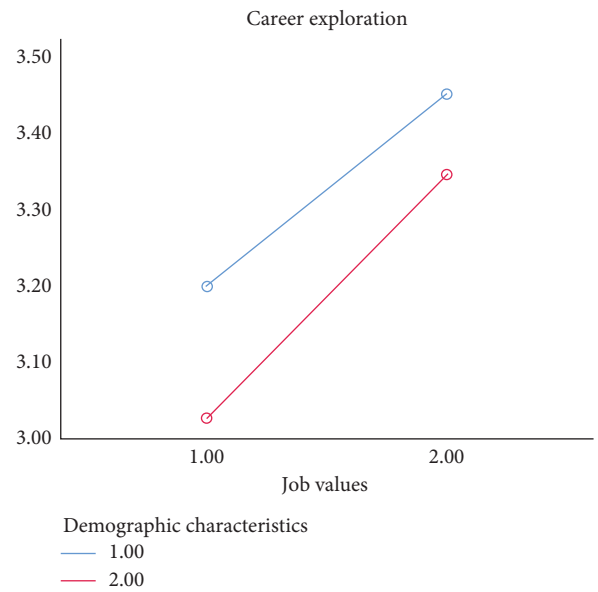

Figure 2: The moderating effect of demographic characteristics on job values and career exploration.

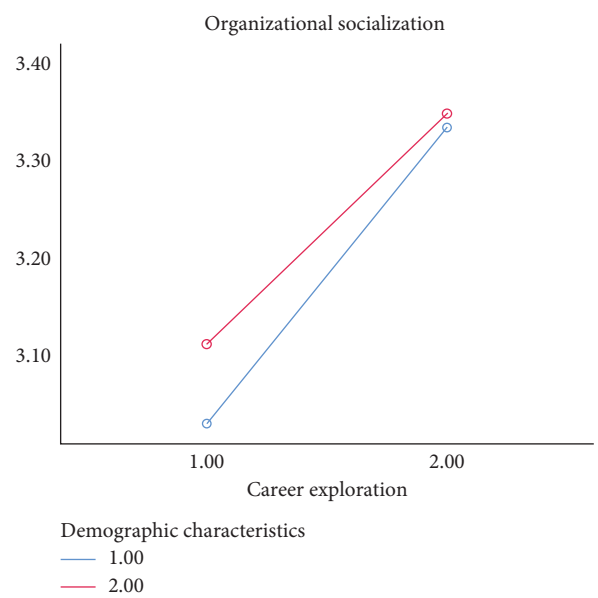

Figure 3: The moderating effect of demographic characteristics on career exploration and organizational socialization.

development of young people in Guangdong, Hong Kong, and Macao. At the same time, the industry can also use this scale to measure the professional values, career exploration behavior, and perception of organizational work of young and middle-aged employees so as to facilitate timely adjustment of the organization and its human resources strategy. In addition, the study tested the model fitness of the measurement items of young people's career values, career exploration, and organizational socialization in Guangdong, Hong Kong, and Macao by confirmatory factor analysis and class regression analysis and discussed the relationship between them by linear regression. The analysis results are all above the standard, and it is concluded that career exploration plays an intermediary role in career values and organizational socialization, the interaction between industry distribution and career values interferes with career exploration, and the interaction between job types and career exploration interferes with organizational socialization. It is of guiding significance to the industry on how to plan and manage the young people's career choice, career orientation, and development in Guangdong, Hong Kong, and Macao. It is also beneficial to take corresponding development and promotion measures from the perspective of organization and society, promote the career development of the young people in Guangdong, Hong Kong, and Macao, and ensure the virtuous circle of social human resources in the Greater Bay Area.

5.2. Suggestions

5.2.1. Suggestions on Young People's Personal Career Exploration. It is found that the professional values of young people in Guangdong, Hong Kong, and Macao pay more attention to professional status and stability, professional remuneration, respect, and stability guarantee. Due to the relative shortage of the whole labor force in the Greater Bay Area, the employment pressure of young people is not great, their career exploration performance is not active enough, and their job satisfaction is not high. The main reason for this phenomenon is that before entering the workplace, they did not really understand themselves and their occupations, and they often chose a certain occupation with the social trend, rather than choosing according to their actual preferences and specialties. This will inevitably lead to the phenomenon of mismatch, which is not conducive to the development of a personal career and will also cause a waste of resources to the organization and society. Therefore, young people in Guangdong, Hong Kong, and Macao should improve their self-exploration awareness, actively seek their own career anchors, make full use of possible resources to explore suitable occupations and enterprises, and avoid blindly following and drifting with the tide.

Young people in Guangdong, Hong Kong, and Macao can take some measures to explore their career development path according to their actual situation. For example, attending lectures and reports on career planning, participating in discussion or exchange activities with enterprises and institutions, participating in activities such as investigation and research in enterprises and institutions, participating in enterprise human resources management training, participating in school-enterprise cooperation projects, and volunteering in enterprises and institutions, college students can enter the working environment in advance to experience, including taking part in extracurricular activities organized by schools or student associations, taking part-time jobs or internships through summer jobs, taking part-time jobs and internships through their own social relations, etc. They can also take part in induction training organized by enterprises, consciously collect professional and enterprise information, take professional tests in interests, values, personalities, abilities, etc., and discuss career-related issues with friends, relatives, teachers, etc. Their preservice and early career development experience are undoubtedly very important to adapt and integrate into the organization in the future. The more you participate, the deeper you know about yourself and professional organizations, the easier it is to make correct decisions in the process of career choice and ultimately promote personal career development.

5.2.2. Suggestions of the Government. The government should step up publicity efforts to make more young people aware of the importance of career development and career exploration. The government needs to consider the macro labor situation in the region as a whole. The highly mobile human resources situation will have a negative impact on the development of the regional economy, and it is also a factor that leads to social instability. In order to achieve the rational allocation of talents and the sustainable advantage of competition and avoid the waste of social resources. The government should guide the young people in Guangdong, Hong Kong, and Macao to pay attention to the role of career exploration through publicity and guide them to complete the process of career exploration before their employment, instead of making career choices through frequent job-hopping after entering the workplace.

Government departments in all parts of the Greater Bay Area should increase investment in youth career planning and can set up professional career consulting service departments, whose main responsibilities are not only to provide job opportunity information but also to include social practice opportunities, free evaluation tools, and professional guidance. Try to help young people in Guangdong, Hong Kong, and Macao who have problems in the process of career analysis and exploration, and provide professional advice for their career development.

5.2.3. School Suggestions. The survey shows that many young people do not know how to do career exploration. School education is an important part of personal growth and a necessary stage before an individual enters the workplace. Schools should not only impart knowledge but also prepare for careers. Therefore, schools should offer courses related to careers, such as career planning and development, so as to help college graduates successfully realize the socialization transformation from students to workers and successfully realize organizational socialization.

Internship programs are the most recognized in career development, but at present, most of the internship programs that young people in Guangdong, Hong Kong, and Macao participate in the use of interpersonal relationships to get opportunities, and there are few opportunities that they really get through schools. In fact, more students only regard internship programs as a means to make money, which losses the meaning of internship itself. Therefore, colleges and universities should strengthen cooperation with enterprises, make full use of this effective career exploration tool, and help students better understand the career and real enterprise situation.

5.2.4. Suggestions of Enterprises. Enterprises can use their recruitment functions to help young employees make correct choices. The goal of enterprise recruitment is not to find the best talents but to find the most suitable talents. Therefore, in the recruitment process, enterprises should provide true information as much as possible to help candidates make appropriate choices. Any false propaganda will increase the possibility of wrong career choice, which will lead to a higher turnover rate, and eventually, the enterprise will bear greater losses. Therefore, the recruitment of enterprises must pay attention to the real job prediction.

The induction training for new employees in enterprises is also prequalification education and orientation training. It is a training method to introduce new employees to the basic

situation of enterprises, job responsibilities, department personnel, etc. It is a short time for employees employed by enterprises to change from "outsiders" to "enterprise people." In this process, enterprises should clearly convey their organizational culture, rules, and regulations, and job requirements so that employees who do not match the organization and position can leave as soon as possible to avoid unnecessary waste of time, energy, and financial resources. Organizations can also use a tutorial system to promote organizational socialization, mainly including direct supervisors, colleagues, senior employees, and other auxiliary employees of new employees. Through social training and other organizational socialization strategies, the degree of organizational socialization will be continuously improved, and the values of work and life will be constantly affected and adjusted, which will gradually be consistent with the values and behavior patterns advocated by the organization. Therefore, from the above two aspects, the higher the degree of organizational socialization of new employees, the higher the degree of matching between individuals and organizations. However, if new employees perceive that they are more compatible with the organization, the longer they serve in the organization, the higher their job satisfaction, the lower their turnover intention, and the higher the overall performance of the organization.

5.3. Research Limitations and Suggestions for Follow-Up Research. Due to the limitation of research time and cost, the sample size is not enough, and the sample extraction is still a kind of nonrandom probability sampling, and there may be some differences. In addition, only demographic characteristics are added as interference variables in the research variables, and other influencing variables can be discussed in the future to improve the development of this field.

In the follow-up research, personality variables can be added as interference variables. Whether young people with different personality characteristics have different preferences for different career values and career exploration is another question worth exploring.

Data Availability

The data used to support the findings of this study are included within this article.

Conflicts of Interest

The authors declare that there are no conflicts of interest regarding the publication of this paper.

Acknowledgments

This research was supported in part by the project grants from the New Century Excellent Talents Support Plan of Fujian Colleges and Universities (grant number 2018047); Basic Ability Improvement Project of Young and Middle-Aged Teachers in Guangxi Universities by the Department of Education (grant number 2019KY0402); and Guangxi Philosophy and Social Science Planning Research Project (grant number 20FJY028).

References

[1] J. P. Jordaan, "Exploratory behavior: the formation of self and occupational concepts," in *Career Development: Self-Concept Theory: Essays in Vocational Development*, D. E. Super, R. Starishevsky, N. Matlin, and J. P. Jordaan, Eds., College Entrance Board, New York, NY, USA, 1963.

[2] J. D. Krumboltz, "A social learning theory of career decision making," in *Social Learning and Career Decision Making*, A. M. Mitchell, G. B. Jones, and J. D. Krumboltz, Eds., Carroll Press, Cranston, RI, USA, 1979.

[3] J. H. Greenhaus and N. D. Sklarew, "Some sources and consequences of career exploration," *Journal of Vocational Behavior*, vol. 18, no. 1, pp. 1–12, 1981.

[4] H. B. Gelatt, "Decision-making: a conceptual frame of reference for counseling," *Journal of Counseling Psychology*, vol. 9, no. 3, pp. 240–245, 1962.

[5] D. E. Super, *The Psychology of Careers*, pp. 25–36, Harper & Row, New York, NY, USA, 1957.

[6] L. Zhen, H.-T. Song, and J.-T. He, "Recommender systems for personal knowledge management in collaborative environments," *Expert Systems with Applications*, vol. 39, no. 16, pp. 12536–12542, 2012.

[7] M. D. C. Taveira and M. L. R. Moreno, "Guidance theory and practice: the status of career exploration," *British Journal of Guidance & Counselling*, vol. 31, no. 2, pp. 189–208, 2003.

[8] S. Luo, "The factors of youth career planning," *China Youth Study*, vol. 8, p. 9, 2003.

[9] L. Song and G. K. Fai Tso, "Consumers can learn and can forget—modeling the dynamic decision procedure when watching TV," *Journal of Management Science and Engineering*, vol. 5, no. 2, pp. 87–104, 2020.

[10] N. E. Betz and K. K. Voyten, "Efficacy and outcome expectations influence career exploration and decidedness," *The Career Development Quarterly*, vol. 46, no. 2, pp. 179–189, 1997.

[11] J. L. Holland, *Making Vocational Choices: A Theory of Personalities and Work Environments*, Prentice-Hall, Englewood Cliffs, NJ, USA, 1985.

[12] R. B. Cattell, "The description of personality: basic traits resolved into clusters," *The Journal of Abnormal and Social Psychology*, vol. 38, no. 4, pp. 476–506, 1943.

[13] D. P. Goldberg and V. F. Hillier, "A scaled version of the general health questionnaire," *Psychological Medicine*, vol. 9, no. 1, pp. 139–145, 1979.

[14] P. T. Costa and R. R. McCrae, *The NEO Personality Inventory*, Psychological Assessment Resources, Odessa, FL, USA, 1985.

[15] R. R. McCrae and P. T. Costa, "The NEO personality inventory: using the five-factor model in counseling," *Journal of Counseling & Development*, vol. 69, no. 4, pp. 367–372, 1991.

[16] D. L. Blustein and S. D. Phillips, "Individual and contextual factors in career exploration," *Journal of Vocational Behavior*, vol. 33, no. 2, pp. 203–216, 1988.

[17] X. Yang and Y. Ji, "Some theoretical thoughts on college students starting up their own business of Chinese characteristics," *Studies in Ideological Education*, vol. 5, pp. 32–34, 2010.

[18] M. Chen, *Work Values and Their Formation Process*, Fu Ren University, Taipei, Taiwan, 1994.

[19] D. E. Super, "A life-span, life-space approach to career development," *Journal of Vocational Behavior*, vol. 16, no. 3, pp. 282–298, 1980.
[20] G. W. Allport, *Personality: A Psychological Interpretation*, Holt, New York, NY, USA, 1937.
[21] J. B. Rounds, "The comparative and combined utility of work value and interest data in career counseling with adults," *Journal of Vocational Behavior*, vol. 37, no. 1, pp. 32–45, 1990.
[22] A. Kidron, "Work values and organizational commitment," *Academy of Management Journal*, vol. 21, no. 2, pp. 239–247, 1978.
[23] D. Elizur, "Facets of work values: a structural analysis of work outcomes," *Journal of Applied Psychology*, vol. 69, no. 3, pp. 379–389, 1984.
[24] D. M. Cable and C. K. Parsons, "Socialization tactics and person-organization fit," *Personnel Psychology*, vol. 54, no. 1, pp. 1–23, 2001.
[25] P. J. Manhardt, "Job orientation of male and female college graduates in business," *Personnel Psychology*, vol. 25, no. 2, pp. 361–368, 1972.
[26] K. Lovelace and B. Rosen, "Differences in achieving person-organization fit among diverse groups of managers," *Journal of Management*, vol. 22, no. 5, pp. 703–722, 1996.
[27] D. M. Cable and T. A. Judge, "Pay preferences and job search decisions: a person-organization fit perspective," *Personnel Psychology*, vol. 47, no. 2, pp. 317–348, 1994.
[28] J. F. Hair, B. J. Babin, R. E. Anderson, and R. L. Tatham, *Multivariate Data Analysis*, Prentice-Hall, Hoboken, NJ, USA, 2005.
[29] M. Wu, *Structural Equation Model: Operation and Application of AMOS*, Chongqing University Press, Chongqing, China, 2009.
[30] H. Qiu, *Quantitative Research and Statistical Analysis*, Chongqing University Press, Chongqing, China, 2009.
[31] R. M. Baron and D. A. Kenny, "The moderator-mediator variable distinction in social psychological research: conceptual, strategic, and statistical considerations," *Journal of Personality and Social Psychology*, vol. 51, no. 6, pp. 1173–1182, 1986.

Hindawi
Scientific Programming
Volume 2021, Article ID 5601833, 17 pages
https://doi.org/10.1155/2021/5601833

Research Article

Traceability Management Strategy of the EV Power Battery Based on the Blockchain

Yanjin Cheng, Hao Hao, Shipeng Tao, and Yanjun Zhou

School of Economics and Management, Shanghai Polytechnic University, Shanghai 201209, China

Correspondence should be addressed to Hao Hao; haohao@sspu.edu.cn

Received 20 April 2021; Revised 8 July 2021; Accepted 11 August 2021; Published 24 August 2021

Academic Editor: Tingsong Wang

Copyright © 2021 Yanjin Cheng et al. This is an open access article distributed under the Creative Commons Attribution License, which permits unrestricted use, distribution, and reproduction in any medium, provided the original work is properly cited.

Regulating and supervising the energy vehicle (EV) power battery recycling market, improving the utilization rate of EV power battery recycling, and guaranteeing the safety and control of all aspects of recycling treatment require the establishment of an effective traceability system. The decentralization and tamper-proof characteristics of the blockchain can ensure the safety and reliability of relevant data while realizing traceability management. This study establishes the Stackelberg game model to compare and analyze the effects of different government mechanisms on the profits of each subject before and after participating in power battery traceability management. The study further uses the model to explore strategies to improve the enthusiasm of EV power battery recycling subjects to participate in traceability management. The results show that (1) the participation of each recycling subject in EV power battery blockchain traceability can help move more spent power batteries into formal recycling channels; (2) the government should adopt appropriate mechanisms to promote its participation in EV power battery blockchain traceability, the best result being when the government adopts a subsidy mechanism for consumers; and (3) the profit of the EV power battery manufacturer is inversely proportional to the target recycling rate set by the government. Furthermore, the pursuit of a very high target recycling rate is not conducive to the normal implementation of initial EV power battery blockchain traceability management. Therefore, it is crucial for the government to set a reasonable target recycling rate.

1. Introduction

In recent years, China's environmental pollution problem has become increasingly serious, with frequent transportation activities emitting large amounts of pollutants and becoming a major source of environmental pollution and energy consumption [1]. In 2010, the Chinese government listed the "new energy" and "new energy vehicle (NEV)" industries as national strategic emerging industry sectors to accelerate the development of the renewable energy industry and solve the environmental pollution and energy crises [2]. According to the data released by the China Association of Automobile Manufacturers (CAAM), the production and sale of the NEV in China reached 1.366 and 1.367 million units, respectively, in 2020. Of these, 1.105 million and 1.115 million units of energy vehicles (EVs) were produced and sold, with a yearly growth of 5.4% and 11.6%, respectively [3]. The use of power batteries has increased considerably following the continuous development of the EV industry. The 5 to 8 years of use of EV power batteries show that China entered the peak of power battery end of life around 2020 [4]. The improper disposal of spent EV power batteries not only increases the risk of environmental pollution but also leads to the wastage of precious metal resources [5]. Today's deteriorating ecological environment and depleted natural resources and EV power battery recycling-related enterprises and organizations proactively carry out the entire life cycle supply chain management of power batteries to realize the recycling and resource utilization of EV power batteries. These can yield huge economic and ecological benefits [6, 7]. Companies obtain more value from the reverse logistics and remanufacturing process of spent EV power batteries while also protecting the ecological environment [8].

China began recycling spent EV power batteries later than other developed countries; however, the development status is not optimistic. Moreover, the recycling and

government regulatory systems need to be improved [9]. First, informal recycling channels coexist with formal recycling channels. The recycling methods of informal recycling channels are more convenient. Therefore, a large number of spent EV power batteries flow into informal recycling channels. Furthermore, it is difficult for formal recyclers to form large-scale benefits. Second, the synergy of the subjects of production-recycling-echelon use is weak. Moreover, there are data and technical barriers between government departments and other enterprises. These make it more difficult to recycle and process spent EV power batteries as well as supervise each recycling subject.

To regulate the recycling market order of spent EV power batteries, the Ministry of Industry and Information Technology (MIIT) issued the "Interim Regulations on the Traceability Management of the Recycling and Utilization of New Energy Vehicle Power Batteries." This proposed the requirements for the establishment of "the Integrated Management Platform for the National Monitoring of New Energy Vehicles and Traceability of Power Battery Recycling," hoping to realize the information collection and supervision of the entire process of power battery production, sales, use, end of life, recycling, and utilization [10]. Furthermore, the traceability management of EV power batteries in China entered the primary stage. However, the existing EV power battery traceability system cannot guarantee a high level of system reliability, data accuracy, and information transparency. Moreover, some EV power battery manufacturers and formal recyclers are not very active in EV power battery traceability management considering issues such as data privacy and security. Additionally, China's policies and regulations in this field still need to be improved. These result in the slow promotion of China's EV power battery traceability management.

Blockchain technology is characterized by immutability and distributed storage among other characteristics. The data security problem of the power battery traceability system can be solved using computer technologies such as point-to-point transmission, consensus mechanism, and encryption algorithm [11]. After the data are deposited into the blockchain to obtain a consensus of the network nodes, it is difficult to be tampered with, which ensures the authenticity and security of the information related to the power battery [12]. Blockchain can realize the transparency of the data of the entire process of the EV power battery supply chain by using a consensus mechanism, improving the knowledge of government departments and related enterprises on the entire process of power battery recycling and breaking the data barriers, so as to further realize source traceability, process supervision, and risk early warning. The government should simultaneously adopt certain mechanisms to encourage EV power battery recycling and treatment-related enterprises to join this traceability management platform. Therefore, this study aims to explore strategies to improve the enthusiasm of EV power battery recycling subjects to further participate in traceability management by establishing the Stackelberg game model. The game model is of great significance in promoting the high-quality development of the power battery recycling industry.

The potential contributions of the study include the following:

(1) Based on summarizing the research of domestic and foreign scholars in the field of EV power battery recycling, the study innovatively proposed the application of blockchain traceability management to EV power battery recycling, hence filling the research gaps in this research field.

(2) Considering different government guidance mechanisms, a comparative analysis of the influence of government rewards, punishments, and subsidies on the enthusiasm of power battery recycling subjects to participate in traceability management is analyzed; government departments and power battery recycling and processing companies provide decision-making references.

(3) The Stackelberg game model was established considering factors such as consumer willingness and blockchain cost. An empirical analysis verified the effectiveness of the model.

The rest of this paper proceeds as follows. Section 2 introduces the current research status. Section 3 describes the model. Section 4 compares and analyzes the optimal situation under different strategies. Section 5 uses relevant data for empirical research. In conclusion, Section 6 summarizes and discusses the limitations of this research.

2. Literature Review

Currently, research on recycling channels and EV power battery recycling in the domestic and foreign literature mainly involves the selection of recycling channels, pricing decisions under multichannel competition, and the influence of government coordination mechanisms. Research on blockchain traceability management mainly focuses on food and medical care. Furthermore, research in the field of EV power battery recycling is scarce.

Regarding research on recycling channels, Savaskan et al. [13] compared and analyzed three recycling models with manufacturers, distributors, and third-party recyclers as recycling takers. They found that the recycling model with distributors as recycling takers was optimal, all else being equal. Liu et al. [14] analyzed the impact of government subsidies on formal and informal recycling channels while considering the quality of the recycled products. They found that the marginal effect of government subsidies was insignificant when the quality of the recycled products was high. Li et al. [15] developed a Stackelberg game model with dual recycling channels while considering consumer preferences. They concluded that the improvement of environmental benefits under government governance mechanisms depends on subsidies and consumer channel preferences. Tang et al. [16] used social welfare as an indicator for selecting recycling models and built Stackelberg game models under three single-recycling channel models and three competitive dual-recycling channel models based on the government's reward and penalty mechanism. They

found that setting a reasonable minimum power battery recycling rate as a benchmark for the reward and penalty mechanism is crucial. Xia et al. [9] studied the impact of competition between mixed WEEE sales channels and recycling channels on CLSC decisions under the government mechanism. They found the optimal strategy of each company and government based on the Stackelberg game model.

Regarding research on power battery recycling, owing to the increasing depletion of natural resources, the recycling of products and materials is a growing concern [17]. Research in this field can be categorized into two types: qualitative and quantitative. Regarding the qualitative aspects of power battery research, Wang and Wu [18] analyzed the challenges in the recycling process of $LiFePO_4$ batteries in China and proposed improvement strategies to make the recycling chain more environmentally friendly. Zeng et al. [5] analyzed the potential environmental and safety risks in the recycling and disposal processes of used lithium batteries and proposed a comprehensive management scheme regarding policies and regulations, recycling systems, and recycling technology. Beaudet et al. [19] analyzed the main challenges and opportunities for recycling new energy vehicle batteries and made relevant recommendations to address these challenges. Hao et al. [20] combined the current status of reverse logistics of power battery recycling and proposed effective countermeasures to contribute to the development of reverse logistics of power battery recycling. Regarding the quantitative aspects of power batteries, Li et al. [21] studied the coordination strategies of each supply chain subject in a three-tier reverse supply chain consisting of recyclers, remanufacturers, and retailers and conducted a detailed comparative analysis of the optimal decisions under different strategies. Gu et al. [22] studied the optimal pricing strategy for the closed-loop supply chain of power batteries and found that recycling spent power batteries does not benefit the profits of power battery manufacturers. They further suggested some government incentives to improve the economic benefits of recycling. Tang et al. [23] explored the social, economic, and environmental impacts of recycling end-of-life electric vehicle batteries under government subsidies and reward and punishment mechanisms, respectively. Hao et al. [17] established an improved fuzzy neural network evaluation structure model based on the combination of the fuzzy comprehensive evaluation method and particle swarm algorithm- (PSO-) optimized error backpropagation (BP) neural network with the feasibility of reverse logistics of end-of-life automotive power batteries as the target layer. Wang et al. [24] considered the recycling and remanufacturing costs of waste batteries and carbon tax to establish the lowest total cost mixed-integer programming problem model for the recycling network of NEVs. Wang et al. [25] analyzed the impact of multiattribute decision-making (MADM) on the efficiency of the end-of-life vehicle (ELV) reverse logistics industry in the context of a circular economy, hence indirectly providing a basis for management and investment decisions in the new energy vehicle power battery recycling industry. It is beneficial to explore the recycling of waste to promote the construction of ecological civilization against the background of a comprehensive implementation of the "Healthy China" strategy [26].

Research in blockchain traceability management focuses on food and medical care. Dandage et al. [27] analyzed the necessity of traceability management in the food industry and introduced the relevant technologies used with the help of traceability management. Tsang et al. [28] and Lin et al. [29] addressed the problems of opaque information, easy tampering, centralization, and serious information silos in traditional food traceability systems. Caro et al. [30] and Feng et al. [31] proposed a food safety traceability system based on the blockchain and Internet of Things (IoT) based on the analysis of the problems of traditional agricultural product supply chain traceability systems. Gong et al. [32] built a blockchain-based power battery data sharing system for real-time data monitoring and the sharing of the power battery life cycle. Gopalakrishnan et al. [33] proposed a blockchain-based solid waste management (SWM) model to solve the problem of waste traceability. Furthermore, the SWM system with the cost element of the blockchain was optimized.

Through the aforementioned combination of the domestic and foreign research literature, it is evident that various research scholars have studied the selection of recycling channels and EV power battery recycling from different perspectives; however, research on EV power battery traceability management in the context of blockchain is relatively rare. Based on the lack of research in this area, this study examines the blockchain-based EV power battery traceability management strategy and analyzes the influence of different government mechanisms on the unit recycling price, quantity, and profit of each subject. We hope to fill the research gap in this field and provide a relevant basis for the formulation of relevant policies and regulations as well as a reference for the decision-making of EV power battery recycling-related enterprises.

3. Model Description and Construction

3.1. Problem Description. Data barriers and technical barriers exist between EV power battery recycling subjects and government enterprises, which make it more difficult for enterprises to recycle spent EV power batteries and for the government to supervise each recycling subject. The Ministry of Industry and Information Technology requires the establishment of a power battery traceability platform, so as to realize the information collection of the whole process of power battery production, use, end of life, recycling, and utilization. It can also realize the implementation of the monitoring of the responsibility of each link subject to fulfill the recycling. However, the existing EV power battery traceability system for energy vehicles cannot guarantee a high level of system reliability and data security, enterprises are not highly motivated to participate in power battery traceability management, and China's policies and regulations in this field still need to be improved, resulting in the slow promotion of EV power battery traceability management in China. Blockchain technology is characterized by

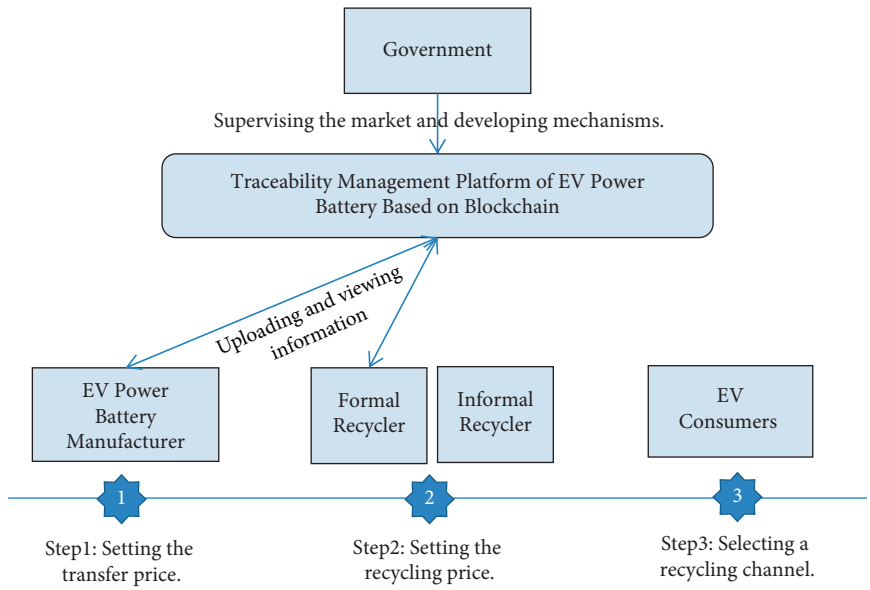

Figure 1: Topological structure diagram of the model.

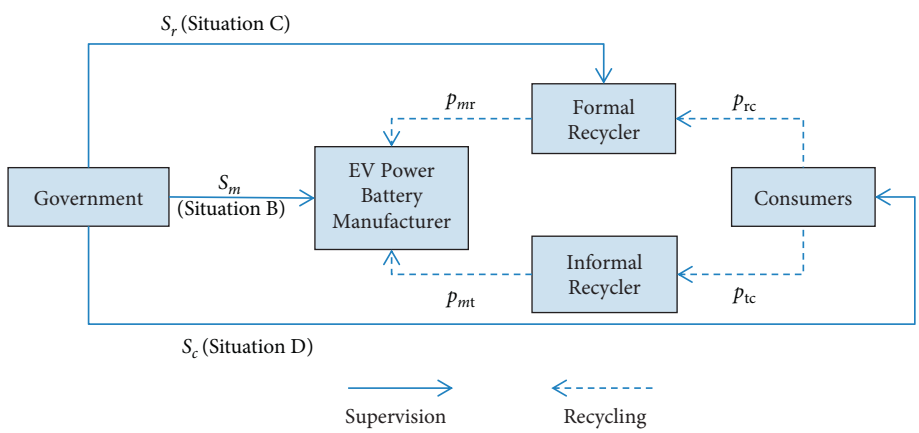

Figure 2: Framework of EV power battery recycling.

immutability and distributed storage among other characteristics. The data security problem of the power battery traceability system can be solved using computer technologies such as point-to-point transmission, consensus mechanism, and encryption algorithm. EV power battery manufacturer can provide technical support to the formal recycler through the traceability management platform to improve the rate of echelon use. And the government can supervise the EV power battery recycling market through the EV power battery traceability management platform and adjust the relevant mechanism, as shown in Figure 1.

In the context of EV power battery traceability management by blockchain technology, this study constructs a reverse supply chain comprising an EV power battery manufacturer, a power battery formal recycler, a power battery informal recycler, and consumers. Figure 2 shows the specific structure. Three government mechanisms are considered in this paper to promote the participation of each recycling subject in power battery traceability management: a reward and punishment mechanism for EV power battery manufacturers (situation B); a subsidy mechanism for formal recyclers (situation C); and a subsidy mechanism for consumers (situation D). EV power battery manufacturers have two channels to choose from: formal recycling channels and informal recycling channels. Informal recycler adopts door-to-door recycling, and formal recycler adopts the method of allowing consumers to send spent EV power batteries to stores or formal recycling stations in the community. This study assumes that $p_{rc} > p_{tc}$ because the relatively inconvenient recycling channels need to attract consumers to participate in recycling by increasing the recycling price [9]. The personnel involved in the recycling process inspect, classify, and discharge the batteries according to the information provided by the EV power battery manufacturer and the status of the actual batteries. The recycled batteries are prioritized for echelon use. Furthermore, materials are extracted from them for remanufacturing batteries that are not available for echelon use.

Table 1: The description of the symbols.

Parameters	Meaning
Q	The potential market size
A	The profit of echelon use
B	The profit of extracting metal materials
θ_r	The rate of echelon use of an EV power battery processed by the formal recycler
θ_t	The rate of echelon use of an EV power battery processed by the informal recycler
k	Increase factor of the echelon use rate of EV power batteries participating in blockchain traceability management
q_{rc}	Number of recycled batteries from the formal recycler
q_{tc}	Number of recycled batteries from the formal recycler
q	Number of EV power batteries delivered by consumers without compensation
α	Sensitivity factor of consumers to the recycling price
β	Recycling competition coefficient between the formal and informal recycler
p_{rc}	Recycling price per unit for the formal recycler
p_{tc}	Recycling price per unit for the informal recycler
p_{mr}	Unit transfer price paid by the power cell manufacturer to the formal recycler
p_{mt}	Unit transfer price paid by the power cell manufacturer to the informal recycler
c_r	Unit recycling disposal cost for the formal recycler
c_t	Unit recycling processing cost for the informal recycler
I	Blockchain operation cost
ξ_0	Minimum target recycling rate set by the government
S_i	$i = m, c, r$
S_m	The amount of incentives and penalties the government issues to the manufacturer participating in blockchain traceability management
S_c	The amount of subsidy the government issues to the consumers participating in blockchain traceability management
S_r	The amount of subsidy the government issues to the recycler participating in blockchain traceability management
Π_m	The profit of the EV power battery manufacturer
Π_r	The profit of the formal recycler
Π_t	The profit of the informal recycler

3.2. Model Assumptions and Parameters' Description. We have made some assumptions about this article based on the research of related scholars:

(1) For simplification, we assume that the recycling market comprises an EV power battery manufacturer, a formal recycler, and an informal recycler [34].

(2) This study only considers the power batteries sold with EVs. Moreover, all the EV power batteries sold can be recycled. Therefore, the total supply of the EV power battery recycling market is the total supply of the EV sales market Q.

(3) A recycled EV power battery is a single type [22].

(4) The EV power battery traceability management platform established based on the blockchain allows only government-certified enterprises with recycling and processing qualifications to participate. This study classifies such enterprises as formal recyclers. The government cannot regulate the market transactions between the power battery manufacturer and informal recycler. Therefore, the recycling rate θ calculated from the government's perspective is the ratio of the recycling quantity q_{rc} from formal recycling channels to the total supply quantity Q.

(5) The recycling volume under each recycling channel is affected by the recycling price. The recycling function of the informal recycler is $q_{tc} = q + \alpha p_{tc} - \beta p_{rc}$, while that of the formal recycler is $q_{rc} = \alpha p_{rc} - \beta p_{tc}$, where $\alpha > \beta > 0$.

(6) The residual value of the recycled EV power battery is not 0; that is, $A + B > 0$. To ensure the profit of each subject, let $p_{mr} > p_{rc}$ and $p_{mt} > p_{tc}$.

(7) EV power battery manufacturer as the producer bears the main responsibility of recycling, consumers are the source of recycling, and formal recyclers are the main recycling enterprises. Therefore, the initial stage can be assumed that $S_c > S_r > S_m$. The above rewards and penalties and subsidies can be adjusted later according to the actual situation.

(8) EV power battery manufacturer acts as the leader of Stackelberg, and the recycler modifies the strategy to be adopted according to the EV power battery manufacturer.

The symbols are described in the text as shown in Table 1.

3.3. Stackelberg Game Model

3.3.1. Mode A: Nonparticipation in Blockchain Traceability Management. In the process of EV power battery recycling, EV power battery manufacturer sets the transfer price of EV power batteries according to the market supply and demand situation firstly; then, the EV power battery formal recycler and informal recycler set the recycling recovery price according to the transfer price; finally, consumers pursue utility maximization and choose the recycling channel

according to the recycling price and convenience of recycling given by each recycler. Therefore, in the case of no government mechanism intervention (situation A), the profit functions of the EV power battery manufacturer, formal recycler, and informal recycler can be expressed, respectively, as follows.

The profit function of the EV power battery manufacturer can be expressed as

$$\begin{aligned}\Pi_m^A = &\left[A\theta_r + B(1-\theta_r) - p_{mr}\right](\alpha p_{rc} - \beta p_{tc}) \\ &+ \left[A\theta_t + B(1-\theta_t) - p_{mt}\right](q + \alpha p_{tc} - \beta p_{rc}), \\ &A\theta_r + B(1-\theta_r).\end{aligned} \tag{1}$$

The EV power battery manufacturer needs to pay the cost of transfer p_{mr} or p_{mt} to the recycler and make profits from the batteries by echelon use A or extracting metal materials B.

The profit function of the formal recycler can be expressed as

$$\Pi_r^A = (p_{mr} - p_{rc} - c_r)(\alpha p_{rc} - \beta p_{tc}). \tag{2}$$

The profit function of the informal recycler can be expressed as

$$\Pi_t^A = (p_{mt} - p_{tc} - c_t)(q + \alpha p_{tc} - \beta p_{rc}). \tag{3}$$

The profit of recyclers is the revenue received from the EV power battery manufacturer p_{mr} or p_{mt} minus the cost of recycling p_{rc} or p_{tc}.

Proposition 1. *Equation (1) is a concave function regarding p_{mt} and p_{mr}; there exists a unique optimal solution.*

Proof. The second-order partial derivatives of equation (1) for p_{mt} and p_{mr}, respectively, give

$$\begin{aligned}H\left(\Pi_m^A\right) &= \begin{bmatrix} \dfrac{\partial^2 \Pi_m^A}{\partial p_{mr}^2} & \dfrac{\partial^2 \Pi_m^A}{\partial p_{mr} p_{mt}} \\ \dfrac{\partial^2 \Pi_m^A}{\partial p_{mt} p_{mr}} & \dfrac{\partial^2 \Pi_m^A}{\partial p_{mt}^2} \end{bmatrix} \\ &= \begin{bmatrix} \dfrac{2\alpha\left(\beta^2 - 2\alpha^2\right)}{4\alpha^2 - \beta^2} & \dfrac{2\alpha^2\beta}{4\alpha^2 - \beta^2} \\ \dfrac{2\alpha^2\beta}{4\alpha^2 - \beta^2} & \dfrac{2\alpha\left(\beta^2 - 2\alpha^2\right)}{4\alpha^2 - \beta^2} \end{bmatrix}.\end{aligned} \tag{4}$$

Because $H_{11} = (2\alpha(\beta^2 - 2\alpha^2)/4\alpha^2 - \beta^2) < 0$, det $(H) = (4\alpha^2(\alpha^2 - \beta^2)/4\alpha^2 - \beta^2) > 0$, and then the Hessian matrix of equation (1) is negative definite; therefore, equation (1) is a concave function regarding p_{mt} and p_{mr}; there exists a unique optimal solution. □

Proposition 2. *Equations (2) and (3) are concave functions regarding p_{rc} and p_{tc}; there exists a unique optimal solution.*

Proof. The first-order partial derivatives and second-order partial derivatives of equations (2) and (3) regarding p_{rc} and p_{tc}, respectively, give

$$\begin{aligned}\frac{\partial \Pi_r^A}{\partial p_{rc}} &= -\alpha c_r + \alpha p_{mr} - 2\alpha p_{rc} + \beta p_{tc}, \\ \frac{\partial^2 \Pi_r^A}{\partial p_{rc}^2} &= -2\alpha, \\ \frac{\partial \Pi_t^A}{\partial p_{tc}} &= -q - \alpha c_t + \alpha p_{mt} + \beta p_{rc} - 2\alpha p_{tc}, \\ \frac{\partial^2 \Pi_t^A}{\partial p_{tc}^2} &= -2\alpha.\end{aligned} \tag{5}$$

From the partial derivatives of the above solution, $(\partial^2 \Pi_r^A / \partial p_{rc}^2) = (\partial^2 \Pi_t^A / \partial p_{tc}^2) = -2\alpha < 0$. Therefore, equations (2) and (3) are concave functions regarding p_{rc} and p_{tc}, respectively: there exists a unique optimal solution.

The solution of equations (1)–(3) is solved using the inverse induction method; Appendix shows the results. □

3.3.2. Mode B: Participate in Blockchain Traceability Management—Adopt a Reward and Punishment Mechanism for the Manufacturer. Spent EV power batteries need to go through steps such as dismantling and testing before being used in the echelon, and informal recyclers face many technical difficulties in processing. Through the blockchain traceability management platform, formal recycler can obtain the status information of EV power batteries and technical support provided by the battery manufacturer, which can improve the gradient utilization rate to a certain extent. The increased gradient echelon use rate is expressed in terms of k; the utilization rate is $(k + \theta_r)$. Meanwhile, when participating in EV power battery blockchain traceability management, EV power battery manufacturer and formal recycler need to pay management costs I, including network costs and labor costs. Therefore, in the situation of the government adopts a reward and punishment mechanism for the EV power battery manufacturer participating in blockchain traceability management (situation B), the profit functions of the EV power battery manufacturer, formal recycler, and informal recycler can be expressed, respectively, as follows.

The profit function of the EV power battery manufacturer can be expressed as

$$\Pi_m^B = [A(k+\theta_r) + B(1-\theta_r-k) - p_{mr}](\alpha p_{rc} - \beta p_{tc}) + [A\theta_t + B(1-\theta_t) - p_{mt}](q + \alpha p_{tc} - \beta p_{rc}) + S_m(\alpha p_{rc} - \beta p_{tc} - \xi_0 Q) - I. \tag{6}$$

Through the blockchain traceability management platform, the government can regulate the EV power battery manufacturer and formal recycler. In situation B, the government gives rewards to the EV power battery manufacturer when the actual recycling quantity is greater than the target recycling quantity; on the contrary, the government gives punishments to power battery manufacturers when the actual recycling quantity is less than the target recycling quantity.

The profit function of the formal recycler can be expressed as

$$\Pi_r^B = (p_{mr} - p_{rc} - c_r)(\alpha p_{rc} - \beta p_{tc}) - I. \tag{7}$$

The profit function of the informal recycler can be expressed as

$$\Pi_t^B = (p_{mt} - p_{tc} - c)_t(q + \alpha p_{tc} - \beta p_{rc}). \tag{8}$$

As in Propositions 1 and 2, equations (4)–(6) are solved using the inverse induction method; Appendix shows the solution results.

3.3.3. Mode C: Participate in Blockchain Traceability Management—Adopt a Subsidy Mechanism for the Formal Recycler. As situation B, the echelon use rate can be improved when the EV power battery manufacturer and formal recycler participate in blockchain traceability management, while they need to pay a certain management cost I. Therefore, in the situation of the government adopts a subsidy mechanism for formal recyclers who participate in blockchain traceability management (situation C), the profit functions of the EV power battery manufacturer, formal recycler, and informal recycler can be expressed, respectively, as follows.

The profit function of the EV power battery manufacturer can be expressed as

$$\Pi_m^C = [A(k+\theta_r) + B(1-\theta_r-k) - p_{mr}](\alpha p_{rc} - \beta p_{tc}) + [A\theta_t + B(1-\theta_t) - p_{mt}](q + \alpha p_{tc} - \beta p_{rc}) - I. \tag{9}$$

The profit function of the formal recyclers can be expressed as

$$\Pi_r^C = (p_{mr} - p_{rc} - c_r + S_r)(\alpha p_{rc} - \beta p_{tc}) - I. \tag{10}$$

In situation C, the formal recycler may receive additional government subsidies S_r.

The profit function of the informal recycler can be expressed as

$$\Pi_t^C = (p_{mt} - p_{tc} - c_t)(q + \alpha p_{tc} - \beta p_{rc}). \tag{11}$$

As in Propositions 1 and 2, equations (7)–(9) are solved using the inverse induction method; Appendix shows the solution results.

3.3.4. Mode D: Participate in Blockchain Traceability Management—Adopt a Subsidy Mechanism for Consumers. As situation B, the echelon use rate can be improved when the EV power battery manufacturer and formal recycler participate in blockchain traceability management, while they need to pay a certain management cost I. Therefore, in the situation of the government adopts a subsidy mechanism for consumers who hand over spent EV power batteries to the formal recycler (situation D), the profit functions of the power battery manufacturer, formal recycler, and informal recycler can be expressed as follows, respectively.

The profit function of the EV power battery manufacturer can be expressed as

$$\Pi_m^D = [A(k+\theta_r) + B(1-\theta_r-k) - p_{mr}][\alpha(p_{rc} + S_c) - \beta p_{tc}] + [A\theta_t + B(1-\theta_t) - p_{mt}][q + \alpha p_{tc} - \beta(p_{rc} + S_c)] - I. \tag{12}$$

The profit function of the formal recycler can be expressed as

$$\Pi_r^D = (p_{mr} - p_{rc} - c_r + S_r)[\alpha(p_{rc} + S_c) - \beta p_{tc}] - I. \tag{13}$$

In situation D, the government gives subsidies to consumers through formal recyclers.

The profit function of the informal recycler can be expressed as

$$\Pi_t^D = (p_{mt} - p_{tc} - c_t)(q + \alpha p_{tc} - \beta p_{rc}). \tag{14}$$

As in Propositions 1 and 2, equations (10)–(12) are solved using the inverse induction method; Appendix shows the solution results.

4. Model Analysis

4.1. Analysis of the Impact of Participation in Blockchain Traceability Management on Recycling Prices

Proposition 3. $p_{mt}^A = p_{mt}^B = p_{mt}^C = p_{mt}^D$.

Proof. According to the result of the inverse induction method of solving, we obtain

$$p_{mt}^A = p_{mt}^B = p_{mt}^C = p_{mt}^D = \frac{-q\alpha + B\alpha^2 - B\beta^2 + (\alpha^2 - \beta^2)c_t + (A-B)(\alpha^2 - \beta^2)\theta_t}{2(\alpha^2 - \beta^2)}. \tag{15}$$

Proposition 3 illustrates that the transfer price paid by the EV power battery manufacturer to the informal recycler is unaffected regardless of whether the EV power battery manufacturer and formal recycler participate in blockchain traceability and the mechanism adopted by the government. □

Proposition 4. *When* $(A-B)k+2c_r>S_c$, $p_{mr}^B>p_{mr}^C>p_{mr}^D>p_{mr}^A$.

Proof. When $(A-B)k+2c_r>S_c$,

$$p_{mr}^B-p_{mr}^C=\frac{1}{2}\left(S_m+S_r\right)>0,$$
$$p_{mr}^C-p_{mr}^D=\frac{1}{2}\left(S_c+S_r\right)>0, \tag{16}$$
$$p_{mr}^D-p_{mr}^A=\frac{1}{2}\left((A-B)k+2c_r-S_c>0\right).$$

When $(A-B)k+2c_r<S_c$, $p_{mr}^D-p_{mr}^A=(1/2)\left((A-B)k+2c_r-S_c<0\right)$.

Proposition 4 illustrates that, after the EV power battery manufacturer and formal recycler participate in blockchain traceability, when $(A-B)k+2c_r>S_c$, the transfer price paid by the EV power battery manufacturer to the formal recycler is greater than the transfer price when they do not participate in blockchain traceability management, and it is greatest when incentives and penalties are adopted for the EV power battery manufacturer. This is because an increase in the transfer price by the EV power battery manufacturer can help the formal recycler to recycle EV power batteries, hence recycling more EV power batteries, avoiding penalties, and obtaining more government subsidies. When $(A-B)k+2c_r<S_c$, the government pays more subsidies to consumers through the formal recycler. The formal recycler has a stronger competitive advantage in recycling prices and can recycle more EV power batteries, at which time the EV power battery manufacturer will appropriately reduce the transfer price paid to the formal recycler. □

Proposition 5. *When* $((A-B)k\alpha^2/3\alpha^2-\beta^2)>S_c$, $p_{rc}^C>p_{rc}^B>p_{rc}^D>p_{rc}^A$.

Proof. When $((A-B)k\alpha^2/3\alpha^2-\beta^2)>S_c$,

$$p_{rc}^C-p_{rc}^B=\frac{\alpha^2\left(S_r-S_m\right)}{4\alpha^2-\beta^2}>0,$$
$$p_{rc}^B-p_{rc}^D=\frac{\left(3\alpha^2-\beta^2\right)S_c+\alpha^2S_m}{4\alpha^2-\beta^2}>0, \tag{17}$$
$$p_{rc}^D-p_{rc}^A=\frac{(A-B)k\alpha^2-\left(3\alpha^2-\beta^2\right)S_c}{4\alpha^2-\beta^2}>0.$$

When $((A-B)k\alpha^2/3\alpha^2-\beta^2)<S_c$, $p_{rc}^D-p_{rc}^A=((A-B)k\alpha^2-(3\alpha^2-\beta^2)S_c/4\alpha^2-\beta^2)<0$.

Proposition 5 illustrates that, after the EV power battery manufacturer and formal recycler participate in blockchain traceability, when $((A-B)k\alpha^2/3\alpha^2-\beta^2)<S_c$, the recycling price paid by the formal recycler to consumers is greater than that when they do not participate in blockchain traceability management. The recycling price is greatest when the subsidy mechanism is adopted for the formal recycler. This is because the increase in the recycling price by the formal recycler will increase the competitive advantage, which can help consumers to deliver spent EV power batteries to the formal recycler and consequently receive more government subsidies. When $((A-B)k\alpha^2/3\alpha^2-\beta^2)<S_c$, the government pays more subsidies to consumers through the formal recycler. The formal recycler has a stronger competitive advantage in recycling price in this case. Therefore, the formal recycler can also recycle EV power batteries by appropriately reducing the recycling price paid to consumers. □

Proposition 6. $p_{tc}^D>p_{tc}^C>p_{tc}^B>p_{tc}^A$.

Proof.

$$p_{tc}^D-p_{tc}^C=\frac{\alpha\beta\left(S_c-S_r\right)}{8\alpha^2-2\beta^2}>0,$$
$$p_{tc}^C-p_{tc}^B=\frac{\alpha\beta\left(S_r-S_m\right)}{8\alpha^2-2\beta^2}>0, \tag{18}$$
$$p_{tc}^B-p_{tc}^A=\frac{\alpha\beta\left((A-B)k+S_m\right)}{8\alpha^2-2\beta^2}>0.$$

Proposition 6 illustrates that, after the EV power battery manufacturer and formal recycler participate in blockchain traceability, the recycling price paid by the informal recycler to consumers is greater than the recycling price when they do not participate in blockchain traceability management. The recycling price paid to consumers is greatest when a subsidy mechanism is adopted by consumers. At this time, the formal recycler has a stronger competitive advantage. Therefore, the informal recycler must increase the recycling price to be more competitive and further obtain more EV power batteries. □

4.2. Analysis of the Impact of Participation in Blockchain Traceability Management on the Number of Recycling

Proposition 7. $q_{rc}^D>q_{rc}^C>q_{rc}^B>q_{tc}^A$; $q_{tc}^A>q_{tc}^B>q_{tc}^C>q_{tc}^D$.

Proof.

Table 2: Summary of the values of the parameters.

Parameter	Q	A	B	θ_r	θ_t	k	α	β	q	c_r	c_t	I	ξ_0	S_m	S_r	S_c
Value	111,509	11,388	1541	0.56	0.3	0.14	3.1	1.2	500	340	200	101,257	0.2	1500	1700	2000

Table 3: The profit of each recycling subject.

	Π_m	Π_r	Π_t
Situation A	1.99×10^7	6.13×10^6	1.68×10^6
Situation B	1.99×10^6	1.35×10^7	1.08×10^6
Situation C	3.68×10^7	2.86×10^6	1.05×10^6
Situation D	3.88×10^7	1.51×10^7	9.95×10^5

$$\begin{aligned}
q_{rc}^D - q_{rc}^C &= \frac{\alpha\left(2\alpha^2 - \beta^2\right)\left(S_c - S_r\right)}{8\alpha^2 - 2\beta^2} > 0,\\
q_{rc}^C - q_{rc}^B &= \frac{\alpha\left(2\alpha^2 - \beta^2\right)\left(S_r - S_m\right)}{8\alpha^2 - 2\beta^2} > 0,\\
q_{rc}^B - q_{rc}^A &= \frac{\alpha\left(2\alpha^2 - \beta^2\right)\left((A - B)k + S_m\right)}{8\alpha^2 - 2\beta^2} > 0,\\
q_{tc}^A - q_{tc}^B &= \frac{\alpha^2\beta\left((A - B)k + S_m\right)}{8\alpha^2 - 2\beta^2} > 0,\\
q_{tc}^B - q_{tc}^C &= \frac{\alpha^2\beta\left(S_r - S_m\right)}{8\alpha^2 - 2\beta^2} > 0,\\
q_{tc}^C - q_{tc}^D &= \frac{\alpha^2\beta\left(S_c - S_r\right)}{8\alpha^2 - 2\beta^2} > 0.
\end{aligned} \tag{19}$$

Proposition 7 illustrates that, after the EV power battery manufacturer and formal recycler participate in blockchain traceability, the formal recycler obtains more EV power batteries than when they do not participate in blockchain traceability management, while the informal recycler does the opposite. Furthermore, the formal recycler obtains the most EV power batteries, and the informal recycler obtains the least EV power batteries when the subsidy mechanism is adopted for consumers. Therefore, the participation of the EV power battery manufacturer and formal recycler in blockchain traceability helps promote the flow of retired EV power batteries to the formal recycling market and reduces black market transactions. The results are optimal when the government adopts the subsidy mechanism for consumers.

Considering that the profit of each recycling subject is complex, it cannot be analyzed directly using the method of analyzing profit expressions. Therefore, it is compared after solving in the arithmetic part. □

5. Numerical Analysis

5.1. Numerical Example. In this study, taking the Beijing New Energy Vehicle (BJEV) as an example, according to the Annual Production and Sales Snapshot of BJEV (2018–2020, three-year average sales), the potential market size Q is assumed to be 111,509. According to [16, 22, 23, 33], we obtained the relevant data of the EV power battery recycling shown in Table 2.

Table 3 shows the profits of the EV power battery manufacturer, formal recycler, and informal recycler under different scenarios.

As shown in Table 3, $\Pi_m^D > \Pi_m^C > \Pi_m^A > \Pi_m^B$, $\Pi_r^D > \Pi_r^B > \Pi_r^A > \Pi_r^C$, and $\Pi_t^A > \Pi_t^B > \Pi_t^C > \Pi_t^D$.

The profit of the EV power battery manufacturer after participating in blockchain traceability management is smaller when the government adopts the reward and punishment mechanism for the manufacturer than when they do not participate in blockchain traceability management. The profit is, however, larger when the government adopts the subsidy mechanism for consumers and the subsidy mechanism for the formal recycler than when they do not participate in blockchain traceability management. The profit is the largest when the government adopts the subsidy mechanism for consumers.

The profit of the formal recycler after participating in blockchain traceability management is smaller when the government adopts the subsidy mechanism for the formal recycler than when they do not participate in blockchain traceability management. The profit is, however, larger when the government adopts the subsidy mechanism for consumers and the reward and punishment mechanism for the EV power battery manufacturer than when they do not participate in blockchain traceability management. It is the largest when the government adopts the subsidy mechanism for consumers.

The profit of the informal recycler after each recycling subject participates in blockchain traceability management is smaller than when they do not participate in blockchain traceability management. The profit of the informal recycler is smaller than when they do not participate in blockchain traceability management; it is the smallest when the government adopts a subsidy mechanism for consumers.

In summary, it is evident that when the government adopts a subsidy mechanism for consumers, the EV power battery manufacturer and formal recycler realize the largest profits, while the informal recycler realizes the smallest profit. This promotes the participation of the EV power battery manufacturer and formal recycler in EV power battery blockchain traceability management.

5.2. Sensitivity Analysis. When the subsidy mechanism is adopted for the formal recycler and the subsidy mechanism is adopted for consumers, the expressions of the relationship between the profit of the EV power battery manufacturer Π_m^C and government subsidy S_r and those between the profit of the power battery manufacturer Π_m^D and government subsidy S_c are similar (see Appendix). Therefore, the images reflected in Figure 3 overlap.

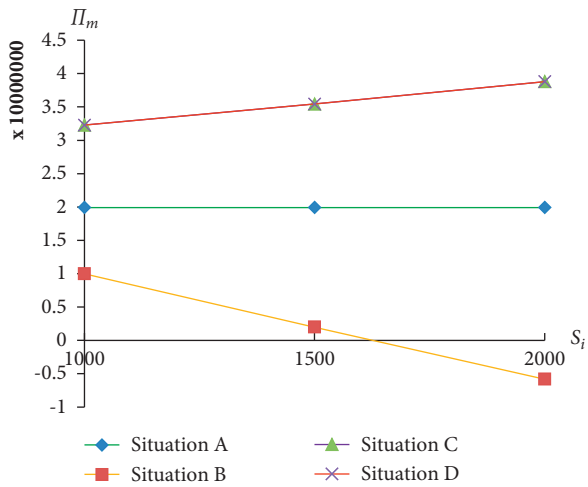

Figure 3: Impact of government mechanisms on the profits of the power cell manufacturer.

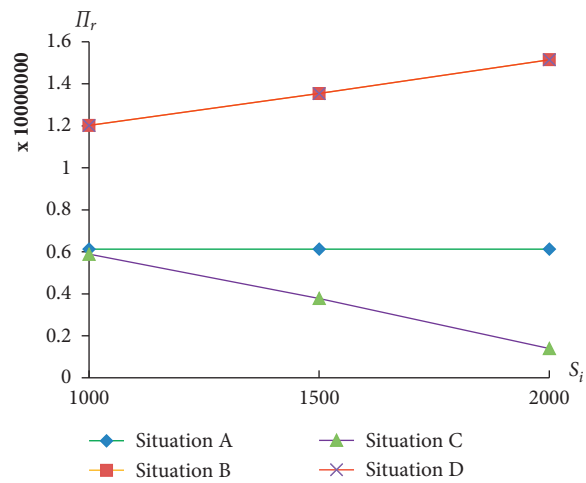

Figure 4: Impact of government mechanisms on the profits of the formal recycler.

The expressions of the relationship between the profit Π_r^B of the formal recycler and the government subsidy S_m and the expressions of the relationship between the profit Π_r^D of the formal recycler and the government subsidy S_c are similar when the incentive and punishment mechanism is adopted for the EV power battery manufacturer and the subsidy mechanism is adopted for the consumer (see Appendix). Therefore, the images reflected in Figure 4 overlap.

The expression of the relationship between the profit of informal recyclers Π_t^B and government subsidy S_m, the expression of the relationship between the profit of formal recyclers Π_t^C and government subsidy S_r, and the expression of the relationship between the profit of the formal recycler Π_t^D and government subsidy S_c are similar when the incentive and punishment mechanism is adopted for the EV power battery manufacturer, the subsidy mechanism is adopted for formal recyclers, and the subsidy mechanism is adopted for consumers (see Appendix). Therefore, the images reflected in Figure 5 overlap.

Figures 3–5 show that, after each recycling subject joins the blockchain traceability management, when the reward and punishment mechanism is adopted for EV power battery manufacturers, the profits of the EV power battery manufacturer and formal recycler are positively proportional to the amount of reward and punishment. The profit of the informal recycler, however, is inversely proportional to the amount of reward and punishment. When the subsidy mechanism is adopted for the formal recycler, the profit of the EV power battery manufacturer is positively proportional to the amount of subsidy, and the profits of formal and informal recyclers are inversely proportional to the amount of subsidy. When the subsidy mechanism is adopted for consumers, the profits of the EV power battery manufacturer and formal recycler are proportional to the amount of rewards and penalties. Moreover, the profit of the informal recycler is inversely proportional to the amount of rewards and penalties.

In summary, when the subsidy mechanism is adopted for formal recyclers, increasing the subsidy amount reduces the

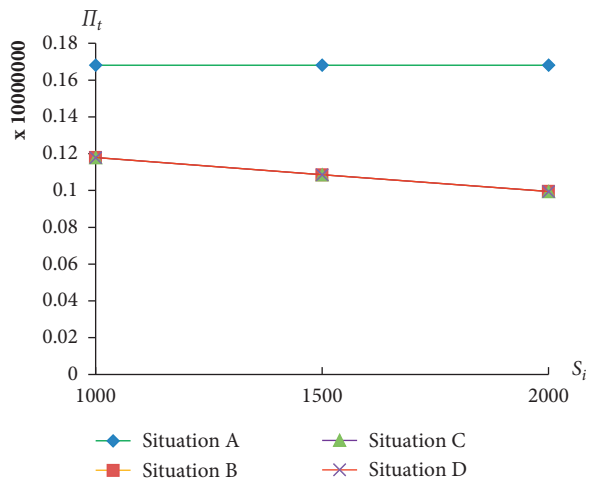

Figure 5: Impact of government mechanisms on the profits of the informal recycler.

profits of formal recyclers, which does not promote the participation of the formal recycler in blockchain traceability management and affects the normal implementation of EV power battery traceability management. However, increasing the amount of rewards and punishments for the EV power battery manufacturer and the amount of subsidies for consumers helps to increase the profits of the EV power battery manufacturer and formal recycler, suppressing the informal recycler and consequently reducing black market transactions and promoting the participation of each recycling subject in EV power battery blockchain traceability management; the results are optimal when consumers adopt the subsidy mechanism.

Figure 6 shows that, after each recycling subject joins blockchain traceability management, the profit of the EV power battery manufacturer is inversely proportional to the target recycling rate set by the government when the government adopts a reward and punishment mechanism for the EV power battery manufacturer. However, when the

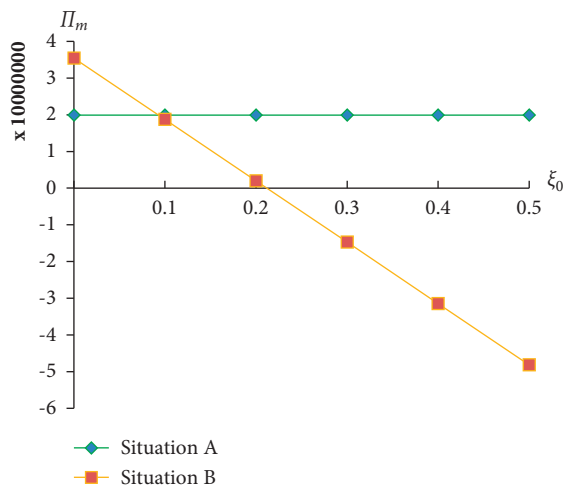

Figure 6: Impact of target recycling rate on the profit of the EV power battery manufacturer.

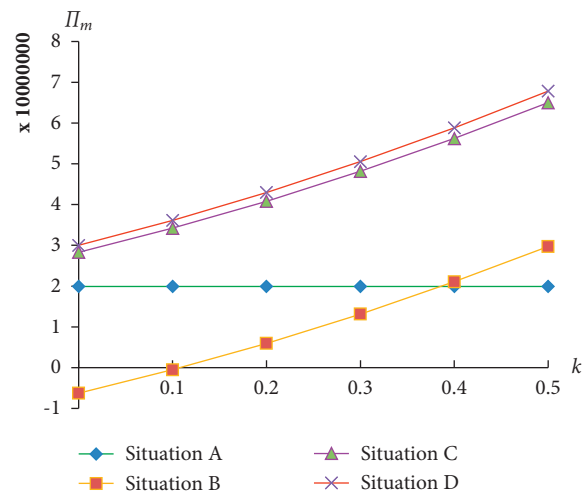

Figure 7: Effect of the increase factor of echelon use rate on the profit of the EV power battery manufacturer.

target recycling rate set by the government $\xi_0 \geq 0.0928$, the profit of the EV power battery manufacturer after participating in blockchain traceability management is smaller than that when they do not participate in blockchain traceability management. Moreover, the profit of the EV power battery manufacturer is negative when $\xi_0 \geq 0.212$. This is because the power battery manufacturer can only receive subsidies if their actual recycling rate is higher than the target recycling rate set by the government; otherwise, they will be penalized. Therefore, when the government adopts the reward and punishment mechanism for the EV power battery manufacturer, it should not pursue an excessively high target recycling rate at the primary stage. The government should set an appropriate target recycling rate to promote the participation of the EV power battery manufacturer in the blockchain traceability management and therefore ensure the normal implementation of the traceability management of EV power batteries. After the EV power battery manufacturer participates in blockchain traceability management, the government can adjust the target recycling rate according to the actual situation.

Figure 7 shows that the profit of EV power battery manufacturers is proportional to the increase factor of the echelon use rate. Therefore, EV power battery manufacturers can improve the echelon use rate by providing relevant technical support to EV power battery recyclers to increase the profit. When the increase factor of the echelon use rate is certain, the profit of the EV power battery manufacturer is the largest when the government adopts the subsidy mechanism for consumers, followed by the subsidy mechanism for the formal recycler. When the increase factor of the echelon use rate $k \leq 0.385$, the profit of EV power battery manufacturers when the reward and punishment mechanism is adopted is smaller than the profit when they do not participate in blockchain traceability management; when $k \leq 0.108$, the profit of EV power battery manufacturers is negative. Therefore, the enthusiasm of the manufacturer to participate in blockchain traceability management is smaller, which is not

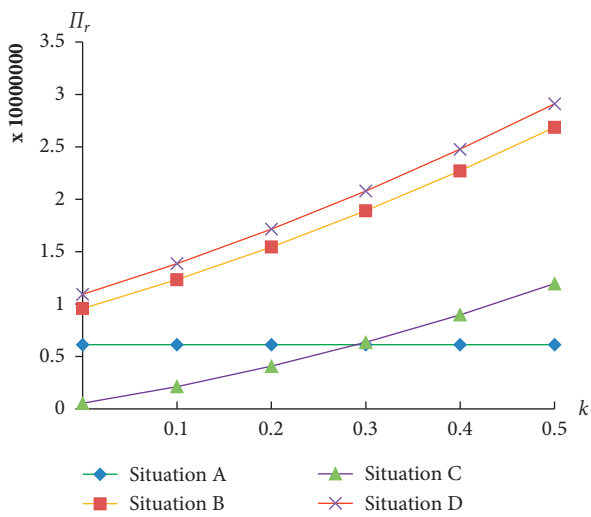

Figure 8: Effect of the increase factor of echelon use rate on the profit of the formal recycler.

conducive to the normal implementation of EV power battery traceability management.

Figure 8 shows that the profit of formal recyclers is proportional to the increase in the echelon use rate; therefore, the formal recycler can improve the echelon use rate by improving the recycling processing technology, hence increasing the profit. When the increase factor of the echelon use rate is certain, the profit of the formal recycler is the largest when the government adopts the subsidy mechanism for consumers, followed by the incentive and punishment mechanism for the EV power battery manufacturer. When the subsidy mechanism is adopted for the formal recycler, the profits of the formal recycler are smaller than those when they do not participate in blockchain traceability management when the echelon use rate increase factor $k < 0.291$, and the enthusiasm of formal recyclers to participate in blockchain traceability

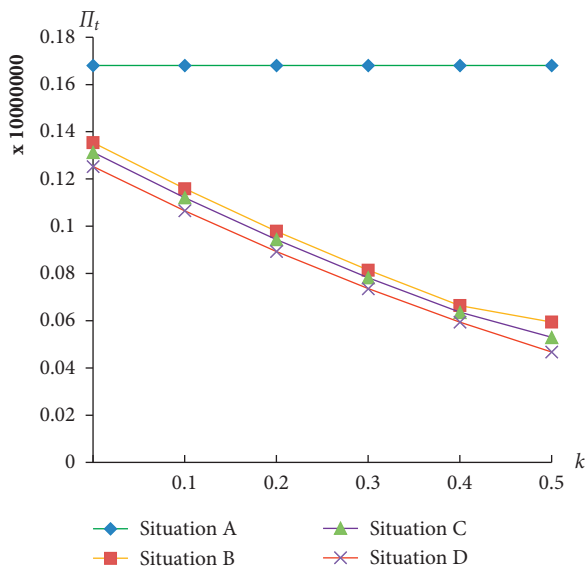

Figure 9: Effect of the echelon use increase factor on profits of the informal recycler.

management is smaller in this case, which is not conducive to the normal implementation of EV power battery traceability management.

Figure 9 shows that the profit of the informal recycler is inversely proportional to the echelon use increase factor, and the profit of the informal recycler is smaller than the profit realized when they do not participate in blockchain traceability management after each recycling subject participates in blockchain traceability management. When the echelon use rate increases by a certain factor, the profit of the informal recycler is the smallest when the government adopts a subsidy mechanism for consumers, followed by the profit when the subsidy mechanism is adopted for the formal recycler. Therefore, it can be proved that the government's adoption of mechanisms to promote the participation of each recycler in blockchain traceability management can play a role in suppressing informal recyclers, hence reducing black market transactions and promoting the transformation of the informal recycler.

6. Conclusions

To explore the strategies to improve the enthusiasm of EV power battery recycling subjects to participate in traceability management, this study considers factors such as the echelon use rate, government mechanism, and blockchain cost and constructs a Stackelberg game model comprising the power battery manufacturer, formal recycler, and informal recycler. Based on this model, the changes in the unit recycling price, recycling quantity, and profit of each recycling subject under different government mechanisms before and after each recycling subject participates in power battery traceability management are compared and analyzed. The main findings of this study are as follows:

(1) The participation of each recycling subject in EV power battery blockchain traceability helps improve the competitive advantage of formal recyclers, suppress informal recyclers, promote more retired power batteries into formal recycling channels and markets, and further reduce black market transactions. Additionally, the adoption of appropriate mechanisms by the government promotes the participation of each recycling subject of EV power batteries in blockchain traceability management, with the best result when the government adopts a subsidy mechanism for consumers.

(2) After each recycling subject participates in blockchain traceability management, the profits of the formal recycler and EV power battery manufacturer when the government adopts the reward and punishment mechanism for EV power battery manufacturers are positively proportional to the amount of government rewards and punishments, and the profits of the informal recycler are inversely proportional to the amount of government rewards and punishments. Therefore, the government increases the amount of rewards and punishments, which promotes the participation of each recycling subject in blockchain traceability management. Therefore, when the government adopts the reward and punishment mechanism for the EV power battery manufacturer, it should not pursue an excessively high target recycling rate at the primary stage. The government should set an appropriate target recycling rate to promote the participation of the EV power battery manufacturer in blockchain traceability management and consequently ensure the normal implementation of the traceability management of EV power batteries.

(3) After each recycling subject participates in blockchain traceability management, the profits of the formal recycler and EV power battery manufacturer when the government adopts the reward and punishment mechanism for formal recyclers are positively proportional to the amount of government subsidies, and the profits of the informal recycler are inversely proportional to the amount of government rewards and punishments. The profits of the formal recycler after participating in blockchain traceability management are smaller than the profits realized when they do not participate in blockchain traceability management. This does not promote the participation of formal recyclers in blockchain traceability management of EV power batteries and cannot ensure the normal implementation of traceability management of EV power batteries.

(4) The profits of power battery manufacturers and formal recyclers are positively proportional to the increase in the echelon use rate. Furthermore, the profits of informal recyclers are inversely proportional to the increase factor of the echelon use rate; therefore, the results are optimal when the subsidy mechanism is adopted for consumers. However, when the increase factor of the echelon use rate is

small, the profit after adopting the reward and punishment mechanism for EV power battery manufacturers or adopting a subsidy mechanism for formal recyclers is smaller than the profit realized when participating in blockchain traceability management. Therefore, the government should adopt a mechanism to encourage EV power battery manufacturers to provide relevant technical support to EV power battery recyclers to improve the echelon use rate, so as to consequently increase the profit of each recycling subject and promote the participation of each recycling subject in EV power battery blockchain traceability.

In summary, in the initial stage of blockchain traceability management of EV power batteries, the government should play a leading role in establishing an institutional system that promotes the participation of various recycling subjects in the blockchain traceability management of EV power batteries. Additionally, it should set a reasonable target recycling rate and the amount of rewards and penalties, which can be adjusted according to the actual situation at a later stage. Simultaneously, formal recycling enterprises should be encouraged to adopt various ways to provide convenient recycling services for EV consumers, so as to prompt consumers to hand over EV power batteries to formal recycling enterprises. Under the guarantee of the government mechanism, the EV power battery recycling enterprises should actively participate in the EV power battery blockchain traceability management work to truly realize that the source of the EV power battery and the destination can be traced and consequently ensure that the spent EV power battery can be safely and environmentally friendly recycled and disposed and reused. Additionally, battery manufacturing enterprises should strengthen cooperation with formal recycling and processing enterprises, improve the echelon use rate of the spent EV power battery gradient, achieve safe recycling and environmental protection treatment, and continuously improve the EV power battery recycling industry chain.

This study has several limitations. First, for the sake of simple calculation, the EV power battery is regarded as a single type. Second, the study does not consider government and environmental benefits. Finally, the competition between multiple formal and informal recyclers is not considered. Therefore, in future research, we will consider more influencing factors and participants.

Appendix

The proofs of Propositions 1 and 2 show that there is a unique optimal solution for each profit function, so it can be solved by using the inverse induction method.

By setting $(\partial \Pi_r^A / \partial p_{rc}) = (p_{mr} - p_{rc} - c_r)(\alpha p_{rc} - \beta p_{tc}) = 0$ and $(\partial \Pi_t^A / \partial p_{tc}) = (p_{mt} - p_{tc} - c_t)(q + \alpha p_{tc} - \beta p_{rc}) = 0$ simultaneously, the following results can be obtained:

$$p_{rc}^A = -\frac{q\beta + 2\alpha^2 c_r + \alpha\beta c_t - 2\alpha^2 p_{mr} - \alpha\beta p_{mt}}{4\alpha^2 - \beta^2}, \tag{A.1}$$

$$p_{tc}^A = \frac{\alpha\left(-2q - \beta c_r - 2\alpha c_t + \beta p_{mr} + 2\alpha p_{mt}\right)}{4\alpha^2 - \beta^2}. \tag{A.2}$$

Finding the first-order derivatives of Π_m^A to p_{mr}^A and p_{mt}^A after substituting equation (1) into equations (A.1) and (A.2) and by setting $(\partial \Pi_m^A / \partial p_{mr}^A)$ and $(\partial \Pi_t^A / \partial p_{mt}^A)$ to zero simultaneously, the following results can be obtained:

$$p_{mr}^A = \frac{B\alpha^2 - q\beta - B\beta^2 + \left(\alpha^2 - \beta^2\right)c_r + (A - B)\left(\alpha^2 - \beta^2\right)\theta_r}{2\left(\alpha^2 - \beta^2\right)}, \tag{A.3}$$

$$p_{mt}^A = \frac{-q\alpha + B\alpha^2 - B\beta^2 + \left(\alpha^2 - \beta^2\right)c_t + (A - B)\left(\alpha^2 - \beta^2\right)\theta_t}{2\left(\alpha^2 - \beta^2\right)}. \tag{A.4}$$

Then, substituting equations (A.3) and (A.4) into equations (A.1) and (A.2), p_{rc}^A and p_{tc}^A can be obtained.

$$p_{rc}^A = \frac{\alpha\left(B(\alpha - \beta)(\alpha + \beta)(2\alpha + \beta) + 3q\left(-2\alpha^2 + \beta^2\right) - (\alpha - \beta)(\alpha + \beta)\left(\beta c_r + 2\alpha c_t - (A - B)\left(\beta\theta_r + 2\alpha\theta_t\right)\right)\right)}{2\left(4\alpha^4 - 5\alpha^2\beta^2 + \beta^4\right)}, \tag{A.5}$$

$$p_{tc}^A = \frac{\alpha\left(B(\alpha - \beta)(\alpha + \beta)(2\alpha + \beta) + 3q\left(-2\alpha^2 + \beta^2\right) - (\alpha - \beta)(\alpha + \beta)\left(\beta c_r + 2\alpha c_t - (A - B)\left(\beta\theta_r + 2\alpha\theta_t\right)\right)\right)}{2\left(4\alpha^4 - 5\alpha^2\beta^2 + \beta^4\right)}. \tag{A.6}$$

By substituting equations (A.5) and (A.6) into $q_{tc} = q + \alpha p_{tc} - \beta p_{rc}$ and $q_{rc} = \alpha p_{rc} - \beta p_{tc}$, q_{rc}^A and q_{tc}^A can be obtained.

$$q_{rc}^A = \frac{\alpha\left(2B\alpha^2 + q\beta - B\alpha\beta - B\beta^2 + \left(-2\alpha^2 + \beta^2\right)c_r + \alpha\beta c_t + 2A\alpha^2\theta_r - 2B\alpha^2\theta_r - A\beta^2\theta_r + B\beta^2\theta_r - A\alpha\beta\theta_t + B\alpha\beta\theta_t\right)}{8\alpha^2 - 2\beta^2}, \tag{A.7}$$

$$q_{tc}^A = \frac{\alpha\left(2q\alpha + 2B\alpha^2 - B\alpha\beta - B\beta^2 + \alpha\beta c_r + \left(-2\alpha^2 + \beta^2\right)c_t - A\alpha\beta\theta_r + B\alpha\beta\theta_r + 2A\alpha^2\theta_t - 2B\alpha^2\theta_t - A\beta^2\theta_t + B\beta^2\theta_t\right)}{8\alpha^2 - 2\beta^2}. \tag{A.8}$$

Substituting equations (A.3)–(A.8) into equations (1)–(3), respectively, we can obtain the optimal solution for each subject's profit.

$$\begin{aligned}\Pi_m^A = {} & \frac{1}{4\left(4\alpha^4 - 5\alpha^2\beta^2 + \beta^4\right)}\alpha\left(\left(-q\beta + B\left(-\alpha^2 + \beta^2\right)\right) + (\alpha - \beta)(\alpha + \beta)\left(c_r + (-A + B)\theta_r\right)\right) \\ & \cdot\left(-q\beta + B\left(-2\alpha^2 + \alpha\beta + \beta^2\right) + \left(2\alpha^2 - \beta^2\right)c_r - \alpha\beta c_t - (A + B)\left(\left(2\alpha^2 - \beta^2\right)\theta_r - \alpha\beta\theta_t\right)\right) \\ & + \left(q\alpha + B(\alpha - \beta)(\alpha + \beta) - (\alpha - \beta)(\alpha + \beta)\left(c_t + (-A + B)\theta_t\right)\right) \\ & \cdot\left(2q\alpha + B(\alpha - \beta)(2\alpha + \beta) + \alpha\beta c_r + \left(2\alpha^2 - \beta^2\right)c_t + (A - B)\left(-\alpha\beta\theta_r + \left(2\alpha^2 - \beta^2\right)\theta_t\right)\right).\end{aligned} \tag{A.9}$$

Similarly, the optimal solutions in other situations can be obtained.

$$\Pi_r^A = \frac{\alpha\left(q\beta + B(\alpha - \beta)(2\alpha + \beta) + \left(-2\alpha^2 + \beta^2\right)c_r + \alpha\beta c_t + (A - B)\left(\left(2\alpha^2 - \beta^2\right)\theta_r - \alpha\beta\theta_t\right)\right)^2}{4\left(-4\alpha^2 + \beta^2\right)^2},$$

$$\Pi_t^A = \frac{\alpha\left(-2\alpha(q + B\alpha) + B\alpha\beta + B\beta^2 - \alpha\beta c_r + \left(2\alpha^2 - \beta^2\right)c_t - (A - B)\left(-\alpha\beta\theta_r + \left(2\alpha^2 - \beta^2\right)\theta_t\right)\right)^2}{4\left(-4\alpha^2 + \beta^2\right)^2},$$

$$\begin{aligned}\Pi_m^B = {} & \frac{1}{4}\Bigg(\frac{1}{4\alpha^4 - 5\alpha^2\beta^2 + \beta^4}\alpha\left(-q\beta + (B(-1 + k) - Ak)(\alpha - \beta)(\alpha + \beta) + (\alpha - \beta)(\alpha + \beta)\left(c_r + S_m + (-A + B)\theta_r\right)\right) \\ & \left(2(B(-1 + k) - Ak))\alpha^2 - qB + B\alpha\beta + (B + Ak - Bk)\beta^2 + \left(2\alpha^2 - \beta^2\right)c_r - \alpha\beta c_t - \left(2\alpha^2 - \beta^2\right)\left(S_m + (A - B)\theta_r\right) + (A - B)\alpha\beta\theta_t\right) \\ & + \frac{1}{4\alpha^4 - 5\alpha^2\beta^2 + \beta^4}\alpha\Big(-2\alpha(q + B\alpha) + (B + Ak - Bk)\alpha\beta + B\beta^2 - \alpha\beta c_r + \left(2\alpha^2 - \beta^2\right)c_t \\ & + \alpha\beta\left(S_m + (A - B)\theta_r\right) - (A - B)\left(2\alpha^2 - \beta^2\right)\theta_t\Big)\left(-\alpha(q + B\alpha) + B\beta^2 + (\alpha - \beta)(\alpha + \beta)\left(c_t + (-A - B)\theta_t\right)\right) \\ & - 4I_m + \frac{1}{4\alpha^2 - \beta^2}2S_m\Big(\alpha\Big(2(B + Ak - Bk)\alpha^2 + (q - B\alpha)\beta + (B(-1 + k) - Ak)\beta^2 + \left(-2\alpha^2 + \beta^2\right)c_r + \alpha\beta c_t \\ & + \left(2\alpha^2 - \beta^2\right)\left(S_m + (A - B)\theta_r\right) + (-A + B)\alpha\beta\theta_t\Big) + 2Q\left(-4\alpha^2 - \beta^2\right)\xi_0\Big)\Bigg),\end{aligned}$$

$$\Pi_r^B = \frac{1}{4\left(-4\alpha^2+\beta^2\right)^2}\alpha\Big(2\left(B(-1+k)-Ak\right)\alpha^2 - q\beta + B\alpha\beta + (B+Ak-Bk)\beta^2 + \left(-2\alpha^2+\beta^2\right)c_r - \alpha\beta c_t - 2\alpha^2 S_m + \beta^2 S_m$$
$$- 2A\alpha^2\theta_r + 2B\alpha^2\theta_r + A\beta^2\theta_r - B\beta^2\theta_r + (A-B)\alpha\beta\theta_t\Big)$$
$$\cdot\left(2\left(B(-1+k)-Ak\right)\alpha^2 - q\beta + B\alpha\beta + (B+Ak-Bk)\beta^2 + \left(2\alpha^2-\beta^2\right)c_r - \alpha\beta c_t - \left(2\alpha^2-\beta^2\right)\right)$$
$$\cdot\left(S_m + (A-B)\theta_r + (A-B)\alpha\beta\theta_t\right) - I_r,$$
$$\Pi_t^B = \frac{\alpha\left(-2\alpha(q+B\alpha) + (B+Ak-Bk)\alpha\beta + B\beta^2 - \alpha\beta c_r + \left(-2\alpha^2-\beta^2\right)c_t + \alpha\beta\left(S_m + (A-B)\theta_r\right) - (A-B)\left(2\alpha^2-\beta^2\right)\theta_t\right)^2}{4\left(-4\alpha^2+\beta^2\right)^2},$$
$$\Pi_m^C = \frac{1}{4}\Big(\frac{1}{4\alpha^4-5\alpha^2\beta^2+\beta^4}\alpha\left(-q\beta + (B(-1+k)-Ak)(\alpha-\beta)(\alpha+\beta) + (\alpha-\beta)(\alpha+\beta)\left(c_r - S_r + (-A+B)\theta_r\right)\right)$$
$$\cdot\left(2\left(B(-1+k)-Ak\right)\alpha^2 - q\beta + B\alpha\beta + (B+Ak-Bk)\beta^2 + \left(2\alpha^2-\beta^2\right)c_r - \alpha\beta c_t - \left(2\alpha^2-\beta^2\right)\right.$$
$$\left.\cdot\left(S_r + (A-B)\theta_r\right) + (A-B)\alpha\beta\theta_t\right)$$
$$+\frac{1}{4\alpha^4-5\alpha^2\beta^2+\beta^4}\alpha\Big(\Big(-2\alpha(q+B\alpha) + (B+Ak-Bk)\alpha\beta + B\beta^2 - \alpha\beta c_r + \left(2\alpha^2-\beta^2\right)c_t$$
$$+\alpha\beta\left(S_r + (A-B)\theta_r\right) - (A-B)\left(2\alpha^2-\beta^2\right)\theta_t\Big)\Big(-\alpha(q+B\alpha) + B\beta^2 + (\alpha-\beta)(\alpha+\beta)\left(c_t + (-A+B)\theta_t\right)\Big)\Big) - 4I_m\Big),$$
$$\Pi_r^C = \frac{1}{4\left(-4\alpha^2+\beta^2\right)^2}\alpha\Big(2\left(B(-1+k)-Ak\right)\alpha^2 - q\beta + B\alpha\beta + (B+Ak-Bk)\beta^2 + \left(2\alpha^2-\beta^2\right)c_r - \alpha\beta c_t$$
$$+6\alpha^2 S_r - \beta^2 S_r - 2A\alpha^2\theta_r + 2B\alpha^2\theta_r + A\beta^2\theta_r - B\beta^2\theta_r + (A-B)\alpha\beta\theta_t\Big)$$
$$\cdot\left(2\left(B(-1+k)-Ak\right)\alpha^2 - q\beta + B\alpha\beta + (B+Ak-Bk)\beta^2 + \left(2\alpha^2-\beta^2\right)c_r - \alpha\beta c_t\right.$$
$$\left.-\left(2\alpha^2-\beta^2\right)\left(S_r + (A-B)\theta_r\right) + (A-B)\alpha\beta\theta_t\right) - I_r,$$
$$\Pi_t^C = \frac{\alpha\left(-2\alpha(q+B\alpha) + (B+Ak-Bk)\alpha\beta + B\beta^2 - \alpha\beta c_r + \left(2\alpha^2-\beta^2\right)c_t + \alpha\beta\left(S_r + (A-B)\theta_r\right) - (A-B)\left(2\alpha^2-\beta^2\right)\theta_t\right)^2}{4\left(-4\alpha^2+\beta^2\right)^2},$$
$$\Pi_m^D = \frac{1}{4}\Big(\frac{1}{4\alpha^4-5\alpha^2\beta^2+\beta^4}\alpha\left(-q\beta + (B(-1+k)-Ak)(\alpha-\beta)(\alpha+\beta) + (\alpha-\beta)(\alpha+\beta)\left(c_r - S_c + (-A+B)\theta_r\right)\right)$$
$$\cdot\left(2\left(B(-1+k)-Ak\right)\alpha^2 - q\beta + B\alpha\beta + (B+Ak-Bk)\beta^2 + \left(2\alpha^2-\beta^2\right)c_r\right.$$
$$\left.-\alpha\beta c_t - \left(2\alpha^2-\beta^2\right)\left(S_c + (A-B)\theta_r\right) + (A-B)\alpha\beta\theta_t\right)$$
$$+\frac{1}{4\alpha^4-5\alpha^2\beta^2+\beta^4}\alpha\Big(\Big(-2\alpha(q+B\alpha) + (B+Ak-Bk)\alpha\beta + B\beta^2 - \alpha\beta c_r + \left(2\alpha^2-\beta^2\right)c_t + \alpha\beta\left(S_c + (A-B)\theta_r\right)$$
$$-(A-B)\left(2\alpha^2-\beta^2\right)\theta_t\Big)\Big(-\alpha(q+B\alpha) + B\beta^2 + (\alpha-\beta)(\alpha+\beta)\left(c_t + (-A+B)\theta_t\right)\Big)\Big) - 4I_m\Big),$$
$$\Pi_r^D = \frac{1}{4\left(-4\alpha^2+\beta^2\right)^2}\alpha\Big(2\left(B(-1+k)-Ak\right)\alpha^2 - q\beta + B\alpha\beta + (B+Ak-Bk)\beta^2 + \left(2\alpha^2-\beta^2\right)c_r$$
$$-\alpha\beta c_t - 2\alpha^2 S_c + \beta^2 S_c - 2A\alpha^2\theta_r + 2B\alpha^2\theta_r + A\beta^2\theta_r - B\beta^2\theta_r + (A-B)\alpha\beta\theta_t\Big)$$
$$\cdot\left(2\left(B(-1+k)-Ak\right)\alpha^2 - q\beta + B\alpha\beta + (B+Ak-Bk)\beta^2 + \left(2\alpha^2-\beta^2\right)c_r - \alpha\beta c_t - \left(2\alpha^2-\beta^2\right)\right.$$
$$\left.\cdot\left(S_c + (A-B)\theta_r\right) + (A-B)\alpha\beta\theta_t\right) - I_r,$$
$$\Pi_t^D = \frac{\alpha\left(-2\alpha(q+B\alpha) + (B+Ak-Bk)\alpha\beta + B\beta^2 - \alpha\beta c_r + \left(2\alpha^2-\beta^2\right)c_t + \alpha\beta\left(S_c + (A-B)\theta_r\right) - (A-B)\left(2\alpha^2-\beta^2\right)\theta_t\right)^2}{4\left(-4\alpha^2+\beta^2\right)^2}.$$

(A.10)

Data Availability

The simulation data used to support the findings of this study are included within this article.

Conflicts of Interest

The authors declare that there are no conflicts of interest regarding the publication of this paper.

Acknowledgments

This research was supported by the National Social Science Foundation of China (Grant no. 20BGL200).

References

[1] L. Zhen, L. Huang, and W. Wang, "Green and sustainable closed-loop supply chain network design under uncertainty," *Journal of Cleaner Production*, vol. 227, pp. 1195–1209, 2019.

[2] S. Council, "State council's decision on accelerating the cultivation and development of strategic emerging industry," 2010, https://www.gov.cn/zwgk/2010-10/18/content_1724848.htm.

[3] CAAM, "Overview of the production and sales of the automotive industry in December 2020," 2021, https://www.autostats.org.cn/ReadArticle.asp?NewsID=10926.

[4] L. Zhang, Y. Liu, B. Pang, B. Sun, and A. Kokko, "Second use value of China's new energy vehicle battery: a view based on multi-scenario simulation," *Sustainability*, vol. 12, no. 1, 2020.

[5] X. Zeng, J. Li, and L. Liu, "Solving spent lithium-ion battery problems in China: opportunities and challenges," *Renewable and Sustainable Energy Reviews*, vol. 52, pp. 1759–1767, 2015.

[6] H. Hao, "Fifth profit source: commercial value and mode of reverse logistics in China," *Logistics Technology*, vol. 36, no. 8, pp. 47–50, 2017.

[7] L. Zhen, "Modeling of yard congestion and optimization of yard template in container ports," *Transportation Research Part B: Methodological*, vol. 90, pp. 83–104, 2016.

[8] L. Zhen, Z. Liang, D. Zhuge, L. H. Lee, and E. P. Chew, "Daily berth planning in a tidal port with channel flow control," *Transportation Research Part B: Methodological*, vol. 106, pp. 193–217, 2017.

[9] X. Xia, Q. Zhu, and H. Wang, "Game model for end-of-life vehicles between formal recycling channels and informal recycling channel based on governmental different policies," *Journal of Systems Management*, vol. 24, no. 1, pp. 82–90, 2016.

[10] MIIT, "Interim regulations on the traceability management of the recycling and utilization of new energy vehicle power batteries," 2018, https://www.miit.gov.cn/jgsj/jns/gzdt/art/2020/art_c1a708247cc54b068ea60ceaff0b044d.html.

[11] M. Kouhizadeh and J. Sarkis, "Blockchain practices, potentials, and perspectives in greening supply chains," *Sustainability*, vol. 10, no. 10, 2018.

[12] J. Leng, R. Guolei, P. Jiang et al., "Blockchain-empowered sustainable manufacturing and product lifecycle management in industry 4.0: a survey," *Renewable and Sustainable Energy Reviews*, vol. 132, 2020.

[13] R. C. Savaskan, S. Bhattacharya, and L. N. Van Wassenhove, "Closed-loop supply chain models with product remanufacturing," *Management Science*, vol. 50, no. 2, pp. 239–252, 2004.

[14] H. Liu, M. Lei, H. Deng, G. Keong Leong, and T. Huang, "A dual channel, quality-based price competition model for the WEEE recycling market with government subsidy," *Omega*, vol. 59, pp. 290–302, 2016.

[15] Y. Li, F. Xu, and X. Zhao, "Governance mechanisms of dual-channel reverse supply chains with informal collection channel," *Journal of Cleaner Production*, vol. 155, pp. 125–140, 2017.

[16] Y. Tang, Q. Zhang, Y. Li, G. Wang, and Y. Li, "Recycling mechanisms and policy suggestions for spent electric vehicles' power battery–a case of Beijing," *Journal of Cleaner Production*, vol. 186, pp. 388–406, 2018.

[17] H. Hao, Q. Zhang, and Z. Wang, "Feasibility evaluation for reverse logistics of end-of-life vehicles battery–based on improved fuzzy neural network," *China Business and Market*, vol. 32, no. 6, pp. 15–24, 2018.

[18] W. Wang and Y. Wu, "An overview of recycling and treatment of spent LiFePO 4 batteries in China," *Resources, Conservation and Recycling*, vol. 127, pp. 233–243, 2017.

[19] A. Beaudet, F. Larouche, K. Amouzegar, P. Bouchard, and K. Zaghib, "Key challenges and opportunities for recycling electric vehicle battery materials," *Sustainability*, vol. 12, no. 14, 2020.

[20] H. Hao, J. Zhang, and Q. Zhang, "Development strategy of power battery recycling reverse logistics under circular economy in China," *Ecological Economy*, vol. 36, no. 1, pp. 86–91, 2020.

[21] J. Li, Z. Wang, B. Jiang, and T. Kim, "Coordination strategies in a three-echelon reverse supply chain for economic and social benefit," *Applied Mathematical Modelling*, vol. 49, pp. 599–611, 2017.

[22] X. Gu, P. Ieromonachou, L. Zhou, and M.-L. Tseng, "Developing pricing strategy to optimise total profits in an electric vehicle battery closed loop supply chain," *Journal of Cleaner Production*, vol. 203, pp. 376–385, 2018.

[23] Y. Tang, Q. Zhang, Y. Li, H. Li, X. Pan, and B. McLellan, "The social-economic-environmental impacts of recycling retired EV batteries under reward-penalty mechanism," *Applied Energy*, vol. 251, 2019.

[24] L. Wang, X. Wang, and W. Yang, "Optimal design of electric vehicle battery recycling network–from the perspective of electric vehicle manufacturers," *Applied Energy*, vol. 275, 2020.

[25] Z. Wang, H. Hao, F. Gao, Q. Zhang, J. Zhang, and Y. Zhou, "Multi-attribute decision making on reverse logistics based on DEA-TOPSIS: a study of the Shanghai end-of-life vehicles industry," *Journal of Cleaner Production*, vol. 214, pp. 730–737, 2019.

[26] H. Hao, J. Zhang, Q. Zhang, L. Yao, and Y. Sun, "Improved gray neural network model for healthcare waste recycling forecasting," *Journal of Combinatorial Optimization*, vol. 39, pp. 1–18, 2019.

[27] K. Dandage, R. Badia-Melis, and L. Ruiz-García, "Indian perspective in food traceability: a review," *Food Control*, vol. 71, pp. 217–227, 2017.

[28] Y. P. Tsang, K. L. Choy, C. H. Wu, G. T. S. Ho, and H. Y. Lam, "Blockchain-driven IoT for food traceability with an integrated consensus mechanism," *IEEE Access*, vol. 7, pp. 129000–129017, 2019.

[29] Q. Lin, H. Wang, X. Pei, and J. Wang, "Food safety traceability system based on blockchain and EPCIS," *IEEE Access*, vol. 7, pp. 20698–20707, 2019.

[30] M. P. Caro, M. S. Ali, M. Vecchio, and R. Giaffreda, "Blockchain-based traceability in Agri-Food supply chain

management: a practical implementation," in *Proceedings of the 2018 IoT Vertical and Topical Summit on Agriculture–Tuscany (IOT Tuscany)*, Tuscany, Italy, May 2018.

[31] H. Feng, X. Wang, Y. Duan, J. Zhang, and X. Zhang, "Applying blockchain technology to improve agri-food traceability: a review of development methods, benefits and challenges," *Journal of Cleaner Production*, vol. 260, 2020.

[32] S. Gong, P. Ding, X. Yan, Y. Wang, and B. Huang, "Design of power battery data monitoring and sharing system based on blockchain," in *Proceedings of the 2019 3rd International Conference on Electronic Information Technology and Computer Engineering (EITCE)*, pp. 830–833, IEEE, Xiamen, China, October 2019.

[33] P. K. Gopalakrishnan, J. Hall, and S. Behdad, "Cost analysis and optimization of blockchain-based solid waste management traceability system," *Waste Management*, vol. 120, pp. 594–607, 2021.

[34] L. Shao, J. Yang, and M. Zhang, "Subsidy scheme or price discount scheme? mass adoption of electric vehicles under different market structures," *European Journal of Operational Research*, vol. 262, no. 3, pp. 1181–1195, 2017.

Hindawi
Scientific Programming
Volume 2021, Article ID 9945583, 10 pages
https://doi.org/10.1155/2021/9945583

Research Article

Application of FWA-Artificial Fish Swarm Algorithm in the Location of Low-Carbon Cold Chain Logistics Distribution Center in Beijing-Tianjin-Hebei Metropolitan Area

Liyi Zhang,[1] **Mingyue Fu**,[2] **Teng Fei**,[1] **and Xuhua Pan**[1]

[1]*School of Information Engineering, Tianjin University of Commerce, Tianjin 300134, China*
[2]*School of Economics, Tianjin University of Commerce, Tianjin 300134, China*

Correspondence should be addressed to Xuhua Pan; panxuhua@tjcu.edu.cn

Received 29 March 2021; Accepted 7 July 2021; Published 2 August 2021

Academic Editor: Xiaobo Qu

Copyright © 2021 Liyi Zhang et al. This is an open access article distributed under the Creative Commons Attribution License, which permits unrestricted use, distribution, and reproduction in any medium, provided the original work is properly cited.

Green development is the hot spot of cold chain logistics today. Therefore, this paper converts carbon emission into carbon emission cost, comprehensively considers cargo damage, refrigeration, carbon emission, time window, and other factors, and establishes the optimization model of location of low-carbon cold chain logistics in the Beijing-Tianjin-Hebei metropolitan area. Aiming at the problems of the fish swarm algorithm, this paper makes full use of the fireworks algorithm and proposes an improved fish swarm algorithm on the basis of the fireworks algorithm. By introducing the explosion, Gaussian mutation, mapping and selection operations of the fireworks algorithm, the local search ability and diversity of artificial fish are enhanced. Finally, the modified algorithm is applied to optimize the model, and the results show that the location scheme of low-carbon cold chain logistics in Beijing-Tianjin-Hebei metropolitan area with the lowest total cost can be obtained by using fireworks-artificial fish swarm algorithm.

1. Introduction

With the rapid development of economy and the increase of people's disposable income, the demand for cold chain food such as vegetables, fruits, and dairy products is constantly increasing, and people have higher and higher requirements for the quality of cold chain food. With fresh electricity as the symbol, the cold chain industry develops rapidly, creating a huge space for the development of cold chain products. In 2020, the outbreak of COVID-19 and the closed management will further promote the development of China's online fresh e-commerce market, which is both an opportunity and a challenge for the cold chain logistics industry. On the one hand, the growth of online consumption of fresh products will promote the growth of cold chain transportation in the logistics industry and increase investment, so the cold chain logistics industry is expected to accelerate its development. On the other hand, the outbreak has also exposed problems in cold chain logistics. While the epidemic forces the fresh food industry chain to carry out a big reform, it also shows the importance of strengthening the construction of the cold chain logistics system.

In the 1980s, the United States, Japan, Western Europe, and other developed countries have basically completed the construction of the cold chain, and their food cold chain logistics is also basically perfect. However, the development of China's cold chain market lags behind that of developed countries, and there are some problems in cold chain logistics, such as low information level, insufficient infrastructure construction, and high cost. Zhou Yuan, an academician at the Chinese Academy of Sciences, pointed out that China's cold chain circulation rate is only 19 percent, while almost all foreign countries are above 85 percent [1]. The level of cold chain logistics in China is low. It is estimated that the annual loss of meat, vegetables, fruits, and aquatic products in China reaches 1.2121 million tons, 253.629 million tons, 21.957 million tons, and 8.244 tons, respectively [2].

Compared with normal temperature logistics, cold chain logistics is characterized by high carbon emission due to its

higher requirements on transportation conditions. The CPC Central Committee with General Secretary Xi Jinping as the core has put forward the concepts of "green development" and "low-carbon economy" and emphasized the construction of ecological civilization for many times, which requires the cold chain logistics industry to reduce energy consumption and carbon emissions and promote green and low-carbon development.

Reasonable location of cold chain logistics distribution center is not only conducive to improving distribution efficiency and sales volume of fresh products, thereby reducing costs, improving the profitability of enterprises, and improving the operation efficiency and economic benefits of the whole social logistics system, but also improves service level and customer satisfaction and enhances the social influence of enterprises. This paper establishes a location model of cold chain logistics distribution center in the Beijing-Tianjin-Hebei metropolitan area with the goal of minimizing the total cost, including manufacturers, distribution centers, and customers.

The rest of this paper is as follows. In Section 2, a literature review is presented. In Section 3, a location model of low-carbon cold chain logistics distribution center is established. In Section 4, the reformative artificial fish swarm algorithm, FWA-artificial fish swarm algorithm, is elaborated in detail. In Section 5, taking the Beijing-Tianjin-Hebei metropolitan area as an example, the basic fish swarm algorithm, FWA-artificial fish swarm algorithm, and DNA-artificial fish swarm algorithm are used to solve the model, and the results are analyzed. In Section 6, the conclusion is made.

2. Literature Review

Cold chain logistics distribution center connects manufacturers and customers, which affects the distribution efficiency of the whole logistics system. Moreover, as the most important infrastructure in cold chain logistics, distribution center has high construction cost and long recovery cycle. Once built, it will be used for a long time and difficult to migrate. Therefore, the location of distribution center has been concerned and studied by many scholars at home and abroad. Marinakis [3] integrated topological structure into the particle swarm optimization algorithm to solve the discrete optimization problem about location path. Li et al. [4] proposed a low-carbon path problem with the goal of minimizing energy consumption, carbon emissions, and total cost of car rental and proposed a tabu search algorithm based on path division to solve it. Sadjadi et al. [5] set the demand and lead time that are subject to Poisson distribution and exponential distribution, respectively, to make the problem more in line with the actual situation. On the basis of queuing analysis, a mixed integer nonlinear programming model is established to study the location problem of three-stage supply chain. Ma et al. [6] considered the change of vehicle load during driving and its influence on fuel consumption and carbon emissions and took the regional delivery network of Zhuhai Express Company as an example to analyze the low-carbon VRP model for multivehicle in a small urban area. Since the change of altitude in mountainous areas could affect the change of temperature and relative humidity and then affect the quality of perishable food, Orjuela-Castro et al. [7] took the capital of Colombia as an example and proposed a site selection model for the transportation of perishable food in mountainous areas. El-Sobky et al. [8] used the trust region method to improve the ability of global convergence and combined the penalty method and active set strategy to determine the number and scale of warehouses with the goal of minimal cost. Simic et al. [9] analyzed the problem of facility location, proposed the methodology based on the fuzzy C-means method, analytic hierarchy process, and hybrid genetic algorithm, and explained how to analyze the multicriteria decision making problem with this model. Wang et al. [10] used the improved genetic and particle swarm algorithm and the minimum and maximum cost-benefit distribution model to solve the benefit distribution problem of multicenter joint distribution. Kang et al. [11] established a research on the optimization of low-carbon distribution path of cold chain logistics of fresh agricultural products and analyzed it with the improved ant colony algorithm. Liang et al. [12], respectively, built the path models of traditional gasoline vehicles and electric vehicles in a low-carbon environment to study the impact of electric vehicles on economic cost and carbon emissions. Bilisik et al. [13] used interval valued trapezoidal fuzzy grey relational degree analysis to solve the distribution location problem of fresh food in urban areas. Zhang et al. [14] used the input-output method to calculate the carbon emission cost, and combined with customers' time satisfaction and quality satisfaction, they compared and analyzed the difference of distribution cost between the single model and multimodel. Sheng [15] proposed the quantum particle swarm optimization algorithm and used it to optimize the logistics management system. Park et al. [16] analyzed the factors influencing the intelligent distribution center, which provided a certain theoretical basis for the construction of intelligent distribution center. Setiawan et al. [17] established three resource allocation models to enable the selected distribution center to allocate rescue resources effectively and quickly in the face of sudden disasters. Zhou et al. [18] proposed a new urban distribution model based on subway by studying the urban subway network and road network. Song et al. [19] established an emergency logistics system by comprehensively considering the delivery time and cost under the condition of material demand and dynamic road conditions. Li et al. [20], under the multichannel urban network, measured carbon emissions by vehicle speed and load and constructed a low-carbon path optimization model. Meng and Gao [21] improved the moth optimization algorithm by using the nonlinear inertia weight based on control factors and the cross-mutation strategy in the genetic algorithm and optimized the location model of agricultural logistics distribution center with the modified moth optimization algorithm. Li and Dang [22] used the heuristic algorithm to solve the logistics site-optimization model under constraints such as vehicle capacity, cargo operation time, and delivery operation time window in the case of

multiple distribution centers. Li et al. [23] studied the distribution problem of dairy products in Beijing by constructing a two-level distribution site-path model with constraints. Lin et al. [24] adopted stochastic programming theory to study the location of low-carbon logistics distribution center in the case of uncertain demand. Xu et al. [25] proposed a pseudo-reverse spider monkey optimization algorithm based on Laplace distribution to solve the location problem of logistics distribution centers.

From the above literatures, most of them study location models that only include distribution centers and demand points, while few study three-level models that include manufacturers, distribution centers, and customers and also contain fewer types of costs. Therefore, this paper first establishes a three-level model including constant cost, transportation cost, cargo damage cost, cooling cost, carbon emission cost, and penalty cost. Secondly, the fireworks algorithm is integrated into the fish swarm algorithm, and FWA-artificial fish swarm algorithm is proposed and used to solve the model.

3. Model

The total cost of this model includes constant cost, transportation cost, cargo damage cost, cooling cost, carbon emission cost, and penalty cost. The parameters of the model are as follows:

I: the number of manufacturers, $i = 1, 2, \ldots, I$

J: the number of distribution centers, $j = 1, 2, \ldots, J$

M: the number of customers, $m = 1, 2, \ldots, M$

α_j: when the distribution center is selected, it is 1; otherwise, it is 0.

α_{jm}: when customer is delivered by distribution center, it is 1; otherwise, it is 0.

c_j: the cost of distribution center j remains unchanged in the short term

p_2: unit transportation cost

d_{ij}: distance between supplier i and distribution center j

d_{jm}: distance between distribution center j and customer m

q_{ij}: demand of distribution center j

q_{jm}: demand of customer m

p_3: food's unit price

T_m: the time required to uninstall food

v: speed of vehicle

β_1: percentage of food spoilage in transit

β_2: percentage of food spoilage at unloading stage

p_{41}: the cost of keeping the temperature low in transit

p_{42}: the cost of keeping the temperature low at unloading stage

E_1: fuel consumption of vehicle driving 1 km

E_2: the energy consumed per hour due to cooling

p_c: the amount to be paid for generating one unit of carbon dioxide due to energy consumption

e: the amount of carbon dioxide produced per unit of energy consumed

p_{61}: cost of a vehicle arriving one hour earlier

p_{62}: the cost incurred when a vehicle is one hour late

t_m: actual delivery time to customer m

(ET_m, LT_m): the best time for vehicles to reach customer m

(EET_m, LLT_m): the maximum time period for vehicles to arrive. If this time period gets exceeded, food will not be accepted by customers

The location model of low-carbon cold chain logistics distribution center is as follows:

$$\min C_t = C_1 + C_2 + C_3 + C_4 + C_5 + C_6, \tag{1}$$

$$C_1 = \sum_{j=1}^{J} c_j \alpha_j, \tag{2}$$

$$C_2 = p_2 \sum_{i=1}^{I} \sum_{j=1}^{J} \sum_{m=1}^{M} \left(q_{ij} d_{ij} \alpha_j + q_{jm} d_{jm} \alpha_{jm} \right), \tag{3}$$

$$C_3 = p_3 \sum_{i=1}^{I} \sum_{j=1}^{J} \sum_{m=1}^{M} \left(q_{ij} \alpha_j \left(1 - e^{-\beta_1 t_{ij}}\right) + q_{jm} \alpha_{jm} \left(1 - e^{-\beta_1 t_{jm}}\right) + q_{jm} \alpha_{jm} \left(1 - e^{-\beta_2 T_m}\right) \right), \tag{4}$$

$$C_4 = \sum_{i=1}^{I} \sum_{j=1}^{J} \sum_{m=1}^{M} \left(p_{41} \left(t_{ij} \alpha_j + t_{jm} \alpha_{jm} \right) + p_{42} T_m \alpha_{jm} \right), \tag{5}$$

$$C_5 = p_c e E_1 \sum_{i=1}^{I} \sum_{j=1}^{J} \sum_{m=1}^{M} \left(d_{ij}\alpha_j + d_{jm}\alpha_{jm}\right) + p_c e E_2 \sum_{i=1}^{I} \sum_{j=1}^{J} \sum_{m=1}^{M} \left(t_{ij}\alpha_j + t_{jm}\alpha_{jm}\right), \tag{6}$$

$$C_6(m) = \begin{cases} \text{inf}, & t_m < EET_m, \\ p_{61}\left(ET_m - t_m\right), & EET_m < t_m < ET_m, \\ 0, & ET_m < t_m < LT_m, \\ p_{62}\left(t_m - LT_m\right) & LT_m < t_m < LLT_m, \\ \text{inf}, & t_m > LLT_m, \end{cases} \tag{7}$$

$$C_6 = \sum_{m=1}^{M} C_6(m). \tag{8}$$

Constraints are as follows:

$$\sum_{j=1}^{J} \alpha_{jm} = 1, \quad m \in M, \tag{9}$$

$$\sum_{j=1}^{J} \alpha_j \le N, \tag{10}$$

$$\sum_{i=1}^{I} \sum_{j=1}^{J} q_{ij} = \sum_{j=1}^{J} \sum_{m=1}^{M} q_{jm}, \tag{11}$$

$$\sum_{n=1}^{N} V_n \ge \sum_{m=1}^{M} q_m. \tag{12}$$

Formula (1) is an objective function, which aims at minimizing the total cost C_t. In formula (2), C_1 represents the total constant cost in the system; in equation (3), C_2 represents the total transportation cost from the manufacturer to distribution centers and from distribution centers to the customers; in formula (4), the total cost of cargo damage C_3 refers to the sum of the cost of spoilage in transit and the cost of spoilage when unloading at customers; in equation (5), the total cooling cost C_4 refers to the total cooling cost during transportation and unloading. In formula (6), the total carbon emission cost C_5 is the cost of carbon dioxide caused by the consumption of fuel by vehicles and energy consumption by refrigeration equipment. Equation (7) represents the penalty cost caused by the vehicle arriving at the customer m late or early; in formula (8), C_6 is the total penalty cost. Formula (9) indicates that a customer's demand can only be delivered once. Formula (10) specifies distribution centers' maximum number N. Equation (11) means that the total demand of distribution centers and customers is equal. Formula (12) indicates that the total capacity of the selected distribution centers is not less than the total demand for customers.

4. FWA-Artificial Fish Swarm Algorithm

4.1. Artificial Fish Swarm Algorithm's Behavior Description. Let rand be a number that is randomly selected from the digital range (0, 1), δ be crowding factor, and $X = (x_1, x_2, \ldots, x_n)$ be every artificial fish's present state. $Y = \mathrm{f}(X)$ represents the amount of food that exist in the fish's present state, where $x_i\,(i = 1, 2, \ldots, n)$ is defined as the desired optimization variate and Y represents objective function value.

(1) *Prey Behavior.* At time t, the artificial fish's location is x_i, and another uncertainly chose position within the visual field is set as x_j. In maximum value problem, if $Y_i < Y_j$ holds, then go forward in the orientation of x_j; otherwise, choose again randomly and identify if the advancing criterion is met. If advancing criterion is still not met when the maximum number of attempts is reached, it can be randomly moved one step.

$$\begin{cases} x_i^{t+1} = x_i^t + \text{rand} \times \text{step} \times \dfrac{x_j - x_i^t}{\left\| x_j - x_i^t \right\|}, & Y_i < Y_j, \\ x_i^{t+1} = x_i^t + \text{rand} \times \text{step}, & \text{else}. \end{cases} \tag{13}$$

(2) *Swarm Behavior.* At time t, $x_i$is the artificial fish's present location and Y_i is set as corresponding food concentration. At present, the number of artificial fish in vision field is n_f, and central position is x_c, and Y_c is the matching food concentration. If $Y_c/n_f > \delta Y_i$ is satisfied, which means that there are more artificial fish at the central position x_c and they are uncrowded, then the fish will move toward the central location x_c by one step. If not, the fish will perform prey behavior.

$$\begin{cases} x_i^{t+1} = x_i^t + \text{rand} \times \text{step} \times \dfrac{x_c - x_i^t}{\left\| x_c - x_i^t \right\|}, & \dfrac{Y_c}{n_f} > \delta Y_i, \\ \text{prey behavior}, & \text{else}. \end{cases} \tag{14}$$

(3) *Follow Behavior*. At time t, x_i is the artificial fish's current location and Y_i is set as corresponding food concentration. In its field of vision, the food concentration Y_m is the highest when the artificial fish state is x_m. If $Y_m/n_f > \delta Y_i$ is satisfied, which means that there exists a high food concentration in position x_m and the position is uncrowded, then the fish in x_i will move in the direction of x_m by one step; otherwise, it will perform prey behavior.

$$\begin{cases} x_i^{t+1} = x_i^t + \text{rand} \times \text{step} \times \dfrac{x_m - x_i^t}{\left\| x_m - x_i^t \right\|}, & \dfrac{Y_m}{n_f} > \delta Y_i, \\ \text{prey behavior}, & \text{else}. \end{cases} \tag{15}$$

(4) *Random Behavior*. Random behavior is the act of randomly selecting a location in the field of vision and moving one step in that direction to expand its range of food and companions.

4.2. FWA-AFSA. The basic fish swarm algorithm has the advantages of simplicity, flexibility, and strong parallel processing capabilities. However, in the late stage of operation, the optimization speed of the algorithm is slow, and it is easy to fall into the vicinity of the local extreme value, resulting in low solution accuracy. Therefore, considering the problems of the fish swarm algorithm in the late stage, this paper introduces the fireworks algorithm into the fish swarm algorithm. The basic idea is that after multiple iterations, if the state of the optimal artificial fish does not change or the change is extremely small, the optimal artificial fish individual is retained, and explosion and Gaussian mutation operators are performed on the remaining artificial fish with a certain probability. After the explosion and Gaussian mutation operations, keep all individuals within the defined range through the mapping rule. Finally, according to the distance-based selection strategy, the better individuals are selected from the newly generated individuals to form the next-generation population with the best individuals retained from the previous generation. The explosion operator enhances the local search ability of the algorithm by enhancing the degree of information exchange in the fish school and then increases the convergence speed. The Gaussian mutation operator can generate individuals far away from the current optimal position and increase the diversity of the population.

4.2.1. Explosion Operator. Explosion operator refers to the fireworks in its vicinity to find fireworks with better fitness value. Fireworks have different explosion radius and explosion spark number. Fireworks with good fitness value can produce more sparks in a smaller explosion radius, which makes the local search ability stronger. Fireworks with poor fitness value can generate fewer sparks in a larger explosion radius, thus enabling the algorithm to have better global search capability [26].

4.2.2. Gaussian Variation. Gaussian mutation operator can generate Gaussian sparks, which can enhance the diversity of the population, thereby improving the optimization efficiency of the algorithm and avoiding falling into local extremes to a certain extent.

4.2.3. Mapping Rule. When the sparks generated by the explosion and Gaussian mutation operation exceeds the value range of the problem to be solved, the mapping rule is used to modify it.

4.2.4. Selection Strategy. After ensuring that fireworks, explosion sparks, and Gaussian mutation sparks (candidate set) are all in the search space, some of them need to be selected as the next-generation fireworks so that the excellent information in the population can be retained.

5. Simulation

In this paper, the Binhai New Area (117.68, 39.03) is selected as the manufacturer, and 13 municipal administrative units in the Beijing-Tianjin-Hebei metropolitan area are selected as the alternative distribution centers to provide service to customers. Tables 1 and 2 represent information about customers and alternative distribution centers, respectively.

Suppose the price of cold chain food is 3000 yuan/t, the transportation cost of unit food is 0.3 yuan/km, percentage of food spoilage in transit and at unloading stage are 0.03 and 0.05, respectively, the unloading time is proportional to the unloading volume, and the proportional coefficient is 5/60, the costs of vehicle arriving early and arriving late for vehicles are 10 yuan/h and 30 yuan/h, respectively, and the cooling cost in order to reduce loss during transportation and unloading is 20 yuan/h and 30 yuan/h, respectively. The vehicle departs from the distribution center at 4 : 30, the driving speed is 60 km/h, the fuel consumption of the vehicle is 0.225 L/km, the energy consumption of the refrigeration equipment is 0.0025 L/t.km, the carbon dioxide emission coefficient is 2.66 kg/L, and the unit carbon tax price is 20 yuan/kg [27].

In this paper, the basic fish swarm algorithm (AFSA), DNA-artificial fish swarm algorithm (DNA-AFSA) [28], and FWA-artificial fish swarm algorithm (FWA-AFSA) are used to solve the location problem of the logistics center, respectively. Parameters of algorithms are set as follows. The number of artificial fish fishnum = 20, crowding factor $\delta = 0.618$, maximum number of trials try_number = 20, step size step = 25, viewable size visual = 80, the probability of DNA crossing $P_c = 0.9$, the probability of DNA mutation

Table 1: Information about customers.

No.	Customer	Longitude and latitude	Maximum time period	Best time period	Quantity demand
1	Huairou District, Beijing	(116.63, 40.32)	5:00–8:45	5:10–8:15	5
2	Fangshan District, Beijing	(116.13, 39.75)	4:30–9:10	4:50–8:30	4.5
3	Jinghai District, Tianjin	(116.92, 38.93)	4:30–9:15	4:45–9:00	4.5
4	Ninghe County, Tianjin	(117.82, 39.33)	4:30–9:30	4:50–9:10	5
5	Pingshan County, Shijiazhuang	(114.20, 38.25)	4:45–8:20	5:00–8:00	2.5
6	Xinji City, Shijiazhuang	(115.22, 37.92)	5:10–8:00	5:20–7:30	4
7	Fengning County, Chengde	(116.65, 41.20)	5:45–9:20	6:00–8:50	3
8	Longhua County, Chengde	(117.72, 41.32)	4:30–9:30	4:40–9:15	4
9	Chongli County, Zhangjiakou	(115.27, 40.97)	5:00–9:40	5:15–9:00	4.5
10	Huai'an County, Zhangjiakou	(114.42, 40.67)	4:45–9:40	5:15–9:15	5
11	Changli County, Qinhuangdao	(119.17, 39.70)	4:30–9:15	4:45–8:45	2
12	Qinglong County, Qinhuangdao	(118.95, 40.40)	4:40–9:00	5:00–8:30	4.5
13	Gu' an County, Langfang	(116.30, 39.43)	4:30–9:30	4:40–8:50	3
14	Xianghe County, Langfang	(117.00, 39.77)	4:45–8:50	4:50–8:30	2.5
15	Zunhua City, Tangshan	(117.95, 40.18)	5:00–9:15	5:10–9:00	4
16	Tanghai County, Tangshan	(118.45, 39.27)	4:30–9:30	4:40–9:00	2
17	Laisyuan County, Baoding	(114.68, 39.35)	4:30–9:45	4:40–9:15	5.5
18	Shunping County, Baoding	(115.13, 38.83)	4:30–8:45	4:35–8:15	4.5
19	Renqiu City, Cangzhou	(116.10, 38.72)	4:30–9:10	4:45–8:30	4
20	Haixing County, Cangzhou	(117.48, 38.13)	5:00–9:40	5:15–9:00	4.5
21	Fucheng County, Hengshui	(116.15, 37.87)	4:50–8:30	5:15–8:00	3.5
22	Gucheng County, Hengshui	(115.97, 37.35)	4:45–9:15	5:10–9:00	5.5
23	Lincheng County, Xingtai	(114.50, 37.43)	4:30–9:30	4:50–8:40	4.5
24	Guangzong County, Xingtai	(115.15, 37.07)	4:40–9:15	5:15–8:40	4
25	Shexian County, Handan	(113.67, 36.57)	4:30–9:30	4:50–8:45	4.5
26	Wei County, Handan	(114.93, 36.37)	4:40–9:40	5:00–8:50	5

Table 2: Information about distribution centers.

Distribution center	Longitude and latitude	Capacity	Constant cost
Beijing City	(116.42, 39.92)	22	8000
Tianjin City	(117.20, 39.13)	26	8500
Shijiazhuang City	(114.30, 38.02)	27	7500
Chengde City	(117.57, 40.59)	21	5000
Zhangjiakou City	(114.53, 40.48)	24	7000
Qinhuangdao City	(119.35, 39.55)	22	5000
Langfang City	(116.70, 39.52)	24	6000
Tangshan City	(118.11, 39.36)	22	5500
Baoding City	(115.30, 38.51)	27	6500
Cangzhou City	(116.52, 38.18)	22	5000
Hengshui City	(115.42, 37.44)	26	6500
Xingtai City	(114.30, 37.04)	22	5500
Handan City	(114.28, 36.36)	24	6000

Table 3: The running results of three algorithms.

	Minimum value	Maximum value	Mean value	Mean convergence algebra	Standard deviation
AFSA	167060.58	235106.86	195877.54	87.87	16249.64
DNA-AFSA	163934.82	211482.97	186939.75	67.63	12195.75
FWA-AFSA	157539.41	204585.40	182149.97	54.70	11229.78

$P_m = 0.01$, maximum number of sparks produced by fireworks explosion $E_n = 20$, the limiting factor for the number of explosion $a = 0.3$ and $b = 0.8$, explosion radius $E_r = 500$, variation spark number $M = 8$, maximum number of iterations maxgen = 100, and threshold of the maximum number of iterations when there is no change Maxbest = 5.

The three algorithms select 5 from 13 alternative distribution centers to deliver goods to 26 customers, and the results of running the algorithms for 30 times are shown in Table 3.

According to Table 3, in terms of solving accuracy, the minimum value, maximum value, and mean value obtained

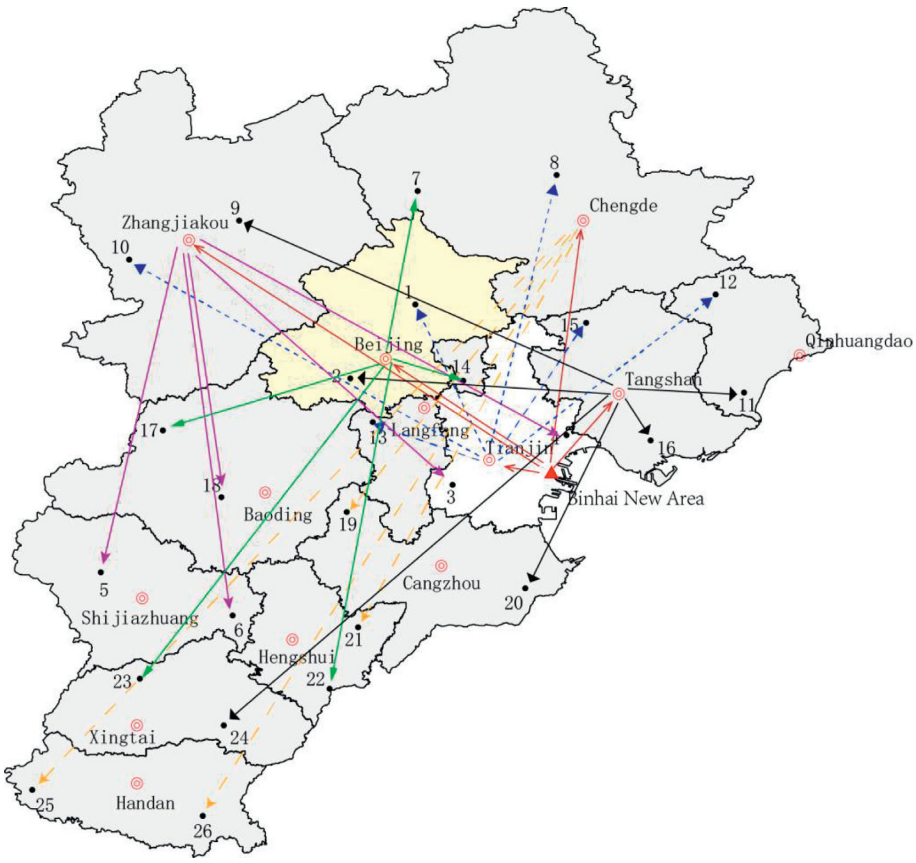

Figure 1: Schematic diagram of location selection of the basic artificial fish swarm algorithm.

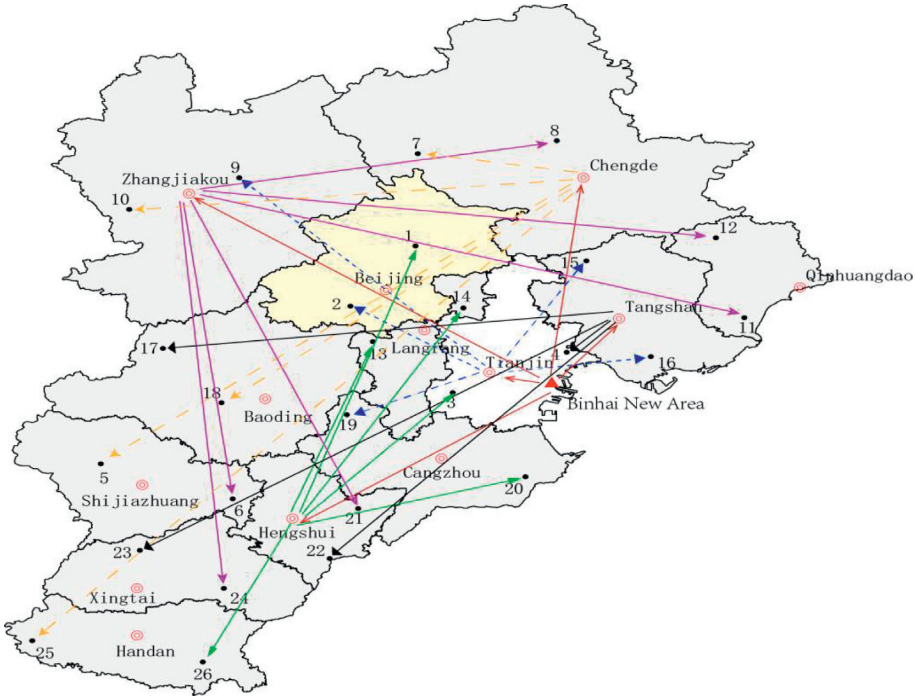

Figure 2: Schematic diagram of location selection of the DNA-artificial fish swarm algorithm.

Figure 3: Schematic diagram of location selection of the FWA-artificial fish swarm algorithm.

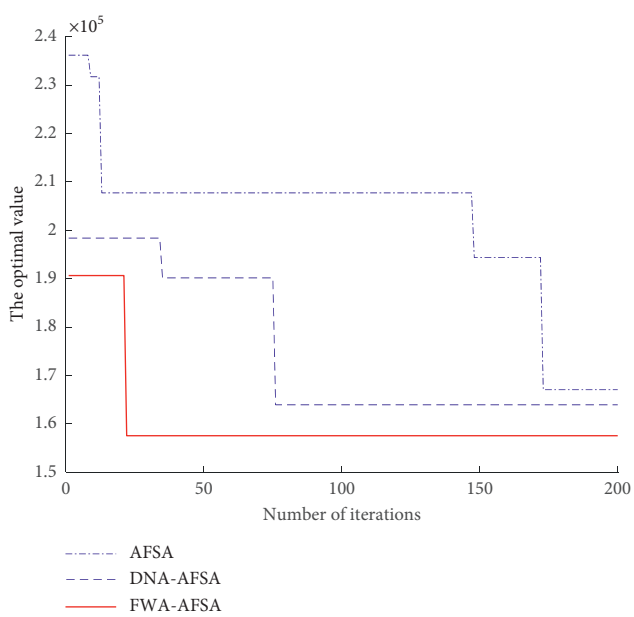

Figure 4: Comparison of optimization curves of the three algorithms.

by FWA-AFSA are, respectively, reduced by 9520.87, 30521.46 and 13727.57 compared with those of the basic artificial fish swarm algorithm and, respectively, reduced by 6395.41, 6897.57 and 4789.78 compared with those of DNA-AFSA, indicating that FWA-AFSA can obtain a lower total cost. In terms of stability, FWA-AFSA has a smaller standard deviation, which proves its stability. In terms of convergence rate, the FWA-AFSA's average convergence algebra is smallest, indicating its faster convergence rate.

The schematic diagrams of optimal location solved by the basic artificial fish swarm algorithm, DNA-artificial fish swarm algorithm, and FWA-artificial fish swarm algorithm are shown in Figures 1–3, respectively.

According to Figure 1, the optimal site selection scheme obtained by the basic artificial fish swarm algorithm is as follows: first of all, food is transported from the supplier, Binhai New Area, to 5 distribution centers: Beijing, Tianjin, Chengde, Zhangjiakou, and Tangshan. Next, the food is transported by distribution centers to customers: (1) customers transported by Beijing: 7 (Fengning County, Chengde), 14 (Xianghe County, Langfang), 17 (Laiyuan County, Baoding), 22 (Gucheng County, Hengshui), and 23 (Lincheng County, Xingtai); (2) customers transported by Tianjin: 1 (Huairou District, Beijing), 8 (Longhua County, Chengde), 10 (Huai'an County, Zhangjiakou), 12 (Qinglong County, Qinhuangdao), 13 (Gu' an County, Langfang), and 15 (Zunhua City, Tangshan); (3) customers transported by Chengde: 19 (Renqiu County, Cangzhou), 21 (Fucheng County, Hengshui), 25 (Shexian County, Handan), and 26 (Wei County, Handan); (4) customers transported by Zhangjiakou: 3 (Jinghai District, Tianjin), 4 (Ninghai

County, Tianjin), 5 (Pingshan County, Shijiazhuang), 6 (Xinji City, Shijiazhuang), and 18 (Shunping County, Baoding); (5) customers transported by Tangshan: 2 (Fangshan District, Beijing), 9 (Chongli County, Zhangjiakou), 11 (Changli County, Qinhuangdao), 16 (Tanghai County, Tangshan), 20 (Haixing County, Cangzhou), and 24 (Guangzong County, Xingtai).

According to Figure 2, the optimal site selection scheme solved by DNA-artificial fish swarm algorithm is as follows: first of all, food is transported from the supplier, Binhai New Area, to 5 distribution centers: Tianjin, Chengde, Zhangjiakou, Tangshan, and Hengshui; next, the food is transported by distribution centers to customers: (1) customers transported by Tianjin: 2 (Fangshan District, Beijing), 9 (Chongli County, Zhangjiakou), 15 (Zunhua City, Tangshan), 16 (Tanghai County, Tangshan), and 19 (Renqiu County, Cangzhou); (2) customers transported by Chengde: 5 (Pingshan County, Shijiazhuang), 7 (Fengning County, Chengde), 10 (Huai' an County, Zhangjiakou), 18 (Shunping County, Baoding), and 25 (Shexian County, Handan); (3) customers transported by Zhangjiakou: 6 (Xinji City, Shijiazhuang), 8 (Longhua County, Chengde), 11 (Changli County, Qinhuangdao), 12 (Qinglong County, Qinhuangdao), 21 (Fucheng County, Hengshui), and 24 (Guangzong County, Xingtai); (4) customers transported by Tangshan: 4 (Ninghai County, Tianjin), 17 (Laiyuan County, Baoding), 22 (Gucheng County, Hengshui), and 23 (Lincheng County, Xingtai); (5) customers transported by Hengshui: 1 (Huairou District, Beijing), 3 (Jinghai District, Tianjin), 13 (Gu' an County, Langfang), 14 (Xianghe County, Langfang), 20 (Haixing County, Cangzhou), and 26 (Wei County, Handan).

According to Figure 3, the optimal site selection scheme solved by FWA-artificial fish swarm algorithm is as follows: First, food is transported from the supplier, Binhai New Area, to 5 distribution centers: Tianjin, Chengde, Zhangjiakou, Tangshan, and Xingtai; Next, the food is transported by distribution centers to customers: (1) customers transported by Tianjin: 2 (Fangshan District, Beijing), 8 (Longhua County, Chengde), 14 (Xianghe County, Langfang), 17 (Laiyuan County, Baoding), 21 (Fucheng County, Hengshui), and 23 (Lincheng County, Xingtai); (2) customers transported by Chengde: 6 (Xinji City, Shijiazhuang), 11 (Changli County, Qinhuangdao), 13 (Gu' an County, Langfang), 16 (Tanghai County, Tangshan), and 22 (Gucheng County, Hengshui); (3) customers transported by Zhangjiakou: 1 (Huairou District, Beijing), 7 (Fengning County, Chengde), 12 (Qinglong County, Qinhuangdao), 24 (Guangzong County, Xingtai), and 26 (Wei County, Handan); (4) customers transported by Tangshan: 3 (Jinghai District, Tianjin), 5 (Pingshan County, Shijiazhuang), 9 (Chongli County, Zhangjiakou), 10 (Huai' an County, Zhangjiakou), and 25 (Shexian County, Handan); (5) customers transported by Xingtai: 4 (Ninghai County, Tianjin), 15 (Zunhua City, Tangshan), 18 (Shunping County, Baoding), 19 (Renqiu County, Cangzhou), and 20 (Haixing County, Cangzhou).

The comparison of the optimization curves of the three algorithms is shown in Figure 4. As can be seen from Figure 4, the FWA-artificial fish swarm algorithm has a faster optimization speed and a higher accuracy.

6. Conclusion

At first, this paper aims at minimizing the total cost and establishes a location model of low-carbon cold chain logistics distribution center, including cargo damage, refrigeration, carbon emission, and other factors, in combination with various factors affecting cold chain food. Secondly, the explosion operator, mutation operator, mapping rule, and selection strategy of the fireworks algorithm are introduced into the artificial fish swarm algorithm, and the FWA-artificial fish swarm algorithm is proposed. At the same time, the FWA-artificial fish swarm algorithm is applied to the location model of low-carbon cold chain logistics distribution center in the Beijing-Tianjin-Hebei metropolitan area. The simulation results show the effectiveness of the FWA-artificial fish swarm algorithm.

Optimizing the location of low-carbon cold chain logistics in the Beijing-Tianjin-Hebei metropolitan area not only makes the links between cities in the circle closer and promotes the integration of resources in the region but also is conducive to realizing the goal of low-carbon development; moreover, it is helpful to promote the economic development and economic integration process of the Beijing-Tianjin-Hebei region.

Data Availability

The data used for research and analysis are included within the article.

Conflicts of Interest

The authors declare that there are no conflicts of interest regarding the publication of this paper.

Acknowledgments

This work was supported by the Tianjin Natural Science Foundation (Grant no. 20JCYBJC00320).

References

[1] Z. Shuiyun: Thinking of "chain Breaking" behind cold chain logistics, 2019, http://www.zgsyb.com/news.html?aid=530826.

[2] Guangming, What is the potential of saving food, 2020, https://www.sohu.com/a/414789580_162758.

[3] Y. Marinakis, "An improved particle swarm optimization algorithm for the capacitated location routing problem and for the location routing problem with stochastic demands," *Applied Soft Computing*, vol. 37, pp. 680–701, 2015.

[4] J. Li, P. H. Fu, X. L. Li, J. H. Zhang, and D. L. Zhu, "Study on vehicle routing problem and tabu search algorithm under low-carbon environment," *Chinese Journal of Management Science*, vol. 23, no. 10, pp. 98–106, 2015.

[5] S. J. Sadjadi, A. Makui, E. Dehghani, and M. Pourmohammad, "Applying queuing approach for a stochastic location-inventory problem with two different mean inventory considerations," *Applied Mathematical Modelling*, vol. 40, no. 1, pp. 578–596, 2016.

[6] Q. Z. Ma, J. Wang, and H. Q. Song, "Small-scaled low carbon multi-vehicle routing problem in urban area: an example from the regional picking-up network of Zhuhai express Company," *Jonrnal of Industrial Engineering/Engineering Management*, vol. 30, no. 4, pp. 153–159, 2016.

[7] J. A. Orjuela-Castro, L. A. Sanabria-Coronado, and A. M. Peralta-Lozano, "Coupling facility location models in the supply chain of perishable fruits," *Research in Transportation Business & Management*, vol. 24, pp. 73–80, 2017.

[8] B. El-Sobky, Y. Abo-Elnaga, and L. Al-Naser, "An active-set trust-region algorithm for solving warehouse location problem," *Journal of Taibah University For Science*, vol. 11, no. 2, pp. 353–358, 2017.

[9] D. Simic, V. Ilin, V. Svircevic, and S. Simic, "A hybrid clustering and ranking method for best positioned logistics distribution centre in balkan peninsula," *Logic Journal of IGPL*, vol. 25, no. 6, pp. 991–1005, 2017.

[10] Y. Wang, Y. J. Ren, and M. Z. Xu, "Optimization of profit allocation based on multi-center joint distribution," *Computer Integrated Manufacturing Systems*, vol. 23, no. 7, pp. 1571–1580, 2017.

[11] K. Kang, J. Han, W. Pu, and Y. F. Ma, "Optimization research on cold chain distribution routes considering carbon emissions for fresh agricultural products," *Computer Engineering and Applications*, vol. 55, no. 2, pp. 259–265, 2019.

[12] F. T. Liang, J. K. Hu, and Y. F. Huang, "Electric vehicle routing problem under low carbon condition," *Journal of Shanghai Maritime University*, vol. 39, no. 2, pp. 34–40, 2018.

[13] O. N. Bilisik, U. R. Tuzkaya, H. Baracli, and M. Tanyas, "Fruits and vegetables market Hall location selection by using interval-valued trapezoidal fuzzy grey relational analysis an application for istanbul," *International Journal of Industrial Engineering Theory Application and Practice*, vol. 26, no. 5, pp. 719–736, 2019.

[14] Y. M. Zhang, Y. M. Li, and H. O. Liu, "Research on VRP optimization of multi-type vehicle cold-chain logistics with satisfaction constraint," *Statistics & Decisions*, vol. 35, no. 4, pp. 176–181, 2019.

[15] L. J. Sheng, "Location of logistics distribution center based on quantum particle swarm optimization," *Science Technology and Engineering*, vol. 19, no. 11, pp. 183–187, 2019.

[16] J. H. Park, J. G. Oh, D. M. Kim, and G. T. Yeo, "A study on the establishment direction of smart distribution logistics center in the era of the fourth industrial revolution," *Journal of Digital Convergence*, vol. 17, no. 2, pp. 59–71, 2019.

[17] E. Setiawan, J. Liu, and A. French, "Resource location for relief distribution and victim evacuation after a sudden-onset disaster," *IISE Transactions*, vol. 51, no. 8, pp. 830–846, 2019.

[18] F. T. Zhou, G. H. Zhou, and J. Zhang, "Study on location of trans shipment points in urban distribution system based on subway network," *Journal of the China Railway Society*, vol. 41, no. 7, pp. 16–25, 2019.

[19] Y. H. Song, B. B. Su, F. Z. Huo, J. J. Ning, and D. H. Fang, "Research on rapid location selection of emergency materials distribution center considering dynamic demand," *China Safety Science Journal*, vol. 29, no. 8, pp. 172–177, 2019.

[20] S. Y. Li, B. Dan, and X. L. Ge, "Optimization model and algorithm of low carbon vehicle routing problem under multi-graph time-varying network," *Computer Integrated Manufacturing Systems*, vol. 25, no. 11, pp. 2973–2982, 2019.

[21] J. Meng and J. H. Gao, "Location strategy of agricultural logistics distribution center based on improved moth optimization algorithm," *Journal of Chinese Agricultural Mechanization*, vol. 41, no. 4, pp. 207–214, 2020.

[22] B. Li and J. J. Dang, "Fresh agricultural cargoes location-routing optimization with simultaneous pickup and delivery for multiple distribution centers," *CAAI Transactions on Intelligent Systems*, vol. 15, no. 1, pp. 50–58, 2020.

[23] Z. P. Li, Y. W. Zhao, and Y. W. Zhang, "Optimization model and algorithm of location-routing for joint distribution," *Journal of Chongqing University*, vol. 43, no. 1, pp. 28–43, 2020.

[24] D. S. Lin, Z. Y. Zhang, J. X. Wang, X. Liang, and Y. Q. Shi, "Low-carbon logistics distribution center location with uncertain demand," *Control and Decision*, vol. 35, no. 2, pp. 492–500, 2020.

[25] X. Q. Xu, Z. Yang, and L. Liu, "Spider monkey optimization algorithm for solving location problem of logistics distribution center," *Computer Engineering and Applications*, vol. 56, no. 1, pp. 150–157, 2020.

[26] W. Zhang, Y. Ma, H. D. Zhao et al., "Obstacle avoidance path planning of intelligent mobile based on improved fireworks-ant colony hybrid algorithm," *Control and Decision*, vol. 34, no. 2, pp. 335–343, 2019.

[27] C. Xiao, L. Y. Zhang, and T. Fei, "Research on bacteria foraging ant colony optimization algorithm for cold chain low carbon logistics distribution routing optimization," *Mathematics in Practice and Theory*, vol. 47, no. 21, pp. 98–107, 2017.

[28] T. Fei, L. Y. Zhang, Y. Bai, and L. Chen, "Improved artificial fish swarm algorithm based on DNA," *Journal of Tianjin University*, vol. 49, no. 6, pp. 581–588, 2016.

Hindawi
Scientific Programming
Volume 2021, Article ID 9949565, 10 pages
https://doi.org/10.1155/2021/9949565

Research Article

The Price Impact of Order Book Events from a Dimension of Time

Wentao Chi,[1] **Xuemei Zhao**,[2] **and Lufei Huang**[1]

[1]*School of Financial Technology, Shanghai Lixin University of Accounting and Finance, Shanghai 201209, China*
[2]*Shandong Management University, Jinan, Shandong 250357, China*

Correspondence should be addressed to Lufei Huang; lufei.huang@lixin.edu.cn

Received 16 April 2021; Accepted 19 July 2021; Published 27 July 2021

Academic Editor: Xiaobo Qu

Copyright © 2021 Wentao Chi et al. This is an open access article distributed under the Creative Commons Attribution License, which permits unrestricted use, distribution, and reproduction in any medium, provided the original work is properly cited.

We propose a new linear model to explain the price move by Level-2 high-frequency data in Chinese mainland stock market. In Chinese stock market, the cancellation ratio is very low, and imbalanced order flow prevails most of the time in the trading periods. From time dimension viewpoint, we find the difference of efficiency of limit orders executed, respectively, in bid/ask limit order book, order execution imbalance (OEI), could improve the classic model of Cont et al. (2014) based on market microstructure of Chinese mainland stock market. In particular, when market's liquidity is booming, our model's explanatory power and R-squared increased sharply. And the correlations of OEI are very high that may be exploited to predict the price move in the next time window for doing high-frequency trading.

1. Introduction

Excessive order cancelations are scrutinized by regulators who view such excess as a possible indicator of manipulative quoting activity by potential stock market manipulators. In US stock market, Hasbrouck and Saar [1] investigate trading of 100 NASDAQ-listed equity securities on INET, an electronic limit order book, and find that over 35% of limit orders are cancelled within two seconds of submission compared with only 5%, which we computed from most liquidity stocks in Shenzhen stock exchange in Chinese stock market. The market microstructure from China will contribute very different order flows from US market composed of limit orders, market orders, and cancellation orders, which are usually discussed in high-frequency trading.

The field of market microstructure, in which reasons could cause price moving in continuous trading period, is a research mainstream, because many factors affect price variation like big market orders, clouded market orders on the same side, breaking news, market liquidity, and number of participant members. Until recently, there are no clear factors and models to determine price moving direction and altitude from high-frequency trading data especially in Chinese mainland stock exchange market. First, we test the order flow imbalance (OFI) factor whether or not it can contribute most R-squared for price moving in every ten seconds from the most liquidity 50 stocks in Shenzhen stock market for one month and compare the results within another month, in which trading volume blooming in recent years. Then, we find that although statistical results derived from OFI are coherent to findings of Cont et al. [2], the R-squared is not as high as NYSE's based on the research of Cont et al. [2]. In practical high-frequency trading, we find that analysis of actions on order book from time dimension is critical for HFT especially in the period of intensive trading activity. Like the reverse of limit orders trade duration, or difference between ratios of arrived buy and sell limit executed, respectively, in a short and fixed timespan, order execution imbalance (OEI) is a time dimension reflecting potential market force to move price up/down. And the time dimension factor model based on Level-2 data of Chinese stock market effectively improves the R-squared compared with Cont's model, and our theory is coherent to principles of market microstructure. In the end, we show that when total market liquidity is surging, these explanatory power and R-squared of our model will be augmented sharply.

Motivated by the above research, we show the price impact model with a time dimension of these orders. The time dimension factor model based on Level-2 data of Chinese stock market effectively improves the R-squared

compared with Cont's model, and our theory is coherent to principles of market microstructure. In the end, we show that when total market liquidity is surging, this explanatory power and R-squared of our model will be augmented sharply.

The paper is structured as follows. In Section 2, the related literature is reviewed. In Section 3, we compare Chinese stock market with US stock market with perspective of proportion of balanced/imbalanced order flow and order cancellation ratio. And then, we provide a new method from time dimension viewpoint, which shows that out of synchronization for limit order books or order queues constructed and deleted by market orders in the bid and ask side respectively could lead to price changes, and other features of order book are unchanged. After that, based on Cont's definition about OFI, we specify a linear model to explain price changes about OFI and OEI. In Section 4, we use 50 most liquid stocks from Shenzhen stock exchange of Chinese mainland to estimate the coefficients of variables and analyze what we find in a normal month compared with a trading volume booming month recently, and then we get statistical results for eight different time periods of a trading day. In Section 5, based on the empirical results, we find high correlations of order execution imbalance (OEI) in high-frequency trading to predict price moves before adverse selection, which is caused by price changes when we placed limit orders waiting a long time in the order book. In Section 6, we conclude possible reasons why OFI and OEI still have deficiencies in explaining price changes and finally propose potential methods for further improvement.

2. Related Literature

2.1. Related Work of Macrofinancial Markets. The moving direction and altitude of prices in financial markets result from the interaction of buy and sell orders through a complex dynamic process. The availability of high-frequency records of orders, trades, and quotes has reported statistical regularities in limit order book (LOB) data from a wide variety of different markets. LOBs are subject to frequent shocks in order flow that cause them to display nonstationary behavior, thus, in the result cause price impact. Ellul et al. [3] reported a positive correlation between higher midprice realized volatility and the percentage of arriving orders that were limit orders. The intuition behind price moving is an imbalance between supply and demand order flows. Cont et al. [2] show that, over short time intervals, price changes are mainly driven by the order flow imbalance (OFI), defined as the imbalance between supply and demand at the best bid and ask prices. But the state space of order book is very large conditioning on the fact that the most recent event is still problematic. Findings from Cont et al. [2] seem to give an intuitive picture of the price impact of order book events, which is somewhat simpler than the ones conveyed by previous studies. Meanwhile, Cont's linear model with average high R-squared also excludes trades, which seem to carry little to no information about price changes after the OFI is taken into account simultaneously.

2.2. Related Work of Trading Strategies. Achab et al. [4] introduce a new nonparametric method that allows for a direct, fast, and efficient estimation of the matrix of kernel norms of a multivariate Hawkes process. Dugast [5] studied the same model and proposed a prediction that positive (negative) market order imbalance, negative (positive) depth, and cancellation imbalances contribute a positive (negative) change in price. Following market news, he found that order flows become unbalanced, and market depth is consumed, leading to positive covariance between price variability and order book unbalances. Prior to news arrival, trading occurs because of differences in private valuations, though at prices generally in line with the asset value. Yet when news arrives, trading prices no longer accord with the new asset value. This mismatch generates imbalances, in both order book and order flows, that disappear once prices have adjusted. Huang et al. [6] are interested in whether the combined estimator may be used to form a combined forecast to improve the RE forecast (forecast made using the RE estimator) and the FE forecast (forecast using the FE estimator) in out-of-sample forecasting.

Since imbalances anticipate a change in price, it follows that they could be exploited, especially by algorithmic trading strategies. Cartea et al. [7] document the predictive power of order book imbalances for future price movements on the Nasdaq exchange. Goldstein et al. [8] show that HFTs on the Australian Securities Exchange take advantage of this predictability. Silantyev [9] conducts an in-depth analysis on the trade and quote data of the XBTUSD perpetual contract and demonstrates that the trade flow imbalance is better at explaining contemporaneous price changes than the aggregate order flow imbalance. Niu et al. [10] studied the valuation of vulnerable European options incorporating the reduced-form approach, which models the credit default of the counterparty. Fosset et al. [11] proposed an actionable calibration procedure for general Quadratic Hawkes models of order book events and found that the Zumbach kernel is a power-law of time, as are all other feedback kernels.

2.3. Literature Summary. From Chinese mainland stock market, we found that the order flow imbalance cannot explain much for price change. Here, today, more and more automated or algorithms trading institutions and professional traders enter Chinese stock market to do T-0 trading (close holding positions everyday) with established stock positions one day ago because of Chinese T-1 trading limitations. Most professional T-0 traders submit limit orders with anticipation of their limit orders that could be matched as soon as possible, epically in 30 minutes after market opened or 30 minutes before market closing, in which most market trading volume accumulated in these periods. With orders' time priority rule, time creates new incentives to use trading information extending Cont's model that would be a worthwhile contribution in its own right. Computing orders' execution timespan once limit orders are submitted into Cont's classical linear model contributes more explanation power for price changes in a 10-second interval from Chinese mainland stock market.

Thus, adding the factor of difference between the ratio of sell limit orders and buy limit orders executed in a fixed timespan proportional to total sell/buy limit orders' arriving at order book in every 10 seconds is a time dimension reflecting potential force to move price up/down. And empirical results illustrated that this is effective.

3. Price Impact Model

3.1. New York Stock Exchange and Nasdaq versus Chinese Mainland Stock Exchanges. Every day, 70% trading volume is from high-frequency trading in US exchange market. Technology has changed financial markets, altering the trading behavior of limit order traders. High-speed computerized trading strategies, and electronic order-driven trading exchanges, let traders better monitor their orders and make faster, more accurate decisions. The increase in trading speed coincides with an explosion in order cancellation activity (Hasbrouck and Saar, 2013). Trading in financial markets has entered the nanosecond age in US financial market, where liquidity is added and subtracted in billionths of a second.

In Chinese stock market, the algorithm and high-frequency trading are at most 10 percent in everyday trading volume analyzed by stock exchanges. And the solution of time stamp from limit orders, market orders, or other kinds is correct to 10 milliseconds both in Shenzhen stock exchange and Shanghai stock exchange. This data resolution would be an obstacle for high-frequency traders in Chinese market. And moreover, Chinese SEC and stock exchanges limit orders' cancellation. Table 1 shows that cancellation ratio is as low as 5% or less.

Table 1 shows the estimation for ratios of orders' cancellation (column 3 for bid side and column 5 for sell side) and ratios of order flow imbalance (column 2 for bid side and column 4 for sell side) from Shenzhen stock exchange; $\lambda(b)$, $\mu(b)$, and $\theta(b)$ stand for limit orders arriving rate, market orders arriving rate, and orders' cancelling rate, respectively, in number of shares per second on March, 2019, by averaging 50 stocks. And the same parameters' descriptions are for sell side.

The order cancellation rate is represented with theta θ, limit order arrival rate is represented with λ, and market order arrival rate is represented with μ. Because, in different periods of a trading day, the liquidity and trading activity variates vastly, Table 1 summarizes cancellation ratios (columns 3 and 5) and unbalanced order flow ratios (columns 2 and 4) for eight trading periods, in which the intensities of cancelled orders and executed orders are compared with limit orders for bid side and sell side (ask side), respectively.

In contrast to Chinese financial market, Hasbrouck and Saar [12] investigate trading of 100 NASDAQ-listed equity securities on INET, an electronic limit order book, and find that over 35% of limit orders are cancelled within two seconds of submission.

Cont and de Larrard [13] consider the case of a balanced order flow, for which the arriving intensities of market orders and cancelations are equal to arriving intensity of limit orders. The study of high-frequency quote data indicates that this is an empirically relevant case for many liquid stocks. For the buy side, they find that the imbalance between arriving intensity of limit orders and intensities of market orders + cancelations is around 5% or less for these stocks. But Table 1 shows that the imbalance is around 33% in Chinese mainland stock market.

So, controlled by Chinese SEC on limit orders' cancellation, the state of imbalanced order flow dominates the market since the proportion of cancellation is low compared with total limit orders in Chinese stock market. The order flow imbalance (OFI), proposed by Cont et al. [2], is defined as the imbalance between supply and demand at the best bid, and ask prices better explain price changes. Their linear model's goodness of fit is surprising for high-frequency data with a R-squared of 65% on average across 50 stocks in S&P 500 constituents.

Hence, in the environment of imbalanced order flow dominated in Chinese stock market, maybe we cannot establish a stable linear relationship or with high R-squared model between OFI and price changes because imbalanced order flow is so prevailing in market whenever price changes. And further OFI is constructed from order book events taking place only at the best bid/ask, and results of Cont et al. [2] show that activity at the top of the order book is the most important factor driving price changes. So, the OFI did not try to explain the latitudes of price changes. In particular, in the morning of market open, some stocks could pump and dump lots of ticks in seconds or in milliseconds in Chinese stock market.

Since the limitation on orders' cancellation, algorithms, and high-frequency trading firms in Chinese mainland hopes that their limit orders can be filled as soon as possible to avoid adverse selection when trading span or duration of limit orders, which is difference between arriving time and first filling time of limit orders, is getting longer, some algorithms trading firms usually use TWAP or VWAP methods to open or cover their positions by optimal placement strategies, which switch between limit orders and market orders. To ensure saving costs from trading stocks, they will use limit orders as much as possible, and with strict limitation on orders' cancellation, they should estimate orders' filling probability more accurately.

3.2. A Time Dimension Viewpoint and Model of the Limit Order Book. Many high-frequency trading mainly uses market making strategy to place limit orders on different layers into order book for capturing the variance of price. They hope that their placed bid limit orders and ask limit orders within a time interval can be executed almost simultaneously to get bid-ask spread for profits. Like TWAP or VWAP of algorithms trading, traders also try to place limit orders when market price has the potential to move towards to the placed prices for saving costs from slippage or using market orders.

In every trade day, the automated or manual high-frequency trading usually happens at the open of stock markets since, in this period, the prices change quickly, and variance

Table 1: In eight different time periods of a trading day, bid(b)/ask(s) side imbalance ratio of orders' arrival (column 2/4) and cancelling ratio of orders (column 3/5).

Time period	$(\lambda(b)-\mu(b)-\theta(b))/\lambda(b)$	$\theta(b)/\lambda(b)$	$(\lambda(s)-\mu(s)-\theta(s))/\lambda(s)$	$\theta(s)/\lambda(s)$
9:30–10:00	0.370073879	0.03662	0.48266014	0.03417
10:00–10:30	0.383481915	0.06472	0.43961763	0.04746
10:30–11:00	0.359117126	0.08013	0.43537183	0.05688
11:00–11:30	0.291588197	0.08751	0.44505638	0.05835
13:00–13:30	0.358005535	0.08612	0.43203355	0.05679
13:30–14:00	0.278926993	0.11276	0.48520687	0.06282
14:00–14:30	0.326217539	0.11834	0.43248183	0.06079
14:30–14:57	0.317330298	0.15007	0.41677333	0.05012

is high, which could cover trading fees. Once they place a limit order, the order may have high possibility to be filled; if the filling possibilities computed are different from the real ones, they have to cancel the previous orders to wait the next execution opportunity.

Execution duration of limit orders is defined as

$$\begin{aligned} \mathrm{ED} = {} & \text{timestamp of first filled} \\ & - \text{timestamp of arriving into market queue.} \end{aligned} \tag{1}$$

We can see from Figure 1 that if some limit orders arrived at the 5th second at both bid and ask queue, most of them are filled around the 10th second on ask side, and on bid side, the limit buy orders are "consumed" relatively gentle, and the curve represented for matching rate is flat between 5 seconds and 15 seconds. If there are no new limit orders arriving on both sides, at time 10, the midprice will pump suddenly since lots of limit ask orders are deleted from ask queues that make the best ask price move upward, even though the total number of filled orders on bid/ask side is the same on average for interval [5 s, 15 s]. The cluster effect for market orders like in environment of Figure 1 is demonstrated by the fact that the majority proportion of orders in the ask queue filled in a short time interval could cause midprice shift towards to the price higher (market buy orders clustering) or lower (market sell orders clustering).

Then, we use order execution imbalance (OEI) to represent the different ratios of new arriving limit orders, respectively, in bid order book and ask order book if they could be filled in a fixed time interval proportional to total arriving ones. We use two time grids $\{T_0, \ldots, T_I\}$ and $\{t_0, 0, \ldots, t_{I,K}\}$ with time steps $T_i - T_{i-1} = 30\,\mathrm{min}$ and $t_{k,i} - t_{k-1,i} = \Delta t = 10\,\mathrm{s}$, $[t_{k-1,i}, t_{k,i}] \subset [T_{i,1}, T_i]$. Within each long-time interval $[T_{i-1}, T_i]$, we compute 180 price changes and OEIs indexed by k [14]:

$$\mathrm{OEI}_k = \frac{\sum_{n=L_{(t_{k-1})}+1}^{L_{(t_k)}} 1^s_{\{ED_n \le 10\}}}{L^s_k} - \frac{\sum_{n=L_{(t_{k-1})}+1}^{L_{(t_k)}} 1^b_{\{ED_n \le 10\}}}{L^b_k}, \tag{2}$$

where OEI_k is the order execution imbalance in the kth interval; L^s_k is the total limit orders arrived in the kth interval for the sell side; L^b_k is the total limit orders arrived in the kth interval for the buy side; $L_{(t_{k-1})} + 1$ is the first limit order in the kth interval; $L_{(t_k)}$ is the last limit order in the kth interval; and $1^s_{\{ED_n \le 10\}}$ is the indicator function for ED_n less than or equal to 10 seconds in sell side, and the same definition for bid side.

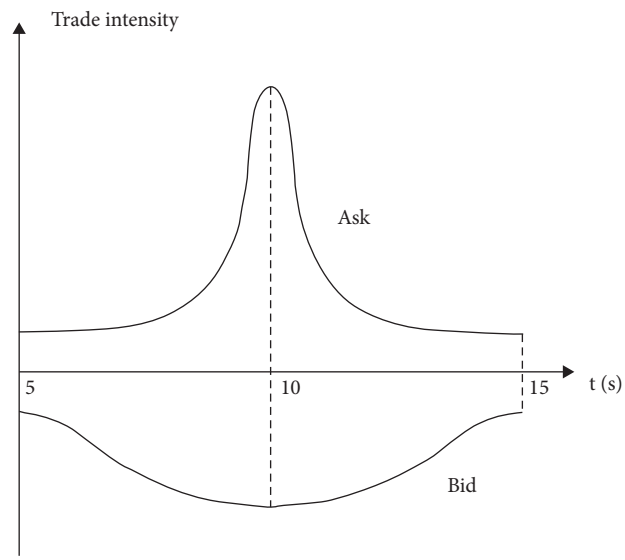

Figure 1: Trading intensity evolves differently at bid and ask queue.

Define price changes as in a time interval $[t_{k-1,i}, t_{k,i}]$ the midprice difference between start and end time point.

$$P_{k,i} = \frac{P^b_{N(t_{k,i})} + P^s_{N(t_{k,i})}}{2\delta} - \frac{P^b_{N(t_{k-1,i})} + P^s_{N(t_{k-1,i})}}{2\delta}, \tag{3}$$

where $N(t_{k-1,i})$ and $N(t_{k,i})$ are the index of the first and the last order book events in the interval $[t_{k-1,i}, t_{k,i}]$. The tick size $\delta$is equal to 1 cent in our data. And s stands for sell (ask) side of order book, and b stands for bid (buy) side of order book.

To get OEI, we first add together the number of limit orders arriving at time interval $[t_{k-1,i}, t_{k,i}]$, which will be first filled less than or equal to 10 seconds (execution duration ≤10 seconds), and then we compute the ratio of these orders proportional to total limit orders arriving, respectively, for bid and ask side; finally, we get the difference of ratios between sell and buy side. Here, we not only concentrate the orders on best bid/ask queue, but also measure the orders on all different price levels. The OEI reflects which side has more potential willingness to trade, in other words, if part of orders placed by high-frequency traders or algorithms traders are executed in a shorter interval, which provides a sign of whether bid (ask) side is more efficient than the other and has more liquidity for trading than the other. If one of two sides was more efficient for providing "service" higher execution speed for incoming limit orders, then order books

of that side will induce more "customers" limit orders to arrive at this line more frequently. With time elapsing, the denominator L_k^s or L_k^b is getting larger and larger making the "service rate" for further incoming limit orders lower and lower. At last, the queuing system will rebalance to a new state, in which the OEI gets balanced, presented with its absolute value shrinking. Then, prices change contributed by orders' ED and OEI of order books measured from a time dimension will cease.

Based on the model of Cont et al. [2], the price changes are mainly caused by order flow imbalance:

$$\mathrm{OFI}_k = \frac{L_k^b - C_k^b - M_k^s}{D_b} - \frac{L_k^s - C_k^s - M_k^b}{D_s}, \tag{4}$$

where L_k^b and L_k^s stand for the number of limit orders in the kth interval for bid and ask side, respectively; C_k^b and C_k^s stand for the number of cancelations in the kth interval for bid and ask side, respectively; M_k^s and M_k^b stand for the number of market orders; and D stands for order book depth. In the regression model of Cont et al. [2], they rewrite OFI_k for formula (5) as a variable in empirical findings.

$$\mathrm{OFI}_k = L_k^b - C_k^b - M_k^s - L_k^s + C_k^s + M_k^b. \tag{5}$$

3.3. Model Specification. Here, we establish two linear models: one is the linear model from Cont et al. [2].

$$\Delta P_{k,i} = \beta_i \mathrm{OFI}_{k,i} + \varepsilon_{k,i}, \tag{6}$$

where β_i is a price impact coefficient for an i-th time interval and $\varepsilon_{k,i}$ is a noise term summarizing influences of other factors. It allows β_i and the distribution of $\varepsilon_{k,i}$ to change with index i because of the well-known intraday seasonality effects.

Then, we construct a new linear model including OFI and OEI.

$$\Delta p_{k,i} = \beta_i \mathrm{OFI}_{k,i} + \gamma_i \mathrm{OEI}_{k,i} + \varepsilon_{k,i}. \tag{7}$$

Comparing the statistical results of model (7) with model (6) will show whether or not there is an improvement for model (7) in the environment of high ratio of imbalance order flow and low cancellation rate prevailing in most time of trading day in Chinese mainland stock market.

4. Estimation and Results

4.1. Data. In Chinese mainland, there are two stock exchanges. One is Shanghai stock exchange, and the other is Shenzhen Stock exchange. Totally, around 3000 companies are listed on these two exchanges.

Here, we use the data usually used for high-frequency trading from Shenzhen stock exchange because Shanghai stock exchange does not provide trade by trade files even though there is electronic connection to it from other institutions. So, we lack the trading timestamp of limit orders from Shanghai for computing execution timespan.

Shenzhen stock exchange has three kinds of data to describe what happened in detail when stocks are trading. The first is the tick file; every three seconds, a new tick will update and disseminate, including tick time with resolution of seconds, newest trade price, best bid price, best bid volume in shares waiting in the queue, best ask price, best ask volume in shares waiting in the queue, and second best bid price. The second is order by order file; every file includes one stock of all orders arriving in the market, including order time stamp with resolution of 10 milliseconds, order price, order volume, index of orders, kinds of orders, and order direction on bid or ask. By the way, all orders cannot be corrected once submitted in Chinese mainland stock market, so if one trader wants to change their previous orders, he/she must cancel them first and then replace orders with new price or volume. The third is trade by trade file; every file includes one stock of all trades happened in the market, including trade timestamp with resolution of 10 milliseconds, trade price, trade volume in shares, label for orders traded or cancelled, index of active orders, and index of passive orders of every trade with the rule of time first and price first; it is a first in first out (FIFO) queuing system, in which every trade happens with a matched pair of one passive order with one active order (usually the market order).

For general, we select 50 stocks with highest liquidity in Shenzhen Stock exchange based on statistics of a month. As shown in Table 2, they summarize 50 most liquidity stocks from Shenzhen stock exchange in July 2018 and March 2019, respectively; in March 2019, the trading volume everyday was booming as high as 150 billion US dollars lasting the whole month.

For comparison, we select data of two months, respectively; one is the month with normal trading volume, and the other is the month with highest trading volume and booming liquid in recent years.

In July 2018, 50 highest liquidity stocks are listed on Shenzhen stock exchange in Table 3 in Appendix, a total of 22 trading days.

We get statistics of stock name, average price in one month, average trading volume in shares for every day, total counts of best bid price updated in one month, total counts of best ask price updated in one month, total counts of trading happened in one month, average bid-ask spread, maximum of spread, and average length of best bid/ask queue in shares for every day.

In March 2019, there are also 50 highest liquid stocks listed on Shenzhen exchange in Table 4 with a total of 21 trading days.

Compared with the two tables, we can see that, in March 2019, even with a total of 21 trading days, the trading frequency and the frequency of best bid/ask price changes are much higher than these in July 2018.

4.2. Empirical Findings. This section reports statistical results of average values across 50 stocks in July 2018 from Shenzhen stock exchange in eight different time periods in a trading day. Model (6) is estimated by an ordinary least squares regression:

Table 2: p values, R-squared, and coefficients of $\widehat{\gamma}_i$ estimated by model (9) for averaging 50 stocks in March 2019.

Item	9:30–10:00	10:00–10:30	14:30–15:00
p value	0.02157613	0.053005478	0.037117952
R-squared	0.26616222	0.254128669	0.234105648
OEI's coefficient	0.16536644	0.095379223	0.049151509

Table 3: Statistical values of highest liquid 20 stocks out of 50 stocks discussed above from Shenzhen stock exchange in July 2018.

Stock name	Price	Volumes	Bidupdates	Iskupdates	Trades	Spread	Max spread	Bidquote	Askquote
"000001"	8.949474	90633922	8584	8585	691911	0.010166	0.05	208784.8	186256.2
"000002"	23.42526	42181755	24764	24490	846306	0.012046	0.17	30181.26	24192.15
"000063"	14.70474	218000000	26186	26151	3877441	0.010325	0.18	7137346	65453.27
"000066"	7.202699	57395362	14472	14450	538278	0.010516	0.07	91451.34	62865.07
"000100"	2.87187	63856220	1674	1670	324921	0.010034	0.02	1231807	1111930
"000333"	47.28303	42269439	43235	42562	1359732	0.014887	0.37	11623.25	9514.582
"000338"	8.516816	62818118	13079	12515	588959	0.010655	0.07	100782.8	95706.92
"000413"	6.029873	53789801	5089	5042	430600	0.010073	0.06	219929.3	199012.8
"000425"	4.045993	69059015	3225	3203	449036	0.010051	0.05	522062.8	460059.8
"000636"	20.15651	94733981	44409	43234	1583531	0.014642	0.41	534288.8	202639.3
"000651"	44.98734	44439886	40025	39113	1510799	0.013861	0.24	12384.81	12172.45
"000709"	2.858653	45590018	954	932	199636	0.010006	0.02	1332800	1342154
"000717"	6.79423	57997266	10213	9987	359260	0.010401	0.09	394507.6	85874.07
"000725"	3.54558	507000000	2397	2389	1970126	0.010006	0.06	4230589	3886116
"000735"	12.02583	111000000	28138	27924	1846659	0.01089	0.18	159588.4	38211.69
"000790"	7.136104	41304190	15006	14632	518929	0.01077	0.1	50848.03	598766.3
"000830"	17.61107	42223402	24782	24311	696922	0.011286	0.1	23583.17	22383.69
"000839"	4.735201	39000627	4820	4731	289843	0.010107	0.05	200474.7	169123.2
"000868"	5.34697	46274097	13327	12987	491337	0.010563	0.12	482389.5	52117.99
"000932"	8.902737	86635903	16526	16407	532922	0.010707	0.08	80327.97	72852.96

Table 4: Statistical values of highest liquid 20 stocks out of 50 discussed above stocks from Shenzhen stock exchange in March 2019.

Stock name	Price	Volumes	Bidupdates	Iskupdates	Trades	Spread	Max spread	Bidquote	Askquote
"000001"	12.54927	126000000	17488	17463	1059145	0.01066	0.08	112559.7	108647.9
"000002"	28.63796	74954324	35847	35491	1359969	0.013032	0.15	23236.36	25846.48
"000063"	29.24184	140000000	41597	41023	2894819	0.012885	0.17	1160519	26272.13
"000066"	8.717627	168000000	26081	25436	1249161	0.012592	0.37	3569660	53256.85
"000100"	3.844991	493000000	5356	5305	2378005	0.010047	0.05	8653295	1451183
"000333"	47.81191	35576311	34704	34508	1003728	0.014848	0.25	14357.82	14197.87
"000338"	10.93427	96004436	22551	22309	990645	0.011147	0.1	63859.75	60373.95
"000413"	6.164903	190000000	10079	10029	1246611	0.010096	0.05	283759.9	248469.5
"000425"	4.266872	135000000	5503	5495	744533	0.010089	0.04	457575.5	467730.4
"000636"	15.38505	86504891	30368	29851	1315250	0.011175	0.15	36598.62	31015.7
"000651"	46.03232	55785464	32959	32395	1647012	0.012225	0.21	19192.34	21113.85
"000709"	3.460779	81331901	2176	2085	432321	0.010028	0.02	930606.8	922097.6
"000717"	5.863062	59962873	6285	6181	345876	0.01015	0.09	191616.1	163426.1
"000725"	4.017527	1390000000	4420	4405	6170115	0.010009	0.03	4509817	4258081
"000735"	12.91924	101000000	24138	23801	1428595	0.010654	0.11	47920.45	45534.02
"000790"	5.386573	26622979	10210	9866	189760	0.010711	0.13	51580.23	51269.71
"000830"	13.09964	78158583	20499	20213	937589	0.010673	0.1	50154.7	47131.92
"000839"	5.914253	239000000	18407	18086	1492968	0.010551	0.17	2961527	525416.3
"000868"	3.992471	36396440	6204	6076	270629	0.010229	0.25	129570.5	116579.2
"000932"	7.69376	69250545	8615	8395	444436	0.010203	0.05	152788.6	132695.1

$$\Delta P_{k,i} = \widehat{\beta}_i \mathrm{OFI}_{k,i} + \widehat{\varepsilon}_{k,i}. \quad (8)$$

For ease of show, we get it from the original data to let $\Delta P_{k,i} = \Delta P_{k,i} * \delta$.

Figure 2 presents a scatter plot of ΔP_k against OFI_k of one stock for every 10 seconds in a whole month. There is a representative stock with an index of SZE.000001, the most liquidity stock in Shenzhen stock exchange.

We can see that the linear effect is not as apparent as the estimations from constituents of S&P 500 by Cont et al. [2]. And the R-squared is relatively much lower compared with stocks in US stock market.

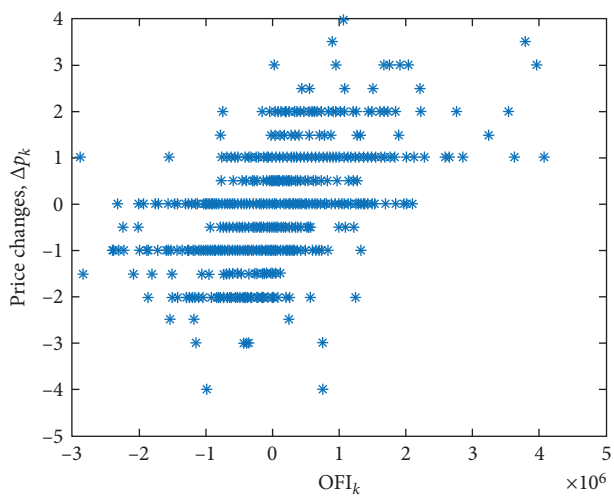

Figure 2: Scatter plot of ΔP_k against OFI_k for stock SZE.000001, July 2018.

Table 5 shows that the R-squared is an average of 50 stocks in 22 trading days for 8 different time periods.

The average order book depths for 8 different time periods evolve with time in Figure 3.

And the $\widehat{\beta}_i$ of OFI_i changes with time, as shown in Figure 4.

We can see that both $\widehat{\beta}_i$ and R-squared of model (8) are decreasing when order book depth gets higher.

And Table 6 shows that p values for coefficient of OFI are all significant at 0.1 threshold. Based on Cont's model, in the second part, we add OEI factor into the linear model to estimate model (7) with improving R-squared efficiently.

Adding values of 8 different time periods together to compute average values of regression model in a trading day is unrealistic. In every different time period, market participants, liquidity, and trading activity are totally different. Usually, high-frequency trading concentrates on open moment of market, at which they were searching trading opportunities that contribute most profits to HFT strategies. Adding the new factor OEI into model (8), we only discuss the statistical results for higher liquidity periods of trading days, such as 9:30 am–10:30 am and 14:30 pm–14:57 pm. In these periods, the most events of order book happened. Then, we estimated the model of

$$\Delta p_{k,i} = \widehat{\beta}_i \mathrm{OFI}_{k,i} + \widehat{\gamma}_i \mathrm{OEI}_{k,i} + \widehat{\varepsilon}_{k,i}. \tag{9}$$

Table 7 shows that the p values are all significant at 0.1 threshold. And the R-squared increases by 34.3%, 26.8%, and 35.5%, respectively, in model (9) compared to those in model (8).

The curve of Figure 5 for coefficients $\widehat{\gamma}_i$ of OEI_i at eight periods is a U-shape showing that when liquidity and trade activities are adequate and intense, the explanatory power of $\widehat{\gamma}_i$ is much higher than that in relatively quiet periods of trading.

Table 5: The R-squared of estimation in model (8).

Time	R-squared
9:30–10:00	0.205776
10:00–10:30	0.190855
10:30–11:00	0.167759
11:00–11:30	0.157325
13:00–13:30	0.156407
13:30–14:00	0.158184
14:00–14:30	0.158095
14:00–14:57	0.144615

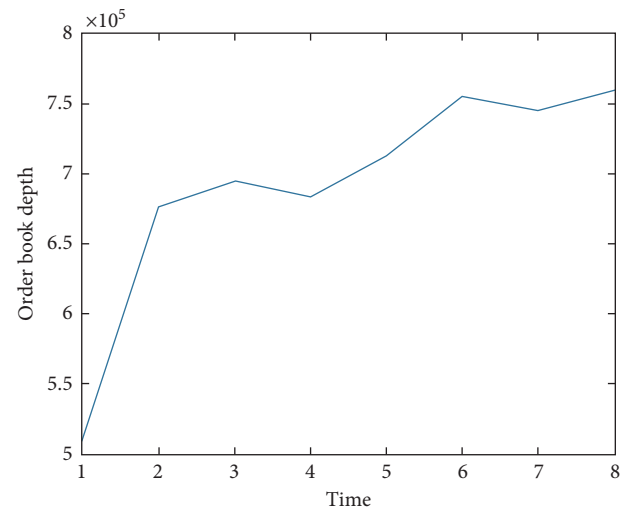

Figure 3: The average order book depth at 8 different time periods.

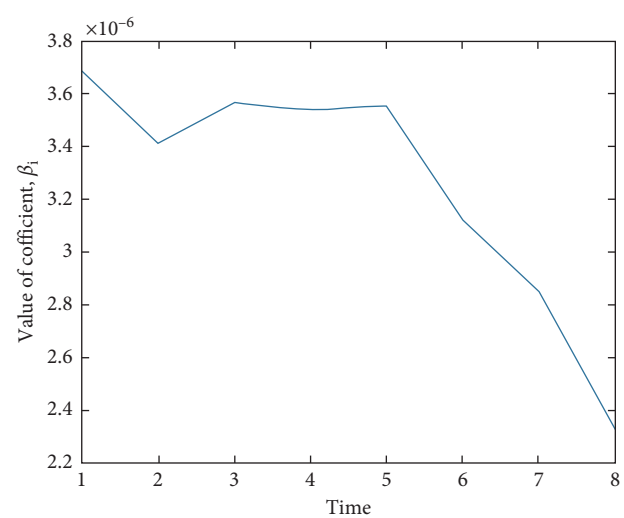

Figure 4: The average coefficients of OFI_i for 50 stocks at 8 different time periods.

4.3. Empirical Findings in the Period of Highest Liquidity of Stock Market. The trading volumes and liquidity of stock in Chinese mainland boomed in March 2019, and the statistical results and coefficients of model (8) and (9) change rapidly in this month. We find that the more the liquidity, the smaller the p values of OEI_i. The R-squared of model (8) is nearly the same as the R-squared in July 2018. But the R-squared of model (9) and coefficients of $\mathrm{OEI}_{k,i}$ increase sharply compared with previous ones in July 2018. Table 8 shows R-squared of model (8) of Cont et al. [2].

Table 6: p values for coefficients of OFI_i from model (8) for 8 different trading periods.

No.	p values for coefficient of OFI
1	0.0041350
2	0.0092107
3	0.0160284
4	0.0157925
5	0.0170173
6	0.0181213
7	0.0168114
8	0.0175921

Table 7: The R-squared for factor OEI_i and p values for $\widehat{\gamma}_i$ in model (9).

Item	9:30–10:00	10:00–10:30	14:30–15:00
p value	0.05385032	0.082507492	0.06868157
R-squared	0.27636538	0.241916241	0.19599882

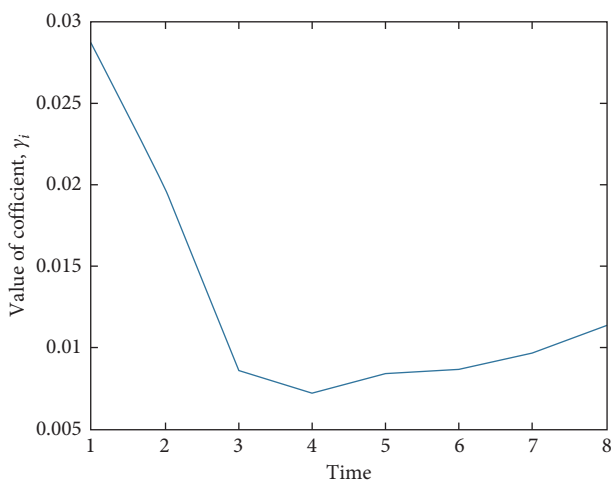

Figure 5: The line for values of $\widehat{\gamma}_i$ changes along with time.

Table 8: The R-squared of model (8) estimated in March 2019.

Time	R-squared
9:30–10:00	0.180138511
10:00–10:30	0.185777441
10:30–11:00	0.175824568
11:00–11:30	0.171979626
13:00–13:30	0.173095659
13:30–14:00	0.173196812
14:00–14:30	0.177265851
14:00–14:57	0.160464719

The values are nearly the same as those in July 2018.

And Table 2 shows the R-squared, p values, and coefficient $\widehat{\gamma}_i$ of the factor $\mathrm{OEI}_{k,i}$ in model (9), respectively.

From Table 2, we can see that the R-squared is increased by 47.8%, 36.8%, and 45.9%, respectively, in the three actively trading time periods compared with these values in July 2018. And the explanatory power of OEI_i is increased by 477.2%, 387.6%, and 333.9%, respectively, compared with the values (Figure 5) in July 2018.

4.3.1. Summary

(1) The coefficients of OEI are much higher in actively trading time periods such as the very open moment of market or near closing time of market.

(2) Within a whole month, the liquidity was booming in March 2019; then the R-squared of our model (9) is enhanced much by near a half of previous values. And more importantly, the coefficients of OEI, explanatory power, are much more than the previous ones.

5. Application of High-Frequency Trading by Prediction of OEI

Predicting price changes in advance is a direct method for trading, but it is too hard to predict if lots of market environment and order book dynamics are included. Whether or not the prediction could be with high rate of winning, market conditions between $[t_{k-1,i}, t_{k,i}]$ and $[t_{k,i}, t_{k+1,i}]$ must have a stable relationship or interplay with each other. And the higher the trading frequency and monitoring frequency for signals, the easier to predict next time direction and momentum of price changes.

In the above discussion of price changes and OFI, we find that price changes in every 10 seconds interval, the autocorrelations are too low to make predictions in next interval, and it is the same situation for OFI even if their autocorrelations are higher compared with price changes in the same period.

But the autocorrelations of OEI are surprisingly high, which reflects that when limit orders waiting on one side could be executed in shorter duration than the other side, the same trend can hold for a while or continue causing the market orders cluster in this side. Thus, we could use the OEI as an indicative of whether or not market orders come to one side order book frequently and densely to form cluster effect in the present and near future moments.

There are high autocorrelations of OEI like Figure 6 for stock SZE.000100 in every 10-second interval.

But autocorrelations of price changes for stock SZE.000100 are nearly ignorable. Figure 7 shows that all the levels of autocorrelations for price changes are very low.

And OFI's autocorrelations still cannot provide enough evidence for there is strong relationship between OFI in the previous time and the OFI in next time as shown in Figure 8. And the autocorrelations in Figure 8 are not only small but also swinging.

For doing high-frequency trading, switch at the right time between market orders and limit orders before the market price changes, which could cause adverse selection to HFT traders, which is what orders management strategies or optimal placement is doing in real time. How to set and monitor threshold values of market conditions such as OFI, OEI, or other high-frequency indicatives along with peculiarities of the microstructure of Chinese mainland stock market is a future work.

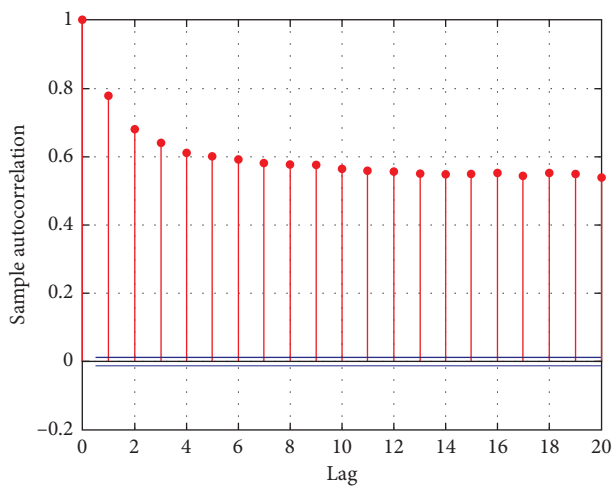

Figure 6: Autocorrelations of OEIs for stock SZE.000100 in March 2019.

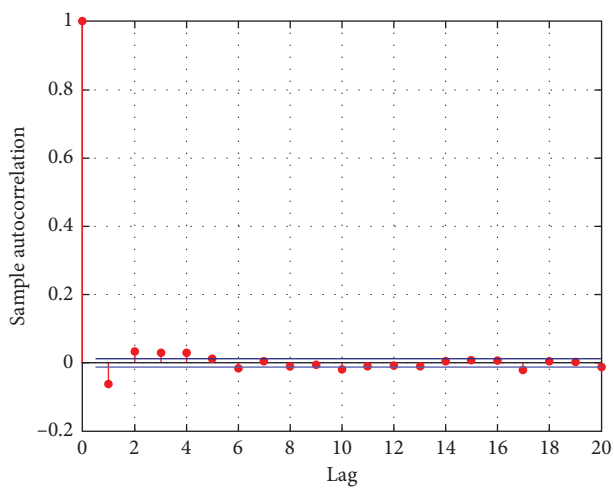

Figure 7: Autocorrelations of price changes for stock SZE.000100 in March 2019.

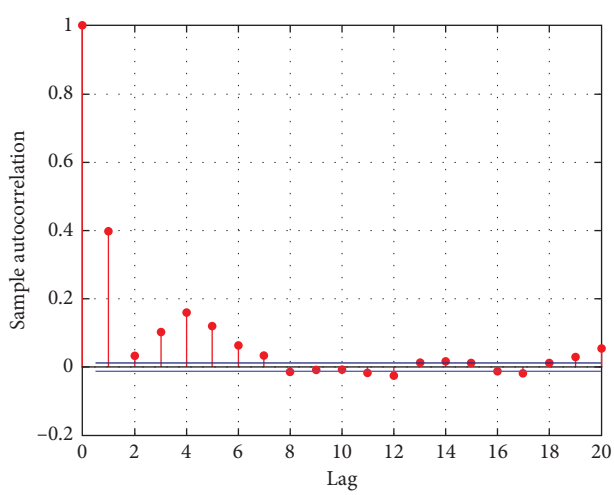

Figure 8: Autocorrelations of OFI for stock SZE.00100 in March 2019.

6. Conclusion

In essence, to predict or prescribe price changes is to study the conditional behavior, which is a problem in which the state space of limit order book is huge, and future order flow changes so quickly. Furthermore, in some situations, there is long memory in order flow, and in other situations, they are nearly independent. Therefore, a key modelling task is to find a way to simplify the evolving, high-dimensional state space, while retaining LOB's key features.

Analyzing and predicting the price changes in above discussions are nonstationary since the R-squared of our model is still not high. Conditioning on most recent events, such as in a 10-second moving window, is problematic. In practice, the most recent events recorded by the exchange may not be the most recent events given a trader observing these data via the trading platform. And in theory, usually, we build a model based on averaging computational results from market conditions for a fix interval but ignoring the prices jump or dump at a particular time point or missing particular distribution information of orders' properties through taking them averaging into uniform values in a time interval. The missing information such as instantaneous volatility or volatility clustering effect should only be observed from event by event order books. In future work, we could use other methods such as Hawkes process to estimate and analyze the clustering and interplay effects between different orders, which could reflect other conditional information.

Observations of price changes from our model give a brand new viewpoint to capture features of order book dynamics from time dimension of orders' execution. Not only the R-squared of Cont's model is enhanced based on Chinese developing stock market, but also, to show it in a different stock market, statistical results gotten from developed stock market uncertainly give us accurate estimations about how the prices, order books, and volatility evolve because some unique features about market microstructure exist in different stock exchanges or markets, although they have the same order-driven matching mechanism.

There are still some limitations in multimethod integration. Many areas that can be further expanded in this study; for example, sustainable development [15], risk interactions [16], multifaceted dimension [17], and innovation network [18] are also the direction of future research.

Data Availability

Data sharing is not applicable to this article as no data sets were generated or analyzed during the current study.

Conflicts of Interest

The authors declare that no conflicts of interest exist regarding this publication.

Acknowledgments

This work was supported in part by the 2020 Shanghai University Key Undergraduate Education Reform Project

"Exploration and Practice of the Construction of New Fintech Majors from the Perspective of the Development of Fintech Industry".

References

[1] H. Joel and G. Saar, "Low-latency trading," *Journal of Financial Markets*, vol. 16, no. 4, pp. 646–679, 2013.
[2] R. Cont, A. Kukanov, and S. Stoikov, "The price impact of order book events," *Journal of Financial Econometrics*, vol. 12, no. 1, pp. 47–88, 2014.
[3] A. Ellul, C. W. Holden, P. Jain, and R. Jennings, "Order dynamics: recent evidence from the NYSE," *Journal of Empirical Finance*, vol. 14, no. 5, pp. 636–661, 2007.
[4] M. Achab, E. Bacry, J. F. Muzy, and M. Rambaldi, "Analysis of order book flows using a non-parametric estimation of the branching ratio matrix," *Quantitative Finance*, vol. 18, no. 2, pp. 199–212, 2018.
[5] J. Dugast, "Unscheduled news and market dynamics," *The Journal of Finance*, vol. 73, no. 6, pp. 2537–2586, 2018.
[6] B. Huang, T.-H. Lee, and A. Ullah, "A combined random effect and fixed effect forecast for panel data models," *Journal of Management Science and Engineering*, vol. 4, no. 1, pp. 28–44, 2019.
[7] Á. Cartea, R. Donnelly, and S. Jaimungal, "Enhancing trading strategies with order book signals," *Applied Mathematical Finance*, vol. 25, no. 1, pp. 1–35, 2018.
[8] M. A. Goldstein, A. Kwan, and R. Philip, "High-frequency trading strategies," *SSRN Electronic Journal*, 2018.
[9] E. Silantyev, "Order flow analysis of cryptocurrency markets," *Digital Finance*, vol. 1, no. 1, pp. 191–218, 2019.
[10] H. Niu, Y. Xing, and Y. Zhao, "Pricing vulnerable European options with dynamic correlation between market risk and credit risk," *Journal of Management Science and Engineering*, vol. 5, no. 2, pp. 125–145, 2020.
[11] A. Fosset, J.-P. Bouchaud, and M. Benzaquen, "Non-parametric estimation of quadratic Hawkes processes for order book events," *The European Journal of Finance*, pp. 1–16, 2021.
[12] J. Hasbrouck and G. Saar, "Technology and liquidity provision: the blurring of traditional definitions," *Journal of Financial Markets*, vol. 12, no. 2, pp. 143–172, 2009.
[13] R. Cont and A. De Larrard, "Price dynamics in a Markovian limit order market," *SIAM Journal on Financial Mathematics*, vol. 4, no. 1, pp. 1–25, 2013.
[14] K. Chan and W.-M. Fong, "Trade size, order imbalance, and the volatility-volume relation," *Journal of Financial Economics*, vol. 57, no. 2, pp. 247–273, 2000.
[15] L. Zhen, L. Huang, and W. Wang, "Green and sustainable closed-loop supply chain network design under uncertainty," *Journal of Cleaner Production*, vol. 227, pp. 1195–1209, 2019.
[16] C. Bao, D. Wu, and J. Li, "Measuring systemic importance of banks considering risk interactions: an ANOVA-like decomposition method," *Journal of Management Science and Engineering*, vol. 5, no. 1, pp. 23–42, 2020.
[17] A. Díaz and A. Escribano, "Measuring the multi-faceted dimension of liquidity in financial markets: a literature review," *Research in International Business and Finance*, vol. 51, Article ID 101079, 2020.
[18] L. Huang, Y. Xu, X. Pan, and T. Zhang, "Green technology collaboration network analysis of China's transportation sector: a patent-based analysis," *Scientific Programming*, vol. 2021, Article ID 9961071, 12 pages, 2021.

Hindawi
Scientific Programming
Volume 2021, Article ID 2657918, 7 pages
https://doi.org/10.1155/2021/2657918

Research Article

Optimal Fixed Route for Multimodal Transportation of Vehicle Logistics in Context of Soft Time Windows

Wanying Zhao

Institute of Logistics Science & Engineering, Shanghai Maritime University, Shanghai, China

Correspondence should be addressed to Wanying Zhao; wyzhao@shmtu.edu.cn

Received 20 April 2021; Accepted 13 July 2021; Published 26 July 2021

Academic Editor: Lu Zhen

Copyright © 2021 Wanying Zhao. This is an open access article distributed under the Creative Commons Attribution License, which permits unrestricted use, distribution, and reproduction in any medium, provided the original work is properly cited.

In order to improve customer satisfaction and reduce the cost of vehicle logistics transportation, this paper adopts the mixed-integer programming model to analyze the delivery routes of vehicle logistics and make simulation and analysis based on the real delivery case. The results show that, compared with a single transportation scheme, the vehicle logistics optimization scheme based on the mixed-integer programming model is able to produce the optimal multimodal transportation plan, which can reduce the transportation costs, improve the service of transportation enterprises, and enhance their core competitiveness.

1. Introduction

The data of 2020 China automobile production and sales released by the China Association of Automobile Manufacturers on January 13, 2021, showed that production volume in 2020 stood at 25.225 million vehicles and sales volume at 25.311 million. All the automobiles produced and sold by China throughout the year are transported through vehicle logistics (VL). Based on the agile automotive supply chain environment focusing on time competition, vehicle logistics is to make quick response and punctual delivery by the object of vehicle logistics, which meets the requirements for delivery time, delivery place, and quality assurance according to customer order. Vehicle logistics has evolved from simple cargo movement to a new type of logistics featured by transportation-dominance, warehousing, distribution, and end-user value-added services as supplementary parts.

The newly issued regulation "Limits of dimensions, axle and mass for motor vehicles, trailers and combination vehicles (GB1589-2016)," as one of the most fundamentals in automobile standards, exerts an important influence on automobile transportation, traffic management, logistics transportation, playing a vital leading role in the development of automobiles. The standard limits the length of the central axle trailer loaded with the whole vehicle to 22 meters, the width to 2.55 meters, and the height to 4 meters, and loading more than 8 vehicles at one time is not allowed. In the case of unchanged freight rates, compared with the original large pallet trucks carrying more than a dozen trucks at the same time, this regulation cuts off the profits of the transportation company by a large margin, which brought a major blow to the vehicle transportation company.

Vehicle logistics is comprised of land transport, water transport, air transport, and so forth. Land transport can be divided into highway transport and railway transport while water vehicle logistics can be applied to container-vehicle logistics and roll-on roll-off VL. As for truck logistics companies, the optimization of distribution routes in the context of time windows, the selection of optimized routes from the road transportation, and water transportation and railway transportation are the focus of this study. This study attempts to find ways to effectively reduce the logistic costs of automobile manufacture by the use of mass, low-cost water transport, and railway transport, by which companies can improve their service and efficiency and enhance their core competitiveness. As a result, the optimal transportation mode based on the model of the vehicle operation of fixed

routes is significant to improve the operation and management of automobile logistics enterprises.

Generally, the problem of vehicle logistics in the context of time windows refers to the handling approaches in reaction to the requirements for vehicle's arrival time, service time, and subsequent noncompliance.

There are two scenarios of vehicle logistics in the context of hard time windows: if the customer requires that the vehicle arrives at the earliest or the deadline time, the vehicle begins to provide service after the arrival of the vehicle within the time window and the service time upon completion shall not exceed the specified deadline. If there is noncompliance, that service will be flatly declined or refused. And such a problem is called vehicle logistics with a hard time window. The second scenario is that the customer requires the vehicle to arrive within the specified early and late time, including the earliest time prior to the ready-to-serve time and the late time of arrival later than the ready-to-serve time. In the context of early arrival, the vehicles have to wait for the service till the specified time. In the context of late arrival, that service will be flatly declined or refused. Such a problem is also referred to as vehicle logistics in the context of hard time windows.

As such, the problems of the vehicle logistics in the context of soft time windows are more complex, including the direct loss of profit caused by nonpunctual demand requirements and the indirect customer loss caused by declined customer satisfaction. However, rich experience and continuous practice verification are needed to calculate these loss costs. And there are three specific scenarios with respect to the time window: first, if the vehicle arrives within the time window, but subsequent to completion of service, the time exceeds the latest service acceptance time in the customer-specified time window. In this case, service is still allowed, but it may be affected when the vehicle reaches the next node. Secondly, if the vehicle arrives prior to the earliest service acceptance time under the time window, the customer will accept the service, but a penalty cost is added for the vehicle's early arrival. In the last case, if the vehicle arrives later than the deadline service time of the time window, the customer not only accepts the service but also adds a penalty for the vehicle's late arrival.

A host of scholars have researched the optimization of vehicle routing of vehicle logistics in the context of time windows from different perspectives. Normasari [1] formulated the mathematical model of the CGVRP and propose simulated annealing (SA) heuristic for its solution in which the CGVRP is set up as a mixed-integer linear program (MILP). Li and Fu [2] proposed a two-layer order allocation model for order allocation in vehicle logistics service supply chain, considering the multiple transportation modes. With the principle of cost minimization, Hu and Yuhong [3] started from route optimization and determined the multimodal transportation scheme within the limitation of time. Jiang et al. [4] put forward the vehicle logistics route optimization network in terms of the two resources, the distribution centers of shared vehicles and shared vehicles, respectively; constructed a mathematical optimization model aiming to minimize the total cost of vehicle logistics transportation; and developed a heuristic algorithm based on genetic algorithm. Cordeau et al. [5] designed a rolling horizon algorithm to dynamically dispatch road transport vehicles in response to the uncertainty of delivery and achieved the goal of minimizing transport vehicle costs. Hou et al. [6] constructed an optimal route for vehicle logistics distribution by using an adaptive genetic algorithm. Dell'Amico et al. [7] verified the search algorithm for the loading of auto-carrier transportation and optimal selection route. Liu and Ma [8] analyzed the plan for vehicle leasing and vehicle sharing within the range of time windows. Cheng et al. [9] raised an improved genetic annealing algorithm to optimize transportation with an adaptive cross-variance rate strategy. Ma et al. [10] analyzed the issue of time-dependent vehicle running speed in practice and studied the solution of time-dependent vehicle routing. Liu et al. [11] studied vehicle routing under sudden-onset disasters. Baldacci [12] established a cost model on the optimization of the vehicle logistics network, used heuristic algorithm and exact algorithm to solve the problem, and found that the heuristic algorithm for multinode network optimization problem can obtain an effective solution in a short time. Xiong et al. [13] analyzed the optimization of multimodal transportation and multiagent operation in the context of time windows. Ceschia et al. [14] designed a tabu exploration algorithm for the heterogeneous vehicle routing problem in the context of time windows. Lin et al. [15] improved the ant colony algorithm for the vehicle routing problem with time windows. Jin et al. [16] used a piecewise linear pricing mechanism to establish a piecewise linear model, taking into account the impact of the difference in price discounts of different railway transportation volumes on the structure of the vehicle distribution network.

From the literature review mentioned above, it is apparent that scholars at home and abroad have made some achievements in the vehicle routing problem in the context of time window, but the research on vehicle logistics optimization in terms of multimodal transportation is insufficient yet. Most of the studies only take into consideration the objective function of minimizing transportation costs but fail to consider the problem of time constraints. As to vehicle logistics, we believe that it is inadequate to consider the only factor of the transportation route optimization; instead, it may be more sensible to choose a reasonable multimodal transport scheme according to the real situation. This study focuses on vehicle logistics optimization of multimodal transportation in the context of time window, which is a complement and improvement compared with previous research, as it takes customers' demand into account and enriches the results of vehicle logistics transportation reoptimization.

In this study, we explore the distribution optimization problem of vehicle logistics in the context of transport time limit. It establishes a mathematical model based on the goal, to make the transportation cost optimization as low as possible, and develops an optimal solution to the vehicle logistics multimodal transport while leveraging the CPLEX (Branch and Bound Algorithm) to precede the model. Real

cases prove that the route solution is effective in solving the practical problems of transportation enterprises.

2. Problem Descriptions and Modeling

2.1. Problem Description. Vehicle logistics in the context of time windows provides customers in different cities with the quantity of vehicles they need to purchase. The logistics and transportation company dispatches vehicles from OEMs to meet customer needs. Generally, customers have requirements for vehicle arrival time, that is, time window. The paper considers an OEM, multiple demand points, and the demand and time windows of each demand point. The specific situation is as follows.

Every city generally has a demand for vehicles from the original equipment manufacturer (OEM) to the destination city via multiple cities. The vehicle logistics network composed of the OEM, transit cities, and destination cities is shown in Figure 1. Every city has different requirements for vehicles. The vehicle logistics from OEM to other cities may bypass highway, railway, or water transportation. If transporting vehicles satisfies the requirements of cities along the route and destination cities, it is necessary to consider the cost of transshipment between cities and the time limit incurred by each city. If overtime occurs, there will be delay costs. It is essential to choose the optimized transportation route as a whole.

2.2. Model Hypothesis. There is one and only one mode of transportation for each distance travelled. There are sufficient means of transport; that is, each mode of transport that is selected for each distance can cover the whole distance without resorting to other modes, not considering the round trip.

Use the mixed integer programming model for calculations.

2.3. Model Parameters and Definitions

o: point of departure

i: the ith supply point, which is the ith distance travelled corresponding to the supply point

d_i: the demand at the ith supply point

t_i^s: the sth transportation time of the ith distance travelled

c_i^s: the unit transportation cost of the sth transportation mode on the ith distance travelled (unit: per vehicle)

tt_{sh}^i: the transit time of the ith supply points and for the s, h transportation ways

ct_{sh}^i: the unit transfer cost of the ith supply point and s, h two modes of transport (yuan/(per vehicle per kilometer))

pp_i: time limit for the ith supply point

cs_i: overtime unit cost of the ith supply point (yuan/vehicle)

$p_i = \sum_{j=i}^{n} d_i$: the ith transportation volume

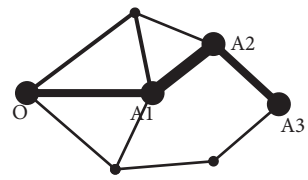

Figure 1: The vehicle logistics network.

$q_i = \sum_{j=i+1}^{n} d_i$: the ith node transfer volume $(1 \le i \le n-1)$

Decision variables:

x_i^s: 0-1 variables, whether the ith distance travelled is the s transportation mode; 1 is yes and 0 is no

y_{sh}^i: 0-1, whether the ith supply point is s, h for transshipment; 1 is yes and 0 is no

T_i: arrival time of the ith supply point

w_i: delay time of the ith supply point

y_i: 0-1 variable, whether the ith supply point is delayed; 1 is yes and 0 is no

2.4. Mathematical Formulation.

$$\min \sum_{s=1}^{3}\sum_{i=1}^{n} c_i^s p_i x_i^s + \sum_{h=1}^{3}\sum_{s=1}^{3}\sum_{i=1}^{n} ct_{sh}^i q_i tt_{sh}^i y_{sh}^i + \sum_{i=1}^{n} cs_i w_i. \quad (1)$$

Minimize the total cost, including transportation cost, transshipment cost, and delay cost:

$$\sum_{s=1}^{3} x_i^s = 1, \quad i = 1, \ldots, n. \quad (2)$$

Choose one and only one mode of transportation for the distance travelled:

$$x_i^s \le \sum_{h=1}^{3} y_{sh}^i, \quad i = 1, \ldots, n-1, \quad (3)$$

$$x_{i+1}^s \le \sum_{h=1}^{3} y_{hs}^i, \quad i = 1, \ldots, n-1, \quad (4)$$

$$\sum_{h=1}^{3}\sum_{s=1}^{3} y_{sh}^i = 1, \quad i = 1, \ldots, n-1. \quad (5)$$

Transshipment is required if the transportation mode at both ends of the supply point (3)–(5) is different:

$$T_i = \begin{cases} \sum_{s=1}^{3} t_1^s x_1^s, & i = 1, \\ \sum_{s=1}^{3}\sum_{j=1}^{i} t_j^s x_j^s + \sum_{h=1}^{3}\sum_{s=1}^{3} tt_{sh}^{i-1} y_{sh}^{i-1}, & 2 \le i \le n, \end{cases} \quad (6)$$

$$T_i - pp_i \le M ys_i, \quad i = 1, \ldots, n, \quad (7)$$

$$w_i - (T_i - pp_i) \le M(ys_i - 1), \quad i = 1, \ldots, n, \quad (8)$$

$$x_i^s \in \{0,1\}, \quad i = 1,\ldots,n, s = 1,2,3, \tag{9}$$

$$y_{sh}^i \in \{0,1\}, \quad i = 1,\ldots,n-1,\ s,h = 1,2,3, \tag{10}$$

$$y_i \in \{0,1\}, \quad i = 1,\ldots,n. \tag{11}$$

Whether the arrival at the supply points (7) and (8) is delayed: if it is delayed, calculate the delay time.

3. Case Analyses

A company needs to send vehicles from the Shanghai car factory to Tianjin, Beijing, and Dalian every month. At the same time, the time limit of vehicles' arrival is required to meet customer's demand for orders. The transport from Shanghai to Beijing transits at Tianjin, and the transport from Shanghai to Dalian transits at Tianjin and Beijing. The car factory uses KPI to access the performance of the time limit of the transport company. KPI includes vehicle damage rate, on-time delivery rate, on-time arrival rate, and data accuracy. In this simulation, on-time arrival rate, part of the KPI is converted into penalty costs.

3.1. Data of the Car of a Certain Brand Sent from Shanghai to Tianjin, Beijing, and Dalian. The demand for the car of brand A in Tianjin, Beijing, and Dalian is $D1$, $D2$, and $D3$, respectively:

$$\begin{aligned} D1 &= 966; \\ D2 &= 3855; \\ D3 &= 121. \end{aligned} \tag{12}$$

See Table 1 for the transportation time rate from Shanghai to Tianjin, Tianjin to Beijing, Beijing to Dalian, Shanghai to Beijing, and Shanghai to Dalian.

The unit transportation cost of Shanghai to Tianjin, Tianjin to Beijing, Beijing to Dalian, Shanghai to Beijing, and Shanghai to Dalian is shown in Table 2.

The transit time in Tianjin and Beijing when transporting vehicles from Shanghai to Tianjin and Beijing is shown in Table 3.

The unit transshipment costs per two modes of transport for vehicles departing from Shanghai via Tianjin and Beijing are shown in Table 4.

The arrival time limit of transport vehicles departing from Shanghai to Tianjin, Beijing, and Dalian (due date) is shown in Table 5.

Penalty for arriving at the destination city for one hour overtime: RMB 10/vehicle (cs_i).

The vehicle transport volume from Shanghai to Tianjin, Beijing, and Dalian is 4942, 3976, and 121, respectively, $p_i = \sum_{j=i}^{n} d_i$.

The transport volume in Tianjin and Beijing is 3976 and 121. respectively. ($q_i = \sum_{j=i+1}^{n} d_i$).

3.2. Computational Results. For road transportation time, we have calculated the effective transportation time, and the sleep time of the driver is not considered. The calculation results with cplex_studio125.win-x86-32 are as follows:

Using the data provided, the Shanghai–Tianjin waterway unit transportation cost 600 is the lowest, while the Shanghai–Tianjin section uses water transportation, and the Tianjin–Beijing and Beijing–Dalian sections use railway transportation, which has the lowest cost.

There will be transshipment charges in Tianjin.

As the transit time from Tianjin waterway to railway is waiting for the train for 3–48 hours, the calculation was carried out in three cases:

(1) Transshipment takes 3 hours:

Therefore, if the transshipment in Tianjin is not overtime, the lengths of time to reach Tianjin, Beijing, and Dalian are 48, 52, and 58 hours, respectively. The total cost is 3,847,300,300 yuan.

(2) Transshipment takes 24 hours:

Therefore, if the transshipment in Tianjin is not overtime, the lengths of time to reach Tianjin, Beijing, and Dalian are 48, 73, and 79 hours, respectively. The total cost is 3,947,508,800 yuan.

(3) Transshipment takes 48 hours:

Therefore, the transshipment in Tianjin will be overtime in Beijing, and the lengths of time to reach Tianjin, Beijing, and Dalian are 48, 97, and 103 hours respectively, and the overtime cost for 1 hour in Beijing is 38550 yuan. The total cost is 4,105,676 million yuan.

Based on the above results, the analysis and discussion are as follows.

In terms of other transportation modes, for example, in the first case, direct transportation from Shanghai to Beijing, the other two multimodal transportation routes are unchanged, and the longest transmit time from Tianjin waterway to railway is 48 hours. The minimum cost of direct transportation from Shanghai to Beijing is 3.084 million yuan for railway transportation. The demand for Beijing in the model is changed to 0, and the transportation mode remains unchanged. The multimodal transportation cost is 75,596,960 yuan, and the total logistics cost is 3,839,696 yuan. In the second case, direct transportation from Shanghai to Dalian and multimodal transportation in the other two places, we can get to know that there is no change in the first two sections of the transportation mode. A direct railway transport from Shanghai to Dalian and the minimum total logistics cost is 405.7298 yuan. In the third case, the three places all adopt the mode is direct transportation. Obviously, the total freight rate is the lowest at 3,784,600 yuan, if we take the water transport from Shanghai to Tianjin and Dalian and the railway from Shanghai to Beijing.

From the above analysis, it is noticeable that the cost of direct transportation is the lowest; thus, this mode is highly recommended. But this is the result according to data

Table 1: Transportation time of each distance (unit: hours).

t_i^s	Road transportation time	Railway transportation time (hours)	Waterway transportation time
Shanghai to Tianjin	16 hours + 8 sleep hours	6	48 hours
Tianjin to Beijing	2 hours	1	N/A
Beijing to Dalian	12 hours + 8 sleep hours	6	N/A
Shanghai to Beijing	18 hours + 8 sleep hours	6	N/A
Shanghai to Dalian	30 hours + 16 sleep hours	11	48 hours

Table 2: Unit transportation cost of each route (unit: CNY/vehicle).

c_i^s	Highway unit cost	Railway unit cost	Waterway unit cost
Shanghai to Tianjin	1500	700	600
Tianjin to Beijing	350	200	N/A
Beijing to Dalian	1000	600	N/A
Shanghai to Beijing	1700	800	N/A
Shanghai to Dalian	2400	1100	1000

Table 3: Transit time of two transport modes at each point (unit: hours).

tt_{sh}^i	Transit time of highway to waterway	Transit time of waterway to railway	Transit time of railway to highway (hours)
Tianjin	Wait 3–24 hours for ship	Wait 3–48 hours for train	3
Beijing	N/A	N/A	3

Table 4: Transshipment costs per unit of two transport modes at each demand point (unit: yuan/vehicle/km).

ct_{sh}^i	Transit costs from road to waterway	Transit costs from waterway to railway	Transit costs from railway to road
Tianjin	0	1.2	0
Beijing	0	1.2	0

Table 5: The arrival time limit at each demand point (unit: hours).

pp_i	Transit time (due date)
Shanghai to Tianjin	72
Shanghai to Beijing	96
Shanghai to Dalian	120

calculation. In fact, the cost of multimodal transportation is generally the lowest due to its scale effect. Therefore, the result of this study may be contrary to the general theory without considering the scale effect.

Some of the data collected, such as transmit time, are uncertain, so it may lead to slightly inaccurate calculations, such as unit transportation cost, overtime penalty cost, and quantity demand. Therefore, the fluctuation margin of the following sensitivity analysis against various data is about 10%.

There is a huge gap among the three direct transportation modes in terms of both unit transportation cost and transportation time, so the smaller fluctuations do not have an impact on the transportation mode, and the following analysis is mainly against multimodal transportation.

First, the unit transportation cost and transportation time are analyzed. According to the given data in Table 6 and the practical operation, it is found that the unit transportation cost of truck-load is not related to time, but merely to the transportation volume. Therefore, the fluctuation of transportation time does not affect the selection of transportation modes. Thus, the fluctuation of the unit transportation cost is analyzed. There are three sections of transportation and the last two parts are Tianjin–Beijing and Beijing–Dalian sections. The unit transportation cost and transportation time of railway transport have their advantages, and smaller fluctuations will not have an impact on the results. Therefore, this study mainly focuses on the analysis of fluctuations in unit transportation costs from Shanghai to Tianjin. The upward fluctuation of the unit transportation of the railway will not affect the result of choosing cheaper waterway transport. Therefore, this study mainly considers 10% of the downward fluctuation of railway unit transportation.

The analysis results show that when the unit transportation cost of the railway fluctuates slightly. It is not enough to make up for the cost of water transport, especially the overtime cost, which has no effect on the result. When the unit transportation cost of the railway (e.g., 640 yuan/vehicle) is close to that of water transportation, when the unit transportation cost is not much higher, the advantage of railway transportation time becomes prominent. Although the cost is still higher than water transport, the higher part is lower than the overtime cost of water transport. Therefore, it has a greater impact on the results.

Table 6: Sensitivity analysis of railway unit transportation cost from Shanghai to Tianjin.

Unit transportation cost (yuan/unit)	690	680	670	650	640	630	620
Total cost (10,000 RMB)	406.20176	406.20176	406.20176	406.20176	403.068	398.126	393.184
Transportation mode	Waterway-railway-railway	Waterway-railway-railway	Waterway-railway-railway	Waterway-railway-railway	Railway-railway-railway	Railway-railway-railway	Railway-railway-railway

Note. Waterway-railway-railway means the first section is waterway transportation and the last two parts are railway transportation.

Then, 10% fluctuation in transit and transshipment costs is analyzed. Based on the previous analysis, the possibility of transshipment in Tianjin is relatively high, especially from water transport to railway transport. There is no need to consider transshipment elsewhere. In the previous discussion on the transmit time of 3, 12, and 48 hours, the transportation mode has not changed. As a result, the transshipment cost is the only consideration. Obviously, the reduction in transshipment costs will not affect the results, and the upward fluctuations are mainly considered.

The results demonstrated that the fluctuation of Tianjin's transshipment cost will not affect the change of transportation mode, but the total logistics cost will change proportionally due to the change of unit transshipment costs.

In addition, the overtime penalty cost and the 10% fluctuation in demand are analyzed. As a consequence, the transportation mode does not change. In this mission, the main situation is that overtime of 1 hour occurred in Beijing. The logistics cost caused by the small fluctuation of the penalty cost is too small for the entire multimodal transportation to affect the entire decision-making. As for demand, the main unit transportation costs and unit transshipment costs are high or low due to the influence of decision-making. Thus, demand fluctuations cannot play a role in the change of transportation modes but can only increase or decrease the total logistics cost in direct proportion to the number of demand fluctuations.

4. Conclusions

The above sensitivity analysis shows that the smaller fluctuations have basically no effect on calculating results, and the sensitivity is low. Most of the data fluctuate because the three transportation modes, regardless of the unit transportation cost and transportation time, have a relatively large difference, except for the water transport and railway transport in the Shanghai–Tianjin section. Some data, such as transshipment undergoes a short time against the entire multimodal transportation (such as transshipment), cannot pose a remarkable impact, and the sensitivity is also very low. Or some data, such as transit time data, have little impact on the results: because of the long intermodal transport time and the short transit time, the transit time may not have a greater impact on the overall multimodal transport results, resulting in the low sensitivity. Since the unit price of water transport from Shanghai to Tianjin and railway transport has a great influence on this multimodal transport, the decision-making should take into account the price change of railway transport and waterway transportation.

For the problem of excessively high logistics costs in the process of long-distance transportation of vehicle logistics, a mixed integer programming model is used for calculation, and a vehicle logistics vehicle optimization path model in the context of a soft time window is established to obtain the optimal multimodal transportation that meets the time requirements, which saves costs for enterprises. We select a fixed line and prove the feasibility of the model through simulation calculations on a company's real transportation vehicles. Therefore, for logistics companies, the research results of this article are somewhat significant in reducing energy consumption, offsetting business operating costs, and improving efficiency. At the same time, it has reference value for similar transportation companies.

It should be noted that, for the overtime arrival of vehicles, the automotive OEM (original equipment manufacturer) uses the method to assess the transportation company's monthly KPI to decide whether to punish or not, which is converted into a penalty for calculation in this study.

Data Availability

The data are available upon request to the author.

Conflicts of Interest

The author declares no conflicts of interest.

References

[1] N. M. E. Normasari, V. F. Yu, C. Bachtiyar, and Sukoyo, "A simulated annealing heuristic for the capacitated green vehicle routing problem," *Mathematical Problems in Engineering*, vol. 2019, no. 2, 18 pages, Article ID 2358258, 2019.

[2] L. Li and H. Fu, "Order allocation problem of vehicle logistics service supply chain considering multiple modes of transportation," *Journal of Computer Applications*, vol. 39, no. 6, pp. 1836–1841, 2019, (in Chinese).

[3] Y. Hu and S. Yuhong, "Multimodal transportation and route optimization of vehicle logistics," *Journal of Transportation Engineering and Information*, vol. 7, no. 1, pp. 13–18, 2019, (in Chinese).

[4] Y. Jiang, X. Qi, H. Ren, and Z. Jin, "Automobile logistics routing problem optimization under resource sharing mode," *Journal of Highway and Transportation Research and Development*, vol. 34, no. 6, pp. 114–121, 2017, (in Chinese).

[5] J.-F. Cordeau, M. Dell'Amico, S. Falavigna, and M. Iori, "A rolling horizon algorithm for auto-carrier transportation," *Transportation Research Part B: Methodological*, vol. 76, pp. 68–80, 2015.

[6] Y. Hou, Z. Jia, X. Tian, and W. Fangfang, "Research on the optimization on the vehicle logistics distribution wih soft time windows," *Journal of Systems Engineering*, vol. 30, no. 2, pp. 240–249, 2015, (in Chinese).

[7] M. Dell'Amico, S. Falavigna, and M. Lori, "Optimization of a real-world auto-carrier transportation problem," *Transportation Science*, vol. 49, no. 2, pp. 402–419, 2014.

[8] J. Liu and Z. Ma, "Multi-depot open vehicle routing problem with time windows based on vehicle leasing and sharing," *Systems Engineering: Theory and Practice*, vol. 33, no. 3, pp. 666–675, 2013, (in Chinese).

[9] B. Cheng, Y. Yang, and A. Liu, "Highway transportation route selection optimization based on improved genetic annealing algorithm," *Computer Integrated Manufacturing Systems*, vol. 19, no. 4, pp. 879–887, 2013, (in Chinese).

[10] H. Ma, P. Jin, and S. Yang, "Heuristic methods for time-dependent vehicle routing problem," *Journal of Systems Engineering*, vol. 27, no. 2, pp. 256–262, 2012, (in Chinese).

[11] T. Liu, W. Xu, and Q. Wu, "Modeling of multi-vehicle route searching with soft time windows under sudden-onset disaster," *Journal of Tongji University:Natural Science*, vol. 40, no. 1, pp. 109–115, 2012, (in Chinese).

[12] R. Baldacci, "Recent exact algorithms for solving the vehicle routing problem under capacity and time window constraints," *European Journal of OperafionM Research*, vol. 6, no. 37, pp. 1–6, 2011.

[13] G. Xiong and W. Yong, "Optimization algorithm of multimodal transportation with time windows and job integration of multi-agent," *Journal of System Engineering*, vol. 26, no. 3, pp. 379–386, 2011, in Chinese.

[14] S. Ceschia, L. Di Gaspero, and A. Schaerf, "Tabu search techniques for the heterogeneous vehicle routing problem with time windows and carrier-dependent costs," *Journal of Scheduling*, vol. 14, no. 6, pp. 601 ~ 605–615, 2011.

[15] L. Lin, S. Liu, and J. Tang, "Improved ant colony algorithm for solving vehicle touting problem with time window," *Control and Decision*, vol. 25, no. 9, pp. 1379–1383, 2010, (in Chinese).

[16] M. Jin, S. D. Eksioglu, B. Eksioglu, and H. Wang, "Mode selection for automotive distribution with quantity discounts," *Networks and Spatial Economics*, vol. 10, no. 1, pp. 1–13, 2010.

Hindawi
Scientific Programming
Volume 2021, Article ID 9181912, 10 pages
https://doi.org/10.1155/2021/9181912

Research Article

Sales Strategy considering Advertising in Advance-Selling and Spot-Selling Integration Mode for Fresh Product

Bo Zhang,[1] **Lan Yang**,[2] **Meng Zhang**,[2] **and Yanhui Li**[2]

[1]*School of Economics, Wuhan Business University, Wuhan 430056, China*
[2]*School of Information Management, Central China Normal University, Wuhan 430079, China*

Correspondence should be addressed to Yanhui Li; yhlee@mail.ccnu.edu.cn

Received 22 April 2021; Revised 12 June 2021; Accepted 13 July 2021; Published 21 July 2021

Academic Editor: Tingsong Wang

Copyright © 2021 Bo Zhang et al. This is an open access article distributed under the Creative Commons Attribution License, which permits unrestricted use, distribution, and reproduction in any medium, provided the original work is properly cited.

In this paper, we look into the optimal sales strategy of e-commerce platform which sells fresh-product advertising in advance-selling period and spot-selling period, respectively, when advance-selling and spot-selling integration mode is applied. The study found that, with the increase of advertising investment, the marginal benefit of e-commerce platform is declining; whether advertising during the advance-selling period or the advertising during the spot-selling period, the e-commerce platform can improve its profit, but under the same advertising effect factor, the optimal advertising investment for the sale period is smaller, and the profit when advertising in the advance-selling period is greater. When advertising in different periods, the optimal advertising and price strategy depends on the maximum valuation of consumers about the product and the advertising effect factor.

1. Introduction

In recent years, e-commerce developed rapidly. Especially, during the COVID-19, e-commerce retailers all over the world have increased their sales volume due to its unique advantages. E-commerce of fresh agricultural products accounts for a large proportion. Taking the Chinese market as an example, in 2020, the transaction volume of China's fresh e-commerce was $56.04 billion, and it is expected to reach $123.1148 billion in 2023 [1]. As a flexible sales mode, advance selling is widely used in various e-commerce retailers. For example, on September 21, 2017, "T-mall advance-selling" sold 140,000 "fresh" hairy crabs in one minute, setting a record in China's fresh industry. Advance selling is affected not only by commodity price factors but also by other nonprice factors (advertising, quality, etc.) [2, 3]. With the development of media channels and information technology, advertising has an increasing impact on consumers' purchase decisions [4]. In reality, e-commerce retailers mostly adopt the mode of combining advance selling and spot selling, and some research studies have shown that the integration of the two modes not only can expand demand and reduce risk but also can effectively solve the problem of high inventory cost [2, 5].

Many scholars focus on the pricing strategy, consumer behavior, and advance-selling time strategy of products in the advance-selling period. For example, Prasad et al. [6] have studied the advance-selling price and inventory decisions in the advance-selling period and the spot-selling period and believe that retailers should apply different sales strategies according to the consumer parameters and market parameters. Xiao et al. [7] studied the seller's equilibrium pricing strategy under two classical early-selling pricing schemes (dynamic pricing scheme and price commitment scheme). Cheng et al. [8] considered the presale strategy of the newsvendor model under the influence of dual marketing. The above papers have analyzed the optimal sales strategy of pricing. While the suppliers increase profits, the consumers become more and more intelligent. Therefore, considering the behavior of the consumer has become a new research direction in the field of advance selling. Yu et al. [9] studied the optimal decisions of presale and cash sale of new products and innovative products considering consumer differences and

strategic consumer response. Lim and Tang [10] considered the market composed of short-sighted consumers, forward-looking consumers, and investors, explored the presale strategy of monopoly sellers, and then proposed a dynamic behavior model of investors. Zhao and Stecke [11] studied the choice of three preorder strategies (no presale, moderate presale and deep presale) of retailers considering consumption loss aversion. In the case of presale, time is an important factor. How retailers choose the presale time to accurately grasp the market demand is a new problem. Chew et al. [12] discussed the problem of the multistage perishable product-ordering strategy. Schaaf and Skiera [13] studied the effect of time preferences on optimal prices and profitability of advance selling. Reviewing the papers on presale strategy, we can see that the research content of presale strategy has been relatively rich, the presale mode has been successfully applied to the online sales of many commodities, and the application of fresh agricultural products is in the exploratory stage. Maihami and Kamalabadi [14] studied the joint pricing and inventory control of noninstantaneous deteriorating items by establishing a time-dependent function model. From the perspective of competition, He et al. [15] analyzed the online presale mode of fresh products. Fan et al. [16] focused on the business strategy of fresh products' retailers and studied the dynamic pricing strategy and supplement policy of multibatch fresh agricultural products with real-time freshness through the revenue management dynamic programming model of consumer choice behavior. Zhang et al. [17] studied three presale strategies and service efforts of the fresh seasonal agricultural products' supply chain. Research on the presale strategy of fresh agricultural products is ascending. It is mainly focusing on presale pricing and fresh agricultural product ordering. Few scholars consider advertising investment as a decision variable in this field though it is an important factor influencing consumers' purchase decisions.

To sum up, few studies took both advance-selling advertising and pricing into account and set the fresh agricultural products' market as the research background. In addition, few scholars consider the impact of consumer behavior and consumer heterogeneity on sales strategy.

Therefore, based on the integrated environment of advance selling and spot selling, this paper discusses the pricing and advertising investment strategies of fresh agricultural products' e-commerce retailers considering consumers' knowledge and demand randomness. Considering the limited investment amount of most enterprises in the real environment, this paper studies the optimal sales strategies of e-commerce retailers for advertising investment in the advance-selling period or the spot-selling period, so as to provide decision-making reference for enterprises to formulate reasonable sales methods.

2. Problem Formulation and Symbol Explanation

This paper assumes that the e-commerce retailers of fresh agricultural products sell in two stages: the first stage is the advance-selling period, in which consumers can order fresh agricultural products in advance; the second stage is the spot-selling period, in which consumers can purchase directly, and the consumers participating in the advance selling and spot selling are getting the real products. Before the product is officially on the market, that is, in the advance-selling period, e-commerce retailers can advertise the product to expand the sales in the advance-selling period; after the product is on the market, that is, in the spot-selling period, consumers will actively search for the sales information of fresh agricultural products, and sellers can also choose to rely on their larger demand base to expand the sales in the spot-selling period. Therefore, this paper studies the optimal pricing, optimal advertising investment, and optimal order quantity of e-commerce retailers in different periods.

The research in this paper is consistent with the following assumptions:

(1) The advertising investment of e-commerce retailers is x, $x \in (0, 1)$, the advertising effect factor is b, and the influence of advertising on demand is $b\sqrt{x}$ [18].

(2) The consumers' number of the product without advertising is 1. According to whether the consumers know the advance-selling information of the e-commerce retailer, the consumers are divided into two categories. One is the informed consumers, whose proportion is γ, and the other is the uninformed consumers, whose proportion is $1-\gamma$ [4,19]. After the advance-selling period, the proportion of informed consumers is $\gamma + b\sqrt{x}$.

(3) In the spot-selling period, the unit price of the products is p and the unit cost is c_2. In the advance-selling period, the unit price of the products is αp, $0 \le \alpha \le 1$, and the unit cost is c_1. At the end of the advance-selling period, the e-commerce retailer decides the order quantity Q of the whole sales period. Considering that fresh agricultural products are easy to rot, e-commerce retailers need to invest in fresh-keeping costs in the spot-selling period to ensure the consistent quality of the products sold. Therefore, $c_1 < c_2$.

(4) After the end of the sales period, the quality of the product decreases rapidly, the demand disappears, and the residual value of the product is 0.

(5) Suppose that the consumer's valuation of the product, v, obeys the uniform distribution $U(0, v_0)$, the density function is $u(v)$, and the distribution function is $U(v)$. When informed consumers enter the market in the advance-selling period, $v \ge \alpha p$, they buy products in the advance selling; $v \ge p$, at that time, and they buy products in the spot-selling period. ε is a demand random variable which belongs to $[A, B]$; its density function is $f(\varepsilon)$, and the distribution function is $F(\varepsilon)$. Without losing generality, it is assumed that $c_1 < p < v_0$.

3. Optimal Strategy Analysis

3.1. The Optimal Decision of Advertising Investment in Advance-Selling Period (A). We assume x_A is the advertising investment of e-commerce retailers in the advance-selling period and $\alpha_A p_A$ is the product price. The consumer demand function in the advance-selling period is as follows:

$$D_{A1} = \left(\gamma + b\sqrt{x_A}\right)\int_{\alpha_A p_A}^{v_0} u(v)\mathrm{d}v. \tag{1}$$

The profit function of e-commerce retailers at this stage is as follows:

$$\pi_{A1} = \left(\alpha_A p_A - c_1\right)\left(\gamma + b\sqrt{x_A}\right)\int_{\alpha_A p_A}^{v_0} u(v)\mathrm{d}v - x_A. \tag{2}$$

In the spot-selling period, e-commerce retailers do not invest in advertising, and the price of products is p_A. The consumer demand function is

$$D_{A2} = (1-\gamma)\int_{p_A}^{v_0} u(v)\mathrm{d}v + \varepsilon. \tag{3}$$

The total demand under the integrated mode of advertising in the advance-selling period is $D_A = D_{A1} + D_{A2} + \varepsilon$, so the total profit is

$$\pi\pi_A = \begin{cases} (\alpha_A p_A - c_1)D_{A1} - x_A + p_A D_{A2} - c_2(Q - D_{A1}), & D_A \le Q, \\ (\alpha_A p_A - c_1)D_{A1} - x_A + (p_A - c_2)(Q - D_{A1}), & D_A > Q. \end{cases} \tag{4}$$

Let $z = Q - (D_1 - D_2)$; then,

$$\pi_A = \begin{cases} (\alpha_A p_A - c_1)D_{A1} - x_A + p_A(D_{A2} + \varepsilon) - c_2(D_{A2} + z), & \varepsilon \le z, \\ (\alpha_A p_A - c_1)D_{A1} - x_A + (p_A - c_2)(D_{A2} + z), & \varepsilon > z. \end{cases} \tag{5}$$

After simplification, it is as follows:

$$\pi_A = \left(\alpha_A p_A - c_1\right)\left(\gamma + b\sqrt{x_A}\right)\int_{\alpha_A p_A}^{v_0} u(v)\mathrm{d}v - x_A + (p_A - c_2)\left((1-\gamma)\int_{p_A}^{v_0} u(v)\mathrm{d}v + z\right) - p_A\int_A^Z F(u)\mathrm{d}u. \tag{6}$$

From the negative definite of the Hessian Matrix, we can see that the function π_A is a joint concave function of α_A and x_A, and the optimal solution can be obtained by the first-order condition.

Proposition 1. *When $b\sqrt{x_A} < 2v_0(\alpha_A p_A - c_1)(v_0 - \alpha_A p_A)/b(v_0 - 2\alpha_A p_A - c_1)^2$, the optimal discount, advertising investment, and profit in the advance-selling period are as follows:*

$$\begin{aligned} \alpha_A^* &= \frac{v_0 + c_1}{2p_A}, \\ \pi_{A_1}^* &= \frac{\gamma(v_0 - c_1)^2}{4v_0} + \frac{b^2(v_0 - c_1)^4}{64{v_0}^2}, \\ x_A^* &= \frac{(v_0 - \alpha_A p_A)^2(\alpha_A p_A - c_1)^2 b^2}{4{v_0}^2}. \end{aligned} \tag{7}$$

Proof.
$(\partial\pi_{A1}/\partial\alpha_A) = (\gamma + b\sqrt{x_A})(p_A(v_0 - 2\alpha_A p_A - c_1)/v_0)$,

$$\begin{aligned} \frac{\partial^2\pi_{A1}}{\partial\alpha_A^2} &= -2p_A^2 < 0, \\ \frac{\partial\pi_{A1}}{\partial x_A} &= \frac{b(\alpha_A p_A - c)_1(v_0 - \alpha_A p_A)}{2v_0\sqrt{x_A}} - 1, \\ \frac{\partial^2\pi_{A1}}{\partial x_A^2} &= -\frac{b(\alpha_A p_A - c_1)(v_0 - \alpha_A p_A)}{4v_0}x_A^{-3/2} < 0, \\ \frac{\partial^2\pi_{A1}}{\partial\alpha_A\partial x_A} &= \frac{bp_A(v_0 - 2\alpha_A p_A - c_1)}{2v_0}. \end{aligned} \tag{8}$$

When $b\sqrt{x_A} < (2v_0(\alpha_A p_A - c_1)(v_0 - \alpha_A p_A)/b(v_0 - 2\alpha_A p_A - c_1)^2)$,

$$\frac{\partial^2\pi_{A1}}{\partial{\alpha_A}^2}\frac{\partial^2\pi_{A1}}{\partial{x_A}^2} - \left(\frac{\partial^2\pi_{A1}}{\partial\alpha_A\partial x_A}\right)^2 > 0. \tag{9}$$

It shows that π_{A1} is a joint concave function of α_A and x_A, so the optimal solution of α_A and x_A can be obtained by $\partial\pi_{A1}/\partial\alpha_A = 0$ and $\partial\pi_{A1}/\partial x_A = 0$:

$$\alpha_A^* = \frac{v_0 + c_1}{2p_A},$$

$$x_A^* = \frac{(v_0 - \alpha_A p_A)^2 (\alpha_A p_A - c_1)^2 b^2}{4v_0^2}, \tag{10}$$

$$\pi_{A1}^* = \frac{\gamma (v_0 - c_1)^2}{4v_0} + \frac{b^2 (v_0 - c_1)^4}{64v_0^2}.$$

Proposition 1 shows that in the advance-selling period, the impact of advertising investment on profit is limited, and there is the best advertising investment. Among them, advertising investment x_A is positively correlated with the advertising effect factor b, indicating that e-commerce retailers tend to increase advertising investment when the advertising effect of products on consumers increases. The optimal discount in the advance-selling stage is inversely proportional to the price in the second stage (spot-selling period), which indicates that when the spot-selling price is higher, the discount coefficient set by the e-commerce retailer in the advance-selling period should be smaller, which can attract more customers; while when the spot-selling price is lower, the e-commerce retailer does not need to provide a large discount in the advance-selling period, which can also obtain the best profit. □

Proposition 2. *The optimal price in the spot-selling period is as follows:*

$$p_A(z)^* = \frac{(1-\gamma)(v_0 + c_2) + \alpha_A (\gamma + b\sqrt{x_A})(v_0 + c_1) + v_0 z - \left(\int_A^Z F(u)\mathrm{d}u\right)}{2\left((1-\gamma) + \alpha_A^2 (\gamma + b\sqrt{x_A})\right)}. \tag{11}$$

The optimal price increases with the increase of z, that is, with the increase of random variables. The optimal order quantity in the spot period is

$$Q(z)_A^* = \frac{v_0 - c_1}{2v_0}\left(\gamma + \frac{b^2 (v_0 - c_1)^2}{8v_0}\right) + (1+\gamma)\frac{v_0 - p_A(z)^*}{v_0}. \tag{12}$$

Proof. From the first derivative $\partial \pi_A / \partial p_A = 0$, the optimal price of the spot-selling period can be obtained, and there is $\partial p_A(z)^* / \partial z = v_0 \overline{F}(z)/2(1-\gamma) > 0$, which shows that $p_A(z)^*$ is a monotone increasing function of z, that is, the optimal price increases with the increase of z.

The optimal solution of Q can be obtained by taking the optimal solution of the first stage into $Q = D_1 + D_2 + z$ and $(\partial Q\ (z)_A^* / \partial z) = 1 - \overline{F}(z) > 0$. It shows that $Q(z)_A^*$ is a monotone increasing function of z, that is, the optimal order quantity increases with the increase of z.

Proposition 2 shows that the optimal price is positively correlated with the demand random variable ε because when ε increases, the demand increases. To ensure that the demand is met to the maximum extent, the optimal order quantity will increase accordingly. In order to compensate for the inventory cost and preservation cost caused by the increase of inventory, e-commerce retailers will increase the sales price. □

Proposition 3. *When the point satisfies formula (12), it is the only extreme point that maximizes the total profit function:*

$$\frac{\partial \pi_A(z)}{\partial z} = \frac{v_0 \overline{F}(z)(z + (1-\gamma)(1 - p_A(z)^*))}{2\left(1 - \gamma + {\alpha_A}^2 (\gamma + b\sqrt{x_A})\right)} + (p_A(z)^* - c_2)\left(1 - \frac{v_0 \overline{F}(z)}{2}\right) - p_A(z)^* F(z) = 0. \tag{13}$$

That is, there is a unique maximum of the total profit when the e-commerce retailer invests in advertising in the advance-selling period.

Proof. Put the optimal solution of $p(z)$ brought into the total profit function; if the solution with the first derivative of 0 exists and is unique, this point is the point with the largest total profit function:

$$\frac{\partial \pi_A(z)}{\partial z} = \frac{v_0 \overline{F}(z)(z + (1-\gamma)(1 - p_A(z)^*))}{2\left(1 - \gamma + {\alpha_A}^2 (\gamma + b\sqrt{x_A})\right)} + (p_A(z)^* - c_2)\left(1 - \frac{v_0 \overline{F}(z)}{2}\right) - p_A(z)^* F(z) = 0. \tag{14}$$

Let the above formula be $S(z)$. Let $v_0 = 1$ to make the calculation convenient, and it can be proved that

$$\frac{\partial^2 S(z)}{\partial z^2} = -3f(z) - f(z)\overline{F}(z) + 2f(z)F(z) - \frac{\partial f(z)}{\partial z}\left(f(z) + (1-\gamma)(1+c_2) + z - \int_A^Z F(u)\mathrm{d}u < 0\right). \tag{15}$$

It is shown that $S(z)$ is a convex function about z, that is, $S(z) = 0$ has two solutions. If $F(A) = 0$ and $F(B) = 1$ are known, $S(A) > 0$ and $S(B) > 0$ can be obtained, so $S(z) = 0$ has a unique solution. Since $\partial\pi_A(z)/\partial z = S(z)$, $\pi_A(z)$ is a function of z increasing first and then decreasing, and when $\partial\pi_A(z)/\partial z = 0$, the maximum value is obtained.

Proposition 3 shows that the model has an optimal solution and the optimal solution is unique. It shows that e-commerce retailers can have the optimal sales strategy and get the maximum revenue when they invest in advertising in the advance-selling period. The detailed analysis results will be described in Section 4. □

3.2. Optimal Decision of Advertising Investment in Spot-Selling Period (R). We assume x_R is the advertising costs in spot-selling period, $\alpha_R p_R$ is the selling price of the products in advance-selling period, and p_R is the selling price of the products in the spot-selling period. The demand in the advance-selling period D_{R1} and the spot-selling period D_{R2} are, respectively, as follows:

$$\begin{aligned} D_{R1} &= \frac{\gamma(v_0 - \alpha_R p_R)}{v_0}, \\ D_{R2} &= \left(1 - \gamma + b\sqrt{x_R}\right)\frac{v_0 - p_R}{v_0} + \varepsilon. \end{aligned} \tag{16}$$

Thus, the profit of the advance-selling period and spot-selling period are as follows:

$$\begin{aligned} \pi_{R1} &= \gamma(\alpha_R p_R - c_1)\frac{(v_0 - \alpha_R p_R)}{v_0}, \\ \pi_{R2} &= (p_R - c_2)\left(z + \left(1 - \gamma + b\sqrt{x_R}\right)\frac{v_0 - p_R}{v_0}\right) - p_R\int_A^Z F(u)\mathrm{d}u - x_R. \end{aligned} \tag{17}$$

Let $z = Q - D_{R1} - D_{R2}$.

Then, the total profit of the e-commerce retailer under the integrated mode of advertising in the spot-selling period is as follows:

$$\pi_R = \gamma(\alpha_R p_R - c_1)\frac{(v_0 - \alpha_R p_R)}{v_0} + (p_R - c_2)\left(\left(z + \left(1 - \gamma + b\sqrt{x_R}\right)\frac{v_0 - p_R}{v_0}\right) - p_R\int_A^Z F(u)\mathrm{d}u - x_R. \tag{18}$$

Proposition 4. *When advertising strategy is put into the spot-selling period, the optimal discount is*

$$\alpha_R^* = \frac{v_0 + c_1}{2p_R}. \tag{19}$$

When $\sqrt{x_R} < 2(p_R - c_2)(v_0 - p_R)$ $(1 - \gamma + \alpha_R^2\gamma)/b(v_0 - 2p_R + c_2)^2 - 2(p_R - c_2)(v_0 - p_R)$, *the optimal advertising investment, price, and order quantity are as follows:*

$$\begin{aligned} x_R^* &= \left(\frac{b(p_R - c_2)(v_0 - p_R)}{2v_0}\right)^2, \\ p_R^* &= \frac{\left(1 - \gamma + b\sqrt{x_R}\right)(v_0 + c_2) + v_0\left(z - \int_A^Z F(u)\mathrm{d}u\right)}{2\left(1 - \gamma + b\sqrt{x_R}\right)}, \\ Q_R^* &= \frac{\gamma(v_0 - c_1)}{2v_0} + \left(1 - \gamma + \frac{b^2(p_R^* - c_2)(v_0 - p_R^*)}{2v_0}\right)\frac{v_0 - {p_R}^*}{v_0} + z. \end{aligned} \tag{20}$$

Proof. The optimal discount $\alpha_R{}^*$ is obtained by finding the first derivative of π_R on α_R:

$$\begin{aligned}
\frac{\partial \pi_R}{\partial p_R} &= \frac{\alpha_R \gamma (v_0 + c_1) + (1 - \gamma + b\sqrt{x_R})(v_0 + c_2)}{v_0} - p\frac{2\alpha_R{}^2\gamma + 2(1 - \gamma + b\sqrt{x_R})}{v_0} + z - \int_A^Z F(u)\mathrm{d}u, \\
\frac{\partial^2 \pi_R}{\partial p_R{}^2} &= -\frac{2\alpha_R{}^2\gamma + 2(1 - \gamma + b\sqrt{x_R})}{v_0} < 0, \\
\frac{\partial \pi_R}{\partial x_R} &= \frac{b(p_R - c_2)(v_0 - p_R)}{2v_0\sqrt{x_R}}, \\
\frac{\partial^2 \pi_R}{\partial x_R{}^2} &= -\frac{b(p_R - c_2)(v_0 - p_R)}{2v_0 x_R{}^{3/2}} < 0, \\
\frac{\partial^2 \pi_R}{\partial x_R \partial p_R} &= \frac{b(v_0 + c_2 - 2p_R)}{2v_0\sqrt{x_R}}.
\end{aligned} \tag{21}$$

When $\sqrt{x_R} < 2(p_R - c_2)(v_0 - p_R)\ (1 - \gamma + \alpha_R^2\gamma)/b((v_0 + c_2 - 2p_R)^2 - 2(p_R - c_2)(v_0 - p_R))$,

$$\frac{\partial^2 \pi_R}{\partial p_R{}^2}\frac{\partial^2 \pi_R}{\partial x_R{}^2} - \left(\frac{\partial^2 \pi_R}{\partial x_R \partial p_R}\right)^2 > 0, \tag{22}$$

and it shows that π_R is a joint concave function of x_R and p_R, so the optimal solution of x_R and p_R can be obtained by $\partial \pi_R / \partial p_R = 0$ and $\partial \pi_R / \partial x_R = 0$, and the optimal solution has been given.

Proposition 4 shows that in the spot-selling period, the impact of advertising investment on the total profit is limited, and there is the best advertising investment, in which the advertising investment x_R is positively correlated with the advertising effect factor b, indicating that when the advertising effect of products on consumers increases, e-commerce retailers tend to increase advertising investment. □

Proposition 5. *We can prove Proposition 5 uses the same method as Proposition 3. When the point satisfies formula (23), it is the only extreme point that maximizes the total profit function:*

$$\frac{\partial \pi_R}{\partial z} = (p_R - c_2)\left(1 - \frac{(1-\gamma)\overline{F}(z)}{2\left(1 - \gamma + b\sqrt{x_R}\right)} + \frac{\left(b^2(v_0 - p_R) - \left(1 + b^2\right)(p_R - c_2)\right)(v_0 - p_R)\overline{F}(z)}{4v_0(1 - \gamma + b\sqrt{x_R})}\right), \tag{23}$$

$$-\frac{b^2\overline{F}(z)\left((p_R - c_2)(v_0 - p_R)^2 - (p_R - c_2)^2(v_0 - p_R)\right)}{2v_0(1 - \gamma + b\sqrt{x_R})} - \frac{z^2 v_0 \overline{F}(z)}{4\left(1 - \gamma + b\sqrt{x_R}\right)} - p_R, \quad z = 0. \tag{24}$$

That is, there is a unique maximum of the total profit of e-commerce retailers when they invest in advertising in the spot-selling period.

Proposition 5 shows that there is also a unique optimal solution for advertising strategy in the spot-selling period. No matter if advertising investment is put in the advance-selling or spot-selling period, the optimal solution exists, but it is inconsistent. The optimal solution is affected by numerous parameters. Once these parameters are determined, the optimal solution can be obtained. The advertising strategy can provide an important reference value for solving practical problems.

The specific analytical formula of the optimal solution in these two cases cannot be given, but it can be analyzed by numerical simulation, so the strategy comparative analysis is described in the part of example analysis.

4. Strategy Analysis

The results of this paper are verified and further analyzed by numerical examples. Using MATLAB 2014 for numerical analysis, referring to the previous research studies [20, 21] on parameter settings, we assume that the maximum estimated value of consumer product $v_0 = 1$, the unit cost of fresh agricultural products $c_1 = 0.2$ in the advance-selling period, the unit cost of fresh agricultural products $c_2 = 0.3$ in the spot-selling period, the advertising effect factor $b = 0.8$, the initial ratio of informed consumers $\gamma = 0.3$, and

the random demand factor ε obeys the uniform distribution of [0,1].

4.1. Analysis of Advertising Strategy. This paper studies the advertising strategy considering consumer valuation and the comparative analysis of the two cases. Consider the case of advertising investment in the advance-selling period, keep other parameters unchanged, and the maximum consumer valuation values are 0.5, 0.8, and 1.0, respectively, and the influence of advertising effect factor b on the optimal advertising investment x is shown in Figure 1.

Figure 1(a) shows that when consumers' valuation of products is large, the advertising investment increases with the increase of the advertising effect factor. With the increase of the maximum valuation, the proportion of consumers whose product valuation is greater than the sales price will increase; when the advertising effect factor is larger, it shows that advertising can effectively improve consumers' demand for fresh agricultural products. Therefore, with the increase of consumers' product valuation, e-commerce retailers should increase their advertising investment.

Figure 1(b) shows that, under the same advertising effect factor, the optimal advertising investment in the spot-selling period is greater than that in the advance-selling period. This shows that, in the spot-selling period, advertising needs to pay more cost. This is because there is an increase in demand due to price discounts in the advance-selling period, so there is no need to invest too much advertising cost.

4.2. Comparative Analysis of Profit. The time of advertising investment would influence the profit. Figure 2 shows the impact of advertising investment on profit in different periods (advance-selling period and spot-selling period).

Figure 2(a) shows that when there is no advertising investment in the advance-selling period, the profit in the spot-selling period is greater than that in the advance-selling period, but the total profit is lower. After the advertising investment, the profits in the spot-selling period and the advance-selling period increase. With the increase of advertising investment, the profit in the advance-selling period gradually approaches that in the spot-selling period, and the total profit increases greatly.

Figure 2(b) shows the following. (1) When advertising is put in the advance-selling period, the total profit will increase with the increase of advertising investment and tend to be stable, indicating that the increased range of total profit with advertising investment is limited, and the marginal benefit decreases, which is consistent with Proposition 1. (2) When advertising is put in the spot-selling period, the total profit will first increase and then decrease with advertising investment, indicating that excessive advertising investment in the spot-selling period will cause profit loss. (3) With the increase of advertising investment, the total profit of advertising in the advance-selling period is greater than that in the spot-selling period.

The profit function is influenced by many factors, among which the demand random factor is uncontrollable. Therefore, we compare the total profit of advertising in the advance-selling period with that in the spot-selling period with the change of demand random factor, as shown in Figure 3.

Figure 3 shows

(1) When the demand stochastic factor $z > 0$, the total profit of advertising in the advance-selling period and the total profit of advertising in the spot-selling period first increases and then decreases with the increase of the demand stochastic factor; a certain range of demand uncertainty can increase the e-commerce retailer's revenue, but once the uncertainty is too large, the e-commerce retailer will not be able to estimate the order quantity, resulting in some losses.

(2) From the trend of profit function, we can see that there are optimal profit points for the total profit of advertising in the advance-selling period and the total profit of advertising in the spot-selling period, which verifies Propositions 3 and 5 of this paper.

(3) When the demand stochastic factor $z > 0$, e-commerce retailers should choose to invest in the advertising cost in the cash period; at this time, the profit is greater; when the demand stochastic factor $z < 0$, e-commerce retailers should choose to invest in the advertising cost in the advance-selling period; at this time, they can get more profits.

4.3. Comparative Analysis of Price and Order Quantity. In order to study the influence of advertising investment on the optimal price and the optimal order quantity, this paper draws the influence of the optimal price and the optimal order quantity changing with the advertising investment, as shown in Figure 4.

Figure 4 shows

(1) In the case of advertising in the advance-selling period, the price and optimal order quantity increase with the increase of advertising investment. When the advertising investment increases, the cost of e-commerce retailers increases, so the price will increase, and the demand will increase, so the order quantity will increase.

(2) When the advertising investment is small, if you choose to put the advertising in the cash period, the optimal pricing of the product in the cash period is higher than that in the advance-selling period. When the advertising investment is large, if you choose to put the advertising in the cash period, the optimal pricing of the product in the cash period is lower than that in the advance-selling period.

(3) With the increase of advertising investment, whether in the advance-selling period or the spot-selling period, the order quantity of products has increased, that is, the demand for products has increased, but the consumer demand is greater in the advance-selling period.

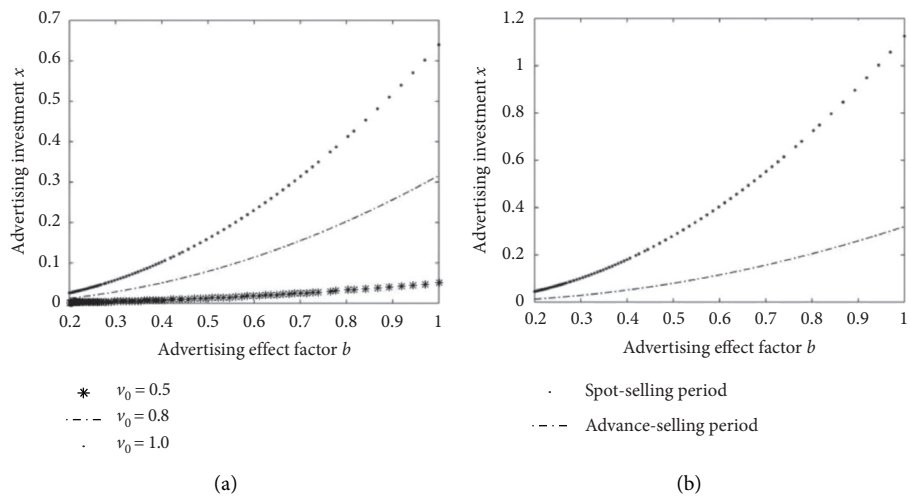

Figure 1: Analysis of advertising strategies under different advertising effect factors.

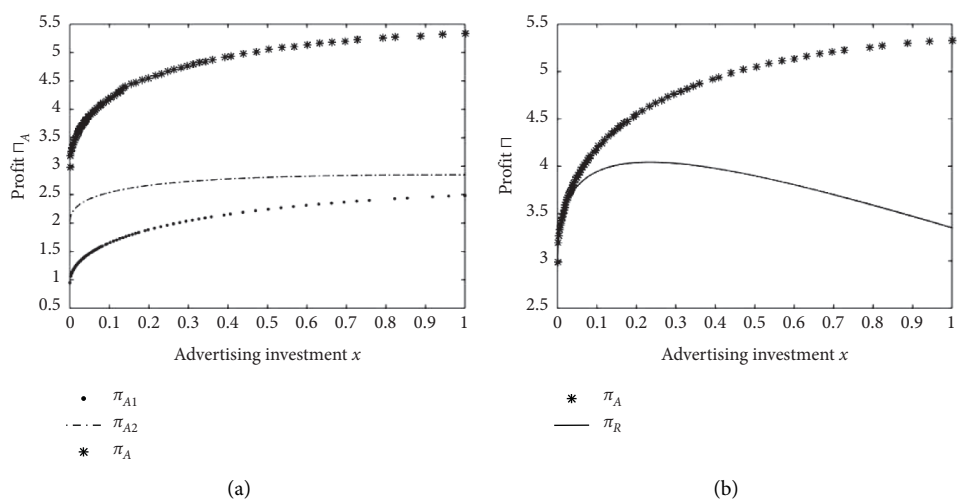

Figure 2: The impact of advertising investment on profit.

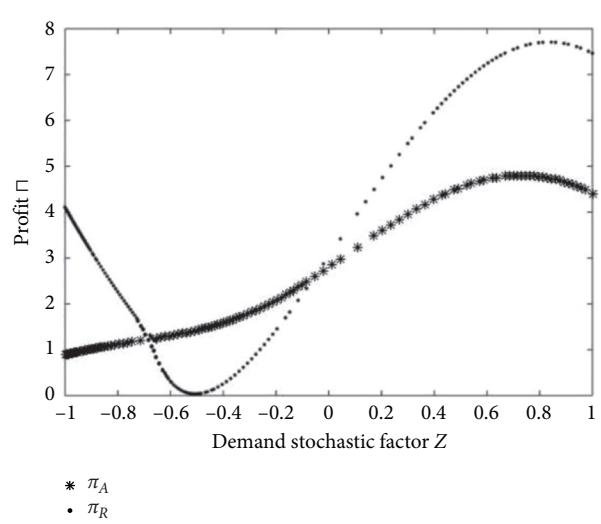

Figure 3: The influence of demand stochastic factor on total profit under different periods of advertising.

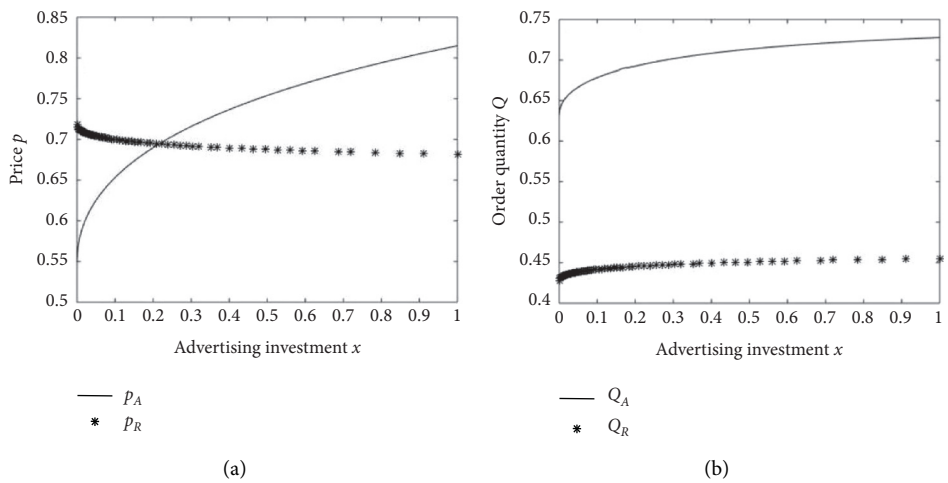

Figure 4: The influence of advertising investment on optimal price and optimal order quantity.

5. Conclusion

Based on the integrated sales model of advance selling and spot selling, this paper distinguishes consumers according to whether they know the advance-selling information of e-commerce retailers, considers the consumers' valuation of products, constructs the revenue function, respectively, under the consideration of e-commerce retailers' advance-selling advertising or spot-selling advertising, and analyzes the optimal strategy of advertising investment, pricing, and order quantity of fresh agricultural products e-commerce retailers. Through the solution of the model and numerical analysis in two modes, the following conclusions are obtained, hoping to provide the basis for the actual market operation of fresh agricultural products' e-commerce retailers in the e-commerce environment.

The conclusions are as follows: (1) e-commerce retailers can increase the total profit by advertising investment in both advance-selling period and spot-selling period; however, the growth of demand by advertising investment is limited, the optimal advertising investment needs to be adjusted according to the advertising effect factor. (2) Uncertainty demand in a certain range can increase the profit of e-commerce retailers. Compared with the case of fixed sales volume, e-commerce retailers' profit is greater when the sales volume is uncertain. However, when this kind of uncertainty becomes too much, it would cause the loss of retailers. Therefore, e-commerce retailers should view the uncertainty in demand correctly. (3) When e-commerce retailers advertise in the advance-selling period, they need to carry out corresponding discount activities. Under the influence of dual marketing means, consumers' demand is greater and the profits are greater. (4) When the demand stochastic factor $z > 0$, e-commerce retailers should choose to invest advertising costs in the spot-selling period; when the demand stochastic factor $z < 0$, e-commerce retailers should choose to invest advertising costs in the advance-selling period. (5) When the advertising investment is small, if you choose to put the advertising in the spot-selling period, the optimal pricing of the product in the spot-selling period should be higher than it in the advance-selling period; when the advertising investment is large, if you choose to put the advertising in the spot-selling period, the optimal pricing of the product in the spot-selling period should be lower than that in the advance-selling period. (6) With the increase of advertising investment, the total profit of advertising in the advance-selling period is greater than that in the cash sale period.

Further research of this paper can be carried out from the following aspects:

(1) This paper only considers the sales strategy of a single e-commerce retailer, and further study can consider the presale pricing problem in the competitive environment

(2) This paper only considers the case that consumers' risk preference is neutral, and further study can analyze the case that consumers' risk preference is different

(3) As many researchers have done with algorithm optimization [22], there are also some problems under complex and uncertain business environment which can be taken into consideration in future research.

Data Availability

All data, models, and code generated or used during the study are available within the article.

Conflicts of Interest

The authors declare that they have no conflicts of interest.

Acknowledgments

This work was supported by the National Natural Science Foundation of China, under Grant no. 71471073, and Fundamental Research Funds for the Central Universities, under Grant no. CCNU19TS078.

References

[1] iResearch inc, *Report on China's Fresh E-Commerce Industry in 2020*, iResearch inc, Shanghai, China, 2020.

[2] S. M. Shugan and J. H. Xie, "Advance-selling as a competitive marketing tool," *International Journal of Research in Marketing*, vol. 22, no. 3, pp. 351–373, 2004.

[3] J. X. Zhang, J. Li, L. Lu, and R. Dai, "Supply chain performance for deteriorating items with cooperative advertising," *Journal of Systems Science and Systems Engineering*, vol. 26, no. 1, pp. 23–49, 2017.

[4] L. Yang and H. Li, "Research on retailers advance selling strategy considering the influence of advertising on demand," *Advances in Social Science, Education and Humanities Research*, vol. 237, pp. 38–42, 2018.

[5] S. H. Cho and S. C. Tang, "Advance selling in a supply chain under uncertain supply and demand," *Operations Research*, vol. 54, no. 5-6, pp. 531–532, 2014.

[6] A. Prasad, K. E. Stecke, and X. Zhao, "Advance selling by a newsvendor retailer," *Production and Operations Management*, vol. 20, no. 1, pp. 129–142, 2011.

[7] L. Xiao, M. Xu, M. Chen, and X. Guan, "Optimal pricing for advance selling with uncertain product quality and consumer fitness," *Journal of the Operational Research Society*, vol. 70, no. 9, pp. 1457–1474, 2019.

[8] Y. Cheng, H. Li, and A. Thorstenson, "Advance selling with double marketing efforts in a newsvendor framework," *Computers & Industrial Engineering*, vol. 118, pp. 352–365, 2018.

[9] Y. Yu, J. Liu, X. Han, and C. Chen, "Optimal decisions for sellers considering valuation bias and strategic consumer reactions," *European Journal of Operational Research*, vol. 259, no. 2, pp. 599–613, 2016.

[10] W. S. Lim and C. S. Tang, "Advance selling in the presence of speculators and forward-looking consumers," *Production and Operations Management*, vol. 22, no. 3, pp. 571–587, 2013.

[11] X. Zhao and K. E. Stecke, "Pre-orders for new to-be-released products considering consumer loss aversion," *Production and Operations Management*, vol. 19, no. 2, pp. 198–215, 2010.

[12] E. P. Chew, C. Lee, R. Liu, K. Hong, and A. Zhang, "Optimal dynamic pricing and ordering decisions for perishable products," *International Journal of Production Economics*, vol. 157, pp. 39–48, 2014.

[13] R. Schaaf and B. Skiera, "Effect of time preferences on optimal prices and profitability of advance selling," *Customer Needs and Solutions*, vol. 1, no. 2, pp. 131–142, 2014.

[14] R. Maihami and I. N. Kamalabadi, "Joint pricing and inventory control for non-instantaneous deteriorating items with partial backlogging and time and price dependent demand," *International Journal of Production Economics*, vol. 136, no. 1, pp. 116–122, 2012.

[15] B. He, X. H. Gan, and K. F. Yuan, "Entry of online presale of fresh produce: a competitive analysis," *European Journal of Operational Research*, vol. 272, no. 1, pp. 339–351, 2018.

[16] T. J. Fan, X. Chang, and T. Feng, "Dynamic pricing and replenishment policy for fresh produce," *Computers & Industrial Engineering*, vol. 139, pp. 106127.1–106127.14, 2020.

[17] H. Y. Zhang, H. Y. Xu, and X. J. Pu, "Comparisons of pre-sale strategies for a fresh agri-product supply chain with service effort," *Agriculture*, vol. 10, no. 8, 324 pages, 2020.

[18] J. Xie and J. C. Wei, "Coordinating advertising and pricing in a manufacturer-retailer channel," *European Journal of Operational Research*, vol. 197, no. 2, pp. 785–791, 2009.

[19] M. Nerlove and K. J. Arrow, "Optimal advertising policy under dynamic conditions," *Economica*, vol. 29, no. 114, pp. 129–142, 1962.

[20] S. Ray, "An integrated operations-marketing model for innovative products and services," *International Journal of Production Economics*, vol. 95, no. 3, pp. 327–345, 2005.

[21] J. Wang, Y. Li, F. Ye, and Q. Chen, "Optimal introduction time decision for holiday products with uncertain market demand," *International Journal of Production Research*, vol. 55, no. 1, pp. 161–175, 2017.

[22] L. Wang, L. Peng, S. Wang, and S. Liu, "Advanced backtracking search optimization algorithm for a new joint replenishment problem under trade credit with grouping constraint," *Applied Soft Computing*, Article ID 105953, 2020.

Hindawi
Scientific Programming
Volume 2021, Article ID 9939805, 12 pages
https://doi.org/10.1155/2021/9939805

Research Article

A Distributed Algorithm for Large-Scale Linearly Coupled Resource Allocation Problems with Selfish Agents

Dian Yu and Tongyao Wang

Shanghai Jiao Tong University, Department of Automation, Shanghai, China

Correspondence should be addressed to Dian Yu; deaniiyu@sjtu.edu.cn

Received 22 March 2021; Accepted 2 July 2021; Published 15 July 2021

Academic Editor: Xiaobo Qu

Copyright © 2021 Dian Yu and Tongyao Wang. This is an open access article distributed under the Creative Commons Attribution License, which permits unrestricted use, distribution, and reproduction in any medium, provided the original work is properly cited.

A decentralized randomized coordinate descent method is proposed to solve a large-scale linearly constrained, separable resource optimization problem with selfish agent. This method has a cheap computational cost and can guarantee an improvement of selected objective function without jeopardizing the others in each iteration. The convergence rate is obtained using an alternative gap benchmark of objective value. Numerical simulations suggest that the algorithm will converge to a random point on the Pareto front.

1. Introduction and Motivation

Distributed and parallel optimization techniques have become a powerful tool in solving large-scale resource optimization problems [1–4]. Different from the consensus-based distributed optimization model ([2, 5]), where all agents collectively share the same decision variables, the resource optimization problem usually has a separable structure, i.e., each agent has its own decision variable and own objective function, but all the agents are weakly coupled by equality or inequality constraints [6]. The overall target is to minimize the summation of the agents' objective functions. One typical example of this kind of model is the optimal coordination problem of the distributed energy resources [4, 5], in which each generator decides the power generation by minimizing the cost function and meeting the overall demand. Recently, Li et al. [6] extended such method to the model of a global inequality constraint.

This work is motivated by the observation that resource allocation problems in the digital age are often subject to some new limitations unseen in traditional resource allocation problems. For example, in the area of content distribution or video streaming, many researchers have explored a scheme called parallel access [7] or multiple content distribution servers [8, 9] in a bid to optimize servers' work load and enhance users' quality of experience (QoE). Similar problems can also arise in the so-called multihoming problem when users start to compete for resources [10, 11]. This scheme first divides the original content/video into fragments, the replicas of these fragments are stored in a number of servers (often geographically diverse), and then the users are allowed to access/download fragments from multiple servers concurrently. This scheme is characterized by the following features:

(i) Large scale: the number of users could easily hit hundreds of thousands or even millions.
(ii) Bandwidth limit: each server has a total bandwidth limit, so that each user is only given a quota of the total bandwidth.

However, there are some practical concerns about this scheme. Specifically, user utilization of bandwidth quota of different servers may vary due to the physical distance or the access quality of different Internet service providers. In this

sense, there is a need to reallocate bandwidth quotas of the servers among users to improve user QoE. Unfortunately, there are three major difficulties underlying this optimization problem:

(1) The information necessary (gradients of objective functions, etc.) for the quota optimization is scattered among users and may be only partially available at a given time (e.g., users are inactive or unresponsive).

(2) Even if all the information is readily available, considering the large scale of the problem, an overall one-shot optimization could be computationally prohibitive and may lack timeliness, which is especially crucial for the enhancement of video viewing experience.

(3) Considering (2), a distributed algorithm that adaptively and progressively optimizes quota allocation among users should be preferred; however, here the crux is that the users in no way can accept a deteriorating QoE during the optimizing process, i.e., the users (agents) are selfish: one would not be too happy when he knows his own QoE is compromised for the QoE of someone else or for the "greater good" of the overall system.

The goal of this paper is to develop an efficient distributed method for solving resource allocation problem with selfish agents. Since the complete information of first and second order information necessary for a one-shot optimization is usually not available in many real world large-scale applications, we develop a randomized coordinate descent (RCD) algorithm that partially updates a pair of objective functions in each iteration (the RCD algorithm coincides with the distributed network optimization model, where only a subset of nodes can communicate with each other and can be optimized in one iteration). Our algorithm can be vaguely viewed as a multiobjective (MO) extension of the single-objective randomized coordinate descent algorithm [12]. Different from the single-objective optimization problem, the MO problem aims to optimize multiple objectives simultaneously in the sense of Pareto optimality (see [13, 14]).

Our RCD method has the following prominent features: first, it optimizes the selected objective functions in each iteration without affecting other objective functions, and the optimization at each iteration is required to be such that none of the selected objective functions should deteriorate. As a result, the value of each objective function should be non-deteriorating over the whole optimizing process, and the solution of each iteration can be applied in real time to progressively improve the objective function of each agent. Second, compared to the centralized MO methods such as [15, 16], our algorithm takes full advantage of the separability of the problem structure, and the update has a very cheap cost per iterate and can be easily implemented in a parallel setting. Perhaps more significantly, this work also focuses on the convergence analysis of the multiobjective RCD algorithm. Although the convergence results of single-objective algorithms are well established ([17, 18]), similar discussions for its MO counterparts are unexpectedly scarce. It was not until very recently that a few works have succeeded in obtaining the convergence rates for certain unconstrained MO algorithms ([19–21]). In fact, as will be evident in our analysis, the limiting point generated by our RCD algorithm will converge to a random point on the Pareto front; as a result, all the tools used in single-objective algorithm analysis are generally rendered useless. To conquer this difficulty and complete the missing piece, we develop a framework of convergence analysis for the RCD method, which generalizes the existing analysis for scalar optimization problem [12]. Under a mild condition, we show that the RCD algorithm has a sublinear convergence rate. If agents' cost functions are all strongly convex, then the RCD algorithm has a linear convergence rate.

The paper is organized as follows. In Section 2, we present the constrained MO optimization problem. In Section 3, we present the RCD algorithm. An analysis of the convergence rate of this RCD algorithm for different cases is given in Section 4. Some numerical examples are given in Section 5. We conclude the paper and discuss the future research in Section 6. Throughout this paper, the following notations are used. The vector is denoted by the bold letter. We use the following notation to denote the order of the vectors. Given $\mathbf{u} = [u_1 \dots u_n]^T$ and $\mathbf{v} = [v_1 \dots v_n]^T$, $\mathbf{u} \preceq \mathbf{v}$ means that $u_i \le v_i$, for all $i = 1, \dots, n$ and $\mathbf{u} \prec \mathbf{v}$ means that $u_i < v_i$, for $i = 1, \dots, n$.

2. Problem Formulation

Consider the following standard multiobjective (MO) optimization problem with linear equality constraints:

$$\begin{aligned} \mathscr{P}_{\mathrm{mo}}\colon\ & \min F(\mathbf{X}) \equiv \left[f_1(\mathbf{x}_1) \dots f_M(\mathbf{x}_M)\right]^T \\ & (s.t)\, \mathbf{X} \in \mathscr{C} := \left\{ \mathbf{X} \in \mathbb{R}^{kM} \mid \sum_{m=1}^{M} \mathbf{x}_m = 0 \right\} \end{aligned}, \tag{1}$$

where $\mathbf{X} = \begin{bmatrix} \mathbf{x}_1 \\ \vdots \\ \mathbf{x}_M \end{bmatrix} \in \mathbb{R}^{kM}$ with $\mathbf{x}_m \in \mathbb{R}^k$ and $f_m\colon \mathbb{R}^k \longrightarrow \mathbb{R}$ is a continuous function satisfying certain conditions for $j \in \mathbb{M} := \{1, 2, \dots, M\}$ (notation 0 denotes the vector with all elements being zero). Clearly, function $F(\cdot)\colon \mathbb{R}^{kM}\colon \longrightarrow \mathbb{R}^M$ is separable, i.e., $\mathbf{x}_m$ only affects $f_m(\mathbf{x}_m)$. However, these decision variables are weakly coupled by the global equality constraint. Note that although the right-hand side of the equality constraint is 0, there is no difficulty to generalize the results to the non-zero case using some affine transformation. In the context of the above bandwidth allocation problem, here $\mathbf{x}_m$ can be viewed as the bandwidth quotas of k servers allocated to agent m; f_m is a function that represents the negative of the utility (QoE) brought by quotas $\mathbf{x}_m$; and the equality constraint represents the total bandwidth limitation of each server $1, \dots, k$. Model $(\mathscr{P}_{mo})$ arises in various network optimization problems (see, e.g., [22–27]).

Problem $(\mathscr{P}_{mo})$ aims to optimize the multiple objectives simultaneously in the sense of Pareto optimality (see [13, 14]). Indeed, a feasible point $\mathbf{X}^* \in \mathscr{C}$ is a Pareto optimal solution of problem $(\mathscr{P}_{mo})$ if there exists no other feasible solution such that $\mathbf{F}(\mathbf{X}') \prec \mathbf{F}(\mathbf{X}^*)$ and $\mathbf{F}(\mathbf{X}') \neq \mathbf{F}(\mathbf{X}^*)$. The

traditional way to solve ($\mathscr{P}_{mo}$) is to aggregate objective functions f_m into a weighted summation social welfare, say, $\sum_m \omega_m f_m(\mathbf{x}_m)$ with $\omega_m > 0, \forall m = 1, \ldots, M$; then, solve the following single-objective optimization problem using classical methods (e.g., gradient descent method, Newton method, etc.):

$$\begin{aligned} &\min \sum_m \omega_m f_m(\mathbf{x}_m) \\ &(s.t)\, \mathbf{X} \in \mathscr{C} := \left\{ \mathbf{X} \in \mathbb{R}^{kM} \mid \sum_{m=1}^{M} \mathbf{x}_m = 0 \right\}. \end{aligned} \tag{2}$$

But this scheme suffers two major drawbacks for the reasons we stated previously: first, the large scale of the underlying problem (a very large M) may prevent this scheme from responding in a timely manner; second, this scheme does not guarantee a progressively non-deteriorating allocation evolution during the optimizing process, so that it is possible that the individual welfares of some agents get sacrificed for the "greater good," i.e., the maximization of social welfare $\sum_m \omega_m f_m(\mathbf{x}_m)$, and hence they could become discontent and discard the service for good. Therefore, to address these issues, we present the following randomized block coordinate descent method.

3. Randomized Block Coordinate Descent Method

3.1. The RCD Algorithm. Throughout this paper, we assume that the following condition holds true.

Assumption 1. Each $f_m(\cdot)$ has Lipschitz continuous gradient with constant $L > 0$, i.e., for all $\mathbf{x}_m, \mathbf{y}_m \in \mathbb{R}^k, m \in \mathbb{M}$, it has

$$\left\| \nabla f_m(\mathbf{x}_m) - \nabla f_m(\mathbf{y}_m) \right\| \le L \left\| \mathbf{x}_m - \mathbf{y}_m \right\|, \tag{3}$$

where $\|\cdot\|$ is the Euclidean norm (note that here the Lipschitz coefficient can be agent-specific, e.g., $L_1, \ldots, L_M$; in this case, we can let $L = \max\{L_1, \ldots, L_M\}$; on the other hand, one can also modify our algorithm scheme accordingly with respect to these agent-specific Lipschitz coefficients and obtain an improved convergence rate).

Note that the Lipschitz property implies the following inequality:

$$f_m(\mathbf{x}_m + \mathbf{d}) \le f_m(\mathbf{x}_m) + \nabla f_m(\mathbf{x}_m)^T \mathbf{d} + \frac{L}{2} \|\mathbf{d}\|^2, \tag{4}$$

for any $\mathbf{d} \in \mathbb{R}^k$ and $m \in \mathbb{M}$. Given the current solution $\mathbf{X}$, the classical gradient-based method needs to compute the whole Jacobian to generate a feasible step that simultaneously decreases all objectives. Obviously, this step is expensive when the problem size is large. To conquer this difficulty, we propose the following RCD method. In each iteration, we randomly select two objectives pair $\{i, j\}$ with probability $p_{i,j}$ to update their objective values for $i, j \in \mathbb{M}$. To ensure convergence of the algorithm, we need the following condition on the sampling probability, $\{p_{i,j}\}_{i,j=1}^{M}$.

Assumption 2. For any $p_{i,j}$, there exists $i_1, i_2, \ldots, i_k \in \mathbb{M}$ such that sampling probabilities $p_{i,i_1}, p_{i_1,i_2}, \ldots, p_{i_k,j}$ are all strictly positive.

Graphically, one can think of a strictly positive $p_{i,j} > 0$ as an "edge" between node i and j, and if $p_{i,j} = 0$, it means that there is no edge between node i and j. Assumption 2 means that the communication network among the nodes is connected, i.e., any two nodes in the network are either directly connected by an edge or indirectly connected by at least one path formed by several intermediate edges. If the network is complete, i.e., each node is directly connected to every other node, $p_{i,j} > 0$ for all edges, the above condition is automatically satisfied. Some other options are available, for example, the cyclic network (see Figure 1). In a cyclic network, each node is connected in a circular fashion: Node 1 $\longrightarrow$ Node 2 $\longrightarrow$ Node 3 $\longrightarrow$ Node 4 $\longrightarrow$ Node 1 .... Another one is the so-called central coordinator network, in which one node is chosen as a central coordinator (see Figure 2), and the rest of the nodes are connected to this central coordinator while do not share direct connections among themselves. The implication of a connected network is that any local change can eventually ripple through the whole network instead of being contained.

Once a pair $\{i, j\}$ is chosen, the following problem for the convex optimization problem is solved:

$$\mathscr{P}_{i,j}(\mathbf{X}): \min_{\mathbf{d}_{i,j}, t_{i,j}} t_{i,j}, \tag{5}$$

$$s.t.\ \nabla f_i(\mathbf{x}_i)^T \mathbf{d}_{i,j} + \frac{L}{2} \left\| \mathbf{d}_{i,j} \right\|^2 \le t_{i,j}$$

$$-\nabla f_j(\mathbf{x}_j)^T \mathbf{d}_{i,j} + \frac{L}{2} \left\| \mathbf{d}_{i,j} \right\|^2 \le t_{i,j}. \tag{6}$$

It is not hard to see that due to inequality (4), the solution of problem $\mathscr{P}_{i,j}(\mathbf{X})$ provides a descent direction to improve the objective values for both i and j. The key difference between $\mathscr{P}_{i,j}$ and its single-objective RCD counterpart is that a single-objective RCD algorithm will aggregate (5) and (6) and attempt to minimize such aggregate cost. Unlike our multiobjective method, this single-objective scheme does not necessarily generate non-deteriorating solution for both agents. We use $\mathbf{d}_{i,j}^*$ to denote the optimal solution of problem $\mathscr{P}_{i,j}(\mathbf{X})$ and use $\mathbf{x}_i^+$ and $\mathbf{x}_j^+$ to denote the updated solution points for the i-th and j-th objective functions, respectively. Let $\mathbf{X}^+ = \begin{bmatrix} \mathbf{x}_1^+ \\ \vdots \\ \mathbf{x}_M^+ \end{bmatrix}$ be the updated solution vector. The RCD algorithm updates the solution points as follows: $\mathbf{x}_i^+ = \mathbf{x}_i + \mathbf{d}_{i,j}^*$, $\mathbf{x}_j^+ = \mathbf{x}_j - \mathbf{d}_{i,j}^*$, and keeps all the others unchanged $\mathbf{x}_m^+ = \mathbf{x}_m$, for $m \ne i, j$ and $m \in \mathbb{M}$. One prominent feature of the method is that problem $\mathscr{P}_{i,j}(\mathbf{X})$ admits explicit solution.

Lemma 1. *Given* $\mathbf{X}$ *and pair* (i, j), *the optimal solution of* $\mathscr{P}_{i,j}(\mathbf{X})$ *is*

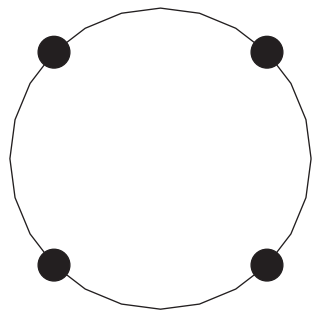

Figure 1: A cyclic network where each node is connected in a circular fashion.

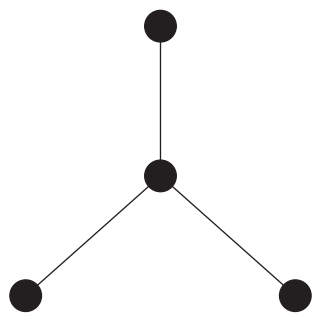

Figure 2: A central coordinator network where nodes do not have direct connections but are connected indirectly by a central node.

$$\mathbf{d}_{i,j}^{*} = -\frac{1}{L}\left(\lambda_{i,j}^{*}\nabla f_i(\mathbf{x}_i) - \left(1-\lambda_{i,j}^{*}\right)\nabla f_j\left(\mathbf{x}_j\right)\right), \tag{7}$$

where

$$\lambda_{i,j}^{*} = \max\left\{0,\ \min\left\{1, \frac{\nabla f_j\left(\mathbf{x}_j\right)^T\left[\nabla f_i(\mathbf{x}_i) + \nabla f_j\left(\mathbf{x}_j\right)\right]}{\left\|\nabla f_i(\mathbf{x}_i) + \nabla f_j\left(\mathbf{x}_j\right)\right\|^2}\right\}\right\}. \tag{8}$$

Furthermore, $\mathbf{X}^*$ is Pareto optimal only if the optimal solution of $\mathscr{P}_{i,j}(\mathbf{X}^*)$ is $\mathbf{d}_{i,j}^{*} = 0$ for all pairs $\{i, j\}$, and the reverse direction holds true if all f_m are convex.

Proof. Checking the Karush–Kuhn–Tucker (KKT) condition of problem $\mathscr{P}_{i,j}(\mathbf{x})$ yields

$$\mathbf{d}_{i,j}^{*} = -\frac{1}{L}\left(\lambda_{i,j}\nabla f_i(\mathbf{x}_i) - \left(1-\lambda_{i,j}\right)\nabla f_j\left(\mathbf{x}_j\right)\right), \tag{9}$$

where $\lambda_{i,j} \in [0,1]$ is the Lagrange multiplier. Substituting $\mathbf{d}_{i,j}^{*}$ back into the constraints gives $t_{i,j}^{*}$ as

$$t_{i,j}^{*} = \min_{\lambda_{i,j}\in[0,1]}\left\{\frac{1}{L}\max\left\{g_i\left(\lambda_{i,j}; \nabla f_i(\mathbf{x}_i), \nabla f_j\left(\mathbf{x}_j\right)\right), g_j\left(\lambda_{i,j}; \nabla f_i(\mathbf{x}_i), \nabla f_j\left(\mathbf{x}_j\right)\right)\right\}\right\}, \tag{10}$$

where

$$\begin{cases} g_i(k; \mathbf{a}_1, \mathbf{a}_2) = \dfrac{1}{2}k^2\left\|\mathbf{a}_1 + \mathbf{a}_2\right\|^2 - k\left\|\mathbf{a}_1 + \mathbf{a}_2\right\|^2 + \mathbf{a}_1^T\mathbf{a}_2 + \dfrac{1}{2}\left\|\mathbf{a}_2\right\|^2 \\ g_j(k; \mathbf{a}_1, \mathbf{a}_2) = \dfrac{1}{2}k^2\left\|\mathbf{a}_1 + \mathbf{a}_2\right\|^2 - \dfrac{1}{2}\left\|\mathbf{a}_2\right\|^2 \end{cases} \tag{11}$$

It can be easily verified that $g_i(k; \mathbf{a}_1, \mathbf{a}_2)$ is strictly decreasing for $k \in [0,1]$ and $g_j(k; \mathbf{a}_1, \mathbf{a}_2)$ is strictly increasing for $k \in [0,1]$; after checking the boundary values, we obtain $\lambda_{i,j}^{*}$ as in (10). Clearly, when each f_m is convex and $\mathbf{d}_{i,j}^{*} = 0$, it implies the Pareto optimality, i.e., $\lambda_{i,j}^{*}\nabla f_i(\mathbf{x}_i) = (1-\lambda_{i,j}^{*})\nabla f_j(\mathbf{x}_j), \lambda_{i,j}^{*} \in [0,1]$ for any pair (i, j), which satisfies the KKT condition of $\mathscr{P}_{mo}$. The other direction is straightforward.

The algorithm is summarized in the following pseudocode.

A distributed algorithm for large-scale linearly-coupled resource allocation problems with selfish agents. Algorithm 1

Since $\mathscr{P}_{mo}$ is assumed to be a large-scale problem, the computational cost of methods [15, 16] could become intimidating because an overall optimization that involves all objectives is required to compute an update direction. Also, the methods of [15, 16] would require all the objective function information to be transmitted to a central coordinating agent, where the optimization is conducted. But

Initialization: set $\mathbf{X} = \mathbf{X}^0$;
while True **do**
  Randomly select a matching pair $\{i, j\}$ according to some network structure
  Solve $\mathbf{d}_{i,j}^{\mathbf{a}st}$ from problem:

$$\mathscr{P}_{i,j}(\mathbf{X}): \min_{\mathbf{d}_{i,j}, t_{i,j}} t_{i,j}$$
$$s.t.\ \nabla f_i(\mathbf{x}_i)^T \mathbf{d}_{i,j} + L/2\|\mathbf{d}_{i,j}\|^2 \le t_{i,j}$$
$$-\nabla f_j(\mathbf{x}_j)^T \mathbf{d}_{i,j} + L/2\|\mathbf{d}_{i,j}\|^2 \le t_{i,j}$$

  Update:

$$\mathbf{x}_i = \mathbf{x}_i + \mathbf{d}_{i,j}^*,$$
$$\mathbf{x}_j = \mathbf{x}_j - \mathbf{d}_{i,j}^*.$$

Algorithm 1: Multiobjective adaptation.

this could create excessive communication overheads in the central coordinating agent. In contrast, our method is able to take advantage of the separability of the problem structure, and the update has an analytical form and can be parallelized by optimizing multiple pairs concurrently; moreover, the pairwise optimization can be easily implemented in a peer-to-peer manner. The cost per iteration is $\mathscr{O}(c_f + c)$, where c_f is the maximum cost of computing the gradient of each f_i, and c is the cost of updating $\mathbf{x}_i$. When compared with the single-objective randomized coordinate descent method, the main difference is that the optimization procedure guarantees that $t_{i,j} \le 0$ for any pair; as a result, the update is always non-deteriorating for each of the agents and hence can be applied in real time. □

Remark 1. When all information is available, one may also consider to follow the idea of [15], that is, to simultaneously optimize all agents, the update directions are given by solving the following problem:

$$\begin{aligned}
&\mathscr{P}_{\text{all}}(\mathbf{X}): \min_{\mathbf{d}_1,\ldots,\mathbf{d}_M, t} t \\
&s.t.\ \nabla f_1(\mathbf{x}_1)^T \mathbf{d}_1 + \frac{L}{2}\|\mathbf{d}_1\|^2 \le t, \\
&\quad\vdots \\
&\nabla f_M(\mathbf{x}_M)^T \mathbf{d}_M + \frac{L}{2}\|\mathbf{d}_M\|^2 \le t, \\
&\sum_{i=0}^{M} \mathbf{d}_i = 0
\end{aligned} \tag{12}$$

However, the cost per iteration of this problem will be $\mathscr{O}(Mc_f + Mc)$. Also note that P_{all} generally does not have an analytical solution form; therefore, an additional algorithm for quadratic programming is needed to find its solution.

4. Convergence Rate Analysis

4.1. Convergence Rate Analysis: Non-convex Case. We investigate the convergence rate of the RCD algorithm in this section. We first introduce the potential function $h: \mathbb{R}^{kM} \longrightarrow \mathbb{R}$ as $h(\mathbf{X}) = \sum_{m=1}^{M} f_m(\mathbf{x}_m)$. For the optimal updating vector $\mathbf{d}_{i,j}^*$ and the associated Lagrange multiplier $\lambda_{i,j}^*$, the Lipschitz continuity of f_m implies

$$\begin{aligned}
&f_i\left(\mathbf{x}_i + \mathbf{d}_{i,j}^*\right) + f_j\left(\mathbf{x}_j - \mathbf{d}_{i,j}^*\right) \\
&\le f_i(\mathbf{x}_i) + f_j(\mathbf{x}_j) + \nabla f_i(\mathbf{x}_i)^T \mathbf{d}_{i,j}^* + \frac{L}{2}\left\|\mathbf{d}_{i,j}^*\right\|^2 - \nabla f_j(\mathbf{x}_j)^T \mathbf{d}_{i,j}^* + \frac{L}{2}\left\|\mathbf{d}_{i,j}^*\right\|^2 \\
&\le f_i(\mathbf{x}_i) + f_j(\mathbf{x}_j) + \lambda_{i,j}^{\mathbf{a}st}\left(\nabla f_i(\mathbf{x}_i)^T \mathbf{d}_{i,j}^* + \frac{L}{2}\left\|\mathbf{d}_{i,j}^*\right\|^2\right) + \left(1 - \lambda_{i,j}^{\mathbf{a}st}\right)\left(-\nabla f_j(\mathbf{x}_j)^T \mathbf{d}_{i,j}^* + \frac{L}{2}\left\|\mathbf{d}_{i,j}^*\right\|^2\right) \\
&\le f_i(\mathbf{x}_i) + f_j(\mathbf{x}_j) - \frac{1}{2L}\left\|\lambda_{i,j}^* \nabla f_i(\mathbf{x}_i) - \left(1 - \lambda_{i,j}^*\right)\nabla f_j(\mathbf{x}_j)\right\|^2,
\end{aligned} \tag{13}$$

where the second inequality follows from the observation that $t_{i,j}^* \le 0$. Therefore, under the preceding updating rule, we can estimate the expected decrease of potential function as

$$\begin{aligned} & h(\mathbf{X}) - \mathbb{E}\left[h\left(\mathbf{X}^+\right)|\mathbf{X}\right] \\ & = \sum_{\{i,j\}} p_{i,j}\left[\left(f_i(\mathbf{x}_i) + f_j\left(\mathbf{x}_j\right)\right) - \left(f_i\left(\mathbf{x}_i + \mathbf{d}_{i,j}^*\right) + f_j\left(\mathbf{x}_j - \mathbf{d}_{i,j}^*\right)\right)\right] \\ & \ge \frac{1}{2L} \sum_{\{i,j\}} p_{i,j}\left\|\lambda_{i,j}^* \nabla f_i(\mathbf{x}_i) - \left(1 - \lambda_{i,j}^*\right)\nabla f_j\left(\mathbf{x}_j\right)\right\|^2. \end{aligned} \tag{14}$$

Now, we introduce the following criteria as a metric, $\mathscr{D}(\cdot)\colon \mathbb{R}^{kM} \longrightarrow \mathbb{R}$, as

$$\mathscr{D}(\mathbf{a}) := \left(\frac{1}{2L}\sum_{(i,j)} p_{i,j}\left\|\lambda_{i,j}(\mathbf{a})\mathbf{a}_i - \left(1 - \lambda_{i,j}(\mathbf{a})\right)\mathbf{a}_j\right\|^2\right)^{1/2}, \tag{15}$$

with $\lambda_{i,j}(\mathbf{a})\max\left\{0, \min\left\{1, \mathbf{a}_j^T(\mathbf{a}_i + \mathbf{a}_j)/\|\mathbf{a}_i + \mathbf{a}_j\|^2\right\}\right\}$ for some $\mathbf{a} = [\mathbf{a}_1^T \ldots \mathbf{a}_M^T]^T \in \mathbb{R}^{kM}$, $\mathbf{a}_m \in \mathbb{R}^k, \forall m$. Using $\mathscr{D}(\cdot)$, the preceding inequality (10) becomes

$$h(\mathbf{X}) - \mathbb{E}\left[h\left(\mathbf{X}^+\right)|\mathbf{X}\right] \ge \mathscr{D}(\nabla h(\mathbf{X}))^2. \tag{16}$$

One can view $\mathscr{D}(\cdot)$ as an improvement potential indicator. Specifically, we have the following lemma.

Lemma 2. *$\mathscr{D}(\nabla h(\mathbf{X}^*)) = 0$ only if $\mathbf{X}^*$ is a Pareto optimal solution of $\mathscr{P}_{mo}$, and the reverse direction holds true if each f_m is convex.*

Proof. We first prove one direction that $\mathscr{D}(\nabla h(\mathbf{X}^*)) = 0$ implies $\mathbf{X}^*$ is a Pareto optimal solution by contraposition. Assume that $\mathbf{X}$ with $\sum_{i=m}^M \mathbf{x}_m = 0$ is not Pareto optimal; then, there exist i and $j \ne i$ such that $\nabla f_i(\mathbf{x}_i) \ne t \cdot \nabla f_j(\mathbf{x}_j)$, $\forall t \in \mathbb{R}_+$, which implies $\mathscr{D}(\nabla h(\mathbf{X})) > 0$. The other direction in this lemma is straightforward. We omit the detail.

We now turn to investigate the convergence rate of the RCD algorithm. Convergence rate of methods for single-objective problem such as $\min_{\mathbf{x}\in\mathscr{C}} f(\mathbf{x})$ is usually measured with respect to the gap from its optimal value f^*. However, different from the single objective-based optimization problem, the generated sequence of the MO algorithm may converge to different points in the Pareto optimal frontier, and there is no a priori way to determine which point the sequence converges to; this property will be further substantiated by the numerical simulations. Therefore, one needs to construct an alternative benchmark that measures the convergence rate (the construction of such alternative gap function for multiobjective optimization problems is also discussed by Dutta et al. and Tanabe et al. [28–30] recently). We define the following two measures (functions):

$$\begin{aligned} h^\dagger(\mathbf{X}) &= \min_{\mathbf{F}(\mathbf{Y})\preccurlyeq\mathbf{F}(\mathbf{X}),\mathbf{Y}\in\mathscr{C}} h(\mathbf{Y}), \\ v^\dagger(\mathbf{X}) &= \max_{\mathbf{F}(\mathbf{Y})\preccurlyeq\mathbf{F}(\mathbf{X}),\mathbf{Y}\in\mathscr{C}} \{h(\mathbf{X}) - h(\mathbf{Y})\} = h(\mathbf{X}) - h^\dagger(\mathbf{X}), \end{aligned} \tag{17}$$

where $h^\dagger(\mathbf{X})$ provides a lower bound of the potential function $h(\mathbf{X})$ and $v^\dagger(\mathbf{X})$ measures the gap between the current value of potential function and such a lower bound. These two measures have the following properties. □

Lemma 3. *For any $\mathbf{X}^1, \mathbf{X}^2 \in \mathscr{C}$, if $\mathbf{F}(\mathbf{X}^2) \prec \mathbf{F}(\mathbf{X}^1)$, it has $h^\dagger(\mathbf{X}^2) \ge h^\dagger(\mathbf{X}^1)$ and $v^\dagger(\mathbf{X}^2) \le v^\dagger(\mathbf{X}^1)$. Furthermore, the solution $\mathbf{X}^*$ is a Pareto optimal point only if $v^\dagger(\mathbf{X}^*) = 0$, and the reverse direction holds true if each f_m is convex.*

Proof. The first half follows directly from the observation that $\mathbf{F}(\mathbf{X}^2) \prec \mathbf{F}(\mathbf{X}^1)$ implies $\{\mathbf{Y} \in \mathscr{C}\colon \mathbf{F}(\mathbf{Y}) \prec \mathbf{F}(\mathbf{X}^2)\} \subseteq \{\mathbf{Y} \in \mathscr{C}\colon \mathbf{F}(\mathbf{Y}) \prec \mathbf{F}(\mathbf{X}^1)\}$. The rest of the proof is straightforward, and we omit the details.

Although $h^\dagger, v^\dagger$ are only tangential to the following convergence result for non-convex objective functions, they are pivotal to obtain convergence rate for convex and strongly convex objective functions. Then, we have the following preliminary convergence rate result for generally non-convex objective functions given as follows. □

Theorem 1. *If level set $\mathscr{L} := \{\mathbf{X} \in \mathscr{C}\colon \mathbf{F}(\mathbf{X}) \prec \mathbf{F}(\mathbf{X}^0)\}$ is bounded, then the following holds:*

$$\min_{k=1,\ldots,n} \mathbb{E}\left[\mathscr{D}\left(\nabla h\left(\mathbf{X}^k\right)\right)|\mathbf{X}^0\right] \le \sqrt{\frac{h\left(\mathbf{X}^0\right) - h^\dagger\left(\mathbf{X}^0\right)}{n}}. \tag{18}$$

Proof. Taking expectation of both sides of (17) with respect to $\mathbf{X}^0$ and summing up to n, we arrive at the following:

$$
\begin{aligned}
& n \cdot \left(\min_{k=1,\ldots,n} \mathbb{E}\left[\mathscr{D}\left(\nabla h\left(\mathbf{X}^k\right)\right)|\mathbf{X}^0\right]\right)^2 \\
& \leq \sum_k \mathbb{E}^2\left[\mathscr{D}\left(\nabla h\left(\mathbf{X}^k\right)\right)|\mathbf{X}^0\right] \\
& \leq \sum_k \mathbb{E}\left[\mathscr{D}^2\left(\nabla h\left(\mathbf{X}^k\right)\right)|\mathbf{X}^0\right] \\
& \leq h\left(\mathbf{X}^0\right) - \mathbb{E}\left[h\left(\mathbf{X}^1\right)|\mathbf{X}^0\right] \\
& \quad + \mathbb{E}\left[h\left(\mathbf{X}^1\right)|\mathbf{X}^0\right] - \mathbb{E}\left[h\left(\mathbf{X}^2\right)|\mathbf{X}^0\right] + \cdots \\
& \quad + \mathbb{E}\left[h\left(\mathbf{X}^{n-1}\right)|\mathbf{X}^0\right] - \mathbb{E}\left[h\left(\mathbf{X}^1\right)|\mathbf{X}^0\right] \\
& = h\left(\mathbf{X}^0\right) - \mathbb{E}\left[h\left(\mathbf{X}^1\right)|\mathbf{X}^0\right] \\
& \leq h\left(\mathbf{X}^0\right) - h^{\dagger}\left(\mathbf{X}^0\right),
\end{aligned} \tag{19}
$$

where the second inequality follows from Jensen's Inequality. Since $\mathscr{L}$ is bounded, we know that $h(\mathbf{X}^0) - h^{\dagger}(\mathbf{X}^0)$ is also bounded, and hence (18) follows.

Note that in the non-convex case, the stationary point could only be a local minimum. □

4.2. Convergence Rate: Convex Case. When each f_m is convex, an accelerated convergence rate can be obtained. But first we need some preliminary results. In the same spirit of the dual norm, for a non-empty compact set $\mathscr{B} \subset \mathbb{R}^{kM}$, we define the dual function of $\mathscr{D}(\cdot)$ on $\mathscr{B}$ as

$$
\mathscr{D}^*_{\mathscr{B}}(\mathbf{d}) = \max_{\mathbf{Y} \in \mathscr{A}_{\mathscr{B}}(\mathbf{d})} \mathbf{Y}^T \mathbf{d}, \tag{20}
$$

where $\mathscr{A}_{\mathscr{B}}(\mathbf{d}) = \left\{\mathbf{Y} = [\mathbf{y}_1^T \ldots \mathbf{y}_M^T]^T \in \mathscr{B}\colon 0 \leq \mathscr{D}(\mathbf{Y}) \leq 1, \mathbf{y}_m^T \mathbf{d}_m \geq 0, \forall m \in \mathbb{M}\right\}$. Then, the following lemma gives the counterpart of Cauchy–Schwarz inequality with respect to the feasible set $\mathscr{C}$ of problem p_{mo}.

Lemma 4. *Given $\mathbf{d} \in \mathscr{C}$ and a non-empty compact set $\mathscr{B} \subset \mathbb{R}^{kM}$, for all $Y \in \mathscr{B} \cap \left\{Y = [y_1^T \ldots y_M^T]^T \in \mathbb{R}^{kM} | y_m^T d_m \geq 0, \forall m \in \mathbb{M}\right\}$, the following inequality holds true:*

$$
\mathbf{Y}^T \mathbf{d} \leq \mathscr{D}(\mathbf{Y}) \cdot \mathscr{D}^*_{\mathscr{B}}(\mathbf{d}). \tag{21}
$$

Furthermore, there exists a number $\Gamma_{\mathscr{B}} \leq 0$ such that $\mathscr{D}^*_{\mathscr{B}}(\mathbf{d}) \leq \Gamma_{\mathscr{B}} \|\mathbf{d}\|$ for all $\mathbf{d} \in \mathscr{C}$.

Proof. Since $\mathscr{A}_{\mathscr{B}}(\mathbf{d})$ is a compact set, then $\mathscr{D}^*_{\mathscr{B}}(\cdot)$ is well defined. Depending on the value of $\mathscr{D}(\mathbf{Y})$, we have two cases as follows:

(1) If $\mathscr{D}(\mathbf{Y}) = 0$, from (17), we know $\mathbf{Y}$ must be in form of $\mathbf{Y} = \begin{bmatrix} t_1 \mathbf{g} \\ \vdots \\ t_M \mathbf{g} \end{bmatrix}$ for some $g \in \mathbb{R}^k$ and $t_1, \ldots, t_M \in \mathbb{R}_+$. Suppose there exists a $\mathbf{d} \in \mathscr{C}$ such that $\mathbf{Y}^T \mathbf{d} > 0$, which implies $\mathbf{g}^T \mathbf{d}_m > 0$ for some m. However, this leads to $\sum_{m=1}^M \mathbf{g}^T \mathbf{d}_m = \mathbf{g}^T (\sum_{m=1}^M \mathbf{d}_m) > 0$, which is a contradiction to the fact that $\mathbf{d} \in \mathscr{C}$. Therefore, $\mathscr{D}(\mathbf{Y}) = 0$ implies $\mathbf{Y}^T \mathbf{d} = 0$ for all $\mathbf{d} \in \mathscr{C}$ such that $\mathbf{y}_m^T \mathbf{d}_m \geq 0$, $\forall m \in \mathbb{M}$.

(2) If $\mathscr{D}(\mathbf{Y}) > 0$, let $\widetilde{\mathscr{A}}_{\mathscr{B}}(\mathbf{d}) = \{\mathbf{Y} \in \mathscr{B} | 0 < \mathscr{D}(\mathbf{Y}) \leq 1, \mathbf{y}_m^T \mathbf{d}_m \geq 0, \forall m \in \mathbb{M}\}$. Clearly, it has $\widetilde{\mathscr{A}}_{\mathscr{B}}(\mathbf{d}) \subseteq \mathscr{A}_{\mathscr{B}}(\mathbf{d})$. Then, inequality (21) follows from

$$
\begin{aligned}
\mathbf{Y}^T \mathbf{d} &= \mathbf{Y}^T \mathbf{d} \cdot \frac{\mathscr{D}(\mathbf{Y})}{\mathscr{D}(\mathbf{Y})} \\
&\leq \mathscr{D}(\mathbf{Y}) \cdot \left(\sup_{\mathbf{Y} \in \widetilde{\mathscr{A}}_{\mathscr{B}}(\mathbf{d})} \mathbf{Y}^T \mathbf{d} \right) \\
&\leq \mathscr{D}(\mathbf{Y}) \cdot \left(\max_{\mathbf{Y} \in \mathscr{A}_{\mathscr{B}}(\mathbf{d})} \mathbf{Y}^T \mathbf{d} \right) \\
&= \mathscr{D}(\mathbf{Y}) \cdot \mathscr{D}^*_{\mathscr{B}}(\mathbf{d}),
\end{aligned} \tag{22}
$$

where the second equality follows from the fact that $\lambda_{i,j}(k\mathbf{Y}) = \lambda_{i,j}(\mathbf{Y})$, $\forall k \in \mathbb{R}$, and hence it has $\mathscr{D}(k\mathbf{Y}) = |k| \mathscr{D}(\mathbf{Y})$.

As for the last part of the lemma, we can compute the lower bound value $\Gamma_{\mathscr{B}}$ as

$$
\begin{aligned}
\Gamma_{\mathscr{B}} &= \sup_{\|\mathbf{d}\|>0} \frac{\mathscr{D}^*_{\mathscr{B}}(\mathbf{d})}{\|\mathbf{d}\|} \\
&\leq \max_{\mathbf{d}:\|\mathbf{d}\| \leq 1} \mathscr{D}^*_{\mathscr{B}}(\mathbf{d}) \\
&= \max_{\mathbf{d}:\|\mathbf{d}\| \leq 1} \left\{ \max_{\mathbf{a} \in \mathscr{A}_{\mathscr{B}}(\mathbf{d})} \mathbf{a}^T \mathbf{d} \right\},
\end{aligned} \tag{23}
$$

where $\mathscr{A}_{\mathscr{B}} = \left\{(\mathbf{Y}, \mathbf{d}) | \mathbf{Y} \in \mathscr{A}_{\mathscr{B}}(\mathbf{d}), \mathbf{d} \in \mathscr{C}, \|\mathbf{d}\| \leq 1\right\}$ is a compact set. □

Theorem 2. *Given an initial solution $\mathbf{X}^0$, if the level set $\mathscr{L} := \left\{\mathbf{X} \in \mathscr{C} | \mathbf{F}(\mathbf{X}) \prec \mathbf{F}(\mathbf{X}^0)\right\}$ is bounded, then the solution $\mathbf{X}^n$ generated by the n-th iteration of RCD algorithm satisfies*

$$
\mathbb{E}\left[v^{\dagger}(\mathbf{X}^n) | \mathbf{X}^0\right] \leq \frac{\Gamma^2_{\mathscr{B}} R\left(\mathbf{X}^0\right)^2}{n}, \tag{24}
$$

where $R(\mathbf{X}^0) := max_{\mathbf{Y}\in\mathscr{L}}\|\mathbf{X}^0 - \mathbf{Y}\|$ and $\Gamma_{\mathscr{B}}$ is defined with respect to $\mathscr{D}^*_{\mathscr{B}}$ in Lemma 4 with $\mathscr{B} := \{\nabla h(\mathbf{X}): \mathbf{X} \in \mathscr{L}\}$. Furthermore, $\Gamma_{\mathscr{B}}$ is bounded by

$$\begin{aligned}\Gamma_{\mathscr{B}} &\le \left\|\nabla h\left(\mathbf{X}^0\right)\right\| + L \cdot \max_{\mathbf{Z}\in\mathscr{L}} \sum_{m=1}^{M} \left\|\mathbf{x}_m^0 - \mathbf{z}_m\right\| \\ &\le \left\|\nabla h\left(\mathbf{X}^0\right)\right\| + L\sqrt{M} \cdot R\left(\mathbf{X}^0\right)\end{aligned}. \tag{25}$$

Proof. As the level set $\mathscr{L}$ is bounded, problem p_{mo} always admits solution. On the other hand, the Lipschitz property in Assumption 1 implies

$$\begin{aligned}&\|\nabla h(\mathbf{X}) - \nabla h(\mathbf{Z})\| \\ &\le \sum_{m=1}^{M} \left\|\nabla f_m(\mathbf{x}_m) - \nabla f_m(\mathbf{z}_m)\right\| \\ &\le L \sum_{m=1}^{M} \left\|\mathbf{x}_m - \mathbf{z}_m\right\|,\end{aligned} \tag{26}$$

which further implies the boundedness of the set $\mathscr{B}$. Therefore, $\Gamma_{\mathscr{B}}$ satisfies the following inequality:

$$\Gamma_{\mathscr{B}} = \max_{(\mathbf{Y},\mathbf{d})\in\mathscr{A}_{\mathscr{B}}} \mathbf{Y}^T\mathbf{d} \le \max_{(\mathbf{Y},\mathbf{d})\in\mathscr{A}_{\mathscr{B}}} \|\mathbf{Y}\| \cdot \|\mathbf{d}\| \le \max_{\mathbf{Y}\in\mathscr{B}} \|\mathbf{Y}\| \le \left\|\nabla h\left(\mathbf{X}^0\right)\right\| + \max_{\mathbf{Z}\in\mathscr{L}} \left\|\nabla h\left(\mathbf{X}^0\right) - \nabla h(\mathbf{Z})\right\|. \tag{27}$$

Then, it has

$$\begin{aligned}0 &\le v^\dagger\left(\mathbf{X}^n\right) \\ &= \max_{\mathbf{F}(\mathbf{Y})\preccurlyeq\mathbf{F}(\mathbf{X}^n),\mathbf{Y}\in\mathscr{C}} \left\{h\left(\mathbf{X}^n\right) - h(\mathbf{Y})\right\} \\ &\le \max_{\mathbf{F}(\mathbf{Y})\preccurlyeq\mathbf{F}(\mathbf{X}^n),\mathbf{Y}\in\mathscr{C}} \left\{\nabla h\left(\mathbf{X}^n\right)^T\left(\mathbf{X}^n - \mathbf{Y}\right)\right\} \\ &\le \max_{\mathbf{F}(\mathbf{Y})\preccurlyeq\mathbf{F}(\mathbf{X}^n),\mathbf{Y}\in\mathscr{C}} \mathscr{D}\left(\nabla h\left(\mathbf{X}^n\right)\right) \cdot \mathscr{D}^{\mathbf{a}st}_{\mathscr{B}}\left(\mathbf{X}^n - \mathbf{Y}\right), \\ &= \mathscr{D}\left(\nabla h\left(\mathbf{X}^n\right)\right) \cdot \max_{\mathbf{F}(\mathbf{Y})\preccurlyeq\mathbf{F}(\mathbf{X}^n),\mathbf{Y}\in\mathscr{C}} \mathscr{D}^{\mathbf{a}st}_{\mathscr{B}}\left(\mathbf{X}^n - \mathbf{Y}\right) \\ &\le \mathscr{D}\left(\nabla h\left(\mathbf{X}^n\right)\right) \cdot \Gamma_{\mathscr{B}} \cdot R\left(\mathbf{X}^0\right),\end{aligned} \tag{28}$$

where the second inequality is from the convexity of $h(\cdot)$, and the third inequality is from (24). Inequality (28) together with (17) gives

$$\begin{aligned}&h\left(\mathbf{X}^n\right) - \mathbb{E}\left[h\left(\mathbf{X}^{n+1}\right)|\mathbf{X}_n\right] \ge \frac{\left(v^\dagger\left(\mathbf{X}^n\right)\right)^2}{\Gamma^2_{\mathscr{B}} R\left(\mathbf{X}^0\right)^2} \\ &\Longrightarrow \mathbb{E}\left[h\left(\mathbf{X}^{n+1}\right) - h^\dagger\left(\mathbf{X}^n\right)|\mathbf{X}_n\right] \le v^\dagger\left(\mathbf{X}^n\right) - \frac{\left(v^\dagger\left(\mathbf{X}^n\right)\right)^2}{\Gamma^2_{\mathscr{B}} R\left(\mathbf{X}^0\right)^2}.\end{aligned} \tag{29}$$

Since it has $\mathbf{F}(\mathbf{X}^{n+1}) \prec \mathbf{F}(\mathbf{X}^n)$, applying Lemma 3 to the preceding inequality gives

$$\begin{aligned}\mathbb{E}\left[v^\dagger\left(\mathbf{X}^{n+1}\right)|\mathbf{X}_n\right] &\le \mathbb{E}\left[h\left(\mathbf{X}^{n+1}\right) - h^\dagger\left(\mathbf{X}^n\right)|\mathbf{X}_n\right] \\ &\le v^\dagger\left(\mathbf{X}^n\right) - \frac{\left(v^\dagger\left(\mathbf{X}^n\right)\right)^2}{\Gamma^2_{\mathscr{B}} R\left(\mathbf{X}^0\right)^2}\end{aligned}. \tag{30}$$

Taking expectation of both sides of the above inequality and applying Jensen's inequality, $\mathbb{E}[(v^\dagger(\mathbf{X}^n))^2|\mathbf{X}_0]$ $\mathbf{g}e(\mathbb{E}[v^\dagger(\mathbf{X}^n)|\mathbf{X}_0])^2$, it has

$$\Delta_{n+1} \le \Delta_n - \frac{\Delta_n^2}{\Gamma^2_{\mathscr{B}} R\left(\mathbf{X}^0\right)^2}, \tag{31}$$

where $\text{Delta}_n = \mathbb{E}[v^\dagger(\mathbf{X}^n)|\mathbf{X}_0]$. Since $\Delta_{n+1} \le \Delta_n$, it has

$$\begin{aligned}&\frac{1}{\Delta_n} \le \frac{1}{\Delta_{n+1}} - \frac{\Delta_n}{\Delta_{n+1}} \cdot \frac{1}{\Gamma^2_{\mathscr{B}} R\left(\mathbf{X}^0\right)^2} \\ &\Longrightarrow \frac{1}{\Gamma^2_{\mathscr{B}} R\left(\mathbf{x}^0\right)^2} \le \frac{1}{\Delta_{n+1}} - \frac{1}{\Delta_n} \\ &\Longrightarrow \Delta_n \le \frac{\Gamma^2_{\mathscr{B}} R\left(\mathbf{X}^0\right)^2}{n}.\end{aligned} \tag{32}$$

□

4.3. Convergence Rate: Strongly Convex Case. In this section, we investigate the convergence rate when function $f_m(\cdot)$ is σ-strongly convex for all $m \in \mathbb{M}$.

Assumption 3. There exists a $\sigma > 0$ such that

$$f_m(\mathbf{y}_m) \geq f_m(\mathbf{x}_m) + \nabla f_m(\mathbf{x}_m)^T(\mathbf{y}_m - \mathbf{x}_m) + \frac{\sigma}{2}\|\mathbf{y}_m - \mathbf{x}_m\|^2, \tag{33}$$

for all $\mathbf{x}_m, \mathbf{y}_m \in \mathbb{R}^k$.

Summing up f_m leads to the strong convexity of the Lyapunov function, i.e.,

$$h(\mathbf{Y}) \geq h(\mathbf{X}) + \nabla h(\mathbf{X})^T(\mathbf{Y} - \mathbf{X}) + \frac{\sigma}{2}\|\mathbf{Y} - \mathbf{X}\|^2, \forall \mathbf{Y}, \mathbf{X} \in \mathbb{R}^{kM}. \tag{34}$$

Theorem 3. *Given an initial feasible solution $\mathbf{X}^0$, if level set $\mathscr{L} := \{\mathbf{X} \in \mathscr{C}: \mathbf{F}(\mathbf{X}) \prec \mathbf{F}(\mathbf{X}^0)\}$ is bounded, then the RCD algorithm satisfies*

$$\mathbb{E}\left[v^\dagger(\mathbf{X}^n)|\mathbf{X}^0\right] \leq \left(1 - \frac{2\sigma}{\Gamma_{\mathscr{B}}}\right)^n \cdot v^\dagger\left(\mathbf{X}^0\right), \tag{35}$$

where $\Gamma_{\mathscr{B}}$ is defined in Lemma 4 with respect to the set $\mathscr{B} = \{\nabla h(\mathbf{X}): \mathbf{X} \in \mathscr{L}\}$.

Proof. Applying Lemma 4 to (34), it has

$$\begin{aligned} h(\mathbf{Y}) &\geq h(\mathbf{Y}) + \nabla h(\mathbf{Y})^T(\mathbf{Y} - \mathbf{X}) + \frac{\sigma}{2}\|\mathbf{Y} - \mathbf{X}\|^2 \\ &\Rightarrow h(\mathbf{Y}) \geq h(\mathbf{X}) + \nabla h(\mathbf{X})^T(\mathbf{Y} - \mathbf{X}) + \frac{\sigma}{2\Gamma_{\mathscr{B}}}\left(\mathscr{D}^*_{\mathscr{B}}(\mathbf{Y} - \mathbf{X})\right)^2 \\ &\Rightarrow \nabla h(\mathbf{X})^T(\mathbf{X} - \mathbf{Y}) - \frac{\sigma}{2\Gamma_{\mathscr{B}}}\left(\mathscr{D}^*_{\mathscr{B}}(\mathbf{X} - \mathbf{Y})\right)^2 \geq h(\mathbf{X}) - h(\mathbf{Y}). \end{aligned} \tag{36}$$

Let

$$\begin{cases} \mathscr{C}_L(\mathbf{X}) & = \left\{\mathbf{Y} \in \mathscr{C} | \nabla f_m(\mathbf{x}_m)^T(\mathbf{x}_m - \mathbf{y}_m) \geq 0, \forall m \in \mathbb{M}\right\}, \\ \mathscr{C}_R(\mathbf{X}) & = \{\mathbf{Y} \in \mathscr{C} | \mathbf{F}(\mathbf{Y}) \prec \mathbf{F}(\mathbf{X})\}. \end{cases} \tag{37}$$

Then, one can easily verify that $\mathscr{C}_R(\mathbf{X}) \subseteq \mathscr{C}_L(\mathbf{X})$ by using the convexity of f_m. Maximizing the left-hand side of (36) with respect to $\mathscr{C}_L(\mathbf{X})$ and the right-hand side with respect to $\mathscr{C}_R(\mathbf{X})$ yields

$$\begin{aligned} &\frac{\Gamma_{\mathscr{B}}}{2\sigma}\mathscr{D}(\nabla h(\mathbf{X}))^2 \\ &= \max_{t \in \mathbb{R}}\left\{\mathscr{D}(\nabla f(\mathbf{X}))t - \frac{\sigma}{2\Gamma_{\mathscr{B}}}t^2\right\} \\ &\geq \max_{\mathbf{Y} \in \mathscr{C}_L(\mathbf{X})}\left\{\mathscr{D}(\nabla f(\mathbf{x})) \cdot \mathscr{D}^*_{\mathscr{B}}(\mathbf{X} - \mathbf{Y})\frac{\sigma}{2\Gamma_{\mathscr{B}}}\left(\mathscr{D}^*_{\mathscr{B}}(\mathbf{X} - \mathbf{Y})\right)^2\right\} \\ &\geq \max_{\mathbf{Y} \in \mathscr{C}_L(\mathbf{X})}\left\{\nabla h(\mathbf{X})^T(\mathbf{X} - \mathbf{Y}) - \frac{\sigma}{2\Gamma_{\mathscr{B}}}\left(\mathscr{D}^*_{\mathscr{B}}(\mathbf{X} - \mathbf{Y})\right)^2\right\} \\ &\geq \max_{\mathbf{Y} \in \mathscr{C}_R(\mathbf{X})}\left\{\nabla h(\mathbf{X})^T(\mathbf{X} - \mathbf{Y}) - \frac{\sigma}{2\Gamma_{\mathscr{B}}}\left(\mathscr{D}^*_{\mathscr{B}}(\mathbf{X} - \mathbf{Y})\right)^2\right\} \\ &\geq \max_{\mathbf{Y} \in \mathscr{C}_R(\mathbf{X})}\{h(\mathbf{X}) - h(\mathbf{Y})\} = v^\dagger(\mathbf{X}), \end{aligned} \tag{38}$$

where the second inequality follows from Lemma 4. Letting $\mathbf{X} = \mathbf{X}^n$, combining $\mathscr{D}(\nabla f(\mathbf{X}^n))^2 \geq 2\sigma/\Gamma_{\mathscr{B}} v^\dagger(\mathbf{X}^n)$ with (17) yields

$$\begin{aligned} h(\mathbf{X}^n) - \mathbb{E}\left[h\left(\mathbf{X}^{n+1}\right)|\mathbf{X}_n\right] &\geq \frac{2\sigma}{\Gamma_{\mathscr{B}}}v^\dagger(\mathbf{X}^n) \\ \Rightarrow \mathbb{E}\left[v^\dagger\left(\mathbf{X}^{n+1}\right)|\mathbf{X}^n\right] &\leq \left(1 - \frac{2\sigma}{\Gamma_{\mathscr{B}}}\right)v^\dagger(\mathbf{X}^n). \end{aligned} \tag{39}$$

Taking expectation of both sides and applying the resulting inequality iteratively leads to (35). □

4.4. Convergence Rate in Probability. Again with the aid of gap benchmark $v^\dagger$, in this section, we are able to establish the convergence rate in probability for the RCD algorithm. First we introduce the following lemma [31].

Lemma 5 (see [31]). *Let $\mathbf{x}i^0 > 0$ be a constant, consider a $0 < \epsilon < \mathbf{x}i^0$, and let $\{\mathbf{x}i^n\}_n$ be a non-negative, non-increasing*

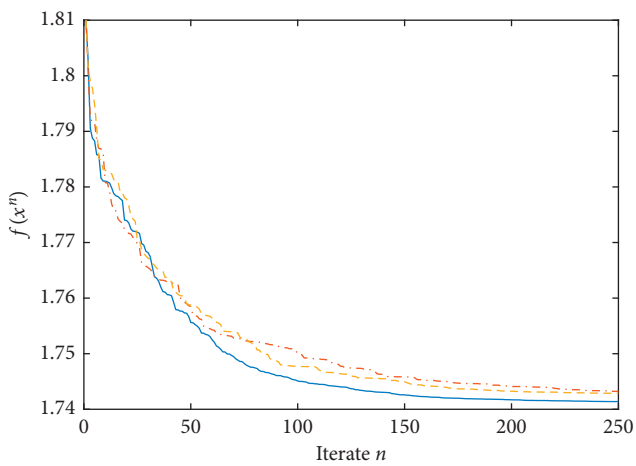

Figure 3: The potential function values for the three runs all stabilize eventually, but they converge to different limiting levels.

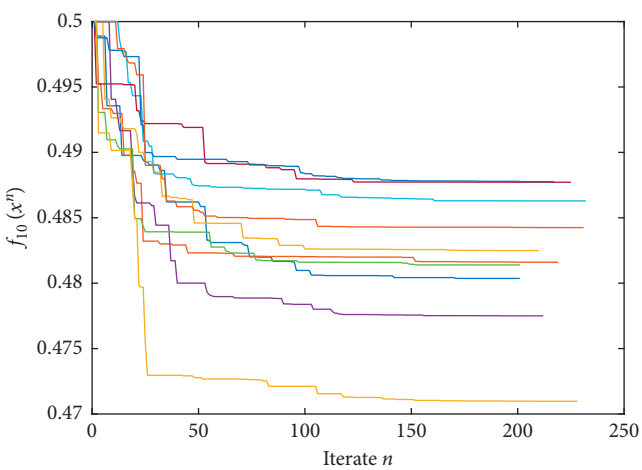

Figure 4: In a complete network, the limiting potential function value varies dramatically from each other.

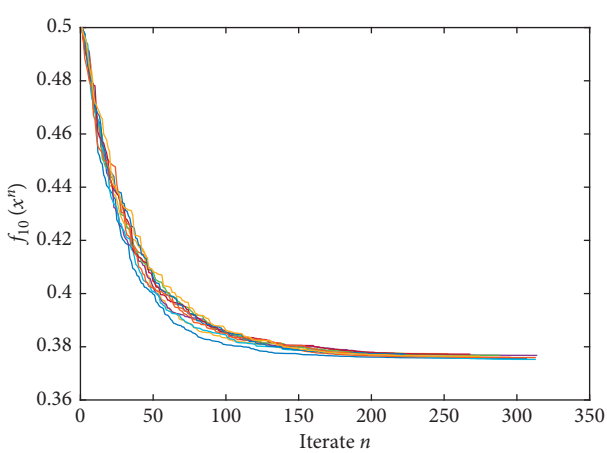

Figure 5: In a central coordinator network, the limiting potential function value is much more stable, and notably the central coordinator is able to achieve a significantly lower limiting value than in a complete network.

sequence of random variables with one of the following properties:

(1) $\mathbb{E}[\xi^{n+1}|\xi^n] \le \xi^n - (\xi^n)^2/c$ *for all* $n > 0$ *and* $r > \epsilon$.

(2) $\mathbb{E}[\xi^{n+1}|\xi^n] \le (1 - 1/c)\xi^n$ *for all* n *such that* $\xi^n \ge \epsilon$ *and* $c > 1$ *is a constant.*

Then, given confidence level $\rho \in (0, 1)$, if property (1) holds, we can choose $\epsilon < c$ and

$$N \ge \frac{c}{\epsilon}\left(1 + \log\left(\frac{1}{\rho}\right)\right) + 2 - \frac{c}{\xi^0}. \tag{40}$$

If property (2) holds, we choose

$$N \ge c \log\left(\frac{\xi^0}{\varepsilon\rho}\right). \tag{41}$$

Then, we have

$$\mathbb{P}\left(\xi^N \le \varepsilon\right) \ge 1 - \rho. \tag{42}$$

Proof (see [31], Theorem 1). This proof is done by applying Markov inequality.

Then, we have the following theorem that quantifies the confidence of reducing the improvement of potential function to no more than ϵ. □

Theorem 4. *If* $\mathscr{L} = \{\mathbf{X} \in \mathscr{C}: \mathbf{F}(\mathbf{X}) \prec \mathbf{F}(\mathbf{X}^0)\}$ *is bounded and each* f_m *is convex, let* $\mathscr{B} = \{\nabla h(\mathbf{X}): \mathbf{X} \in \mathscr{L}\}$*; then, we can choose*

$$N \ge \frac{\Gamma_{\mathscr{B}}^2 R^2(\mathbf{X}^0)}{\varepsilon}\left(1 + \log\left(\frac{1}{\rho}\right) - \frac{\Gamma_{\mathscr{B}}^2 R^2(\mathbf{X}^0)}{v^\dagger(\mathbf{X}^0)}\right) + 2, \tag{43}$$

where $\Gamma_{\mathscr{B}}$ *is the corresponding bounding coefficient with respect to* $\mathscr{B}$*; if each* f_m *is* σ*-strongly convex, then we may choose*

$$N \ge \frac{\Gamma_{\mathscr{B}}}{2\sigma}\log\left(\frac{v^\dagger(\mathbf{X}^0)}{\varepsilon\rho}\right). \tag{44}$$

Under either way, it has

$$\mathbb{P}\left(v^\dagger(\mathbf{X}^N) \le \varepsilon\right) \ge 1 - \rho. \tag{45}$$

Proof. This result follows directly from the observation that the gap sequence generated by RCD: $\{v^\dagger(\mathbf{X}^n)\}$, satisfies the properties mentioned in Lemma 5, according to (32) and (39). □

5. Numerical Simulation

In this section, we use simulation method to demonstrate our theoretical results. Consider the following example with 10 quadratic objective functions, each objective function taking the form of (46), for $m = 1, \ldots, 10$

$$f_m(\mathbf{x}_m) = \frac{1}{2}\pi_{m1}x_{m1}^2 + \frac{1}{2}\pi_{m2}x_{m2}^2 + \frac{1}{2}\pi_{m3}x_{m3}^2, \quad (46)$$

for $m = 1, \ldots, 10$. The coefficients $[\pi_{m1}, \pi_{m2}, \pi_{m3}]$ are randomly generated in each trial of test. The 10-th objective (agent) is selected as a central coordinator, i.e., at each iteration, one of the first 9 objectives is randomly picked with equal probability to communicate with the 10-th objective. For a given initial point $\mathbf{X}^0$, we run the algorithm 3 times and record their corresponding potential function value trajectories. The results are summarized in Figure 3.

As is clearly seen, although each of the three runs is convergent, their limiting levels of potential function value differ, indicating that they converge to different points on the Pareto front.

To further highlight this point, we run two extra sets of simulations. With the same setting as the preceding simulation (10 quadratic objectives, randomly generated π_m), again we fix an initial point at $\mathbf{X}^0$. For the first set of simulation, the communication network is designed to be complete, i.e., at each iterate, any pair $\{i, j\}$ can be chosen with equal probability. For the second test, the communication network is the same as the preceding simulation, i.e., the 10-th objective being a central coordinator and one of the rest of the objectives is randomly selected with equal probability to communicate with 10-th objective at each iterate. For each test, we run the RCD algorithm for 10 times, and the resulting value trajectories for the 10-th objective function are recorded in the following figures.

As is clearly indicated in Figure 4, the limiting levels of the 10 runs differ dramatically from each other. As for the central coordinator network (see Figure 5), the limiting level of the coordinator is relatively more stable at around 0.38. What is interesting is that when compared to the complete network with random pairing, the central coordinator somehow manages to achieve a significantly better level of objective value. Indeed, the lowest level of the 10-th objective in the complete network barely touches 0.47. This is probably because the central coordinator is involved in every single iterate; as a result, its corresponding objective is more heavily optimized.

6. Discussion and Concluding Remarks

We propose a randomized coordinate descent algorithm to solve the large-scale, linearly coupled resource allocation problem with selfish agents. This method has a low computational cost in each iteration and can guarantee convergence to the Pareto optimal solution under mild conditions, and then we derive the convergence rate of such an algorithm. As the sampling probability is fixed exogenously in the current framework, one potential extension is to identify these sampling probabilities with respect to the problem's parameter, which may further enhance the efficiency of the algorithm. Specifically, it is known in the literature that the selfish/greedy behavior of the individual agents generally leads to efficiency loss from a systemic perspective [27, 32], and hence the design of a sampling probability that will narrow this efficiency gap would be an interesting direction of future research.

Data Availability

No data were used to support this study. The MATLAB code used in this article is available from the corresponding author upon request.

Conflicts of Interest

The authors declare that they have no conflicts of interest.

Acknowledgments

This study was partially supported by the National Natural Science Foundation of China under grant nos. 71971132 and 61573244.

References

[1] Y. Cao, W. Ren, and G. Chen, "An overview of recent progress in the study of distributed multi-agent coordination," *IEEE Transactions on Industrial Informatics*, vol. 9, no. 9, pp. 427–438, 2013.

[2] D. K. Molzahn, F. Dorfler, H. Sandberg et al., "A survey of distributed optimization and control algorithms for electric power systems," *IEEE Transactions on Smart Grid*, vol. 8, no. 6, pp. 2941–2962, 2017.

[3] A. Nedich, "Convergence rate of distributed averaging dynamics and optimization in networks," *Foundations and Trends in Systems and Control*, vol. 2, no. 1, pp. 1–100, 2015.

[4] P. Yi, Y. Hong, and F. Liu, "Initialization-free distributed algorithms for optimal resource allocation with feasibility constraints and application to economic dispatch of power systems," *Automatica*, vol. 74, pp. 259–269, 2016.

[5] A. Nedić and J. Liu, "Distributed optimization for control," *Annual Review of Control, Robotics and Autonomous Systems*, vol. 1, pp. 77–103, 2018.

[6] P. Li, Y. Zhao, J. Hu, Y. Zhang, and B. K. Ghosh, "Distributed initialization-free algorithms for multi-agent optimization problems with coupled inequality constraints," *Neurocomputing*, vol. 407, pp. 155–162, 2020.

[7] P. Rodriguez and E. W. Biersack, "Dynamic parallel access to replicated content in the internet," *IEEE/ACM Transactions on Networking*, vol. 10, no. 4, pp. 455–465, 2002.

[8] V. K. Adhikari, Y. Guo, F. Hao et al., "Unreeling netflix: understanding and improving multi-cdn movie delivery," in *2012 Proceedings IEEE INFOCOM*, pp. 1620–1628, IEEE, Orlando, FL, USA, March 2012.

[9] W. Pu, Z. Zou, and C. W. Chen, "Dynamic adaptive streaming over http from multiple content distribution servers," in *Proceedings of IEEE Global Telecommunications Conference-GLOBECOM 2011*, December 2011.

[10] D. K. Goldenberg, L. Qiuy, H. Xie, Y. R. Yang, and Y. Zhang, "Optimizing cost and performance for multihoming," *ACM SIGCOMM - Computer Communication Review*, vol. 34, no. 4, pp. 79–92, 2004.

[11] M. Ismail and W. Weihua Zhuang, "Decentralized radio resource allocation for single-network and multi-homing services in cooperative heterogeneous wireless access

medium," *IEEE Transactions on Wireless Communications*, vol. 11, no. 11, pp. 4085–4095, 2012.

[12] I. Necoara, Y. Nesterov, and F. Glineur, "A random coordinate descent method on large optimization problems with linear constraints," Forestry Report, University Politehnica Bucharest, Bucharest, Romania, 2011.

[13] A. Mas-Colell, M. D. Whinston, J. R. Green et al., *Microeconomic Theory*, Oxford University Press, New York, NY, USA, 1995.

[14] K. Miettinen, *Nonlinear Multiobjective Optimization*, Springer, New York, NY, USA, 1998.

[15] J. Fliege and B. F. Svaiter, "Steepest descent methods for multicriteria optimization," *Mathematical Methods of Operations Research*, vol. 51, no. 3, pp. 479–494, 2000.

[16] E. H. Fukuda and L. M. Graña Drummond, "Inexact projected gradient method for vector optimization," *Computational Optimization and Applications*, vol. 54, no. 3, pp. 473–493, 2013.

[17] D. P. Bertsekas, *Convex Optimization Algorithms*, Athena Scientific, New York, NY, USA, 2015.

[18] Y. Nesterov, *Introductory Lectures on Convex Optimization: A basic Course*, Springer Science & Business Media, New York, NY, USA, 2013.

[19] L. M. G. Drummond, F. M. P. Raupp, and B. F. Svaiter, "A quadratically convergent Newton method for vector optimization," *Optimization*, vol. 63, no. 5, pp. 661–677, 2014.

[20] J. Fliege, A. I. F. Vaz, and L. N. Vicente, "Complexity of gradient descent for multiobjective optimization," *Optimization Methods and Software*, vol. 34, no. 5, pp. 949–959, 2019.

[21] G. N. Grapiglia, J. Yuan, and Y.-x. Yuan, "On the convergence and worst-case complexity of trust-region and regularization methods for unconstrained optimization," *Mathematical Programming*, vol. 152, no. 1-2, pp. 491–520, 2015.

[22] R. Frongillo and M. D. Reid, "Convergence analysis of prediction markets via randomized subspace descent," in *Advances in Neural Information Processing Systems*, C. Cortes, N. D. Lawrence, D. D. Lee, M. Sugiyama, and R. Garnett, Eds., Curran Associates, Inc, New York, NY, USA, 2015.

[23] G. M. Heal, "Planning without prices," *The Review of Economic Studies*, vol. 36, no. 3, pp. 347–362, 1969.

[24] V. Jalaparti and G. D. Nguyen, "Cloud resource allocation games," Technical report, 2010.

[25] J. F. Kurose and R. Simha, "A microeconomic approach to optimal resource allocation in distributed computer systems," *IEEE Transactions on Computers*, vol. 38, no. 5, pp. 705–717, 1989.

[26] E. A. Pazner and D. Schmeidler, "Egalitarian equivalent allocations: a new concept of economic equity," *Quarterly Journal of Economics*, vol. 92, no. 4, pp. 671–687, 1978.

[27] T. Roughgarden and É. Tardos, "How bad is selfish routing?" *Journal of the ACM*, vol. 49, no. 2, pp. 236–259, 2002.

[28] J. Dutta, P. Kesarwani, and S. Gupta, "Gap functions and error bounds for nonsmooth convex vector optimization problem," *Optimization*, vol. 66, no. 11, pp. 1807–1836, 2017.

[29] H. Tanabe, E. H. Fukuda, and N. Yamashita, "Convergence rates analysis of multiobjective proximal gradient methods," 2020a, https://arxiv.org/abs/2010.08217.

[30] H. Tanabe, E. H. Fukuda, and N. Yamashita, "New merit functions and error bounds for non-convex multiobjective optimization," 2020b, https://arxiv.org/abs/2010.09333.

[31] P. Richtárik and M. Takáč, "Iteration complexity of randomized block-coordinate descent methods for minimizing a composite function," *Mathematical Programming*, vol. 144, no. 1-2, pp. 1–38, 2014.

[32] D. Acemoglu and A. Ozdaglar, "Competition and efficiency in congested markets," *Mathematics of Operations Research*, vol. 32, no. 1, pp. 1–31, 2007.

Hindawi
Scientific Programming
Volume 2021, Article ID 4313749, 12 pages
https://doi.org/10.1155/2021/4313749

Research Article

AGV Scheduling Optimization for Medical Waste Sorting System

Xueting He,[1] **Hao Quan**,[2] **Wanlong Lin**,[3] **Weiliang Deng**,[1] **and Zheyi Tan**[1]

[1]*School of Management, Shanghai University, Shanghai, China*
[2]*Shibei Hospital, Jing'an District, Shanghai, China*
[3]*Shanghai No. 3 Rehabilitation Hospital, 100 Jiaocheng Road, Jing'an District, Shanghai 200072, China*

Correspondence should be addressed to Wanlong Lin; wanlong.lin@yahoo.com

Received 22 April 2021; Revised 10 May 2021; Accepted 22 May 2021; Published 15 June 2021

Academic Editor: Tingsong Wang

Copyright © 2021 Xueting He et al. This is an open access article distributed under the Creative Commons Attribution License, which permits unrestricted use, distribution, and reproduction in any medium, provided the original work is properly cited.

The dramatic increase in medical waste has put a severe strain on sorting operations. Traditional manual order picking is extremely susceptible to infection spread among workers and picking errors, while automated medical waste sorting systems can handle large volumes of medical waste efficiently and reliably. This paper investigates the optimization problem in the automated medical waste sorting system by considering the operational flow of medical waste. For this purpose, a mixed-integer programming model is developed to optimize the assignment among medical waste, presorting stations, and AGVs. An effective variable neighborhood search based on dynamic programming algorithm is proposed, and extensive numerical experiments are conducted. It is found that the proposed algorithm can efficiently solve the optimization problem, and the sensitivity analysis gives recommendations for the speed setting of the conveyor.

1. Introduction

Medical waste carries a large number of pathogenic microorganisms and harmful chemicals, making it an important risk factor for the spread of disease. Medical waste, if not properly recycled and disposed of, poses a great threat to the environment and human health. In recent years, the rapid development of China's healthcare industry has inevitably caused the problem of a sharp increase in medical waste. The recent outbreak of the novel coronavirus has stimulated the demand for medical services and protective equipment, causing the amount of medical waste to increase exponentially. The medical waste generated during an epidemic is highly infectious and prone to secondary contamination if not timely and correctly disposed of. Additionally, the current disposal rate of medical waste cannot meet the growth rate of medical waste. Therefore, how to collect and dispose of medical waste safely and efficiently is particularly important to protect human health, maintain ecological safety, and promote sustainable social development.

The disposal process of medical waste mainly includes classification and collection, transportation, and recycling. As the last segment of the medical waste disposal process, the recycling, which comprises sorting and reuse or incineration to landfill, occupies a significant role. The recycling of medical waste can reduce the infection rate as well as improving the utilization of resources. For example, recycling decreases the utilization of forests, mined metals, and oil, and it also reduces greenhouse gas emissions by decreasing the amount of waste disposed of in landfills [1]. For traditional reasons, quite a few medical waste disposal centers still use the manual sorting method. However, the dramatic increase in medical waste has put a severe strain on sorting operations, and traditional manual sorting is no longer capable of handling large volumes of medical waste efficiently and safely.

With the rapid development of automation technology and information technology, the application of automatic sorting systems is becoming more and more widespread. Besides, automated sorting systems are currently used in a variety of industries, such as the postal industry, warehouses, cross docks, and airports, due to their fast processing speed, ability to efficiently handle large volumes of goods, and reliable processes. Considering that medical waste is infectious, toxic, and hazardous, the application of automated

sorting systems can greatly reduce the infection rate of operators and improve the efficiency of medical waste disposal compared with traditional manual sorting.

Due to the large amount of medical waste that needs to be sorted, medical waste recycling and processing centers (MWRPC) face the requirements for small orders, high volume, and strict work schedules, which are similar to e-commerce warehouses. Nowadays, automated sorting systems, such as automated picking workstations, robots, and AGV-assisted order picking systems, are widely used in e-commerce warehouses to process a huge number of parcels quickly and accurately [2]. Among the various automated sorting systems, vertical sorting systems can be used in MWRPC to reduce staff infection rates and improve the efficiency of medical waste sorting due to the high level of automation and the efficient and reliable handling of packages. Therefore, based on the operational flow of medical waste in an automated sorting system, this paper develops a mixed-integer linear programming model with the objective of minimizing the time to finish processing a batch of medical waste by optimizing the allocation of resources such as presorting table, sorting AGV, and resorting area in the sorting system. To improve the computational efficiency, a variable neighborhood search (VNS) algorithm based on dynamic programming (DP) is designed for the problem. The validity of the model and algorithm is verified by numerical experiments, and a sensitivity analysis is performed to derive management insights.

The remainder of this paper is organized as follows. The related literature review is presented in Section 2. Section 3 gives a detailed description of the proposed problem; then, a mathematical model is formulated in Section 4. A variable neighborhood search algorithm based on dynamic programming is designed to solve this problem in Section 5. Extensive numerical experiments are conducted in Section 6, and conclusions are drawn in Section 7.

2. Literature Review

This study is related to the AGV scheduling optimization problem for a specific kind of object, medical waste. Here some closely related studies are discussed as follows.

A comprehensive summary of research on medical waste management in China was provided by He et al. [3], which found that the existing studies are mainly from a macro-perspective and defined that medical waste recycling consists of two main aspects: collection and disposal. Mantzaras and Voudrias [4] developed a model to optimize the design of a whole process system for infectious medical waste. Fraifeld et al. [5] discovered that failure to properly segregate medical waste could lead to the misuse, environmental pollution, and increased costs to institutions. Taslimi et al. [6] designed a weekly inventory routing schedule to transport medical wastes to disposal centers, and a heuristic algorithm was devised to solve this problem. Ghannadpour et al. [7] focused on the real-life medical waste collection vehicle routing problem of small medical centers in Iran and aimed to reduce public health risks by minimizing the waste collection time. During the disposal process of medical waste, Liu et al. [8, 9] designed a medical waste classified disposal system based on the RFID technology, and the application of this system model can strictly supervise the classification and disposal of medical waste, effectively reduce the spread of germs, and protect the environment.

The vertical sorting system mainly consists of cross-belt conveyor, AGVs, picking station, etc., and previous scholars have done various studies in all aspects. As for the conveyor-based system, Boysen et al. [10] provided a comprehensive review about various types of fully automated conveyor-based sorting system and divided decision problems into the following four areas: layout design, inbound problems, outbound problems, and short-term scheduling decisions. Fedtke and Boysen [11] stressed that the number of loading stations and its correlation with inbound and outbound destinations were shown to influence the throughput of a hub terminal. Briskorn et al. [12] investigated the short-term decision problem to minimize the makespan and derived some basic design rules. In warehouses, order consolidation processes are inevitable when zoning and batching process is performed. To enable fast assembly of picking orders to their packing stations, Boysen et al. [13, 14] optimized bins released from automated storage/retrieval system in their specific warehouse setting. Chen et al. [15] studied the integrated order batching, sequencing, and routing problem in warehouses. An algorithm integrating hybrid coded genetic algorithm and ant colony optimization was developed to solve the nonlinear mixed-integer model.

Besides, robots and AGVs are the critical resources in RMFS and AGV-based picking systems, so the research on robot routing, driving behavior, and operational strategies has received much attention. Vis [16] discussed literature related to design and control issues of AGV systems at manufacturing, distribution, transshipment, and transportation systems. Xie et al. [17] concentrated on decisions about the assignment of shelves to stations and orders to stations in robotic mobile fulfillment systems, and they presented a new MIP model to integrate both decision problems. Gharehgozli and Zaerpour [18] studied the operational problem of scheduling a mobile robot fulfilling a set of customer orders from a pick station. They formulated the basic problem as an asymmetric traveler problem and extended the model by adding priority constraints to provide different priorities for customer orders depending on their urgency.

Metaheuristics are crucial to accelerate convergence, and some local search heuristics are used to avoid trapping in local optimum, like Critical-Searching Neighborhood Search [19, 20] and Squeaky Wheel Optimization [21, 22]. Two variable neighborhood search algorithms are used to solve joint order batching and picker routing problem and clustered vehicle routing problem [23, 24]. Hintsch and Irnich [25] proposed that the standard approach for the shortest-path problem with resource constraints was based on dynamic programming labeling algorithms. Cimen and Soysal [26] used hybrid genetic algorithm with variable neighborhood search to solve vehicle routing problem.

The review of the literature reveals that many works have been done to reduce the infection rate and improve medical

waste disposal efficiency. While most studies on medical waste management have focused on the medical waste transportation aspect, studies on MWRPC are rare. Considering that medical waste and parcel have many similar characteristics, such as large quantity and strict timetable, it is highly feasible to apply the automatic sorting system to the MWRPC. The novelty of our work is fourfold. First, we study the sorting process in the medical waste recycling and processing center based on the automatic sorting system. Second, we investigate the operational problem of a vertical sorting system and transform the problem into a mixed-integer programming model. Third, we proposed VNS/DP algorithm for problem solving. Finally, some managerial insights are concluded according to numerical experiment.

3. Problem Description

The disposal process of medical waste mainly includes classification and collection, transportation, and recycling. Firstly, medical waste is generated and placed by medical personnel in designated recycling bags and recycling bins according to its category. Then, the medical waste temporarily stored in the hospital is transported to a medical waste disposal center. Finally, medical waste is sorted and disposed for reprocessing or incineration to landfill. Medical waste is usually divided into five categories: infectious waste, pathological waste, injury waste, pharmaceutical waste, and chemical waste. However, in the actual recycling activities, medical waste usually needs to be classified again according to its composition. For example, it can be divided into waste glass, waste metal, waste plastic, waste rubber, paper, pharmaceuticals, etc. [3]. Medical wastes are briefly classified and represented in Figure 1.

The vertical sorting system consists of an induction station, a cross-belt conveyor, several presorting stations, some trailers, and a fleet of AGVs. The induction station is used to capture information on the type of medical waste which would be used in sorting. The cross-belt conveyor is used to transfer different categories of medical waste to the corresponding presorting tables. A presorting station has a slide for receiving medical waste from the cross-belt conveyor and a mechanical arm for placing parcels onto AGV. The AGV fleet is assigned to transport medical waste to the trailers and complete the sorting. Trailers are used to collect different types of medical waste.

Therefore, the sorting process for medical waste is as follows. Firstly, medical waste enters the system through the induction station in turn, while the induction station identifies medical waste information. Secondly, medical waste proceeds along the conveyor and is led by the conveyor to chutes of presorting stations as soon as it reaches the designated presorting station. Thirdly, once the medical waste arrives at the presorting station, it is carried by the mechanical arm on the presorting station to an AGV that has already arrived at the presorting station in advance. Finally, the AGV loaded with medical waste travels to the location of the designation trailer and drops the package into the trailer. Then, the AGV moves to the next designated sorting station to transport the next medical waste.

Figure 2 illustrates the sorting process in vertical sorting system. From the above sorting procedures, we can summarize several decision problems that are crucial for the sorting process in vertical sorting system. First, different categories of medical waste need to be assigned to the suitable presorting stations to accomplish the initial sorting process of medical waste. Second, the transportation routes of AGVs require reasonable allocation and scheduling to complete the final sorting of medical waste. In addition, there is a tight limit on the processing time of medical waste, and large batches of medical waste need to be sorted urgently, so the completion time of the last medical waste is used as the optimization objective in this paper.

Before modeling the sorting problem, several assumptions need to be cleared.

(a) The destination information of the medical waste and the trailer designated for the medical waste are known in advance.

(b) There is no waiting time for the processing of medical waste. This means that when medical waste arrives at the presorting table, it needs to be immediately carried by the mechanical arm to the AGV that arrives at the presorting table in advance.

(c) A presorting table can process no more than one defined category of medical waste, and the medical waste belonging to the same category can only be processed by a certain presorting station.

4. Mathematical Model

In this section, a mixed-integer programming model for the sorting problem is presented. The objective of the model is to minimize the completion time of last medical waste.

4.1. Notations. The following notations are introduced to the model:

Indices and sets are given as follows:

P: set of medical waste
P_1: a subset of medical waste, $P_1 \subseteq P, 2 \leq |P_1| \leq |P|$
I: set of presorting stations
J: set of AGVs
T: set of medical waste categories

Parameters are given as follows:

$e, \hat{e}$: dummy points for the start point and end point of AGV routes
h: the handling time for the mechanical arm at the presorting station
$m_{p,p'}$: set to one when medical wastes p and p' belong to the same category and medical waste p' enters the induction station after medical waste p, and to zero otherwise
f_p: category of medical waste p
c_i^1: medical waste travel time of conveyor from induction station to presorting station

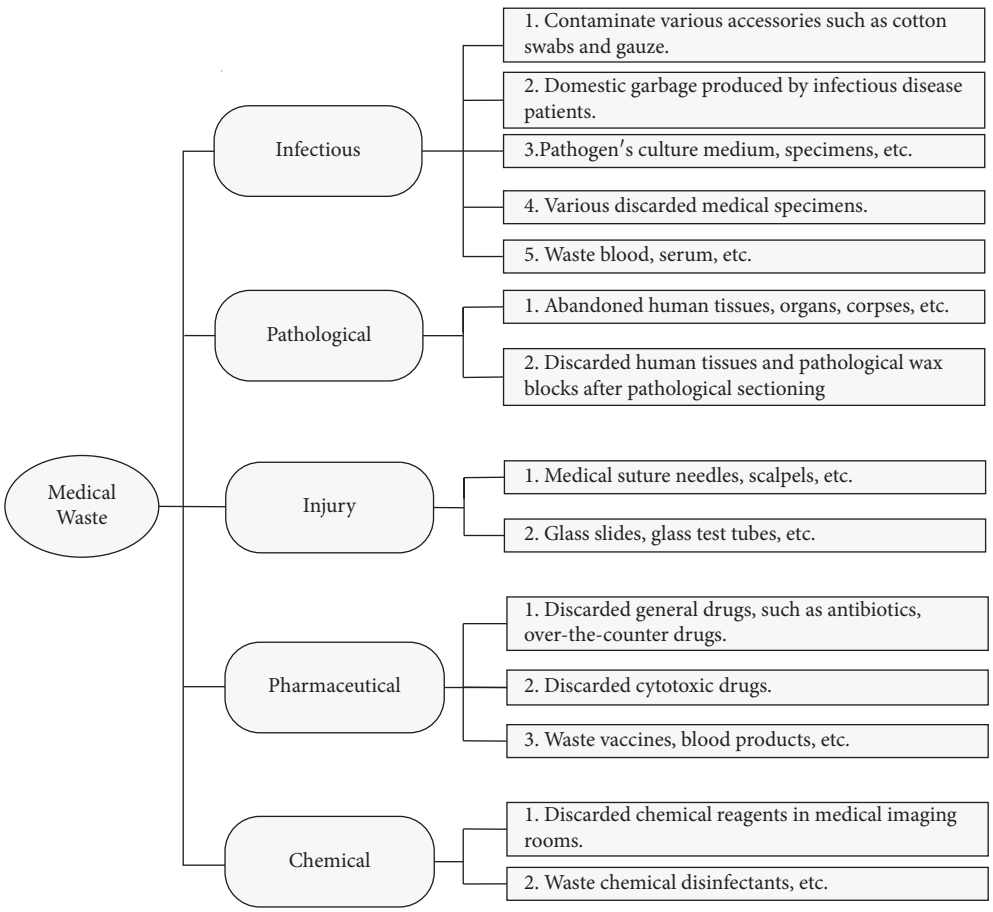

Figure 1: Classification of medical wastes.

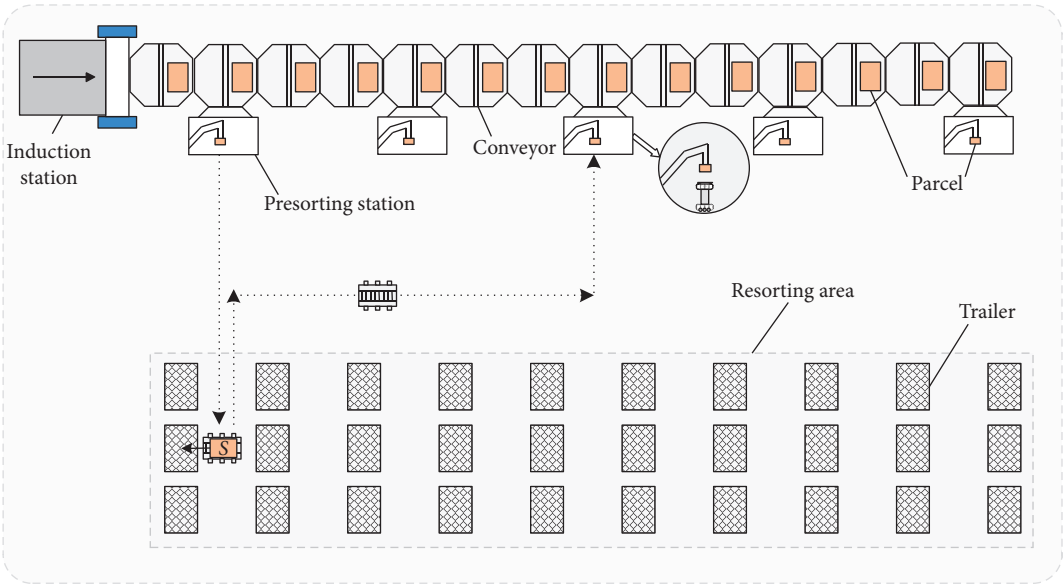

Figure 2: A top view of automated medical waste sorting system.

$c^2_{i,p}$: AGV travel time from presorting station i to trailer for medical waste p

g_p: the time of medical waste p released to the induction station

Decision variables are as follows:

$\mu_{i,t}$: set to one if medical wastes belonging to category t are allocated to presorting station i, and to zero otherwise

$\nu_{p,p',j}$: set to one if medical waste p' is transported by AGV j right after medical waste p, and to zero otherwise

$\rho_{p,j}$: set to one if medical waste p is transported by AGV j, and to zero otherwise

$\varphi_{p,j}$: the arrival time of AGV j to the presorting station which handles medical waste p

$\tau_{p,j}$: the start time of medical waste p being transported by AGV j

ζ_j: the time of AGV j finishing all its transporting tasks

4.2. Mathematical Model

$$\text{Minimize } \max_{j\in J}\{\zeta_j\}, \tag{1}$$

s.t.

$$\sum_{i\in I}\mu_{i,t} = 1, \quad \forall t \in T, \tag{2}$$

$$\sum_{t\in T}\mu_{i,t} \le 1, \quad \forall i \in I, \tag{3}$$

$$\sum_{j\in J}\rho_{p,j} = 1, \quad \forall p \in P, \tag{4}$$

$$\sum_{p\in P\cup\{e\}}\nu_{p,p',j} = \sum_{p\in P\cup\{\widehat{e}\}}\nu_{p',p,j} = \rho_{p',j}, \quad \forall p' \in P, j \in J, \tag{5}$$

$$\sum_{p\in P\cup\{\widehat{e}\}}\nu_{e,p,j} = \sum_{p\in P\cup\{e\}}\nu_{p,\widehat{e},j} = 1, \quad \forall j \in J, \tag{6}$$

$$\sum_{p\in P_1}\sum_{p'\in P_1}\nu_{p,p',j} \le |P_1| - 1, \quad P_1 \subseteq P, 2 \le |P_1| \le |P|, \forall j \in J, \tag{7}$$

$$\varphi_{p',j} \ge \tau_{p,j} + h + \sum_{i\in I}c^2_{i,p}\mu_{i,f_p} + \sum_{i\in I}c^2_{i,p}\mu_{i,f_{p'}} + M\left(1 - \nu_{p,p',j}\right), \quad \forall p \in P, p' \in P, j \in J, \tag{8}$$

$$\varphi_{p',j} \ge \tau_{p,j} + h + \sum_{i\in I}c^2_{i,p}\mu_{i,f_p} + \sum_{i\in I}c^2_{i,p}\mu_{i,f_{p'}} - M\left(1 - \nu_{p,p',j}\right), \quad \forall p \in P, p' \in P, j \in J, \tag{9}$$

$$\tau_{p',j'} \ge \tau_{p,j} + h - M\left(3 - m_{p,p'} - \rho_{p,j} - \rho_{p',j}\right), \quad \forall p, p' \in P, j, j' \in J, \tag{10}$$

$$\tau_{p,j} \ge g_p + \sum_{i\in I}c^1_i\mu_{i,f_p} + M\left(\rho_{p,j} - 1\right), \quad \forall p \in P, j \in J, \tag{11}$$

$$\tau_{p,j} \le g_p + \sum_{i\in I}c^1_i\mu_{i,f_p} - M\left(\rho_{p,j} - 1\right), \quad \forall p \in P, j \in J, \tag{12}$$

$$\varphi_{p,j} \le \tau_{p,j}, \quad \forall p \in P\cup\{e,\widehat{e}\}, j \in J, \tag{13}$$

$$\tau_{p,j} \le M\rho_{p,j}, \quad \forall p \in P, j \in J, \tag{14}$$

$$\zeta_j \ge \tau_{p,j} + h + \sum_{i\in I}c^2_{i,p}\mu_{i,f_p} + M\left(\rho_{p,j} - 1\right), \quad \forall p \in P, j \in J, \tag{15}$$

$$\mu_{i,t}, \nu_{p,p',j}, \rho_{p,j} \in \{0,1\}, \quad \forall p, p' \in P\cup\{e,\widehat{e}\}, j \in J, t \in T, \tag{16}$$

$$\varphi_{p,j}, \tau_{p,j} \ge 0, \quad \forall p, p' \in P\cup\{e,\widehat{e}\}, j \in J, \tag{17}$$

where objective (1) minimizes the latest completion time for a particular batch of medical waste sorting. Constrains (2) ensure that medical waste with the same category is allocated to only one presorting station. Constraint (3) guarantees that each presorting station handles at most one category of medical waste. Constraint (4) stipulates that each medical waste is transported by only one AGV. Constraints (5) and (6) ensure the continuity of the AGV transportation routes. Constraint (7) prevents the transportation routes of AGVs from forming loops. Constraints (8) and (9) indicate that if medical waste p' is transported by the AGV j right after medical waste p, the arrival time of the AGV to the presorting station serving medical waste p' cannot be earlier than the travel time at which AGV j transports medical waste p and then travels to the presorting station serving medical waste p'. Constraints (10) guarantee that if parcel p' is handled right after parcel p by the same presorting station, the start time of parcel p' being transported by AGV j needs to be later than the time at which parcel p is transported by AGV plus the handling time of mechanical arm. Constraints (11) and (12) enforce the rule that medical waste p is transported by the AGV as soon as it arrives at the presorting station. Constraint (13) ensures that the start time of AGV transporting medical waste is later than the time medical waste arrives the presorting station. Constraints (14) link two decision variables $\tau_{p,j}$ and $\rho_{p,j}$. Constraint (15) states the finishing time of processing the last medical waste.

Constraints (16) and (17) define the domains of decision variables.

5. Solution Methodology

For some small-scale problem instances, the proposed model in Section 4 can be solved directly by commercial solver, such as CPLEX. However, when facing large-scale problem instances, the model becomes too intractable for CPLEX to solve. This study designs a variable neighborhood algorithm (VNS) based on dynamic programming (DP) for solving this model. Section 5.1 addresses the VNS framework. Then, Section 5.2 elaborates on the DP algorithm.

5.1. Variable Neighborhood Search. From constraints (11) and (12) of the proposed model, the medical waste p is transported by the AGV as soon as it arrives at the presorting station. Besides, from constraint (15), it can be seen that the completion time of the sorting task for all medical wastes mainly depends on the allocation of presorting stations and the arrival time of medical waste to the assigned presorting station. Clearly, the allocation of presorting stations relies on the decision variable $\mu_{i,t}$. We denote the arrival time of medical waste p to the presorting station by U_p; then, $U_p = g_p + c_i^1$. Furthermore, the assigned presorting station i relies on the decision variable $\mu_{i,t}$, where $t = f_p$. Therefore, we find that once the decision variable $\mu_{i,t}$ is determined, the objective function is determined.

However, the routes of the AGVs interact with the allocation of presorting stations, making this problem difficult to solve. In order to determine the better $\mu_{i,t}$, an effective VNS algorithm based on DP is designed in this paper. The VNS algorithm is mainly used to generate distribution schemes of presorting stations. Besides, DP algorithm is mainly used to generate the feasible routes of AGVs under a certain presorting station allocation plan generated by VNS algorithm.

In addition, on the basis of the VNS framework, the critical issues to solve the proposed model include the following.

5.1.1. Initial Solution Generation. According to Zhen [27, 28], it can be seen that prioritizing the destinations with a larger number of parcels to the presorting station close to the induction station can effectively improve the sorting efficiency. Therefore, this article first generates the initial solution according to this rule. If the solution is not feasible, a heuristic algorithm is used to find a feasible solution. An example result is shown in Figure 3. Medical wastes belonging to categories 1, 2, 3, 4, and 5 are allocated to presorting stations 2, 1, 5, 3, and 4, which means $\mu_{1,2}, \mu_{2,1}, \mu_{3,5}, \mu_{4,3}, \mu_{5,4} = 1$.

5.1.2. The Design of Neighborhood Structures. Considering the characteristics of $\mu_{i,t}$, the following two neighborhood structures are designed in this paper.

(1) Neighborhood structure 1: interval reversal: the process of interval reversal is shown in Figure 4. First, a subinterval of the medical waste categories sequence is randomly selected, and then we invert the corresponding relationship between the medical waste category and the presorting station in the interval.

(2) Neighborhood structure 2: exchange: we will randomly select two medical waste categories and exchange their corresponding presorting stations, as shown in Figure 5.

e	1	2	3	4	5
i	2	1	5	3	4

Figure 3: Initial solution generation.

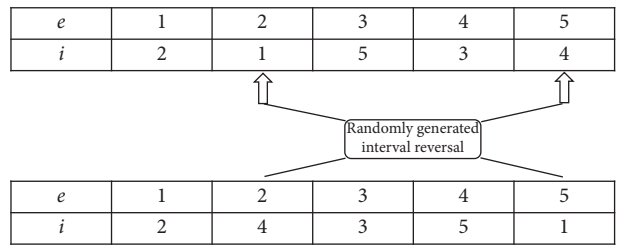

Figure 4: Neighborhood structure: interval reversal.

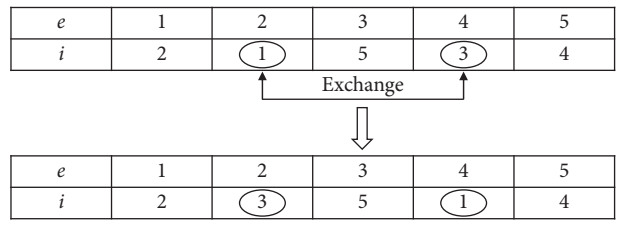

Figure 5: Neighborhood structure: exchange.

5.1.3. The Framework of Variable Neighborhood Descent. Variable neighborhood descent is the framework of the neighborhood search, which is used to search different neighborhood structures. The algorithm will completely explore one neighborhood structure and then move to the next neighborhood when no solution better than the optimal solution can be found (Algorithm 1).

5.1.4. Shaking Procedure. To avoid falling into local optimization, we design a shaking procedure. The medical waste categories sequence is randomly divided into two parts, and the corresponding presorting station is shuffled by part, as shown in Figure 6.

In summary, based on the description about initial solution, neighborhood structure, and shaking procedure, the table provides the pseudocode of VNS (Algorithm 2).

5.2. Dynamic Algorithm. The dynamic programming method is a mathematical method for solving the optimization of decision-making processes. Besides, DP algorithm is mainly used to generate the feasible routes of AGVs (Algorithm 3).

```
Input: s, s', l←1//s' is the optimal solution and s is the current solution, and l is used to record the neighborhood structure
s ⟵ s'
While(true)
  Switch(l)
    case 1:
      FindBestNeighborhood_one(s)
      If (f(s') < f(s))then//f(s) is the fitness of solution s, calculated by DP.
      s ⟵ s';
      l = 0;
    End if
    Break;
      case 2:
    FindBestNeighborhood_two(s)
    If (f(s') < f(s))then
    s ⟵ s';
    l = 0;
    End if
    break;
  default;
return;
l++;
End while
```

Algorithm 1: Variable neighborhood descent (VND).

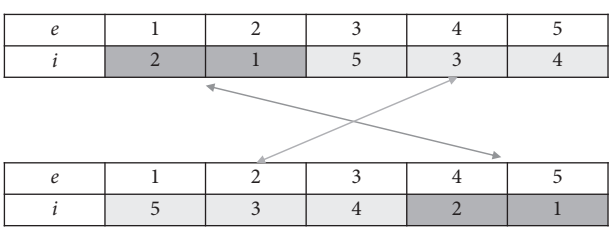

Figure 6: Shaking procedure.

The core idea is to divide a complex system problem into several stages and transform the multistage process into a series of single-stage problems. These single-stage problems are solved one by one by selecting appropriate decision variables and constructing indicator functions and optimal value functions. When using the idea of dynamic programming to solve the actual problem, it is necessary to abstract the corresponding terms of dynamic programming according to the actual situation of the problem, so as to facilitate the analysis and calculation.

5.2.1. Stage. In this problem, the route of the AGV transporting medical waste is divided into different stages, denoted by k. The kth stage represents the kth medical waste transported by the AGV.

5.2.2. State. The state represents the condition at the beginning of each phase. The state variables s_k is used to describe the state at stage k, which means that the kth medical waste transported by AGV is s_k.

5.2.3. Decision. When the state of a stage is determined, the decision to make a choice to move to the next stage is called a decision. Commonly $u_k(s_k)$ indicates the decision set in state s_k at stage k. $u_k(s_k)$ denotes the set of medical waste that can be transported by the vehicle at stage $k+1$.

5.2.4. State Transition Equation. If the state and decision of a stage are given, the state of the next stage can be determined, and the state transition equation can be set as

$$s_{k+1} = u_k(s_k) = u_k(\min T_k). \tag{18}$$

5.2.5. Indicator Function. The indicator function is used to measure each state's degree of excellence in order to achieve better decision-making. In the proposed problem, $t(k-1,k)$ represents the sum of the time it takes the AGV to transport the medical waste $k-1$ to a designated trailer and the time it takes to travel to the medical waste k from the trailer. In this paper, the indicator function is set to

$$f(k) = \begin{cases} 0, & k = 0, \\ \min\{f(k-1) + h + t(k-1,k)\}, & k > 0. \end{cases} \tag{19}$$

6. Numerical Experiment

To validate the effectiveness of the proposed model and efficiency of the proposed algorithm, we conduct extensive numerical experiments on different instances. All experiments are performed on a workstation equipped with Intel i5-10210U CPU @1.60 GHz and 16 GB RAM. The proposed model and algorithm are implemented in C# (VS2019) concert technology with the solver IBM ILOG CPLEX 12.6.1.

```
Input: G, g, s, s', g = 0, G = 10 //g represents the current iteration number, G represents the maximum iteration number, s' is the
optimal solution, and s is current solution
s^0 //generate the initial solution;
s' ⟵ s^0;
While (iteration < G)
    s ⟵ s';
    Shaking(s);
    Variable neighborhood descent(s);
If (f(s) < f(s'))Then
    s' ⟵ s;
    g = 0;
End if
    g++;
End while
Output: best found solution.
```

Algorithm 2: Variable neighborhood search (VNS).

```
Input: P, J//P: set of medical waste. J: set of AGVS.
Interpretations: L_p: set to 1 if medical waste p has been transported, and to zero otherwise. j.route.count indicates the number of
medical wastes transported by AGV j. j · f(k) denotes the time for AGV j to transport the kth medical waste
    For j ∈ J
        Select a medical waste p with an L_p = 0;
        j.route.Add(p);//add medical waste p to the route of AGV j
        j · f(0) = U_p;
        L_p = 1;
End For
For j ∈ J
    For p ∈ P
        k = j.route.count;
        j · f(k) = j · f(k − 1) + h + t(k − 1, k);
If (L_p = 0&&j · f(k) < U_p)
        j.route.Add(p);
            L_p = 1;
        End for
    End for
For p ∈ P
    If (L_p = 1)
        Return obj = MaxValue;
End for
Output: obj = max_{j∈J}{j.f(j.route.count − 1)}
```

Algorithm 3: Dynamic programming (DP).

6.1. Generation of Test Instances. Numerical examples of small, medium and large scale are designed to validate the performance of proposed algorithms, and each scale contains several groups of examples which can avoid accidental results.

Since medical waste is mainly classified into five categories in Chinese hospitals, the number of medical waste categories and the number of presorting stations are both set to 5; i.e., $|E| = |I| = 5$. The category of medical waste f_p is generated randomly. The release time of medical waste is related to the operation of induction station, and we use the formula $g_p = p$ to generate the release time. The handling time h for the mechanical arm is set to 1 second. According to the layout of the MWRPC, we can use the Manhattan distance to calculate the distance between the trailer and the presorting station, and the distance between induction station and the presorting station. Then we use the speed of conveyor and AGV to calculate the values of c_i^1 and $c_{i,p}^2$, respectively.

6.2. Algorithm Performance. Extensive experiments are conducted to test the performance of the proposed VNS algorithm based on DP. The results are shown in Tables 1 and 2, with the objective function obtained by different methods, the calculation time, and the gap listed. The maximum calculation time is set to 7200 seconds. In our experiment, a heuristic algorithm is proposed for comparison. Besides, in order to artificially improve the solution

Table 1: Algorithm performance for small-scale instances.

Instances		CPLEX		VNS		Comparison	Heuristic			Comparison	
Scale	ID	Z_C	T_C	Z_V	T_V	GAP_V (%)	$\lvert J_H \rvert$	Z_H	T_H	$JGAP_H$ (%)	$ZGAP_H$ (%)
	1	40.0	21.45	40.0	0.003	0.00	10	37.0	0.009	25.00	−7.50
	2	39.0	6.61	39.0	0.003	0.00	10	47.0	0.015	25.00	20.51
$\lvert J \rvert = 8 \lvert P \rvert = 10$	3	41.0	7.43	41.0	0.003	0.00	10	42.0	0.005	25.00	2.44
	4	41.0	10.89	41.0	0.002	0.00	10	41.0	0.013	25.00	0.00
	5	40.0	10.92	40.0	0.003	0.00	10	40.0	0.023	25.00	0.00
Avg.		40.2	11.46	40.2	0.003	0.00	10	41.4	0.013	25.00	3.09
	1	46.0	31.62	46.0	0.002	0.00	15	52.0	0.011	25.00	13.04
	2	47.0	39.98	47.0	0.004	0.00	15	47.0	0.006	25.00	0.00
$\lvert J \rvert = 12 \lvert P \rvert = 15$	3	41.0	39.64	41.0	0.002	0.00	13	41.0	0.010	8.33	0.00
	4	44.0	31.43	44.0	0.002	0.00	12	44.0	0.013	0.00	0.00
	5	42.0	31.43	42.0	0.005	0.00	13	40.0	0.007	8.33	−4.76
Avg.		44.0	34.82	44.0	0.003	0.00	13.6	44.8	0.009	13.33	1.66
	1	47.0	132.32	47.0	0.003	0.00	16	47.0	0.026	14.29	0.00
	2	46.0	41.26	46.0	0.006	0.00	15	46.0	0.007	7.14	0.00
$\lvert J \rvert = 14 \lvert P \rvert = 20$	3	51.0	416.43	51.0	0.005	0.00	20	51.0	0.012	42.86	0.00
	4	50.0	799.37	50.0	0.004	0.00	16	48.0	0.003	14.29	−4.00
	5	52.0	99.75	52.0	0.006	0.00	15	52.0	0.008	7.14	0.00
Avg.		49.2	297.826	49.2	0.005	0.00	16.4	48.8	0.011	17.14	−0.80
	1	61.0	>7200	61.0	0.003	0.00	18	59.0	0.006	12.50	−3.28
	2	57.0	>7200	57.0	0.003	0.00	30	58.0	0.007	87.50	1.75
$\lvert J \rvert = 16 \lvert P \rvert = 30$	3	54.0	>7200	54.0	0.006	0.00	16	54.0	0.010	0.00	0.00
	4	58.0	>7200	58.0	0.006	0.00	26	62.0	0.010	62.50	6.90
	5	62.0	>7200	62.0	0.006	0.00	21	62.0	0.007	31.25	0.00
Avg.		58.4	>7200	58.4	0.005	0.00	22.2	59.0	0.008	38.75	1.07

Notes. (1) Z_C denotes the optimal solution obtained by CPLEX. For the instance scale $|J| = 16, |P| = 30$, Z_C denotes the feasible solution obtained by CPLEX in 7200 seconds. Z_V, Z_H denote the feasible solution obtained by VNS algorithm and heuristic algorithm, respectively. (2) J_H represents the number of AGVs required when the heuristic algorithm obtains a feasible solution. T_C, T_V, T_H are the computation time of CPLEX, VNS algorithm, and heuristic algorithm in seconds, respectively. (3) $GAP_V = (Z_{VNS} - Z_{CPLEX})/Z_{CPLEX}$, $JGAP_H = (|J_H| - |J|)/|J|$, $ZGAP_H = (Z_H - Z_V)/Z_V$.

Table 2: Algorithm performance for large-scale instances.

Instances		VNS		Heuristic			Comparison	
Scale	ID	Z_V	T_V	$\lvert J_H \rvert$	Z_H	T_H	$JGAP_H$ (%)	$ZGAP_H$ (%)
	1	74.0	0.006	21	74.0	0.008	5.00	0.00
	2	86.0	0.008	36	86.0	0.007	80.00	0.00
$\lvert J \rvert = 20 \lvert P \rvert = 50$	3	81.0	0.005	37	81.0	0.003	85.00	0.00
	4	78.0	0.006	36	78.0	0.003	80.00	0.00
	5	73.0	0.008	21	73.0	0.006	5.00	0.00
Avg.		78.4	0.007	30	78.4	0.005	51.00	0.00
	1	125.0	0.014	24	125.0	0.005	20.00	0.00
	2	127.0	0.015	23	126.0	0.003	15.00	−0.79
$\lvert J \rvert = 20 \lvert P \rvert = 100$	3	126.0	0.010	24	126.0	0.007	20.00	0.00
	4	132.0	0.012	27	131.0	0.007	35.00	−0.76
	5	130.0	0.024	27	128.0	0.004	35.00	−1.54
Avg.		128.0	0.015	25	127.2	0.005	25.00	−0.62
	1	228.0	0.026	26	228.0	0.003	23.81	0.00
	2	224.0	0.025	27	224.0	0.003	28.57	0.00
$\lvert J \rvert = 21 \lvert P \rvert = 200$	3	232.0	0.026	29	232.0	0.008	38.10	0.00
	4	227.0	0.026	26	227.0	0.011	23.81	0.00
	5	226.0	0.030	27	226.0	0.003	28.57	0.00
Avg.		227.4	0.027	27	227.4	0.006	28.57	0.00
	1	527.0	0.098	29	527.0	0.011	31.82	0.00
	2	529.0	0.096	29	529.0	0.003	31.82	0.00
$\lvert J \rvert = 22 \lvert P \rvert = 500$	3	525.0	0.094	29	525.0	0.004	31.82	0.00
	4	531.0	0.092	31	531.0	0.003	40.91	0.00
	5	530.0	0.097	32	529.0	0.003	45.45	−0.19
Avg.		528.4	0.095	30	528.2	0.005	36.36	−0.04

```
Input: P, I // P: set of medical waste. I: set of presorting stations;
L_p: set to 1 if medical waste p has been transported, and to zero otherwise.
U_p: time to enter the presorting table for medical waste p. i.agv.count: indicates the number of AGVs serving presorting station i,
set the initial value to 1.
j · t(p): denotes the finish time of AGV j transporting medical waste p, set j = 0 initially.
(1)  For i ∈ I
(2)    For j ∈ i.agv.count
(3)      Select a medical waste with minimize U_p in p ∈ {P | L_p = 0};
(4)    If (L_p = 0 && j · t(p) < U_p)
(5)      Update j · t(p);
(6)      L_p = 1;
(7)    End if
(8)    If (L_p = 0)
(9)    j = i.agv.count; Update j · t(p);
(10)   i.agv.count + +;
(11)   End If
(12) End For
(13) End For
Output: Σ_{i∈I} i.agv.count and max_{j∈J}{j · t(p)}
```

Algorithm 4: Heuristic algorithm.

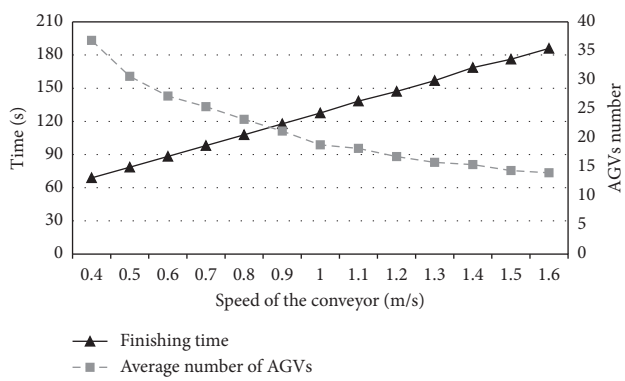

Figure 7: Sensitivity analysis about AGVs number and finishing time.

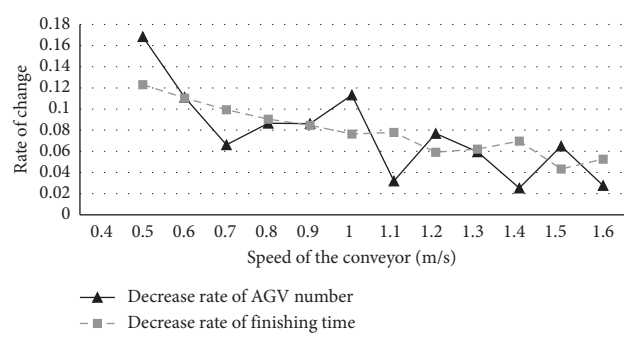

Figure 8: Sensitivity analysis about speed of the conveyors and number of AGVs.

quality of the heuristic algorithm, this paper will use the heuristic algorithm to solve the same instance five times and record the optimal solution in Tables 1 and 2. The procedure of the heuristic is listed as follows:

Step 1: the corresponding relationship between medical waste categories and presorting stations is given randomly; i.e., the decision variable $\mu_{i,t}$ is assumed to be known.

Step 2: each AGV is dedicated to a specific category of medical waste. Due to the limitation of a category of medical waste to be processed by only one presorting station, an AGV can only service a designated presorting station.

Step 3: the greedy algorithm is designed to generate the route of AGVs transporting medical waste. The

pseudocode of greedy algorithm is shown in Algorithm 4.

For experiments of small-scale and medium-scale instances, we compare the result obtained by VNS algorithm and the heuristic. From Table 1, we can see that VNS algorithm can obtain near-optimal results. The average gap between the objective values of the VNS algorithm and CPLEX is close to 0. What is more, CPLEX can only solve some small-scale problems within reasonable time period. When the number of medical wastes grows to 16 and the number of AGVs grows to 14, CPLEX is incapable of calculating the result under 7200 seconds. The computation time of VNS algorithm is much shorter than CPLEX when the scale of instances increases, where the average computing time for VNS is 0.009 seconds. It can be seen that the gap between the feasible solution obtained by heuristic algorithm and the optimal solution is about 1.26% on average. However, the number of AGVs required by the heuristic algorithm is 23.56% more than that of CPLEX on average.

For experiments of large-scale instances, we compare the result obtained by VNS algorithm and the heuristic in Table 2. It is obvious that the average computing time of the heuristic algorithm and the VNS algorithm is steadily less than 1 second. The objective function gap between heuristic algorithm and VNS algorithm is −0.16% on average; i.e., $ZGAP_H = -0.16\%$. However, the objective function of the heuristic is 1% lower than the objective function of the VNS algorithm; i.e., $ZGAP_H = -0.16\%$. However, the number of AGVs required by the heuristic is greater than that of the VNS algorithm by 23%; i.e., $JGAP_H = 35.23\%$. That is to say, VNS algorithm results in much greater performance in solving large-scale problem than heuristic.

6.3. Sensitivity Analysis. The speed of the conveyor has a significant impact on the finishing time of medical waste sorting. Therefore, we calculate the minimum number of AGVs required to complete the sorting of 100 medical wastes in a timely manner at different conveyor speeds. In addition, the finishing time for medical waste sorting at different conveyor speeds is also calculated. Different sets of instances under the same scale are calculated, and the average value is taken to avoid unexpected results.

From Figure 7, we can see that there is an approximate positive correlation between conveying speed and finishing time, and an approximate negative correlation between conveyor speed and number of AGVs. Figure 7 illustrates the change rate of AGVs number and finishing time as the conveyor speed increases.

However, in the process of increasing the conveyor speed, the change rate of AGVs number is different. It can be seen that a conveyor speed of 1 m/s is a critical point. It is noticeable that the decrease rate in the number of AGVs when the conveyor speed increases from 0.4 m/s to 0.9 m/s is generally higher than the decrease rate when the conveyor speed increases from 1.1 m/s to 1.4 m/s. Similarly, there are differences in the change rate of the completion time. When the conveyor speed increases from 0.4 m/s to 0.9 m/s, the change rate is steadily decreasing while the change rate fluctuates and decreases when the conveyor speed increases from 1.1 m/s to 1.4 m/s.

In this proposed problem, the completion time of medical waste sorting is regarded as the only objective function. However, in reality, managers often need to trade off the fixed cost of AGVs and the completion time of medical waste sorting. Therefore, Figure 8 gives some recommendations to managers on how to set the conveyor speed when the number of AGVs is limited.

7. Conclusion

Existing MWRPC have difficulty in processing large volumes of medical waste efficiently. Considering the similarity between medical waste and parcels, we propose that the vertical sorting system can be applied in medical waste processing and sorting center. A mixed-integer linear programming model is established which aims to optimize the assignments of presorting stations and AGVs to improve the efficiency of medical waste sorting. Besides, we designed a VNS algorithm based on DP for problem solving. Compared with related works, the main contributions of this work are summarized as follows:

(1) This paper expands the medical waste sorting way in the medical waste processing and sorting center. The application of the automated sorting system can greatly reduce manual operations, thereby reducing the infection rate of medical waste. In addition, a reasonable and effective classification of medical waste can improve the recycling rate of resources.

(2) VNS algorithm is applied in problem solving, which is competent in solving both small- and large-scale problems. VNS algorithm improves computational efficiency, so the research finding provides a decision support tool for medical waste processing and sorting center.

(3) Different conveyor speeds will result in different operating efficiencies. The faster the conveyor speed, the greater the AGVs number required, and the shorter the finishing time of the medical waste sorting. Managers can adjust the conveyor speed to complete the medical waste sorting according to the number of AGVs and the urgency of medical waste disposal.

This research also has its limitations. In our research, we only consider a relatively simple medical waste classification method, but there may be a variety of different classification requirements in reality, such as classification according to different treatment methods and classification according to the material. In addition, the objective of the model (i.e., to minimize the finishing time of the last medical waste) only considers the processing time but does not take account of the fixed cost of AGV. The start-up cost and maintenance cost of AGV and the finishing time of medical waste need to be considered simultaneously to achieve a balance of cost

and utility. All of these issues can be our research directions in the future.

Data Availability

No data were used to support this study.

Disclosure

Xueting He and Hao Quan are co-first authors of the article.

Conflicts of Interest

The authors declare that they have no conflicts of interest.

References

[1] L. M. Riedel, "Environmental and financial impact of a hospital recycling program," *American Association of Nurse Anesthetists Journal*, vol. 79, no. 4, pp. S8–S14, 2011.

[2] N. Boysen, R. de Koster, and F. Weidinger, "Warehousing in the e-commerce era: a survey," *European Journal of Operational Research*, vol. 277, no. 2, pp. 396–411, 2019.

[3] Z.-G. He, Q. Li, and J. Fang, "The solutions and recommendations for logistics problems in the collection of medical waste in China," *Procedia Environmental Sciences*, vol. 31, pp. 447–456, 2016.

[4] G. Mantzaras and E. A. Voudrias, "An optimization model for collection, haul, transfer, treatment and disposal of infectious medical waste: application to a Greek region," *Waste Management*, vol. 69, pp. 518–534, 2017.

[5] A. Fraifeld, A. N. Rice, M. J. Stamper, and V. C. Muckler, "Intraoperative waste segregation initiative among anesthesia personnel to contain disposal costs," *Waste Management*, vol. 122, pp. 124–131, 2021.

[6] M. Taslimi, R. Batta, and C. Kwon, "Medical waste collection considering transportation and storage risk," *Computers & Operations Research*, vol. 120, 2020.

[7] S. F. Ghannadpour, F. Zandieh, and F. Esmaeili, "Optimizing triple bottom-line objectives for sustainable health-care waste collection and routing by a self-adaptive evolutionary algorithm: a case study from tehran province in Iran," *Journal of Cleaner Production*, vol. 287, 2021.

[8] H. Liu and Z. Yao, "Study of an rfid-based medical waste classified disposal model," *Fresenius Environmental Bulletin*, vol. 28, no. 3, pp. 1752–1763, 2019.

[9] H. Liu, Z. Yao, and Q. Zhang, "A temporary storage systematic model for medical waste based on rfid technology," *Fresenius Environmental Bulletin*, vol. 27, no. 9, pp. 6152–6161, 2018.

[10] N. Boysen, D. Briskorn, S. Fedtke, and M. Schmickerath, "Automated sortation conveyors: a survey from an operational research perspective," *European Journal of Operational Research*, vol. 276, no. 3, pp. 796–815, 2019.

[11] S. Fedtke and N. Boysen, "Layout planning of sortation conveyors in parcel distribution centers," *Transportation Science*, vol. 51, no. 1, pp. 3–18, 2017.

[12] D. Briskorn, S. Emde, and N. Boysen, "Scheduling shipments in closed-loop sortation conveyors," *Journal of Scheduling*, vol. 20, no. 1, pp. 25–42, 2017.

[13] N. Boysen, D. Briskorn, and S. Emde, "Parts-to-picker based order processing in a rack-moving mobile robots environment," *European Journal of Operational Research*, vol. 262, no. 2, pp. 550–562, 2017.

[14] N. Boysen, S. Fedtke, and F. Weidinger, "Optimizing automated sorting in warehouses: the minimum order spread sequencing problem," *European Journal of Operational Research*, vol. 270, no. 1, pp. 386–400, 2018.

[15] T.-L. Chen, C.-Y. Cheng, Y.-Y. Chen, and L.-K. Chan, "An efficient hybrid algorithm for integrated order batching, sequencing and routing problem," *International Journal of Production Economics*, vol. 159, pp. 158–167, 2015.

[16] I. F. A. Vis, "Survey of research in the design and control of automated guided vehicle systems," *European Journal of Operational Research*, vol. 170, no. 3, pp. 677–709, 2006.

[17] L. Xie, N. Thieme, R. Krenzler, and H. Li, "Introducing split orders and optimizing operational policies in robotic mobile fulfillment systems," *European Journal of Operational Research*, vol. 288, no. 1, pp. 80–97, 2021.

[18] A. Gharehgozli and N. Zaerpour, "Robot scheduling for pod retrieval in a robotic mobile fulfillment system," *Transportation Research Part E-Logistics and Transportation Review*, vol. 142, 2020.

[19] L. Zhen, "Tactical berth allocation under uncertainty," *European Journal of Operational Research*, vol. 247, no. 3, pp. 928–944, 2015.

[20] L. Zhen, E. P. Chew, and L. H. Lee, "An integrated model for berth template and yard template planning in transshipment hubs," *Transportation Science*, vol. 45, no. 4, pp. 483–504, 2011.

[21] L. Zhen, "Modeling of yard congestion and optimization of yard template in container ports," *Transportation Research Part B: Methodological*, vol. 90, pp. 83–104, 2016.

[22] L. Zhen, Z. Xu, K. Wang, and Y. Ding, "Multi-period yard template planning in container terminals," *Transportation Research Part B: Methodological*, vol. 93, pp. 700–719, 2016.

[23] B. Aerts, T. Cornelissens, and K. Sorensen, "The joint order batching and picker routing problem: modelled and solved as a clustered vehicle routing problem," *Computers & Operations Research*, vol. 129, p. 19, 2021.

[24] C. Defryn and K. Sörensen, "A fast two-level variable neighborhood search for the clustered vehicle routing problem," *Computers & Operations Research*, vol. 83, pp. 78–94, 2017.

[25] T. Hintsch and S. Irnich, "Exact solution of the soft-clustered vehicle-routing problem," *European Journal of Operational Research*, vol. 280, no. 1, pp. 164–178, 2020.

[26] M. Çimen and M. Soysal, "Time-dependent green vehicle routing problem with stochastic vehicle speeds: an approximate dynamic programming algorithm," *Transportation Research Part D: Transport and Environment*, vol. 54, pp. 82–98, 2017.

[27] L. Zhen, Z. Y. Tan, L. Y. Xiao, and C. L. Ma, "Research on parcel sorting optimization model and algorithm for double-layer automatic sorting systems," *Chinese Journal of Management Science*, vol. 25, pp. 1–12, 2018.

[28] L. Zhen, Z. Liang, D. Zhuge, L. H. Lee, and E. P. Chew, "Daily berth planning in a tidal port with channel flow control," *Transportation Research Part B: Methodological*, vol. 106, pp. 193–217, 2017.

Hindawi
Scientific Programming
Volume 2021, Article ID 3058472, 17 pages
https://doi.org/10.1155/2021/3058472

Research Article

Solving a Real-World Urban Postal Service System Redesign Problem

Hao Yu,[1] **Xu Sun**,[1] **Wei Deng Solvang**,[1] **and Gilbert Laporte**[2,3]

[1]*Department of Industrial Engineering, UiT The Arctic University of Norway, Lodve Langsgate 2, Narvik 8514, Norway*
[2]*Department of Decision Sciences, HEC Montréal, 3000 Chemin de la Côte-Sainte-Catherine, Montréal H3T 2A7, Canada*
[3]*School of Management, University of Bath, Bath, UK*

Correspondence should be addressed to Hao Yu; hao.yu@uit.no

Received 22 April 2021; Revised 16 May 2021; Accepted 20 May 2021; Published 28 May 2021

Academic Editor: Tingsong Wang

Copyright © 2021 Hao Yu et al. This is an open access article distributed under the Creative Commons Attribution License, which permits unrestricted use, distribution, and reproduction in any medium, provided the original work is properly cited.

Due to recent technological advancements, more diversified customer demand, and increasingly harder competition, traditional postal service systems have experienced significant changes all over the world. In Norway, through a strategic reform called post-in-shop, undertaken in 2013, most postal services are now provided at postal service counters located in retailer stores in order to improve accessibility, operational efficiency, and cost-effectiveness. This has led to a complex decision-making problem for the redesign of urban postal service networks across the country. In this paper, a two-stage method is proposed to solve a real-world urban postal service network redesign problem. First, two location models are employed to determine the optimal locations of postal service counters. In the second stage, a simulation model is built to evaluate the urban postal service system with different location and demand allocation plans under a realistic and stochastic environment. Among other insights, our results show that the proposed two-stage method can be used to effectively improve the accessibility of postal service networks by making optimal location-allocation decisions.

1. Introduction

In recent years, with the rapid development and increasing use of computer technologies, the traditional postal service system has experienced significant changes in order to better satisfy customer demand and to survive in a more competitive market [1, 2]. The wide adoption of digitalization and information and communication technology (ICT) across businesses, public sectors, and individuals has led to two major challenges in the postal service system. On the one hand, customer demand for traditional letter delivery services has declined drastically due to the extensive use of electronic platforms, e.g., e-mail and digital mailboxes [1, 3]. However, on the other hand, the technological development has also altered customer behavior, and the customer demand fulfilled by online channels has increased unprecedentedly [4]. At the same time, the growth of online shopping has generated a significant increase in customer demand for parcel delivery [5]. Furthermore, due to the increased labor cost and the emergence of international competitors for parcel delivery, e.g., DHL, UPS, and FedEx, the traditional postal service system faces a much harder competition [6]. Hence, worldwide postal service providers need to shift their focus and replan their postal service systems to improve operational efficiency and accessibility.

In Norway, an ambitious strategic reform and structural change of the urban postal service network, named post-in-shop, was launched by Posten Norge in 2013. The scheme has been implemented across the whole country with the aim of converting the traditional centrally located post offices into smaller postal service counters at local supermarkets and grocery stores [3]. Through a partnership with retailers, Posten Norge can not only reduce the cost of opening and operating large dedicated post offices in city centers but also can improve the accessibility of postal service by locating a larger number of postal service counters that are closer to customer demand. Meanwhile, the utilization of space and personnel at local supermarkets and grocery stores can also be improved.

To implement this scheme optimally, an analysis of the urban postal service network redesign problem is essential. The problem can be modeled as a service facility location problem, which aims at selecting the optimal facility locations to provide services and determining the allocation of customer demand. Facility location is one of the most crucial decisions in strategic management throughout a wide range of businesses and public sectors [7, 8]. Mathematical models, as well as other qualitative and quantitative approaches, such as analytical hierarchy process (AHP) [9, 10], geographical information systems (GIS) [11, 12], and simulation [13], have been investigated and applied to the optimization of facility locations with respect to different criteria.

In service facility location problems, one widely formulated objective is to maximize the accessibility of a service network to targeted customer demand [14]. Accessibility can be measured either by the coverage of customer segments [15] or by the distance or travel time [14, 16]. To improve the accessibility of an urban postal service system, we proposed a two-stage optimization-simulation approach, where two classical location models were first employed to choose the best locations of postal service counters, and a simulation model was then applied to evaluate different facility location and demand allocation strategies. One reason for applying simulation after the optimization phase is that several real-life features, namely, stochasticity, cannot be readily incorporated into the mathematical models. In addition, the output of the optimization models depends on the aggregation levels used for the inputs.

This paper aims at effectively using the strengths of both optimization and simulation to solve a real-world urban postal service network redesign problem. Even though the problem is motivated and derived from a specific problem in Norway, the methodological framework can be adopted in a wide range of applications. The remainder of this paper is organized as follows. With a focus on practical applications, Section 2 presents an extensive literature review on the location models and on simulation for network optimization problems. This is followed by the problem description in Section 3. Section 4 introduces the methodology. Section 5 is devoted to data generation, results, and discussions. Conclusions follow in Section 6.

2. Literature Review

The redesign of postal networks has been the object of attention in recent years. Mathematical models were developed to analyze cost efficiency [17] and optimize network replanning decisions, i.e., postbox locations [1, 2]. The urban post office relocation problem was modeled by Šarac et al. [18] who used a set covering location problem (SCLP) to determine the minimum number of permanent post offices required for providing a certain level of service. However, due to the resource limitation in a large number of real-world problems, the urban postal network may not be able to provide a desired level of coverage to all customers. Thus, this paper focuses on improving the accessibility of an urban postal service system with a limited number of postal service counters installed.

The redesign of an urban postal service network belongs to service facility location problems, which have been investigated by a large number of researchers [19]. In this paper, we proposed a two-stage method where service facility location models with budgetary constraints were first used to generate optimal locations. Then, a simulation model was developed and used for performance evaluation. Hence, our literature review focuses on the recent development and applications with respect to the aforementioned methods.

2.1. Maximal Covering Location Problem. The maximal covering location problem (MCLP) was put forward by Church and ReVelle [20]. Over the years, the MCLP has become one of the most extensively investigated location models due to its applicability to a wide range of practical problems [21]. In the MCLP, the distance or the travel time between customers and facilities is the measurement of the satisfaction of customer demand [20]. The MCLP aims at maximizing the coverage of weighted customer demand with limited facilities [22].

Recent research has focused on the development of improved models and computational algorithms for the MCLP [23]. Seyhan et al. [24] proposed a new model and heuristic for a MCLP under competition between different players. Janković et al. [25] improved the formulation and solution approach of an uncapacitated single or multiple allocation p-hub MCLP. Combining both exact and metaheuristic methods, Pereira et al. [26] investigated an efficient solution approach for a probabilistic maximal covering location-allocation problem. Cordeau et al. [27] developed an enhanced Benders decomposition approach to solve large maximal covering models.

Real-world applications of the MCLP have also been documented. The improvement of the accessibility of healthcare facilities with improved MCLPs was studied by Murawski and Church [28]; Verter and Lapierre [29]; and Sorensen and Church [30]. Recently, Frade and Ribeiro [31] investigated the optimal design of an urban bike-sharing system under a budget constraint. Pasandideh et al. [32] proposed a multiobjective hub MCLP to simultaneously maximize both network reliability and commodity flow. Taking into account the uncertainty related to the impact of disasters, Li et al. [33] formulated a cooperative MCLP for the design of a humanitarian relief logistics network. Paul et al. [34] formulated an improved biobjective MCLP for the network redesign of a large-scale emergency response system. The model aims at simultaneously maximizing the demand coverage and minimizing the efforts needed for modifying the existing system.

2.2. p-Median Location Problem. The p-median problem (PMP) was first formulated by Hakimi [35, 36], where it was used to determine the optimal locations of switching centers in a telecommunications network. The PMP aims at minimizing the total travel distance or travel time by opening a fixed number p of service facilities [37]. To better cope with practical problems, several extensions of the classic PMP have been formulated, e.g., the capacitated PMP [38], the

Hamiltonian PMP [39], the p-hub median problem [40], and the competitive PMP [41].

The PMP is NP-hard (see, e.g., [42]), so the computational performance with both improved heuristics and commercial solvers has been tested in recent works [43]. Hale et al. [44] solved a large-scale classic PMP with an improved Lagrangian search approach. Erdoğan et al. [45] and Bektaş et al. [46] tested different exact and approximation methods to solve a Hamiltonian PMP. Stefanello et al. [47] proposed an iterated reduction matheuristic combining both mathematical programming techniques and local search metaheuristics to solve a capacitated PMP. Drezner and Salhi [48] solved a planar PMP using efficient neighborhood reductions combined with metaheuristics. Colmenar et al. [49] put forward an enhanced greedy randomized adaptive search approach for an obnoxious PMP.

Focusing on real-world applications, De Azevedo and Pizzolato [50] investigated an urban real estate location problem in Rio de Janeiro modeled as a PMP. To cope with the rapid increases in demands, Adler et al. [51] used the p-hub median model to evaluate expansion alternatives for an existing airline network in Africa. Wheeler [52] improved the location decisions on police patrol areas with a modified PMP so that both the total travel distance and the inequality of call allocation can be reduced. Cintrano et al. [53] applied a neighborhood search algorithm to determine the best locations of public bike stations in Malaga. In addition, comparisons between both the MCLP and the PMP were reported in several practical applications, e.g., healthcare services [54], printer locations in an university campus [55], and public charging stations for the electric vehicle [16].

2.3. Computer-Based Simulation. Real-world decisions are rarely made without uncertainty [56]. To capture the stochasticity of a decision-making problem, one may need to employ several assumptions and stochastic parameters, which may either reduce the accuracy of the analysis [30] or increase the computational complexity. The rapid development of computer-based simulation has provided opportunities to solve this problem and to explore the system's performance at a more detailed level [57]. Recently, the use of simulation has become an attractive tool to evaluate a model's output in several problems, e.g., factory flow optimization [58], production planning [57], service accessibility [59], and intermodal transportation under uncertainty [60].

Even though computer-based simulation has already been used in a wide variety of industries and in the public sector [61–63], its application in facility location problems has been less common until recently. Considering the flow of customer demands and demographical data, Rouzafzoon and Helo [64] and Helo et al. [65] investigated agent-based simulation modeling to compare different network configurations of service supply chains in Southern Finland. Li et al. [66] simulated a facility fortification problem in order to mitigate the supply chain risk caused by both natural and human-related disasters. Kim et al. [67] tackled the network design problem of a biomass supply chain by using a two-phase simulation method. Elia et al. [68] developed a simulation-based framework to evaluate both economic and environmental performances of a reverse logistics system.

2.4. Summary and Scientific Contributions. In strategic location problems, the idea of using the hybrid optimization-simulation method originated from the mid-1990s (see, e.g., [69]) and was mostly used in emergency medical service (EMS) location problems, where the vehicle busyness and the rate of call response were analyzed with discrete-event simulation [30, 70]. However, in service network design problems, the potential of combining both optimization and simulation has not been fully exploited. For this reason, we propose a two-stage optimization-simulation method in this paper to solve a real-world urban postal service network redesign problem, where the focus is accessibility. In the first stage, the MCLP and the PMP are used to select the optimal facility locations. In the second stage, a simulation model is built with AnyLogic to evaluate the location decisions with respect to different demand allocation strategies.

Our scientific contributions are summarized as follows:

(1) We develop a two-stage optimization-simulation method to improve the accessibility of an urban service system with continuous demand distribution

(2) We show the applicability and effectiveness of the proposed method to a real-world urban postal service system redesign problem

(3) With the simulation tool, the network accessibility is evaluated under the stochasticity of time, location, and demand volume

3. Problem Description

3.1. Background. The post-in-shop scheme aims to provide postal services in retail outlets where a postal service counter and a storage space for parcels and letters will be installed. In this paper, the problem under investigation is inspired by a real-world case of the post-in-shop relocation problem in Narvik, which is a small but strategically important town in Northern Norway. With one of the largest ice-free deep-water ports inside the Arctic Circle and the world's northernmost railway connection, Narvik is an important transportation hub in the Arctic region, especially for the shipment of high-quality iron ore mined in northern Sweden.

The original post office in Narvik was located at a large shopping mall in the city center, but it was closed in 2013 with the implementation of the post-in-shop scheme. Instead of the original large and centrally located post office in Narvik, two postal service counters were relocated at two supermarkets, Coop Extra Bolaget and SPAR Finnbekken, as shown in Figures 1 and 2. The customers were assigned to different postal service counters based only on their postcodes (the customers with postcode 8514 were assigned to SPAR Finnbekken, and those with postcode 8517 were assigned to Coop Extra Bolaget). The relocation of post offices expands the urban postal service network by opening more facilities closer to the customers. However, many

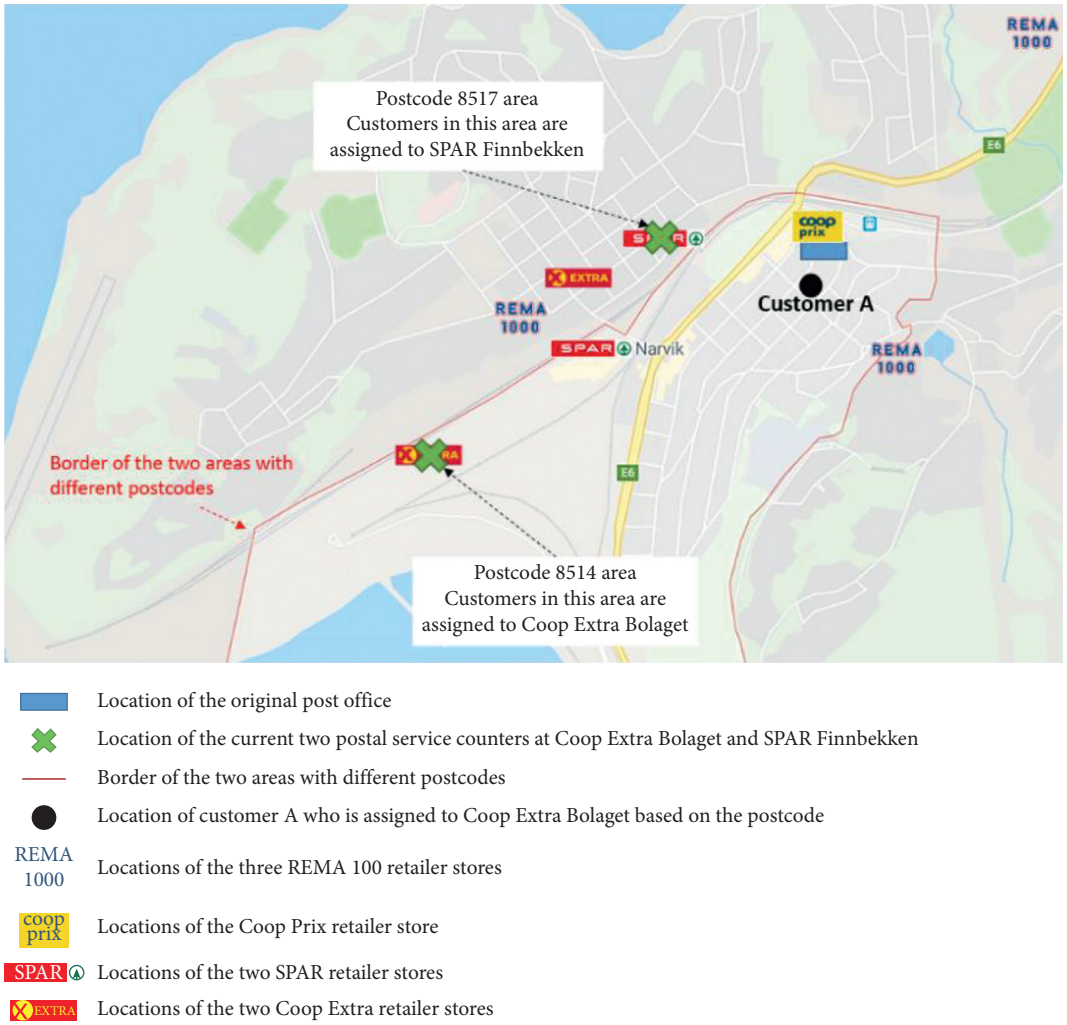

Figure 1: Locations of the original post offices, the current postal service counters, and the candidates for postal service counters.

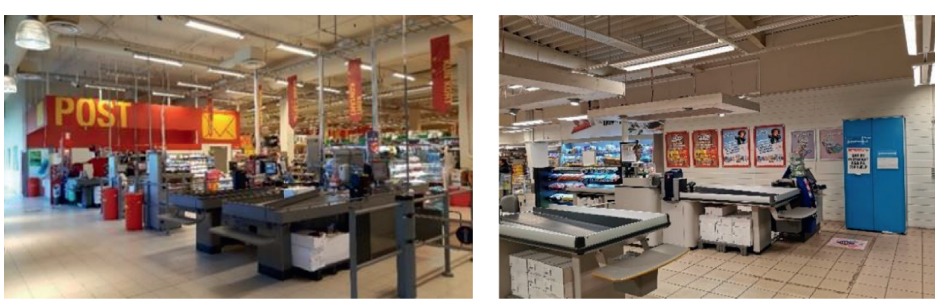

(a) (b)

Figure 2: Post-in-shop at Coop Extra Bolaget and SPAR Finnbekken in Narvik. (a) Coop Extra Bolaget. (b) SPAR Finnbekken.

customers will need to travel a larger distance than before in order to pick up their parcels due to the postcode-based demand allocation. For instance, as shown in Figure 1, customer A located in the postcode 8514 area needs to go to a much further postal service counter (Coop Extra Bolaget) to pick up a parcel instead of going to the closest one (SPAR Finnbekken).

3.2. The Problem. The urban postal service system redesign is, by nature, a service network design problem that determines the locations of service facilities and allocates customers to different locations. In the design of some service systems, e.g., petrol stations and ATM networks, only facility locations need to be determined, and customers are free to choose the facilities for respective services. However,

for an urban postal service system, customers need to be assigned to specific locations to pick up their parcels. Thus, both facility location and customer allocation decisions are of essential importance to determine the overall performance of this service system in terms of accessibility, convenience, and customer satisfaction. An improperly designed service system, as illustrated in Figure 1, may result in increased travel distance for customers and reduced accessibility. Moreover, this may further increase fuel consumption and hence greenhouse gas emissions. To solve this problem, both facility location and customer allocation decisions need to be optimized.

Designing a service system consists of two-stage decision-making. First, the number and locations of service facilities are selected from a set of candidate points. In an urban postal service system, taking into account the storage space requirement for parcels, the candidate points can only be located at large- and medium-size shops. Figure 1 depicts the candidate locations for potential postal service counters in the urban area of Narvik (three REMA 1000, two SPAR, two Coop Extra, and one Coop Prix). In order to provide a high accessibility to customer demand under budgetary constraints, the determination of the number and locations of service facilities is usually done with the objective either to maximize the demand coverage (the MCLP) or to minimize the total travel distance by customers (the PMP).

Based on the first-stage decisions, the demand allocation can be determined in the second stage, where customers can be either assigned to a specific location or to the nearest facility. In the urban postal system redesign problem, we are interested in the comparison of both postcode-based and distance-based demand allocation strategies, and their implications to the overall system's accessibility are evaluated.

4. Methodology

In order to solve the problems of traditional mathematical methods such as demand aggregation and oversimplified assumptions, we proposed a two-stage optimization-simulation method for the service system design problem with special focus on the urban area and tested it with a real-world case study of the urban postal service system redesign in Narvik. We first describe the framework of the two-stage method. Then, the two classical optimization models and the simulation method are briefly introduced.

4.1. Methodological Framework. Figure 3 illustrates a two-stage methodological framework for the service system design problem. In the first stage, we apply the MCLP and the PMP to obtain an optimal network configuration with different objectives and requirements. In the second stage, the AnyLogic simulation is used for performance measurement. To set up the simulation model, the GIS information is given based on the optimal locations obtained, and the generation intervals of stochastic parameters are determined in accordance with the data used in the first stage. The agent's behavior is set up based on different demand allocation strategies. It is noted that a stability and quality check is performed so that the proposed method can be used with a high level of confidence in order to solve large problem instances.

In this research, we exploit the strengths of both mathematical optimization and computer-based simulation. The terms of optimization and simulation are used interchangeably in several cases [71]. However, they are two very different techniques that should be properly applied in different problems. Optimization aims, through a model and an algorithm, at searching an optimal objective value within the feasible domain of a problem. It is capable of solving combinatorial optimization problems with a large number of alternatives. However, due to the simplifications made in the models, e.g., demand aggregation, the results obtained may not be sufficiently accurate [30]. Furthermore, the incorporation of input stochasticity into a mathematical model may significantly increase its computational complexity [72].

Simulation, on the contrary, aims at the performance evaluation of a set of alternatives under different conditions [73], which can better reproduce real-world problems with stochastic parameters, real-world GIS, and real planning horizon. Moreover, it is also a powerful tool to create an animation of the physical installations and flows of the system modeled. However, while the primary objective of simulation is for performance evaluation, it can neither solve a complex combinatorial optimization problem nor generate proven optimal decisions when the number of potential alternatives is large. Tables 1 and 2 show the strengths and weaknesses of the two approaches.

4.2. The Location Optimization Models. Both the MCLP and the PMP optimize the network performance under budgetary constraints through installing a limited number of facilities. The sets, parameters, and variables used in the model formulation are first given in Table 3.

The MCLP measures accessibility with the level of demand coverage and aims at establishing a service system to ensure that a maximum number of customers can find a service facility within their preferred distance. In this regard, objective function (1) maximizes the overall weighted customer demand coverage. Constraints (2) guarantee that the demand of customer i is covered only if a service facility is installed within its preferred distance. Constraint (3) specifies the number of facilities to be installed. Constraints (4) define the domain of the variables.

$$\text{Maximize} \sum_{i \in I} d_i z_i, \tag{1}$$

subject to

$$z_i \leq \sum_{j \in N_i} y_j, \quad \forall i \in I, \tag{2}$$

$$\sum_{j \in J} y_j = p, \tag{3}$$

$$z_i, y_j \in \{0, 1\}, \quad \forall i \in I, j \in J. \tag{4}$$

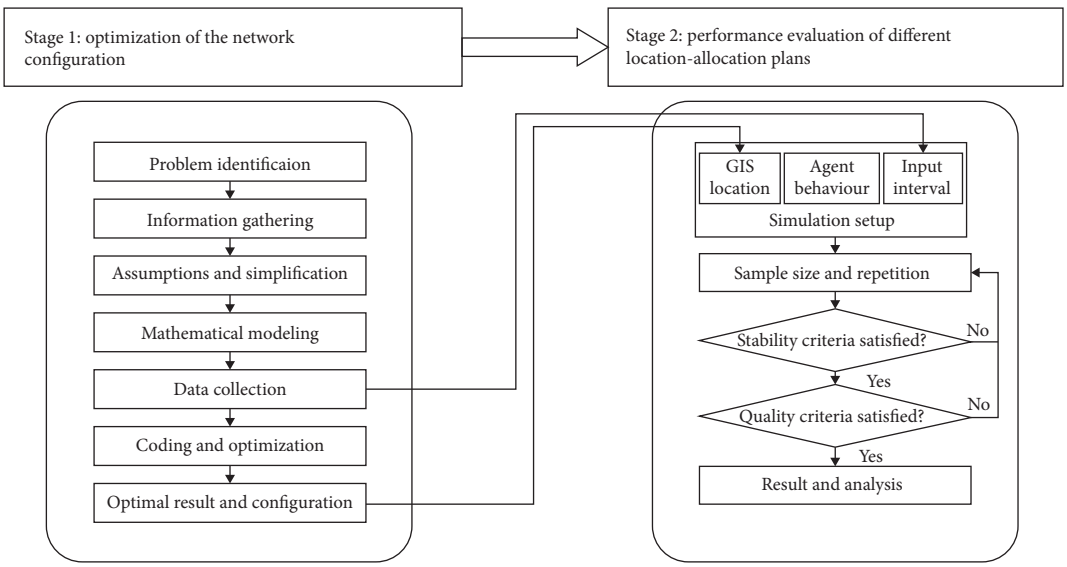

Figure 3: Methodological framework.

Table 1: Strengths and weaknesses of optimization.

Optimization	
Strengths	(1) Capability of selecting an optimal solution among a large number of alternatives (2) Capability of generating high-quality solutions to complex decision-making problems
Weaknesses	(1) Inaccurate analytical results due to the simplifications made (2) Increased complexity in modeling and computation due to the inclusion of uncertainty (3) The numerical results may be difficult to be understood by decision makers who do not possess the relevant knowledge

Table 2: Strengths and weaknesses of simulation.

Simulation	
Strengths	(1) Capability of evaluating different predetermined alternatives under a realistic environment (2) Capability of incorporating the uncertainty, real-world GIS, and time horizon of a decision-making problem (3) Capability of generating high-quality animation of the physical system
Weaknesses	(1) Ineffectiveness and incapability of selecting an optimal solution among a large number of alternatives (2) Ineffectiveness and incapability of generating high-quality solutions to complex decision-making problems

Table 3: Sets, parameters, and variables.

Sets	
I	Set of customers, indexed by i
J	Set of candidate locations for the service facility, indexed by j
Parameters	
d_i	Demand of customer i
c_{ij}	Distance between customer i and service facility j
r	The coverage distance of a service facility
$j_i = \{j \in J: c_{ij} \leq r\}$	The set of candidate locations j of the service facility within the coverage distance of customer i
p	The number of service facilities to be installed
Variables	
y_j	Binary variable: $y_j = 1$ if a service facility is installed at candidate location j; $y_j = 0$, otherwise
z_i	Binary variable: $z_i = 1$ if the demand from customer i is covered; $z_i = 0$, otherwise

The PMP aims at minimizing the total weighted travel distance by all customers. It not only selects the locations of the service facility but also determines the allocation of customer demands. Hence, an additional variable for demand allocation is defined as follows.

x_{ij}: binary variable: $x_{ij} = 1$ if customer i is assigned to service facility j; $x_{ij} = 0$, otherwise.

$$\text{Minimize} \sum_{i \in I} d_i c_{ij} x_{ij}, \tag{5}$$

subject to

$$\sum_{j \in J} x_{ij} = 1, \quad \forall i \in I, \tag{6}$$

$$x_{ij} \leq y_j, \quad \forall i \in I, j \in J, \tag{7}$$

$$\sum_{j \in J} y_j = p, \tag{8}$$

$$x_{ij}, y_j \in \{0, 1\}, \quad \forall i \in I, j \in J. \tag{9}$$

Objective function (5) minimizes the total weighted travel distance of all customers. Constraints (6) assign each customer i to a single service facility. Constraints (7) guarantee that the demand of a customer is allocated to a service facility only if it has been located. Constraint (8) sets the number of service facilities to be installed. Constraints (9) define the domain of the variables. Clearly, in the PMP, the demand is assigned to a facility based only on the travel distance.

4.3. The Simulation Method. Real-world decision-making is usually affected by uncertainties, so an agent-based simulation model was built with AnyLogic to evaluate the network performance under input stochasticity. AnyLogic is one of the most powerful simulation packages, and by using multiple methods including system dynamics and agent-based and discrete-event modeling, it can be used to simulate complex systems with different features [61]. In our case study, we consider demand stochasticity in performance evaluation. The customer demands for postal service are generated in the real-world GIS with random locations, random time, and random demand. This will affect the objective values of the optimization model due to the stochasticity in parameters d_i, c_{ij}, and N_i. The movement of individual customers or agents is governed by the demand allocation strategy, which can be to go to a specific service facility or to travel to the nearest one for service.

The simulation model is, by nature, a stochastic form of the optimization model. It can be written as a generic objective function $f(y_j, \xi(d_i, c_{ij}, N_i))$ to calculate either coverage (to be maximized) or distance (to be minimized), where y_j is the location decision and ξ is the scenario tree. With given probability distributions for the stochastic parameters, an infinite number of decision trees can be generated. However, we focus on the model's behavior but not on the scenario generation procedures [56], so the output of the simulation model should be stable with different scenario trees [74], as shown in equation (10). Therefore, a Monte Carlo simulation method is used, which runs the AnyLogic model for $|S|$ times in order to test the stability of the analytical results:

$$f\left(\hat{y}_j, \xi_p\left(d_i, c_{ij}, N_i\right)\right) \approx f\left(\hat{y}_j, \xi_q\left(d_i, c_{ij}, N_i\right)\right), \quad \forall p, q \in S. \tag{10}$$

Real-world problems can be extremely large and may therefore lead to a significant computational challenge. In this regard, instead of performing a full-size simulation with a large number of agents and a long-time horizon, a reliable sampling method may be used to approximate the objective value of the real problem, as shown in equation (11), where the sampling problem γ is much smaller than that of the real problem ξ:

$$f\left(\hat{y}_j, \gamma\left(d_i, c_{ij}, N_i\right)\right) \approx f\left(\hat{y}_j, \xi\left(d_i, c_{ij}, N_i\right)\right), \quad \forall p \in S. \tag{11}$$

When a smaller size simulation is used to analyze the real problem, both the stability and the quality of the sampling procedures must be checked. This idea is based on the sample average approximation (SAA) [75]. For a location decision $\hat{y}_j$ and a given sample size, stability is checked with $|S|$ repetitions, as shown in equation (12). Then, the simulation is run with a set of increased samples generated from the same probability distribution. The gap between the objective values obtained is used to measure the quality of the approximation. If the gap estimators satisfy the quality criteria, the given sample size can be used to approximate the result of the real problem, as shown in equation (13). Otherwise, an increased sample size or repetition is needed.

$$f\left(\hat{y}_j, \gamma_p\left(d_i, c_{ij}, N_i\right)\right) \approx f\left(\hat{y}_j, \gamma_q\left(d_i, c_{ij}, N_i\right)\right), \quad \forall p, q \in S, \tag{12}$$

$$f\left(\hat{y}_j, \gamma_p\left(d_i, c_{ij}, N_i\right)\right) \approx f\left(\hat{y}_j, \xi\left(d_i, c_{ij}, N_i\right)\right), \quad \forall p, q \in S. \tag{13}$$

5. Application and Results

In this section, the data generation procedures for both optimization and simulation are first introduced. Then, discussions are given based on the numerical results.

5.1. Data Generation and Model Implementation. To implement the optimization models for the urban postal service network redesign problem in Narvik, input data were first generated based on the following assumptions:

(1) The urban area of Narvik is divided into 40 same-size customer segments (A1, A2,..., E8), as shown in Figure 4.

(2) The customer demands for postal service are directly proportional to the population size of each customer segment.

Figure 4: Customer demand aggregation and candidate locations for postal service counters.

(3) The population size is determined by the demographic distribution and by the portion of the residential area of each customer segment. Thus, the customer segments with very low coverage of the residential area, e.g., A1, are eliminated from the analysis. In total, 29 customer segments are included in the optimization.

(4) The weighted customer demands are aggregated into the center point of each customer segment.

The demand of each customer segment is first estimated. Customers need to go to the postal service counters to pick up their parcels and registered letters. Compared with the volume of registered letters delivered for individuals, the volume of parcel delivery for individuals is much higher. Therefore, the demand estimation is based mainly on parcel delivery with customer pickup at postal service counters. The total volume of parcel delivery in Norway is 59.9 million units [5], among which 60% is assumed to be parcel delivery for individuals with customer pickup at postal service counters, and the others are related to business demands and value-added home delivery. The total population in Norway is 5.296 million [76]. Hence, the average demand for parcel delivery with customer pickup per capita is approximately six to seven times a year, based on which the aggregated annual customer demand for postal service of each customer segment can be estimated by demand = demand per capita × population.

The distance matrix between the center point of each customer segment and the candidate locations for postal service counters is calculated on Google Maps. The customer-preferred distance to the postal service counter is considered as the facility coverage radius, which was determined by interviews with randomly selected customers in Narvik. For a detailed discussion on the coverage radius of postal services in European countries, see [18]. In this study, the coverage radius of a postal service counter is set to 900 m. Based on the distance matrix and coverage radius, the coverage matrix can be established as in Table 4. The optimization problems consist of 29 customer segments and eight candidate locations for postal service counters. Both MCLP and PMP were solved using LINGO 18.0. Since the sizes of the optimization problems are very small, the models can be solved within two seconds.

In the second stage, an agent-based simulation model was built in AnyLogic 8.4 to test different combinations of location plans and allocation strategies. Agent-based modeling (ABM) is able to simulate the behaviors of individuals within a system as well as the interactions among them [77]. Hence, the characteristics of the urban postal system redesign problem can be better represented in the simulation. The simulation model was implemented under the following assumptions:

(1) The average number of people per family in Narvik is 2.13 [78], and the demand for postal services is seven times per person per year. In the simulation, one agent represents the customer demands from the same family. Considering uncertainty, customer demands were randomly generated from a continuous uniform distribution with an upper bound calculated by $c^{\text{upper}} = (1+\beta)c^m$ and a lower bound calculated as $c^{\text{lower}} = (1-\beta)c^m$ [79], where $c^m = 14$ and $\beta = 0.15$ were used.

(2) The map of Narvik was created with a real GIS (OSM classic), in which the customer demand points were

Table 4: The coverage matrix.

Candidate	Demand coverage
1	A6, B5, B6
2	A4, A5, B3, B4, B5, B6, C3, C4, C5, C6, D4, D5
3	A3, B2, B3, B4, C2, C3, C4, C5, D2, D4
4	A4, B4, B5, C3, C4, C5, C6, D4, D5, E4
5	A5, A6, B4, B5, B6, C4, C5, C6, C7, D5, D6
6	B6, C5, C6, C7, C8, D5, D6, D7, E6
7	C3, D1, D2, D4
8	B4, B5, C3, C4, C5, C6, D4, D5, D6, E4

Table 5: Scenarios with different location and demand allocation strategies.

Scenarios	Number of facilities	Facility locations		Allocation plan
		Location plan	Candidate	
S1	1	Original	5	
S2	1	Optimal	4	
S3	2	Current	2, 7	Current allocation plan
S4	2	Current	2, 7	Optimal allocation plan
S5	2	Optimal	3, 5	Current allocation plan
S6	2	Optimal	3, 5	Optimal allocation plan

Table 6: Performance evaluation of different scenarios.

Scenarios	Demand coverage (%)	Travel distance (m)		Standard deviation (m)
		Mean	Overall median	
S1	32.9	1220.3	1176.5	525.8
S2	31.7	1221	1175.5	532.8
S3	25.2	1271	1301.1	505.9
S4	35.6	1219.3	1177.4	557.2
S5	37.1	1227	1165.7	609
S6	49.2	945.5	918.3	417.5

randomly generated over the residential area. The locations of the postal service counters in different scenarios were obtained from the optimization models. Besides, the travel distance between two points was calculated with real road information.

(3) Two demand allocation strategies were modeled. In the first one, customers are assigned to a postal service counter based only on their postcodes. For the other one, customers choose their nearest postal service counter.

(4) In the simulation, the sample size of demand points was set to 1,000, and the virtual time for simulation was set to one year. For the stability check, 20 repetitions were performed for each scenario. The coefficient of variation (CV) was used for stability check, and the confidence level was set equal to 90%.

(5) Due to the computational challenge, the full simulation could not be efficiently completed with the hardware configuration and software package used in the experiment. Therefore, instead of conducting a full-size simulation, four other scenarios with an increase in either the sample size (2,000 and 3,000) or in the virtual time of simulation (three and five years) were tested for quality check. The expectation on the level of confidence in this step was set to 90%.

All simulation models were run on a PC with the same configuration as that used in the first stage. The CPU time varies from 300 to 1,100 seconds with respect to different sample sizes and virtual time for simulation.

5.2. Results and Discussion. When the number of postal service counters installed is equal to one or two, both the MCLP and the PMP yield the same optimal location decisions. Considering several combinations of location-allocation plans, six scenarios were first compared, as shown in Table 5. When only one postal service counter is installed in scenarios S1 and S2, all customers are obviously assigned to the same location. Scenarios S3, S4, S5, and S6 are two-facility scenarios with different location and demand allocation strategies.

Table 6 shows the performance evaluation of the network accessibility with respect to two criteria: demand coverage and travel distance. When only one postal service counter is installed, the simulation result suggests that the difference between the original location and the optimal location is small, and the accessibility cannot be noticeably improved through location optimization. Next, the accessibility of the current two locations of the postal service counters and the current postcode-based demand allocation strategy is evaluated in S3. The performance of both

Table 7: Estimators for the stability and quality checks.

Performance evaluation	Indicator	Sample		Scenarios											
				S1		S2		S3		S4		S5		S6	
		Size	Time (year)	Coverage (%)	Distance (%)	Coverage (%)	Distance (%)	Coverage (%)	Distance (%)	Coverage (%)	Distance (%)	Coverage (%)	Distance (%)	Coverage (%)	Distance (%)
Stability check	CV of 20 repetitions	1,000	1	7	2.2	9.9	2.5	9	1.3	6.5	1.6	9.1	2.5	4.8	2
Quality check	Gap from the basic sample (1000 agents and one year)	1,000	3	6.5	−3.3	5.9	−2.7	−7.1	0.4	5.4	−4.2	4.7	−2.5	6.7	−6.2
		1,000	5	5.6	−4.1	2.8	−5.4	−1.1	−4.4	4.5	−7	8.5	−1.9	0.6	−4.6
		2,000	1	−9.8	1.3	−8.7	0	−3.5	−1	6.3	−1.7	−0.2	2.5	8	−3.6
		3,000	1	−2	−1.1	−2.4	−1.9	2.4	−2.3	5.9	−0.6	6.4	2.2	−2.3	−0.7

Table 8: Optimal decisions of the MCLP and the PMP with an increased number of facilities to be installed.

Number of facilities (p)	Optimal locations	
	MCLP	p-median location problem
1	Candidate 4	Candidate 4
2	Candidates 3 and 5	Candidates 3 and 5
3	Candidates 1, 4, and 6	Candidates 3, 4, and 6
4	Candidates 1, 2, 6, and 7	Candidates 1, 3, 4, and 6
5	Candidates 1, 2, 3, 6, and 7	Candidates 1, 3, 4, 5, and 6
6	Candidates 1, 2, 3, 6, 7, and 8	Candidates 1, 3, 4, 5, 6, and 7
7	Candidates 1, 2, 3, 4, 6, 7, and 8	Candidates 1, 3, 4, 5, 6, 7, and 8
8	Candidates 1, 2, 3, 4, 5, 6, 7, and 8	Candidates 1, 2, 3, 4, 5, 6, 7, and 8

demand coverage and travel distance is reduced compared with the one-facility scenarios, which shows that installing a larger number of facilities may not improve the network accessibility if an improper demand allocation strategy is implemented. When either the allocation strategy (S4) or the location decision (S5) is optimized, the result suggests that an improvement in the performance indictors may be achieved. Finally, when both the optimal location decision and the distance-based allocation strategy are implemented in S6, the accessibility of the urban postal service network can be drastically improved. Compared with the current plant, the demand coverage increases by 95.2%, and the average travel distance reduces by 25.6%. This result illustrates that the accessibility of a service network is determined not only by the number of facilities installed but also by the facility locations and by the demand allocation strategies implemented.

Due to the stochastic nature of the problem, the effective use of the simulation results depends on the stability and quality of the sample with respect to the real problem. Table 7 shows the stability and quality checks. First, the CV ($= \sigma/\mu$) of the 20 repetitions with sample size 1,000 is used for the stability check, which ranges from 1.3% to 9.9%. The average value of 20 repetitions is used as the benchmark. With an increase in either sample size or virtual time for simulation, the estimators for the quality check are calculated and normalized to the same scale of the benchmark scenario. The absolute values of these estimators range from 0 to 9.8%. The evaluation result shows that both stability and quality fulfill the requirement of the level of confidence. In addition, we observe that the absolute values of the gap estimators for demand coverage are larger than those of the travel distance in most cases. This can be explained by the fact that the distance between customer locations and postal service counters is the only indicator for calculating the demand coverage, which may be significantly affected by the randomness related to the generation of customer locations and hence result in a high variation. However, on the contrary, the aggregation of the uncertainty related to both customer demand and geographical location in the calculation of total travel distance in the PMP may lead to a more stable result.

The sensitivity of the system performance with respect to the number of postal service counters opened is of interest. Table 8 shows the location decisions obtained by the MCLP and the PMP with an increase in the number of facilities opened. In the sensitivity analysis, only the optimal distance-based demand allocation strategy is considered. When $p = 3$, 4, 5, 6, and 7, the MCLP and the PMP yield different location decisions. Table 9 shows the gap estimators for the stability and the quality checks, which exhibit a pattern similar to that of the previous scenarios. Herein, the expected level of confidence for the quality check is relaxed to 87% in order to maintain the computational efficiency. In addition, it is noted that the change of virtual time may have more impact on the simulation results. Table 10 presents the computational performance of the simulation model in the sensitivity analysis. Compared with the change of the virtual time for simulation, the increase in the sample size has much more influence on the computational performance. Therefore, we have shown that the proposed method can effectively maintain its computational efficiency while providing, at the same time, a high level of confidence in the simulation results.

As shown in Figure 5, the result of the sensitivity analysis suggests that the accessibility of the urban postal service system in Narvik evaluated by both indicators can be improved when p increases from one to three. However, accessibility may not be significantly improved by installing more than three postal service counters. This provides important information to the decision makers on the proper number of postal service counters to install under both accessibility and budget constraints. In addition, we observe that, in most cases, the optimal solution obtained by the PMP may outperform the one calculated by the MCLP in both demand coverage and travel distance.

Table 9: Estimators for the stability and quality check in sensitivity analyses.

Performance evaluation	Indicators	Sample		Three facilities				Four facilities				Five facilities				Six facilities				Seven facilities				Eight facilities	
				MCLP		p-median		MCLP		p-median		MCLP	p-median	MCLP	p-median	MCLP	p-median	MCLP	p-median	MCLP	p-median	MCLP	p-median	MCLP	p-median
		Size	Time (year)	Coverage (%)	Distance (%)	Coverage (%)	Distance (%)	Coverage (%)	Distance (%)	Coverage (%)	Distance (%)	Coverage (%)	Distance (%)	Coverage (%)	Distance (%)	Coverage (%)	Distance (%)	Coverage (%)	Distance (%)	Coverage (%)	Distance (%)	Coverage (%)	Distance (%)	Coverage (%)	Distance (%)
Stability check (lower bound)	CV of 20 repetitions	1,000	1	3.3	2	3.5	1.7	5.9	2.8	4.3	3	3.3	2.1	3.3	2.6	3.6	2.6	2.9	3.2	2.6	2.4	3.7	3.5	4.2	2.1
Quality check (upper bound)	Gap from the basic sample (1000 agents and one year)	1,000	3	6.5	−3.2	6.5	−3.2	1.6	−2.6	3.1	−2.7	7.6	−2.8	10.7	−6.1	−2.6	1.7	11.9	−0.8	3.7	−1.8	11.7	−11.2	7.5	−5.4
		1,000	5	9.5	−5.5	9.5	−5.5	9.4	−5.3	10.1	−6.3	13.1	−9.3	10.9	−8.7	8.6	−6.9	6.6	−2.3	7.5	−7.2	7.7	−5.5	1.6	−2.6
		2,000	1	−4	0.9	−4	0.9	−3.9	4.3	12.1	−0.8	−3.8	2.5	−0.6	−0.5	2.6	0.9	−5.3	−0.8	−2.4	1.3	−3.9	3.6	−2.8	2.9
		3,000	1	−2	−0.5	−2	−0.5	−3.2	0	1.4	1.9	−3.7	1.4	−2.9	0.7	−2.1	3	0.4	−0.8	−3.9	2.7	−2.0	2.7	−1	2.6

Table 10: CPU time of the simulations.

Sample size and virtual time for simulation	One facility		Two facilities		Three facilities		Four facilities		Five facilities		Six facilities		Seven facilities		Eight facilities
	Original	Optimal	Current	Optimal	MCLP	p-median	MCLP	p-median	MCLP	p-median	MCLP	p-median	MCLP	p-median	
Sample 1000 for 1 year (average CPU time)	335	334	357	370	365	364	324	351	366	351	339	358	362	338	334
Sample 1000 for 3 years	352	359	367	365	363	364	361	365	334	368	386	385	368	391	360
Sample 1000 for 5 years	382	369	381	369	367	372	379	405	375	378	405	418	373	404	378
Sample 2000 for 1 year	708	689	687	705	682	666	659	672	670	685	707	721	718	720	708
Sample 3000 for 1 year	1,063	1,025	1,039	1,059	1,010	1,004	1,016	1,000	1,025	1,050	1,039	1,074	1,094	1,082	1,081

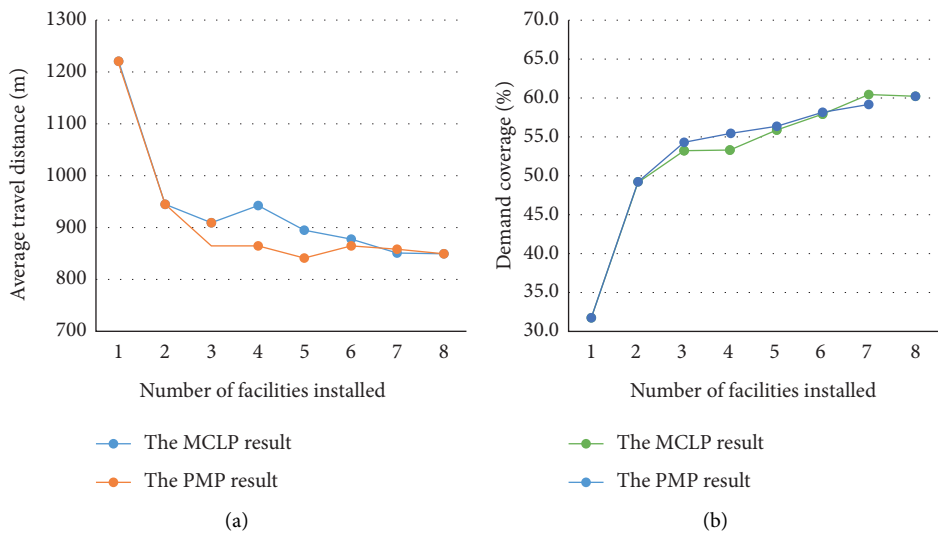

Figure 5: Result of the sensitivity analysis.

6. Conclusions

Facility location and demand allocation strategies are the most important factors affecting the accessibility of a service system. In this paper, we have proposed a two-stage approach for service system design and tested it with a real-world urban postal service system redesign problem in Norway. First, two mathematical models were used to determine the optimal number and locations of service facilities. Then, a simulation model was built to evaluate different location-allocation strategies. Considering the tradeoff between the quality of analytical results and the computational effort required, instead of performing full-size simulations, sampling procedures based on the SAA were developed for solving large instances. The results of the case study in Narvik reveal that even if another postal service counter had been opened in the current system, the accessibility would have been reduced significantly due to the implementation of the postcode-based demand allocation strategy. When either the location or the demand allocation strategy is optimized, the impacts on the accessibility are relatively insignificant. However, when both optimal location decision and demand allocation strategy are implemented, the accessibility of the urban postal service network can be drastically improved. In addition, the experimental results also suggest that the proper number of facilities for maximizing the accessibility of the urban postal service system is three, beyond which the accessibility cannot be effectively improved with an increase in the number of postal service counters.

Among other insights, the research shows that both facility location and demand allocation strategies may play an important role in determining the accessibility of a service system. Besides, the accessibility may not be improved by increasing the number of facilities when the break-even point of the system performance is reached. From a methodological perspective, the proposed two-stage approach uses the strengths of both optimization and simulation. Mathematical models can effectively obtain optimal decisions with several simplifications. For instance, the aggregation of customer demands into a few points may work well in large systems with discrete customer locations such as investigating the performance of a rural healthcare network [28, 54]. In these systems, the distances between different customer locations are very large, and the demands of a city or a town can be properly aggregated at a higher level. However, in an urban area, this is more complicated due to the continuous distribution of residential areas from which customer demands are generated randomly in terms of time, location, and demand. In this case, aggregating customer demands into a large number of discrete points and taking into account the stochasticity may improve the accuracy of the analytical results, but, on the contrary, the modeling complexity and the computational requirements will be increased dramatically. In this regard, the simulation model can be effectively and efficiently used as a performance evaluation tool of the optimal location decisions and to analyze the system behavior under a more realistic environment with minimal assumptions and simplifications. Even though the proposed method is based on a specific problem, it can be applied to a wide range of service network planning problems, especially in urban areas.

Future work may be conducted to improve the current research in the following aspects:

(i) To better reflect the real-world situation, customers' trips for postal service may be categorized in more detail, and multitype tours with different purposes, origins, and destinations may be modeled in the simulation.

(ii) The system performance may further be investigated and compared with more criteria, e.g., equity of service [54] and facility utilization.

(iii) The current research only considers accessibility. However, when strategic alliance decisions with retailer stores are to be made, other influencing

factors, i.e., the possible demand increase at shops due to combined customer trips, employee's satisfaction with increased demand, and multiple tasks, may also be considered in order to have a holistic analysis.

Data Availability

The data used in the experiment are available from the corresponding author upon request.

Disclosure

This paper is an extended and significantly modified version of "A Comparison of Two Location Models in Optimizing the Decision-Making on the Relocation Problem of Post Offices at Narvik, Norway" published at the IEEE International Conference on Industrial Engineering and Engineering Management, 2018, Bangkok, Thailand [80].

Conflicts of Interest

The authors declare that they have no conflicts of interest.

References

[1] G. Bruno, M. Cavola, A. Diglio, G. Laporte, and C. Piccolo, "Reorganizing postal collection operations in urban areas as a result of declining mail volumes—a case study in Bologna," *Journal of the Operational Research Society*, pp. 1–16, 2020.

[2] M. Šelmić, M. Nikolić, and A. Čupić, "Postboxes quantitative optimization model," *Sustainability*, vol. 12, no. 5, p. 1945, 2020.

[3] P. Norge, "Posten Norge: because people change Posten Norge much also change," 2013, https://nsd.no/polsys/data/filer/aarsmeldinger/AE_2012_8608.pdf.

[4] S. Bellman, G. Lohse, and E. J. Johnson, "Predictors of online buying behavior," *Communications of the ACM*, vol. 42, pp. 32–48, 2009.

[5] P. Norge, "Posten Norge: annual and sustainability report 2019," 2019, https://www.postennorge.no/en/report-archive/_/attachment/inline/2371ea4b-000c-4c2f-a4f8-6f0004f1c12c:becff691661c9172f74c3677f9c327921c8845d4/Annual%20and%20sustainability%20report%202019_Posten%20Norway%5B1%5D.pdf.

[6] J. Confraria, F. Silva, F. Pereira, and A. Franco, "Postal users' needs regarding accessibility to the postal network," in *The Contribution of the Postal and Delivery Sector, Topics in Regulatory Economics and Policy*, P. Parcu, T. Brennan, and V. Glass, Eds., Springer, Cham, Switzerland, pp. 187–205, 2018.

[7] S. H. Owen and M. S. Daskin, "Strategic facility location: a review," *European Journal of Operational Research*, vol. 111, no. 3, pp. 423–447, 1998.

[8] A. Klose and A. Drexl, "Facility location models for distribution system design," *European Journal of Operational Research*, vol. 162, no. 1, pp. 4–29, 2005.

[9] J. Yang and H. Lee, "An AHP decision model for facility location selection," *Facilities*, vol. 15, no. 9-10, pp. 241–254, 1997.

[10] B. Sennaroglu and G. Varlik Celebi, "A military airport location selection by AHP integrated PROMETHEE and VIKOR methods," *Transportation Research Part D: Transport and Environment*, vol. 59, pp. 160–173, 2018.

[11] F. Zhang, D. M. Johnson, and J. W. Sutherland, "A GIS-based method for identifying the optimal location for a facility to convert forest biomass to biofuel," *Biomass and Bioenergy*, vol. 35, pp. 3951–3961, 2011.

[12] B. Bozkaya, S. Yanik, and S. Balcisoy, "A GIS-based optimization framework for competitive multi-facility location-routing problem," *Networks and Spatial Economics*, vol. 10, no. 3, pp. 297–320, 2010.

[13] R. McCormack and G. Coates, "A simulation model to enable the optimization of ambulance fleet allocation and base station location for increased patient survival," *European Journal of Operational Research*, vol. 247, no. 1, pp. 294–309, 2015.

[14] R. Li and D. Tong, "Incorporating activity space and trip chaining into facility siting for accessibility maximization," *Socio-Economic Planning Sciences*, vol. 60, pp. 1–14, 2017.

[15] S. Davari, M. H. Fazel Zarandi, and A. Hemmati, "Maximal covering location problem (MCLP) with fuzzy travel times," *Expert Systems with Applications*, vol. 38, no. 12, pp. 14535–14541, 2011.

[16] S. Y. He, Y.-H. Kuo, and D. Wu, "Incorporating institutional and spatial factors in the selection of the optimal locations of public electric vehicle charging facilities: a case study of Beijing, China," *Transportation Research Part C: Emerging Technologies*, vol. 67, pp. 131–148, 2016.

[17] M. Blagojević, P. Ralević, and D. Šarac, "An integrated approach to analysing the cost efficiency of postal networks," *Utilities Policy*, vol. 62, Article ID 101002, 2020.

[18] D. Šarac, M. Kopić, K. Mostarac, M. Kujačić, and B. Jovanović, "Application of set covering location problem for organizing the public postal network," *PROMET-Traffic&Transportation*, vol. 28, no. 4, pp. 403–413, 2016.

[19] G. Laporte, S. Nickel, and F. Saldanha da Gama, *Location Science*, Springer, Cham, Switzerland, 2nd edition, 2019.

[20] R. Church and C. ReVelle, "The maximal covering location problem," *Papers of the Regional Science Association*, vol. 32, no. 1, pp. 101–118, 1974.

[21] C. S. ReVelle and H. A. Eiselt, "Location analysis: a synthesis and survey," *European Journal of Operational Research*, vol. 165, no. 1, pp. 1–19, 2005.

[22] S. Atta, P. R. Sinha Mahapatra, and A. Mukhopadhyay, "Solving maximal covering location problem using genetic algorithm with local refinement," *Soft Computing*, vol. 22, no. 12, pp. 3891–3906, 2018.

[23] S. García and A. Marín, "Covering location problems," in *Location Science*, G. Laporte, S. Nickel, and F. Saldanha da Gama, Eds., pp. 99–119, Springer, Cham, Switzerland, Second Edition, 2019.

[24] T. H. Seyhan, L. V. Snyder, and Y. Zhang, "A new heuristic formulation for a competitive maximal covering location problem," *Transportation Science*, vol. 52, no. 5, pp. 1156–1173, 2018.

[25] O. Janković, S. Mišković, Z. Stanimirović, and R. Todosijević, "Novel formulations and VNS-based heuristics for single and multiple allocation p-hub maximal covering problems," *Annals of Operations Research*, vol. 259, pp. 191–216, 2017.

[26] M. A. Pereira, L. C. Coelho, L. A. N. Lorena, and L. C. De Souza, "A hybrid method for the probabilistic maximal covering location-allocation problem," *Computers & Operations Research*, vol. 57, pp. 51–59, 2015.

[27] J.-F. Cordeau, F. Furini, and I. Ljubić, "Benders decomposition for very large scale partial set covering and maximal

covering location problems," *European Journal of Operational Research*, vol. 275, no. 3, pp. 882–896, 2019.

[28] L. Murawski and R. L. Church, "Improving accessibility to rural health services: the maximal covering network improvement problem," *Socio-Economic Planning Sciences*, vol. 43, no. 2, pp. 102–110, 2009.

[29] V. Verter and S. D. Lapierre, "Location of preventive health care facilities," *Annals of Operations Research*, vol. 110, no. 1–4, pp. 123–132, 2002.

[30] P. Sorensen and R. Church, "Integrating expected coverage and local reliability for emergency medical services location problems," *Socio-Economic Planning Sciences*, vol. 44, no. 1, pp. 8–18, 2010.

[31] I. Frade and A. Ribeiro, "Bike-sharing stations: a maximal covering location approach," *Transportation Research Part A: Policy and Practice*, vol. 82, pp. 216–227, 2015.

[32] S. H. R. Pasandideh, S. T. A. Niaki, and M. Sheikhi, "A biobjective hub maximal covering location problem considering time-dependent reliability and the second type of coverage," *International Journal of Management Science and Engineering Management*, vol. 11, no. 4, pp. 195–202, 2016.

[33] X. Li, M. Ramshani, and Y. Huang, "Cooperative maximal covering models for humanitarian relief chain management," *Computers & Industrial Engineering*, vol. 119, pp. 301–308, 2018.

[34] N. R. Paul, B. J. Lunday, and S. G. Nurre, "A multiobjective, maximal conditional covering location problem applied to the relocation of hierarchical emergency response facilities," *Omega*, vol. 66, pp. 147–158, 2017.

[35] S. L. Hakimi, "Optimum locations of switching centers and the absolute centers and medians of a graph," *Operations Research*, vol. 12, no. 3, pp. 450–459, 1964.

[36] S. L. Hakimi, "Optimum distribution of switching centers in a communication network and some related graph theoretic problems," *Operations Research*, vol. 13, no. 3, pp. 462–475, 1965.

[37] A. Marín and M. Pelegrín, "p-median problems," in *Location Science*, G. Laporte, S. Nickel, and F. Saldanha da Gama, Eds., pp. 20–50, Springer, Cham, Switzerland, 2nd edition, 2019.

[38] L. A. N. Lorena and E. L. F. Senne, "Local search heuristics for capacitated p-median problems," *Networks and Spatial Economics*, vol. 3, no. 4, pp. 407–419, 2003.

[39] I. M. Branco and J. D. Coelho, "The Hamiltonian p-median problem," *European Journal of Operational Research*, vol. 47, no. 1, pp. 86–95, 1990.

[40] J. F. Campbell, "Hub location and the p-hub median problem," *Operations Research*, vol. 44, no. 6, pp. 923–935, 1996.

[41] E. Alekseeva, N. Kochetova, Y. Kochetov, and A. Plyasunov, "A hybrid memetic algorithm for the competitive p-median problem," *IFAC Proceedings Volumes*, vol. 42, no. 4, pp. 1533–1537, 2009.

[42] N. Mladenović, J. Brimberg, P. Hansen, and J. A. Moreno-Pérez, "The p-median problem: a survey of metaheuristic approaches," *European Journal of Operational Research*, vol. 179, pp. 927–939, 2007.

[43] R. L. Church and S. Wang, "Solving the p-median problem on regular and lattice networks," *Computers & Operations Research*, vol. 123, p. 105057, 2020.

[44] J. Q. Hale, E. Zhou, and J. Peng, "A Lagrangian search method for the P-median problem," *Journal of Global Optimization*, vol. 69, no. 1, pp. 137–156, 2017.

[45] G. Erdoğan, G. Laporte, and A. M. Rodríguez Chía, "Exact and heuristic algorithms for the Hamiltonian p-median problem," *European Journal of Operational Research*, vol. 253, pp. 280–289, 2016.

[46] T. Bektaş, L. E. Gouveia, and D. Santos, "Revisiting the Hamiltonian p-median problem: a new formulation on directed graphs and a branch-and-cut algorithm," *European Journal of Operational Research*, vol. 276, pp. 40–64, 2019.

[47] F. Stefanello, O. C. B. de Araújo, and F. M. Müller, "Matheuristics for the capacitated p-median problem," *International Transactions in Operational Research*, vol. 22, no. 1, pp. 149–167, 2015.

[48] Z. Drezner and S. Salhi, "Incorporating neighborhood reduction for the solution of the planar p-median problem," *Annals of Operations Research*, vol. 258, no. 2, pp. 639–654, 2017.

[49] J. M. Colmenar, P. Greistorfer, R. Martí, and A. Duarte, "Advanced greedy randomized adaptive search procedure for the obnoxious p-median problem," *European Journal of Operational Research*, vol. 252, no. 2, pp. 432–442, 2016.

[50] B. F. De Azevedo and N. D. Pizzolato, Satoru Ochi, "Proposal for analysis of location of popular residential using the p-median," in *Smart and Digital Cities*, V. Nazário Coelho, I. Machado Coelho, and T. Aparecida de Oliveira, Eds., Springer, Cham, Switzerland, pp. 65–77, 2019.

[51] N. Adler, E. T. Njoya, and N. Volta, "The multi-airline p-hub median problem applied to the African aviation market," *Transportation Research Part A: Policy and Practice*, vol. 107, pp. 187–202, 2018.

[52] A. P. Wheeler, "Creating optimal patrol areas using the p-median model," *Policing: An International Journal*, vol. 42, no. 3, pp. 318–333, 2019.

[53] C. Cintrano, F. Chicano, T. Stützle, and E. Alba, "Studying solutions of the p-median problem for the location of public bike stations," *Lecture Notes in Computer Science*, Springer, Berlin, Germany, pp. 198–208, Article ID 11160, 2018.

[54] M. L. Burkey, J. Bhadury, and H. A. Eiselt, "A location-based comparison of health care services in four U.S. states with efficiency and equity," *Socio-Economic Planning Sciences*, vol. 46, no. 2, pp. 157–163, 2012.

[55] H. Yu, W. D. Solvang, and J. G. Yang, "Improving accessibility and efficiency of service facility through location-based approach: a case study at Narvik university college," *Advanced Materials Research*, vol. 1039, pp. 593–602, 2014.

[56] A. J. King and S. W. Wallace, *Modeling with Stochastic Programming*, Springer-Verlag, New York, NY, USA, 2012.

[57] J. Li, M. González, and Y. Zhu, "A hybrid simulation optimization method for production planning of dedicated remanufacturing," *International Journal of Production Economics*, vol. 117, no. 2, pp. 286–301, 2009.

[58] S. Lidberg, T. Aslam, L. Pehrsson, and A. H. C. Ng, "Optimizing real-world factory flows using aggregated discrete event simulation modelling," *Flexible Services and Manufacturing Journal*, vol. 32, no. 4, pp. 888–912, 2019.

[59] X. Sun, H. Yu, and W. D. Solvang, "Solving the location problem of printers in a university campus using p-median location model and AnyLogic simulation," in *Proceedings of the International Workshop of Advanced Manufacturing and Automation*, pp. 577–584, Springer, Plymouth, UK, November 2019.

[60] M. Hrušovský, E. Demir, W. Jammernegg, and T. Van Woensel, "Hybrid simulation and optimization approach for green intermodal transportation problem with travel time uncertainty," *Flexible Services and Manufacturing Journal*, vol. 30, pp. 486–516, 2018.

[61] Y. Yang, J. Li, and Q. Zhao, "Study on passenger flow simulation in urban subway station based on anylogic," *Journal of Software*, vol. 9, pp. 140–146, 2014.

[62] D. Mourtzis, M. Doukas, and D. Bernidaki, "Simulation in manufacturing: review and challenges," *Procedia CIRP*, vol. 25, pp. 213–229, 2014.

[63] S. Lupin, K. N. Z. Lin, H. Tun, A. M. Thike, and H. H. Linn, "Data structure for GIS based firefighting stations simulations," in *Proceeding of the IEEE Conference of Russian Young Researchers in Electrical and Electronic Engineering (EIConRus)*, pp. 1545–1548, Moscow, Russia, January 2018.

[64] J. Rouzafzoon and P. Helo, "Developing service supply chains by using agent based simulation," *Industrial Management & Data Systems*, vol. 116, no. 2, pp. 255–270, 2016.

[65] P. Helo, J. Rouzafzoon, and A. Gunasekaran, "Service supply chain design by using agent-based simulation," in *Practices and Tools for Servitization*, M. Kohtamäki, T. Baines, R. Rabetino, and A. Bigdeli, Eds., Palgrave Macmillan, Cham, Switzerland, pp. 387–403, 2018.

[66] X. Li, R. Kizito, and T. I. Paula, "An agent-based simulation framework for supply chain disruptions and facility fortification," in *Proceedings of the 2018 Winter Simulation Conference*, pp. 821–832, Gothenburg,, December 2018.

[67] S. Kim, S. Kim, and J. R. Kiniry, "Two-phase simulation-based location-allocation optimization of biomass storage distribution," *Simulation Modelling Practice and Theory*, vol. 86, pp. 155–168, 2018.

[68] V. Elia, M. G. Gnoni, and F. Tornese, "Designing a sustainable dynamic collection service for WEEE: an economic and environmental analysis through simulation," *Waste Management & Research: The Journal for a Sustainable Circular Economy*, vol. 37, no. 4, pp. 402–411, 2019.

[69] V. Marianov and C. ReVelle, "The queueing maximal availability location problem: a model for the siting of emergency vehicles," *European Journal of Operational Research*, vol. 93, no. 1, pp. 110–120, 1996.

[70] R. Swamy, J. E. Kang, R. Batta, and Y. Chung, "Hurricane evacuation planning using public transportation," *Socio-Economic Planning Sciences*, vol. 59, pp. 43–55, 2017.

[71] E. Tekin and I. Sabuncuoglu, "Simulation optimization: a comprehensive review on theory and applications," *IIE Transactions*, vol. 36, no. 11, pp. 1067–1081, 2004.

[72] S. Ahmed, "Two-stage stochastic integer programming: a brief introduction," in *Wiley Encyclopedia of Operations Research and Management Science*, J. J. Cochran, L. A. Cox, P. Keskinocak et al., Eds., Wiley, Hoboken, NJ, USA, 2010.

[73] S. Attia, E. Gratia, A. De Herde, and J. L. M. Hensen, "Simulation-based decision support tool for early stages of zero-energy building design," *Energy and Buildings*, vol. 49, pp. 2–15, 2012.

[74] H. Yu, X. Sun, W. D. Solvang, G. Laporte, and C. K. M. Lee, "A stochastic network design problem for hazardous waste management," *Journal of Cleaner Production*, vol. 277, Article ID 123566, 2020.

[75] A. J. Kleywegt, A. Shapiro, and T. Homem-De-Mello, "The sample average approximation method for stochastic discrete optimization," *SIAM Journal on Optimization*, vol. 12, no. 2, pp. 479–502, 2002.

[76] SSB, "Key figures for the population," 2019, https://www.ssb.no/en/befolkning/nokkeltall/population.

[77] B. Wang, S. Brême, and Y. B. Moon, "Hybrid modeling and simulation for complementing lifecycle assessment," *Computers & Industrial Engineering*, vol. 69, pp. 77–88, 2014.

[78] Municipality of Narvik, "Demography," 2016, https://ugeo.urbistat.com/AdminStat/en/no/demografia/dati-sintesi/narvik/20485108/4.

[79] M. S. Pishvaee and S. A. Torabi, "A possibilistic programming approach for closed-loop supply chain network design under uncertainty," *Fuzzy Sets and Systems*, vol. 161, no. 20, pp. 2668–2683, 2010.

[80] H. Yu and W. D. Solvang, "A comparison of two location models in optimizing the decision-making on the relocation problem of post offices at Narvik, Norway," in *Proceedings of the IEEE International Conference on Industrial Engineering and Engineering Management (IEEM)*, pp. 814–818, Bangkok, Thailand, December 2018.

Hindawi
Scientific Programming
Volume 2021, Article ID 5561357, 15 pages
https://doi.org/10.1155/2021/5561357

Research Article

Decision and Coordination of Cross-Border E-Commerce Supply Chain: Based on Four Modes of Cooperation

Wei Yan,[1] Huijun Zhou,[2] and Hui Li[3]

[1]*Logistics Engineering College, Shanghai Maritime University, Shanghai 201306, China*
[2]*School of Economics and Management, Shanghai Maritime University, Shanghai 201306, China*
[3]*School of Management, Guangxi University for Nationalities, Nanning 530006, China*

Correspondence should be addressed to Huijun Zhou; hjzhou@shmtu.edu.cn and Hui Li; lihui_1011@163.com

Received 6 February 2021; Accepted 26 April 2021; Published 7 May 2021

Academic Editor: Lu Zhen

Copyright © 2021 Wei Yan et al. This is an open access article distributed under the Creative Commons Attribution License, which permits unrestricted use, distribution, and reproduction in any medium, provided the original work is properly cited.

Due to the explosive growth trend of cross-border e-commerce, a series of problems such as high transportation costs and insufficient publicity are to be solved urgently by researching on supply chain from both decision-making and coordination perspectives. Under the four-incomplete cooperative Stackelberg decision-making modes of cross-border e-commerce supply chain members, the transportation cost of overseas suppliers and the promotion strategy of domestic retailers determine the profit of the supply chain together and further influence the choice of the optimal decision-making plan. Furthermore, the Shapley value method and full cooperative income incremental sharing mechanism are used to redistribute the profits under different cooperation modes, and it is expected to provide scientific decision-making reference for domestic cross-border e-commerce enterprises to rationally choose cooperative relationships.

1. Introduction

With the increasing popularity of Internet technology and the improvement in payment system and the influence of new coronavirus (COVID-19), more and more consumers are buying imported goods through cross-border e-commerce platforms. Therefore, the import cross-border e-commerce shows an explosive growth trend. According to the data released by China E-Commerce Research Center (100%) EC, the transaction volume of China's import cross-border e-commerce market in 2019 is 2.47 trillion yuan, an increase of nearly 30% over 2018, and it is expected to reach 29.66 trillion yuan in 2020.

The vigorous development of cross-border e-commerce has not only greatly enriched the product supply in the domestic market but also exposed a series of problems in the supply chain management of cross-border e-commerce in China [1]. On the one hand, the high transportation cost of cross-border e-commerce (accounting for about 20%~30% of the total cost) not only increases the purchase cost of consumers but also reduces the profits of middlemen; on the other hand, due to the insufficient publicity of cross-border e-commerce, the single channel of commodity promotion, it is difficult for retailers to avoid the third-party e-commerce platform, which increases the intermediate links and weakens the profits of domestic cross-border e-commerce enterprises ability [2].

Therefore, in order to solve the vicious competition cycle caused by the non-cooperative game between overseas e-commerce and domestic retailers, it is urgent to study the influence of changes in transportation costs and propaganda strategy on the pricing strategy and member profit distribution of cross-border e-commerce supply chain. In this paper, we focus on the following question: first, in the decentralized and centralized scenario, how do the members in the cross-border e-commerce supply chain make decisions; second, how do the influences of transport cost and advertising cost on the decisions; finally, which can coordination mechanism effectively balance the stakeholders to make the total performance maximization.

From the existing literature, the research related to the above contents mainly focuses on the following two aspects:

(1) Influence of advertising strategy on supply chain decision-making

Based on the supply chain of manufacturers and retailers, study the problems of price promotion and advertising strategy of manufacturers [3]; considering the problem that advertising investment restricts market demand, discuss the optimal decision-making and coordination mechanism under the mode of concentration and dispersion of single- and double-channel supply chain [4]; by using the consumer demand function, explore the cooperative advertising and supply chain coordination of pricing [5]; from the perspective of the dynamic influence of advertising on market demand, discuss the issues of manufacturer's advertisement competition and manufacturer-retailer channel price competition [6]; on the basis of the influence of innovation and advertising on the demand of commodity market, probe into the optimal decision-making of supply chain members under cooperative and non-cooperative mechanisms [7].

(2) Influence of transport costs on supply chain decision-making

To reduce transport costs and divide the cross-border e-commerce costs into management cost, logistics cost, and sale cost [8]; different supply chain logistics cost-sharing strategies are applied to explore the influence on supply chain profit through the study of the impact of tariffs, transport costs on global value chains, find that the rise of trade costs such as tariffs will increase the investment of enterprises and the purchase price of raw materials [9]; based on the game model of cross-border supply chain led by retailers, introduce the index of tariff and international transportation cost to analyze the influence of tariff change in commodity pricing and member profit of cross-border supply chain [10]; the optimized countermeasure is applied to how to use overseas warehouse to realize the timeliness of cross-border logistics in order to reduce transportation cost; consider that logistics cost has an important impact on cross-border e-commerce imports and then make a deep study on the cost optimization of cross-border e-commerce logistics [11, 12].

(3) Influence of coordination contract on supply chain decision-making

Through the supply chain contract to coordinate the decision-making behavior among the members, the profit can be optimized. Under the uncertain environment, Peng et al. [13] proposed a unidirectional option contract and bidirectional option contract to coordinate supply chain members and analyze their different impacts on members. Xu et al. [14] introduced the revenue sharing and cost sharing into designing an improved contract to coordinate the participates effectively. Designed the decision model for the nongreen and green products pricing to ensure the supply chain's participants achieve Pareto improvement. Dai et al. [15] designed the delivery-time-dependent quantity flexibility contract and late-rebate contract to balance the stakeholders under the uncertain demand. Liu et al. [16] discussed whether an option contract coordinated the members effectively when express delivery was provided from retailer.

Through the analysis of the above literature, it is found that the research methods of supply chain are rich and mature, which provide a specific reference for this paper from the technical point of view. However, most of the research results on supply chain publicity and transportation costs are concentrated in the traditional production enterprises. There are few studies on the influence of publicity strategy and transportation cost on cross-border e-commerce pricing strategy. There is little research on the influence of supplier retailer cooperation mode on supply chain pricing at home and abroad.

Based on this, from the perspective of cross-border e-commerce supply chain pricing and publicity strategies under different cooperation modes, this paper discusses the coordination of cross-border e-commerce supply chain pricing strategy and member profit distribution, as well as how cross-border e-commerce enterprises cope with the impact of changes. In terms of transportation cost and publicity level, this paper makes optimization decisions for cross-border e-commerce supply chain members to optimize cross-border e-commerce supply chain e-commerce supply chain member's profit. Cross-border e-commerce supply chain provides a scientific reference for the rapid and healthy development of China's e-commerce industry.

2. Model Hypothesis

Hypothesis 1. Domestic retailers use a variety of promotional tools to enable consumers to buy their goods, and according to [17], the demand function is not only affected by retail price but also by propaganda strategy, so suppose the demand function $d(p, \theta_2) = a - p + \lambda\theta_2$, in which "$a$" for the potential market demand, "p" for the retail prices per unit product of domestic retailers, "λ" for consumer sensitivity to retailer propaganda ($\lambda > 0$), and "θ_2" for the domestic retailer's propaganda strategy.

Hypothesis 2. According to [18], wholesale price for unit products of overseas suppliers is w, and the transportation cost per unit product is a linear relationship of monotone decreasing with the volume of transport, so $c_d = c - \rho\ d(p, \theta_2)$, in which "$\rho$" is for marginal transport cost factor for unit product ($\rho > 0$) and "c" is fixed transport costs per unit product (i.e., fixed transport costs per unit product regardless of economies of scale).

Hypothesis 3. Domestic retailers promote the extra cost of product propaganda. Assume the publicity costs of domestic retailers $C(\theta_2) = K_2\theta_2^2/2$, in which K_2 indicates the scale of domestic retailer propaganda activity.

Hypothesis 4. If only the cost of transportation of products from overseas suppliers to domestic suppliers is considered, the cost of transportation from domestic retailers to consumers is ignored.

Hypothesis 5. Overseas suppliers and domestic retailers are completely rational persons, and the decision information of both sides is completely symmetrical.

3. Construction of Cross-Border E-Commerce Supply Chain Decision Model

In view of the space limitation, this paper mainly studies the decision-making problem under the two-level cross-border supply chain cooperation mode composed of a single overseas supplier and a single domestic retailer; that is, the overseas supplier sells the goods to the domestic retailer and bears the transportation cost. Clearly, the overseas supplier and the domestic retailer form a kind of Stackelberg cooperation relationship, and the overseas supplier is the decision-maker, while the domestic retailer is the decision follower.

By constructing decision-making models of non-cooperation, semi-cooperation (including two kinds of one-way cooperation modes of retailers sharing transportation cost and supplier sharing propaganda cost), and full cooperation between overseas suppliers and domestic retailers, it can clarify the influence of pricing and propaganda strategy on profit of cross-border e-commerce supply chain and provide scientific decision reference for rational selection of cooperative relationship.

Furthermore, the introduction of Shapley value method and the incremental benefit sharing mechanism for full cooperation is beneficial to the rational redistribution of profits of overseas suppliers and domestic retailers under different cooperation modes.

3.1. Decision-Making in the Non-Cooperative Model of Suppliers and Retailers (N). Under this model, overseas suppliers usually set wholesale prices w^N first, and then, domestic retailers determine retail prices P^N and publicity strategies θ_2^N.

Thus, the profits of overseas suppliers and domestic retailers under the non-cooperation mode are as follows:

$$\begin{aligned} \pi_m^N &= (w-c)(a-p+\lambda\theta_2) + \rho(a-p+\lambda\theta_2)^2, \\ \pi_r^N &= (p-w)(a-p+\lambda\theta_2) - \frac{1}{2}K_2\theta_2^2. \end{aligned} \tag{1}$$

Proposition 1. *Under the non-cooperation structure of overseas suppliers and domestic retailers, the optimal decision of cross-border e-commerce supply chain is*

$$w^{N*} = \frac{2(a+c-a\rho)K_2 - (a+c)\lambda^2}{2\left[(2-\rho)K_2 - \lambda^2\right]}, \tag{2}$$

$$P^{N*} = \frac{(c+3a-2a\rho)K_2 - (a+c)\lambda^2}{2\left[(2-\rho)K_2 - \lambda^2\right]}, \tag{3}$$

$$\theta_2^{N*} = \frac{(a-c)\lambda}{2\left[(2-\rho)K_2 - \lambda^2\right]}. \tag{4}$$

Proof. The reverse induction method is used to solve the problem.

Firstly, determine the Hessian matrix for the domestic retailer profit function π_r^N:

$$H(p,\theta_2) = \begin{bmatrix} \dfrac{\partial^2\pi_r^N}{\partial\left(P^N\right)^2} & \dfrac{\partial^2\pi_r^N}{\partial P^N\partial\theta_2^N} \\ \dfrac{\partial^2\pi_r^N}{\partial\theta_2^N\partial P^N} & \dfrac{\partial^2\pi_r^N}{\partial\left(\theta_2^N\right)^2} \end{bmatrix} = \begin{bmatrix} -2 & \lambda \\ \lambda & -K_2 \end{bmatrix}. \tag{5}$$

It is not difficult to see from the above Hessian matrix: $(\partial^2\pi_r^N/\partial(P^N)^2) = -2 < 0$ and $|H| = 2K_2 - \lambda^2 > 0$; π_r^N is a strictly joint concave function about P^N and $c\ \theta_2^N$, and there is an optimal solution to maximize profits.

Secondly, first-order partial derivative conditions are as follows: $\overline{p^N} = ((a+w)K_2 - w\lambda^2/2K_2 - \lambda^2)$ and $\overline{\theta_2^N} = ((a-w)\lambda/2K_2 - \lambda^2)$ substituted into formula (1), and the second-order derivative function of profit function of overseas suppliers can be obtained as $(\partial^2\pi_m^N/\partial(w^N)^2) = -(2K_2[(2-\rho)K_2 - \lambda^2]/(2K_2 - \lambda^2)^2) < 0$.

It can be seen that π_m^N is a strict concave function about w^N, and there is an optimal solution to maximize profit, and thus, the first-order partial derivative condition is $w^{N*} = (2[a(1-\rho)+c)K_2 - (a+c)\lambda^2/2[(2-\rho)K_2 - \lambda^2])$; decisions available to domestic retailers are $P^{N*} = ((c+3a-2a\rho)K_2 - (a+c)\lambda^2/2[(2-\rho)K_2 - \lambda^2])$ and $\theta_2^{N*} = ((a-c)\lambda/[2(2-\rho)K_2 - \lambda^2])$. Now, the commodity market demand and the profits of the members of the cross-border e-commerce supply chain are

$$d^{N*} = \frac{(a-c)K_2}{2\left[(2-\rho)K_2 - \lambda^2\right]}, \tag{6}$$

$$\pi_m^{N*} = \frac{(a-c)^2K_2}{4\left[(2-\rho)K_2 - \lambda^2\right]}, \tag{7}$$

$$\pi_r^{N*} = \frac{(a-c)^2\left(2K_2 - \lambda^2\right)K_2}{8\left[(2-\rho)K_2 - \lambda^2\right]^2}. \tag{8}$$

From the above equilibrium results, we can see that the pricing of cross-border e-commerce supply chain is inversely proportional to the unit transportation cost, while the propaganda strategy of domestic retailers and the profits of supply chain members are all proportional to the unit

transportation cost; that is, $(\partial w^{N*}/\partial\rho) < 0$, $(\partial p^{N*}/\partial\rho) < 0$, $(\partial\theta_2^{N*}/\partial\rho) < 0$, $(\partial\pi_m^{N*}/\partial\rho) < 0$, $(\partial\pi_r^{N*}/\partial\rho) < 0$. □

3.2. Decision-Making under the One-Way Cooperation Mode for Retailers Sharing Suppliers' Transportation Costs (M). Based on their own profit maximization under this mode, domestic retailers will share the transportation costs of overseas suppliers in proportion of $\theta_m\,(0 \le \theta_m \le 1)$.

Obviously, when $\theta_m = 0$, domestic retailers are unwilling to share the transportation costs of overseas suppliers, and when $\theta_m = 1$, domestic retailers are willing to share the full transportation costs of overseas suppliers.

Under established θ_m, overseas suppliers usually set wholesale prices w^M, and then, domestic retailers determine retail price P^M and publicity strategy θ_2^M.

Therefore, the profits of overseas suppliers and domestic retailers under this cooperation model are

$$\pi_m^M = \{w - (1-\theta_m)[c - \rho(a - p + \lambda\theta_2)]\}(a - p + \lambda\theta_2),$$
$$\pi_r^M = \{p - w - \theta_m[c - \rho(a - p + \lambda\theta_2)]\}(a - p + \lambda\theta_2) - \frac{1}{2}K_2\theta_2^2. \tag{9}$$

Proposition 2. *Under the one-way cooperation mode of domestic retailers sharing the transportation cost of overseas suppliers, the optimal decision of cross-border e-commerce supply chain is as follows:*

$$\theta_m^{M*} = 1, \tag{10}$$

$$w^{M*} = \frac{a-c}{2}, \tag{11}$$

$$p^{M*} = \frac{[c + a(3-4\rho)]K_2 - (a+c)\lambda^2}{2\left[2(1-\rho)K_2 - \lambda^2\right]}, \tag{12}$$

$$\theta_2^{M*} = \frac{(a-c)\lambda}{2\left[2(1-\rho)K_2 - \lambda^2\right]}. \tag{13}$$

Proof. The reverse induction method is used to solve the problem.

Firstly, determine Hessian matrix for the domestic retailer profit function π_r^M:

$$H(p,\theta_2) = \begin{bmatrix} \dfrac{\partial^2\pi_r^M}{\partial\left(P^M\right)^2} & \dfrac{\partial^2\pi_r^M}{\partial P^M\partial\theta_2^M} \\ \dfrac{\partial^2\pi_r^M}{\partial\theta_2^M\partial P^M} & \dfrac{\partial^2\pi_r^M}{\partial\left(\theta_2^M\right)^2} \end{bmatrix} = \begin{bmatrix} -2(1-\rho\theta_m) & \lambda(1-\rho\theta_m) \\ \lambda(1-\rho\theta_m) & -K_2 + 2\lambda^2\rho\theta_m \end{bmatrix}. \tag{14}$$

It is not difficult to see from the above Hessian matrix: $(\partial^2\pi_r^M/\partial(P^M)^2) = -2(1-\rho\theta_m) < 0$ and $|H| = 2K_2(1-\rho\theta_m) - \lambda^2 > 0$; π_r^M is a strictly joint concave function about P^M and θ_2^M, and there is an optimal solution to maximize profits.

Secondly, first-order partial derivative conditions are as follows: $p^M = (K_2[a + w + (c - 2a\rho)\theta_m] - \lambda^2(w + c\theta_m)/2K_2(1-\rho\theta_m) - \lambda^2)$ and $\theta_2^M = (\lambda(a - w - c\theta_m)/2K_2(1-\rho\theta_m) - \lambda^2)$ substituted into formula (2), and the second-order derivative function of profit function of overseas suppliers can be obtained as $(\partial^2\pi_m^M/\partial(w^M)^2) = -(2K_2\{K_2[2-\rho(1+\theta_m)] - \lambda^2\}/[2K_2(1-\rho\theta_m) - \lambda^2]^2) < 0$.

It can be seen that π_m^M is a strict concave function about w^M, and there is an optimal solution to maximize profit; thus, the first-order partial derivative condition is $w^M(\theta_m) = (2K_2[a(1-\rho) + c(1 - 2\theta_m + \rho\theta_m^2)] - \lambda^2(a + c - 2c\theta_m)/2\{K_2[2-\rho(1+\theta_m)] - \lambda^2\})$, and decisions available to domestic retailers are $p^M(\theta_m)$ and $\theta_2^M(\theta_m)$. The profits of domestic retailers are $\pi_r^M(\theta_m) = ((a-c)^2K_2[2K_2(1-\rho\theta_m) - \lambda^2]/8\{K_2[2-\rho(1+\theta_m)] - \lambda^2\}^2)$.

Moreover, according to $(\partial^2\pi_r^M(\theta_m)/\partial(\theta_m)^2) < 0$, π_r^M is a strict concave function about θ_m, which has the optimal solution to maximize the profit of domestic retailers, so substituting the first-order partial derivative condition $\theta_m^{M*} = 1$ into formula $w^M(\theta_m)$, $p^M(\theta_m)$, and $\theta_2^M(\theta_m)$, the optimal decisions of overseas suppliers and domestic retailers are w^{M*}, p^{M*}, and θ_2^{M*}.

Finally, it can be concluded that the market demand of commodities and the profits of each member of cross-border e-commerce supply chain are as follows:

$$d^{M*} = \frac{(a-c)K_2}{2\left[2(1-\rho)K_2 - \lambda^2\right]},$$
$$\pi_m^{M*} = \frac{(a-c)^2K_2}{4\left[2(1-\rho)K_2 - \lambda^2\right]}, \tag{15}$$
$$\pi_r^{M*} = \frac{(a-c)^2K_2}{8\left[2(1-\rho)K_2 - \lambda^2\right]}.$$

It can be seen that, in the semi-cooperative mode of retailers sharing the transportation costs with suppliers, domestic retailers are generally willing to share the total transportation costs of overseas suppliers in order to maximize their profits. Also, the cost of transportation will eventually be passed on to consumers by domestic retailers. □

3.3. Decision-Making under the One-Way Cooperation Model for Suppliers Sharing Retailers' Publicity Costs (R). Based on their own profit maximization under this mode, most of the overseas suppliers in this model will share the publicity cost with domestic retailers in proportion of $\theta_r\,(0 \le \theta_r \le 1)$.

Obviously, when $\theta_r = 0$, overseas suppliers are unwilling to share the promotional costs of domestic retailers; when $\theta_r = 1$, overseas suppliers are willing to share the full promotional costs of domestic retailers. Under established condition θ_r, overseas suppliers usually set wholesale prices w^R first, and then, domestic retailers determine retail prices P^R and publicity strategies θ_2^R.

Therefore, the profits of overseas suppliers and domestic retailers under this cooperation model are

$$\pi_m^R = (w-c)(a-p+\lambda\theta_2) + \rho(a-p+\lambda\theta_2)^2 - \frac{1}{2}\theta_r K_2 \theta_2^2,$$

$$\pi_r^R = (p-w)(a-p+\lambda\theta_2) - \frac{1}{2}(1-\theta_r)K_2\theta_2^2. \tag{16}$$

Proposition 3. *Under the one-way cooperation mode of overseas suppliers sharing the propaganda cost of domestic retailers, the optimal decision of cross-border e-commerce supply chain is as follows:*

$$\theta_r^{R*} = \frac{1}{3}, \tag{17}$$

$$w^{R*} = \frac{8(a+c-a\rho)K_2 - 3(a+2c)\lambda^2}{8(2-\rho)K_2 - 9\lambda^2}, \tag{18}$$

$$p^{R*} = \frac{4[c+a(3-2\rho)]K_2 - 3(a+2c)\lambda^2}{8(2-\rho)K_2 - 9\lambda^2}, \tag{19}$$

$$\theta_2^{R*} = \frac{6(a-c)\lambda}{8(2-\rho)K_2 - 9\lambda^2}. \tag{20}$$

Proof. Proof. The reverse induction method is used to solve the problem.

Firstly, determine the π_r^R Hessian matrix for the domestic retailer profit function:

$$H(p,\theta_2) = \begin{bmatrix} \dfrac{\partial^2 \pi_r^R}{\partial (P^R)^2} & \dfrac{\partial^2 \pi_r^R}{\partial P^R \partial \theta_2^R} \\ \dfrac{\partial^2 \pi_r^R}{\partial \theta_2^R \partial P^R} & \dfrac{\partial^2 \pi_r^R}{\partial (\theta_2^R)^2} \end{bmatrix} = \begin{bmatrix} -2(1-\rho\theta_m) & \lambda(1-\rho\theta_m) \\ \lambda(1-\rho\theta_m) & -K_2 + 2\lambda^2\rho\theta_m \end{bmatrix}. \tag{21}$$

It is not difficult to see from the above Hessian matrix, $(\partial^2 \pi_r^R/\partial (P^R)^2) = -2(1-\rho\theta_m) < 0$ and $|H| = 2K_2(1-\rho\theta_m) - \lambda^2 > 0$; π_r^R is a strictly joint concave function about P^R and θ_2^R, and there is an optimal solution to maximize profits; thus, the first-order partial derivation condition is $\overline{p^R} = ((a+w)K_2(1-\theta_r) - w\lambda^2/2K_2(1-\theta_r) - \lambda^2)$ and $\overline{\theta_2^R} = ((a-w)\lambda/2K_2(1-\theta_r) - \lambda^2)$. Substituting $\overline{p^R}$ and $\overline{\theta_2^R}$ into formula (2), the second-order derivative function of profit function of overseas suppliers can be obtained. When $0 < \rho < (4K_2(1-\theta_r)^2 - \lambda^2(2-3\theta_r)/2K_2(1-\theta_r)^2)$, $(\partial^2 \pi_m^R/\partial (w^R)^2) = -(K_2[2(2-\rho)K_2(1-\theta_r)^2 - \lambda^2(2-3\theta_r)]/[2K_2(1-\theta_r) - \lambda^2]^2) < 0$.

It can be seen that π_m^M is the strict concave function about w^M, and there is an optimal solution to maximize profits. Therefore, the first-order partial derivative condition is $w^R(\theta_r) = (2(a+c-a\rho)K_2(1-\theta_r)^2 - \lambda^2[a+c-(2a+c)\theta_r]/2(2-\rho)K_2(1-\theta_r)^2 - \lambda^2(2-3\theta_r))$, decisions of domestic retailers are $p^R(\theta_r)$ and $\theta_2^R(\theta_r)$, and profits from overseas suppliers at this time are $\pi_m^R(\theta_r) = ((a-c)^2 K_2(1-\theta_r)^2/2[2(2-\rho)K_2(1-\theta_r)^2 - \lambda^2(2-3\theta_r)])$.

According to $(\partial^2 \pi_m^R(\theta_r)/\partial(\theta_r)^2) < 0$, π_r^R is the strict concave function about θ_r, and there is an optimal solution to maximize the profits of overseas suppliers, so the first-order partial derivative condition is $\theta_r^{R*} = (1/3)$.

Substituting θ_r^{R*} into formula $w^R(\theta_r)$, $p^R(\theta_r)$, and $\theta_2^R(\theta_r)$, respectively, optimal decision-making available for overseas suppliers and domestic retailers can be obtained as w^{R*}, p^{R*}, and θ_2^{R*}.

Finally, the market demand for commodities and the profits of members of cross-border e-commerce supply chains are

$$d^{R*} = \frac{4(a-c)K_2}{8(2-\rho)K_2 - 9\lambda^2},$$

$$\pi_m^{R*} = \frac{2(a-c)^2 K_2}{8(2-\rho)K_2 - 9\lambda^2}, \tag{22}$$

$$\pi_r^{R*} = \frac{4(a-c)^2 K_2 (4K_2 - 3\lambda^2)}{[8(2-\rho)K_2 - 9\lambda^2]^2}.$$

In the semi-cooperative mode of supplier sharing retailer's propaganda cost, foreign suppliers are mostly willing to share 1/3 propaganda cost of domestic retailers in order to maximize their profits. □

3.4. Decision-Making under the Two-Way Cooperation Mode in Which Retailers Share Transportation Costs and Suppliers Share Publicity Costs (MR). The domestic retailers in this mode share the transportation costs of overseas suppliers in proportion of $\theta_m (0 \le \theta_m \le 1)$ based on their own profit maximization considerations, and the overseas suppliers share the propaganda costs of domestic retailers in proportion of $\theta_r (0 \le \theta_r \le 1)$ based on their own profit maximization considerations.

Under established condition θ_m and θ_r, overseas suppliers will first determine wholesale prices, and then, domestic retailers determine retail prices P^{MR} and publicity strategies θ_2^{MR}.

Under this condition, the profit of overseas suppliers and domestic retailers under the cooperation mode is

$$\pi_m^{\mathrm{MR}*} = \{w - (1-\theta_m)[c - \rho(a - p + \lambda\theta_2)]\}(a - p + \lambda\theta_2) - \frac{1}{2}\theta_r K_2 \theta_2^2,$$
$$\pi_r^{\mathrm{MR}*} = \{p - w - \theta_m[c - \rho(a - p + \lambda\theta_2)]\}(a - p + \lambda\theta_2) - \frac{1}{2}(1-\theta_r)K_2\theta_2^2. \tag{23}$$

Proposition 4. *Under the two-way cooperation mode between overseas suppliers and domestic retailers, the optimal decision of cross-border e-commerce supply chain is*

$$\theta_m^{\mathrm{MR}*} = \left(1 - \frac{3\lambda^2}{8\rho K_2}\right), \tag{24}$$

$$\theta_r^{\mathrm{MR}*} = \frac{1}{3}, \tag{25}$$

$$w^{\mathrm{MR}*} = \frac{4(a-c)\rho K_2 + 3c\lambda^2}{8\rho K_2}, \tag{26}$$

$$p^{\mathrm{MR}*} = \frac{2[c + a(3-4\rho)]K_2 - 3c\lambda^2}{8(1-\rho)K_2 - 3\lambda^2}, \tag{27}$$

$$\theta_2^{\mathrm{MR}*} = \frac{3(a-c)\lambda}{8(1-\rho)K_2 - 3\lambda^2}. \tag{28}$$

Proof. The reverse induction method is used to solve the problem.

Firstly, determine the π_r^{MR} Hessian matrix for the domestic retailer profit function:

$$H(p,\theta_2) = \begin{bmatrix} \dfrac{\partial^2 \pi_r^{\mathrm{MR}}}{\partial (P^{\mathrm{MR}})^2} & \dfrac{\partial^2 \pi_r^{\mathrm{MR}}}{\partial P^{\mathrm{MR}} \partial \theta_2^{\mathrm{MR}}} \\ \dfrac{\partial^2 \pi_r^{\mathrm{MR}}}{\partial \theta_2^{\mathrm{MR}} \partial P^{\mathrm{MR}}} & \dfrac{\partial^2 \pi_r^{\mathrm{MR}}}{\partial (\theta_2^{\mathrm{MR}})^2} \end{bmatrix} = \begin{bmatrix} -2(1-\rho\theta_m) & \lambda(1-\rho\theta_m) \\ \lambda(1-\rho\theta_m) & -K_2 + 2\lambda^2\rho\theta_m \end{bmatrix}. \tag{29}$$

It is not difficult to see from the above Hessian matrix: $(\partial^2 \pi_r^{\mathrm{MR}}/\partial (P^{\mathrm{MR}})^2) = -2(1-\rho\theta_m) < 0$ and $|H| = 2K_2(1-\rho\theta_m)(1-\theta_r) - \lambda^2 > 0$. Thus, π_r^R is a strictly joint concave function about P^R and θ_2^R, and there is an optimal solution to maximize profits.

Secondly, first-order partial derivation conditions are as follows:

$$\overline{p^{\mathrm{MR}}} = \frac{K_2[a + w + (c - 2a\rho)\theta_m](1-\theta_r) - \lambda^2(w + c\theta_m)}{2K_2(1-\rho\theta_m)(1-\theta_r) - \lambda^2},$$
$$\overline{\theta_2^{\mathrm{MR}}} = \frac{\lambda(a - w - c\theta_m)}{2K_2(1-\rho\theta_m)(1-\theta_r) - \lambda^2}. \tag{30}$$

Substituting $\overline{p^{\mathrm{MR}}}$ and $\overline{\theta_2^{\mathrm{MR}}}$ into formula (7), the second-order derivative of the profit function of overseas suppliers can be obtained.

When $0 < \rho < (4K_2(1-\theta_r)^2 - \lambda^2(2-3\theta_r)/2K_2(1+\theta_m)(1-\theta_r)^2)$,

$$\frac{\partial^2 \pi_m^R}{\partial (w^R)^2} = -\frac{K_2\{2K_2[2-\rho(1+\theta_m)](1-\theta_r)^2 - \lambda^2(2-3\theta_r)\}}{[2K_2(1-\rho\theta_m)(1-\theta_r) - \lambda^2]^2} < 0. \tag{31}$$

It can be seen that π_m^{MR} is the strict concave function about w^{MR}, and there is an optimal solution to maximize profits. Therefore, the first-order partial derivative condition is $w^{\mathrm{MR}}(\theta_m,\theta_r) = (2K_2[a(1-\rho) + c(1-2\theta_m + \rho\theta_m^2)](1-\theta_r)^2 - \lambda^2[a + c - c\theta_m(2-3\theta_r) - (2a+c)\theta_r]/2K_2[2-\rho(1+\theta_m)](1-\theta_r)^2 - \lambda^2(2-3\theta_r))$, so decision-making by domestic retailers is $p^{\mathrm{MR}}(\theta_m,\theta_r)$ and $\theta_2^{\mathrm{MR}}(\theta_m,\theta_r)$.

At this point, the profits of the cross-border e-commerce supply chain are

$$\pi_m^{\mathrm{MR}}(\theta_m,\theta_r) = \frac{(a-c)^2 K_2(1-\theta_r)^2}{2(2K_2(2-\rho(1+\theta_m))(1-\theta_r)^2 - \lambda^2(2-3\theta_r))},$$
$$\pi_r^{\mathrm{MR}}(\theta_m,\theta_r) = \frac{(a-c)^2 K_2[2K_2(1-\rho\theta_m)(1-\theta_r) - \lambda^2](1-\theta_r)^3}{2\{2K_2[2-\rho(1+\theta_m)](1-\theta_r)^2 - \lambda^2(2-3\theta_r)\}^2}. \tag{32}$$

According to $(\partial \pi_r^{\mathrm{MR}}(\theta_m,\theta_r)/\partial\theta_m) = 0$ and $(\partial \pi_m^{\mathrm{MR}}(\theta_m,\theta_r)/\partial\theta_r) = 0$, the optimal proportion of overseas suppliers and domestic retailers sharing each other's corresponding costs, under this cooperation mode, is $\begin{cases} \theta_m^{\mathrm{MR}*} = 1 - (3\lambda^2/8\rho K_2) \\ \theta_r^{\mathrm{MR}*} = (1/3) \end{cases}$.

Substituting $\theta_m^{\mathrm{MR}*}$ and $\theta_r^{\mathrm{MR}*}$ into $w^{\mathrm{MR}}(\theta_m,\theta_r)$, $p^{\mathrm{MR}}(\theta_m,\theta_r)$, and $\theta_2^{\mathrm{MR}}(\theta_m,\theta_r)$, respectively, optimal decisions for overseas suppliers and domestic retailers can be obtained as $w^{\mathrm{MR}*}$, $p^{\mathrm{MR}*}$, and $\theta_2^{\mathrm{MR}*}$.

Finally, it can be determined that the commodity market demand and the profits of the members of the cross-border e-commerce supply chain are as follows:

$$d^{\mathrm{MR}*} = \frac{2(a-c)K_2}{8(1-\rho)K_2 - 3\lambda^2},$$
$$\pi_m^{\mathrm{MR}*} = \frac{(a-c)^2 K_2}{8(1-\rho)K_2 - 3\lambda^2}, \tag{33}$$
$$\pi_r^{\mathrm{MR}*} = \frac{(a-c)^2 K_2}{2(8(1-\rho)K_2 - 3\lambda^2)}.$$

Under the two-way cooperation mode between overseas suppliers and domestic retailers, retailers are no longer willing to share the total transportation costs of suppliers, but suppliers are still willing to share one-third of the promotional costs of retailers. □

4. Comparative Analysis

Proposition 5. *Under the specific unit transportation cost, the pricing decisions of different cooperation modes satisfy the following:*

$$\begin{aligned} w^{R*} > w^{N*} > w^{\mathrm{MR}*} > w^{M*}, \\ p^{R*} > p^{N*} > p^{\mathrm{MR}*} > p^{M*}. \end{aligned} \tag{34}$$

Proof. According to the above proposition, comparing the optimal solutions under the four different cooperation modes, the following relationships can be found:

$$\begin{aligned} w^{R*} - w^{N*} &= \frac{(a-c)\lambda^2\left[(6-4\rho)K_2 - 3\lambda^2\right]}{2\left[(2-\rho)K_2 - \lambda^2\right]\left[8(2-\rho)K_2 - 9\lambda^2\right]} > 0, \\ w^{N*} - w^{MR*} &= \frac{4\rho[4c-(c+a)\rho]K_2^2 - c\lambda^2(6+5\rho)K_2 + 3c\lambda^4}{8\rho K_2\left[(2-\rho)K_2 - \lambda^2\right]} > 0, \\ w^{MR*} - w^{M*} &= \frac{3c\lambda^2}{8\rho K_2} > 0, \\ p^{R*} - p^{N*} &= \frac{(a-c)\lambda^2\left[(7-4\rho)K_2 - 3\lambda^2\right]}{2\left[(2-\rho)K_2 - \lambda^2\right]\left[8(2-\rho)K_2 - 9\lambda^2\right]} > 0, \\ p^{N*} - p^{MR*} &= \frac{(a-c)\left[4\rho K_2^2 - \lambda^2(5+2\rho)K_2 + 3\lambda^4\right]}{2\left[(2-\rho)K_2 - \lambda^2\right]\left[8(1-\rho)K_2 - 3\lambda^2\right]} > 0, \\ p^{MR*} - p^{M*} &= \frac{(a-c)\lambda^2\left[(5-4\rho)K_2 - 3\lambda^2\right]}{2\left[2(1-\rho)K_2 - \lambda^2\right]\left[8(1-\rho)K_2 - 3\lambda^2\right]} > 0. \end{aligned} \tag{35}$$

It is found from Proposition 5 that, when overseas suppliers share part of the publicity costs of domestic retailers, the premise of raising or lowering wholesale prices is that domestic retailers are willing to share all or part of their transportation costs. Also, the retail price ranking of domestic retailers is consistent with the wholesale price ranking of overseas suppliers. More importantly, in the pricing decision of cross-border e-commerce supply chain, the cost of upstream enterprises will be transferred directly to downstream enterprises and eventually apportioned to each consumer. □

Proposition 6. *Under the specific unit transportation cost, the propaganda strategy of different cooperation modes satisfies the following:*

When $0 < \rho < (8K_2 - 3\lambda^2/16K_2)$, $\theta_2^{MR} > \theta_2^R > \theta_2^M > \theta_2^N$.

When $(8K_2 - 3\lambda^2/16K_2) < \rho < 1$, $\theta_2^{MR} > \theta_2^M > \theta_2^R > \theta_2^N$.

Proof. According to the above proposition, comparing the optimal solutions under the four different cooperation modes, the following relationships can be found:

$$\begin{aligned} \theta_2^{\mathrm{MR}*} - \theta_2^{R*} &= \frac{3(a-c)\lambda\left(8\rho K_2 - 3\lambda^2\right)}{\left[8(2-\rho)K_2 - 9\lambda^2\right]\left[8(1-\rho)K_2 - 3\lambda^2\right]} > 0, \\ \theta_2^{\mathrm{MR}*} - \theta_2^{M*} &= \frac{(a-c)\lambda\left[4(1-\rho)K_2 - 3\lambda^2\right]}{2\left[2(1-\rho)K_2 - \lambda^2\right]\left[8(1-\rho)K_2 - 3\lambda^2\right]} > 0, \\ \theta_2^{R*} - \theta_2^{M*} &= \frac{(a-c)\lambda\left[8(1-2\rho)K_2 - 3\lambda^2\right]}{2\left[8(2-\rho)K_2 - 9\lambda^2\right]\left[2(1-\rho)K_2 - \lambda^2\right]}. \end{aligned} \tag{36}$$

When $0 < \rho < (8K_2 - 3\lambda^2/16K_2)((a-c)\lambda(8(1-2\rho)K_2 - 3\lambda^2)/2[8(2-\rho)K_2 - 9\lambda^2][2(1-\rho)K_2 - \lambda^2]) > 0$, i.e., $\theta_2^{R*} > \theta_2^{M*}$.

When $(8K_2 - 3\lambda^2/16K_2) < \rho < 1$, $((a-c)\lambda(8(1-2\rho)K_2 - 3\lambda^2)/2[8(2-\rho)K_2 - 9\lambda^2][2(1-\rho)K_2 - \lambda^2]) < 0$, i.e., $\theta_2^{R*} < \theta_2^{M*}$; $\theta_2^{R*} - \theta_2^{N*} = ((a-c)\lambda[4(2-\rho)K_2 - 3\lambda^2]/2[(2-\rho)K_2 - \lambda^2][8(2-\rho)K_2 - 9\lambda^2]) > 0$, and $\theta_2^{M*} - \theta_2^{N*} = ((a-c)\lambda\rho K_2/2[(2-\rho)K_2 - \lambda^2][2(1-\rho)K_2 - \lambda^2]) > 0$.

It is found from Proposition 6 that the two-way cooperation mode between overseas suppliers and domestic retailers can most effectively enhance the product publicity strategy of domestic retailers. However, for the two one-way

cooperation modes, with the increase in unit transportation cost, the initial one-way cooperation of the supplier sharing the retailer's propaganda cost will become the one-way cooperation of the retailer sharing the supplier's transportation cost. □

Proposition 7. *Under the specific unit transportation cost, the profits of cross-border e-commerce supply chain members of different cooperation modes satisfy, respectively, the following:*

$$\begin{aligned} \pi_m^{M*} > \pi_m^{\mathrm{MR}*} > \pi_m^{R*} > \pi_m^{N*}, \\ \pi_r^{M} > \pi_r^{\mathrm{MR}} > \pi_r^{N} > \pi_r^{R}. \end{aligned} \tag{37}$$

Proof. According to the above proposition, comparing the profits of cross-border e-commerce supply chain members under four different cooperation modes, we can get the following relationship:

$$\begin{aligned} \pi_m^{M*} - \pi_m^{\mathrm{MR}*} &= \frac{(a-c)^2\lambda^2 K_2}{4\left[2(1-\rho)K_2-\lambda^2\right]\left[8(1-\rho)K_2-3\lambda^2\right]} > 0, \\ \pi_m^{\mathrm{MR}*} - \pi_m^{R*} &= \frac{(a-c)^2 K_2\left(8\rho K_2-3\lambda^2\right)}{\left[8(2-\rho)K_2-9\lambda^2\right]\left[8(1-\rho)K_2-3\lambda^2\right]} > 0, \\ \pi_m^{R*} - \pi_m^{N*} &= \frac{(a-c)^2\lambda^2 K_2}{4\left[(2-\rho)K_2-\lambda^2\right]\left[8(2-\rho)K_2-9\lambda^2\right]} > 0, \\ \pi_r^{M*} - \pi_r^{\mathrm{MR}*} &= \frac{(a-c)^2\lambda^2 K_2}{8\left[2(1-\rho)K_2-\lambda^2\right]\left[8(1-\rho)K_2-3\lambda^2\right]} > 0, \\ \pi_r^{\mathrm{MR}*} - \pi_r^{N*} &= \frac{(a-c)^2 K_2\left(4\rho^2K_2^2-2\lambda^2K_2+\lambda^4\right)}{8\left[(2-\rho)K_2-\lambda^2\right]^2\left[8(1-\rho)K_2-3\lambda^2\right]} > 0, \\ \pi_r^{N*} - \pi_r^{R*} &= \frac{(a-c)^2\lambda^2 K_2\left[32\left(2-3\rho+\rho^2\right)K_2^2-2\lambda^2\left[31-24\rho)K_2+15\lambda^4\right]\right.}{8\left[(2-\rho)K_2-\lambda^2\right]^2\left[8(2-\rho)K_2-9\lambda^2\right]^2} > 0. \end{aligned} \tag{38}$$

It is found from Proposition 7 that both overseas suppliers and domestic retailers will choose the one-way cooperation mode of retailers sharing the transportation costs of suppliers and the two-way cooperation mode to improve their profits, and the former is more effective than the latter. □

5. Coordination Analysis

In cross-border e-commerce, even if overseas suppliers and domestic retailers choose the decision-making mode of semi-cooperation (between non-cooperation and full cooperation), the two parties will still keep some room for profit. Therefore, it is necessary to introduce the Shapley value method and full cooperative decision profit incremental sharing mechanism to coordinate non-cooperation and the three semi-cooperation modes, but before that, it is necessary to analyze the problem of full cooperative decision-making between suppliers and retailers.

5.1. Coordination of the Full Cooperation Mode between Overseas Suppliers and Domestic Retailer (C). In the mode of full cooperation, the members of the supply chain of cross-border e-commerce pay great attention to the maximization of the overall benefit, so they generally make joint decisions on the retail price P^C and propaganda strategy θ_2^C of the goods at the same time.

Therefore, the profit of cross-border e-commerce supply chain under the mode of full cooperation is as follows:

$$\pi_{\mathrm{sc}}^C = (p-c)(a-p+\lambda\theta_2) + \rho(a-p+\lambda\theta_2)^2 - \frac{1}{2}K_2\theta_2^2. \tag{39}$$

Proposition 8. *Under the mode of full cooperation between overseas suppliers and domestic retailers, the optimal decision of cross-border e-commerce supply chain is*

$$\begin{aligned} p^{C*} &= \frac{(a+c-2a\rho)K_2-c\lambda^2}{2(1-\rho)K_2-\lambda^2}, \\ \theta_2^{C*} &= \frac{(a-c)\lambda}{2(1-\rho)K_2-\lambda^2}. \end{aligned} \tag{40}$$

Proof. Solved by reverse induction.

Firstly, determine Hessian matrix of π_{sc}^{C} for the domestic retailer profit function:

$$H(p,\theta_2)=\begin{bmatrix}\dfrac{\partial^2\pi_{sc}^{C}}{\partial\left(P^{C}\right)^2} & \dfrac{\partial^2\pi_{sc}^{C}}{\partial P^{C}\partial\theta_2^{C}}\\[2ex] \dfrac{\partial^2\pi_{sc}^{C}}{\partial\theta_2^{C}\partial P^{C}} & \dfrac{\partial^2\pi_{sc}^{C}}{\partial\left(\theta_2^{C}\right)^2}\end{bmatrix}=\begin{bmatrix}-2(1-\rho) & \lambda(1-2\rho)\\ \lambda(1-2\rho) & -K_2+2\lambda^2\rho\end{bmatrix}. \tag{41}$$

It is not difficult to see from the above Hessian matrix: when $0<\rho<(2K_2-\lambda^2/2K_2)$, $(\partial^2\pi_r^{\mathrm{MR}}/\partial(P^{\mathrm{MR}})^2)=-2(1-\rho)<0$ and $|H|=2(1-\rho)K_2-\lambda^2>0$. Thus, π_{sc}^{C} is a strictly joint concave function about P^{C} and θ_2^{C}, and there is an optimal solution to maximize profits. So the first-order partial derivation conditions are as follows: $p^{C*}=((a+c-2a\rho)K_2-c\lambda^2/2(1-\rho)K_2-\lambda^2)$ and $\theta_2^{C*}=((a-c)\lambda/\,2(1-\rho)K_2-\lambda^2)$, and the market demand for commodities and the profits of cross-border e-commerce supply chain can be determined as

$$\begin{aligned} d^{C*}&=\frac{(a-c)K_2}{2(1-\rho)K_2-\lambda^2},\\ \pi_{sc}^{C*}&=\frac{(a-c)^2K_2}{2\left[2(1-\rho)K_2-\lambda^2\right]}.\end{aligned} \tag{42}$$

□

5.2. Shapley Value Method Coordination (S). Shapley value method is a method of fair distribution of cooperative income based on the marginal contribution of individuals to the whole.

For the non-cooperation mode and 3 semi-cooperation modes between overseas suppliers and domestic retailers, the Shapley value method is used to distribute the overall supply chain profits when the two fully cooperate, and the profits distributed by both sides under different cooperation modes can be obtained:

(1) Non-cooperative coordination between overseas suppliers and domestic retailers (SN)

At this point,

$$\begin{aligned}\pi_m^{\mathrm{SN}*}&=\frac{1}{2}\pi_m^{N*}+\frac{1}{2}\left(\pi_{sc}^{C*}-\pi_r^{N*}\right)=\frac{(a-c)^2K_2}{4\left[2(1-\rho)K_2-\lambda^2\right]}+\frac{(a-c)^2K_2\left[2(1-\rho)K_2-\lambda^2\right]}{16\left[(2-\rho)K_2-\lambda^2\right]^2},\\ \pi_r^{\mathrm{SN}*}&=\frac{1}{2}\pi_r^{N*}+\frac{1}{2}\left(\pi_{sc}^{C*}-\pi_m^{N*}\right)=\frac{(a-c)^2K_2}{4\left[2(1-\rho)K_2-\lambda^2\right]}-\frac{(a-c)^2K_2\left[2(1-\rho)K_2-\lambda^2\right]}{16\left[(2-\rho)K_2-\lambda^2\right]^2}.\end{aligned} \tag{43}$$

(2) One-way cooperative coordination of domestic retailers sharing transportation costs for overseas suppliers (SM)

At this point,

$$\begin{aligned}\pi_m^{\mathrm{SM}*}&=\frac{1}{2}\pi_m^{M*}+\frac{1}{2}\left(\pi_{sc}^{C*}-\pi_r^{M*}\right)=\frac{5(a-c)^2K_2}{16\left[2(1-\rho)K_2-\lambda^2\right]},\\ \pi_r^{\mathrm{SM}*}&=\frac{1}{2}\pi_r^{M*}+\frac{1}{2}\left(\pi_{sc}^{C*}-\pi_m^{M*}\right)=\frac{3(a-c)^2K_2}{16\left[2(1-\rho)K_2-\lambda^2\right]}.\end{aligned} \tag{44}$$

(3) One-way cooperative coordination of domestic retailers sharing publicity costs for overseas suppliers (SR)

At this point,

$$\begin{aligned}\pi_m^{\mathrm{SR}*}&=\frac{1}{2}\pi_m^{R*}+\frac{1}{2}\left(\pi_{sc}^{C*}-\pi_r^{R*}\right)=\frac{(a-c)^2K_2}{4\left[2(1-\rho)K_2-\lambda^2\right]}+\frac{(a-c)^2K_2\left[8(1-\rho)K_2-3\lambda^2\right]}{\left[8(2-\rho)K_2-9\lambda^2\right]^2},\\ \pi_r^{\mathrm{SR}*}&=\frac{1}{2}\pi_r^{R*}+\frac{1}{2}\left(\pi_{sc}^{C*}-\pi_m^{R*}\right)=\frac{(a-c)^2K_2}{4\left[2(1-\rho)K_2-\lambda^2\right]}-\frac{(a-c)^2K_2\left[8(1-\rho)K_2-3\lambda^2\right]}{\left[8(2-\rho)K_2-9\lambda^2\right]^2}.\end{aligned} \tag{45}$$

(4) Two-way cooperative coordination of domestic retailers sharing transportation costs of overseas suppliers and overseas suppliers sharing promotional costs of domestic retailers (SMR)

At this point,

$$\pi_m^{\mathrm{SMR}*} = \frac{1}{2}\pi_m^{\mathrm{MR}*} + \frac{1}{2}\left(\pi_{\mathrm{sc}}^{\mathrm{C}*} - \pi_r^{\mathrm{MR}*}\right) = \frac{(a-c)^2K_2}{4\left(2(1-\rho)K_2-\lambda^2\right)} + \frac{(a-c)^2K_2}{4\left(8(1-\rho)K_2-3\lambda^2\right)},$$
$$\pi_r^{\mathrm{SMR}*} = \frac{1}{2}\pi_r^{\mathrm{MR}*} + \frac{1}{2}\left(\pi_{\mathrm{sc}}^{\mathrm{C}*} - \pi_m^{\mathrm{MR}*}\right) = \frac{(a-c)^2K_2}{4\left(2(1-\rho)K_2-\lambda^2\right)} - \frac{(a-c)^2K_2}{4\left(8(1-\rho)K_2-3\lambda^2\right)}. \tag{46}$$

5.3. Benefit-Sharing Coordination for Full Cooperation Decision-Making between Suppliers and Retailers (V). The profit increment mechanism of the shared system is based on the profit increment of the whole supply chain under the decision of full cooperation, compared with that under the decision of non-cooperation or semi-cooperation. The system income increment is distributed to each member according to the proportion of the supply chain member's input.

Therefore, the input of overseas suppliers and domestic retailers is as follows, respectively:

$$T_m = c(a-p+\lambda\theta_2), \tag{47}$$

$$T_r = w(a-p+\lambda\theta_2) + \frac{1}{2}K_2\theta_2^2. \tag{48}$$

5.3.1. Non-Cooperative Coordination between Suppliers and Retailers (VN). Under this structure, the income increment of supply chain is as follows:

$$\Delta\pi^{\mathrm{VN}} = \pi_{\mathrm{sc}}^{\mathrm{C}*} - \left(\pi_m^{N*} + \pi_r^{N*}\right) = \frac{(a-c)^2\left(2K_2-\lambda^2\right)^2K_2}{8\left[(2-\rho)K_2-\lambda^2\right]^2\left[2(1-\rho)K_2-\lambda^2\right]}. \tag{49}$$

Substituting the aforementioned values of P^{N*}, θ_2^{N*} into (47) and (48), the proportion of input from overseas suppliers and domestic retailers to the total input of the supply chain is

$$\theta_m^{\mathrm{VN}*} = \frac{T_m^N}{T_m^N + T_r^N} = \frac{4c\left[(2-\rho)K_2-\lambda^2\right]}{4[c(3-\rho)+a(1-\rho)]K_2-(a+7c)\lambda^2},$$
$$\theta_r^{\mathrm{VN}*} = \frac{T_r^N}{T_m^N + T_r^N} = \frac{4[a(1-\rho)+c]K_2-(a+3c)\lambda^2}{4[c(3-\rho)+a(1-\rho)]K_2-(a+7c)\lambda^2}. \tag{50}$$

Thus, the profits of overseas suppliers and domestic retailers after coordination are

$$\pi_m^{\mathrm{VN}*} = \frac{(a-c)^2K_2}{4\left[(2-\rho)K_2-\lambda^2\right]} + \theta_m^{\mathrm{VN}*}\left(\Delta\pi^{\mathrm{VN}}\right),$$
$$\pi_r^{\mathrm{VN}*} = \frac{(a-c)^2\left(2K_2-\lambda^2\right)K_2}{8\left[(2-\rho)K_2-\lambda^2\right]^2} + \theta_r^{\mathrm{VN}*}\left(\Delta\pi^{\mathrm{VN}}\right). \tag{51}$$

5.3.2. Coordination of One-Way Cooperation of Retailers Sharing Suppliers' Transport Costs (VM). In this mode, the income increment of supply chain system is as follows:

$$\Delta\pi^{\mathrm{VM}} = \pi_{\mathrm{sc}}^{C*} - \left(\pi_m^{M*} + \pi_r^{M*}\right) = \frac{(a-c)^2K_2}{8\left[2(1-\rho)K_2-\lambda^2\right]}. \tag{52}$$

Substituting formulas (12) and (13) P^{M*}, θ_2^{M*} into (47) and (48), the proportion of input from overseas suppliers and domestic retailers to the total input of the supply chain is

$$\theta_m^{\mathrm{VM}*} = \frac{T_m^M}{T_m^M + T_r^M} = \frac{4c\left[2(1-\rho)K_2-\lambda^2\right]}{4(a+c)(1-\rho)K_2-(a+3c)\lambda^2},$$
$$\theta_r^{\mathrm{VM}*} = \frac{T_r^M}{T_m^M + T_r^M} = \frac{(a-c)\left[4(1-\rho)K_2-\lambda^2\right]}{4(a+c)(1-\rho)K_2-(a+3c)\lambda^2}. \tag{53}$$

Thus, the profits of overseas suppliers and domestic retailers after coordination are as follows:

$$\pi_m^{\mathrm{VM}*} = \frac{(a-c)^2K_2}{4\left[2(1-\rho)K_2-\lambda^2\right]} + \theta_m^{\mathrm{VM}*}\left(\Delta\pi^{\mathrm{VM}}\right),$$
$$\pi_r^{\mathrm{VM}*} = \frac{(a-c)^2K_2}{8\left[2(1-\rho)K_2-\lambda^2\right]} + \theta_r^{\mathrm{VM}*}\left(\Delta\pi^{\mathrm{VM}}\right). \tag{54}$$

5.3.3. Coordination of One-Way Cooperation of Suppliers Sharing Retailers' Publicity Costs (VR). In this mode, the income increment of supply chain system is

$$\Delta\pi^{\mathrm{VR}} = \pi_{\mathrm{sc}}^{C*} - \left(\pi_m^{R*} + \pi_r^{R*}\right) = \frac{(a-c)^2 K_2\left[21\lambda^4 - 8\lambda^2(9+\rho)K_2 + 64K_2^2\right]}{2\left[8(2-\rho)K_2 - 9\lambda^2\right]^2\left[2(1-\rho)K_2 - \lambda^2\right]}. \tag{55}$$

Substituting formulas (19) and (20) P^{R*}, θ_2^{R*} into (47) and (48), the proportion of input from overseas suppliers and domestic retailers to the total input of the supply chain is

$$\begin{aligned}\theta_m^{\mathrm{VR}*} &= \frac{T_m^R}{T_m^R + T_r^R} = \frac{2c\left[8(2-\rho)K_2 - 9\lambda^2\right]}{3(a-13c)\lambda^2 + 16[c(3-\rho) + a(1-\rho)]K_2},\\ \theta_r^{\mathrm{VR}*} &= \frac{T_r^R}{T_m^R + T_r^R} = \frac{16[a(1-\rho)+c]K_2 + 3(a-7c)\lambda^2}{3(a-13c)\lambda^2 + 16[c(3-\rho) + a(1-\rho)]K_2}.\end{aligned} \tag{56}$$

Thus, the profits of overseas suppliers and domestic retailers after coordination are

$$\begin{aligned}\pi_m^{\mathrm{VR}*} &= \frac{2(a-c)^2 K_2}{8(2-\rho)K_2 - 9\lambda^2} + \theta_m^{\mathrm{VR}*}\left(\Delta\pi^{\mathrm{VR}}\right),\\ \pi_r^{\mathrm{VR}*} &= \frac{4(a-c)^2 K_2\left(4K_2 - 3\lambda^2\right)}{\left[8(2-\rho)K_2 - 9\lambda^2\right]^2} + \theta_r^{\mathrm{VR}*}\left(\Delta\pi^{\mathrm{VR}}\right).\end{aligned} \tag{57}$$

5.3.4. Coordination of Two-Way Cooperation of Retailers Sharing Suppliers' Transport Costs and Suppliers Sharing Retailers' Publicity Costs (VMR). In this mode, the income increment of supply chain system is

$$\Delta\pi^{\mathrm{VMR}} = \pi_{\mathrm{sc}}^{C*} - \left(\pi_m^{\mathrm{MR}*} + \pi_r^{\mathrm{MR}*}\right) = \frac{(a-c)^2(1-\rho)K_2^2}{\left[2(1-\rho)K_2 - \lambda^2\right]\left[8(1-\rho)K_2 - 3\lambda^2\right]}. \tag{58}$$

Substituting formulas (27) and (28) $P^{\mathrm{MR}*}, \theta_2^{\mathrm{MR}*}$ into (47) and (49), the proportion of input from overseas suppliers and domestic retailers to the total input of the supply chain is

$$\begin{aligned}\theta_m^{\mathrm{VMR}*} &= \frac{T_m^{\mathrm{MR}}}{T_m^{\mathrm{MR}} + T_r^{\mathrm{MR}}} = \frac{8c\rho K_2\left[8(1-\rho)K_2 - 3\lambda^2\right]}{32(a+c)(1-\rho)\rho K_2^2 + 6\lambda^2[c(4-9\rho) + a\rho]K_2 - 9c\lambda^4},\\ \theta_r^{\mathrm{VMR}*} &= \frac{T_r^{\mathrm{MR}}}{T_m^{\mathrm{MR}} + T_r^{\mathrm{MR}}} = \frac{32(a-c)(1-\rho)\rho K_2^2 + 6\lambda^2[c(4-5\rho) + a\rho]K_2 - 9c\lambda^4}{32(a+c)(1-\rho)\rho K_2^2 + 6\lambda^2[c(4-9\rho) + a\rho]K_2 - 9c\lambda^4}.\end{aligned} \tag{59}$$

Thus, the profits of overseas suppliers and domestic retailers after coordination are

$$\begin{aligned}\pi_m^{\mathrm{VMR}*} &= \frac{(a-c)^2 K_2}{8(1-\rho)K_2 - 3\lambda^2} + \theta_m^{\mathrm{VMR}*}\left(\Delta\pi^{\mathrm{VMR}}\right),\\ \pi_r^{\mathrm{VMR}*} &= \frac{(a-c)^2 K_2}{2\left[8(1-\rho)K_2 - 3\lambda^2\right]} + \theta_r^{\mathrm{VMR}*}\left(\Delta\pi^{\mathrm{VMR}}\right).\end{aligned} \tag{60}$$

6. Example Analysis

In order to further analyze and compare the rationality and effectiveness of decision-making in different cooperation modes, this paper verifies the above proposition by example analysis. Based on the investigated data, the relevant parameters can be set as the scale of domestic retailers' publicity activities $K_2 = 50$, potential market demand $a = 100$, fixed transportation costs per unit product $c = 5$, and the sensitivity of consumers to retailers' publicity $\lambda = 0.6$. The value range of marginal transportation cost factor per unit product ρ can be limited to range $[0.1, 0.7]$.

Substituting the above parameters into the profit algebraic formula of supply chain members of Propositions 1–4 and the corresponding algebraic formula after coordination, as ρ increases gradually in the range of values, the profits of the members of cross-border e-commerce will change accordingly. In order to observe the law of concrete change, the results of operations in different cooperative modes can be mapped to graphs to analyze the

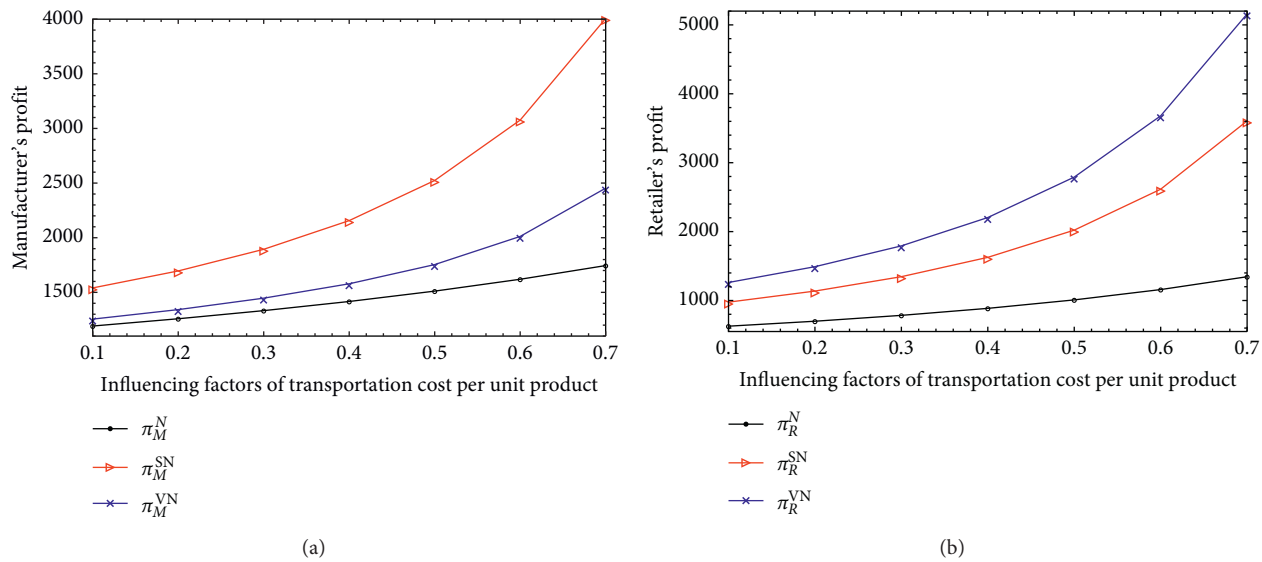

Figure 1: Impact of unit transport costs on member profits in the N mode.

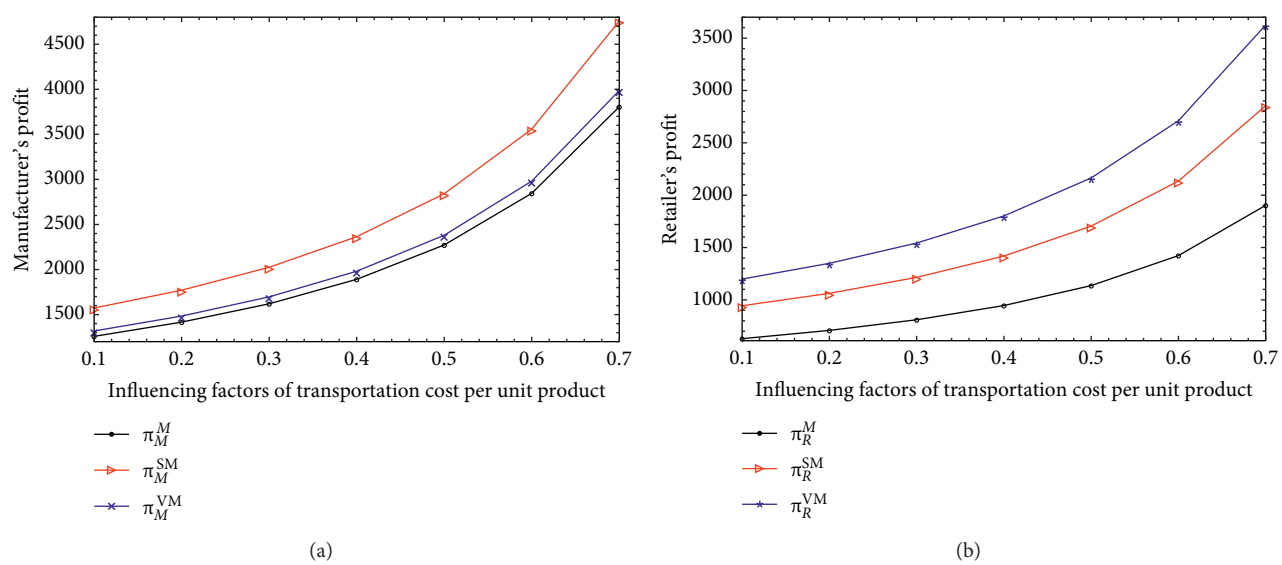

Figure 2: Impact of unit transport costs on member profits in the M mode.

coordinating effect of the two coordination mechanisms, as shown in Figures 1–4.

It can be seen from Figures 1–4 that, under different cooperation modes, the Shapley value method and full cooperation revenue increment sharing coordination mechanism can improve the profits of overseas suppliers and domestic retailers. Firstly, overseas suppliers under different cooperation modes are more willing to choose the Shapley value method for profit redistribution, while domestic retailers are more willing to choose the full cooperation incremental revenue sharing mechanism for profit redistribution; secondly, the larger the unit transportation cost is, the more obvious the profit redistribution is; the impact of these two coordination mechanisms on the profits of cross-border e-commerce supply chain members will be different; Finally, under the two semi-cooperation modes of domestic retailers participating in the sharing of transportation costs of overseas suppliers, the profit coordination effect of full cooperation benefits is increasing, which is generally not important for the sharing mechanism of overseas suppliers. Taking different coordination mechanisms as units, the results can be drawn into tables to analyze the changing trend of profit under different cooperation modes before and after coordination, as shown in Tables 1 and 2.

It can be seen from Tables 1 and 2 that, under different cooperation modes, after the profits of supply chain members are coordinated by the Shapley value method and

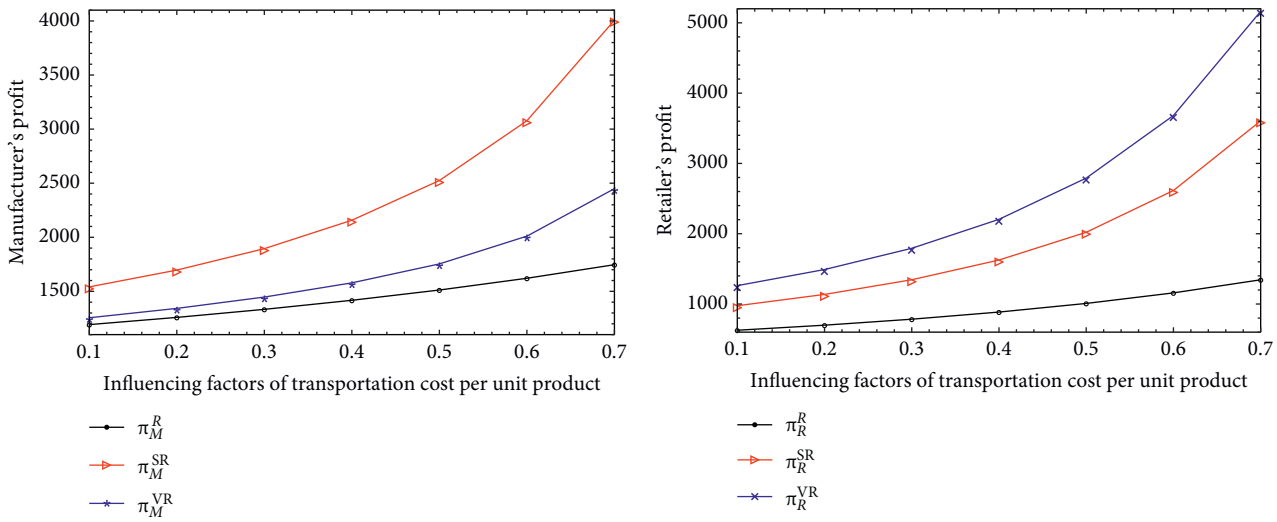

(a) (b)

Figure 3: Impact of unit transport costs on member profits in the R mode.

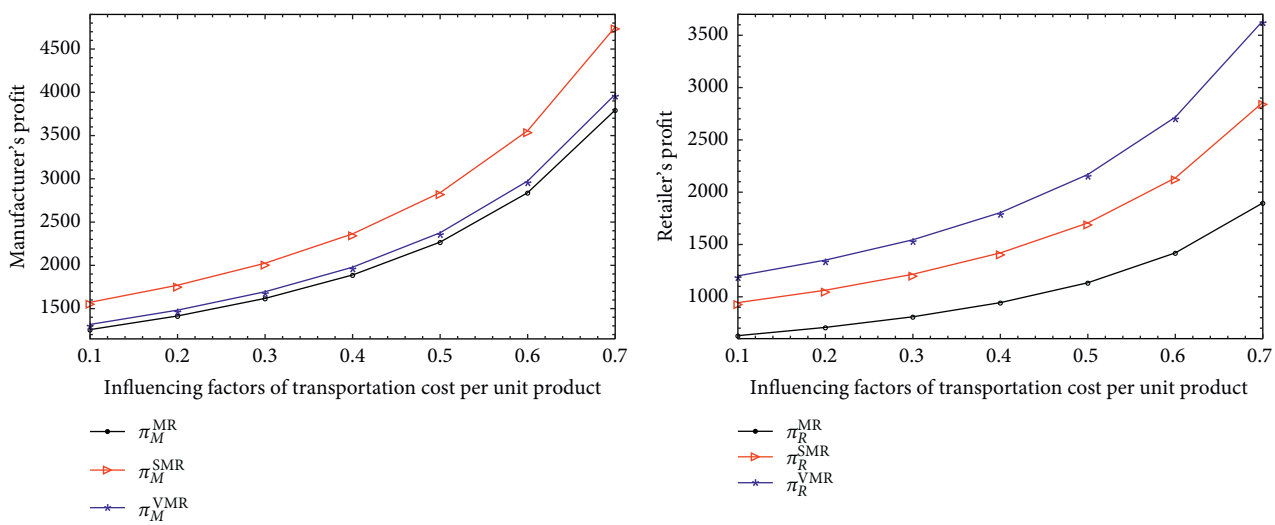

(a) (b)

Figure 4: Impact of unit transport costs on member profits in the MR mode.

Table 1: Profits of members of different cooperation modes under the Shapley value method mechanism.

	ρ						
	0.1	0.2	0.3	0.4	0.5	0.6	0.7
π_M^{SN*}	1540.77	1696.06	1894.10	2156.76	2523.91	3076.45	4006.16
π_M^{SM*}	1573.13	1770.66	2024.92	2364.45	2840.77	3557.41	4757.61
π_M^{SR*}	1541.32	1696.66	1894.75	2157.46	2524.67	3077.27	4007.04
π_M^{SMR*}	1572.82	1770.26	2024.40	2363.73	2839.74	3555.80	4754.73
π_R^{SN*}	976.24	1137.00	1345.78	1626.36	2021.32	2615.40	3606.02
π_R^{SM*}	943.88	1062.40	1214.95	1418.67	1704.46	2134.44	2854.57
π_R^{SR*}	975.69	1136.41	1345.13	1625.66	2020.5	2614.58	3605.14
π_R^{SMR*}	944.19	1062.80	1215.48	1419.38	1705.49	2136.06	2857.45

Table 2: Profits of members of different cooperative modes under the full cooperation income incremental mechanism.

	ρ						
	0.1	0.2	0.3	0.4	0.5	0.6	0.7
π_M^{VN*}	1255.33	1342.17	1446.97	1578.58	1754.20	2011.89	2453.71
π_M^{VM*}	1318.33	1483.85	1696.90	1981.39	2380.48	2980.89	3986.34
π_M^{VR*}	1255.69	1342.50	1447.20	1578.63	1753.80	2010.44	2449.38
π_M^{VMR*}	1316.96	1482.22	1694.82	1978.53	2376.46	2974.62	3975.16
π_R^{VN*}	1261.68	1490.89	1792.91	2204.53	2791.03	3679.96	5158.47
π_R^{VM*}	1198.69	1349.21	1542.98	1801.73	2164.75	2710.96	3625.84
π_R^{VR*}	1261.32	1490.56	1792.67	2204.49	2791.43	3681.41	5162.8
π_R^{VMR*}	1200.06	1350.84	1545.06	1804.54	2168.77	2717.24	3637.02

full cooperation revenue sharing mechanism, when the domestic retailers share the transportation costs of overseas suppliers, the suppliers get the maximum profits, while the domestic retailers get the maximum profits when the overseas suppliers and domestic retailers do not cooperate.

7. Conclusion

By constructing a cooperative game model of cross-border e-commerce supply chain composed of a single overseas supplier and a single domestic retailer, this paper explores how the propaganda strategy and transportation cost impact the pricing strategy of cross-border e-commerce. Meanwhile, the Shapley value method and the full cooperative income incremental sharing mechanism are introduced to redistribute the profits of supply chain members under different cooperation modes.

By verifying the decision results of different cooperation modes, the following conclusions can be drawn:

(1) If domestic retailers pursue lower wholesale prices, they need to share the transportation costs of overseas suppliers and attract more consumers at lower retail prices. Therefore, retailers sharing transport risks with overseas suppliers can significantly reduce the cost of cross-border e-commerce to expand customer groups to enhance product sales and ultimately achieve an increase in profitability.

(2) The whole cross-border e-commerce supply chain is pursuing the most efficient commodity promotion strategy, and it needs two-way cooperation between overseas suppliers and domestic retailers; that is, domestic retailers share the transportation costs of overseas suppliers and overseas suppliers share the publicity costs of domestic retailers. This indicates that, in the cross-border e-commerce supply chain, domestic retailers share overseas suppliers as a win-win strategy.

(3) When the members of cross-border e-commerce supply chain choose the mode of first coordination and then cooperation, overseas suppliers generally choose retailers to share the total transportation costs of suppliers, while domestic retailers choose the non-cooperation mode; when the members of the cross-border e-commerce supply chain choose the mode of cooperation before coordination, most of the overseas suppliers will choose the Shapley value method to redistribute the profits, while the domestic retailers will choose the full cooperative income incremental sharing mechanism to redistribute the profits.

(4) Overseas suppliers under different cooperation modes are more willing to choose the Shapley value method for profit redistribution, while domestic retailers are more willing to choose the full cooperative income incremental sharing mechanism for profit redistribution. In addition, the greater the unit transportation cost is, the more obvious the effect of the two coordination mechanisms on the profits of the members of the cross-border e-commerce supply chain will be.

Although our article has made a lot of contributions around these problems, there are still many places to continue to study. When the demand is uncertain, whether the same result will be obtained and what kind of change will happen when the supply chain structure changes are very interesting research issues.

Data Availability

There are not empirical data in this paper. The equilibrium solution of the model is obtained by Mathematics software.

Conflicts of Interest

The authors declare that they have no conflicts of interest.

Acknowledgments

This work was sponsored by the National Natural Science Foundation of China (Grant nos. 72072112, 71602114, 72002125, and 72001135), Shanghai Rising-Star Program (Grant no. 19QA1404200), Shanghai Sailing Program (Grant nos. 19YF1418800 and 20YF1416600), Middle-Aged and Young Teachers' Basic Ability Promotion Project of Guangxi (Grant no. 2020KY04036), and Talent Introduction Research Project of Guangxi University for Nationalities (Grant no. 2018SKQD16).

References

[1] L. Xu, Z. Di, and J. Chen, "Evolutionary game analysis on behavior strategies of multiple stakeholders in maritime shore power system," *Ocean & Coastal Management*, vol. 202, Article ID 105508, 2021.

[2] L. Xu, J. Shi, and J. H. Chen, "Platform encroachment with price matching: introducing a self-constructing online platform into the sea-cargo market," *Computers & Industrial Engineering*, vol. 156, Article ID 107266, 2021.

[3] Y. Malekian and M. Rasti-Barzok, "A game theoretic approach to coordinate price promotion and advertising policies with reference price effects in a two-echelon supply chain," *Journal of Retailing and Consumer Services*, vol. 51, pp. 114–128, 2019.

[4] J. Xie, L. Liang, L. Liu et al., "Coordination contracts of dual-channel with cooperation advertising in closed-loop supply chains," *International Journal of Production Economics*, vol. 183, pp. 528–538, 2017.

[5] J. Chaab and M. Rasti-Barzoki, "Cooperative advertising and pricing in a manufacturer-retailer supply chain with a general demand function: a game-theoretic approach," *Computers & Industrial Engineering*, vol. 99, pp. 112–123, 2017.

[6] T. Y. Chan, C. Narasimhan, and Y. Yoon, "Advertising and price competition in a manufacturer-retailer channel," *International Journal of Research in Marketing*, vol. 34, no. 3, pp. 694–716, 2017.

[7] J. Song, F. Li, D. Wu et al., "Supply chain coordination through integration of innovation effort and advertising support," *Applied Mathematical Modelling*, vol. 49, pp. 108–123, 2017.

[8] P. Rodríguez-Torrico, R. S. J. Cabezudo, and S. San-Martín, "Tell me what they are like and I will tell you where they buy. An analysis of omnichannel consumer behavior," *Computers in Human Behavior*, vol. 68, pp. 465–471, 2017.

[9] A. James and V. W. Eric, "Trade costs," *Journal of Economic Literature*, vol. 42, no. 3, pp. 691–751, 2004.

[10] X. Liang and L. Liang, "Retailer-led cross-border dual-channel supply chain pricing decision under the change of tariff and cost," *China Management Science* 2020, in Chinese.

[11] Y. Zhang, "A study on the cost control of cross-border E-commerce logistics," *National Circulation Economy*, no. 33, pp. 18-19, 2018, in Chinese.

[12] D. Zi, "Cost control of cross-border E-commerce logistics under overseas warehouse mode," *Logistics Technology*, vol. 34, no. 16, pp. 175–180, 2015, in Chinese.

[13] Q. Y. Peng, C. X. Wang, and L. Xu, "Emission abatement and procurement strategies in a low-carbon supply chain with option contracts under stochastic demand," *Computers & Industrial Engineering*, vol. 144, Article ID 106502, 2020.

[14] L. Xu, C. X. Wang, and J. J. Zhao, "Decision and coordination in the dual-channel supply chain considering cap-and-trade regulation," *Journal of Cleaner Production*, vol. 197, pp. 551–561, 2018.

[15] T. Dai, S. H. Cho, and F. Zhang, "Contracting for on-time delivery in the US influenza vaccine supply chain," *Manufacturing & Service Operations Management*, vol. 18, pp. 332–346, 2016.

[16] X. Liu, Q. Gou, L. Alwan et al., "Option contracts: a solution for overloading problems in the delivery service supply chain," *Journal of Operational Research Society*, vol. 67, pp. 187–197, 2016.

[17] Q. Wang and D. Zhao, "Co-operative strategies on emission reduction and promotion of two-level supply chain," *Control and Decision-Making*, vol. 29, no. 2, pp. 307–314, 2014, in Chinese.

[18] J. Chen, L. Liang, D. Yao et al., "Price and quality decisions in dual-channel supply chains," *European Journal of Operational Research*, vol. 259, no. 3, pp. 935–948, 2017.

Hindawi
Scientific Programming
Volume 2021, Article ID 9974235, 10 pages
https://doi.org/10.1155/2021/9974235

Research Article

Replacing Management or Not: Contract Renegotiation to Prevent Double Moral Hazards of Venture Capital Investments

Linsen Yin[1] and Ane Pan[2]

[1]*School of Financial Technology, Shanghai Lixin University of Accounting and Finance, Shanghai 201209, China*
[2]*School of Management, Wuhan University of Technology, Wuhan 430070, China*

Correspondence should be addressed to Ane Pan; panane@whut.edu.cn

Received 29 March 2021; Revised 15 April 2021; Accepted 19 April 2021; Published 5 May 2021

Academic Editor: Tingsong Wang

Copyright © 2021 Linsen Yin and Ane Pan. This is an open access article distributed under the Creative Commons Attribution License, which permits unrestricted use, distribution, and reproduction in any medium, provided the original work is properly cited.

During the venture capital development, replacing the management work team or keeping up the status quo is a key strategy choice for venture capitalist and venture entrepreneur about the long-term development of enterprise and the control right transferring. In fact, the contract designing focuses on the distribution of cash flow to encourage both efforts in order to avoid double moral hazard, and the strategy behavior has similar effects according to the developing condition of venture enterprise. In this paper, we consider both contract design and strategic behavior, regarding this strategic behavior choice as a motivator and combining strategic behavior with financial instrument options. The main innovation is to redesign and optimize the contract based on dynamic perspective, which will analyze initial contract designed to motivate both sides' effort if a venture enterprise is in good state, and then renegotiate whether to replace the management work team or keep up the status quo according to the venture enterprise's development state in the process of venture investment cooperation. The paper also puts forward some conclusions: joint effort of both sides can be motivated through strategic behavior choice and then lead to increasing the overall value of the venture enterprise; after the venture enterprise has gained private benefits in the early stage, the venture capitalist needs to make appropriate assignments and demisability in benefits to remotivate the venture enterprise's efforts, aiming to further balance venture enterprise's private benefits and the earnings redistributed by venture capitalist.

1. Introduction

Funding difficulties of startup firms can be mitigated by venture capitalists' initial or multiple stage investments, after which the value of venture capital backed firm is shared by venture capitalists and entrepreneurs. However, due to information asymmetry, venture entrepreneurs or management team may take advantage of the actual control right to maximize personal benefits instead of firm value. One typical case is that even entrepreneurs are not well qualified; entrepreneurs tend to continue to operate the firm for private benefits, rather than to be replaced by professional managers, thus causing entrepreneurs' moral hazard that holds up venture capitalists [1–5]. Therefore, it presents a key challenge to venture capitalists to motivate entrepreneurs to maximize the value of the firm and thus the benefits shared by both entrepreneurs and capitalists [6].

Contract instruments selection and arrangements are important means to solve the problem of double moral hazard in the field of venture capital. Previous studies developed models to use financial instruments such as common stock and convertible bonds to motivate both efforts and to prevent double moral hazard [7]. The focus of these studies is to choose and compare different financial tools to motivate the efforts of both sides.

However, contract is not complete as future situation of enterprises cannot be completely predicted. After the venture capitalist and entrepreneur sign an initial contract, they usually will take further actions after they observe situation of the enterprise in its development process. One typical example is that the capitalist who has controlling rights can

select to keep up the status quo if he observes a good development state of the enterprise or to replace entrepreneur management team by professional managers if he observes a bad development state of the enterprise. Therefore, the enterprise's natural state (as an important uncertain factor) not only affects the efforts level of both sides but also affects or even determines the further strategic choices of both sides, such as whether to maintain the entrepreneur management team and to continue cooperation between both sides.

In this paper, we propose a potential solution for capitalists, that is, an optional choice on replacing managers or keeping up the status quo in initial contract design. This design of renegotiation contract provides capitalists an optional choice to remotivate entrepreneurs after the company has developed to a certain stage and entrepreneurs have attained personal benefits. The remotivation leads entrepreneurs to operate the firm targeted with long-term performance and to keep align their interest with capitalists, thus ensuring the interests of venture capitalists.

Extending the model of Casamatta [2], we redesign and optimize the contract in a dynamic setting. More specifically, we analyze initial contract designed to motivate both sides' efforts from entrepreneurs and capitalists and then renegotiate whether to replace the management team or keep up the status quo according to the enterprise's development state in the process of cooperation between capitalists and entrepreneurs.

The structure of the remainder of this paper is as follows: Section 2 discusses related literature. Section 3 offers basic model description and model assumption. Section 4 presents the contract model combined strategic behavior choice and the corresponding scheme to mitigate double moral hazard. Section 5 describes "Alibaba" case to demonstrate our model. Section 6 concludes the paper.

2. Literature Review

There is a growing body of research on the double moral hazard in venture capital investment [8]. In practice, the efforts made by venture capitalist and entrepreneurs cannot be observed due to the incomplete information [9]. Consequently, venture capitalists and entrepreneurs tend to shirk and optimize their own interest and behavior after their own incentives, which leads to less than the first-best level of effort [10]. It brings about double moral hazard between venture capitalists and entrepreneurs.

Some literature suggests using suitable financial instruments to alleviate moral hazard. Admati and Pfleiderer [7] show that a fixed fraction of equity contract can provide robust optimal incentives as it can allocate efficient control rights to venture capitalists. Berglof [11] considers a framework of convertible debt in incomplete contracts to transfer control rights to the value-maximizing party. Based on the work of Hart and Moore [12], the option of the entrepreneur to repudiate her financial obligations limits the feasible amount of outsider claims. Kaplan and Stromberg [13] find that venture capitalists are usually willing to take preferred stock, which can be more suitable to motivate double efforts. Additionally, some literature argues that, in many corporate venturing deals, investors tend to take a majority of equity stake in the startup [13–15]. Overall, these literature focus on designing financing instruments, such as equity and convertible debt, to alleviate moral hazard.

On the other hand, some literature proposes using other approaches for mitigating moral hazard. Neher [16] put forward stage financing as an instrument to implement the optimal investment path. Aghion et al. [17] and Hart et al. [12] propose the contract arrangement combining with contingent control right. They argue that contingent control right allocation can be used as an effective alternative to cash flow rights arrangement, which can make up for the inadequacy of simple contract arrangement of distributing cash flow to prevent double moral hazard.

However, control rights held by venture capitalists cannot be described by the standard array of securities; it should develop a financial contracting model to investigate the joint allocation of control and cash-flow rights attained through contractual covenants in venture capital deals [14, 15]. Thus, stage financing and contingent control right can be used as important measures according to the development situation of venture enterprise to prevent double moral hazard.

Another issue is what leads to double moral hazard. For example, Cornelli and Yosha [18] analyze the problem of an entrepreneur manipulating short-term results for the purpose of "window-dressing." Inderst et al. [19] find the forming mechanism and fundamental reason of the moral hazard about venture capitalist and venture entrepreneur, which focus on the private gains grabbed by venture capitalist and venture entrepreneur. Bachmann and Schindele [20] argue that venture capitalists try to have theft for commercial secret or invention of venture enterprise, which may damage the profit of venture enterprise.

Recently, scholars show a growing interest in different exit methods of venture capital, attempting to understand the impact of various exit methods on the gains of venture capital company and venture enterprise. For instance, in an empirical analysis of venture capital exit, Cumming [21] found that financing contract differs a lot in terms of cash flow and control, and it differs even more when it comes to considering types of exit (IPO, acquisition, or liquidation) choosing and investment earnings with risk, which not only depends on the characteristics of the venture enterprise but also depends on the distribution of cash flow and control right. Tian et al. [22] design a novel approach that considers both the bounded rationality of venture capitalists and the uncertain circumstance of venture capital in decision-making which is urgent to select the promising enterprise in China.

In a separate research, Thomas [23] found that exit clause "investment relationship between the two sides" encouraged venture capitalists to lock the capital into the venture in initial stage. In later stages until the exit, venture capitalists managed to gain more and more control over exit methods by setting up additional seats on the board and gained exit control right in the contract. As a result, the control right was gradually transferred from venture

entrepreneurs to venture capitalists with the increase of venture capital. Babich et al. [8] model a bargaining game with a moral-hazard problem between an entrepreneur and a bank and a double-sided moral-hazard problem between the entrepreneur and a VC with respect to their non-contractible efforts. The research decomposes the economic value of crowdfunding into cash gains or losses, costs of bad investments avoided, and project-payoff probability update.

Based on the distribution structure and evolution rules of decision-making right and control right of German venture capital samples, Bienz and Walz [24] found that venture capitalists could gain valuable exit right when they return the operation right to entrepreneurs in the investment and cooperation period. An additional finding is that the shorter the contract term is, the more control right is transferred to the hands of the venture capitalists.

Combining the strategy choice behavior of venture capital, it is important and deserves much research work on the contract designing and optimization under the framework with various strategy choices, which is also a new research angle of view. In present research, the aims are to design contract or compare and choose contract to motivate more effort of venture capitalist and venture entrepreneur and to choose strategy behavior to threaten venture capitalist and venture entrepreneur in order to motivate their effort, but it goes blank to study on the contract designing and optimization under the framework with various strategy choices. Therefore, the paper will focus on making up the deficiency, which will design contract considering various strategy choices.

3. Model Description and Basic Assumptions

Based on the model developed by Casamatta and Haritchabalet [25], venture capitalist and entrepreneur sign a contract. In the contract, the capitalist invests money, while the entrepreneur invests expertise in each stage. The investment and expertise from both sides determine the total revenue of the venture enterprise. The incentive arrangement is set by the equity allocation scheme, which forms the income distribution to both sides. In this paper, we consider adding a term in the contract, in which the capitalist has an optional strategic choice; that is, he can maintain the status quo or replace venture entrepreneurs with professional managers according to the state of the enterprise after investment. The strategic choice not only relieves the capitalist the worry on the reducing effort of the entrepreneur but also increases the total income of the enterprise, thus increasing the incentive of the entrepreneur.

Consider a venture entrepreneur (hereafter EN) endowed with an innovative investment project. The EN has the creativity and technical skills, but, due to wealth constraint, he needs a sum of investment fund I from a venture capitalist (hereafter VC). The entrepreneur EN and capitalist VC sign an initial contract, which requires VC to provide the fund I to cooperate with the entrepreneurial project. The contract also formulates an income distribution arrangement according to which VC and EN share the benefits after the termination of the project and the realization of earnings.

Assume that two sides have made detailed due diligence and investigation on the project and have a common understanding for the future development of the project. Both sides think that the project is worth investing before signing the initial contract. These above are all common knowledge.

Investment process is roughly divided into the five following stages:

Stage 1: sign the initial contract (I, ϕ), in which I is the initial capital invested by VC and $qW_s + b \geq W_r \geq b$ is the income shared by both sides.

Stage 2: both sides exert efforts. e and a are the efforts exerted by EN and VC, respectively.

Stage 3: the state of the enterprise θ can be observed step by step, but it cannot be confirmed.

Stage 4: according to the state θ of the enterprise, both sides take the corresponding strategic behavior.

Stage 5: final revenue of the enterprise is realized, and both sides share the benefits according to the initial contract or renegotiation contract.

Project schedule is shown in Figure 1.

3.1. Assumption of State. Assuming that the natural state is discrete with only two states, $\theta = \{\theta_g; \theta_b\}$, which denote that the venture enterprise is in a good condition θ_g or in a bad condition θ_b, respectively. The probability is as follows:

$$\theta = \begin{cases} \theta_g, & \text{Prob} = p(e, a), \\ \theta_b, & \text{Pro}b = 1 - p(e, a). \end{cases} \tag{1}$$

In stage 3, whether the enterprise is in a good condition or not is influenced by the efforts devoted by both sides. Assume that the efforts devoted by EN are only of two types: exertion or inexertion, denoted as $e = \{0; 1\}$. "$e = 1$" indicates making efforts while "$e = 0$" indicates no efforts. Since we focus on how to motivate the efforts of EN in this paper, we assume that the efforts devoted by VC are a fixed level a; $\Omega = \pi^{VC} + \lambda_1 (qW_s - W_r - (C_{EN}/\mu) + b) + \lambda_2 (W_r - b) + \lambda_3 (\pi_s - W_s) + \lambda_4 (\pi_r - W_r)$. Assume that the probability in good state is $p(e, a) = u * (e + a)$, where λ_2. Due to λ_3 and λ_4, then suppose a constant $(\partial\Omega/\partial W_s) = 0$ is to ensure the probability $(\partial\Omega/\partial W_r) = 0$ is not larger than 1.

3.2. Assumption of Efforts. Assuming that VC devotes a fixed level effort λ_3 to the enterprise, the cost is λ_4. If the effort EN devoted is W_s, that is, making no efforts, then its cost is W_r; otherwise, if the effort EN devoted is $\lambda_1 = \mu(1 + a) > 0$, that is, making efforts, then the cost is $\lambda_2 = 1 > 0$. Therefore, EN can save its opportunity cost $\lambda_3 = 0$ if he makes no effort.

3.3. Assumption of Project Revenue under Different Strategic Behaviors. After observing the natural state θ, VC determines by himself or negotiates with EN to select strategic behaviors. One strategic choice is to maintain the status quo; that is, EN continues with the operation according to the business plan, which is defined as A_s. The other choice is to employ professional managers to replace EN, which is

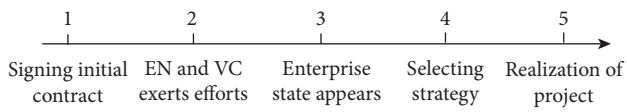

Figure 1: Game event sequence diagram under the contract arrangement.

defined as A_r. These two different strategic behaviors are denoted as $A = \{A_s; A_r\}$. These two strategic behaviors lead to different project profit and private benefit of EN.

Assume that both VC and EN are risk-neutral. The total revenue of the project is divided into two components: the project revenue shared by VC and EN and the private benefit exclusively owned by EN. It is because EN who is responsible for the daily operation is more familiar with the situation of the project than VC, which leads to the fact that EN can get extra private benefit through his operating over the enterprise.

Consider selecting strategic behavior A_s, that is, maintaining the status quo. EN can always get the private benefit b if he is not replaced. The project revenue depends on the enterprise's natural state. When the enterprise is in a good condition (natural state θ_g), it may obtain a high project revenue π_s with a probability of q; or it may obtain a low project revenue 0 with a probability of $1-q$. When the enterprise's natural state is bad (θ_b), keeping up the status quo will lead to failure of the enterprise project, and the project revenue surely is 0.

If selecting strategic behavior A_r, that is, EN is replaced by professional managers, EN has no private benefit, since he lost the operation of the enterprise. The project revenue will not be affected by the enterprise's natural state because the enterprise is operated by professional managers and the effort devoted by VC is still in a fixed level. So, no matter what the natural condition is (b or A_r), the project revenue is stable, which is denoted as b.

Table 1 summarizes the project revenue of the enterprise and private benefit of EN under different strategic behaviors in two natural conditions.

Chan et al. [3], Hellmann [26], and Gebhardt et al. [27] have provided detailed analyses on how to choose strategic behavior under these two conditions. Their main conclusions are as follows. When the enterprise is in good condition, it should keep the status quo, that is, keep EN continue to operate the enterprise, because the good condition indicates that the enterprise has a good prospect under the operation of EN. However, when the enterprise is in a bad state, EN should be replaced. According to the above conclusion, we make the following assumption on the relationship between the project revenue and private benefit.

$$q\pi_s + b > \pi_r > b, \tag{2}$$

$$q\pi_s > \pi_r. \tag{3}$$

Formula (2) suggests that an optimal strategic behavior will be determined by maximizing the total revenue of the project, that is, the sum of the project revenue shared by EN and VC and private benefit of EN. In the natural state θ_g,

Table 1: Project revenue under different enterprise's natural state and strategic behavior.

State behavior	θ_g		θ_b	
	Project revenue	Private benefit	Project revenue	Private benefit
θ_b	A_r	θ_b	0	b
A_r	π_r	0	π_r	ρ

$A_r + b > \pi_r$ is to ensure that strategic behavior A_s is selected, while $\pi_r > b$ is to ensure that strategic behavior A_r is selected when in natural state A_r.

Formula (3) suggests that optimal strategic behavior is to maximize the project revenue shared by VC and EN, without considering the private benefit of EN. When the enterprise is in good natural state, $A_r > \pi_r$ is to ensure that strategic behavior A_s is selected, while strategic behavior A_r is selected because $\pi_r > 0$.

EN can not only share the monetary revenue of the project but also have private benefit of the enterprise when he operates and controls the enterprise [28]. Thus, EN can gain private benefits if he maintains the status quo. So, even in the natural state W_r, EN may hope to keep up the status quo $\widehat{W_r}$ rather than effective strategic action 0 because of private benefits when the project revenue EN shared is less than the private benefit. This is moral hazard of EN due to pursuing private benefit.

3.4. Description of Social Value Constraints. After exerting fixed level effort a, VC needs to encourage EN to take effort $e = 1$ to maximize his profit, since EN can choose to make effort $e = 1$ or make no effort $e = 0$. To ensure that the behavior exerted by EN $e = 1$ is more effective than the behavior $e = 0$, we formulate a constraint from the aspect of social value as follows:

$$\begin{aligned}&\mu(1+a)(q\pi_s + b) + [1-\mu(1+a)]\pi_r - C_{VC} - C_{EN}\\&\quad > \mu a(q\pi_s + b) + (1-\mu a)\pi_r - C_{VC}.\end{aligned} \tag{4}$$

Formula (4) shows that the social value when EN takes effort is bigger than that when EN takes no efforts.

3.5. Description of Revenue Allocation Scheme of the Contract. The initial contract stipulates the revenue allocation scheme for VC and EN under different strategic behavior choices. The initial contract ϕ is as follows.

Under the strategic action A_s, the project revenue of the enterprise is A_s, and the benefit distributed to EN is θ_b, while under the strategic action $\max \Phi = (\widehat{W_r} - b)^{\rho}(\pi_r - \widehat{W_r})^{1-\rho}$, the project revenue is $\widehat{W_r} \geq \widehat{W}b$, and the benefit distributed to EN is $\pi_r \geq \widehat{W_r}$.

VC and EN both have limited liability, so limited liability (LL) constraint should be met:

$$\begin{aligned}&0 \leq W_s \leq \pi_s,\\&0 \leq W_r \leq \pi_r.\end{aligned} \tag{5}$$

4. Contract Designing with Strategy Behavior Choices

4.1. Initial Contract Designing Based on the Double Moral Hazard. The purpose of designing an initial contract between VC and EN is to improve efforts of both sides based on maximizing their own benefits. In a well-designed initial contract, optimal strategic action A_s is taken by both VC and EN when the enterprise is in a natural state θ_g, while A_r is selected when the enterprise is in the state θ_b.

4.1.1. Constraints Designed to Motivate EN. To maximize his revenue, EN takes strategic action A_s when the natural state of the enterprise is θ_g, while EN takes strategic action A_r when in a natural state θ_b. Thus, the following condition (C-1) should be satisfied:

$$(\mathrm{C}-1): qW_s + b \geq W_r \geq b. \tag{6}$$

On the other hand, to motivate EN to make efforts $e = 1$ instead of $e = 0$, the following incentive compatibility (IC) constraints should be satisfied simultaneously in the initial contract allocation scheme:

$$\begin{aligned}(\mathrm{IC}):\ & \mu(1+a)(qW_s + b) + [1-\mu(1+a)]W_r - C_{EN} \\ & \geq \mu a(qW_s + b) + (1-\mu a)W_r.\end{aligned} \tag{7}$$

Formula (7) is simplified as follows:

$$qW_s - W_r \geq \frac{C_{EN}}{\mu} - b. \tag{8}$$

4.1.2. Optimization of Contract to Motivate VC. When VC and EN negotiate the initial contract allocation scheme, VC maximizes his own benefit through the arrangement of payoff W_s and W_r, while ensuring that EN make efforts $e = 1$ instead of $e = 0$.

Therefore, contract optimization problem of VC can be described as

$$\begin{aligned}\max_{W_s, W_r} \pi^{\mathrm{VC}} &= \mu(1+a)q(\pi_s - W_s) + [1-\mu(1+a)](\pi_r - W_r) \\ &\quad - C_{\mathrm{VC}}, \\ \mathrm{S.T.}\ (\mathrm{IC}):\ & q(W_s - W_r)\frac{C_{EN}}{\mu} - b, \quad W_r \geq b, \\ (\mathrm{LL}):\ & W_s - \pi_s, \quad W_r - \pi_r.\end{aligned} \tag{9}$$

This is a nonlinear programming problem satisfying the Kuhn-Tucker conditions, which can be solved by using the Kuhn-Tucker theorem. Assume that

$$\begin{aligned}\Omega = \pi^{\mathrm{VC}} &+ \lambda_1\left(qW_s - W_r - \frac{C_{\mathrm{EN}}}{\mu} + b\right) + \lambda_2(W_r - b) \\ &+ \lambda_3(\pi_s - W_s) + \lambda_4(\pi_r - W_r),\end{aligned} \tag{10}$$

where λ_1, λ_2, λ_3, and λ_4 are the Lagrange multipliers of each constraint (IC and LL).

Let $(\partial\Omega/\partial W_s) = 0$, and $(\partial\Omega/\partial W_r) = 0$, so we can get the Kuhn-Tucker conditions:

$$\begin{cases} -\mu(1+a)q + \lambda_1 q - \lambda_3 = 0, \\ -[1-\mu(1+a)] - \lambda_1 + \lambda_2 - \lambda_4 = 0, \\ \lambda_1\left(qW_s - W_r - \dfrac{C_{EN}}{\mu} + b\right) = 0, \\ \lambda_2(W_r - b) = 0, \\ \lambda_3(\pi_s - W_s) = 0, \\ \lambda_4(\pi_r - W_r) = 0. \end{cases} \tag{11}$$

By analyzing whether λ_1, λ_2, λ_3, or λ_4 is zero, we can find W_s and W_r which meet the inequality above. The results where the values of λ_1, λ_2, λ_3, and λ_4 satisfy the Kuhn–Tucker conditions are

$$\begin{aligned}\lambda_1 &= \mu(1+a) > 0, \\ \lambda_2 &= 1 > 0, \\ \lambda_3 &= 0, \\ \lambda_4 &= 0.\end{aligned} \tag{12}$$

Thus, the revenue that is allocated to EN is

$$\begin{aligned}W_s &= \frac{C_{\mathrm{EN}}}{\mu q}, \\ W_r &= b.\end{aligned} \tag{13}$$

Formula (13) suggests that, under condition (C-1) in formula (6), $qW_s + b \geq W_r \geq b$, VC and *EN* only stipulate in the initial contract where the income allocated to *EN* is $W_s = (C_{EN}/\mu q)$ when keeping *EN* to operate the enterprise, while the income allocated to *EN* becomes $W_r = b$ when replacing *EN* with professional managers. This allocation scheme ensures that EN takes the effective strategic action actively and makes efforts without renegotiating or redesigning the income allocation scheme. At the same time, it will also relieve *VC* the "hold up" of moral hazard caused by EN selecting alternative ineffective strategic choice through his control of core resources of the enterprise.

4.2. Renegotiation of Contract

4.2.1. The Condition of the Renegotiation of Contract. As noted above, EN may attain large private benefit at the cost of the enterprise's long-term interests. When the private benefit is big beyond a certain threshold, it is necessary for VC to readjust the initial contract.

Consider the condition of readjusting the initial contract: $b > W_r$. When the enterprise is in the natural state θ_b, EN takes the strategic action A_s and maintains the operation of the enterprise. Although the project revenue is zero and *EN* gets zero revenue, EN can attain private benefit b. If the strategic action A_r is taken to replace EN by professional managers, EN loses his private benefit b because of the replacement; thus EN can only get the allocation revenue W_r according to the initial contract. Obviously, if $b > W_r$, it is better for EN to stay in the enterprise instead of being replaced by professional managers.

Therefore, if the revenue allocated to EN W_r is less than the private benefit b in the initial contract, EN will try to stay in the enterprise instead of actively hiring professional managers even when the enterprise is in a bad state. Although this action is at the cost of the interest of VC, it is optimal for EN. This is the moral hazard caused by the nominal control of the entrepreneur, which is also called the moral hazard that entrepreneurs "hold up" venture capitalists in some literature.

4.2.2. Optimization of Renegotiation Contract. To eliminate the moral hazard that holds up VC, an effective solution is VC and EN renegotiates to redesign the initial allocation contract after observing the natural state θ_b. By increasing the entrepreneur's distributed revenue during reallocating the revenue of the enterprise, EN will actively take the effective strategic action A_r when in the natural state θ_b; thus, the moral hazard of EN is eliminated.

The key term in the renegotiation contract is to optimize $\widehat{W_r}$ to realize the Pareto improvement of the benefit of both EN and VC. Let us denote $\widehat{W_r}$ as the revenue of the enterprise in the renegotiation contract to motivate EN actively to take the strategic action A_r, that is, actively hiring professional managers to replace himself. Table 2 describes the distribution of enterprise's revenue under the new allocation scheme when the enterprise is in a bad natural state θ_b.

Table 2: Revenue distributed to EN and VC in the natural state θ_b.

	In the initial contract		In the renegotiation contract
	Revenue under A_s	Revenue under A_r	Revenue under A_r
EN	b	W_r	$\widehat{W_r}$
VC	0	$\pi_r - W_r$	$\pi_r - \widehat{W_r}$

During the negotiation process, the reallocation of the revenue depends on bargain power between VC and EN. We denote fine ρ as the bargaining power of EN, and $1-\rho$ is the bargaining power of VC. Based on Nash equilibrium of bargaining game, we construct the following optimizing problem realizing the Pareto improvement:

$$\begin{aligned} &\max_{\widehat{W_r}} \quad \Phi = \left(\widehat{W_r} - b\right)^{\rho}\left(\pi_r - \widehat{W_r}\right)^{1-\rho}, \\ &\text{S.T.} \quad \widehat{W_r} \geq b, \pi_r \geq \widehat{W_r}. \end{aligned} \tag{14}$$

Let $(\partial\Phi/\partial\widehat{W_r}) = 0$, so we get

$$\begin{aligned} (1-\rho)\left(\widehat{W_r} - b\right) &= \rho\left(\pi_r - \widehat{W_r}\right), \\ \widehat{W_r} &= (1-\rho)b + \rho\pi_r = b + \rho\left(\pi_r - b\right). \end{aligned} \tag{15}$$

Besides ensuring that EN actively hires professional managers to eliminate the moral hazard of "hold up" in the natural state θ_b, VC also needs to motivate EN to make efforts instead of making no efforts in the renegotiation contract. Incentives' compatibility condition is

$$\begin{aligned} \text{(IC)}: &\ \mu(1+a)\left(qW_s + b\right) + \left[1 - \mu(1+a)\right]\left[(1-\rho)b + \rho\pi_r\right] \\ &- C_{EN} \geq \mu a\left(qW_s + b\right) + (1-\mu a)\left[(1-\rho)b + \rho\pi_r\right]. \end{aligned} \tag{16}$$

The above formula can be simplified as

$$qW_s \geq \frac{C_{\text{EN}}}{\mu} + \rho\left(\pi_r - b\right). \tag{17}$$

Therefore, the optimization problem of VC can be described as

$$\begin{aligned} &\max_{W_s} \quad \pi^{\text{VC}} = \mu(1+a)q\left(\pi_s - W_s\right) + \left[1 - \mu(1+a)\right]\left(\pi_r - \widehat{W_r}\right) - C_{\text{VC}}, \\ &\text{S.T. (IC)} \quad qW_s \geq \frac{C_{\text{EN}}}{\mu} + \rho\left(\pi_r - b\right), (1-\rho)\left(\widehat{W_r} - b\right) = \rho\left(\pi_r - \widehat{W_r}\right), \\ &\text{(LL)}: W_s \leq \pi_s, W_r \leq \pi_r. \end{aligned} \tag{18}$$

This is an extreme value problem satisfying Kuhn–Tucker conditions. Similarly, we can get the solution of revenue reallocation in the renegotiation contract as follows:

$$\begin{aligned} W_s &= \frac{C_{\text{EN}}}{\mu q} + \frac{\rho\left(\pi_r - b\right)}{q}, \\ \widehat{W_r} &= b + \rho\left(\pi_r - b\right). \end{aligned} \tag{19}$$

4.2.3. Discussion on the Bargaining Power ρ. Calculating the first derivative of W_s and $\widehat{W_r}$ in formula (19) with respect to ρ, we can get

$$\frac{\partial W_s}{\partial \rho} = \frac{\pi_r - b}{q} > 0,$$
$$\frac{\partial \widehat{W_r}}{\partial \rho} = \pi_r - b > 0. \tag{20}$$

Obviously, we have

$$\frac{\partial W_s}{\partial \rho} > \frac{\partial \widehat{W_r}}{\partial \rho} > 0. \tag{21}$$

From formula (20), we find that the stronger the bargaining power of EN is, the higher the revenue EN required. That is, whether the enterprise is in the good state or in the bad state, the revenue distributed to *EN* (W_s or $\widehat{W_r}$) and his bargaining power ρ are positively correlated. On the other hand, formula (21) shows that the margin increasing rate of W_s to ρ is higher than that of $\widehat{W_r}$ to ρ. It suggests that EN's bargaining power can help EN get more compensation when EN stays in the enterprise compared to when he is replaced.

The above conclusion is also reasonable in practice. EN's negotiating power comes from his specialty of human capital. When EN has a high specialty of human capital, this specialty is important and difficult to be replaced for the development of the enterprise. So this specialty of human capital provides EN a high bargaining power in the renegotiation process. Consequently, *VC* has to distribute more revenue to EN to maximize his benefit.

4.3. Implications. As discussed in Section 4.2, when the enterprise is in a bad operation state, the revenue shared by VC and EN decreases; thus the revenue distributed to EN also decreases. So if the private benefit extracted by EN is greater than a threshold, EN will pursue this private benefit but will not be concerned about the revenue shared by VC and EN. Although this action maximizes EN's benefit, it damages the benefit of VC. This is the reason why VC needs to renegotiate with EN through distributing more revenue to EN. The implication is that it is necessary for VC to restrain EN pursuing the private benefit, which not only directly improves the operation efficiency of the enterprise but also motivates EN to take effective action when the enterprise is in a bad state. The measures of restraining EN's pursuit of private benefit include increasing transparency of the enterprise, reducing information asymmetry between EN and VC, and enhancing financial control on the enterprise during the process of providing services and advices to EN.

Secondly, comparing the revenue distributed to EN in the initial contract expressed in formula (13) and that in the negotiation contract expressed in formula (19), we find that the latter is bigger than the former. This suggests that *VC* needs to distribute more revenue to EN in the negotiation process to remotivate EN when EN can get a large private benefit; thus the higher revenue which EN attained in the negotiation process leads EN to select strategic behavior according to the long-term interests of the enterprises instead of private interests.

Thirdly, in the renegotiation contract, the bargaining power of EN plays a key role in the revenue allocation. Strengthening mutual understanding between both sides, enhancing the information transparency, and reducing the information asymmetry help to weaken the bargaining power of EN, thus improving the efficiency of benefit allocation in designing contract.

5. Case Study

Owing to commercial secrets and other required secrets, the details of the contract signed by venture capitalist and entrepreneur are not public. It is short of detailed operation and financial situations from the public channels. Thus, researchers usually cannot get enough details to empirically investigate the moral hazard problems from the perspective of contract designing. That is the reason why current literature on the double moral hazard between the capitalist and entrepreneur still stays in the stage of making normative analysis and theoretical design. In this section, we use case study to demonstrate our model. The case is about the cooperation and the corresponding fighting for control rights between Alibaba Group and Yahoo Inc.

5.1. Finding of Venture Enterprise Alibaba Group. Alibaba Group is a China-based group of Internet-based e-commerce businesses including business-to-business online web portals, online retail and payment services, a shopping search engine, and data-centric cloud computing services. The company was founded in the apartment of the current CEO, Jack Ma, in 1999. At that time, Jack Ma and 17 other founders released their first online marketplace named "Alibaba Online"; and, in December 2001, Alibaba Online began to achieve profitability. For seeking broad market space, in May 2003, Taobao was founded as a consumer e-commerce platform; and, in December 2004, Alipay, which started as a service on the Taobao platform, became a separate business. These platforms constitute the key elements of Alibaba Group. In 2012, two of Alibaba's portals together handled 1.1 trillion yuan ($170 billion) in sales, more than the competitors eBay and Amazon.com combined. On 18 September 2014, Alibaba's IPO was priced at US$68, raising US$ 21.8 billion for the company and investors. Alibaba was the biggest U.S. IPO in history. At close time, on the date of its initial public offering (IPO), Alibaba's market value was measured at US$ 231 billion.

5.2. Acquiring the Support from Venture Capitalists. When Jack Ma founded the company, it was just an Internet company, owning a good market idea and computer technology but starving for venture capital. From 1999 to 2000, Alibaba Group raised a total of US$ 25 million from SoftBank, Goldman Sachs, Fidelity, and some other institutions, which provided initial capital for Alibaba Online startup.

After 6 years of difficult venture, Alibaba Group provided a broad outline for further development. Meanwhile,

Alibaba Group also met the development bottleneck, starving for a great deal of venture capital and Internet services. Fortunately, Alibaba Group and Yahoo! Inc came together. In October 2005, Alibaba Group formed a strategic partnership with Yahoo! Inc and acquired China Yahoo! (http://www.yahoo.com.cn), a Chinese portal that focuses on Internet services such as news, email, and search. Yahoo became the largest controlling shareholder of Alibaba Group by using $10 billion and Yahoo all business in China to change Alibaba Group's 40% stock rights. Softbank held 29 percent of Alibaba's shares and voting rights.

Thus, Yahoo and Softbank as capitalists of venture enterprise Alibaba Group have formed stable three-side relationship with the entrepreneurs, Jack Ma management team. This stable relationship speeded the development of Alibaba Group. Under the support from the corporation framework of initial contract, Alibaba Group succeeded in making Alipay, Taobao, Taobao mall, Ali cloud, China Yahoo, and so forth into its all wholly owned subsidiaries by the way of acquisition and merge, and Alibaba Group had gotten a rapid development. In 2007, Alibaba.com Ltd. went public on Hong Kong Stock Exchange, which amounted to 15$ billion by Public financing; and in fact the finance amount reached 16.9$ billion if adding the overallotment option at that day, which exceeded the finance amount of 16.7$ billion that Google company went public and get finance and set a new record about finance amount by global Internet company going public. This was a successful investment contract, which promoted the close cooperation between venture capital and venture enterprise and boosted the great success of Alibaba Group.

5.3. Fighting for Control Rights between Capitalists and Entrepreneurs. After Alibaba Group got a great success, the war of interest distribution broke out between capitalists and entrepreneurs. In 2009, when Alibaba Group held the tenth anniversary celebration, Yahoo beyond all expectations undersold its hold share of 1% Alibaba Group's share to improve its sliding in the stock price. Furthermore, Yahoo hoped that Alibaba Group wholly owned subsidiaries, such as Taobao and Alipay, go public, which would bring about high returns and cash flow to Yahoo. This action is to some extent harmful to Alibaba Group as the selling share of its strategic investor released a bad sign to the public.

On the other hand, Alibaba also took a fight back action. As the core of Alibaba Group, Jack Ma and his management team stripped the core business and core subsidiaries, including Alipay and Taobao company from the Alibaba Group, which had not been unauthorized by the shareholder's meeting. This provoked Yahoo that was to use the controlling shareholder's control right to replace Jack Ma and his management team with joint actions of Softbank.

5.4. Renegotiation between Capitalists and Entrepreneurs. Teaming up together again becomes an ideal tendency, when both sides of venture capital and venture enterprise truly understand the idea "Cooperation is a win-win, while fighting leads double defeat."

Yahoo and Alibaba Group have been fighting for themselves about private interests for three years since 2009. They eventually went back to the conference table and renegotiated together. Yahoo began to take some active measures; for example, Yahoo's president stressed that they highly respect Jack Ma's management team and their achievements and promised to devote himself to establishing a good business relationship and continue providing a large amount technical cooperation, including that Yahoo will continue to provide core technology, oversea business, and tunnel and ad-serving platform to help Alibaba Group.

On May 21, 2012, Alibaba announced an agreement with Yahoo. In the agreement, Alibaba would repurchase one-half of the shares held by Yahoo with $6.3 billion in cash and no more than $800 million in newly issued Alibaba preferred stock. In September of that year, the repurchase was completed. After the deal, the voting rights of Yahoo and Softbank have declined to less than 50 percent. In the new board of the company, Alibaba, Yahoo, and Softbank would maintain a ratio of 2:1:1. Yahoo also agreed to give up the veto it had wielded over Alibaba's strategic and business decisions. These actions had ensured Jack Ma's management team could have more of a say in such decisions, paving the way for business restructuring and a potential IPO.

5.5. Case Analysis. This case provides a good example for the renegotiation to mitigate double moral hazard between venture capitalists and entrepreneurs.

At the beginning, Alibaba had a good development with the support of Yahoo and Softbank. But after Alibaba had made some initial success, both sides of capitalists and entrepreneurs took some actions based on their own private interests, which were harmful to each other. This is the situation of stage four, which is described in our model. For the long-term development of Alibaba Group, it is necessary for Yahoo, Softbank, and Jack Ma's management team to cooperate closely with each other. Without the help from Yahoo and Softbank, such as Yahoo's technical support and Softbank's good peripheral channels and overseas business, Alibaba would be difficult to make further expansions of their business, especially overseas business. On the other hand, if Yahoo and Softbank replaced Jack Ma's management team using their control right, Alibaba would be a "shell" lacking the soul of Jack Ma as Alibaba had been branded by the values of Jack Ma and his management team.

For the strategic behavior of capitalists, Yahoo and Softbank had two choices. One is to replace Jack Ma's management team with another professional team. The other is to keep up the status quo, that is, letting Jack Ma and his management team control and manage Alibaba Group.

As discussed in our model, how to choose the strategic choice is determined by the state of the enterprise. According to the good development of Alibaba, the capitalist Yahoo should continue to maintain Jack Ma's management team instead of replacing them. But Yahoo needed to find a solution to prevent the management team pursuing private benefit. In this case, Yahoo renegotiated with the

management team and got a monetary benefit from the exchange between the voting rights and ownership.

From the case, we find that it is normal for the capitalist and entrepreneur try to seek their private benefits. The key is how to choose the strategic behavior to mitigate the double moral hazard. As our model shows, renegotiation of both sides to form a new balance of contract is a good solution, which not only considers mutual interests of both sides but also promotes their efforts. Although this case cannot use empirical data to accurately analyze our contract model, the process of fighting for control rights between Alibaba and Yahoo can still qualitatively describe our idea on mitigating moral hazard by contract designing and optimization under the framework with various strategic behavior choice.

6. Conclusion

In this paper, we consider the further strategic choice (renegotiation contract) after signing an initial contract. In the variety process of venture enterprise's development state, whether to keep up the status quo or to replace management team with professional manager is a painful choice for venture enterprise when there appears a certain unfavorable situation. This is a common phenomenon, but this kind of common phenomenon implies that the venture enterprise can take advantage of this opportunity (as a threat). After signing the contract, venture capitalist may threat venture enterprise by ending cooperation in order to motivate venture entrepreneur's effort level. This is a kind of strategy behavior.

Casamatta & Schmidt's study did not consider using strategic behavior to stimulate the efforts of both sides, while mainly concentrating on the choice of financial instruments. Regarding this strategic behavior choice as a motivator and combining strategic behavior with financial instrument options is an important breakthrough in this paper. Not only is the choice of financial instruments a factor to stimulate efforts of both sides, but also the strategic behavior choice of cooperating or not after contract signing should also be included. This strategic behavior is used as postthreats.

The main breakthrough of this research conclusion is to divide contract into initial contract and renegotiation contract. Initial contract is mainly to motivate effort by the arrangement of financial instruments, while renegotiation contract provides strategic behavior choices of whether to cooperate or replace venture entrepreneur for venture enterprise. On the basis of strategic behavior choices, designing corresponding contract to motivate venture entrepreneur's effort level is an important research frame.

Some conclusions can be reached from renegotiating contract:

(1) Joint effort of both sides can be motivated through strategic behavior choice and then lead to increasing the overall value of venture enterprise. Viewed from the social welfare, it increases social overall benefit and realizes the result of positive-sum game.

(2) After venture enterprise gained private benefits in the early stage, venture capitalist needs to make appropriate assignment and demisability in benefits to remotivate venture enterprise's efforts, aiming to further balance venture enterprise's private benefits and the earnings redistributed by venture capitalist. Once the balance can be greater incentive to venture entrepreneur, he will focus on long-term benefits and give up the private benefits.

(3) There is a close relationship between benefit assignment motivation of venture enterprise's efforts and the bargaining power of venture entrepreneur. Venture capitalist may inhibit the bargaining power of venture entrepreneur appropriately by enhancing information transparency of venture enterprise.

In general, the paper forms a research frame, in which two strategic behavior choices are considered overall to be introduced into contract arrangement, which depends on different conditions to design corresponding contracts optimization, including the non-in-depth analysis of various financial instruments, such as equity contracts and convertible bond contracts. These institutional arrangements have vital significance to motivate both sides' efforts and alleviate double moral hazard.

Follow-up studies can further consider combining strategic behavior choice with contract tools to control or adjust the income distribution between both sides through contingent control, which motivate the efforts of both sides indirectly by combining strategic behavior choice and slow or partly eliminate double moral hazard. This is a more realistic and feasible idea.

Data Availability

Data sharing is not applicable to this article as no data sets were generated or analyzed during the current study.

Conflicts of Interest

The authors declare no conflicts of interest.

Acknowledgments

This work was supported in part by the 2020 Shanghai University Key Undergraduate Education Reform Project "Exploration and Practice of the Construction of New Fintech Majors from the Perspective of the Development of Fintech Industry."

References

[1] M. J. Barclay and C. G. Holderness, "Private benefits from control of public corporations," *Journal of Financial Economics*, vol. 25, no. 2, pp. 371–395, 1989.

[2] C. Casamatta, "Financing and advising: optimal financial contracts with venture capitalists," *The Journal of Finance*, vol. 58, no. 5, pp. 2059–2085, 2010.

[3] Y.-S. Chan, D. Siegel, and A. V. Thakor, "Learning, corporate control and performance requirements in venture capital contracts," *International Economic Review*, vol. 31, no. 2, pp. 365–381, 1990.

[4] V. Yerramilli, "Moral hazard, hold-up, and the optimal allocation of control rights," *The RAND Journal of Economics*, vol. 42, no. 4, pp. 705–728, 2011.

[5] S. Mullainathan and Z. Obermeyer, "Does machine learning automate moral hazard and error?" *American Economic Review*, vol. 107, no. 5, pp. 476–480, 2017.

[6] F. Thies, A. Huber, C. Bock, A. Benlian, and S. Kraus, "Following the crowd-does crowdfunding affect venture capitalists' selection of entrepreneurial ventures?" *Journal of Small Business Management*, vol. 57, no. 4, pp. 1378–1398, 2019.

[7] A. R. Admati and P. Pfleiderer, "Robust financial contracting and the role of venture capitalists," *The Journal of Finance*, vol. 49, no. 2, pp. 371–402, 1994.

[8] V. Babich, S. Marinesi, and G. Tsoukalas, "Does crowdfunding benefit entrepreneurs and venture capital investors?" *Manufacturing & Service Operations Management*, vol. 23, no. 2, pp. 508–524, 2021.

[9] A. Cavallo, A. Ghezzi, C. Dell'Era, and E. Pellizzoni, "Fostering digital entrepreneurship from startup to scaleup: the role of venture capital funds and angel groups," *Technological Forecasting and Social Change*, vol. 145, pp. 24–35, 2019.

[10] H. Fu, J. Yang, and Y. An, "Contracts for venture capital financing with double-sided moral hazard," *Small Business Economics*, vol. 53, no. 1, pp. 129–144, 2019.

[11] E. Berglof, "A control theory of venture capital finance," *Journal of Law Economics & Organization*, vol. 10, no. 2, pp. 247–267, 1994.

[12] O. Hart and J. Moore, "A theory of debt based on the inalienability of human capital," *The Quarterly Journal of Economics*, vol. 109, no. 4, pp. 841–879, 1994.

[13] S. N. Kaplan and P. Stromberg, "Financial contracting theory meets the real world: an empirical analysis of venture capital contracts," *Review of Economic Studies*, vol. 70, no. 2, pp. 281–315, 2003.

[14] D. Cumming and S. A. B. Johan, "Advice and monitoring in venture finance," *Financial Markets and Portfolio Management*, vol. 21, no. 1, pp. 3–43, 2007.

[15] D. J. Cumming and S. A. Johan, *Venture Capital and Private Equity Contracting: An International Perspective*, Elsevier, Amsterdam, Netherlands, 2013.

[16] D. V. Neher, "Staged financing: an agency perspective," *Review of Economic Studies*, vol. 66, no. 2, pp. 255–274, 1999.

[17] P. Aghion and P. Bolton, "An incomplete contracts approach to financial contracting," *The Review of Economic Studies*, vol. 59, no. 3, pp. 473–494, 1992.

[18] F. Cornelli and O. Yosha, "Stage financing and the role of convertible securities," *Review of Economic Studies*, vol. 70, no. 1, pp. 1–32, 2003.

[19] R. Inderst, H. M. Mueller, and F. Münnich, "Financing a portfolio of projects," *Review of Financial Studies*, vol. 20, no. 4, pp. 1289–1325, 2007.

[20] R. Bachmann and I. Schindele, *Theft and Syndication in Venture Capital Finance*, Social Science Electronic Publishing, Rochester, NY, USA, 2006.

[21] D. J. Cumming, "Capital structure in venture finance," *Journal of Corporate Finance*, vol. 11, no. 3, pp. 550–585, 2005.

[22] X. Tian, Z. Xu, J. Gu, and E. Herrera-Viedma, "How to select a promising enterprise for venture capitalists with prospect theory under intuitionistic fuzzy circumstance?" *Applied Soft Computing*, vol. 67, pp. 756–763, 2018.

[23] K. P. Thomas, *Investment Incentives and the Global Competition for Capital*, Palgrave Macmillan UK, London, UK, 2011.

[24] C. Bienz and U. Walz, "Venture capital exit rights," *Journal of Economics & Management Strategy*, vol. 19, no. 4, pp. 1071–1116, 2010.

[25] C. Casamatta and C. Haritchabalet, *Learning and Syndication in Venture Capital Investments*, Elsevier, Amsterdam, Netherlands, 2003.

[26] T. Hellmann, "The allocation of control rights in venture capital contracts," *The RAND Journal of Economics*, vol. 29, no. 1, pp. 57–76, 1998.

[27] G. Gebhardt and K. M. Schmidt, *Conditional allocation of control rights in venture capital finance*, Ludwig Maximilian University of Munich, Ingolstadt, Germany, 2006.

[28] P. Aghion and J. Tirole, "Formal and real authority in organizations," *Journal of Political Economy*, vol. 105, no. 1, pp. 1–29, 1997.

Hindawi
Scientific Programming
Volume 2021, Article ID 9961071, 12 pages
https://doi.org/10.1155/2021/9961071

Research Article

Green Technology Collaboration Network Analysis of China's Transportation Sector: A Patent-Based Analysis

Lufei Huang,[1,2] **Ying Xu**,[2] **Xiaohui Pan**,[3,4] **and Tao Zhang**[5]

[1]*Shanghai Financial Technology Research Centre, Shanghai Lixin University of Accounting and Finance, Shanghai 201209, China*
[2]*School of Financial Technology, Shanghai Lixin University of Accounting and Finance, Shanghai 201209, China*
[3]*School of Management, Shanghai University, Shanghai 200444, China*
[4]*School of Artificial Intelligence and Law, Shanghai University of Political Science and Law, Shanghai 201701, China*
[5]*Department of Computer Engineering and Science, Shanghai University, Shanghai 200444, China*

Correspondence should be addressed to Xiaohui Pan; panxiaohui@shupl.edu.cn

Received 5 March 2021; Revised 19 March 2021; Accepted 25 March 2021; Published 7 April 2021

Academic Editor: Tingsong Wang

Copyright © 2021 Lufei Huang et al. This is an open access article distributed under the Creative Commons Attribution License, which permits unrestricted use, distribution, and reproduction in any medium, provided the original work is properly cited.

The development of green transportation technologies in China has grown rapidly due to increasing concerns about climate change and environmental pollution. Collaboration innovations covering kinds of participating entities and various linked relationships have become one of the critical drivers for the transportation sector. Some researchers have analysed the collaborative innovation of scientific literature in this field. However, fewer studies have investigated the current performance of collaborative technology innovation represented by patents in the transportation sector. In this context, a research framework based on the social network analysis approach is proposed for collaboration green transportation technologies. The purpose of the research is to establish an analytical framework for the green transportation innovation network and seek the key collaboration activities and strategies. Subsequently, a collaborative innovation network based on the patent data of green transportation technologies was built and analysed. Especially, the innovation entities in the collaboration network are divided into four groups: business enterprises, individuals, universities, and research institutions, so that more detailed information in the network could be obtained. The results show that the proposed research framework based on patent data and social network analysis method helps examine the critical nodes and links in the network, as well as their types and characteristics of the collaboration network. The increasing number of green transportation technologies shows active cooperation in this field. The study also found that business enterprises node gradually plays a major role in cooperative innovation. The corresponding policy recommendations are also provided.

1. Introduction

Not surprisingly, China is growing into one of the world's most crucial transportation market. A report conducted by Forbes.com shows that ten transportation enterprises in China made the Forbes Global 2000, with each rising significantly in rank Forbes Global 2000: the World's Largest Transportation Companies 2018 (https://www.forbes.com/sites/antoinegara/2018/06/06/forbes-global-2000-the-worlds-largest-transportation-companies/#6e40011b100f). According to the World Bank database, China's definite advantage in transportation infrastructure prompts its rank rise in the logistics performance index system. The latest report on the logistics performance index shows that China has become the top performer among upper-middle-income economies [1]. Based on the booming development of China's transportation market, research on China's GTTs is also gradually rising. Wang et al. [2] applied the transportation mode-technology-energy-CO_2 model to analyse the energy consumption and CO_2 emissions in China's transportation sector. Wang et al. [3] investigated the impact of three different policies on the implementation of electric vehicle technology. Liu et al. [4]

employed the DEA approach to measure the technological progress and environmental efficiency of China's road transportation industry.

As a complex innovation activity that impacts public transportation and trade flow, transportation technologies (TTs) are undergoing revolutionary upgrades to cope with the changing demand market [5]. There into, green transportation technologies (GTTs) are regarded as practical solutions to improve the sustainable performance of the transportation sector in the increasingly severe environmental crisis [6]. In line with the sustainable requirement, a continuous body of research literature and research applications explored the creation, verification, and adoption of GTTs [7]. For instance, Pelletier et al. [8] presented an overview of the technologies and marketing research in the field of green transportation represented by electric vehicles. Perboli and Rosano [9] employed simulation optimization technology to study business and operational models of traditional and green couriers. OECD promoted the environmentally sustainable transport (EST) initiative to construct a common understanding across the global world on the basic concepts of green transportation [10]. McKinsey & Company released a study on the critical factors of efficient urban transportation in 24 world cities to help leaders understand the knowledge and technologies needed to improve public health [11].

Furthermore, scholars, enterprises, and organizations widely participate in related innovation activities to boost the development of GTTs. The role of collaboration in stimulating the growth of the transportation market has been gradually emphasized. Marra et al. [12] researched green technology companies in San Francisco, New York, and London to recognize their specialization and collaboration field of the transportation sector and forecast the potential emerging technologies. The available literature on the analysis of GTTs collaborative innovation is on the strength of various levels, such as the regional case study [13], advanced model simulation [14], and green operation strategy [15]. Luan et al. [16] constructed an analysis framework that analysed the effect of collaboration among traffic information service providers, local governments, and users. Sun and Rahwan [17] investigated the co-authors' network of scientific collaboration in transport research by using published metadata.

It is worth noting that the above outputs about China's transportation sector and GTTs are achieved through cooperation and collaboration between individuals and/or organizations. In the context of the emerging development of the transportation industry, it is crucial to find out the major players in China's GTTs collaboration activities in the transportation sector and how those collaboration activities among different players influence green collaboration innovation performance. However, few studies analysed the collaborative activities aimed at transportation technology innovation, especially for GTTs in China. Moreover, existing research focused attention on the segment transportation market or specific technology [18, 19] than on the whole transportation industry [20]. Thus, those literature gaps motivate the demand to explore the current performance and future trend of GTTs collaboration innovation activities in China's transportation sector.

From the methodological perspective, the social network analysis approach, which is widely used in bibliometric analysis and complex social analysis, has also been employed to present the collaboration relationship among different organizations and individuals. Key nodes and links in the collaboration can be detected accordingly. Al-Tabbaa and Ankrah [21] applied the social network analysis method to uncover the dynamics of social capacity for university-industry collaboration. Liu et al. [22] used social network analysis to investigate the evolutionary course of the global nanotechnology collaboration network. From the view of research data, patents are recognized as a valid form of transforming knowledge into technology [23]. Chai et al. [24] investigated to empirically examine the intensity and structure of the entire city network in the Yellow River Basin using the social network analysis method and ArcGIS software. More and more individuals and organizations put a large amount of investment in the research of new technology and the declaration of patents, especially green technology patents. Technically, the World Intellectual Property Organization (WIPO), the international organization for intellectual property services, released a guidance list called IPC (International Patent Classification Number) green inventory for facilitating patent searches and applications relating to environmentally sound technologies (ESTs). The list has been applied for energy technologies studies [25] and macroanalysis of green technology innovation [26]. Moreover, the "collaboration effect" of the cooperative patent application by multiple entities has been widely demonstrated and implemented in patent research [27–29].

Motivated by the abovementioned content, our research aims to investigate GTTs collaboration in China's transportation sector based on the social network analysis method and GTTs patent data. This study makes contributions to the transportation field as the following research objectives described.

1.1. Research Objectives.

(i) To measure the evolution and current performance of GTTs collaborative innovation in China's transportation sector with the IPC green inventory and patent data

(ii) To identify the participants who involve the collaborative innovation of GTTs patents and the collaboration relation in China's transportation sector

(iii) To provide relevant policy implications on these results

The rest of this study is arranged as follows. In Section 2, a detailed research framework is depicted. Section 3 provides the results and discussion. The conclusion and future research direction are summarized in Section 4.

2. Materials and Methods

2.1. Research Framework. To clear the research flow of this study, a detailed research framework, including four steps, is illustrated in Figure 1.

Step 1. First, the GTTs-related collaboration patents at the SIPO (State Intellectual Property Office of China) database were collected by a developed Python crawler tool (the source code is available at the github.com https://github.com/huangPark/IPC_patent_collection.git). SIPO database is the official patent database of China that contains the complete patent information in China and frequently used in innovation and technology studying [30]. The survey period is set to 2007–2018. WIPO's green IPC inventory list is used for the filtering of GTTs.

Step 2. A multiattribute index system is constructed to preprocess the patent data and analysed the GTTs' characteristics. Attribute indicators include IPC code classification, patent applicant, approval time, and region information.

Step 3. Subsequently, employing these patent documents, we conducted the patent collaboration networks by the social network analysis tool, Gephi software.

Step 4. Finally, the assessment of the network structure and policy suggestions for the collaboration activities of GTTs innovations were identified via the statistical analysis of patent information and the social network analysis of patent collaboration.

2.2. Data Processing

2.2.1. Data Source. The research data in this study for GTTs analysis are patent data, collected from the SIPO database through a developed web crawler tool. The transportation category of the IPC green inventory (Table S1 in Appendix A) was selected as the green transportation technology list for this study. Five first-level classifications (vehicles in general, vehicles other than rail vehicles, rail vehicles, marine vessel propulsion, and cosmonautic vehicles using solar energy) and 57 second-level classifications of IPCs are regarded as the code of GTTs. Practically, two search methods, IPC taxonomy and keywords searching, are widely used by scholars in the field of patent investigation. Both of them may face some drawbacks. The IPC approach may result in duplication of patent data, as a patent can often be subordinate to multiple IPC classifications. The keywords searching approach can retrieve patents containing specific information. However, the keywords searching method is often subjective, and the keyword coverage area is usually not complete. Here, we choose the IPC taxonomy method because of its full recognition. After crawling all the transportation patents in the IPC green inventory, duplicate data will be deleted according to the patent application number to avoid duplicate collection of patents.

There are three types of patent rights in China, namely, invention, utility model, and design. The "Utility Model" patent is regarded as the main type of patent analysis and technology innovation evaluation by the majority of scholars [28, 31]. Utility models appeal to some users because they provide more accessible, cheaper, and faster patent protection for the traditional invention patent system. Prud'homme [32] developed an evaluation system, including six institutional calibration strategies to investigate the regime and innovation of utility model patents. Zhang et al. [33] employed the data of utility model patents in the field of China's offshore wind power to examine the technological progress and conduct statistical analysis on the evolution.

2.2.2. Collaborative Identification. The focus of this research is the collaborative innovation of patented technologies. Here, patents containing two or more patent application entities are identified as cooperative patents [31]. To conveniently characterize the sorting relationship for the multimember in cooperative patents, the first application entity of the collaborative patent is regarded as the leader node and the second and subsequent application entities of the collaborative patent as the follower node. The reason for this setting is that the first applicant for a patent often has a more significant contribution to the patent [34]. Here, four types of partners are generated, namely, business enterprises (B), individuals(C), research institutions (I), and universities (U), mainly referring to the principles of the previous literature on innovation collaboration [28]. It is noted that the node type attribute represents the category of patent application organization or individual, and it is an indicator that needs further confirmation. The type of an organization (other than an individual client) will be determined by the relevant information corresponding to the organization name in the official enterprise database (National Enterprise Credit Information Publicity System, http://www.gsxt.gov.cn/index.html). The static pattern analysis per year of GTTs patents is extracted by the patents registered between 2007 and 2018, while the evolution pattern analysis is abstracted through patent time-series, which is divided into three 4-year periods (2007–2010, 2011–2014, and 2015–2018). Finally, a directional collaborative network based on the GTTs patent has been constructed.

2.3. The Social Network Analysis Method. The proposed research framework applied social network analysis for the GTTs collaboration patent analysis. A social network is recognized as a set of nodes (e.g., companies, scholars, or other social entities) and links (e.g., topic, cooperation, or other social relations) [35]. As a practical approach to transferring resources and information between nodes, the social network plays a significant function [36]. Social network analysis (SNA) is the process of investigating social structures using networks and graph theory and the mapping and measuring of relationships and flows between people, groups, organizations, and other connected information/knowledge entities. The SNA method is employed to analyse the fundamental nature and structure of network nodes and network links. This analysis method can help to

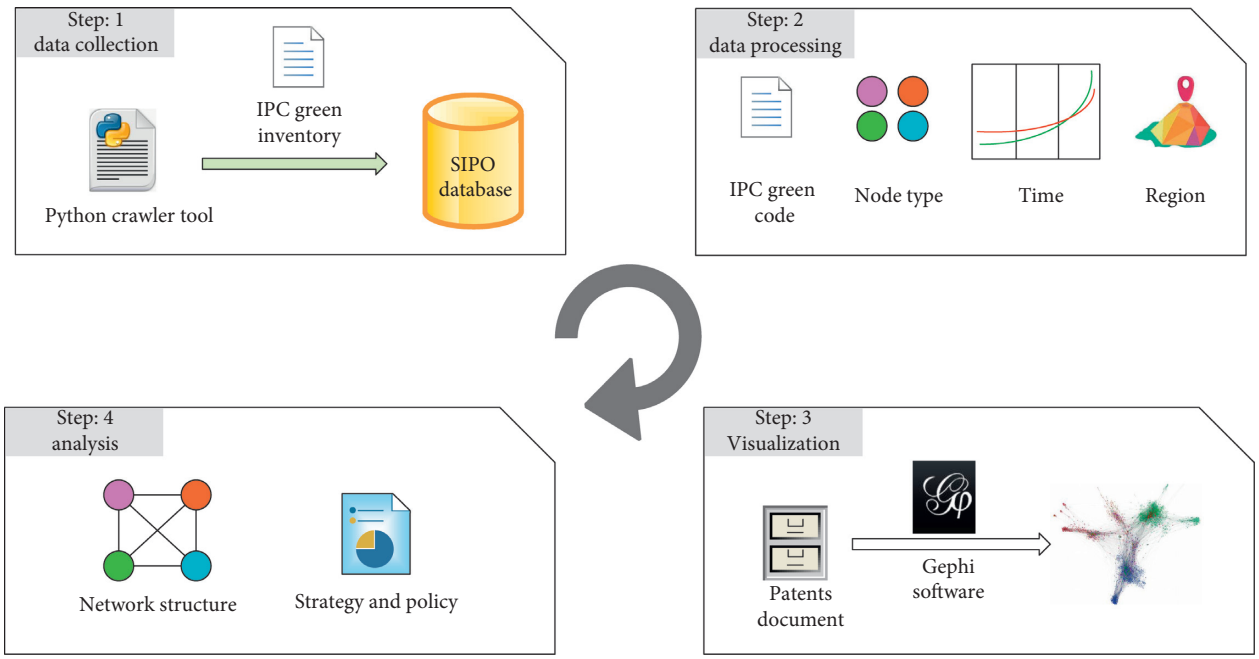

Figure 1: The overall research framework.

identify the global and local patterns in a social network and recognize the influential entities and relationships in a network. Once the time-series patent data are collected, the dynamics of the network can also be illustrated. Due to the interdisciplinary nature, social network analysis has been widely employed in policy analysis [37], risk analysis [38], and industrial innovation analysis [39].

2.3.1. Network Structure Analysis

Network Density. Network density is employed to characterize the denseness of interconnected links between nodes in the network. Also, network density is defined as the ratio of the number of actual links in the network to the upper limit of the number of links that can be accommodated. Here, the calculation formula of degree centrality is as follows:

$$D = \frac{T}{n(n-1)}, \tag{1}$$

where T refers to the number of links in the network, n refers to the number of nodes in the network, and $n(n-1)$ refers to the maximum possible links in the network.

Network Average Degree. The degree of a node refers to the number of links connected to the node. The average degree of the network can be expressed as the average of the degrees of all nodes in the network. The formula for calculating network average degree is

$$a = \frac{1}{N}\sum_{i=1}^{n} \text{degree}(V_i), \tag{2}$$

where N is the number of nodes in the network.

Network Average-Weighted Degree. The weight of a link indicates the number of times the link has been traversed between a pair of nodes. The weighted degree of a node is based on the number of nodes' links. However, the weight of each link is different. The average weighted degree of the network can be expressed as the average of the weighted degrees of all nodes in the network.

Network Diameter. The diameter of the network can be defined as the longest path among all the shortest paths calculated in the network. The diameter of the network is a network characteristic that represents the shortest distance between the two furthest nodes in the network.

Network Average Clustering Coefficient. One node may have K neighbor nodes. The actual number of links between the K neighbor nodes over the maximum possible number of links between the K neighbor nodes is the clustering coefficient of the node, $C_K^2 = K * (K-1)/2$. The average clustering coefficient of the network can be expressed as the average of the clustering coefficient of all nodes in the network.

Network Average Path Length. The average path length is another essential characteristic measure in the network. It is the shortest average distance between all the node pairs in the network. Here, the distance between nodes refers to the minimum number of edges to be experienced from a node, where the maximum distance between all nodes is called the diameter of the network. Average path length and diameter measure the transmission performance and efficiency of the network.

2.3.2. Network Centrality Analysis.

In the field of social network analysis, network centrality is a vital index applied to measure the importance of nodes in a network. Based on

the different centrality algorithms, there are different centrality evaluations for the nodes, as described below.

Degree Centrality. Degree centrality is the most direct metric to describe node centrality in network analysis. The larger the degree of a node and the higher the degree centrality of the node, the more valuable the node is in the network. Generally, such nodes are at the centre of the network being studied and have a higher influence on other nodes. If the research object is a directed network, that is, a link points directionally from one node to another node; then, a node of this has two different types of degrees. Input degree is the number of links input to the node. Output degree is the number of links that the node outputs. Here, the calculation formula of degree centrality is as follows:

$$C_D(n_i) = d(n_i) = \sum_{j=1} x_{ij} = \sum_{j=1} x_{ji} (i \neq j), \tag{3}$$

where $d(n_i)$ refers to the degree centrality, $\sum_{j=1} x_{ji}$ is employed to calculate the number of direct links between node i and other node j ($i \neq j$, excluding the relation of the node i to itself).

Betweenness Centrality. Betweenness centrality requires the average length of the shortest circuit from each node to the other. In other words, for one node, the closer it is to the other nodes, the more centered it is. For instance, this kind of facilities that need to be used by as many people as possible is relatively close to the centre. Here, the calculation formula of betweenness centrality is as follows:

$$C_{ABi} = \sum_{j}^{n} \sum_{k}^{n} b_{jk}(i), \quad j \neq k \neq i, \ j < k, \tag{4}$$

where $b_{jk}(i)$ indicates the power of node to manage the link between node j and k.

Closeness Centrality. Closeness centrality refers to the number of times a node acts as the shortest bridge between the other two nodes. The higher the number of times a node acts as an "intermediary," the higher the centrality of its intermediary. Here, the calculation formula of closeness centrality is as follows:

$$C_{APi}^{-1} = \sum_{j}^{n} d_{ij}, \tag{5}$$

where d_{ij} represents the distance between nodes i and j.

3. Results and Discussion

In this section, two kinds of analysis results are provided. First, Section 3.1 presents an overview development of GTTs' patent in China. The quantity scale of collaborative GTTs patents and the growth trend of various GTTs patents are clearly demonstrated. Second, Section 3.2 provides the structure analysis of the GTTs collaboration network, including network evolution, network properties, key nodes, and link analysis.

3.1. Overview Situation

3.1.1. Patent Number. A search based on IPC green inventory list shows that the total number of utility models for GTTs-related patents from 2007 to 2018 is 59,809, which includes 4,467 cooperative patents. Figure 2 presents two histograms of the selected patents for China's GTTs during the investigation periods. During the study period, the total number of GTTs and the number of cooperative GTTs have steadily grown. It is worth noting that the number of GTTs and cooperative GTTs increased significantly in 2012. Importantly, the number of approved collaborations GTTs remains relatively high. In general, the green transportation innovation activities represented by GTTs and cooperative GTTs are active during the investigation period, especially for the significant growth of total GTTs.

3.1.2. Patent Collaboration Classification. According to the classification principle of cooperative entities in Subsection 2.2.2, the 4,467 cooperative GTTs patents are divided into four leadership groups: type B (business organization lead), type C (individual lead), type U (university organization lead), and type I (institute lead). Results in Figure 3 show that type B and type C cooperative patent applications account for the majority of the total, while the number of type U and type I remains at a lower level. On the one hand, Figure 3(a) illustrates that the dominance of type C and type B changed significantly during the study period. Type C lead was still much more massive than type B lead in the first two years (2008-2009). After 2011, the trend changed radically. Type B keeps an account for more than 50% every year. On the other hand, type U and type I have no advantage in absolute quantity compared with type B and type C. Type I has a slightly higher proportion than type U. In summary, type B (business organization) has gradually grown into a significant leader in the field of cooperative GTTs.

3.1.3. Subsector Classification. Subsection 2.2 points out the subsector classification of IPC green inventory transportation categories; the growth trend of different groups cooperative GTTs patent data are analysed by time accordingly in this subsection. Figure 4 shows GTTs outputs of various transportation subsectors during the investigation period. For the most part, the number of cooperative GTTs patents in the field of rail vehicles has been a leader, and the trend continues to grow. Accidentally, there was a significant spike in approved GTTs volume around vehicles in general in 2012, which found out the reason for the sharp increase in 2012 in Figure 2 from the perspective of the subsector. By contrast, GTTs in the field of marine vessel propulsion have been at a low level, and the green cooperation innovation activities are not active.

3.1.4. Geographic Classification. The cooperative patent data record the province information of the first patent applicant. Patent data and geographic information are combined to form Figure 5, which represents the patent distribution of

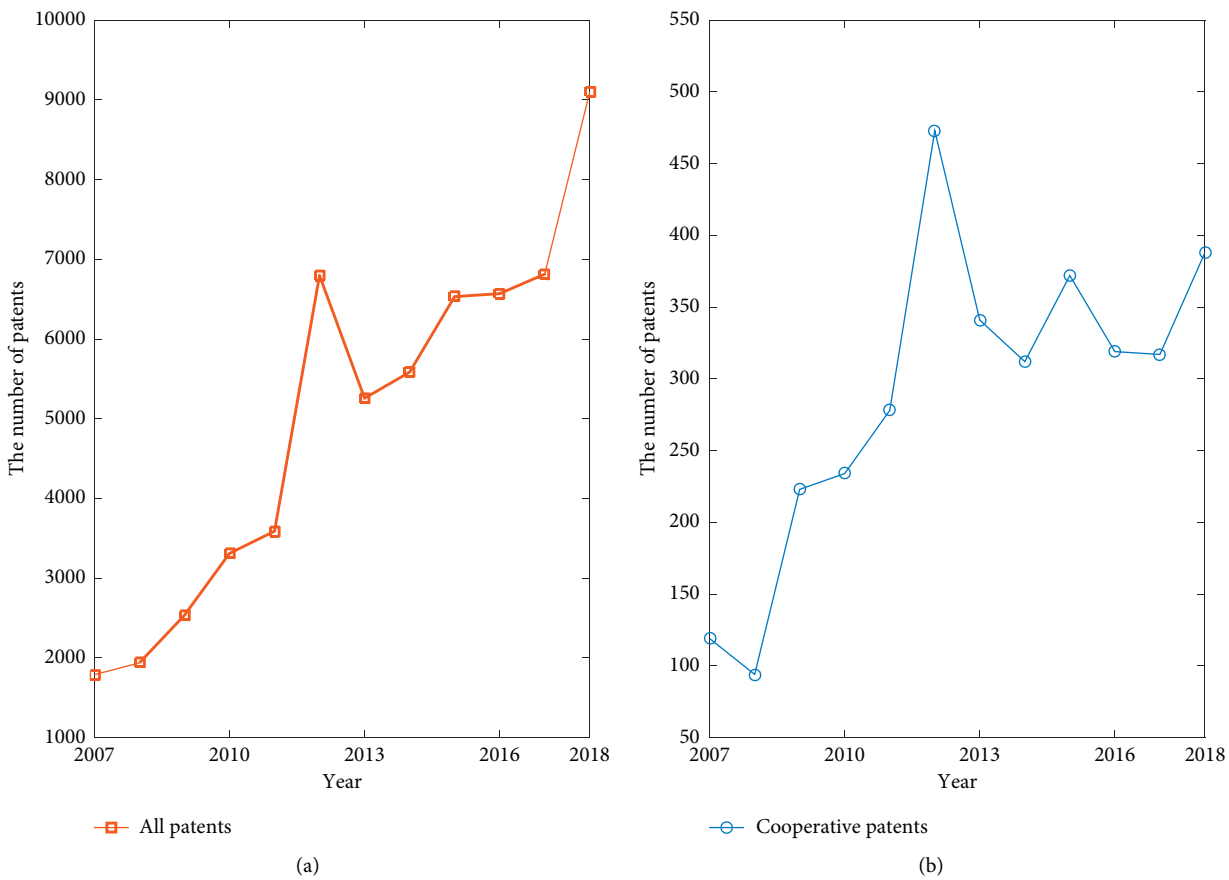

Figure 2: Growth trend of GTTs and cooperative GTTs.

cooperative GTTs. As shown in Figure 5, the number of cooperative GTTs in most coastal provinces of China is far higher than that in other regions. Notably, the GTTs output in Beijing and Jiangsu is outstanding. The outstanding performance of green collaboration innovation activities in both places may benefit from a high number of local universities and enterprises. The creation of such an innovation atmosphere is also conducive to the output of collaboration innovation.

3.2. Patent Collaboration Network

3.2.1. Network Evolution. GTTs patent cooperation in China is divided into three stages: S1(2007–2010), S2 (2011–2014), and S3 (2015–2018). By constructing the GTTs cooperation network with 4,467 cooperative patents in three stages, the evolution of the GTTs cooperation network over time has been presented. Figure 6 shows the patent collaboration networks in three stages. Table 1 provides the performance of key parameters using the social network analysis method. Cooperation innovation is becoming more and more active, which indicates a steady evolution of the patent network. In detail, the number of nodes and links in the network are constantly increasing. Among the two main nodes and two main links, the proportions of B type node and B lead link are increasing, while the proportions of C type node and C lead link are decreasing. The results show the key role of B type node and B lead link in collaborative GTTs. The increase of average degree and average-weighted degree indicates that the capabilities of other nodes connected by a single node in the network are improving, and the GTTs collaborative network is getting closer. The increase of diameter and average path length represents that the speed of knowledge transformed into technology between nodes may slow down; the cost of conversion might be increased.

3.2.2. Node and Link Analysis. In addition to showing the evolution process of the network, the social network analysis method could also identify critical nodes and critical links in the network. Here, the two characteristics of node centrality and link weight are used for analysis. Table 2 provides the top ten nodes of degree centrality, betweenness centrality, and closeness centrality, respectively. The results show that all the three centrality indicators of State Gird rank first, which reflected the critical position of this entity in the GTTs network. Besides, many CRRC subsidiaries appear in the table, which also show that CRRC is also an important node of the network. Table 3 provides the top 10% of weighted links. The results show that the links B-B occur most frequently, illustrating the close cooperation between the two entities, which also indicates the importance of this type of cooperation link in the GTTs network.

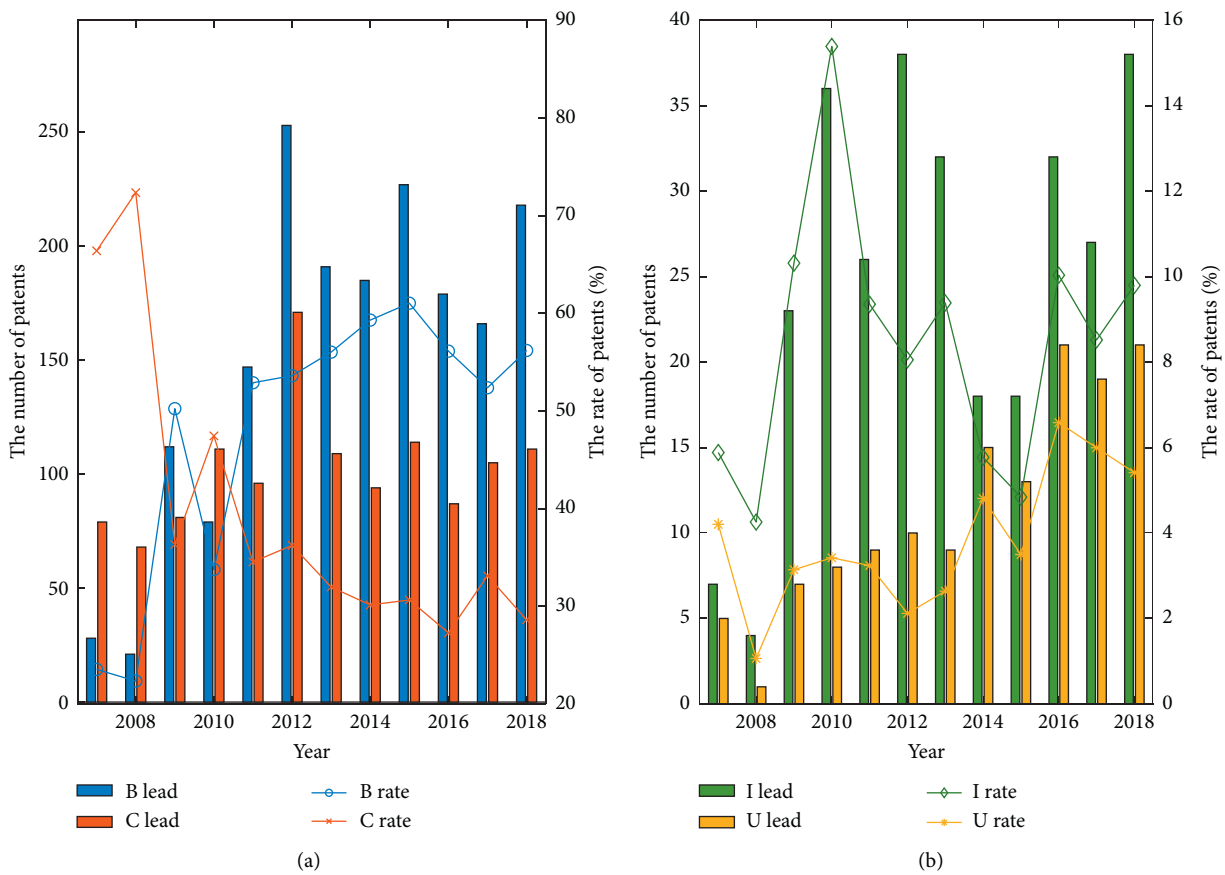

Figure 3: Leading entity trends in cooperative GTTs.

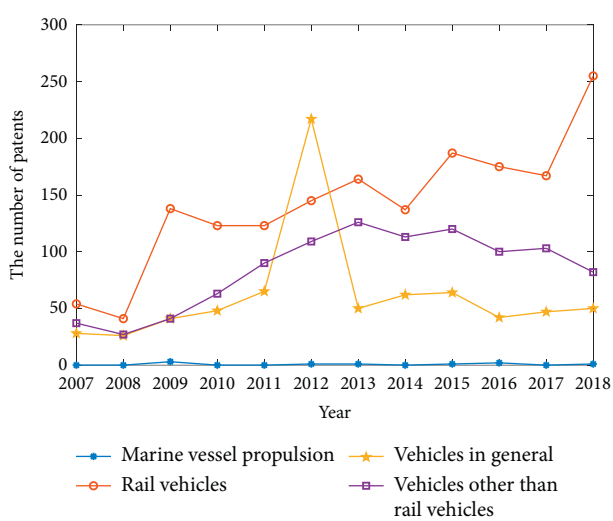

Figure 4: Trends of subarea cooperative GTTs.

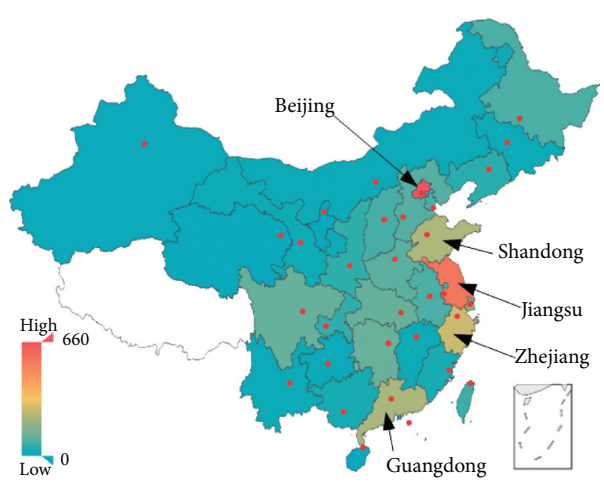

Figure 5: Distribution of cooperative GTTs by province.

3.2.3. Networks of Different Leadership Types. In the previous two subsections, a collaboration network that completely contained four leading entities was analysed. Another interesting question is what are the structural characteristics of the innovation collaboration network led by the four innovation entities, separately. Table 4 illustrates the attributes of the four networks. Figure 7 shows the networks of four different leadership types.

As given in Table 4, the type C network owns the most nodes, while the type B network owns the most links. The type U network has the lowest percentage of its nodes, which indicates that this type of network has the highest willingness to cooperate. The result of the type C network is the opposite of the type U network.

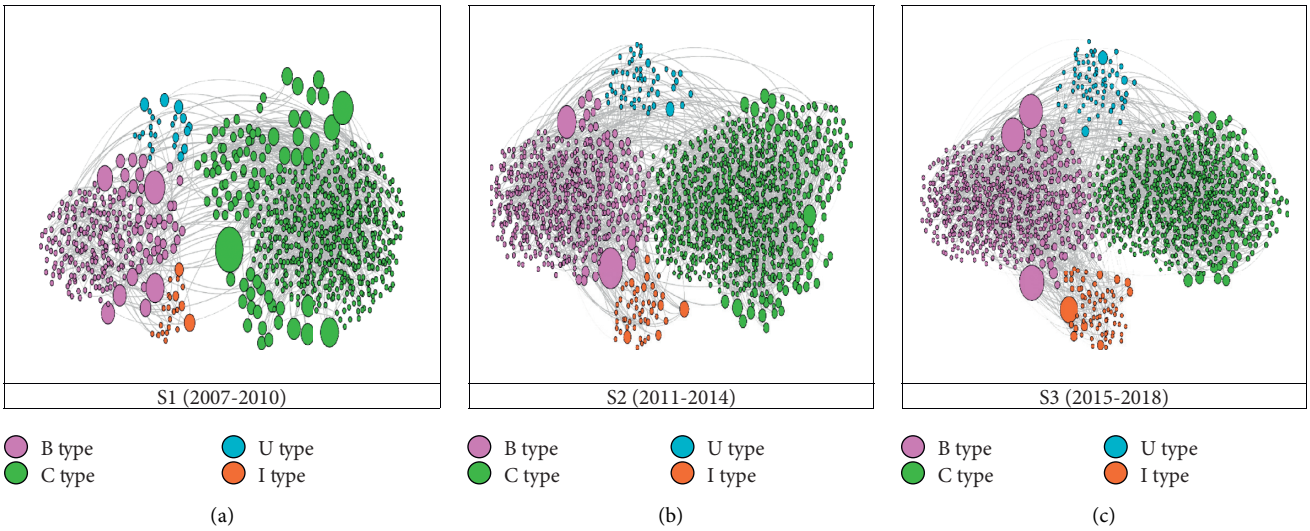

Figure 6: Evolution of the GTTs collaborative network. (a) S1 (2007–2010), (b) S2 (2011–2014), and (c) S3 (2015–2018).

Table 1: Characteristics of GTTs collaborative network in different stages.

Item	S1 (2007–2010)		S2 (2011–2014)		S3 (2015–2018)	
Qty. of nodes	987		1686		1727	
B type node	238	24.11%	572	33.93%	680	39.37%
C type node	703	71.23%	1010	59.91%	903	52.29%
U type node	24	2.43%	55	3.26%	71	4.11%
I type node	22	2.23%	49	2.91%	73	4.23%
Qty. of links	876		1769		1822	
B lead link	288	32.88%	869	49.12%	939	51.54%
C lead link	489	55.82%	716	40.47%	618	33.92%
U lead link	26	2.97%	48	2.71%	79	4.34%
I lead link	73	8.33%	136	7.69%	186	10.21%
Density	0.001		0.001		0.001	
Average degree	0.637		0.657		0.675	
Average weighted degree	0.888		1.049		1.055	
Diameter	5		5		6	
Average clustering coefficient	0.009		0.013		0.009	
Average path length	1.1214		1.265		1.97	

Table 2: Top 10 nodes with degree centrality, betweenness centrality, or closeness centrality in the GTTs collaborative network.

Degree centrality				Betweenness centrality		Closeness centrality	
Node	Degree	Out degree	In degree	Node	Betweenness	Node	Closeness
State Grid	51	17	34	State Grid	575.0	State Grid	1.000
China Shenhua Energy	40	0	40	China Railway	344.0	China Railway 6th Engineering	1.000
China Railway	23	6	17	CRRC Times Electric	309.0	Guangzhou Metro	1.000
Geely Holding Group	11	6	5	CRRC Qingdao Sifang	242.5	CRRC Qingdao Sifang	1.000
Railway Transport Bureau	10	0	10	Zhuzhou Times Electric technology	233.0	Liaoning Chaoyang New Energy	1.000
CRRC Times Electric	7	4	3	Qingdao Yatongda	103.0	Geely Holding Group	0.857
China Railway 12th Bureau	7	3	4	CRRC Qingdao Sifang	101.0	CNPC	0.833
SH Metro Consulting	7	3	4	SH Metro Consulting	84.0	State Grid, Shandong	0.800
Guangzhou Metro	7	2	5	Beijing Huaxing Zhiyuan Technology	78.0	Qiqihar Railway Rolling	0.800
CRRC Qingdao Sifang	7	2	5	Nanjing Kangni Mechanical and Electronical	46.0	China Railway	0.778

Table 3: Top 10% of weighted links in the GTTs collaborative network.

No.	Source	Node type	Target	Node type	Weight
1	Taicang Chezhongbao	B	PANG, Mingfang	C	286
2	China Shenhua Energy	B	Shuohuang Railway Development	B	66
3	Railway Transport Bureau	B	CRRC Qingdao Sifang	B	30
4	Qiqihar Railway Rolling	B	Tuofeng High Tech	B	24
5	China Shenhua Energy	B	Shenhua Huanghua Port	B	19
6	Geely Holding Group	B	Geely Institute	I	16
7	Railway Transport Bureau	B	CRRC Changchun Railway Vehicle	B	15
8	Railway Transport Bureau	B	CRRC Tangshan Railway Vehicle	B	15
9	Xinyu Air Conditioning System	B	Xinyu Group	B	14
10	China Shenhua Energy	B	China Shenhua Energy, Shuohuang branch	B	14
11	Tianlong Transportation Equipment	B	Zhang, Yunkun	C	14
12	Tianlong Transportation Equipment	B	Zhang, Libo	C	14

Table 4: Characteristics of the GTTs collaborative network of different lead types.

Item	Type B network		Type C network		Type U network		Type I network	
Qty. of nodes	1445		2372		208		165	
B type node	1186	82.08%	34	1.43%	66	31.73%	74	44.85%
C type node	166	11.49%	2331	98.27%	48	23.08%	2	1.21%
U type node	40	2.77%	7	0.30%	89	42.79%	7	4.24%
I type node	53	3.67%	0	0.00%	5	2.40%	83	50.30%
Qty. of links	2096		1825		153		395	
Density	0.001		0.001		0.009		0.006	
Average degree	0.694		0.649		0.615		0.782	
Average weighted degree	1.451		0.769		0.736		2.394	
Diameter	10		3		2		3	
Average clustering coefficient	0.007		0.01		0		0.04	
Average path length	2.095		1.575		1.117		1.549	

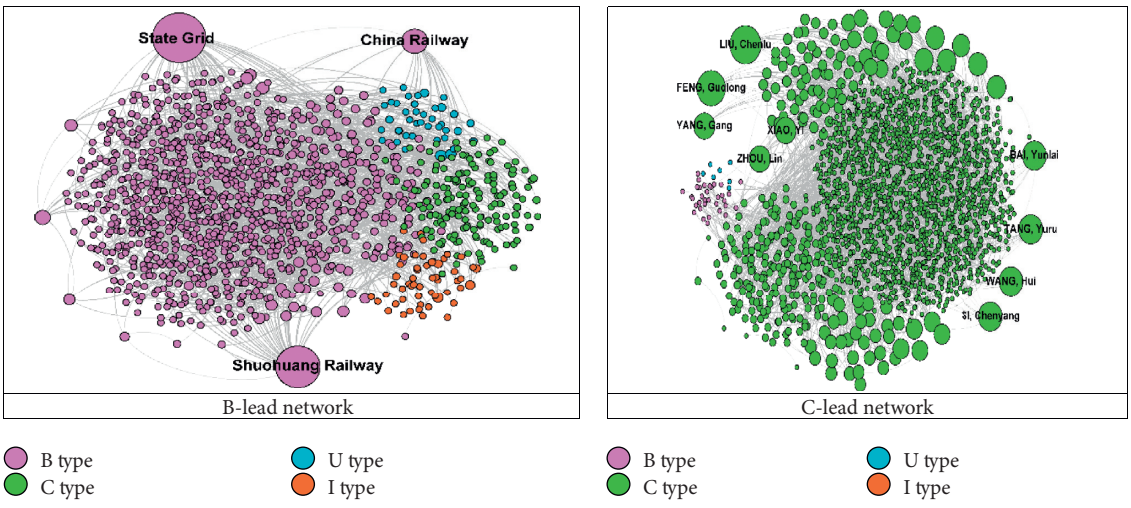

(a) (b)

Figure 7: Continued.

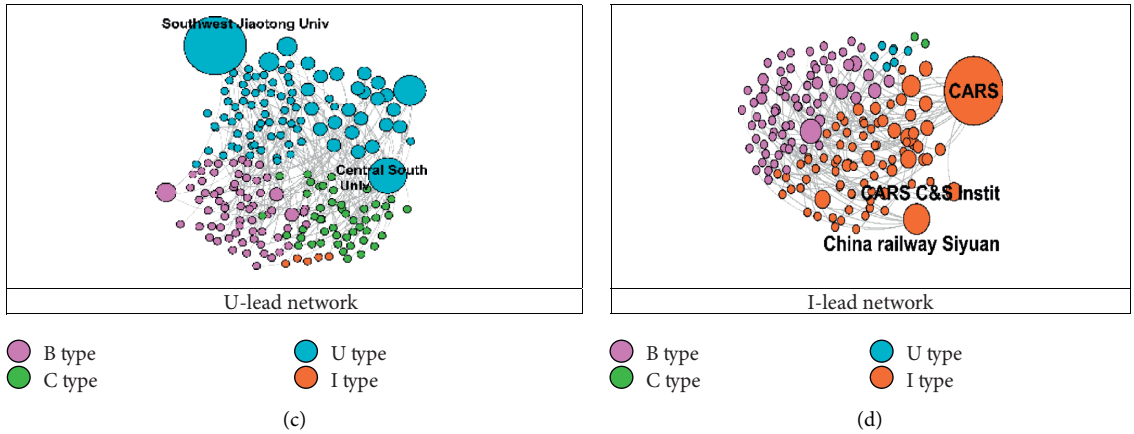

Figure 7: Networks of different leadership types. (a) B lead network, (b) C lead network, (c) U lead network, and (d) I lead network.

From a network topology perspective, the type U network has the most extensive network density, which represents that network members are most closely connected. The type I network has the highest average degree and average-weighted degree, indicating that the nodes in this type of network have the best connectivity with each other. Among the last three network characteristic indicators, the type B network reflects the highest value, which indicates that the spatial scale of this type of network is the largest. These two networks are the most complex on a physical scale. In general, the type B network and type C network are the most complex two types of GTTs collaboration innovation networks.

4. Conclusions

GTTs are the critical driving forces to promote the sustainable development of the transportation industry, in which technical collaboration plays an active role. This study presented the investigation of GTTs collaborative in China's transportation sector based on the social network analysis method and GTTs patent data. The following conclusions are offered.

(1) The collaboration patent data selected in this study are an active measurement indicator of GTTs' progress. The results show that cooperative GTTs continued to grow from 2007 to 2018. The growth of GTTs in the railway subindustry has been particularly marked. The geographic information contained in the patent reflects the substantial GTTs cooperative innovation activities in Beijing and Jiangsu of China.

(2) The SNA method is a simple and efficient method to understand the structure and characteristics of the technical cooperation network. The research framework proposed in this study is feasible. The results show that the cooperation mode of B type leadership has gradually become the main form of cooperation among different entities. State Grid and CRRC are the main nodes of cooperative GTTs technology. B-B is the main mode of GTTs collaboration.

(3) Some policy suggestions can also be derived from the results. The collaboration innovation of GTTs has maintained a high level. Each innovation entity plays a role in the innovation cooperation network. Organizations or individuals need to choose specific areas based on their abilities and decide where to lead or follow. The government should also formulate policies to actively guide organizations or individuals to participate in cooperative innovation activities.

Indeed, this study mainly focuses on patent data on green transportation technologies. There are still limitations in this study. To measure and evaluate the innovation activities in the field of transportation comprehensively, we need to obtain more dimensional data, such as the literature review [40], green transportation research [41, 42], and sustainable green technology inventions [26]. A broader range of data may further improve the robustness of the study.

Data Availability

The data used to support the findings of this study are available from the corresponding author upon request.

Conflicts of Interest

The authors declare that they have no conflicts of interest.

Acknowledgments

This work was supported in part by the Philosophy and Social Science Planning Project of Shanghai (2019BGL028) and in part by Natural Science Foundation of Shanghai (17ZR1409800) and Shanghai Financial Technology Research Centre Project (2020-JK05-B).

Supplementary Materials

Table S1 IPC green inventory list. (*Supplementary Materials*)

References

[1] J. Rezaei, W. S. van Roekel, and L. Tavasszy, "Measuring the relative importance of the logistics performance index indicators using Best Worst Method," *Transport Policy*, vol. 68, pp. 158–169, 2018.

[2] H. Wang, X. Ou, and X. Zhang, "Mode, technology, energy consumption, and resulting CO_2 emissions in China's transport sector up to 2050," *Energy Policy*, vol. 109, pp. 719–733, 2017.

[3] S. Wang, J. Li, and D. Zhao, "The impact of policy measures on consumer intention to adopt electric vehicles: evidence from China," *Transportation Research Part A: Policy and Practice*, vol. 105, pp. 14–26, 2017.

[4] H. Liu, J. Wu, and J. Chu, "Environmental efficiency and technological progress of transportation industry-based on large scale data," *Technological Forecasting and Social Change*, vol. 144, pp. 475–482, 2019.

[5] E. Demir, T. Bektaş, and G. Laporte, "A review of recent research on green road freight transportation," *European Journal of Operational Research*, vol. 237, no. 3, pp. 775–793, 2014.

[6] S. Saberi, J. M. Cruz, J. Sarkis, and A. Nagurney, "A competitive multiperiod supply chain network model with freight carriers and green technology investment option," *European Journal of Operational Research*, vol. 266, no. 3, pp. 934–949, 2018.

[7] Y. Sun, X. Yu, R. Bie, and H. Song, "Discovering time-dependent shortest path on traffic graph for drivers towards green driving," *Journal of Network and Computer Applications*, vol. 83, pp. 204–212, 2017.

[8] S. Pelletier, O. Jabali, and G. Laporte, "50th anniversary invited article-goods distribution with electric vehicles: review and research perspectives," *Transportation Science*, vol. 50, no. 1, pp. 3–22, 2016.

[9] G. Perboli and M. Rosano, "Parcel delivery in urban areas: opportunities and threats for the mix of traditional and green business models," *Transportation Research Part C: Emerging Technologies*, vol. 99, pp. 19–36, 2019.

[10] J. Zawieska and J. Pieriegud, "Smart city as a tool for sustainable mobility and transport decarbonisation," *Transport Policy*, vol. 63, pp. 39–50, 2018.

[11] S. M. Knupfer, V. Pokotilo, and J. Woetzel, *Elements of Success: Urban Transportation Systems of 24 Global Cities*, McKinsey & Company, New York, NY, USA, 2018, https://www.mckinsey.com/%7E/media/McKinsey/Business%20Functions/Sustainability/Our%20Insights/Elements%20of%20success%20Urban%20transportation%20systems%20of%2024%20global%20cities/Urban-transportation-systems_e-versions.ashx.

[12] A. Marra, P. Antonelli, and C. Pozzi, "Emerging green-tech specializations and clusters - a network analysis on technological innovation at the metropolitan level," *Renewable and Sustainable Energy Reviews*, vol. 67, pp. 1037–1046, 2017.

[13] M. Dodgson, D. Gann, S. MacAulay, and A. Davies, "Innovation strategy in new transportation systems: the case of Crossrail," *Transportation Research Part a: Policy and Practice*, vol. 77, pp. 261–275, 2015.

[14] J. Zhang, X. Qu, and S. Wang, "Reproducible generation of experimental data sample for calibrating traffic flow fundamental diagram," *Transportation Research Part a: Policy and Practice*, vol. 111, pp. 41–52, 2018.

[15] R. Dai and J. Zhang, "Green process innovation and differentiated pricing strategies with environmental concerns of South-North markets," *Transportation Research Part E: Logistics and Transportation Review*, vol. 98, pp. 132–150, 2017.

[16] J. Luan, J. Polak, and R. Krishnan, "The structure of public-private sector collaboration in travel information markets: a game theoretic analysis," *Transportation Research Part a: Policy and Practice*, vol. 129, pp. 19–38, 2019.

[17] L. Sun and I. Rahwan, "Coauthorship network in transportation research," *Transportation Research Part a: Policy and Practice*, vol. 100, pp. 135–151, 2017.

[18] L. L. P. De Souza, E. E. S. Lora, J. C. E. Palacio, M. H. Rocha, M. L. G. Renó, and O. J. Venturini, "Comparative environmental life cycle assessment of conventional vehicles with different fuel options, plug-in hybrid and electric vehicles for a sustainable transportation system in Brazil," *Journal of Cleaner Production*, vol. 203, pp. 444–468, 2018.

[19] A. Patel, N. Arora, V. Pruthi, and P. A. Pruthi, "Biological treatment of pulp and paper industry effluent by oleaginous yeast integrated with production of biodiesel as sustainable transportation fuel," *Journal of Cleaner Production*, vol. 142, pp. 2858–2864, 2017.

[20] T. Bektaş, J. F. Ehmke, H. N. Psaraftis, and J. Puchinger, "The role of operational research in green freight transportation," *European Journal of Operational Research*, vol. 274, no. 3, pp. 807–823, 2019.

[21] O. Al-Tabbaa and S. Ankrah, "Social capital to facilitate 'engineered' university-industry collaboration for technology transfer: a dynamic perspective," *Technological Forecasting and Social Change*, vol. 104, pp. 1–15, 2016.

[22] F. Liu, N. Zhang, and C. Cao, "An evolutionary process of global nanotechnology collaboration: a social network analysis of patents at USPTO," *Scientometrics*, vol. 111, no. 3, pp. 1449–1465, 2017.

[23] Y.-C. J. Wu and P.-J. Lee, "The use of patent analysis in assessing ITS innovations: US, Europe and Japan," *Transportation Research Part A: Policy and Practice*, vol. 41, no. 6, pp. 568–586, 2007.

[24] D. Chai, D. Zhang, Y. Sun, and S. Yang, "Research on the city network structure in the Yellow River basin in China based on two-way time distance gravity model and social network analysis method," *Complexity*, vol. 2020, Article ID 6680954, 19 pages, 2020.

[25] V. Albino, L. Ardito, R. M. Dangelico, and A. Messeni Petruzzelli, "Understanding the development trends of low-carbon energy technologies: a patent analysis," *Applied Energy*, vol. 135, pp. 836–854, 2014.

[26] H. Fujii and S. Managi, "Decomposition analysis of sustainable green technology inventions in Chinaa," *Technological Forecasting and Social Change*, vol. 139, pp. 10–16, 2019.

[27] M. Karvonen, R. Kapoor, A. Uusitalo, and V. Ojanen, "Technology competition in the internal combustion engine waste heat recovery: a patent landscape analysis," *Journal of Cleaner Production*, vol. 112, pp. 3735–3743, 2016.

[28] S. Rajalo and M. Vadi, "University-industry innovation collaboration: reconceptualization," *Technovation*, vol. 62-63, pp. 42–54, 2017.

[29] M. De Silva, J. Howells, and M. Meyer, "Innovation intermediaries and collaboration: knowledge-based practices and internal value creation," *Research Policy*, vol. 47, no. 1, pp. 70–87, 2018.

[30] T. W. Tong, K. Zhang, Z.-L. He, and Y. Zhang, "What determines the duration of patent examination in China? an outcome-specific duration analysis of invention patent

applications at SIPO," *Research Policy*, vol. 47, no. 3, pp. 583–591, 2018.

[31] H. Sun, Y. Geng, L. Hu, L. Shi, and T. Xu, "Measuring China's new energy vehicle patents: a social network analysis approach," *Energy*, vol. 153, pp. 685–693, 2018.

[32] D. Prud'homme, "Utility model patent regime 'strength' and technological development: experiences of China and other East Asian latecomers," *China Economic Review*, vol. 42, pp. 50–73, 2016.

[33] H. Zhang, Y. Zheng, D. Zhou, and X. Long, "Selection of key technology policies for Chinese offshore wind power: a perspective on patent maps," *Marine Policy*, vol. 93, pp. 47–53, 2018.

[34] J. Guan and N. Liu, "Exploitative and exploratory innovations in knowledge network and collaboration network: a patent analysis in the technological field of nano-energy," *Research Policy*, vol. 45, no. 1, pp. 97–112, 2016.

[35] S. Wasserman and K. Faust, *Social Network Analysis: Methods and Applications*, Cambridge University Press, Cambridge, UK, 1994.

[36] B. R. Lea, W. B. Yu, N. Maguluru, and M. Nichols, "Enhancing business networks using social network based virtual communities," *Industrial Management & Data Systems*, vol. 106, no. 1, pp. 121–138, 2006.

[37] X. Gan, R. Chang, and T. Wen, "Overcoming barriers to off-site construction through engaging stakeholders: a two-mode social network analysis," *Journal of Cleaner Production*, vol. 201, pp. 735–747, 2018.

[38] J. Yuan, K. Chen, W. Li, C. Ji, Z. Wang, and M. J. Skibniewski, "Social network analysis for social risks of construction projects in high-density urban areas in China," *Journal of Cleaner Production*, vol. 198, pp. 940–961, 2018.

[39] B. Yuan and Q. Xiang, "Environmental regulation, industrial innovation and green development of Chinese manufacturing: based on an extended CDM model," *Journal of Cleaner Production*, vol. 176, pp. 895–908, 2018.

[40] H. Zou, H. Du, Y. Wang et al., "A review of the first twenty-three years of articles published in the Journal of Cleaner Production: with a focus on trends, themes, collaboration networks, low/no-fossil carbon transformations and the future," *Journal of Cleaner Production*, vol. 163, pp. 1–14, 2017.

[41] L. Huang, L. Murong, and W. Wang, "Green closed-loop supply chain network design considering cost control and CO_2 emission," *Modern Supply Chain Research and Applications*, vol. 2, no. 1, pp. 42–59, 2020.

[42] L. Zhen, L. Huang, and W. Wang, "Green and sustainable closed-loop supply chain network design under uncertainty," *Journal of Cleaner Production*, vol. 227, pp. 1195–1209, 2019.

Hindawi
Scientific Programming
Volume 2021, Article ID 5523910, 11 pages
https://doi.org/10.1155/2021/5523910

Research Article

Routing Optimisation of Urban Medical Waste Recycling Network considering Differentiated Collection Strategy and Time Windows

Jiajing Gao, Haolin Li, Jingwen Wu, Junyan Lyu, Zheyi Tan, and Zhufan Jin

School of Management, Shanghai University, Shanghai, China

Correspondence should be addressed to Jingwen Wu; jingwen_wu@shu.edu.cn

Received 11 January 2021; Revised 23 February 2021; Accepted 6 March 2021; Published 18 March 2021

Academic Editor: Tingsong Wang

Copyright © 2021 Jiajing Gao et al. This is an open access article distributed under the Creative Commons Attribution License, which permits unrestricted use, distribution, and reproduction in any medium, provided the original work is properly cited.

The increasing gap between medical waste production and disposal stresses the urgency of further development of urban medical waste recycling. This paper investigates an integrated optimisation problem in urban medical waste recycling network. It combines the vehicle routing problem of medical facilities with different requirements and the collection problem of clinics' medical waste to the affiliated hospital. To solve this problem, a compact mixed-integer linear programming model is proposed, which takes account of the differentiated collection strategy and time windows. Since the medical waste recycling operates according to a two-day pattern, the periodic collection plan is also embedded in the model. Moreover, we develop a particle swarm optimisation (PSO) solution approach for problem-solving. Numerical experiments are also conducted to access the solution efficiency of the proposed algorithm, which can obtain a good solution in solving large-scale problem instances within a reasonable computation time. Based on the results, some managerial implications can be recommended for the third-party recycling company.

1. Introduction

Medical waste contains potentially dangerous microorganisms produced by medical activities. If medical waste is not properly recycled and disposed, it may pollute people's living environment, spread diseases, and sometimes pose threats to public health [1]. It is particularly important to establish a safe, sustainable, and green medical waste recycling system to protect human health, maintain ecological safety, and promote sustainable development. According to the data of the National Bureau of Statistics shown in Figure 1, the production of medical waste in 2008 was about 1.222 million tons, and, in 2017, the production of medical waste was 2.235 million tons, 183% of that in 2008. However, the recycling rate of medical waste is still in a low level, where about two-thirds of the medical waste are not properly disposed. The gap between medical waste production and disposal is still significant. The main problem of medical waste collection is the lack of proper facilities for waste collection, safe storage, and transportation, which stresses the urgency of further development of medical waste recycling [2].

The recycling of medical waste can be divided into two stages, namely, collection stage and recycling and disposing stage. In the collection stage, medical waste is collected from medical facilities. In the recycling and disposing stage, waste is recycled and disposed in the recycling centre. Both stages stress the safe in both transportation and disposal, which will be supervised by the government and the public. The collection stage includes three key steps: classification, temporary storage, and transport. Among those steps, the transportation step consumes much labour and resources. Effective planning is required in the transportation step to improve efficiency and cut down the operational cost for the medical waste collection operators. Vehicle routing problem (VRP) is a well-known optimisation problem in transportation section. In medical waste recycling network, the operator needs to determine the route of collection vehicle. Before applying the vehicle routing problem into the medical

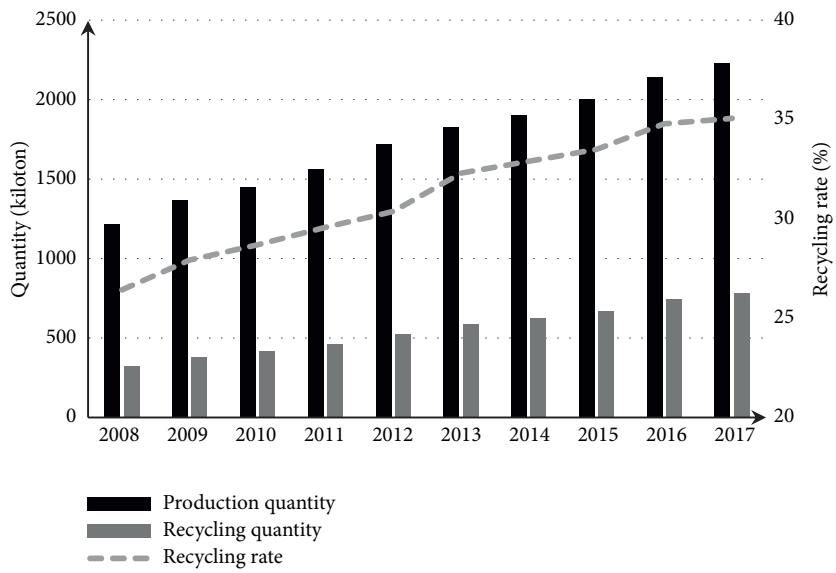

Figure 1: Statistics data of medical waste production.

waste recycling network, we should pay attention to the difference of medical waste collection compared to general waste collection, that is, the potential risk in transportation and storage process of medical waste. To reduce the potential storage risk of storage, a higher service frequency is required in medical waste network. The structure of medical waste collection network may also have some special feature. Based on the differences, some new challenges, such as the periodicity of waste collection, regulations for the storage and transportation of medical waste, and the different waste quantity produced by different medical facilities, need to be tackled. These challenges imply that the medical waste recycler should provide the differentiated waste collection strategy, which can be achieved by different service frequencies. In this paper, we focus on the routing optimisation of a typical urban medical waste recycling network in China and build up a mixed-integer linear programming model to solve the periodic vehicle routing problem with time windows (PVRPTW) with the objective of minimising the total travelling distance. Based on the periodicity of waste collection and the different requirements of medical facilities, we propose a differentiated recycling strategy to collect medical waste. To enhance the computing efficiency, PSO algorithm is applied for problem-solving. Numerical experiments are used to verify the model and the effectiveness of the proposed algorithm, and sensitivity analysis is conducted to explain some related problems.

The rest of this paper is organised as follows: Section 2 provides an exhaustive literature review of related research. Section 3 expounds the research problems of this paper and describes the special features of the routing problem in medical waste network. Section 4 elaborates the mathematical model. Section 5 proposes PSO algorithm for problem-solving. Section 6 conducts a numerical experiment to verify the model and algorithm and puts forward some management insights by sensitivity analysis. Section 7 presents the conclusion.

2. Literature Review

Medical waste collection and recycling problems can be defined as a PVRPTW, which determines minimum distance routes in a reverse logistics network. Among the research problems in reverse logistics, VRP is one of the most important and most widely studied combinatorial optimisation problems because of its complexity and importance in cost minimisation in transportation networks [3]. The spread of COVID-19 puts the whole world into danger and panic, and, of course, the amount of medical waste from COVID-19 encounters explosive growth, which places pressure on the waste disposing systems and poses a great threat of virus infection to the public. When focusing on the research of medical waste recycling, we find that COVID-19 and other public health events have motivated scholars to conduct research about medical waste recycling. Among the previous researches, waste collection problems in previous works are usually modelled as inventory-routing problem, location-routing problem, and supply chain network construction problem. Cost and social objectives like public risk are taken as the objective of optimisation problems.

Inventory-routing problem can be seen as a special form of VRP, where medical waste in medical facilities is waiting to be collected. Nolz et al. [4] investigate the collection of medical waste stored at pharmacies. Stochastic aspects are considered in the inventory-routing problem, and the social objective is applied as the objective. A sampling method and an approach based on an adaptive large neighbourhood search algorithm are developed to solve the proposed problem.

Location-routing problem is another hotspot of medical waste recycling network. Mantzaras and Voudrias [5] develop an optimisation model to minimise the cost of infectious waste management. Location and capacity of treatment plants and transfer stations as well as transport paths of vehicles are determined in this model.

Tirkolaee et al. [6] investigate a sustainable multitrip location-routing problem with time windows for medical waste management. Travelling time, total violation of time windows, service priorities, total infection, and environmental risk are minimised in their model. Fuzzy chance-constrained programming approach is applied to address uncertainty. The model is then tested by a case study in Sari city of Iran.

Some scholars investigate medical waste recycling networks as a supply chain network design and construction problems. Yu et al. [7] propose a multiobjective multiperiod mixed-integer programming model for the epidemic logistics network of medical waste to determine facility locations and transportation strategies. Risk in transportation and treatment and the cost of system establishment are selected as the objectives. Several general policies are obtained by experiments and analysis. Kargar et al. [8] propose a multi-item and multiperiod linear programming model for medical waste reverse supply chain with objectives relevant to total costs, treatment technology selection, and medical waste stored. A robust possibilistic programming approach and a fuzzy goal programming method are employed in modelling.

VRP is a well-known NP-hard problem. To obtain a solution in a reasonable time, researchers try to use heuristic algorithms to solve the models and obtain near-optimal solutions efficiently. Global search algorithms like genetic algorithm, PSO, and simulated annealing are applied because of the strong capability of finding the global optimum [9–11]. For local search heuristics, some metaheuristics are applied in problem-solving to improve search efficiency and avoid trapping in local optimum, like Squeaky Wheel Optimisation [12, 13] and Critical-Shaking Neighbourhood Search [14, 15].

From the literatures reviewed above, we can find that medical waste collection and disposing is an emerging research field in reverse logistics. Although many works have been done about VRP considering time windows and vehicle capacity in the field of waste collection, to the best of our knowledge, there are few works that investigate the differentiated collection strategy for medical facilities. The main contribution of our research can be categorized into three aspects. First, we investigate the PVRPTW of medical waste recycling network considering the differentiated collection strategy based on different grades of medical facilities, in which different collection frequency and collection from clinics to grade 1 hospital are applied. A mixed-integer linear programming model is formulated to minimise the total travelling distance. Second, we propose a PSO algorithm for problem-solving, which can be a tool for solving real-scale problems. Third, some managerial insights about vehicle capacity are concluded according to numerical experiments and sensitivity analysis, which provide a broad view of network operation.

3. Problem Background

This study attempts to investigate the PVRPTW of an urban medical waste recycling network based on a typical urban medical system in China. The urban medical waste recycling network works to recycle waste produced in the daily operations of medical facilities. There are several medical facilities and a recycling centre in the network. The medical facilities are the producers of medical waste, including hospitals in different grades, clinics, and other medical waste producers. Medical waste produced by medical facilities is recycled or disposed by the recycling centre. Once the medical waste is produced, it is stored in temporary storage areas within or adjacent to medical facilities and waits to be collected. Vehicles for medical waste collection start from the recycling centre, go to assigned hospitals to collect waste along the assigned routes, and go back to the recycling centre when all wastes in the assigned hospitals are collected. According to regulations, the medical waste can only be stored in the temporary storage areas for a maximum of 48 hours to minimise the risk of infections [16].

In general, medical facilities have different functions and sizes, and the amount of medical waste produced by different facilities varies. For economic reasons, different waste quantity among medical facilities requires different frequency of waste collection; that is to say, the medical facilities that produce more waste require higher frequency of waste collection. Based on the hospital classification system and the actual operation of the medical system, we classify the medical facilities into the following 4 grades in our research and set the corresponding collection strategies to different grade of medical facilities.

(1) *Grade 2 and Above Hospitals*. These hospitals are the core of the medical system, which will treat more patients and produce more medical waste in daily operation. These hospitals all have temporary storage areas for waste, so the waste can be stored in the temporarily storage areas within the hospitals, and the vehicles need to visit these hospitals to collect waste. To deal with the large amount of waste, we set a higher waste collection frequency for grade 2 and above hospitals as once a day.

(2) *Grade 1 Hospitals*. These hospitals are usually community hospitals and health centres and are distributed more densely in the city. The wastes produced by grade 1 hospitals are stored in their temporary storage area and collected by the vehicles every two days. Grade 1 hospitals are also used as collection points for those clinics without the temporary storage areas because of the denser distribution.

(3) *Clinics*. The clinics are more common in the city and appear as supplements of the medical system. Clinics are usually smaller and generate less medical waste, so there are no medical waste temporary storage areas in clinics. Once waste is produced by clinics, it is sent to temporary storage areas in nearby grade 1 hospitals and waits to be collected. This requires an affiliated relationship between clinics and grade 1 hospitals. The clinics can affiliate a grade 1 hospital only when the clinic locates in the service radius of the hospital. Since the distances between clinics and

their affiliated hospitals are short, the cost incurred by waste collection of clinics is ignored in our research.

(4) *Other Waste Producers*. Some medical waste is produced by some facilities other than hospitals and clinics, including scientific institutions and laboratories, blood banks, and pharmaceutical manufacturers. These facilities have temporary storage areas for waste, and the waste is collected every two days.

Based on the settings above, a two-day period can be set up for waste collection. Each period contains two days, namely, odd day and even day. Waste collection tasks are generated among hospitals according to the waste collection frequency and waste amount. For every waste collection period, grade 2 and above hospitals will generate two waste collection tasks for the waste produced by themselves: one task involves the collection of waste produced on the odd day, and the other task involves the collection of waste produced on the even day. Grade 1 hospitals will generate one collection task in a period, which contains the waste produced by themselves and the affiliated clinics. The task of grade 1 hospitals can be collected on either odd day or even day. The task of other waste producers contains the waste produced in two days and will be collected once in a period. The waste collection and recycling activities follow certain working hours; that is to say, a time window is added to the route of waste collection.

Based on the above process, the medical waste transport network is shown in Figure 2. The above problem setting can be abstracted as a PVRPTW, in which the recycling centre serves as the depot of the network, and medical facilities play the role of the nodes where demands are located. All collection routes are visited on either odd day or even day and start from and end at the recycling centre. Every collection task should be served in one of the two days and assigned to a specific route. The objective of this problem is to minimise the total transportation distance. The decision problem contains the collection routes of vehicles along with the date and time of tasks being served. For the waste collection of clinics, the affiliated relationship also needs to be determined.

4. Mathematical Model

4.1. Notations. The notations used to formulate the model are introduced below.

Indices and Sets

w, w': Index of task, which means the medical waste to be collected in a hospital

W: Set of all tasks

W^0: A subset of task set W, $W^0 \subseteq W, 2 \leq |W^0| \leq |W|$

i: Index of hospitals

I: Set of all hospitals

I_g: Set of grade g hospitals; in detail, I_0 represents other medical facilities, I_1 represents set of grade 1 hospitals, and I_2 represents grade 2 and above hospitals

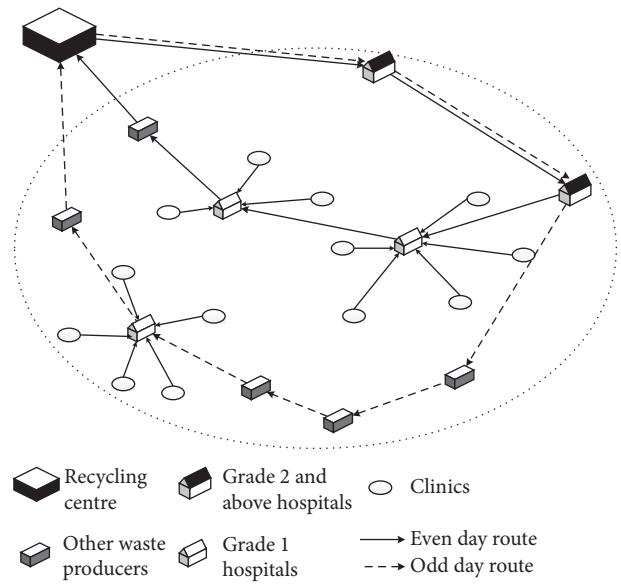

Figure 2: Hierarchy diagram of medical waste recovery network.

j: Index of clinics

J: Set of all clinics

t: Index of date

T: Set of dates in a transport cycle. $T = \{1, 2\}$, where 1 represents odd day, and 2 represents even day

r: Index of vehicles

R: Set of all vehicles

R_t: Set of vehicles working on date t; R_1 represents vehicles working on odd days, and R_2 represents vehicles working on even days.

Parameters

$e(r), e'(r)$: Recycling centre, the start point, and end point for collection route

h_w: Corresponding hospital of task w

g_i: Grade of hospital i, where 0 represents other waste producers, 1 represents grade 1 hospitals, and 2 represents grade 2 and above hospitals

$d_{w,w'}$: Travelling distance between tasks w and w'

$t_{w,w'}$: Travelling time between tasks w and w'

$p_{j,i}$: Set to 1 if the clinic j locates within the service radius of grade 1 hospital i and 0 otherwise

t_w: Task w's processing time

$[a^f, b^f]$: The availability service time of waste collection for all tasks

q_w^1: The amount of medical waste produced by the hospital corresponding to the task w

q_j^2: The amount of medical waste in the clinic j

Q_i^1: Medical waste capacity of grade 1 hospital i, $i \in I_1$

Q_r^2: Maximum capacity of vehicle r, $r \in R$

M: A sufficiently large positive number

H: 24 hours.

Decision Variables

$\mu_{j,i}$: Binary variable, set to 1 if the waste of clinic j is collected to the hospital i and 0 otherwise

$\pi_{w,w',r}$: Binary variable, set to 1 if the vehicle r serves the task w' immediately after serving the task w and 0 otherwise

$\varphi_{w,t}$: Binary variable, set to 1 if the task w is served in date t and 0 otherwise

$\sigma_{w,r}$: Binary variable, set to 1 if the task w is served by the vehicle r and 0 otherwise

$\rho_{w,r}$: Float variable, the start time of the task w being served by vehicle r

τ_w: Float variable, the total medical waste of the task w

$\varepsilon_{w,r}$: Float variable, the amount of medical waste in the task w transported by the vehicle r.

Based on the notations above, to simplify the expression, we define the set W_i to express task set of the hospital i, where $W_i = \{w \mid w \in W, h_w = i\}$.

4.2. Mathematical Model Construction.

$$\text{Minimize} \quad \sum_{r\in R} \sum_{w\in W\cup\{e(r)\}} \sum_{w'\in W\cup\{e'(r)\}} d_{w,w'} \pi_{w,w',r}, \tag{1}$$

$$\text{s.t.} \quad \sum_{i\in I_1} \mu_{j,i} = 1, \forall j \in J, \tag{2}$$

$$\mu_{j,i} \le p_{j,i}, \quad \forall i \in I_1, j \in J, \tag{3}$$

$$\sum_{r\in R} \sigma_{w,r} = 1, \quad \forall w \in W, \tag{4}$$

$$\sigma_{w,r} \le \varphi_{w,t}, \quad \forall w \in W, t \in T, r \in R_t, \tag{5}$$

$$\sum_{w\in W\cup\{e(r)\}} \pi_{w,w',r} = \sum_{w\in W\cup e_l(r)} \pi_{w_l,w,r} = \sigma_{w_l,r}, \quad \forall w' \in W, r \in R, \tag{6}$$

$$\sum_{w\in W\cup\{e'(r)\}} \pi_{e(r),w,r} = \sum_{w\in W\cup\{e(r)\}} \pi_{w,e_l(r),r} = 1, \quad \forall r \in R, \tag{7}$$

$$\sum_{w\in W^0} \sum_{w'\in W^0} \pi_{w,w',r} \le \left|W^0\right| - 1 \; W^0 \subseteq W, \quad 2 \le \left|W^0\right| \le |W|, \forall r \in R, \tag{8}$$

$$\tau_w = q_w^1 + \sum_{j\in J} q_j^2 \mu_{j,i}, \quad \forall w \in W, i \in I_1, \tag{9}$$

$$\tau_w = q_w^1, \quad \forall w \in W, i \in I_0 \cup I_2, \tag{10}$$

$$\tau_w \le Q_i^1, \quad \forall w \in W, i \in I_1, \tag{11}$$

$$\varepsilon_{w,r} \le M\sigma_{w,r}, \quad \forall w \in W, r \in R, \tag{12}$$

$$\varepsilon_{w,r} \le \tau_w, \quad \forall w \in W, r \in R, \tag{13}$$

$$\varepsilon_{w,r} \ge \tau_w - M\left(1 - \sigma_{w,r}\right), \quad \forall w \in W, r \in R, \tag{14}$$

$$\sum_{w\in W} \varepsilon_{w,r} \le Q_r^2, \quad \forall r \in R, \tag{15}$$

$$\varphi_{w,1} + \varphi_{w,2} = 1, \quad \forall w \in W, \tag{16}$$

$$\sum_{w \in W_i} \varphi_{w,t} \leq 1, \quad \forall t \in T, i \in I, \tag{17}$$

$$\sum_{w \in W_i} \varphi_{w,1} + \sum_{w \in W_i} \varphi_{w,2} = 2, \quad \forall i \in I_2, \tag{18}$$

$$\sum_{w \in W_i} \varphi_{w,1} + \sum_{w \in W_i} \varphi_{w,2} \geq 1, \quad \forall i \in I_0 \cup I_1, \tag{19}$$

$$\rho_{w,r} \geq a^f + t_w + H\varphi_{w,2} + M\left(\sigma_{w,r} - 1\right), \quad \forall w \in W, r \in R, \tag{20}$$

$$\rho_{w,r} \leq b^f + H\varphi_{w,2} - M\left(\sigma_{w,r} - 1\right), \quad \forall w \in W, r \in R, \tag{21}$$

$$\rho_{w,r} \leq M\sigma_{w,r}, \quad \forall w \in W, r \in R, \tag{22}$$

$$\rho_{w',r} \geq \rho_{w,r} + t_{w'} + t_{w,w'} - M\left(1 - \pi_{w,w',r}\right), \quad \forall w \in W \cup \{e(r)\}, w' \in W \cup \{e'(r)\}, r \in R, \tag{23}$$

$$\mu_{j,i}, \pi_{w,w_l,r}, \sigma_{w,r} \in \{0,1\}, \quad \forall w \in W \cup \{e(r)\}, w'^{\in} W \cup \{e'(r)\}, r \in R, i \in I, j \in J, t \in T, \tag{24}$$

$$\rho_{w,r}, \tau_w, \varepsilon_{w,r} \geq 0, \quad \forall w \in W \cup \{e(r), e'(r)\}, r \in R. \tag{25}$$

The objective function of this model is to minimise the total transportation distance, which is shown in constraint (1). Constraints (2) determine the affiliation between the clinic and the level 1 hospital, where a clinic must be affiliated to only one grade 1 hospital. Constraints (3) indicate that a clinic can affiliate with a grade 1 hospital only when the clinic is in the coverage area of the hospital. Constraints (4) make sure that all tasks will be served by a vehicle. Constraints (5) state that a vehicle can serve a task only when the vehicle works on the date that the task is assigned. Constraints (6) and (7) ensure the routes' consecutiveness of all vehicles, and constraints (8) prevent the shipping routes of vehicles forming loops. Constraints (9) ensure that, for all tasks of grade 1 hospitals, the total amount of waste to be transported in the corresponding task equals the sum of the wastes produced by itself and collected from the affiliated clinics. Constraints (10) state that, for all tasks of grade 0 and 2 hospitals, the total amount of medical waste to be transported in the corresponding task equals the amount of waste produced by itself. Constraints (11) make sure that the total amount of medical waste in each task cannot exceed the maximum capacity of the corresponding hospital. Constraints (12), (13), and (14) denote the shipping amount of task w by vehicle r. If task w is assigned to be shipped by vehicle r, the shipping amount should be equal to the total waste amount of the task. If the task w will not be shipped by vehicle r, the shipping amount must be zero. Constraints (15) imply that the total amount of medical waste transported by a vehicle should not exceed its maximum capacity. Constraints (16) and (17) ensure that a task should be assigned to only one date. Constraints (18) ensure that a grade 2 and above hospital must have two transportation tasks within a transport cycle. Constraints (19) ensure that level 0 and level 1 hospitals have one transportation task within a transport cycle. Constraints (20) and (21) set the working time limit on vehicles. Constraints (22) denote that the start time of the task w served by vehicle r can exist only if the task w is assigned to be served by vehicle r. Constraints (23) indicate the relationship of start time for adjacent tasks. Constraints (24) and (25) define all decision variables.

5. Solution Method

5.1. PSO Solution Method. For small-scale instances, the proposed model can be solved directly by CPLEX and some other commercial solvers. However, the commercial solver cannot solve large-scale problem instances within a reasonable time. Therefore, we design a PSO solution approach to solve the problem. PSO is widely used for solving continuous nonlinear optimisation problems because of its simple concept, easy implementation, and quick convergence [17]. The PSO algorithm is successfully applied by numerous researchers to solve VRP [18, 19]. For the problem in other logistics sections, PSO can also achieve outstanding performance [20].

For the PSO method, we employ dimensional reduction for the particles to improve the solving efficiency. The first group of particles is defined by variables $\mu_{j,i}$ with the notation μ^n_{mj}. For a particle m in iteration n, μ^n_{mj} denotes the hospital i where the medical waste of the clinic j is collected. Similarly, the second group of particles is defined by variables $\varphi_{w,t}$ with the notation φ^n_{mw}. For a particle m iteration n, φ^n_{mw} denotes the date t where the task w is served. Variables $\pi_{w,w',r}$ and $\sigma_{w,r}$ can be redefined by β^n_{mr} and π_{mrz}, where β^n_{mr} represents the number of tasks which is assigned to the vehicle r and π_{mrz} represents the task w served by vehicle r in sequence z. To determine the sequence of tasks and connect the two particles β^n_{mr} and π_{mrz}, we introduce the priority

attribute χ_w. χ_w represents the priority of task w. The value of χ_w is randomly generated within an interval, which is used to determine the sequence z in particle π_{mrz}. A random sequence can be indicated from the set containing all χ_w; that is, the task with smaller value of χ_w will be processed earlier. For example, there are 3 tasks named w_1, w_2, and w_3 waiting to be served by the vehicle r, or we can express this by $\beta_{mr}^n = 3$. To determine the sequence of the three tasks, $\chi_{w_1} = 53$, $\chi_{w_2} = 72$, and $\chi_{w_3} = 20$ are randomly generated within the interval $[0, 100]$. According to the value of χ_w, the sequence of the vehicle serving those tasks is $w_3 \longrightarrow w_1 \longrightarrow w_2$; that is, $\pi_{mr1} = w_3$, $\pi_{mr2} = w_1$, and $\pi_{mr3} = w_2$. The updating formulas of velocity and position for both groups of particles are presented as follows:

$$\mu V_{mj}^{n+1} = \mu V_{mj}^n + c_1 r_1 \left(\mu p \operatorname{Best}_{mj}^n - \mu_{mj}^n\right) + c_2 r_2 \left(\mu g \operatorname{Best}_j^n - \mu_{mj}^n\right), \tag{26}$$

$$\mu_{mj}^{n+1} = \mu_{mj}^n + \mu V_{mj}^{n+1}, \tag{27}$$

$$\varphi V_{mw}^{n+1} = \varphi V_{mw}^n + c_1 r_1 \left(\varphi p \operatorname{Best}_{mw}^n - \varphi_{mw}^n\right) + c_2 r_2 \left(\varphi g \operatorname{Best}_w^n - \varphi_{mw}^n\right), \tag{28}$$

$$\varphi_{mw}^{n+1} = \varphi_{mw}^n + \varphi V_{mw}^{n+1}, \tag{29}$$

$$\beta V_{mr}^{n+1} = \beta V_{mr}^n + c_1 r_1 \left(\beta p \operatorname{Best}_{mr}^n - \beta_{mr}^n\right) + c_2 r_2 \left(\beta g \operatorname{Best}_r^n - \beta_{mr}^n\right), \tag{30}$$

$$\beta_{mr}^{n+1} = \beta_{mr}^n + \beta V_{mr}^{n+1}, \tag{31}$$

$$\chi V_{mw}^{n+1} = \chi V_{mw}^n + c_1 r_1 \left(\chi p \operatorname{Best}_{mw}^n - \chi_{mw}^n\right) + c_2 r_2 \left(\chi g \operatorname{Best}_w^n - \chi_{mw}^n\right), \tag{32}$$

$$\chi_{mw}^{n+1} = \chi_{mw}^n + \chi V_{mw}^{n+1}. \tag{33}$$

In formulas 26 and 27, μV_{mj}^{n+1} and μV_{mj}^n represent the current velocity and the previous velocity of particle μ_{mj}^n on dimension m, respectively. For dimension m, $\mu p \operatorname{Best}_{mj}^n$ denotes the best position of particle μ_{mj}^n on up to iteration n, and $\mu g \operatorname{Best}_j^n$ denotes the best position of the whole swarm until iteration n; μ_{mj}^{n+1} and μ_{mj}^n denote the current and previous position of the particle. In formulas 28 and 29, φV_{mw}^{n+1} and φV_{mw}^n represent the current velocity and the previous velocity of particle φ_{mw}^n on dimension m, respectively. For dimension m, $\varphi p \operatorname{Best}_{mw}^n$ denotes the best position of particle φ_{mw}^n on up to iteration n, and $\varphi g \operatorname{Best}_w^n$ denotes the best position of the whole swarm until iteration n; φ_{mw}^{n+1} and φ_{mw}^n denote the current and previous position of the particle. In formulas 30 and 31, βV_{mr}^{n+1} and βV_{mr}^n represent the current velocity and the previous velocity of particle β_{mr}^n on dimension m, respectively. For dimension m, $\beta p \operatorname{Best}_{mr}^n$ denotes the best position of particle β_{mr}^n on up to iteration n, and $\beta g \operatorname{Best}_r^n$ denotes the best position of the whole swarm until iteration n; β_{mr}^{n+1} and β_{mr}^n denote the current and previous position of the particle.

In formulas 32 and 33, χV_{mw}^{n+1} and χV_{mw}^n represent the current velocity and the previous velocity of particle χ_{mw}^n on dimension m, respectively. For dimension m, $\chi p \operatorname{Best}_{mw}^n$ denotes the best position of particle φ_{mw}^n on up to iteration n, and $\chi g \operatorname{Best}_w^n$ denotes the best position of the whole swarm until iteration n; χ_{mw}^{n+1} and χ_{mw}^n denote the current and previous position of the particle. For both groups of particles, c_1 and c_2 are acceleration weights; r_1 and r_2 are two random numbers generated within the interval $[0, 1]$.

5.2. Main Framework of the PSO Procedure. Based on the above components, the PSO procedure for the proposed problem is listed in Table 1.

6. Numerical Experiment

We conduct extensive numerical experiments to access the solution efficiency of the proposed algorithm. All experiments are performed on a computer with Intel Xeon E5-2680 v4 CPU @2.40 GHz and 256 GB RAM. The proposed model and algorithm are implemented in C# (VS2019) concert technology with the solver IBM ILOG CPLEX 12.5.1.

6.1. Generation of the Test Instances. In the computational experiments, we test nine instances with different scales. The parameter settings for the instance groups (ISGs) are shown in Table 2. The planning horizon considered is two days. Each task is served from 0 am to 10 am. The service radius of grade 1 hospital is 500 metres. Other input parameters for the experiments are uniformly distributed in the ranges given in Table 3.

For the PSO algorithm, the learning factors r_1 and r_2 are randomly generated within the interval $[0, 1]$. Based on the results of the test runs, the acceleration weights c_1 and c_2 are both set to 0.638.

6.2. Performance of the Proposed Solution Method. To validate the quality and efficiency of the proposed PSO algorithm, we first conduct the experiments on small-scale

Table 1: PSO algorithm procedure.

Parameters: $\mathbf{n}$, $\mathbf{N}$, $|\mathbf{I}_0|$, $|\mathbf{I}_1|$, $|\mathbf{I}_2|$, $|\mathbf{J}|$, $|\mathbf{W}|$, $|\mathbf{R}_1|$, $|\mathbf{R}_2|$, $|\mathbf{T}|$, $\mathbf{c}_1$, $\mathbf{c}_2$, $\mathbf{r}_1$, $\mathbf{r}_2$ //n represents the current iteration number, N represents the maximum iteration number.
Objective: $\sum_{r\in R_1\cup R_2}\sum_{w\in W\cup\{e(r)\}}\sum_{w'\in W\cup e'(r)} d_{w,w'}\pi_{w,w',r}$

Define μ^n_{mj}, φ^n_{mw}, β^n_{mr}, χ^n_{mw}, num_{t_1}, num_{t_2}, π_{mrz}, μV^n_{mj}, φV^n_{mw}, βV^n_{mr}, χV^n_{mw}, $\mu p\,\mathrm{Best}^n_{mj}$, $\varphi p\,\mathrm{Best}^n_{mw}$, $\beta p\,\mathrm{Best}^n_{mr}$, $\chi p\,\mathrm{Best}^n_{mw}$, $\mu g\,\mathrm{Best}^n_{j}$, $\varphi g\,\mathrm{Best}^n_{w}$, $\beta g\,\mathrm{Best}^n_{r}$, $\chi g\,\mathrm{Best}^n_{w}$, $\mathrm{Fitness}^n_m$, $P\,\mathrm{Best}^n_m$, $G\,\mathrm{Best}^n$
For $\mathbf{m}\in\mathbf{M}$ //M is the set of particles
For $\mathbf{j}\in\mathbf{J}$
Set μ^n_{mj} to a random number $i\in I_1$, $p_{j,i}=1$
End for
For $\mathbf{w}\in\mathbf{W}$
Set φ^n_{mw} to a random number of intervals $[0,T]$
End for
Calculate the total number of tasks num_{t_1} and num_{t_2} in different date
For $\mathbf{r}\in\mathbf{R}$
Set β^n_{mr} to a random number of intervals $[0,\mathrm{num}_{t_1}]$ or $[0,\mathrm{num}_{t_2}]$
End for
For $\mathbf{r}\in\mathbf{R}$, $\mathbf{z}\in\beta^{\mathbf{n}}_{\mathbf{mr}}$
Set π_{mrz} to a random number of intervals $[0,W]$
End for
For $\mathbf{w}\in\mathbf{W}$
Set χ^n_{mw} to a random number of intervals $[0,100]$
End for
Reorder π_{mrz} based on χ^n_{mw}
If $\rho_{w,r}\in[a^f,b^f]$, $\tau_w\le Q^1_i$, $\varepsilon_{w,r}\le Q^2_r$, then calculate the fitness value; otherwise calculate the fitness value with penalty cost
Update $P\,\mathrm{Best}^n_m$, $G\,\mathrm{Best}^n$
End for
While $(\mathbf{n}<\mathbf{N})$ **do**
For $\mathbf{m}\in\mathbf{M}$
Update the velocity and position of μ^n_{mj}, φ^n_{mw}, β^n_{mr}, χ^n_{mw}
Make μ^n_{mj}, φ^n_{mw}, β^n_{mr}, χ^n_{mw} feasible, and reorder π_{mrz} based on χ^n_{mw}
Update $P\,\mathrm{Best}^n_m$, $G\,\mathrm{Best}^n$
End for
$\mathbf{n}=\mathbf{n}+1$
End while
Return $G\,\mathrm{Best}^n$

Table 2: Scale of instance groups in experiments.

Group ID	No. of other medical facilities ($\lvert I_0\rvert$)	No. of grade 1 hospitals ($\lvert I_1\rvert$)	No. of grade 2 hospitals ($\lvert I_2\rvert$)	No. of tasks ($\lvert W\rvert$)	No. of clinics ($\lvert J\rvert$)	No. of vehicles ($\lvert R_t\rvert$)
ISG1	2	3	2	9	8	3
ISG2	4	3	2	11	12	4
ISG3	4	5	3	15	12	4
ISG4	6	8	5	24	22	5
ISG5	12	12	7	38	24	6
ISG6	18	14	9	50	26	6
ISG7	20	20	15	70	30	8
ISG8	24	22	17	80	35	8
ISG9	26	24	20	90	40	8

instances by comparing the results using the CPLEX solver. From Table 4, we can observe that the PSO algorithm and the CPLEX solver obtain the same objective results. However, the optimal solutions calculated by CPLEX are achievable within 2 hours only for ISG1 and ISG2, which means the CPLEX can only solve some small-scale instances. The PSO algorithm performs more efficiently than CPLEX in terms of computation time, where the average computing time for PSO is only 15.61 seconds.

For the medium-scale instances in Table 5, we can conclude that, for medium-scale instances, the solutions obtained by PSO are at least as good as the feasible solution obtained by CPLEX in 7200 seconds, while the computation process of PSO algorithm is much faster than CPLEX.

When facing large-scale instances in our experiments, a set of assignment rules are conducted for comparison. The main procedure of the rules is listed as follows.

Table 3: Parameters setting for the experiments.

Parameter	Value
$d_{w,w'}$	[1–3] km
q_j^2	[3–6] kg
$t_{w\in W_0}$	[0.05–0.10] h
$t_{w\in W_1}$	[0.10–0.17] h
$t_{w\in W_2}$	[0.17–0.27] h
Q_i^1	5000 kg
Q_r^2	1500 kg
$q_{w\in W_0}^1$	[20–40] kg
$q_{w\in W_1}^1$	[50–100] kg
$q_{w\in W_2}^1$	[100–200] kg

Table 4: Comparison between CPLEX solver and PSO algorithm on small-scale instances.

Instance		CPLEX		PSO		
Group	ID	F_{CPLEX}	t_{CPLEX}	F_{PSO}	t_{PSO}	Gap_1
ISG1	1	11	1.77	11	8.10	0.00%
	2	11	1.49	11	8.22	0.00%
	3	11	0.80	11	7.83	0.00%
	4	11	1.58	11	8.31	0.00%
	5	12	1.97	12	7.60	0.00%
ISG2	1	13	5.17	13	15.2	0.00%
	2	13	242.43	13	14.45	0.00%
	3	13	132.15	13	14.32	0.00%
	4	13	354.97	13	14.30	0.00%
	5	13	348.38	13	13.19	0.00%
ISG3	1	—	>7200	17	20.83	—
	2	—	>7200	17	21.38	—
	3	—	>7200	17	22.41	—
	4	—	>7200	17	20.79	—
	5	—	>7200	17	37.29	—
Average	—	—	—	—	15.61	—

Notes: (1) F_{CPLEX} represents the optimal solution obtained by CPLEX. F_{PSO} denotes the global best solution obtained by PSO algorithm. (2) t_{CPLEX} and t_{PSO} are the computation time of CPLEX and PSO algorithm in seconds, respectively. (3) $\text{Gap}_1 = ((F_{\text{PSO}} - F_{\text{CPLEX}})/F_{\text{CPLEX}})$.

Step 1. The medical waste of the clinic is collected by the nearest grade 1 hospital without exceeding its capacity. If the waste collected by a hospital has reached the capacity, then find the second nearest hospital for collecting the clinic's waste.

Step 2. The total tasks for each vehicle are proportionally distributed based on its load capacity and time windows.

Step 3. Based on the "Nearest Service" principle, each vehicle serves the closest tasks.

Table 6 illustrates the comparisons between the proposed solution methods and the rules. As can be seen, the PSO algorithm can obtain a good solution in solving the large-scale problem instances, with the average computing time of 1120.28 seconds. More importantly, it is seen that the PSO algorithm outperforms the rules for all instances from ISG7 to ISG9 in terms of solution quality. The average gap between the two solutions is −5.98%; that is, the PSO algorithm can achieve further optimisation of the solution of rules in solving large-scale problems.

Table 5: Comparison between CPLEX solver and PSO algorithm on medium-scale instances.

Instance		CPLEX		PSO		
Group	ID	F_{CPLEX}	t_{CPLEX}	F_{PSO}	t_{PSO}	Gap_1
ISG4	1	29	>7200	28	51.62	−3.45%
	2	29	>7200	29	51.64	0.00%
	3	28	>7200	27	56.50	−3.57%
	4	27	>7200	27	52.08	0.00%
	5	29	>7200	28	51.93	−3.45%
ISG5	1	45	>7200	44	132.59	−2.22%
	2	48	>7200	47	129.94	−2.08%
	3	49	>7200	49	130.73	0.00%
	4	48	>7200	46	132.41	−4.17%
	5	51	>7200	49	130.98	−3.92%
ISG6	1	62	>7200	60	212.95	−3.23%
	2	69	>7200	68	213.59	−1.45%
	3	68	>7200	65	211.06	−4.41%
	4	66	>7200	66	213.97	0.00%
	5	64	>7200	62	215.46	−3.13%
Average	—	—	—	—	132.50	−2.34%

Notes: (1) F_{CPLEX} represents the feasible solution obtained by CPLEX in 7200 seconds. F_{PSO} denotes the global best solution obtained by PSO algorithm. (2) t_{CPLEX} and t_{PSO} are the computation time of CPLEX and PSO algorithm in seconds, respectively. (3) $\text{Gap}_1 = ((F_{\text{PSO}} - F_{\text{CPLEX}})/F_{\text{CPLEX}})$.

6.3. Sensitivity Analysis. The type of vehicle (e.g., capacity) has a significant influence on the optimisation of the transportation network. Therefore, we conduct a sensitivity analysis on the capacity of the vehicle to assess its effect on the objective value. Case 1, Case 2, Case 3, and Case 4 employ single type of vehicles of 500 kg, 1000 kg, 1500 kg, and 2000 kg, respectively, which are the four types of special transport vehicles for medical waste in practice. Case 5 represents a multivehicle fleet, which applies all types of vehicles employed. The proportions of each type of vehicles employed in Case 5 for different scales of instances are 1 : 1:1 : 1, 1 : 1:2 : 1, 1 : 3:3 : 1, respectively. ISG2, ISG4, and ISG7 are employed to represent the small-scale, medium-scale, and large-scale problem instances, respectively.

Figure 3 indicates that the objective value is sensitive to the capacity of the vehicle, especially for large-scale instances. In particular, the total distance shows a downward trend as the increasing capacity of single vehicle (e.g., Case 1–Case 4). There is a remarkable drop in Case 2, which means it is economical to allocate the type of 1000 kg vehicle for the third-party recycling company. It is worthwhile to mention that the performance of Case 5 reaches the better solution among all scale problems. Multiple vehicles can greatly improve the transportation efficiency, and the operator may allocate various types of vehicles to serve different scale tasks.

Table 6: Comparison between the rules and the PSO algorithm on large-scale instances.

Instance		Rules	PSO		
Group	ID	F_{Rules}	F_{PSO}	t_{PSO}	Gap_2
ISG7	1	100	95	899.48	−5.00%
	2	99	91	864.21	−8.08%
	3	96	89	872.12	−7.29%
	4	96	88	864.62	−8.33%
	5	98	93	858.85	−5.10%
ISG8	1	102	100	1107.1	−1.96%
	2	108	102	1111.35	−5.56%
	3	106	98	1104.23	−7.55%
	4	105	98	1143.90	−6.67%
	5	105	101	1116.67	−3.81%
ISG9	1	125	117	1361.83	−6.40%
	2	119	114	1372.91	−4.20%
	3	123	118	1382.82	−4.07%
	4	131	120	1370.40	−8.40%
	5	124	115	1373.64	−7.26%
Average	—	—	—	1120.28	−5.98%

Notes: (1) F_{Rules} represents the feasible solution obtained by rules. F_{PSO} denotes the global best solution obtained by PSO algorithm. (2) t_{PSO} is the computation time of PSO algorithm in seconds. (3) $\text{Gap}_2 = ((F_{\text{PSO}} - F_{\text{Rules}})/F_{\text{Rules}})$.

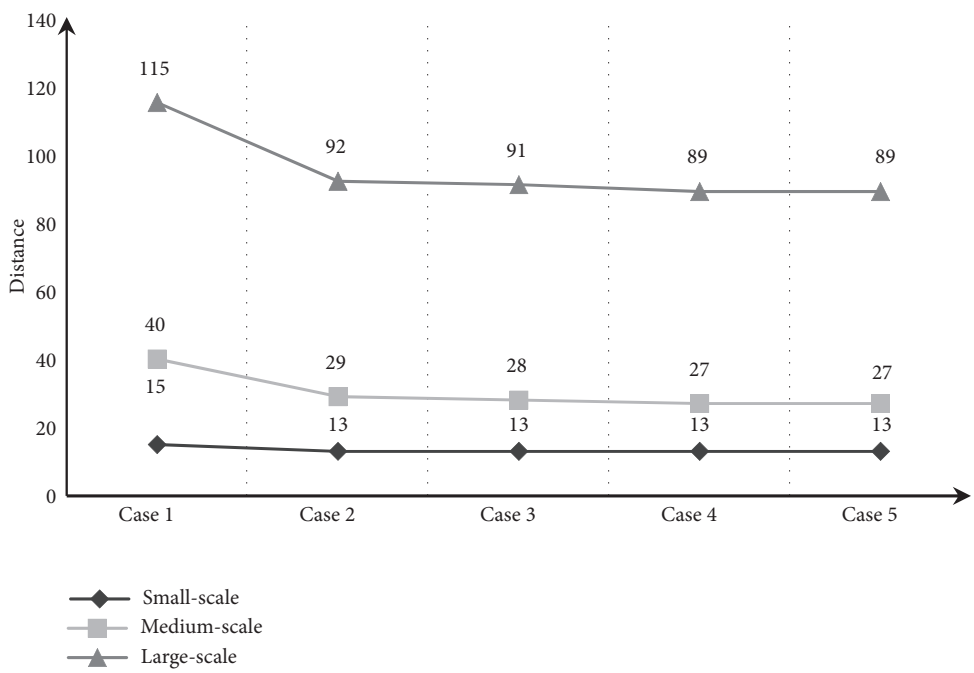

Figure 3: Sensitivity analysis about types of vehicles.

7. Conclusion

This paper studies an integrated optimisation problem of urban medical waste recycling network considering differentiated collection strategies with time windows. In addition, since the medical waste recycling operates according to a two-day pattern, the periodicity of the plan is also embedded in the model. To tackle the optimisation, a compact mixed-integer linear programming model is proposed, which aims to minimise the total distance of the recycling network. Then we develop a PSO solution approach to solve the problem. Based on some realistic instances, extensive numerical experiments are conducted and some managerial implications can be recommended for the third-party recycling company. The major contributions of this study are summarised in the following aspects:

(1) This paper extends the traditional medical waste recycling network problem, which takes the periodicity of medical waste collection and differentiated medical waste collection strategies for medical facilities of various grades into account. Moreover, the affiliated relationships between clinics and grade 1 hospitals are integrated into the whole model.

(2) For solving the proposed integrated problem, this study develops a PSO solution approach, which is validated for both small-scale and large-scale instances. The PSO algorithm can obtain a good solution in solving large-scale problem instances within a reasonable time, which means the algorithm can provide a decision support tool for the operator.

(3) Based on extensive numerical experiments and sensitivity analysis, we can see that multiple vehicles can greatly improve the transportation efficiency in the recycling network. The third-party recycling company's operator may allocate various types of vehicles to serve different scale tasks.

However, there are some limitations for this study. First, the benefit of multivehicle fleet is proved by the sensitivity analysis. Multivehicle transportation can be further explored by investigating the optimal proportion of different vehicle types in a fleet. Second, although the proposed PSO algorithm can obtain solutions of high quality in reasonable time, the computation of large-scale instances still takes a longer time than expected. To improve the computation efficiency in large-scale instances, some acceleration strategies could be addressed to the algorithm. We will focus on these limitations which form the research directions for future studies.

Data Availability

No data were used to support this study.

Conflicts of Interest

The authors declare that they have no conflicts of interest.

Acknowledgments

This research was supported by the National Key R&D Program of China (Grant no. 2018YFE0102700).

References

[1] M. Taslimi, R. Batta, and C. Kwon, "Medical waste collection considering transportation and storage risk," *Computers & Operations Research*, vol. 120, p. 104966, 2020.

[2] B. A. Khan, L. Cheng, A. A. Khan, and H. Ahmed, "Healthcare waste management in Asian developing countries: a mini review," *Waste Management & Research*, vol. 37, no. 9, pp. 863–875, 2019.

[3] H. Rachih, F. Z. Mhada, and R. Chiheb, "Meta-heuristics for reverse logistics: a literature review and perspectives," *Computers & Industrial Engineering*, vol. 127, pp. 45–62, 2019.

[4] P. C. Nolz, N. Absi, and D. Feillet, "A stochastic inventory routing problem for infectious medical waste collection," *Networks*, vol. 63, no. 1, pp. 82–95, 2014.

[5] G. Mantzaras and E. A. Voudrias, "An optimization model for collection, haul, transfer, treatment and disposal of infectious medical waste: application to a Greek region," *Waste Management*, vol. 69, pp. 518–534, 2017.

[6] E. B. Tirkolaee, P. Abbasian, and G.-W. Weber, "Sustainable fuzzy multi-trip location-routing problem for medical waste management during the COVID-19 outbreak," *Science of the Total Environment*, vol. 756, p. 143607, 2021.

[7] H. Yu, X. Sun, W. D. Solvang, and X. Zhao, "Reverse logistics network design for effective management of medical waste in epidemic outbreaks: insights from the coronavirus disease 2019 (COVID-19) outbreak in Wuhan (China)," *International Journal of Environmental Research and Public Health*, vol. 17, no. 5, p. 1770, 2020.

[8] S. Kargar, M. M. Paydar, and A. S. Safaei, "A reverse supply chain for medical waste: a case study in Babol healthcare sector," *Waste Management*, vol. 113, pp. 197–209, 2020.

[9] Y. Shi, Y. J. Zhou, W. H. YE, and Q. Q. Zhao, "A relative robust optimization for a vehicle routing problem with time-window and synchronized visits considering greenhouse gas emissions," *Journal of Cleaner Production*, vol. 275, p. 124112, 2020.

[10] R. EL-Hajj, R. N. Guibadj, A. Moukrim, and M. Serairi, "A PSO based algorithm with an efficient optimal split procedure for the multiperiod vehicle routing problem with profit," *Annals of Operations Research*, vol. 291, no. 1-2, pp. 281–316, 2020.

[11] L. D. C. Martins, P. Hirsch, and A. A. Juan, "Agile optimization of a two-echelon vehicle routing problem with pickup and delivery," *International Transactions in Operational Research*, vol. 28, no. 5, pp. 201–221, 2021.

[12] B. O. Ovstebo, L. M. Hvattum, and K. Fagerholt, "Routing and scheduling of RoRo ships with stowage constraints," *Transportation Research Part C-Emerging Technologies*, vol. 19, no. 6, pp. 1225–1242, 2011.

[13] L. Zhen, "Modeling of yard congestion and optimization of yard template in container ports," *Transportation Research Part B: Methodological*, vol. 90, pp. 83–104, 2016.

[14] L. Zhen, "Tactical berth allocation under uncertainty," *European Journal of Operational Research*, vol. 247, no. 3, pp. 928–944, 2015.

[15] L. Zhen, E. P. Chew, and L. H. Lee, "An integrated model for berth template and yard template planning in transshipment hubs," *Transportation Science*, vol. 45, no. 4, pp. 483–504, 2011.

[16] Z.-G. He, Q. Li, and J. Fang, "The solutions and recommendations for logistics problems in the collection of medical waste in China," *Procedia Environmental Sciences*, vol. 31, pp. 447–456, 2016.

[17] J. Kennedy and R. Eberhart, "Particle swarm optimization," in *Proceedings of ICNN'95-International Conference on Neural Networks*, pp. 1942–1948, Perth, Australia, November, 1995.

[18] N. Norouzi, M. Sadegh-Amalnick, and R. Tavakkoli-Moghaddam, "Modified particle swarm optimization in a time-dependent vehicle routing problem: minimizing fuel consumption," *Optimization Letters*, vol. 11, no. 1, pp. 121–134, 2017.

[19] B. Yao, B. Yu, P. Hu, J. Gao, and M. Zhang, "An improved particle swarm optimization for carton heterogeneous vehicle routing problem with a collection depot," *Annals of Operations Research*, vol. 242, no. 2, pp. 303–320, 2016.

[20] L. Zhen, Z. Xu, K. Wang, and Y. Ding, "Multi-period yard template planning in container terminals," *Transportation Research Part B: Methodological*, vol. 93, pp. 700–719, 2016.

Hindawi
Scientific Programming
Volume 2021, Article ID 5530343, 14 pages
https://doi.org/10.1155/2021/5530343

Research Article

Evaluating the Rail-Based Multimodal Freight Transportation after HSR Entry in Yangtze River Delta Economics Zone

Junliang He,[1,2] **Minghui Wei**,[3] **Hang Yu**,[2] **Jun Yuan**,[2] **and Yanbing Chen**[4]

[1]*Engineering Research Center of Container Supply Chain Technology, Ministry of Education, Shanghai Maritime University, Shanghai, China*
[2]*China Institute of FTZ Supply Chain, Shanghai Maritime University, Shanghai, China*
[3]*School of Economics and Management, Shanghai Maritime University, Shanghai, China*
[4]*Freight Department, China Railway Shanghai Group Co., Ltd., Shanghai, China*

Correspondence should be addressed to Hang Yu; yuhang@shmtu.edu.cn

Received 11 February 2021; Revised 24 February 2021; Accepted 28 February 2021; Published 10 March 2021

Academic Editor: Lu Zhen

Copyright © 2021 Junliang He et al. This is an open access article distributed under the Creative Commons Attribution License, which permits unrestricted use, distribution, and reproduction in any medium, provided the original work is properly cited.

In recent years, China keeps working on restructuring the country's multimodal transport and highly develops the high-speed rail (HSR) infrastructure to improve transport efficiency. As the economic engine of China, the Yangtze River Delta region keeps leading the HSR development and the transporting modal transformation within the whole country. The fast development of HSR on the one hand highly improves passengers' travel efficiency and, on the other hand, releases the capacity of conventional rail infrastructures to support regional multimodal freight transport. This study applies a three-level AHP structure and constructs a comprehensive index to evaluate the development of a rail-based multimodal freight transport network including railway, rail-water, and rail-road. The comprehensive index contains 14 quantitative and 8 qualitative indexes, covering the rail-based infrastructures, multimodal transport capability, freight transport performance, and transport sustainability. The comprehensive index is then applied to analyze the rail-based multimodal freight transport for the Yangtze River Delta region. The operational data of 59 freight stations and more than 200 railway links of the Yangtze River Delta were recorded. About 172 valid questionnaires were collected to score the qualitative indexes, and all the quantitative indexes are scored based on the real-life freight data. The results reveal the impacts of HSR development on rail freight transportation and show that Zhejiang has led rail freight transportation while Shanghai mainly leads the waterway freight transportation. Meanwhile, Anhui performs very well on road-rail transportation and Jiangsu has made a great improvement on water-rail transportation.

1. Introduction

In the past five years, China invested more than 80 billion yuan each year in the construction of high-speed rail (HSR). By the end of 2019, the total revenue length of HSR in China had reached 35,000 km and ranked first place in the world. HSR commanded a share of 64.4% in the total rail passengers by the end of 2019. At the same time, the development of HSR and the shift away from traditional passenger rail services have released the capacity of conventional rail infrastructures to support freight transport including multimodal freight transport. In China State Council's *Three-Year Action Plan for Promoting Transport Restructuring (2018-2020) (The Action Plan)* released in 2018, rail-based freight transport was given unprecedented attention and improved the bulk freight volume via rail and water was set as the priority goal of this action plan.

As the economic engine of China, the Yangtze River Delta region including three provinces, Jiangsu, Zhejiang, and Anhui, and one province-level city (municipality), Shanghai, accounts for about 1/4 of the national GDP with only 2.1% of the nation's land area. Within this area, both the traditional railway and HSR are highly developed and lead the whole country. The total revenue length of HSR in

Yangtze River Delta has already reached 5,000 kilometers, and four main HSR lines go through in this region and join in Shanghai, as shown in Figure 1. The Jinghu, Hukun, and Yanjiang HSR lines all start from Shanghai and link through several main cities in the Yangtze River Delta. Meanwhile, the Yanhai HSR is also being designed to link the main coastal cities of the Yangtze River Delta. As a result, the HSR had already been the main choice for rail travelers, and the released capacity of conventional rail infrastructures is transferred for the use of freight transportation in the Yangtze River Delta. At the same time, with the implementation of *The Action Plan* since 2018, rail-based multimodal transport has been quickly developed. Such revolutionary changes have not been documented and examined by the existing studies. Even in other countries where the HSR network has been developed, the impact of HSR on freight transportation, particularly its impact on rail-based multimodal transportation, has been largely ignored.

Therefore, this study aims to document the current status of the development of rail-based multimodal freight transportation in the Yangtze River Delta due to the capacity freed up by the launch of HSR. In addition, we construct an AHP-based performance index comprising qualitative and quantitative indicators to evaluate the development of the rail-based multimodal freight transportation network including rail-rail, rail-water, and rail-road. This study will inform relevant stakeholders, particularly the policymakers to recognize the current performance of the multimodal transportation in each province in the Yangtze River Delta, which will assist them to design a long-term transport master plan for a multimodal freight transport network in the Yangtze Delta as HSR construction continues in this region.

2. Background

The study targets the multimodal freight transport network among three provinces (Zhejiang, Jiangsu, and Anhui) and one municipality (Shanghai) in The Yangtze River Delta region. Based on the freight transport data in 2018 and 2019, the study chooses 59 rail stations (the chosen stations accounting for 80% of the whole rail transport traffic in 2018 in Yangtze River Delta) as the key nodes to form the evaluation network. The evaluated network includes not only cities from the arterial rail lines but also main cities from the branch lines. This sampling network thus contains 31 cities with HSR stations and more than 200 railway links as shown in Figure 2. In order to capture the booming water-based transportation performance [1] considering sustainable requirements as mentioned in Tan and He [2] and He et al. [3], eight ports with railway freight stations are also evaluated in this research.

All the 59 evaluated rail stations are located in the conventional rail freight network within the Yangtze River Delta. As every city in the Yangtze River Delta has already been linked by the HSR, all the evaluated freight stations are likely affected by the HSR development. To have a closer look at the effects of the HSR development, this study separates the 59 stations into 29 arterial stations and 30 branch stations. All the 29 arterial stations are located along the national *eight vertical and eight horizontal* HSR lines. The distribution of the 59 stations can be found in Table 1.

The freight and container traffic at these stations in 2019 for the three provinces and Shanghai is reported in Table 2. It can be seen that arterial stations recorded the largest increase, particularly in Jiangsu province. However, the freight traffic at the stations in Shanghai slightly dropped from 2018 to 2019. Freight traffic at the arterial stations in Anhui also recorded a slight decrease in 2019.

The freight multimodal network in the Yangtze River Delta is well developed. For the rail-road transport, Anhui outperformed the other three provinces because of the highly developed conventional railway freight network (see Figure 3). Meanwhile, rail-road is rarely used to distribute freight and containers in Shanghai.

Figures 4 and 5 present the market shares of water-based multimodal transportation modes at eight ports in the Yangtze River Delta area in 2019. It can be seen that rail-water mode accounted for a very small share in all the provinces except for Anhui. The region has very developed water transportation systems, and most of these ports mainly focus on water-water freight transportation. For container transportation, road-based transport is still the first choice by customers for most areas in the Yangtze River Delta. There is much room to promote the rail-water model in this region.

3. Literature Review

China's first HSR was launched between Beijing and Tianjin. The first long-haul HSR was the HSR put into use in 2009. A decade later, China has become a world leader in HSR construction [4]. The total length of China's HSR will reach 38,000 km by 2025 and 45,000 by 2030. The impact of HSR on various aspects of the economy has been well studied (for a good survey, see [5]). After more than ten years' construction, the entry of HSR has made a significant impact on the regional development in China. Chen and Haynes [6] propose a conceptual framework to assess the impact of HSR on regional economic disparity. They confirm that the regional economic disparity has been decreased since the development of HSR in China. Zhang et al. [7] studied the impacts of HSR development on regional equity in China and found that the launch of HSR is positively associated with provincial equity. Long et al. [8] report that the entry of HSR accelerates urban expansion and benefit more for the underdeveloped central and western cities in China. Liang et al. [9] hold a similar view. However, Li et al. [10] found that positive impacts are shown to be greater for metropolis than small cities, which implies that HSR also contributes significantly to the economic development of the wealthy eastern region [11] including the Yangtze River Delta Region and Pearl River Delta Region [12]. Despite these positive impacts, Sun and Mansury [13] pointed out that HSR may also contribute to the widening gap between developed and underdeveloped regions. Overall, it seems that the benefits brought about by HSR are significant and unambiguous. However, up to today, there is a

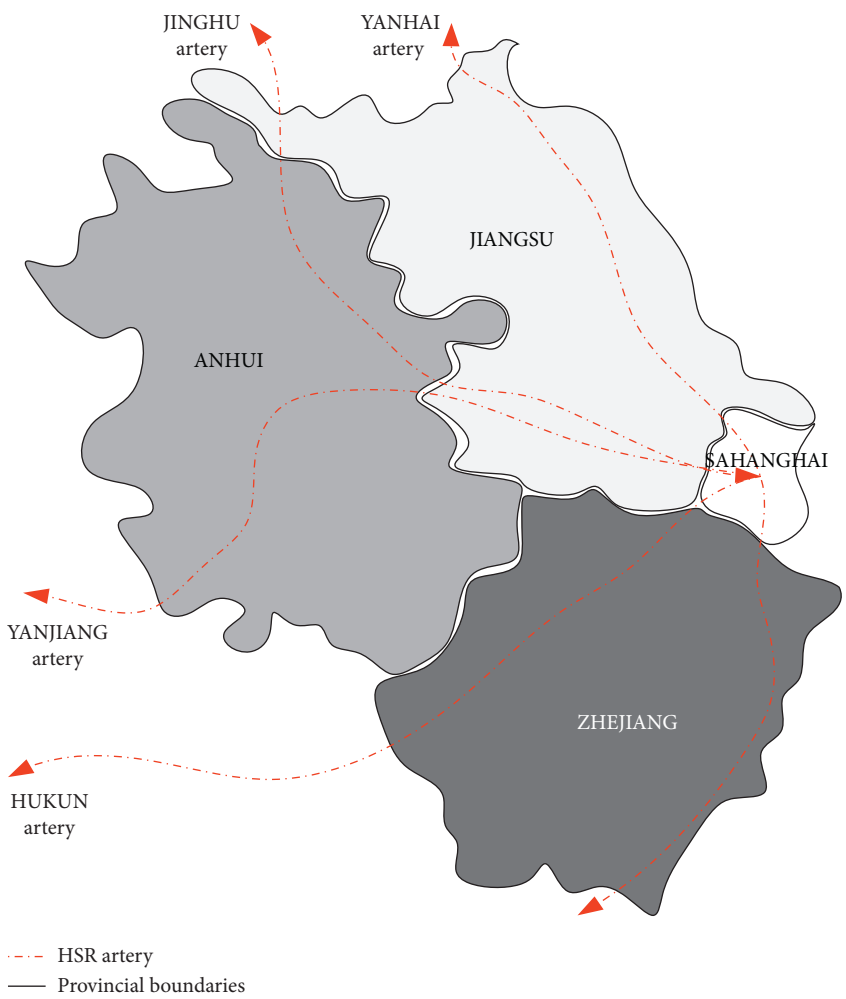

Figure 1: Major HSR lines in Yangtze River Delta.

lack of systematic and comprehensive approaches to quantify the impacts of HSR on the economy as a whole or one particular industry or sector.

International experiences have proven that the HSR development has direct and indirect effects on regional development and creates opportunities to reconstruct the urban system, in both spatial and economic terms [14]. Cascetta et al. [15] evaluated the impact of HSR on economic growth, transport accessibility, and regional quality in Italy ten years after the HSR operation and found significant links between these variables. With the development of the HSR network, the impacts of HSR are also widely received in China. Chen [16] assessed the economic and environmental impact of HSR development from the regional development perspective with proofs where the effects of HSR on the increase of the land value, housing value, and tourism demand are real and significant. From the tourism perspective, Weng et al. [17] revealed that the HSR has become the main choice for short- and medium-range travel distances for tourists. The domestic tourism market improvement due to the presence of HSR is particularly for small- and medium-sized cities. Chen and Haynes [18] and Yang and Li [19] both found that the development of HSR can attract more international tourism and boost inbound tourism.

Furthermore, the development of HSR poses a big challenge to traditional transport markets especially the air transport sector [5, 20]. Zhang et al. [21] and Zhang et al. [22] demonstrated that the negative impacts on air transport are strong with the entry of HSR, particularly for major airline routes. The development of HSR has forced airline companies to reduce their prices and improve services, particularly punctuality to retain existing and attract new passengers [23, 24]. Its threat to low-cost carriers is more prominent due to the close substitution of the two [25]. Meanwhile, the opening of HSR has gradually reshaped the regional freight transport structure. With the entry of HSR, rail-based freight transport becomes more competitive in the regional multimodal transport systems. It is acknowledged that the HSR-based freight transport system is more efficient and cost-effective [26]. However, the development of the HSR-based freight transport network requires a significant investment which is not an easy decision for many governments [27].

Therefore, the conventional railway infrastructure continues to play an important role in rail-based freight transportation. Li et al. [28] indicate that there has been a significant reduction of conventional train services because of the entry of HSR, which makes room for freight

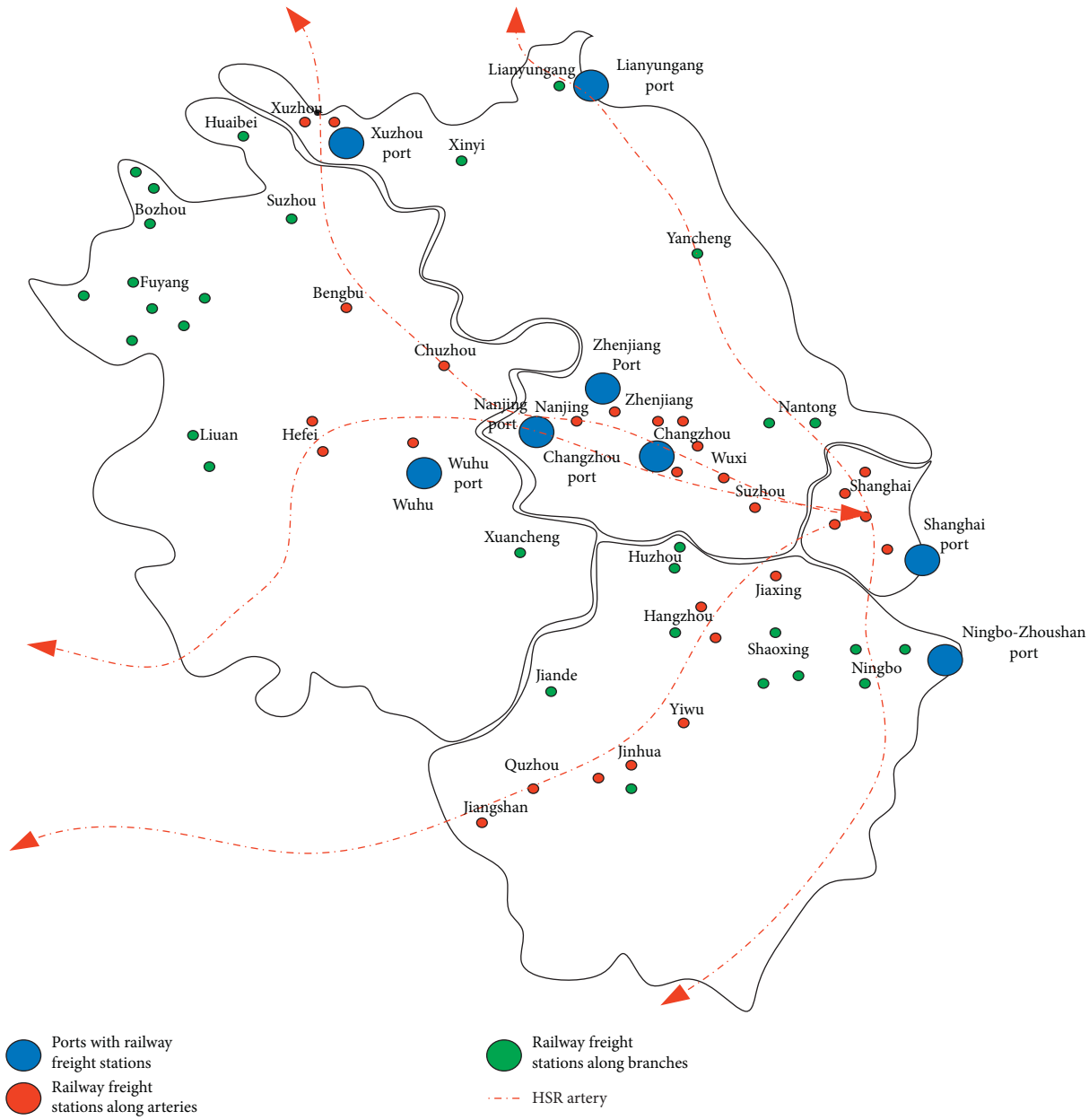

Figure 2: The rail-based multimodal freight transport network in Yangtze River Delta.

Table 1: The distribution of evaluated rail freight stations*.

	Shanghai	Zhejiang	Jiangsu	Anhui
Arterial stations	6	8	10	5
Branch stations	0	11	5	14

*Shanghai is the key node for several HSR arteries; thus, all the stations in Shanghai are classified as arterial stations.

transportation using the traditional train lines. This represents a spillover effect of HSR development. However, in the existing literature on HSR impacts, little has been said about the promotion effect of HSR on the development of rail-based freight transportation. This research aims to fill this literature gap by designing a comprehensive performance index to measure the development of the rail-based freight multimodal transport system, including rail-rail, rail-road, and rail-water in the Yangtze River Delta.

4. Methodology

This study applies a three-level AHP structure and constructs a comprehensive index to evaluate the development of a rail-based multimodal freight transport network. This AHP-based performance index contains 14 quantitative and 8 qualitative indicators, covering the rail-based infrastructures, multimodal transport capability, freight transport performance, and transport sustainability. The index has three levels with the first level including regional distribution network, multimodal transport capacity, and transport operational performance sustainability as shown in Table 3.

Table 2: The 2019 traffic of the evaluated freight stations in Yangtze River Delta.

		Yangtze River Delta	Shanghai	Zhejiang	Jiangsu	Anhui
Freight traffic (000'tonnes)	Arterial stations	44478.29	6936.2	15687.36	19332.22	13717.36
	Year on year	20.91%	−1.39%	19.81%	38.13%	−0.20%
	Branch stations	40050.05	—	14231.31	2668.31	11955.57
	Year on year	14.99%	—	24.63%	−5.06%	25.62%
	Total	84528.34	6936.2	29918.67	22000.54	25672.93
	Year on year	18.03%	−1.39%	22.05%	30.91%	10.36%
Container traffic (000'TEU)	Arterial stations	1369.66	322.57	482.99	531.37	138.32
	Year on year	47.94%	22.25%	37.75%	90.50%	90.21%
	Branch stations	515.46	—	339.75	34.58	35.52
	Year on year	37.34%	—	27.45%	−3.76%	9.28%
	Total	1885.11	322.57	822.75	565.95	173.84
	Year on year	44.88%	22.25%	33.30%	79.75%	65.21%

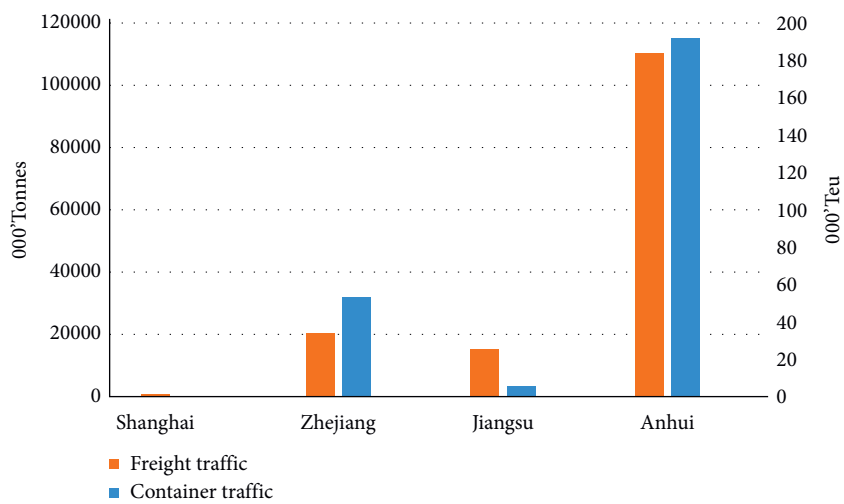

Figure 3: The rail-road freight transport traffic.

All the indicators are selected by the brainstorming meeting with experts experienced with rail-based transport from the Yangtze River Delta region. Meanwhile, a questionnaire was designed to collect transport experts' opinions on the qualitative indicators. The survey includes two parts: the first part is to compare the significance between indicators as shown in Table 4; the second part is to score the qualitative indicators (C11, C12, C13, C21, C22, D31) based on the questions in Table 5. The questionnaires were sent to more than 200 logistics companies that had multimodal freight transport experience and 172 valid questionnaires were collected. Meanwhile, all the quantitative indicators are scored based on real-life freight data.

The single-level ordering method is used to score the three-level index system. To validate the index system's consistency, this study uses the ANC (Asymptotic Normalization Coefficient) method to calculate the maximal eigenvalue of the AHP judgment matrix **B** and its corresponding eigenvector. The judgment matrix **B** is defined as

$$\mathbf{B} = \begin{bmatrix} b_{11} & \cdots & b_{1j} \\ \vdots & \ddots & \vdots \\ b_{i1} & \cdots & b_{ij} \end{bmatrix}, \tag{1}$$

where b_{ij} represents the importance of index i to index j at a certain level. The matrix **B** is obtained by the expert scoring method. Each column of the matrix is then normalized, with the formula as follows:

$$\overline{b}_{ij} = \frac{b_{ij}}{\sum b_{ij}}, \quad i, j = 1, 2, \ldots, n. \tag{2}$$

The matrix after column normalization is added by row to $\overline{W}_i = \sum \overline{b}_{ij}$. Then, the vector $\overline{W} = [\overline{W}_1, \overline{W}_2, \ldots, \overline{W}_n]^T$ can be normalized as

$$W_i = \frac{\overline{W}_i}{\sum \overline{W}_j} \quad , i, j = 1, 2, \ldots, n. \tag{3}$$

The eigenvector can be expressed as $W = [W_1, W_2, \ldots, W_N]^T$, so that the maximal eigenvalue $\lambda_{\max}$ of the judgment matrix can be calculated through

$$\lambda_{\max} = \sum_{i=1}^{n} \frac{(BW)_i}{nW_i}. \tag{4}$$

The solution of the maximal eigenvalue $\lambda_{\max}$ is the basis of the consistency verification, which is carried out by the following formulas:

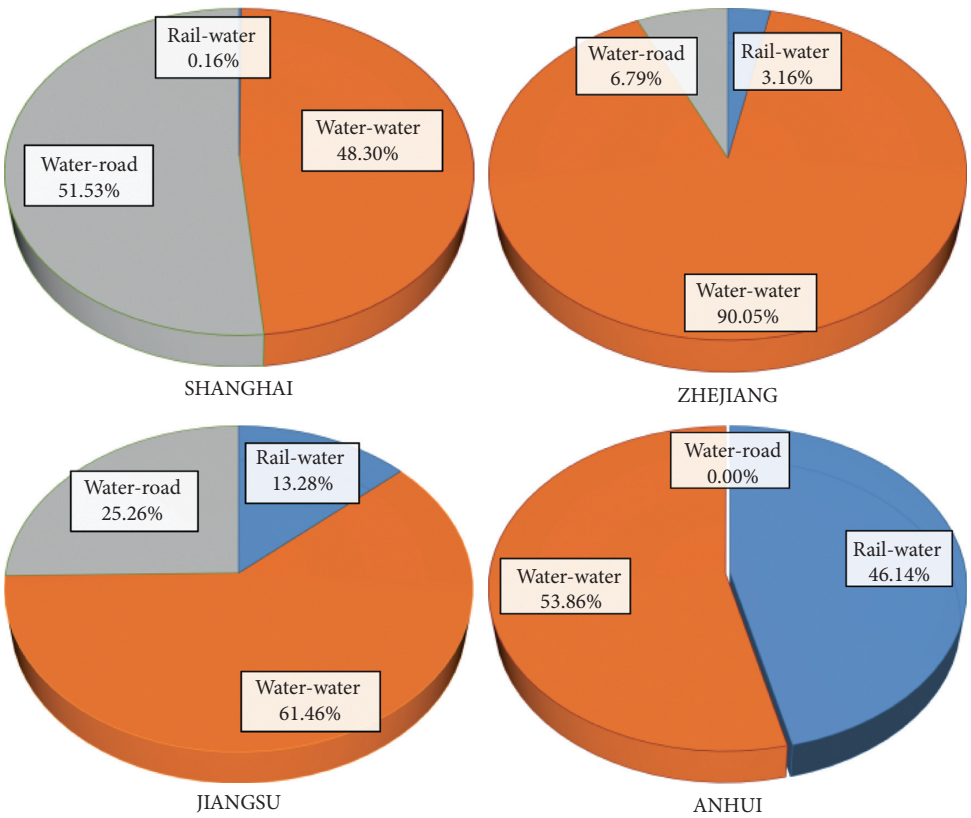

Figure 4: The water-based freight traffic in Yangtze River Delta.

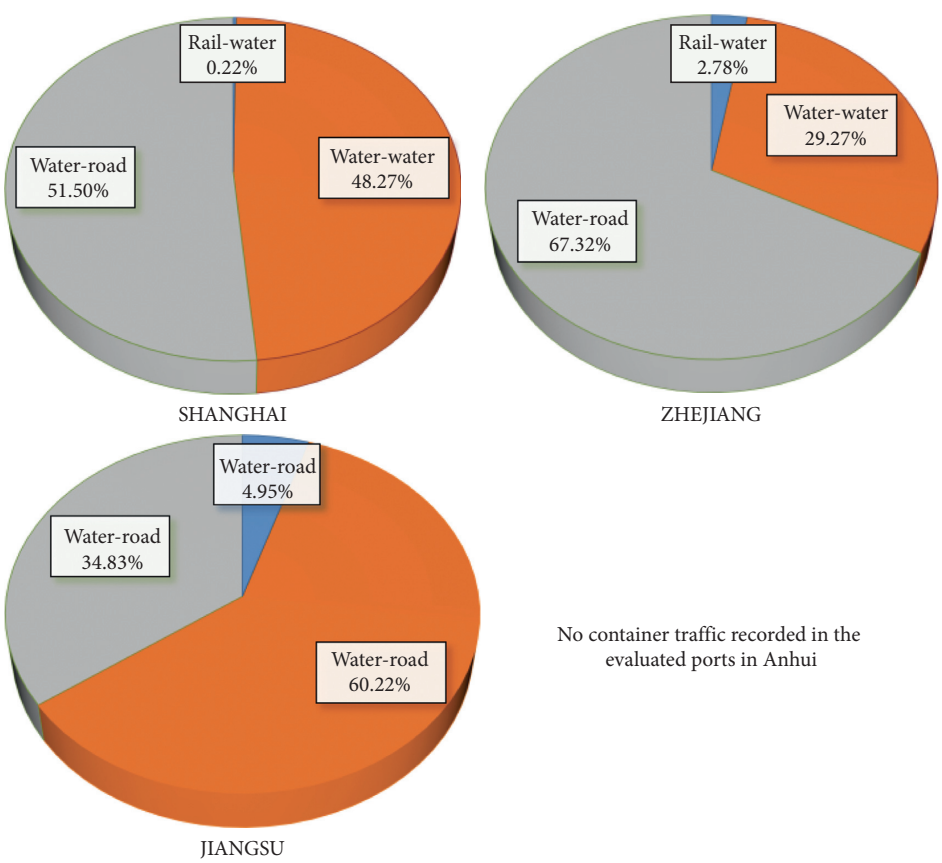

Figure 5: The water-based container traffic in Yangtze River Delta.

Table 3: The framework of the AHP-based index.

First level	Second level	Third level
Regional distribution network (A)	Multimodal transport infrastructure (A1)	Public rail stations and railway links (A11)
		Exclusive railway (A12)
		Port shoreline (A13)
		Highway density (A14)
	Multimodal transport operations (A2)	Public rail freight volume (A21)
		Exclusive rail freight volume (A22)
		Port throughput (A23)
		Highway freight volume (A24)
Multimodal transport capability (B)	Rail-water transport (B1)	Rail-water transport volume (B11)
	Water-water transport (B2)	Water-water transport volume (B21)
	Road-water transport (B3)	Road-water transport volume (B31)
	Road-rail transport (B4)	Road-rail transport volume (B41)
Transport operational performance (C)	Transport performance (C1)	Multimodal transport delay (C11)
		Multimodal transfer efficiency (C12)
		Revenue of multimodal transport (C13)
	Technical improvement (C2)	Informatization (C21)
		Availability (C22)
	Safety control (C3)	Ratio of accidents (C31)
		Average compensation for every accident (C32)
Sustainability (D)	Economic (D1)	Improvement of market share (D11)
	Environment (D2)	Unit energy consumption (D21)
	Social (D3)	Policy implication (D31)

Table 4: The description of the comparison significance between indicators is introduced as Mu and Pereyra-Rojas [29].

Significance (i)	Description
9	Compared with j, indicator i is extremely important
7	Compared with j, indicator i is very strongly more important
5	Compared with j, indicator i is strongly more important
3	Compared with j, indicator i is moderately more important
1	Compared with j, indicator i is equally important
2, 4, 6, 8	The intermediate values between the two adjacent judgments, used when a compromise is needed

$$\mathrm{CI} = \frac{\lambda_{\max} - n}{n-1} \times \frac{1}{\mathrm{RI}} < 0.1. \quad (5)$$

CI represents the consistency verification value. The value of RI depends on the dimensions of the index. Dimensions 1 to 4 are 0, 0, 0.58, and 0.90, respectively.

If the verification results of CI meet the above conditions, the index system meets the consistency requirements. The eigenvector $W = [W_1, W_2, \ldots, W_N]^T$ can be considered as the evaluation index weight that represents the importance ranking of the index to its superior index. The description of the significance comparison between indicators can be found in Table 4. Using equations (1)–(4), the index scores for qualitative indicators (C11, C12, C13, C21, C22, D31) can be calculated. For quantitative indicators, calculations are made using real-life data. The details of the raw data for every indicator can be found in Table 5. It is necessary to normalize the data of different dimensions and then calculate the corresponding scores. By doing so, we can obtain different scores of the third-level indicators. The second-level indicators' scores are obtained by the weighted sum of the corresponding third-level indicators' weights and scores. The first-level indicators' scores are obtained by the weighted sum of the second-level indicators' weights and scores. The scores of different indicators can be applied to analyze the development of multimodal transportation within the evaluated network.

5. Results and Discussion

5.1. The Impact of HSR on Railway Transportation in Yangtze River Delta. To reveal the different features of HSR impacts on the arterial and branch stations, Figures 6–9 compare the transport traffic (both freight and container traffic) in 2019 with the data in 2015 (the vertical axes in these figures indicate the traffic data in 2019 minus the corresponding data in 2015).

Compared with 2015, the rail freight traffic experienced a drop in 2019, probably because, in recent years, China has taken actions to restrict the consumption of coals to protect the environment, which has decreased the demand for bulk transportation. It is also noticed that the drop took place at branch stations. In contrast, the arterial stations recorded a substantial increase in traffic, largely due to the capacity release as a result of the HSR development. It seems that freight traffic has become more concentrated in the arterial stations. Our interviewers note that with the development of the HSR network, more passengers (80% of the total railway

Table 5: The description of original data for every indicator.

Indicators	Original data description
Public rail stations and railway links (A11)	The number of railway stations and links for public freight transport in the evaluated network
Exclusive railway (A12)	The number of railway links of transporting freight for exclusive companies in the evaluated network
Port shoreline (A13)	The length of the berthing line [30] for the evaluated ports
Highway density (A14)	The highway density which equals the total length of a highway divided by the acreage of the area for the evaluated regions (Shanghai, Zhejiang, Jiangsu, Anhui)
Public rail freight volume (A21) Exclusive rail freight volume (A22) Port throughput (A23) Highway freight volume (A24)	The corresponding freight volume of A11 to A14 in 2019
Rail-water transport volume (B11) Water-water transport volume (B21) Road-water transport volume (B31) Road-rail transport volume (B41)	The multimodal transport volume in 2019
Multimodal transport delay * (C11)	How is the performance of multimodal transport? Do you satisfied with the service of the multimodal transport considering the possible delay?
Multimodal transfer efficiency (C12) *	How is the transferring efficiency in the multimodal stations or terminals?
Revenue of multimodal transport (C13) *	Will you choose multimodal transport instead of your former transport choice? Is the cost of multimodal transport competitive?
Informatization (C21) *	How about the operations system of multimodal transport when you try to use it?
Availability (C22) *	Is it convenient for you to get the service for multimodal transport?
Ratio of accidents (C31) Average compensation for every accident (C32)	No railway freight accident recorded in 2019 for the evaluated stations and links
Improvement of market share (D11)	The freight volume improvement (2019 compared with 2018) for multimodal transport in the evaluated network
Unit energy consumption (D21)	The variation of energy consumption for unit freight transport (total consumption divide total freight volume)
Policy implication (D31) *	How about the impacts of governmental policy implication for multimodal transport?

*The target scores for the qualitative indicators are based on the answers to the following questions by invited experts from 0 to 100.

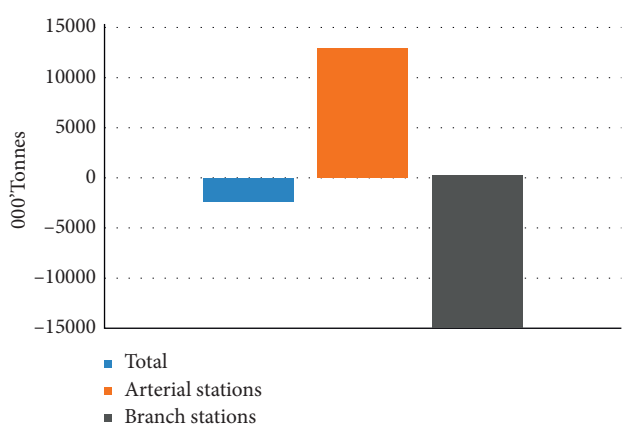

Figure 6: Freight traffic comparison between 2019 and 2015.

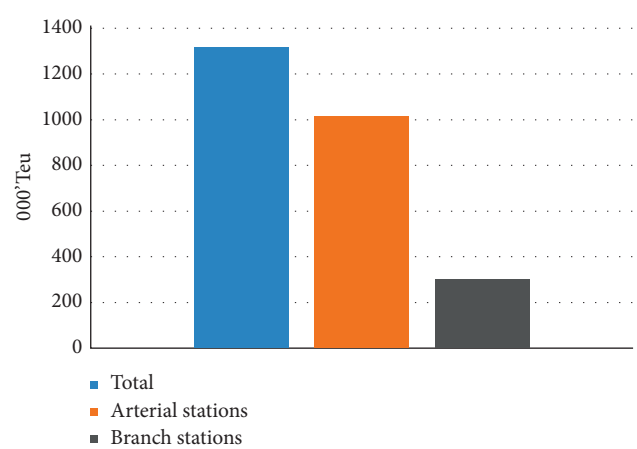

Figure 7: Container traffic comparison between 2019 and 2015.

passengers in 2019) chose HSR instead of the conventional railway services especially those along the arterial stations. As a result, the conventional railway infrastructures were released for handling freight, which can explain the rise in freight traffic at arterial stations. The rise in container traffic is not surprising as, in recent years, incentive policies such as those noted in *The Action Plan* have been implemented to promote containerization transportation.

Figures 8 and 9 further report the changes in freight and container traffic in these two years for Shanghai and three provinces. The same pattern can be observed for each province, suggesting that HSR has promoted the freight traffic at arterial stations. With the impacts of HSR development, the freight transport for arterial stations has been shown with a better opportunity to lead the rail-based freight transport. The results guide policymakers on the one hand focus on optimizing the conventional rail infrastructures to

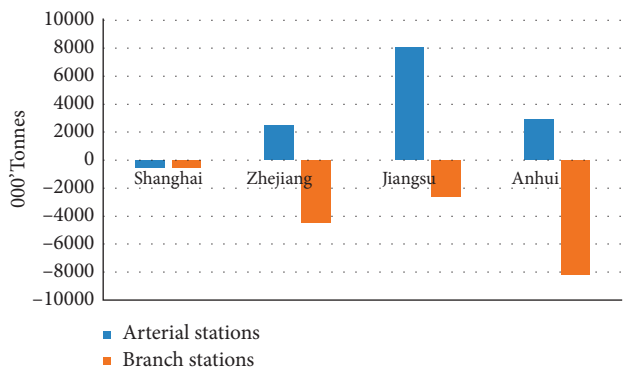

Figure 8: Freight traffic comparison between 2019 and 2015.

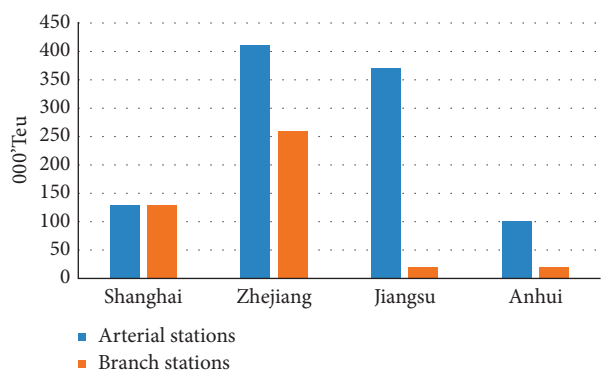

Figure 9: Container traffic comparison between 2019 and 2015.

support rail-based freight transport for arterial stations and, on the other hand, release more incentives for promoting rail-based traffic for branch stations.

5.2. The Current Status of the Rail-Based Multimodal Transport in Yangtze River Delta. The evaluation index weights based on Section 4 are shown in Table 6. The index scores for each indicator and province are reported in Table 7. Zhejiang leads other provinces with the highest overall score, 92.36, followed by Jiangsu, 89.97; Anhui, 88.32; and Shanghai, 88.05.

The scores of the first-level indicators are shown in Figure 10. It can be seen that Zhejiang scores the highest in multimodal transport capacity, transport operational performance, and sustainability, while Anhui has the highest score in the regional distribution network.

The evaluation results of the regional distribution network are shown in Figure 11. Shanghai's transport infrastructures are relatively strong, especially in terms of highway density, port shoreline, and port throughput as shown in Table 7. However, their weights are small based on expert scoring which makes Shanghai lag behind in the rail-based infrastructure and operations. In contrast, Anhui is more developed in exclusive railway and highway freight volume, public rail station, and exclusive railway links, whose weights are relatively higher. As a result, Anhui has the best multimodal transport operations. Meanwhile, Zhejiang has a balanced development in public rail freight volume, port throughput, and its regional distribution network. In terms of multimodal transport capability in Figure 12, Zhejiang and Jiangsu have a better overall performance, and they are well developed in rail-water transport. For Shanghai, water-based transport including water-water transport and road-water transport has developed more prominently, while Anhui has the best road-rail transport performance.

The evaluation results of the transport operational performance can be found in Figure 13. The research has investigated the main multimodal transport market in the Yangtze River Delta. The results show that Zhejiang received relatively higher scores for transport performance and technical improvement. Shanghai and Jiangsu do not lag too far behind in these two indicators because the development of technical improvement and transport performance is well developed in the Yangtze River Delta region. There was no railway freight accident recorded in 2019 and all provinces received 100 points. However, the technical improvement and transport performance of Anhui received relatively lower points, implying that there is room for improvement for the indicators of transport delay, transfer efficiency, revenue, informatization, and availability as shown in Table 7.

In terms of sustainability, the scores can be seen in Figure 14. Shanghai is highly restricted by the strong water-based transport and market, which have affected the

Table 6: The evaluation indicators weight.

First level	Second level	Third level
0.2139 (A)	0.4220 (A1)	0.5561 (A11)
		0.2664 (A12)
		0.1150 (A13)
		0.0626 (A14)
	0.5780 (A2)	0.5438 (A21)
		0.2302 (A22)
		0.1367 (A23)
		0.0894 (A24)
0.1659 (B)	0.5314 (B1)	1.0000 (B11)
	0.1640 (B2)	1.0000 (B21)
	0.1244 (B3)	1.0000 (B22)
	0.1802 (B4)	1.0000 (B23)
0.3972 (C)	0.4390 (C1)	0.4164 (C11)
		0.1867 (C12)
		0.3969 (C13)
	0.2099 (C2)	0.5327 (C21)
		0.4673 (C22)
	0.3511 (C3)	0.4113 (C31)
		0.5887 (C32)
0.2230 (D)	0.3485 (D1)	1.0000 (D11)
	0.3746 (D2)	1.0000 (D21)
	0.2769 (D3)	1.0000 (D31)

Table 7: Index scores of the third-level indicators.

The indicators of the third-level	Shanghai	Zhejiang	Jiangsu	Anhui
Public rail stations and railway links (A11)	82.23	87.00	88.55	94.23
Exclusive railway (A12)	84.09	86.13	85.68	96.09
Port shoreline (A13)	93.77	85.90	90.56	81.77
Highway density (A14)	96.33	85.57	85.77	84.33
Public rail freight volume (A21)	81.71	93.71	87.92	88.65
Exclusive rail freight volume (A22)	84.09	87.19	84.63	96.09
Port throughput (A23)	92.88	91.89	86.36	80.88
Highway freight volume (A24)	81.24	88.12	89.39	93.24
Rail-water transport volume (B11)	82.67	92.76	94.28	82.28
Water-water transport volume (B21)	92.64	92.45	86.27	80.64
Road-water transport volume (B31)	94.64	89.01	85.72	82.64
Road-rail transport volume (B41)	83.73	87.49	85.06	95.73
Multimodal transport delay (C11)	90.26	93.03	87.67	81.03
Multimodal transfer efficiency (C12)	93.72	89.97	86.6	81.72
Revenue of multimodal transport (C13)	86.57	95.04	87.35	83.04
Informatization (C21)	88.18	94.04	87.75	82.04
Availability (C22)	93.43	92.63	84.52	81.43
Ratio of accidents (C31) *	100.00	100.00	100.00	100.00
Average compensation for every accident (C32) *	100.00	100.00	100.00	100.00
Improvement of market share (D11)	84.50	84.87	86.14	96.50
Unit energy consumption (D21)	81.36	91.47	93.36	85.80
Policy implication (D31)	85.85	95.02	88.11	83.02

*As no railway freight accident is recorded in 2019 for the evaluated stations and links, the scores for C31 and C32 are 100.

development of railway freight transport, so the score is significantly lower. Meanwhile, the governmental policies seem too weak to promote the transformation of Shanghai's transport structure. In contrast, the governmental policies in Zhejiang are more active to stimulate rail-based transport. Considering the environmental impacts, Jiangsu has the best performance with less road-based transport and more green modals. Meanwhile, Anhui is developing rapidly in the rail-based multimodal transport based on the well-developed rail infrastructures.

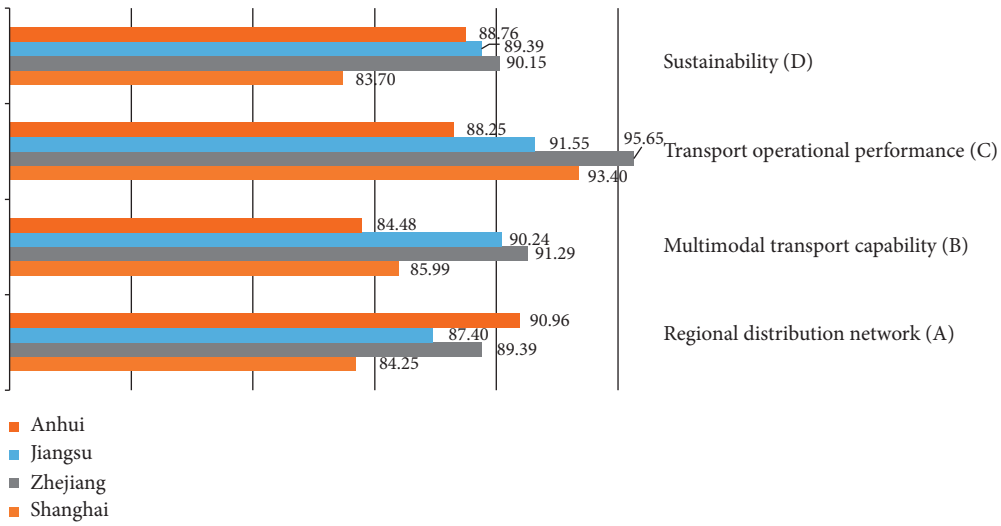

Figure 10: The score of the first-level indicators.

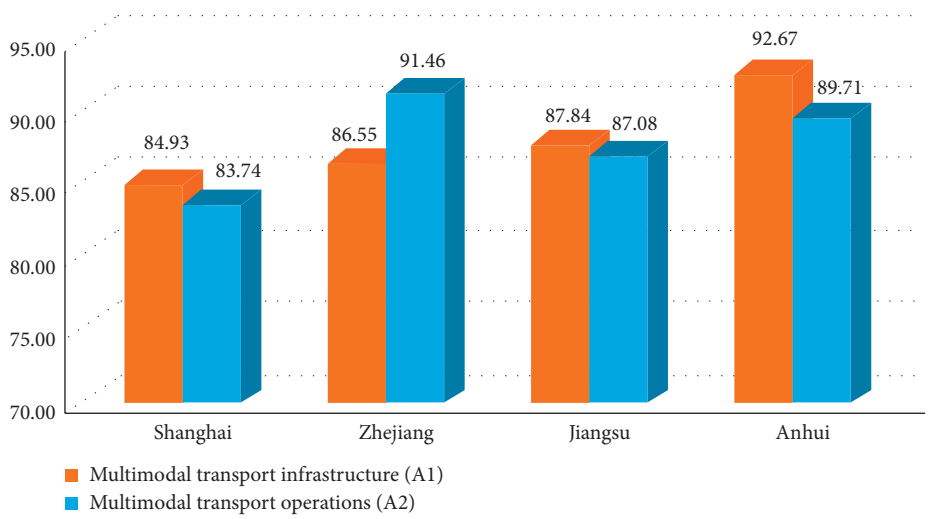

Figure 11: The index scores of the regional distribution network.

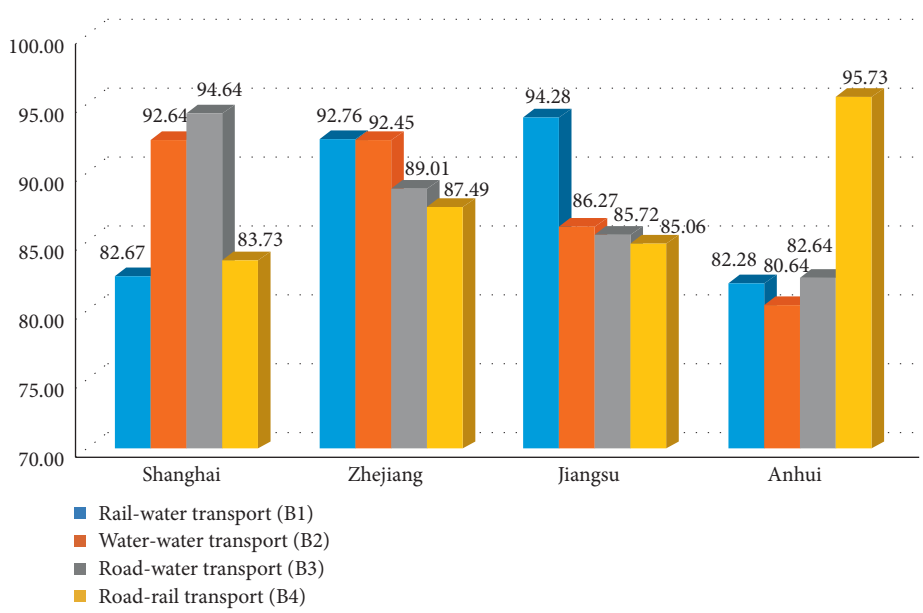

Figure 12: The scores of the multimodal transport capability.

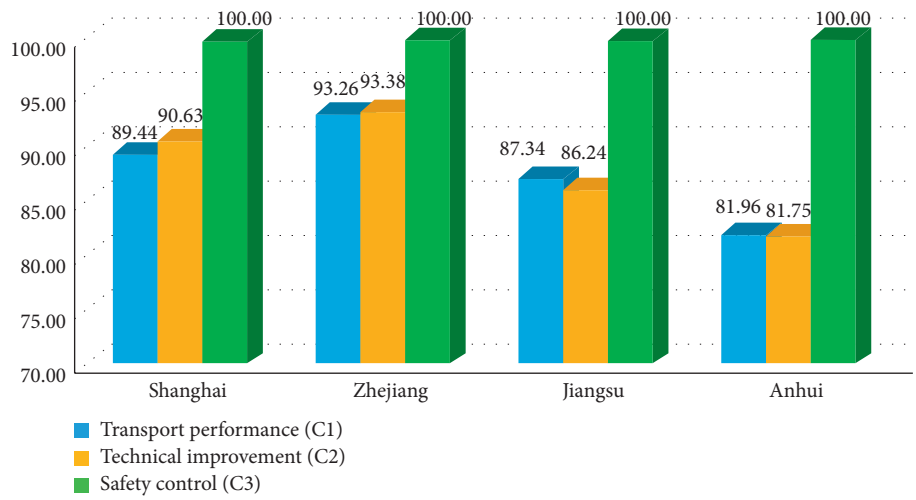

Figure 13: The scores of the transport operational performance.

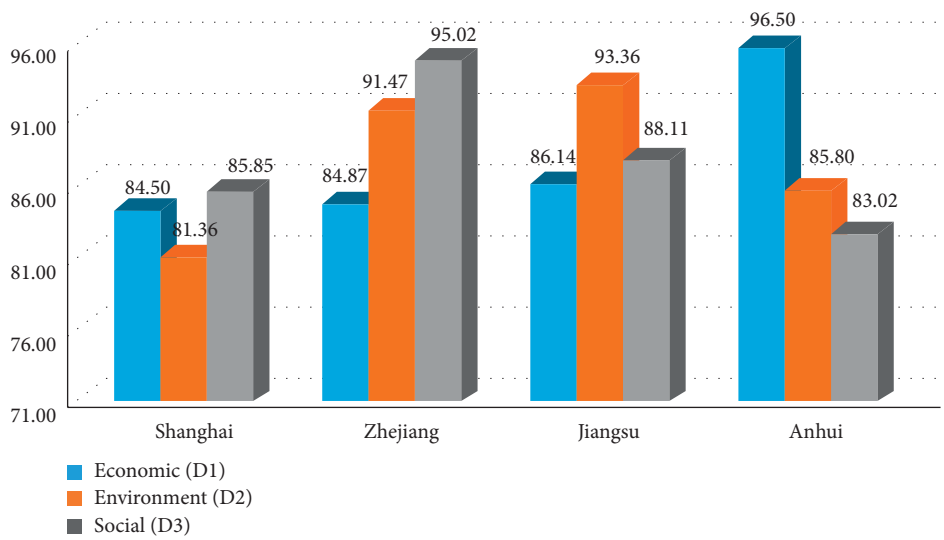

Figure 14: The scores of the sustainability.

6. Conclusions

This research proposes a method to evaluate the current status of the rail-based multimodal freight transport system in the Yangtze River Delta economics zone and reveals the impacts of HSR development on rail-based freight transport. Here are some major findings:

(1) The rail-based freight transport gradually plays a more important role in the multimodal transport in the Yangtze River Delta region due to the capacity releases of the conventional railway with the growth of the HSR network. The development of HSR has a positive impact on the rail-based freight and container traffic especially for the railway stations along the *eight vertical and eight horizontal* arteries. Therefore, the policymaker should pay more attention to optimizing the conventional railway schedules for arterial stations to improve freight transport.

(2) The original transport market and modals still determine the multimodal transport structures. Zhejiang has led the rail freight transport while Shanghai mainly leads the waterway freight transportation. Meanwhile, the road-rail transport in Anhui and water-rail transportation in Jiangsu are also well developing within the Yangtze River Delta region. Thus, the policymaker should design different incentives based on the original transport modals in each region to promote rail-based freight transport.

(3) Overall, the designed comprehensive index is shown to be efficient to evaluate multimodal transport, especially for rail-based freight transport. Currently, rail-based freight transport is still not competitive compared with road-based and water-based transport in the Yangtze River Delta region. However, the timely updates of this evaluation are important for the government to trace the development of rail-

based multimodal transport and release more efficient policies.

Besides, the proposed evaluation method is also available for evaluating the development of rail-based multimodal transport for individual cities and logistic centers, which is also inspiring for developing rail-based freight transport in different levels.

Data Availability

No data were used to support this study.

Conflicts of Interest

The authors declare that they have no conflicts of interest.

Acknowledgments

This work was sponsored by the National Natural Science Foundation of China (grant nos. 72072112, 71602114, 71804108, and 72001135), Shanghai Rising-Star Program (grant no. 19QA1404200), and Shanghai Sailing Program (grant no. 20YF1416600).

References

[1] L. Zhen, Z. Liang, D. Zhuge, L. H. Lee, and E. P. Chew, "Daily berth planning in a tidal port with channel flow control," *Transportation Research Part B: Methodological*, vol. 106, pp. 193–217, 2017.

[2] C. M. Tan and J. L. He, "Integrated proactive and reactive strategies for sustainable berth allocation and quay crane assignment under uncertainty," *Annals of Operations Research*, 2021.

[3] J. He, Y. Wang, C. Tan, and H. Yu, "Modeling berth allocation and quay crane assignment considering QC driver cost and operating efficiency," *Advanced Engineering Informatics*, vol. 47, Article ID 101252, 2021.

[4] W. Ma, Q. Wang, H. Yang, G. Zhang, and Y. Zhang, "Understanding airline price dispersion in the presence of high-speed rail," *Transport Policy*, vol. 95, pp. 93–102, 2020.

[5] A. Zhang, Y. Wan, and H. Yang, "Impacts of high-speed rail on airlines, airports and regional economies: a survey of recent research," *Transport Policy*, vol. 81, pp. A1–A19, 2019.

[6] Z. Chen and K. E. Haynes, "Impact of high-speed rail on regional economic disparity in China," *Journal of Transport Geography*, vol. 65, pp. 80–91, 2017.

[7] F. Zhang, Z. Yang, J. Jiao, W. Liu, and W. Wu, "The effects of high-speed rail development on regional equity in China," *Transportation Research Part A: Policy and Practice*, vol. 141, pp. 180–202, 2020.

[8] F. Long, L. Zheng, and Z. Song, "High-speed rail and urban expansion: an empirical study using a time series of nighttime light satellite data in China," *Journal of Transport Geography*, vol. 72, pp. 106–118, 2018.

[9] Y. Liang, K. Zhou, X. Li, Z. Zhou, W. Sun, and J. Zeng, "Effectiveness of high-speed railway on regional economic growth for less developed areas," *Journal of Transport Geography*, vol. 82, Article ID 102621, 2020.

[10] H. Li, K. Wang, K. Yu, and A. Zhang, "Are conventional train passengers underserved after entry of high-speed rail?-evidence from Chinese intercity markets," *Transport Policy*, vol. 95, pp. 1–9, 2020.

[11] M. Diao, "Does growth follow the rail? The potential impact of high-speed rail on the economic geography of China," *Transportation Research Part A: Policy and Practice*, vol. 113, pp. 279–290, 2018.

[12] J. Cao, X. C. Liu, Y. Wang, and Q. Li, "Accessibility impacts of China's high-speed rail network," *Journal of Transport Geography*, vol. 28, pp. 12–21, 2013.

[13] F. Sun and Y. S. Mansury, "Economic impact of high-speed rail on household income in China," *Transportation Research Record: Journal of the Transportation Research Board*, vol. 2581, no. 1, pp. 71–78, 2016.

[14] M. Yin, L. Bertolini, and J. Duan, "The effects of the high-speed railway on urban development: international experience and potential implications for China," *Progress in Planning*, vol. 98, pp. 1–52, 2015.

[15] E. Cascetta, A. Cartenì, I. Henke, and F. Pagliara, "Economic growth, transport accessibility and regional equity impacts of high-speed railways in Italy: ten years ex post evaluation and future perspectives," *Transportation Research Part A: Policy and Practice*, vol. 139, pp. 412–428, 2020.

[16] Y. Chen, "High speed Rail and China's New Economic Geography: impact assessment from the regional science perspective," *Eurasian Geography and Economics*, Edward Elger, Cheltenham, UK, 2020.

[17] J. Weng, X. Zhu, and X. Li, "Impact of high-speed rail on destination accessibility: a case study of China," *Journal of China Tourism Research*, vol. 16, pp. 494–509, 2020.

[18] Z. Chen and K. E. Haynes, "Impact of high-speed rail on international tourism demand in China," *Applied Economics Letters*, vol. 22, no. 1, pp. 57–60, 2015.

[19] Z. Yang and T. Li, "Does high-speed rail boost urban tourism economy in China?," *Current Issues in Tourism*, vol. 23, no. 16, pp. 1973–1989, 2020.

[20] Z. Chen, Z. Wang, and H. Jiang, "Analyzing the heterogeneous impacts of high-speed rail entry on air travel in China: a hierarchical panel regression approach," *Transportation Research Part A: Policy and Practice*, vol. 127, pp. 86–98, 2019.

[21] Q. Zhang, H. Yang, and Q. Wang, "Impact of high-speed rail on China's Big Three airlines," *Transportation Research Part A: Policy and Practice*, vol. 98, pp. 77–85, 2017.

[22] Q. Zhang, H. Yang, Q. Wang, A. Zhang, and Y. Zhang, "Impact of high-speed rail on market concentration and Lerner index in China's airline market," *Journal of Air Transport Management*, vol. 83, Article ID 101755, 2020.

[23] H. Yang and A. Zhang, "Effects of high-speed rail and air transport competition on prices, profits and welfare," *Transportation Research Part B: Methodological*, vol. 46, no. 10, pp. 1322–1333, 2012.

[24] H. Yang, W. Ma, Q. Wang, K. Wang, and Y. Zhang, "Welfare implications for air passengers in China in the era of high-speed rail," *Transport Policy*, vol. 95, pp. A1–A13, 2020.

[25] C. Wu, M. Liao, Y. Zhang, M. Luo, and G. Zhang, "Network development of low-cost carriers in China's domestic market," *Journal of Transport Geography*, vol. 84, Article ID 102670, 2020.

[26] I. Watson, A. Ali, and A. Bayyati, "Freight transport using high-speed railways," *International Journal of Transport Development and Integration*, vol. 3, no. 2, pp. 103–116, 2019.

[27] J. A. Pazour, R. D. Meller, and L. M. Pohl, "A model to design a national high-speed rail network for freight distribution," *Transportation Research Part A: Policy and Practice*, vol. 44, no. 3, pp. 119–135, 2010.

[28] Y. Li, Z. Chen, and P. Wang, "Impact of high-speed rail on urban economic efficiency in China," *Transport Policy*, vol. 97, pp. 220–231, 2020.
[29] E. Mu and M. Pereyra-Rojas, "Understanding the analytic hierarchy process," *Practical Decision Making*, pp. 7–22, Springer, Berlin, Germany, 2017.
[30] L. Zhen, "Tactical berth allocation under uncertainty," *European Journal of Operational Research*, vol. 247, no. 3, pp. 928–944, 2015.